Strategies for the Synthesis of Bioactive Compounds: Biomimetic Approaches to the Salinosporamides and the Hexadehydro-Diels–Alder Reaction

A DISSERTATION
SUBMITTED TO THE FACULTY OF THE GRADUATE SCHOOL
OF THE UNIVERSITY OF MINNESOTA BY

Patrick Henry Willoughby

IN PARTIAL FULFILLMENT OF THE REQUIREMENTS
FOR THE DEGREE OF
DOCTOR OF PHILOSOPHY

Thomas R. Hoye, Adviser

August 2013

Acknowledgements

As I reflect on reaching this milestone of my career I have so many people to thank. First and foremost, I would like to thank my wife, Amber Willoughby. I would not be where I am today without her unconditional support, encouragement, and, most importantly, love. She embodies the perfect companion and she is my best friend. Because of this, and countless other things for which I probably am not aware of, I love her, and continue to fall more and more in love with her each day.

I would like to thank my parents, Clark and Patricia Willoughby. It was not until my sophomore year of college that I realized I wanted to be a scientist. Too many it was a surprise, however, being raised by a college instructor and a nurse/chiropractor/botanist/ adjunct professor it is less unexpected that my inherited interests might lead me to some form of science in an academic setting. In fact, when I was eleven my father built me a wooden tool bench and gave it to me as a birthday present. It was equipped with notches for me to holster the various tools that I didn't have. To be honest, I was surprised to receive it and its use or intrigue wasn't immediately apparent. However, included with the bench was a toy chemistry set. I spent quite a bit of time mixing the various chemicals together and storing them in well-labeled vials. To those who know my laboratory habits, it is probably not surprising that my mother was not pleased with how quickly the bench became cluttered and untidy. I could ramble with more stories similar to this, but suffice it to say that I had two parents that were passionate about my development and cared deeply about my attitude towards education and its effects on society. For their unending love, support, and encouragement, I also thank my sister Kimberly Lohrer, grandparents Margaret Willoughby, Patrick Enwright, and Jeannine Enwright; in-laws Steve Lohrer, Jennifer Lammers, Nathan Lammers, and Sara Werner. For their clear-minded advice, unending encouragement, and ability to always find a way to take my mind off of research I thank personal friends Jordan Engbers, Chad Bitterman, and Jordan Bathen.

I would next like to thank my adviser, Thomas R. Hoye. Tom has been a phenomenal adviser. The common phrase around lab is always "Tom is the smartest person I know." I can't disagree with this statement, especially so in the context of

chemistry. Every step of my graduate career, Tom has been there with advice and insight. I could scratch my head about an issue for a week, and after a quick, two-minute conversation with Tom, I would have all the guidance and direction I needed. Our conversations have changed the way I think about chemistry and science, and I know that I am not alone in saying that. In addition to being a world-class scientist, he has dedicated himself to becoming an excellent educator, and his students can tell that teaching is what ultimately drives him. Fortunately, I have more or less been a member of the Hoye group since 2007, when I was a bright-eyed, bushy-tailed Lando student. From then until now (and I assume onward into the future), Tom has treated me as a colleague and with the utmost respect. I am sure that has not always been easy. In addition to being intelligent, a good scientist, and a great educator, Tom is very patient. In fact, aside from my mother, I would argue that he is the most patient person I know.

I can't say enough good things about Tom, but I would like to end my acknowledgement to him more professionally. Tom has provided me with an educational opportunity richer and deeper than I could have ever imagined. As a member of the Hoye group, I have been involved with a variety of interesting and creative projects. Often, Tom let me run free and let the course be driven by my own interests. It was fun, exciting, instructional, and, most importantly, rewarding. Tom has fought valiantly in a number of ways to ensure that I had that opportunity, and I will never forget it. Still, I can't help but think I fell short of taking full advantage of just how grand this opportunity was and I make myself feel better by arguing that no one could.

I would next like to thank my committee members, Tom, Wayland Noland, Marc Distefano, and Robert Fecik. They have been helpful, patient, flexible, and supportive as I progressed through the written and oral preliminary examinations, as well as the final Thesis submission and oral defense. I would like to thank Professors Christopher Cramer, Christopher Douglas, Steve Kass, Marc Hillmyer, Valerie C. Pierre, as well as Tom for providing excellent coursework. The material presented was both relevant and helpful in preparing me for the rigors of graduate research. Additionally, I am grateful for the many helpful personal conversations I had with Professor Cramer, Douglas, and Andrew Harned. I would like to thank Letitia Yao for her continued commitment to ensuring that

our NMR facilities are state-of-the-art and always running smoothly. I would like to thank Gregory T. Rohde, Victor G. Young, and the X-Ray Crystallographic Laboratory for their determination of the crystallographic data presented in this Thesis. I would also like to thank my undergraduate professors Russell Wiley, William Harwood, Kirk Manfredi, Jeffrey Elbert, and Ira Simet, whose wisdom I still value and lessons I still reflect on.

Being able to participate with Tom's early efforts into the HDDA reaction was a phenomenal experience and I would like to thank Beeraiah (Beeru) Baire, Dawen Niu, and Brian Woods (a.k.a Team Benzyne). This was one of the best team experiences I've had. The group was very intense and focused, but also supportive and understanding. I think I learned just as much about working on a team-based project as I did about chemistry. I would also like to thank other members of the Hoye group, namely Aaron May, Matthew Jansma, Aaron Burns, Junha Jeon, and Lucas Kopel. All of these individuals played key roles in my development as a chemist. Aaron May taught me everything from using a separatory funnel to acylating an oxazolidinone with 99.7% yield. He was incredibly patient with me while I was a Lando and I still employ many of his 'tricks' on a daily basis. Matt taught me everything I know about computational chemistry. Additionally, Matt and Aaron Burns were great resources for all-things synthesis. Combined, these two know so much about organic chemistry, from basically all named reactions to the details of many obscure organometallic reactions. Junha and Lucas welcomed me to 415 Smith with open arms. They were the first to provide me with glassware, reagents, silica gel, etc. I am grateful for the friendships and helpful conversations I had with other members including Eric Buck, Julian Lo, Adam Wohl, Susan Brown, Josh Marell, Junhua Chen, Tao Wang, Andrew Michel, Sean Ross, Amanda Schmit, and Susanna Emond. I also had the opportunity to work with three excellent undergraduates Stephen Humble, Angelika Neitzel, and Dmitry Kuznetsov. These students were dedicated to undergraduate research and patient with me as I learned to juggle all of our projects. I am also indebted to Eric and Brian for critically reviewing this thesis.

To my son, Logan

My source of joy and inspiration

Abstract

Part I: The salinosporamides are a subset of polyketide-derived marine natural products that have as their key structural feature a fused γ-lactam/β-lactone moiety. These molecules are known to inhibit the 20S proteasome (20SP) by utilizing the β-lactone reactivity, a promising target for cancer therapeutics. We propose that salinosporamide A may be formed biosynthetically by a non-enzymatic bis-cyclization event involving an uncatalyzed intramolecular ketene-ketone [2+2] cycloaddition of an amidoketene precursor. We also propose a transition state that places the C2 substituent pseudo-equatorial, allowing for enhanced stereoselectivity during bis-cyclization. Enolate formation from a thioester followed by internal acylation and concurrent loss of thiolate would form a 5(4H)-oxazolone. It is known that 5(4H)-oxazolones readily tautomerize to 4-hydroxyoxazoles, which are in equilibrium with their mesoionic Münchnone forms. Valence bond isomerism interconverts Münchnones to amidoketenes. Spontaneous ketene-ketone [2+2] cycloaddition would siphon the precursors through such a tautomeric manifold to give the natural product. Progress toward the synthesis of the biosynthetic precursors to salinosporamide A is disclosed in Chapters 3–5.

Part II: The second part of this Thesis describes our recent, serendipitous encounter with the hexadehydro-Diels–Alder (HDDA) reaction. The HDDA reaction is a mode of the Diels–Alder reaction that involves [4+2] cycloaddition between a diyne and an alkyne to form aryne reactive intermediate. In Part II we show the scope of substrates that are capable of generating an aryne via the HDDA reaction. Additionally, we show that HDDA-mediated generation of arynes allows for the discovery of new modes of aryne trapping, for example, the desaturation of hydrocarbons.

Table of Contents

List of Figures

List of Tables

List of Abbreviations

20SP	20S proteasome core particle
4-PPY	4-Pyrrolidinopyridine
Ac_2O	Acetic anhydride
AIBN	Azobisisobutyronitrile
$AlMe_3$	Trimethylaluminum
API	Active pharmaceutical ingredient
Bn	Benzyl
BOP	(Benzotriazol-1-yloxy)tris(dimethylamino)phosphonium hexafluorophosphate
BOPCl	Bis(2-oxo-3-oxazolidinyl)phosphinic chloride
BRSM	Based on recovered starting material
Bz	Benzoyl
CAN	Cerric ammonium nitrate
Cbz	Carbobenzyloxy
CMAE	Corrected mean absolute error
CoA	Coenzyme A
CSA	Camphor sulfonic acid
DBBT	Dibutylboryl trifluoromethanesulfonate
DBU	Diaza(1,3)bicyclo[5.4.0]undecane
DIEA	Diisopropylethylamine
DIBAL	Diisobutylaluminum hydride
DCC	Dicyclohexylcarbodiimide
DCM	Dichloromethane
DCE	Dichloroethane
DFT	Density functional theory
DMAD	Dimethyl acetylenedicarboxylate
DMAP	*N*,*N*-4-Dimethylaminopyridine
DME	Dimethoxyethane

DMP [O]	Standard procedure: Dess–Martin periodinane-mediated oxidation
DMF	*N*,*N*-Dimethylformamide
DMS	Dimethyl sulfide
dr	Diastereomeric ratio
EDCI	*N*-(3-Dimethylaminopropyl)-*N'*-ethylcarbodiimide hydrochloride
ee	Enantiomeric excess
epi	Epimer
EtOAc	Ethyl acetate
Et_3N	Triethylamine
Et_2O	Diethyl ether
MAE	Mean absolute error
GIAO	Gauge-independent atomic orbital
GC/MS	Gas chromatography-mass spectrometry
HATU	1-[Bis(dimethylamino)methylene]-1*H*-1,2,3-triazolo[4,5-*b*]pyridinium 3-oxid hexafluorophosphate
HBTU	*O*-(Benzotriazol-1-yl)-*N,N,N′,N′*-tetramethyluronium hexafluorophosphate
HOBT	1-Hydroxybenzotriazole
HR ESI-MS	High resolution electrospray ionization-mass spectrometry
IEFPCM	Integrated equation formalism polarized continuum model
IR	Infrared
LC/MS	Liquid chromatography-mass spectrometry
LDA	Lithium diisopropylamide
LiHMDS	Lithium *bis*(trimethylsilyl)amide
LUMO	Lowest unoccupied molecular orbital
MeCN	Acetonitrile
MS	Molecular sieve
mp	Melting point
MTBE	*tert*-Butyl methyl ether
NAC	*N*-Acetylcysteamine

NBS	*N*-Bromosuccinimide
NCI	National Cancer Institute
NF-κB	Nuclear factor-kappa B
NMP	*N*-Methyl-2-pyrrolidone
NMR	Nuclear magnetic resonance
PCP	Peptidyl carrier protein
$PhCH_3$	Toluene
PhH	Benzene
PhSH	Benzenethiol
$(PhS)_2$	Diphenyl disulfide
PPh_3	Triphenylphosphine
PMB	4-Methoxybenzyl
PPTS	Pyridinium *para*-toluenesulfonate
psi	Pounds per square inch
Py	Pyridine
PyBOP	(Benzotriazol-1-yloxy)tripyrrolidinophosphonium hexafluorophosphate
SAD	Sharpless asymmetric dihydroxylation
SAR	Structure-activity relationship
SNAC	*S*-(*N*-Acetylcysteamine)
TAL	Tandem aldol-lactonization
TBAF	Tetra-*n*-butylammonium fluoride
TBAI	Tetra-*n*-butylammonium iodide
TBS	*t*-Butyldimethylsilyl
TBDPS	*t*-Butyldiphenylsilyl
TES	Triethylsilyl
Tf	Trifluoromethanesulfonyl
TFA	Trifluoroacetic acid
TIPS	Triisopropylsilyl
THF	Tetrahydrofuran

Thr1O$^{\gamma}$	*N*-Terminal threonine of the 20S proteasome core particle
TLC	Thin layer chromatography
TMAL	Tandem Mukaiyama aldol-lactonization
TMEDA	Tetramethylethylenediamine
TMS	Trimethylsilyl
Tol	4-Methylphenyl
Ts	*p*-Toluenesulfonyl
UA0	United-atomic Radii

◊ Part I ◊

Synthetic Studies Related to the Biosynthesis of Salinosporamide A

Chapter 1. Introduction and Background

1.1. Isolation, Structure Elucidation, and Biological Activity of Salinosporamide A

In 2003, Fenical and co-workers[1] reported the isolation of salinosporamide A (**1**, Figure 1-A, a.k.a NPI-0052 and marizomib[2]), a secondary metabolite of the marine actinomycete *Salinispora tropica*. Cytotoxicity-guided fractionation of several biologically active crude extracts of *Salinispora tropica* produced 7 mg L^{-1} of **1** as a colorless crystalline solid. The core structure of **1** is a fused γ-lactam/β-lactone bicycle containing five contiguous stereogenic centers, two of which are quaternary. Additional functionality of note are the C-2 chloroethyl and C-5 cyclohex-2-enyl groups. The bicyclic core of **1** is similar to that of omuralide (**1003**), which is formed in the extracellular matrix by lactonization of the isolated natural product lactacystin (**1002**) (cf. Figure 1-B). [3,4]

Figure 1 | Structures of interest: A) salinosporamide A (**1**), B) lactacystin (**1002**) and its conversion into omuralide (**1003**), C) X-ray crystal structure of **1**.

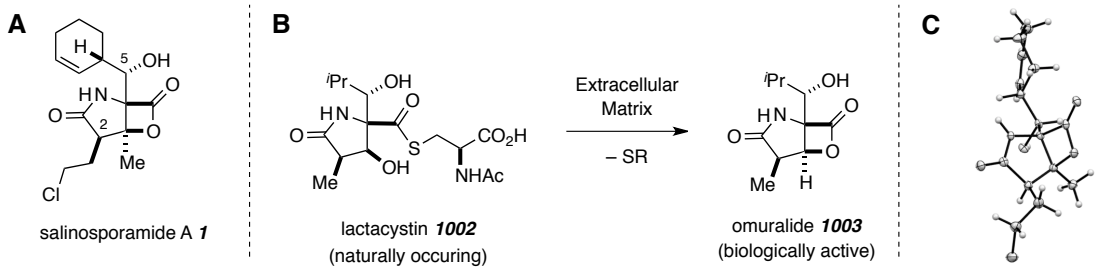

[1] Feling, R. H.; Buchanan, G. O.; Mincer, T. J.; Kauffman, C. A.; Jensen, P. R.; Fenical, W. Salinosporamide A: A highly cytotoxic proteasome inhibitor from a novel microbial source, a marine bacterium of the new genus *Salinospora*. *Angew*. *Chem*. *Int*. *Ed*. **2003**, *42*, 355–357.

[2] Potts, B. C.; Albitar, M. X.; Anderson, K. C.; Baritaki, S.; Berkers, C.; Bonavida, B.; Chandra, J.; Chauhan, D.; Cusack, J. C.; Fenical, W.; Ghobrial, I. M.; Groll, M.; Jensen, P. R.; Lam, K. S.; Lloyd, G. K.; McBride, W.; McConkey, D. J.; Miller, C. P.; Neuteboom, S. T. C.; Oki, Y.; Ovaa, H.; Pajonk, F.; Richardson, P. G.; Roccaro, A. M.; Sloss, C. M.; Spear, M. A.; Valashi, E.; Younes, A.; Palladino, M. A. Marizomib, a proteasome inhibitor for all seasons: Preclinical profile and a framework for clinical trials. *Current Cancer Drug Targets* **2011**, *11*, 254–284.

[3] Ōmura, S.; Fujimoto, T.; Otoguro, K.; Matsuzaki, K.; Moriguchi, R.; Tanaka, H.; Sasaki, Y. Lactacystin, a novel microbial metabolite, induces neuritogenesis of neuroblastoma cells. *J. Antibiot.* **1991**, *44*, 113–116.

[4] Dick, L. R.; Cruikshank, A. A.; Destree, A. T.; Grenier, L.; McCormack, T. A.; Melandri, F. D.; Nunes, S. L.; Palombella, V. J.; Parent, L. A.; Plamondon, L.; Stein, R. L. Mechanistic studies on the inactivation of the proteasome by lactacystin in cultured cells. *J. Biol. Chem.* **1997**, *272*, 182–188.

The structure of **1** was elucidated by analysis of NMR and mass spectrometry data.[1] The ^{1}H NMR spectrum included peaks with chemical shifts characteristic of an amide N-*H*, *Z*-alkene, oxygen-bearing methine, and an isolated methyl group. Additionally, the presence of a chlorine atom was evident from the $[M+2]^+$ molecular ion peak in the high-resolution mass spectrometry measurements, which further supported the molecular formula of the assigned structure. The authors also noted that the IR spectrum included bands at 1702 and 1819 cm^{-1}, the latter of which is diagnostic for a β-lactone carbonyl C=O stretch. The relative configuration was determined from nOe experiments, and other aspects of the structure were assigned following full analysis of various 2D NMR techniques (e.g., COSY, HMQC, and HMBC).[5] Crystallization from ethyl acetate/*iso*-octane afforded **1** as single crystals from which the authors utilized single-crystal X-ray diffraction to assign the absolute configuration and confirm the overall structure (cf. Figure 1-C).

In vitro biological assays demonstrated that **1** possessed cytotoxicity against HCT-116 human colon carcinoma cells (IC_{50} = 11 ng mL^{-1}). When screened against the NCI's 60-cell-line panel, **1** displayed potent activity against NCI-H226 non-small cell lung cancer, SF-539 CNS cancer, SK-MEL-28 melanoma, and MDA-MB-435 breast cancer (overall mean GI_{50} < 10 nM with log LC_{50} > 4). Because the structure of **1** resembles that of known proteasome inhibitor **1003**, the authors also probed **1** for proteasome inhibition activity. The IC_{50} value of **1** was found to be 1.3 nM for the inhibition of chymotrypsin-like proteolytic activity against purified 20S-proteasome core particle (20SP). For comparison, the authors found the IC_{50} value of **1002** to be 49 nM.[1] Shortly after initial isolation, **1** entered Phase I clinical trials for the treatment of patients with multiple myeloma, solid tumors, or lymphoma.[6]

Due to its interesting biological activity and potential therapeutic value, **1** has been intensely studied from a biochemical and medicinal perspective. Additionally, the

---

[5] While nOe analysis allowed for assignment of relative configuration, use of NMR spectroscopy to determine the absolute configuration by was a challenge because derivatization of the hindered C-5 hydroxy failed with either Mosher's reagent or *p*-bromobenzoic acid failed.

[6] Fenical, W.; Jensen, P. R.; Palladino, M. A.; Lam, K. S.; Lloyd, G. K.; Potts, B. C. Discovery and development of the anticancer agent salinosporamide A (NPI-0052). *Bioorg. Med. Chem.* **2009**, *17*, 2175–2180.

unusual, complex, and minimalistic[7] structure has attracted the interest of synthetic chemists as indicated by the numerous total synthesis reports (eight as of this writing). Our interest in this molecule stems from the prospect of developing a biomimetic synthesis to the bicyclic core of **1**. Such studies would present opportunities to both deepen our understanding of the biosynthesis of **1** and gain access to novel and previously inaccessible analogues. In addition, these studies would likely result in the development of new synthetic methodologies to be extended into the preparation of other biologically active molecules. Chapter 1 details previous studies related to the biological activity, biosynthesis, and total synthesis of **1**. While this chapter is extensive, it is not comprehensive and only information necessary for better understanding and/or appreciating the content of this Thesis has been included. For other information related to this family of natural products, the reader is directed to several recent reviews.[8]

1.2. The Proteasome and Its Potential Role in the Treatment of Cancer

The 20SP is part of the larger 26S proteasome protein complex. The main function of the 26S proteasome is to recognize and break down proteins (i.e. proteolysis) that have been polyubiquitinated. The 26S proteasome is a protein complex consisting of one 20S core particle subunit and two 19S regulatory particles.[9] The 20S core particle is comprised of four stacked peptides to form a cylindrical structure with a 53 Å internal diameter.[10] Several of the peptides that line the inner cavity of the 20S core particle possess active sites that are capable of carrying out proteolysis. A peptide chain marked for proteolysis is fed through the cavity of the 20S core particle where proteolysis occurs by reaction with active site threonine resides. The proteolysis function is selective for three different classes of residues to equip the proteasome with chymotrypsin-like,

---

[7] All functional groups have been assigned a unique role for 20SP inhibition (see ref 6).

[8] a) Shibasaki, M.; Kanai, M.; Fukuda, N. Total synthesis of lactacystin and salinosporamide A. *Chem.-Asian J.* **2007**, *2*, 20–38. b) Gulder, T. A. M.; Moore, B. S. Salinosporamide natural products: Potent 20S proteasome inhibitors as promising cancer chemotherapeutics. *Angew. Chem. Int. Ed.* **2010**, *49*, 9346–9367. c) Rentsch, A.; Landsberg, D.; Brodmann, T.; Bülow, L.; Girbig, A.-K.; Kalesse, M. Synthesis and pharmacology of proteasome inhibitors. *Angew. Chem. Int. Ed.* **2013**, *52*, 5450–5488.

[9] Lodish, H.; Berk, A.; Matsudaira, P.; Kaiser, C. A.; Krieger, M.; Scott, M. P.; Zipursky, L.; Darnell, J. *Molecular Cell Biology*, 5th ed.; Scientific American Press, N.Y. 2003, pp. 71–73.

[10] Nandi, D.; Tahiliani, P.; Kumar, A.; Chandu, D. The ubiquitin-proteasome system. *J. Biosci.* **2006**, *31*, 137–155.

trypsin-like, and peptidylglytamyl-peptide hydrolyzing activities. Proteolysis generates small peptide chains with lengths varying from 4-25 residues.[11]

The major role of the proteasome is to regulate the concentration of native proteins and eradicate misfolded proteins. By degrading unnecessary or harmful proteins, the 26S proteasome provides the cell with additional amino acids for the synthesis of new proteins. The products of proteolysis can also be functional in the form of oligopeptide transcription factors. For example, nuclear factor-kappa B (NF-κB) is a transcription factor that is biosynthesized as an inactive protein trimer and is only activated by proteasome-mediated protealytic cleavage of an inhibitor protein IκB. In its active state, the NF-κB protein dimer promotes the transcription of genes that encourage cell survival by preventing apoptosis. In effect, the proteasome acts an important regulator of NF-κB production.[12]

Misregulation of NF-κB has been linked to several types of haematological malignancies and epithelial tumors. This is likely because overproduction of NF-κB leads to increased tumor cell proliferation.[13] Inhibition of the proteasome in tumor cells will also inhibit production of active NF-κB, and, in turn, induce apoptosis.[14] For this and other reasons,[15] proteasome inhibitors have gained intense interest for their potential treatment of cancer. In 2003, the FDA approved the first proteasome inhibitor, bortezomib, for the treatment of relapsing myeloma and mantle cell lymphoma.[16]

1.3. Studies Related to the Therapeutic Potential of Salinosporamide A

The mechanism of proteasome inhibition by **1** is similar to that of the structurally related omuralide **1003**. Namely, *O*-acylation of the catalytic, active site, *N*-terminal,

---

[11] Marques, A. J.; Palanimurugan, R.; Matias, A. C.; Ramos, P. C.; Dohmen, R. J. Catalytic mechanism and assembly of the proteasome. *Chem. Rev.* **2009**, *109*, 1509–1536.

[12] Lodish, H.; Berk, A.; Matsudaira, P.; Kaiser, C. A.; Krieger, M.; Scott, M. P.; Zipursky, L.; Darnell, J. *Molecular Cell Biology*, 5th ed.; Scientific American Press, N.Y. 2003, pp. 602–603.

[13] a) Karin, M.; Cao, Y.; Greten, F. R.; Li, Z.-W. NF-κB in cancer: From innocent bystander to major culprit. *Nature Reviews Cancer* **2002**, *2*, 301–310. b) Liu, J.-J.; Lin, M.; Yu, J.-Y.; Liu, B.; Bao, J.-K. Targeting apoptotic and autophagic pathways for cancer therapeutics. *Cancer Letters* **2011**, *300*, 105–114.

[14] Escárcega, R. O.; Fuentes-Alexandro, S.; García-Carrasco, M.; Gatica, A.; Zamora, A. The transcription factor nuclear factor-kappa B and cancer. *Clinical Oncology* **2007**, *19*, 154–161.

[15] Montagut, C.; Rovira, A.; Albanell, J. The proteasome: A novel target for anticancer therapy. *Clin. Transl. Oncol.* **2006**, *8*, 313–317.

[16] Sánchez-Serrano, I. Success in translational research: Lessons from the development of bortezomib. *Nat. Rev. Drug Disc.* **2006**, *5*, 107–114.

threonine (Thr1O$^{\gamma}$) by the β-lactone carbonyl of **1003** precludes subsequent proteolytic activity, thereby competitively inhibiting the 20SP.[17,18] In 2006, Groll, Huber, and Potts[19] solved the crystal structure of the yeast 20SP in complex with **1** and the biologically active deschloro analogue salinosporamide B (**1004**, Figure 2-A).[20] Through these studies the authors found that similar to **1003**, both **1** and **1004** form covalent bonds to the Thr1O$^{\gamma}$ residue via ester linkages (cf. complexes **1005** and **1007**, Figure 2-B and C). However, **1** is more potent than **1003** by a factor of 37,[1] and **1004** is more potent than **1003** by a factor of 2.[21] The X-ray structures of **1** and **1004** in complex with the 20SP indicate that the C-5 cyclohex-2-enyl moiety of both inhibitors occupies the S1 hydrophobic binding pocket.[19] Previous studies of the X-ray structure of the **1003**/20SP complex showed that the C-5 isopropyl group of **1003** occupies the same S1 binding pocket.[18] It can be argued that the isopropyl group of **1003** occupies the S1 binding pocket to a lesser extent, which leads to a weaker inhibitor-enzyme interaction. The increased potency of **1** and **1004** can then, at least partially, be attributed to tighter binding with the enzyme vis-à-vis enhanced hydrophobic interactions.

---

[17] Fenteany, G.; Standaert, R. F.; Lane, W. S.; Choi, S.; Corey, E. J.; Schreiber, S. L. Inhibition of proteasome activities and subunit-specific amino-terminal threonine modification by lactacystin. *Science* **1995**, *268*, 726–726.

[18] Groll, M.; Ditzel, L.; Löwe, J.; Stock, D.; Bochtler, M.; Bartunik, H. D.; Huber, R. Structure of 20S proteasome from yeast at 2.4 Å resolution. *Nature* **1997**, *386*, 463–471.

[19] Groll, M.; Huber, R.; Potts, B. C. M. Crystal structures of salinosporamide A (NPI-0052) and B (NPI-0047) in complex with the 20S proteasome reveal important consequences of β-lactone ring opening and a mechanism for irreversible binding. *J. Am. Chem. Soc.* **2006**, *128*, 5136–5141.

[20] Williams, P. G.; Buchanan, G. O.; Feling, R. H.; Kauffman, C. A.; Jensen, P. R.; Fenical, W. New cytotoxic salinosporamides from the marine actinomycete *Salinispora tropica*. *J. Org. Chem.* **2005**, *70*, 6196–6203.

[21] Macherla, V. R.; Mitchell, S. S.; Manam, R. R.; Reed, K. A.; Chao, T.-H.; Nicholson, B.; Deyanat-Yazdi, G.; Mai, B.; Jensen, P. R.; Fenical, W. F.; Neuteboom, S. T. C.; Lam, K. S.; Palladino, M. A.; Potts, B. C. M. Structure−activity relationship studies of salinosporamide A (NPI-0052), a novel marine derived proteasome inhibitor. *J. Med. Chem.* **2005**, *48*, 3684–3687.

Figure 2 | The biological mechanism of action of fused γ-lactam-β-lactone proteasome inhibitors: A) salinosporamide B (**1004**), B) mechanism for proteasome acylation and subsequent aqueous hydrolysis by **1003**/**1004**, C) mechanism of proteasome acylation and subsequent irreversible S_N2 reaction to generate a stable THF ring (cf. **1009**).

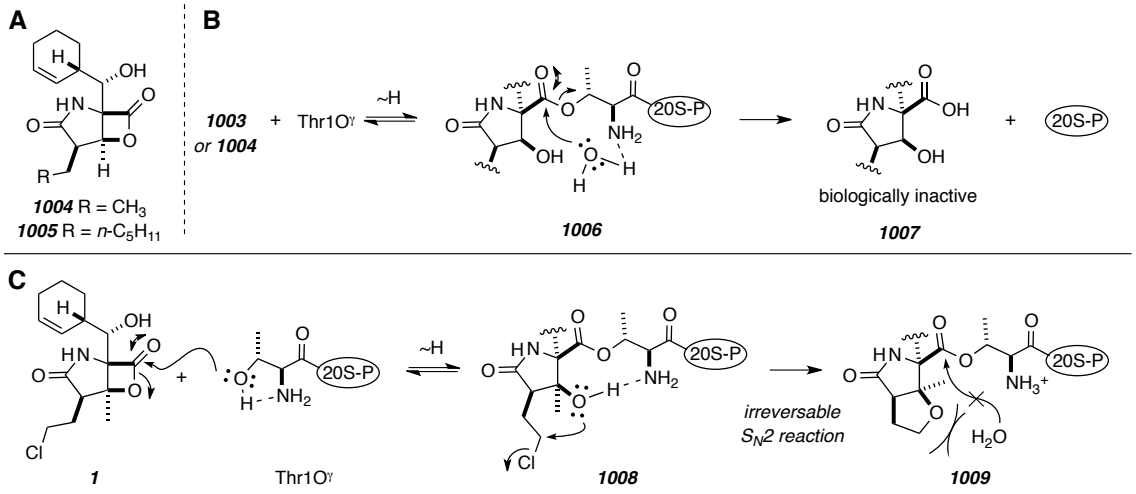

In addition to varying levels of hydrophobic interactions within the enzyme active site, the differing potencies of the structurally related proteasome inhibitors **1**, **1003**, and **1004** can also be explained by the relative stabilities of their respective acyl-Thr1O$^{\gamma}$ complexes. In the case of **1003**, 20SP inhibition can be reversed by ester cleavage of the acyl-Thr1O$^{\gamma}$ complexes to give rise to a fully functional 20SP.[22] Ester cleavage likely occurs by i) hydrolysis by adventitious water molecules that enter the enzyme active site afford a biologically *in*active[23] lactam dicarboxylic acid (cf., conversion of **1006** into **1007** or ii) C-3 OH-mediated deacylation of Thr1O$^{\gamma}$ to regenerate the β-lactone (cf. equilibrium arrow for generation of **1006** and **1008**).[19]

The 20SP relies on a few specific water molecules fortuitously positioned near the catalytic threonine residues to carryout native proteolysis. X-ray crystal structures of **1**,

[22] Nett, M.; Moore, B. S. Exploration and engineering of biosynthetic pathways in the marine actinomycete *Salinispora tropica*. *Pure. Appl. Chem.* **2009**, *81*, 1075–1084.
[23] Manam, R. R.; McArthur, K. A.; Chao, T.-H.; Weiss, J.; Ali, J. A.; Palombella, V. J.; Groll, M.; Lloyd, G. K.; Palladino, M. A.; Neuteboom, S. T. C.; Macherla, V. R.; Potts, B. C. M. Leaving groups prolong the duration of 20S proteasome inhibition and enhance the potency of salinosporamides. *J. Med. Chem.* **2008**, *51*, 6711–6724.

1003, and **1004** complexes with the 20SP show that the C-3 OH has displaced these water molecules from the enzyme active site. The authors propose that the inhibitor displaces water molecules from the active site upon Thr1O$^{\gamma}$ acylation, and subsequent hydrolysis (i.e. conversion of **1006** into **1007**) must arise from water molecules entering the active site through a long, narrow cavity in the enzyme. The crystal structures indicate that this cavity is occupied by the C-2 substituent of the inhibitor after Thr1O$^{\gamma}$ acylation, thus, blocking additional water molecules from entering the enzyme active site.[19] This hypothesis is consistent with bioactivity studies of cinnabaramide A (**1005**), a natural product isolated from a terrestrial *Streptomyces* strain, which differs from **1004** only in the length of the C-2 substituent, yet is reported to inhibit the 20SP at levels as comparable to **1** (ca. IC_{50}=1 nM).[24]

In addition to ester hydrolysis, deacylation of the Thr1O$^{\gamma}$ residue by the C-3 OH also results in ester cleavage and reversal of 20SP inhibition. Analysis of the crystal structure of the **1004**/20SP complex indicates that the C-3 OH is hydrogen bound to the Thr1O$^{\gamma}$, an interaction that could catalyze the deacylation of Thr1O$^{\gamma}$ and release β-lactone. It has been argued that β-lactone reformation does not account for reversing enzyme inhibition because the rate of dissociation from the 20SP cavity is likely much slower than the rate of threonine re-acylation.[19] However, β-lactone-containing inhibitors are inherently susceptible to aqueous hydrolysis,[25] therefore reformation of the β-lactone is likely accompanied by occasional hydrolysis by adventitious water to give rise to biologically inactive **1007** and a fully functional 20SP.

The X-ray crystal structure of the **1**/20SP complex differs from that of **1003** and **1004** by the presence of a THF ring fused to both C-2 and C-3 (cf. **1009**), and the Thr1NH2 is fully protonated. The proposed mechanism for cyclic ether formation involves intramolecular S_N2 chloride displacement by the β-lactone-derived alcohol (cf. **1008**) following Thr1O$^{\gamma}$ acylation. From the X-ray structure the authors propose that the

[24] Stadler, M.; Bitzer, J.; Mayer-Bartschmid, A.; Müller, H.; Benet-Buchholz, J.; Gantner, F.; Tichy, H.-V.; Reinemer, P.; Bacon, K. B. Cinnabaramides A−G: Analogues of lactacystin and salinosporamide from a terrestrial streptomycete. *J. Nat. Prod.* **2007**, *70*, 246–252.

[25] Hogan, P. C.; Corey, E. J. Proteasome inhibition by a totally synthetic β-lactam related to salinosporamide A and omuralide. *J. Am. Chem. Soc.* **2005**, *127*, 15386–15387.

Thr1NH_2 enhances the nucleophilicity of the tertiary hydroxy group by hydrogen bonding to the alcohol OH, to, in effect, catalyze the intramolecular S_N2 reaction. The newly formed THF ring greatly stabilizes the corresponding acyl-Thr1O^{γ} complex by i) C-3 OH incorporation into the cyclic ether, which precludes β-lactone reformation (cf. lactonization of **1006** to **1003**), ii) displacement of water molecules necessary for 20SP-catlayzed ester hydrolysis, and iii) fully protonating Thr1NH2. renders the catalytic *N*-terminus non-basic. Generating a non-basic Thr1NH2 is important to consider because the basic *N*-terminal nitrogen atom is necessary to catalyze native proteolysis, aqueous hydrolysis of the inhibitor/enzyme complex, and reverse inhibition by β-lactone reformation.[19]

In addition to increased potency, Potts and co-workers also reported that **1** also exhibits prolonged proteasome inhibition, which is likely due to increased stability of the corresponding acyl-Thr1O^{γ} complex.[23] The intramolecular chloride displacement is effectively irreversible, so restoring proteasomal activity would require unfavorable aqueous hydrolysis of the THF-containing inhibitor/enzyme complex **1009**. Because **1** is both more potent and exhibits a prolonged duration of proteasome inhibition with respect **1003**, it is considered to be an irreversible inhibitor of the 20SP. Additionally, from these studies the authors determined that acylation of Thr1O^{γ} was rate-limiting as opposed to the subsequent S_N2 displacement necessary for cyclic ether formation.[23]

Additional structure-activity relationship (SAR) studies proteasome inhibition by the salinosporamides are necessary to better understand, for example i) the high selectivity and potency for 20SP inhibition, ii) the unique biological mechanism of action, and iii) the disparity in biological activity between the various congeners. Potts and co-workers prepared a series of salinosporamide derivatives by substitution at chlorine and tested them for 20SP inhibition activities.[21,23] Many of these semisynthetic analogues cf. R^1 = Br, I, OTs, exhibited potencies similar to **1** indicating that substitution by other halide or (pseudohalide) leaving groups are tolerated (Figure 3). This implies that proteasome inhibition involves intramolecular S_N2 displacement, with irreversible cyclic ether formation, following active site acylation when the C-2 substituent contains a leaving group. Substitution by fluoride affords fluorosalinosporamide (R^1 = F), a

congener whose potency falls between **1** and **1004** (R^1 = H, Figure 3). The authors speculate that the intermediate biological activity demonstrates that cyclic ether formation by S_N2 reaction at the alkyl fluoride carbon is still occurring, but at a slower rate.

Figure 3 | Biological activity of γ-lactam-β-lactone proteasome inhibitors: A) effects of substitution at C-2, B) structures and biological activities of salinosporamide F (2-*epi*-**1** or **1010**) and salinosporamide I (**1011**), C) effects of substitution at C-5. (Data from refs 21, 23, and 24)

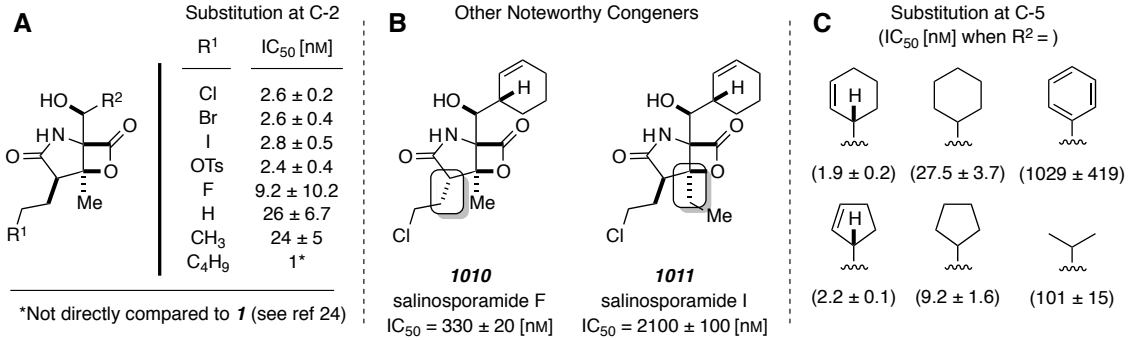

Large-scale fermentation of *Salinospora tropica* has led to efficient isolation of many naturally occurring salinosporamide congeners including, for example, **1004** (Figure 3A, R^1 = H), salinosporamide E ($R^1 = CH_3$), the C-2 epimer of **1** salinosporamide F (**1010**, Figure 3, Panel B), and the C-3 ethyl analogue, salinosporamide I (**1011**).[20,26] In addition to the structurally related cinnabaramides (e.g. $R^1 = C_4H_9$) these substrates collectively provide ample opportunity to study structure-activity relationships for the salinosporamide family of proteasome inhibitors. As previously mentioned, substitution of chloride by hydrogen leads to decreased potency for 20SP inhibition. A similar effect is observed in the case of R^1=CH_3, however cinnabaramide A **1005** ($R^1 = C_4H_9$) was reported[24] to inhibit the 20SP at levels comparable to that of **1** despite not possessing a

[26] Reed, K. A.; Manam, R. R.; Mitchell, S. S.; Xu, J.; Teisan, S.; Chao, T.-H.; Deyanat-Yazdi, G.; Neuteboom, S. T. C.; Lam, K. S.; Potts, B. C. M. Salinosporamides D−J from the marine actinomycete *Salinispora tropica*, bromosalinosporamide, and thioester derivatives are potent inhibitors of the 20S proteasome. *J. Nat. Prod.* **2007**, *70*, 269–276.

leaving group necessary for THF ring formation.[27] These results support the hypothesis that inhibitors possessing either a leaving group or a bulky alkyl chain at C-2 will avoid inhibitor cleavage by blocking adventitious water molecules.

Several investigations[28] from the Moore group indicate that the biosynthesis of **1** proceeds through a hybrid PKS/NRPS system that involves incorporation of a cyclohex-2-enyl analogue of alanine. Through these studies the authors also demonstrated that the enzyme responsible for recognizing the cyclohexene-containing amino acid exhibits relaxed substrate specificity.[28a] This observation provided the authors with an opportunity to perform SAR studies on the C-5 group by studying a series of congeners generated by incorporation of other alanine-derived amino acids (results summarized in Figure 3-C). Substituting the cyclohex-2-enyl group with cyclohexyl or phenyl led to decreased 20SP potency by a factor of 14 and >500 respectively. Changing the ring size of the cyclic alkene from cyclohexenyl to cyclopentenyl led to a small decrease in potency. Substitution with cyclopentyl led to a four-fold decrease in potency, however, the decrease in potency was not as significant as substitution with cyclohexyl. The isopropyl containing analogue (a.k.a. antiprotealide) had an IC_{50} greater than fifty-fold less potent than **1**. Collectively these data likely reflect differences in favorable hydrophobic

[27] While the reported IC_{50} value of **1005** is lower than that of **1**, the authors reported that they were not able to obtain an authentic sample of **1** for direct comparison.

[28] a) Beer, L. L.; Moore, B. S. Biosynthetic convergence of salinosporamides A and B in the marine actinomycete *Salinispora tropica*. *Org. Lett.* **2007**, *9*, 845–848. b) Eustáquio, A. S.; Pojer, F.; Noel, J. P.; Moore, B. S. Discovery and characterization of a marine bacterial SAM-dependent chlorinase. *Nat. Chem. Biol.* **2007**, *4*, 69–74. c) McGlinchey, R. P.; Nett, M.; Eustáquio, A. S.; Asolkar, R. N.; Fenical, W.; Moore, B. S. Engineered biosynthesis of antiprotealide and other unnatural salinosporamide proteasome inhibitors. *J. Am. Chem. Soc.* **2008**, *130*, 7822–7823. d) Eustáquio, A. S.; McGlinchey, R. P.; Liu, Y.; Hazzard, C.; Beer, L. L.; Florova, G.; Alhamadsheh, M. M.; Lechner, A.; Kale, A. J.; Kobayashi, Y.; Reynolds, K. A.; Moore, B. S. Biosynthesis of the salinosporamide A polyketide synthase substrate chloroethylmalonyl-coenzyme A from *S*-adenosyl-L-methionine. *Proc. Natl. Acad. Sci. U.S.A.* **2009**, *106*, 12295–12300. e) Liu, Y.; Hazzard, C.; Eustaquio, A. S.; Reynolds, K. A.; Moore, B. S. Biosynthesis of salinosporamides from α,β-unsaturated fatty acids: Implications for extending polyketide synthase diversity. *J. Am. Chem. Soc.* **2009**, *131*, 10376–10377. f) Nett, M.; Guider, T. A. M.; Kale, A. J.; Hughes, C. C.; Moore, B. S. Function-oriented biosynthesis of β-lactone proteasome inhibitors in *Salinispora tropica*. *J. Med. Chem.* **2009**, *52*, 6163–6167. g) Gulder, T. A. M.; Moore, B. S. Chasing the treasures of the sea-bacterial marine natural products. *Curr. Opin. Microbiol.* **2009**, *12*, 252–260. h) Eustáquio, A. S.; O'Hagan, D.; Moore, B. S. Engineering fluorometabolite production: Fluorinase expression in *Salinispora tropica* yields fluorosalinosporamide. *J. Nat. Prod.* **2010**, *73*, 378–382. i) Mahlstedt, S.; Fielding, E. N.; Moore, B. S.; Walsh, C. T. Prephenate decarboxylases: A new prephenate-utilizing enzyme family that performs nonaromatizing decarboxylation en route to diverse secondary metabolites. *Biochemistry* **2010**, *49*, 9021–9023.

interactions between the C-5 substituent and the S1 binding pocket of the 20SP. The increased potency exhibited by the C-5 cyclohexene- and cyclopentane-containing substrates is likely because the unsaturation changes the shape of the C-5 cyclic hydrocarbon to better match S1 binding pocket.[28f]

Despite thorough investigations into the SAR of **1**, a superior 20SP inhibitor has not been identified. This likely reflects Nature's ability to evolve a 'structurally minimalistic' inhibitor where all heavy atoms are used to enhance the molecule's ability to selectively inhibit the 20SP. The C-5 cyclohexenyl ring has been optimized to form strong hydrophobic interactions. The C-5 OH forms an important hydrogen bond within the active site. The β-lactone 'warhead' represents a highly atom-economical acylating agent for reaction with the enzyme *N*-terminus. The γ-lactam ring and C-2 chloroethyl group ultimately shield the enzyme-inhibitor complex against cleavage of the newly formed ester bond. For these reasons, **1** is the only member of the γ-lactam-β-lactone proteasome inhibitors to enter clinical trials.[6] However, the clinical trials are still ongoing, the formulated drug (marizomib), while likely much more potent than bortezomib for the treatment of multiple myeloma, "gives patients a powerful dose of side effects."[29] This statement suggests that an opportunity still exists for the rational design of analogues by chemical synthesis or biosynthesis engineering. The remainder of this chapter is devoted to reviewing *landmark* studies of **1** with regard to i) early total syntheses, ii) the biosynthesis, and iii) total syntheses based on a biosynthetic model (biomimetic syntheses).

1.4. Early Landmark Synthesis Studies of Salinosporamide A

1.4.1. Corey's Total Synthesis of (–)-Salinosporamide A

One year after Fenical reported the isolation of salinosporamide A, E. J. Corey and co-workers published the first total synthesis of (–)-**1**.[30] For brevity, discussion of the synthesis of enamide **1013** from commercially available serine methyl ester hydrochloride (**1012**, 46% yield over 6 steps) has been omitted. Quinuclidine was used to catalyze an intramolecular Baylis–Hillman-aldol reaction of **1013** to give γ-lactam **1014**

[29] Appel, A. Drugs: More shots on target. *Nature* **2011**, *480*, S40–S42.
[30] Reddy, L. R.; Saravanan, P.; Corey, E. J. A simple stereocontrolled synthesis of salinosporamide A. *J. Am. Chem. Soc.* **2004**, *126*, 6230–6231.

as a 9:1 mixture of C-3 epimers. Treating **1014** with chlorosilane **1015** gave bromoethyl silyl ether **1016**, which was followed by tin hydride-mediated radical cyclization to give the bicyclic lactam **1017** with the desired configuration at C-2. Benzyl ether hydrogenolysis of **1017** followed by Dess–Martin periodinane (DMP) oxidation gave aldehyde **1018**. Addition of cyclohex-2-enylzinc chloride (**1019**) gave alcohol **1020** and set the desired configuration at the C-5 and C-6 stereogenic centers. Tamao–Fleming oxidative cleavage of the silyl ether furnished triol **1021**, which following PMB deprotection and ester hydrolysis, gave the penultimate intermediate **1022**. β-Lactone formation was accomplished with bis(2-oxo-3-oxazolidinyl)phosphinic chloride (BOPCl). Chlorination of the primary alcohol with Ph_3PCl_2 produced 100 mg of the natural product (–)-**1** in 13.6% overall yield over 17 steps.

Scheme 1 | Corey's total synthesis of (–)-**1** (adapted from ref 30).

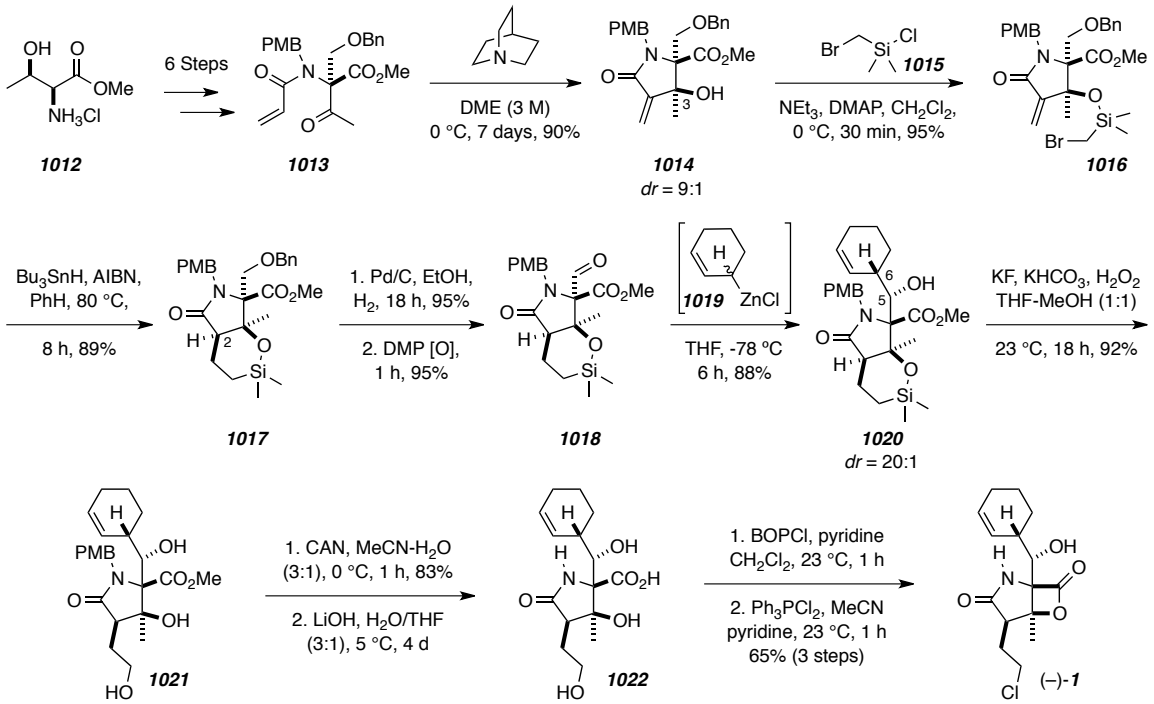

Other research groups have used many of the reactions that were developed for Corey's total synthesis **1** in subsequent synthetic efforts. Most notably is the doubly diastereoselective reaction of 2-cyclohexenylzincate (**1019**) with aldehyde **1018**. The preparation **1019** is depicted in Scheme 2. Pd(0)-catalyzed hydrostannylation of 1,3-

cyclohexadiene with tri-*n*-butyltin hydride gave the allylic stannane **1023** regioselectively.[31] Corey and co-workers then found that sequential treatment of **1023** with *n*-butyllithium and zinc chloride gave a THF solution of **1019**. Addition of aldehyde **1018** to the organozinc solution cleanly afforded alcohol **1020**. A transition structure to account for the observed diastereoselectivity is shown in Scheme 2 (**1024**).[32] Chelation of the zinc metal-center to the dicarbonyl moiety likely directs the allylation to the sterically more accessible face of the aldehyde. Preparation **1019** must result in a racemic mixture, so to account for the stereoselectivity at C-6 the authors propose that the enantiomers of **1019** rapidly equilibrate with one another and the (*S*)-enantiomer is faster reacting with **1018**.[32] While unconventional,[33] this approach has been used in a number of later syntheses for the introduction of the cyclohexene moiety.[8]

Scheme 2 | Preparation of zincate **1019** and its stereoselective reaction with aldehyde **1018** (adapted from refs 31 and 32).

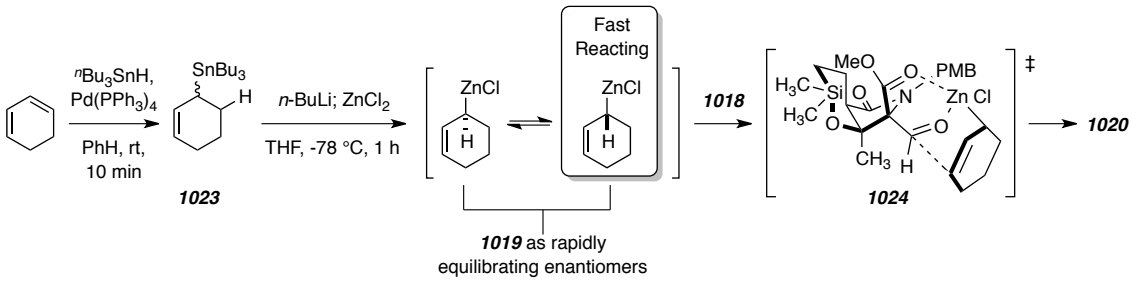

Corey and co-workers subsequently reported alternative conditions for the Bayliss–Hillman-aldol reaction.[34] The authors found that sequentially treating the same enamide precursor **1013** with the prototypical Kulinkovich reagent (**1025**, Scheme 3), molecular iodine, and triethylamine gave the desired γ-lactam **1014** (cf. 1 h vs. 7 days), in

[31] Miyake, H.; Yamamura, K. Pd(0) catalyzed hydrostannation of conjugated dienes. A facile and highly regio- and stereoselective synthesis of (Z)-2-alkenylstannanes. *Chem. Lett.* **1992**, 507–508.
[32] Corey, E. J.; Kürti, L. *Enantioselective Chemical Synthesis*, 1st ed.; Direct Book Publishing, Dallas, Texas, 2010, pp. 218–222.
[33] The authors noted that attempts to react other metallo-cyclohex-2-ene reagents with **1024** were unproductive. For example, no product was observed when cyclohex-2-enyl lithium was, which is likely due to retro-aldol cleavage of the intermediate lithium alkoxide. Direct addition of the organostannane via a Lewis acid-catalyzed approach also failed.
[34] Reddy, L. R.; Fournier, J.-F.; Reddy, B. V. S.; Corey, E. J. New synthetic route for the enantioselective total synthesis of salinosporamide A and biologically active analogues. *Org. Lett.* **2005**, *7*, 2699–2701.

comparable yield, and with excellent diastereoselectivity. To account for this unusual transformation the authors propose that the mechanism involves initial ligand exchange with the α,β-unsaturated alkene of **1013** to form an equilibrating mixture of organotitanium intermediates **1026** and **1027**, which can rearrange to form intermediate **1028**. Quenching the reaction with molecular iodine affords iodolactam **1029**, which is readily converted into desired product **1014** by amine-mediated elimination of HI. This unusual transformation provides a significantly more practical method to produce an early-stage intermediate used in Corey's approach for the synthesis of **1**.

Scheme 3 | Titanium-mediated formal Baylis-Hillman reaction to convert enamide **1013** into **1014** (adapted from refs 32 and 34).

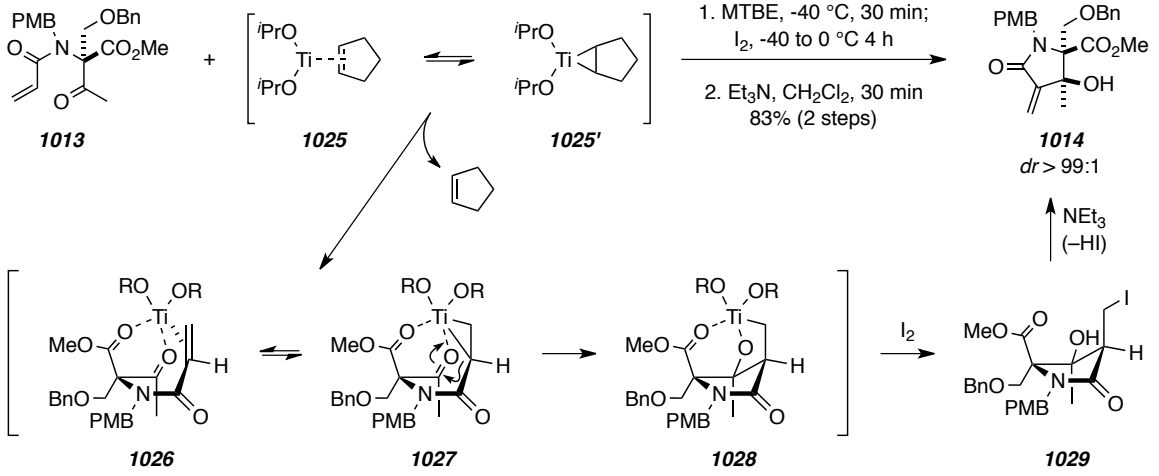

1.4.2. Danishefsky's Total Synthesis of (–)-Salinosporamide A

In 2005, Danishefsky and co-workers reported an alternative approach to the total synthesis of **1**.[35] The synthesis began with conjugate addition of the vinyl cuprate derived from vinylmagnesium bromide to the readily available[36] chiral building block **1030** to give lactam **1031**. The reaction proceeded with high stereoselectivity for α-face addition

[35] Endo, A.; Danishefsky, S. J. Total synthesis of salinosporamide A. *J. Am. Chem. Soc.* **2005**, *127*, 8298–8299.

[36] a) Thottathil, J. K.; Moniot, J. L.; Mueller, R. H.; Wong, M. K.; Kissick, T. P. Conversion of L-pyroglutamic acid to 4-alkyl-substituted L-prolines. The synthesis of *trans*-4-cyclohexyl-L-proline. *J. Org. Chem.* **1986**, *51*, 3140–3143. b) Hamada, Y.; Kawai, A.; Yasushi, K.; Hara, O.; Shioiri, T. Stereoselective total synthesis of AI-77-B, a gastroprotective substance from *Bacillus pumilus* AI-77. *J. Am. Chem. Soc.* **1989**, *111*, 1524–1525.

and established the configuration of the C-3 stereogenic center. Treating the lithium anion of **1031** with 2-iodoethyl benzyl ether gave lactam **1032** with high stereoselectivity at C-2 by β-face enolate alkylation. The authors then converted **1032** into imidate **1033** in six straightforward chemical steps in 1.8% overall yield.

Scheme 4 | Synthesis of imidate **1033** from amide **1032**, which is prepared by two sequential stereoselective alkylations of enamide **1030** (adapted from ref 35).

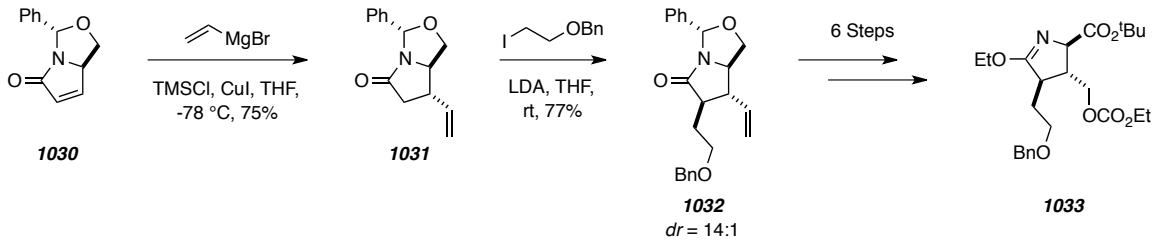

1030 ***1031*** ***1032*** *dr* = 14:1 ***1033***

Treating imidate **1033** with LiHMDS gave lactone **1034** by intramolecular acylation and established the configuration of the C-4 all-carbon, quaternary, stereogenic center with high stereoselectivity. A series of protecting group manipulations were carried out to furnish lactam **1035**. Soft-nucleophile-mediated ring-opening of the γ-lactone by *in situ*-generated phenylselenate followed by esterification of the carboxylic acid intermediate gave the selenium-containing mixed malonate **1036**. Aldehyde **1037** was generated following straightforward peroxide-mediated selenium elimination and oxidation with Dess Martin periodinane. Phenylselenyl bromide and catalytic Ag(I) were used to effect seleno-etherification of a hemi-acetal derived from **1037** to give selenoether **1038**, which, following radical-mediated deselenylation to give **1039**, established the configuration of the C-3 quaternary, methyl-bearing stereogenic center.

Scheme 5 | Synthesis of bicyclic amide **1040** in eleven steps from imidate **1033** (adapted from ref 35).

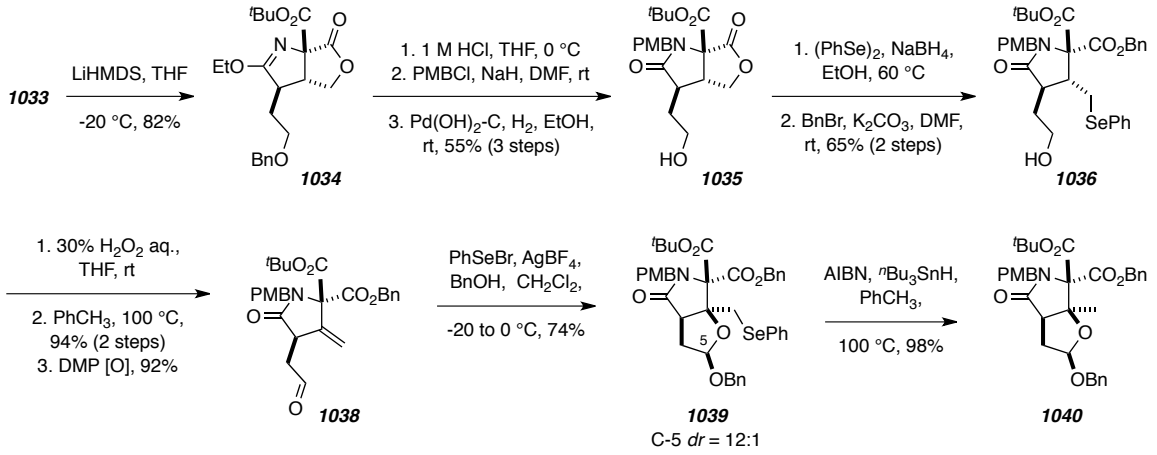

Aldehyde **1041** was prepared by selective reduction of benzyl ester **1040** with $NaBH_4$ followed by oxidation with Dess Martin periodinane. Treating **1041** with the "Corey reagent"[30] introduced the cyclohex-2-ene moiety, which proceeded with high stereoselectivity for the generation of the two stereogenic centers at C-5 and C-6 to give late-stage intermediate **1042**. Interestingly, the authors also commented on the importance of the *N*-PMB group for the stereoselectivity in the organozinc addition:

> "*…the use of the corresponding imidate aldehyde* [**1043**] *instead of* [**1041**] *resulted in poor diastereoselectivity (78% yield, 4:3, configuration not determined). Obviously, the PMB group plays a critical role in diastereo-selection in the novel Corey reaction."*[35]

This observation is consistent with the transition structure proposed by Corey (cf. **1024** in Scheme 2), the PMB group either directs the face of the aldehyde that (*S*)-**1019** adds to or impedes competitive addition by the corresponding (*R*) enantiomer. From intermediate **1042** the authors were able to complete the total synthesis of 6.8 mg of (–)-**1** in 1.8% overall yield over 28 steps from **1030**.

Scheme 6 | Conversion of bicyclic amide **1040** into (–)-**1** in nine steps and completion of the total synthesis.

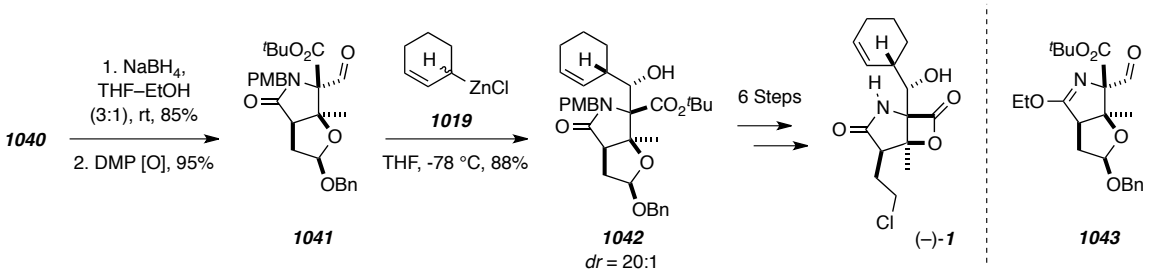

1.5. Investigations Into the Biosynthesis of Salinosporamide A

By performing an extensive array of isotopic labeling experiments, Moore and co-workers found that **1** is biosynthesized from three biosynthetic building blocks: acetyl-CoA (**1046**, Scheme 7), 4-chlorocrotonyl-CoA (**1044**), and alanine-derived peptidyl carrier protein (PCP) thioester **1049**.[28a,e] Feeding C2-^{13}C-labeled **1046** into the polyketide biosynthetic assembly line gave **1** with ^{13}C-encrichment at C14. Feeding **1044** to the biosynthetic cascade furnished **1**, and similar feeding experiments with C1-^{13}C-labeled propionyl-CoA (**1048**) furnished the corresponding β-lactone with ^{13}C-enrichment at the amide carbonyl. These experiments indicate that C1, C2, C12, and C13 arise from **1044**. The remaining portion of **1** most likely arise from PCP-anchored thioester **1049**. The amino acid framework of **1049** is proposed to arise from shikimic acid.[28i]

Scheme 7 | Proposed intermediates in the biosynthesis of **1** (adapted from refs 28a,d,e).

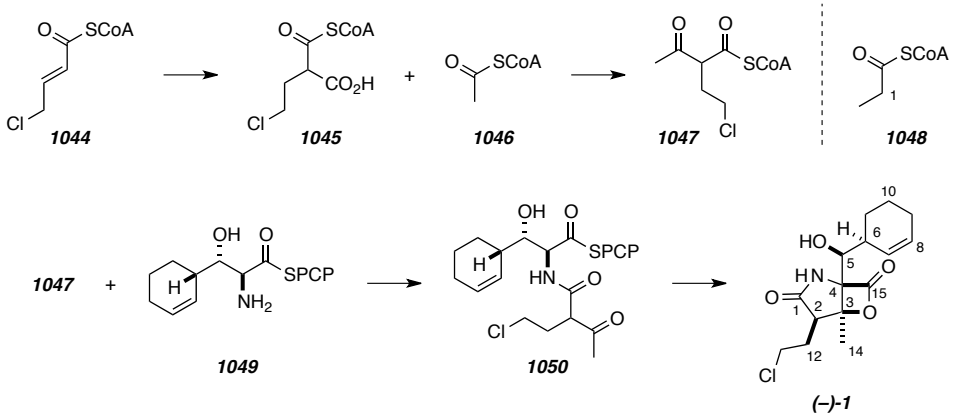

Assembly of the three biosynthetic units is proposed to proceed via a CoA carboxylase-catalyzed oxidation of **1044** to give α-carboxy thioester **1045**. Decarboxylative acylation of **1045** with **1046** then gives the β-keto thioester **1047**. Acyl transfer by condensation of **1047** with amine **1049** gives PCP thioester **1050**. Unprecedented hybrid PKS-NRPS-mediated bis-cyclization of **1050** then forms the natural product, **1**.[28d,e]

The biosynthesis of **1** was further probed by performing experiments involving gene deletion, biochemical analyses, and chemical complementation with relevant intermediates, all of which led the authors to sequence the *Salinispora tropical* genome and assign gene sequences corresponding to the specific enzymes necessary for biosynthetic assembly of **1050**.[28c,e] The conversion of **1050** into the fused bicyclic natural product **1** has yet to be fully elucidated, and the authors comment that the hybrid PKS-NRPS-mediated transformation is a novel and unprecedented biosynthetic event.[37] The authors suggest that cyclization is effected by either the SalC (ketosynthase) or SalO (cyclase) genes to form lactam **1051**, and lactonization is catalyzed by the SalF (α,β-hydrolase or thioesterase) gene (Scheme 8).[37] However, more mutagenesis studies are necessary to confidently assign the corresponding protein-encoding genes. Interestingly, despite the tremendous advances into the biosynthesis of **1** made by the Moore group,[28] the details of the final biscyclization event have not yet been described in the primary literature.

Scheme 8 | Proposed biscyclization event in the biosythesis of **1** (adapted from ref 37).

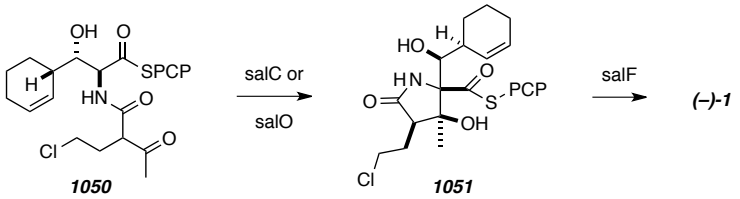

[37] Moore, B. S.; Beer, L.; Eustaquio, A. S. Biosynthesis of salinosporamide A and analogs and methods thereof. U.S. Patent 2009/0325208 A1, December 31, 2009.

1.6. Synthetic Studies Inspired the Biosynthesis of Salinosporamide A

1.6.1. Pattenden Total Synthesis of (–)-Salinosporamide A

In 2006 Pattenden and co-workers[38] reported a total synthesis of (±)-**1** that involved a late-stage biomimetic intramolecular aldol of a β-keto-α-amido ester that is structurally similar to the putative biomimetic intermediate **1050** proposed by Moore. The aldol precursor **1053** was prepared by amide coupling of acid **1052** with dimethyl aminomalonate hydrochloride (Scheme 9). Treating **1053** with a mixture of acetic acid and water effected the deketalization and intramolecular aldol reaction to give lactam **1054** with good stereoselectivity for establishing the C-3 stereogenic center. Silyl ether formation with TMSOTf and PMB protection via routine procedures gave malonate **1055**, which was selectively reduced with lithium triethylborohydride (i.e. superhydride) at the sterically more accessible methyl ester to give aldehyde **1056**. The total synthesis was accomplished from aldehyde **1056** using either routine transformations or methodologies developed by the landmark syntheses presented in Section 1.4. The synthesis of Pattenden and co-workers gave (±)-**1** in 9.6% overall yield over 14 steps. The authors later published a follow-up report detailing alternative conditions that make the intramolecular aldol reaction more practical.[39] Applying these alternative strategies the authors were able to access 3.6 mg of (±)-**1** in a similar yield over 14 steps.

[38] Mulholland, N. P.; Pattenden, G.; Walters, I. A. S. A concise total synthesis of salinosporamide A. *Org. Biol. Chem.* **2006**, *4*, 2845–2846.
[39] Mulholland, N. P.; Pattenden, G.; Walters, I. A. S. A concise and straightforward total synthesis of (±)-salinosporamide A, based on a biosynthesis model. *Org. Biol. Chem.* **2008**, *6*, 2782–2789.

Scheme 9 | Total synthesis of (±)-**1** by Pattenden and co-workers (adapted from refs 38 and 39).

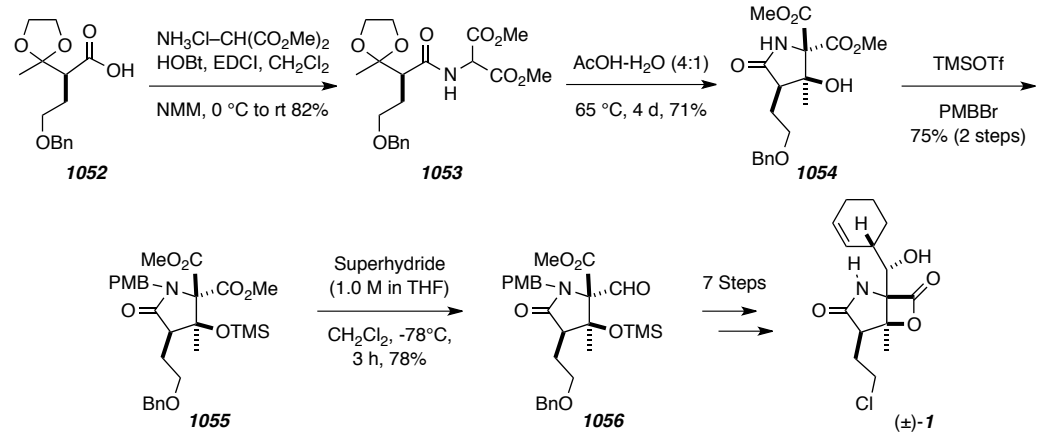

1.6.2. Romo's Total Synthesis of (–)-Salinosporamide A

In a series of reports, Romo and co-workers describe a biomimetic approach to the preparation of the salinosporamides and cinnabaramides that, as of this writing, represents the shortest total synthesis **1**.[40] Starting with protected serine **1057** (Scheme 10), acylation by ketene dimer **1058** gives β-ketoamido ester **1059** as a 1:1 mixture of C-2 epimers. While the mixture of diastereomers might be due to facile C-2 enolization, the authors proposed that it was the use of a racemic mixture of **1058** that led to the epimeric mixture. Previous reports have shown that α-stereocenters in tertiary β-ketoamides are stabile at ambient conditions owing introduction of allylic $A_{1,3}$ strain in the corresponding enols.[41] Consistent with these reports, Romo and co-workers were able to separate the two epimers of **1059** by MPLC to give **1060** as a single enantiomer. Heating a mixture of the undesired diastereomer (C-2-*epi*-**1060**) with *p*-toluenesulfonic acid in a methanol-ethyl acetate gave rise to a mixture of C-2 epimers (dr = 1:1), which could be re-subjected to MPLC purification to give more of the desired diastereomer of **1060**. Pd(0)-

[40] Nguyen, H.; Ma, G.; Gladysheva, T.; Fremgen, T.; Romo, D. Bioinspired total synthesis and human proteasome inhibitory activity of (−)-salinosporamide A, (−)-homosalinosporamide A, and derivatives obtained via organonucleophile promoted bis-cyclizations. *J. Org. Chem.* **2011**, *76*, 2–12, and references cited therein.

[41] Evans, D. A.; Ennis, M. D.; Le, T.; Mandel, N.; Mandel, G. Asymmetric acylation reactions of chiral imide enolates. The first direct approach to the construction of chiral β-dicarbonyl synthons. *J. Am. Chem. Soc.* **1984**, *106*, 1154–1156.

mediated deprotection of the allyl ester revealed the carboxylic acid in **1061**, which was treated with MsCl and 4-PPY to induce the key tandem aldol-lactonization bis-cyclization reaction. This generated the β-lactone-containing late-stage intermediate **1062**.

Scheme 10 | Synthesis of late-stage intermediate β-lactone **1062** (adapted from ref 40).

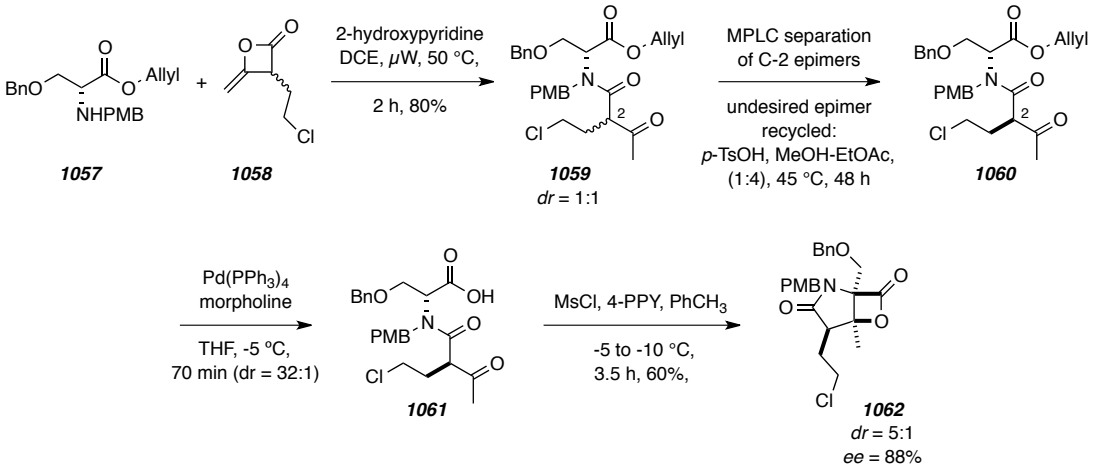

The key step of Romo's approach involved the biscyclization reaction of β-ketoamido acid **1061** to γ-lactam-fused β-lactone **1062**. The mechanism for this transformation is shown in Scheme 11. Carboxylate acylation likely forms mixed anhydride-like intermediate **1063**. Transacylation with 4-PPY forms an acyl ammonium intermediate with increased acidity of the α-proton, which is readily deprotonated by DIEA to give ammonium enolate **1064**. The nucleophilic carbon of enolate **1064** then reacts intramolecularly via an aldol reaction to give lactam **1065**, which rapidly forms β-lactone **1062** by alkoxide acylation and pyridinium displacement to release 4-PPY. The key step proceeds in 52% with good stereoselectivity (*dr* = 5:1) and with good retention of enantiopurity (*ee* = 90%). Because the C-4 stereogenic center is destroyed during the course of the reaction, the configuration at C-2 determines which enantiomer of the product is produced. Only minimal erosion of *ee* was observed. This is consistent with the C-2 stereogenic center being more stable to enolization than a typical α-stereocenter of a β-dicarbonyl system.

Scheme 11 | Mechanism for the tandem aldol-lactonization in the preparation of β-lactone **1062** (adapted from ref 40).

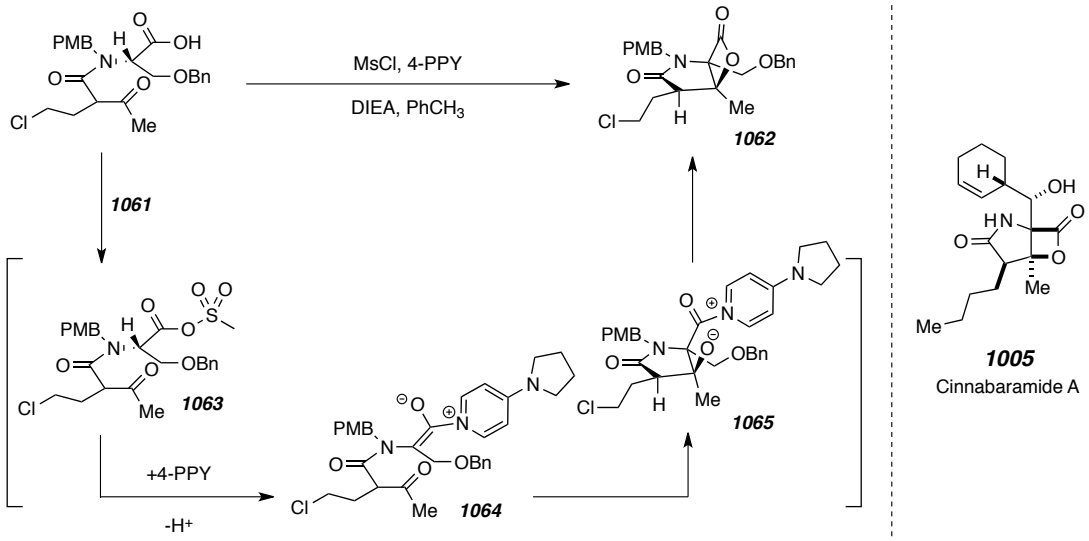

From **1062**, the authors were able to complete the total synthesis of (–)-**1** in 4 steps. Hydrogenolysis of the benzyl ether gave alcohol **1066**. Modified Moffatt oxidation of **1066** gave the corresponding aldehyde, and introduction of the cyclohexene moiety was accomplished by adding Corey's zinc reagent **1019** to give **1067**. This represents the example of Corey's reagent being used to add to an aldehyde in the presence of both β-lactone and the alkyl chloride.[42] CAN-mediated PMB cleavage of **1067** completed the total synthesis of 1.05 g of (–)-**1** in over nine steps.

[42] Ma, G.; Nguyen, H.; Romo, D. Concise total synthesis of (±)-salinosporamide A, (±)-cinnabaramide A, and derivatives via a bis-cyclization process: Implications for a biosynthetic pathway? *Org. Lett.* **2007**, *9*, 2143–2146.

Scheme 12 | Completion of Romo's total synthesis of (–)-**1** (adapted from ref 40).

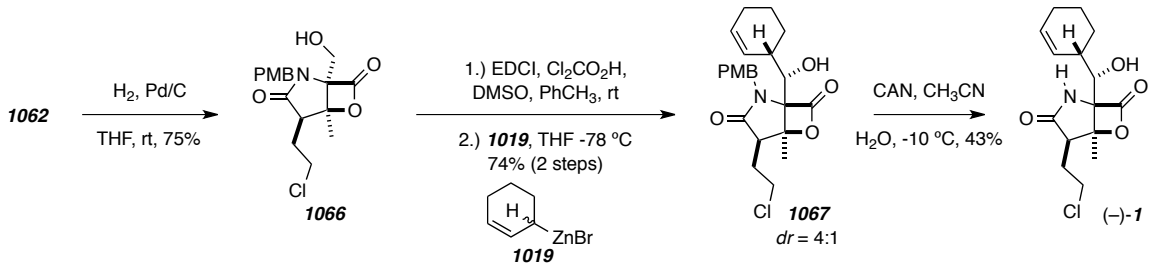

1.6.3. Potts Total Synthesis of (–)-Salinosporamide A

In 2007 Potts and co-workers[43] reported a synthesis of (–)-**1** inspired by the proposed biosynthetic aldol reaction. The synthesis began with a highly stereoselective, biomimetic, intramolecular aldol reaction of β-ketoamido ester **1068** to give bicyclic lactam **1069** (Scheme 13). In four steps **1069** was converted into the tricyclic aldehyde **1070**, to which the authors added the *B*-2-cyclohexen-1-yl-9-BBN (**1071**) to generate alcohol **1072**. This approach for introducing the cyclohexene moiety stereoselectively provided the desired configuration within the cyclohexene (i.e. C-6) and the undesired configuration at C-5. The authors were able to push **1072** though an additional 10 steps to complete the synthesis 5-*epi*-**1**. Epimerization was accomplished by DMP oxidation to ketone **1074** and stereoselective enzymatic reduction to complete the total synthesis of 4.5 mg of **1** in 0.8% overall yield over 18 steps.

[43] Ling, T.; Macherla, V. R.; Manam, R. R.; McArthur, K. A.; Potts, B. C. M. Enantioselective total synthesis of (−)-salinosporamide A (NPI-0052). *Org. Lett.* **2007**, *9*, 2289–2292.

Scheme 13 | Total synthesis of (–)-**1** by Potts and co-workers (adapted from ref 43).

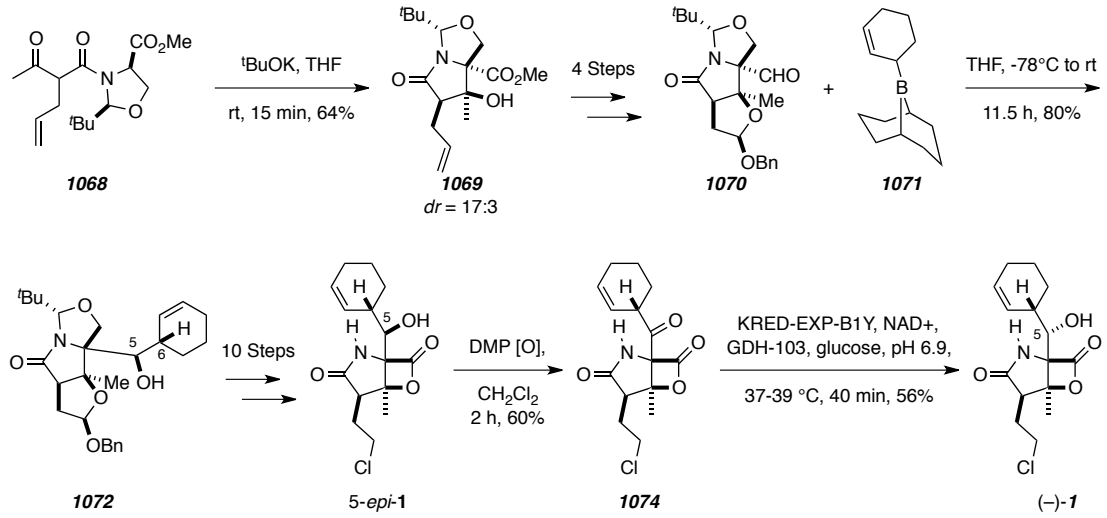

1.6.4. Fukuyama's Total Synthesis of (–)-Salinosporamide A

In 2011 Fukuyama and co-workers[44] reported a total synthesis of (–)-**1**, which as of this writing remains the highest overall yielding total synthesis of **1**. Similar to the approach by Pattenden and co-workers[38,39] (Scheme 9), the key step for the core lactam assembly involved a biomimetic, intramolecular aldol reaction. Preparation of the aldol precursor **1079** (Schemes 14-16) began with condensation between oxazolidinethione chiral auxiliary **1075** and 4-pentenoic acid (**1077**) followed by Ti(IV)-mediated stereoselective alkylation by orthoester **1076** to give imide **1078**. DIBAL-mediated reductive cleavage of the chiral auxiliary gave the corresponding aldehyde, which was immediately subjected to reductive amination with dimethyl aminomalonate hydrochloride to give aminomalonate **1079**.

Scheme 14 | Prepartion of aldol precursor **1079** (adapted from ref 44).

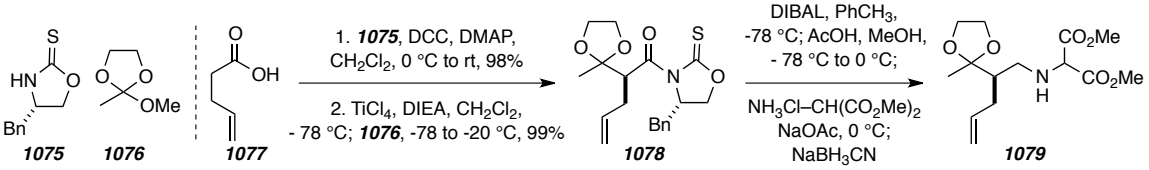

[44] Satoh, N.; Yokoshima, S.; Fukuyama, T. Total synthesis of (−)-salinosporamide A. *Org. Lett.* **2011**, *13*, 3028–3031.

Amine **1079** was formylated with a mixture of formic acid-acetic anhydride mixture followed by acid-mediated deketalization to simultaneously effect an intramolecular aldol reaction to give a mixture of the desired monocyclic **1080**, 3-*epi*-**1080**, and an acyclic formamide. The authors attempted to carry this mixture forward for the preparation of **1085** (Scheme 15), but non-diastereoselective outcomes were accompanied by reduced enantiopurity in the product mixtures. The authors hypothesized that 3-*epi*-**1080** could racemize by a pathway that is inaccessible to the desired diastereomer. Fortunately the authors found that crystallization (from Et_2O) of this complex mixture gave only the desired product **1080** in 71% yield. More thorough control experiments verified that the aldol reaction was reversible for both products and that the dynamic epimerization was driven by crystallization of the desired diastereomer.

Scheme 15 | Prepartion of late-stage intermediate **1085** (adapted from ref 44).

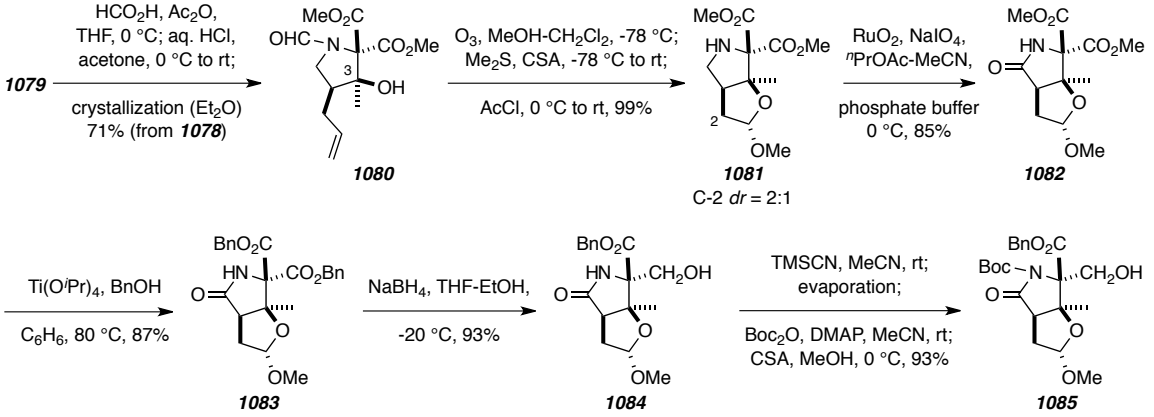

Ozonolysis of **1080** followed by reductive ozonide workup in the presence of CSA led to ketalization of the resulting aldehyde. Reacting the methanol-containing reaction mixture led to HCl-mediated deformylation to give **1081** with moderate stereoselectivity and without observable erosion of enantiopurity (*ee* > 99%). Treating amine **1081** with catalytic amount of RuO_2 in the presence of $NaIO_4$ induced methylene oxidation vicinal to the amine moiety to give amide **1082**. Ti(IV)-mediated transesterification converted amide dimethylmalonate **1082** into dibenzyl ester **1083**. Functional group interconversion and protecting group manipulation by regioselective

ester reduction to alcohol **1084** followed by TMS protection, Boc protection, and acid-mediated silyl ether cleavage gave rise to alcohol **1085**.

DMP oxidation and treatment of the resulting aldehyde with Corey's reagent **1019** gave a mixture of secondary alcohol **1086** and Boc ester **1087** (resulting from transacylation of **1086**, Scheme 16). By treating this mixture with TFA at elevated termperatures followed by reduction with $NaBH_4$ removed the Boc and ketal protecting groups to give triol **1088**. Benzyl ester cleavage, BOPCl-mediated lactonization, and alcohol chlorination completed the total synthesis of 1.54 grams of (–)-**1** in 19% overall yield over 14 steps, repersenting the most efficient total synthesis of **1** to date.

Scheme 16 | Completion of Fukuyama's total synthesis of (–)-**1** (adapted from ref 44).

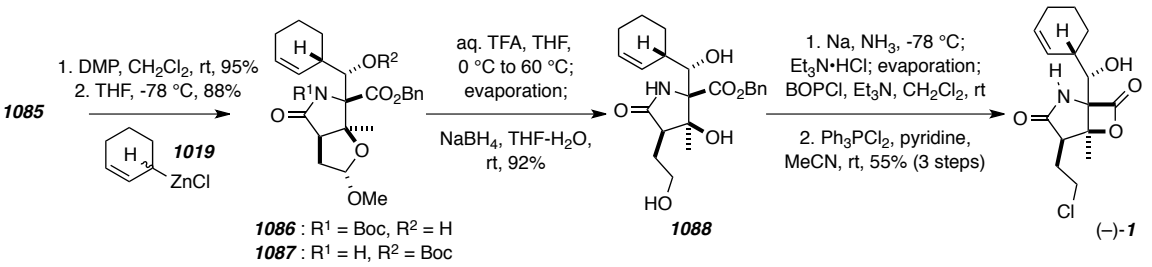

1.7. Concluding Remarks

The studies presented in Chapter 1 demonstrate that **1** is of enormous interest to scientists in the fields of medicinal chemistry, biochemistry, and synthetic organic chemistry. This interest ultimately stems from the unique, minimalistic structure of **1** that renders the natural product with unique biological activities. Potts and co-workers have shown that the proficiency by which **1** inhibits the 20SP is unprecedented and has far-reaching implications into the treatment of cancerous diseases.[2] Furthermore, Moore has demonstrated that the biosynthesis of such a unique structure requires biosynthetic machinery that we do not yet fully understand.[28] Spurred by the developments of Fenical,[1] Potts, and Moore, many of the preeminent leaders in organic chemistry have invested significant effort into developing novel synthetic approaches to the salinosporamides. Collectively, these studies inspired us to probe the mechanistic details of the final biscyclization event in the biosynthesis of **1** and its congeners.

Chapter 2. A Hypothesis for the Non-Enzymatic Biosynthesis of the Salinosporamides

2.1. An Alternative Hypothesis for the Biosynthesis of Salinosporamide A

Despite the numerous and impressive synthetic studies related to **1**, none have directly addressed the means by which the hybrid PKS-NRPS biosynthesis machinery is able to induce biscyclization of thioester **2001** to form **1** (Figure 4). Romo and co-workers[40] reported an approach that closely mimics the proposed biosynthetic biscyclization originally proposed by Moore and co-workers.[28a] The observed diastereoselectivity was much lower (ca. **1**:2-*epi*-**1** dr 5:1)[40] than reported in natural isolation (ca. **1**:2-*epi*-**1** dr 40:1).[26] Our initial hypothesis for the biosynthesis of **1** involves a spontaneous, nonenzymatic, intramolecular ketene-ketone [2+2] cycloaddition via transition structure **2003** from amidoketene **2002**, which is itself derived from thioester **2001**.

Figure 4 | Proposed spontaneous generation of salinosporamide A [(–)-**1**] via ketene intermediate **2002**.

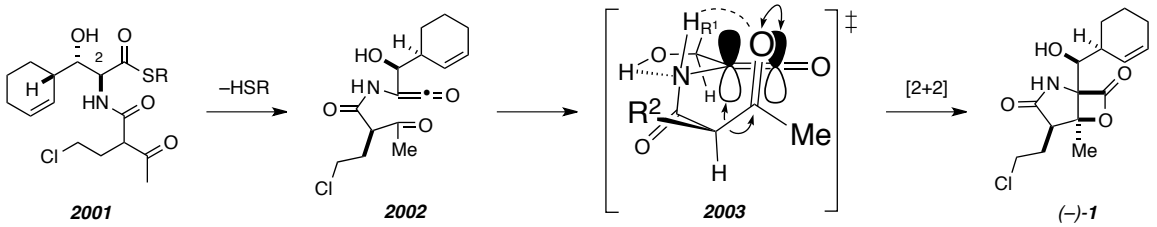

The C-2 diastereoselectivity could be accounted for by pseudo-equatorial positioning of the chloroethyl group (R^2) in transition structure geometry **2003**. An analogous transition structure with pseudo-axial positioning of R_2 is expected to be higher in energy relative to **2003**, which provides a kinetic rationale for the preferred biosynthesis of **1** as opposed to 2-*epi*-**1**. The consideration of both transition structures is necessary because the C-2 stereogenic center of **2001** could readily epimerize to give an equilibrating mixture of **1** and 2-*epi*-**1**. Further consideration of **2003** reveals the

opportunity for useful hydrogen bonding networks. The OH-N hydrogen bond would position the carbinol carbon to minimize $A_{1,3}$-strain and pyramidize the amide nitrogen. Both of these effects would lower the transition structure energy for the formation of the preferred bicyclic system. Additionally, amide pyramidization would introduce the opportunity for NH-CO_{ketone} hydrogen bonding to facilitate the $[2\pi_{s(ketone)} + 2\pi_{a(ketene)}]$ cycloaddition by lowering the lowest unoccupied molecular orbital (LUMO) of the ketone.

Many investigators consider ketenes to be unsuitable biosynthetic intermediates due to their rapid hydrolysis in aqueous media. Our proposed biosynthesis not only utilizes a ketene intermediate, but also does so without an enzyme to protect against adventitious water. We propose that thioester **2001** could serve as a biosynthetic precursor to **2002** by a cascade initiated by deprotonation to form enolate **2004** (Scheme 17). This species could in turn undergo internal acylation that would form azlactone **2005** with concomitant loss of thiolate. Tautomerization to mesoionic Münchnone **2007** by way of 4-hydroxyoxazoles **2006** sets the stage for valence bond isomerism to amidoketenes **2002**. Finally, ketene-ketone [2+2]-cycloaddition would siphon **2002** and all equilibrating intermediates through the tautomeric manifold to give (–)-**1**.

Scheme 17 | Proposed cascade to convert thioeser **2001** into amidoketene **2002**, and ultimately (–)-**1**.

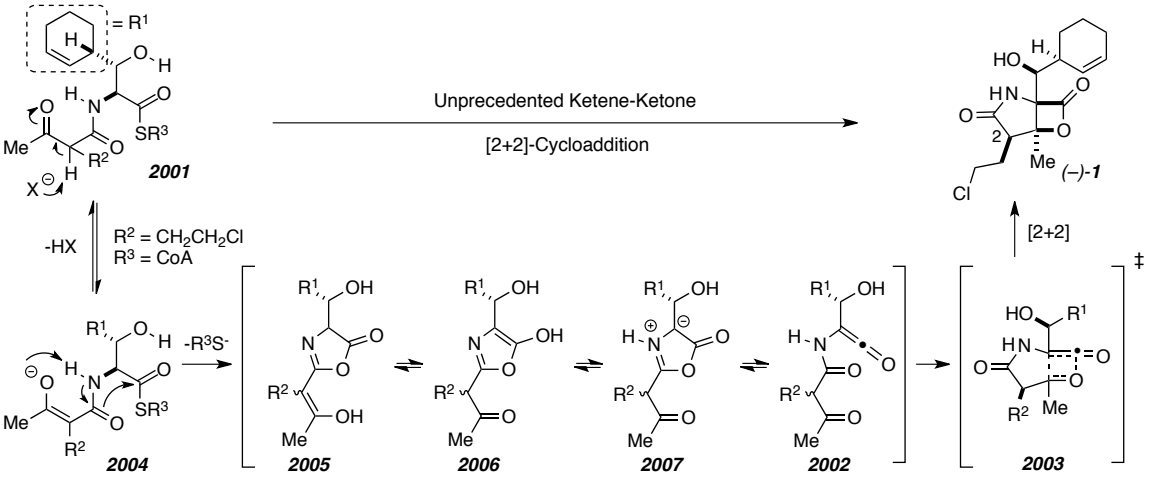

2.2. Previous Studies Relevant to Our Proposed Biosynthesis of Salinosporamide A

2.2.1. Previous Studies that Provide Evidence for Münchnone-Ketene Isomerism

In 1967, Huisgen and co-workers[45] reported the possibility of Münchnone-ketene isomerism by observing that Münchnone **2008** was converted into β-lactam **2011** at 80-100 °C when treated with various azomethine imines (cf. **2010**, Scheme 18). The mechanism for this reaction was assumed to involve valence bond isomerism of the Münchnone to give ketene **2009** as a short-lived intermediate, which underwent [2+2]-cycloaddition with **2010** to give **2011**. Although the authors did not assign the relative stereochemistry of the product, the product mixture was measured to have a narrow melting point, which is consistent with the production of a single diastereomer. A single diastereomer would be predicted if the product was formed by a concerted [2+2] pericyclic reaction via a transition structure similar to **2003** as opposed to the alternative stepwise mechanism, which involves a zwitterionic intermediate. At more elevated temperatures, the authors also reported that Münchnone **2008** reacts with diisopropylcarbodiimide to give azetidindione imine **2012**.

Scheme 18 | Early experiments that demonstrate valence bond isomerization of Münchnones (cf. **2008**) into amido ketenes (cf. **2009**) (adapted from ref. 45).

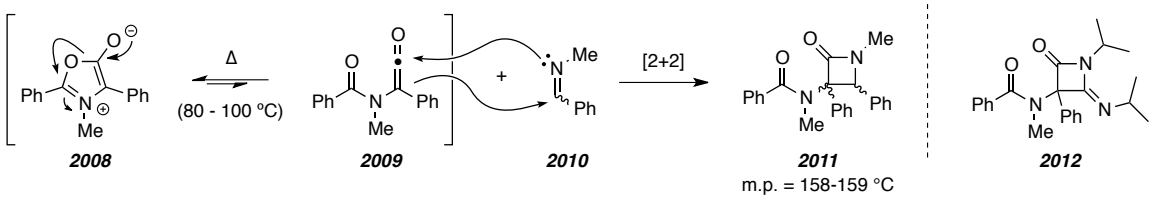

The ketene valence bond isomer has not been observed spectroscopically due to its high reactivity and low equilibrium concentration relative to the corresponding Münchnone. However, Huisgen and co-workers observed further evidence of ketene intermediacy by isolating allene **2014** from heating **2008** at 105 °C in the absence of a ketenophile (Scheme 19). The proposed mechanistic for this transformation involves dimerization of **2009** to form diketene **2013**, a side reaction that often accompanies

[45] Huisgen, R.; Funke, E.; Schaefer, F. C.; Knorr, R. Possible valence tautomerism of a mesoionic oxazol-5-one with an acylaminoketene. *Angew. Chem. Int. Ed.* **1967**, *6*, 367–368.

ketene generation.[46] Subsequent β-lactone decarboxylation then furnishes symmetrical amido allene **2014**.[45]

Scheme 19 | Generation of allene **2014** by dimerization and decarboxylation of amidoketene **2009** (adapted from ref 45).

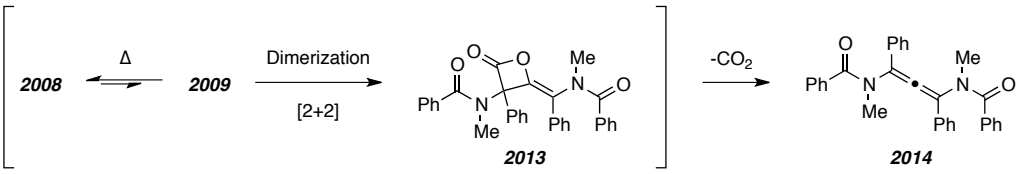

In 1988, Wilde reported evidence for Münchnone-ketene valence bond isomerism in a synthesis of *N*-acyl pyrroles (cf. **2017** and **2018** Scheme 20).[47] Acylation and desilylation of 5-siloxyoxazole **2015** was followed by 1,3-dipolar cycloaddition with acetylenic dipolarophiles to afford pyrroles after decarboxylation. The reaction is assumed to proceed through *N*-acyl Münchnone intermediate **2016**, which produces pyrrole **2017** following treatment with dimethyl acetylenedicarboxylate (DMAD). Interestingly, the authors isolated a second pyrrole product (cf. **2018**) that was structurally similar to the expected product of 1,3-dipolar cycloaddition. The proposed mechanism for generation of **2018** involves isomerism of **2016** to give the *N*-acyl amidoketene **2019**, which is in equilibrium with the rearranged *N*-acyl Münchnone **2020**. Cycloaddition of **2020** with DMAD followed by decarboxylation forms **2018**.

[46] Tidwell, T. T. *Ketenes*, 2nd ed.; Wiley Interscience, Hoboken, New Jersey, 2006.
[47] Wilde, R. G. Generation, cycloadditions, and tautomerism of *N*-acyl munchnones. *Tetrahedron Lett.* **1988**, *29*, 2027–2030.

Scheme 20 | Evidence for Münchnone-ketene equilibrium in *N*-acyl pyrrole synthesis (adapted from ref 47).

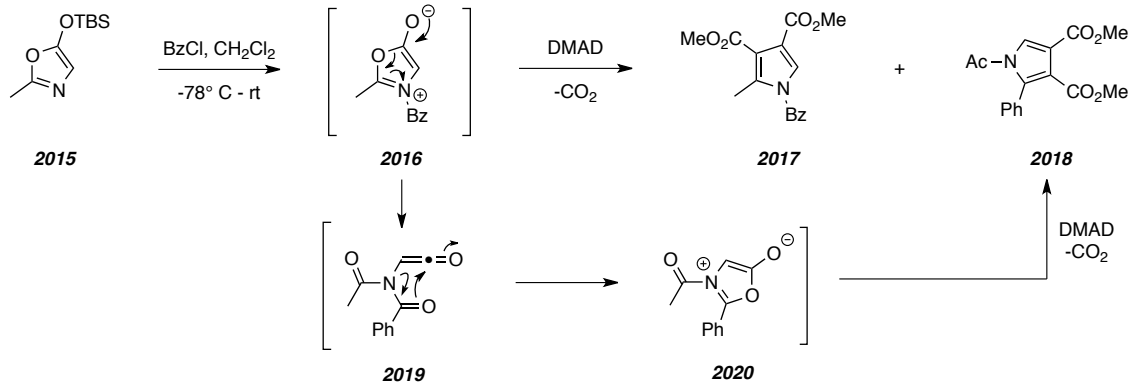

Arndtsen and co-workers[48] have reported a palladium-catalyzed multicomponent reaction that proceeds via a Münchnone intermediate (cf. **2023**, Scheme 21). The reaction involves condensation of an imine (cf. **2021**) with an acid halide (c.f. **2022**) under an atmosphere of CO to give a zwitterionic imidazoline (cf. **2025**). The authors propose that the reaction likely proceeds through an intermediate Münchnone, which reacts with an additional equivalent of imine to give a bicyclic intermediate (cf. **2024**). Spontaneous ring opening gives **2025**. These conditions were further developed to provide efficient routes to the more conventional heterocycles, pyrroles[49] and imidazoles.[50]

[48] a) Dghaym, R. D.; Dhawan, R.; Arndtsen, B. A. The use of carbon monoxide and imines as peptide derivative synthons: A facile palladium-catalyzed synthesis of α-amino acid derived imidazolines. *Angew. Chem. Int. Ed.* **2001**, *40*, 3228–3230. b) Dhawan, R.; Dghaym, R. D.; Arndtsen, B. A. The development of a catalytic synthesis of Münchnones: A simple four-component coupling approach to α-amino acid derivatives. *J. Am. Chem. Soc.* **2003**, *125*, 1474–1475.

[49] Dhawan, R.; Arndtsen, B. A. Palladium-catalyzed multicomponent coupling of alkynes, imines, and acid chlorides: A direct and modular approach to pyrrole synthesis. *J. Am. Chem. Soc.* **2004**, *126*, 468–469.

[50] Siamaki, A. R.; Arndtsen, B. A. A direct, one step synthesis of imidazoles from imines and acid chlorides: A palladium catalyzed multicomponent coupling approach. *J. Am. Chem. Soc.* **2006**, *128*, 6050–6051.

Scheme 21 | Münchnone intermediates for the preparation of zwitterionic imidazolines (adapted from ref 48).

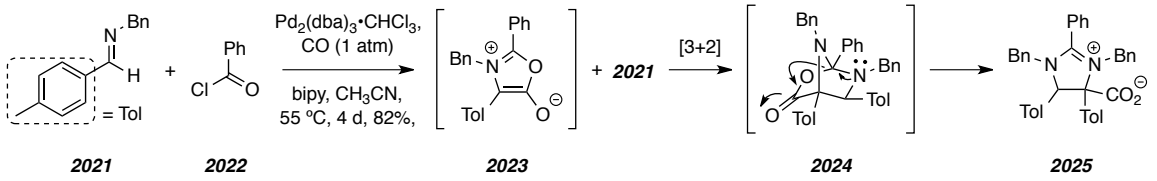

Arndtsen and co-workers subsequently reported[51] that replacing the ligand and adding external base diverted the reaction toward the generation of β-lactams (cf. **2027**, Scheme 22). Heating a 1:2 mixture of imine **2021** and acid halide **2022** at 55 ºC, in the presence of Pd(0) and DIEA, and under an atmosphere of CO gave **2027** in moderate yield. During optimization studies of the reaction presented in Scheme 21, the authors found that addition of external HCl led to increased yields of **2025** with shorter reaction times. However, reactions carried out in the presence of DIEA, unexpectedly, produced β-lactam **2027** and none of zwitterion **2025**. Optimizing for the ligand (cf. ligand in Scheme 22) led to moderate yields of **2027**. The addition of DIEA likely both facilitates HCl elimination and precludes iminium formation by reaction of protonation of imine **2021**. The authors speculate that the conjugate acid of imine **2021** is the active dipolarophile in the synthesis of the zwitterionic imidazoline and not **2021** alone. Formation of β-lactam **2027** then likely proceeds by [2+2] cycloaddition of amidoketene **2026** with imine **2021** to give lactam **2027**.

Scheme 22 | Evidence for Münchnone-ketene valence bond isomerizaiton in the preparation of β-lactams (adapted from ref 51).

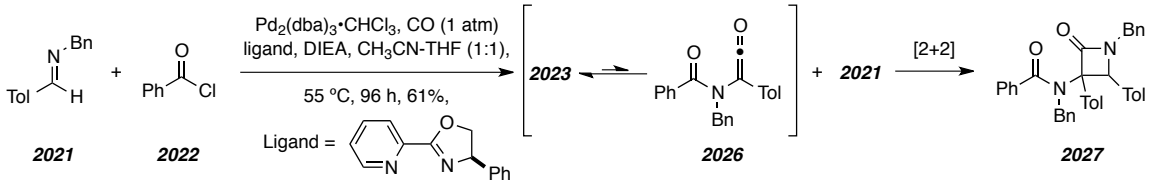

[51] Dhawan, R.; Dghaym, R. D.; St. Cyr, D. J.; Arndtsen, B. A. Direct, palladium-catalyzed, multicomponent synthesis of β-lactams from imines, acid chloride, and carbon monoxide. *Org. Lett.* **2006**, *8*, 3927–3930.

The mechanism for this palladium-catalyzed multicomponent reaction is thought to involve initial condensation of imine **2021** with acid halide **2022** to form acyliminium salt **2028**. Formal oxidative addition by Pd(0) into **2028** then forms *N*-acyl palladium complex **2029** (Scheme 23). Coordination of carbon monoxide forms **2030** and subsequent migratory insertion gives **2031**. Amidoketene **2026** could arise directly from **2031** by sequential β-hydride elimination and reductive elimination of HCl and regeneration of Pd(0). β-Lactam **2027** would be formed directly from **2026** by a bimolecular [2+2] cycloaddition with imine **2021**. The amidoketene would also rapidly equilibrate with the corresponding Münchnone **2023**. Under acidic conditions **2023** is known to undergo 1,3-dipolar cycloaddition with **2021** to form imidazoline **2025**.[48a] Addition of coordinating ligands and DIEA diverts the reactivity from 1,3-dipolar cycloaddition toward β-lactam formation, which is a net [2+2]-cycloaddition that likely involves amidoketene **2026**.[51] The need for ketene intermediacy in either scenario further demonstrates that Münchnones equilibrate with the corresponding ketenes.

Scheme 23 | Proposed mechanism for the Pd(0)-catalyzed synthesis of either zwitterionic imidazoline **2025** or β-lactam **2027** (adapted from refs 48–51).

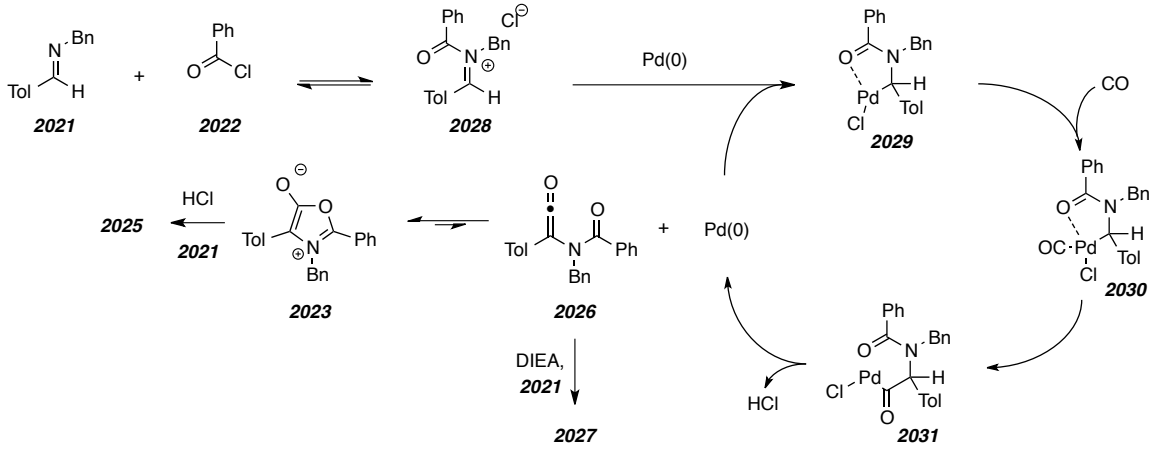

In a series of publications,[52] La Rosa and co-workers have reported evidence for Münchnone-ketene isomerization from thiazolidine-2-carboxylic acids (cf. **2032**, Scheme 24). Treating **2032** with an acid-activating reagent [e.g., acetic anhydride, DCC, or Mukaiyama's reagent (**2033**)], an amine base (e.g., *n*-Pr_3N), and imine **2038** gave spiro-β-lactam **2039** The reaction is thought to proceed through activated acid **2034**, when **2033** is employed. Subsequent elimination of HI and pyridone **2035** under basic conditions generates an equilibrating mixture of Münchnone **2036** and amidoketene **2037**. Ketene-imine [2+2]-cycloaddition of **2037** with imine **2038** then gives spiro-β-lactam **2039** as a mixture of diastereomers.

Scheme 24 | Prepartion of spiro-β-lactam **2039** from thiazolidine-2-carboxylic acid **2032** with by [2+2] cycloaddition of putative amidoketene intermediate **2037** with imine **2038** (adapted from ref 52).

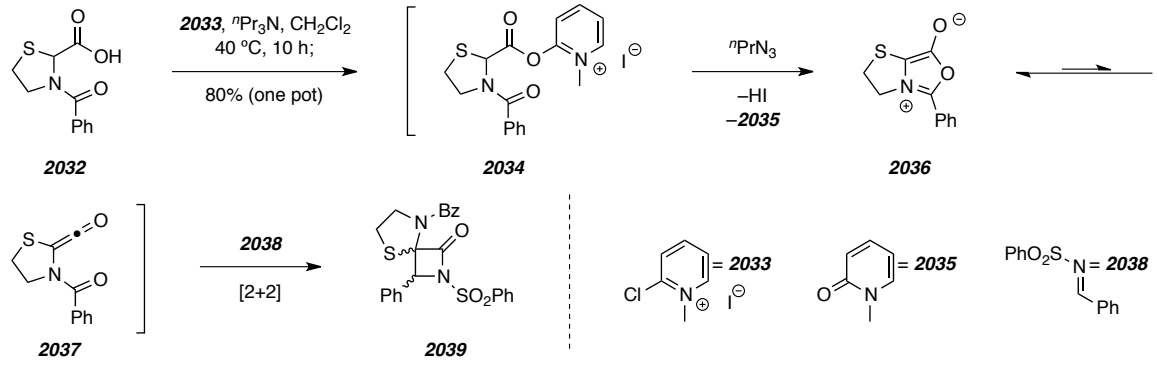

2.2.2. Previous Studies that Involve Ketene-Carbonyl [2+2] Cycloaddition

Experimental and computational studies of ketene-carbonyl [2+2]-cycloaddition reactions have been reported far less often in comparison to their ketene-alkene counterparts, and few examples of inter- or intramolecular variants have been

[52] Croce, P. D.; Ferraccioli, R.; La Rosa, C. Cycloaddition reactions of 5H,7H-thiazolo[3,4-*c*] oxazolium-1-oxides with imines. *Tetrahedron* **1995**, *51*, 9385–9392. (b) Cremonesi, G.; Croce, P. D.; La Rosa, C. Synthesis of imidazo[5,1-*b*]thiazoles or spiro-β-lactams by reaction of imines with mesoionic compounds or ketenes generated from *N*-acyl-thiazolidine-2-carboxylic acids. *Tetrahedron* **2004**, *60*, 93–97. (c) Cremonesi, G.; Dalla Croce, P.; La Rosa, C. [2+ 2] Cycloaddition reactions of imines with cyclic ketenes: Synthesis of 1,3-thiazolidine derived spiro-β-lactams and their transformations. *Helv. Chim. Acta* **2005**, *88*, 1580–1588.

demonstrated. Additionally, there are no known examples of such reactions carried out in aqueous media. Knunyants and Cheburkov[53] reported that warming an ethereal solution of ketene **2040** and hexafluoroacetone (**2041**) induced [2+2]-cycloaddition to form β-lactone **2042** (Scheme 25). The mechanism of this transformation is proposed to involve an uncatalyzed $[2\pi_s + 2\pi_a]$ cycloaddition.

Scheme 25 | First reported uncatalyzed ketene carbonyl [2+2] cycloaddition (adapted from ref 53).

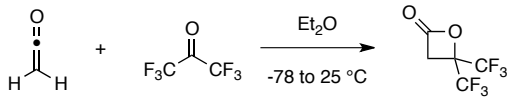

2040 ***2041*** ***2042***

Neidlein and Bernhard[54] later utilized the reactivity of spiro-β-lactones and developed an efficient methenylation strategy and a practical use of ketene-carbonyl $[2\pi_s + 2\pi_a]$ cycloadditions. The authors used the method of Moore[55] to generate dicyanoketene (**2044**) by thermal decomposition of the 2,5-diazido-1,4-quinone **2043** in refluxing benzene (Scheme 26). In the presence of cyclopropenone **2045**, the *in situ*-generated ketene reacts via [2+2] cycloaddition to form spiro-β-lactone intermediate **2046**, which readily decarboxylates to give cyclopropene **2047**.

Scheme 26 | Use of ketene-carbonyl [2+2] cycloadditions as a practical methenylation strategy (adapted from ref 54).

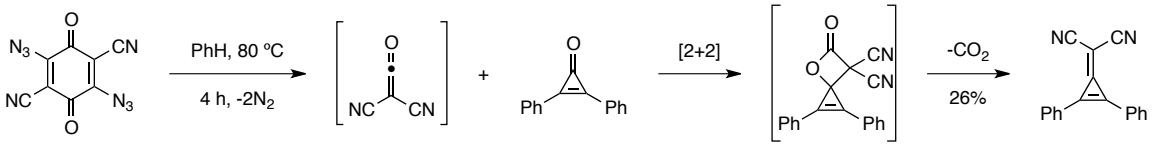

2043 ***2044*** ***2045*** ***2046*** ***2047***

[53] Knunyants, I. L.; Cheburkov, Y. A. Fluorine containing β-lactones I. β,β-Bis(trifluoromethyl)-β-propiolactone and its properties. *Izvest. Akad. Nauk SSSR, Otd. Khim.* **1960**, 678–685.
[54] Neidlein, B. Dicyanoketene. *Angew. Chem. Int. Ed.* **1978**, *17*, 369–370.
[55] Weyler, W., Jr; Duncan, W. G.; Moore, H. W. Rearrangements of azidoquinones. XVI. Thermal and photolytic rearrangements of 2,5-diazido-1,4-quinones. Synthesis and chemistry of cyanoketenes. *J. Am. Chem. Soc.* **1975**, *97*, 6187–6192.

In 1982, Wynberg and Staring[56] reported a chiral alkaloid-mediated, asymmetric, nucleophile-catalyzed, aldehyde-ketene [2+2]-cycloaddition (Scheme 27). Cinchona alkaloids are a class of nucleophilic, chiral amines capable of adding to ketenes to form chiral, reactive intermediates.[46] Use of cinchona alkaloids quinine (**2050**) and quinidine (**2051**) selectively gave the *S*- and *R*-enantiomers of β-lactone **2052** with high enantioselectivity (*ee* = 89%). While the methodology was applied to several substrates, the overall scope was limited to α-chloro aldehydes (e.g., **2048**) and unhindered ketenes (e.g., **2049**).

Scheme 27 | Asymmetric, nucleophile-catalyzed ketene-aldehyde [2+2] cycloaddition of α,α-dichloroaldehyde **2048** with ketene (**2049**) (adapted from ref 56).

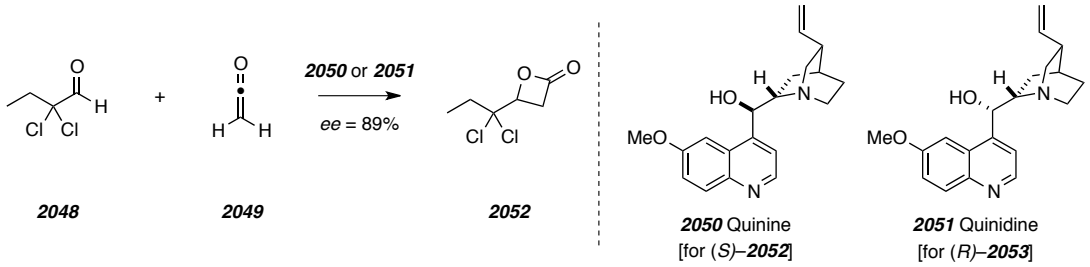

By using a combination of a Lewis acid (e.g., $LiClO_4$) and a chiral amine (e.g., cinchona alkaloid **TMSQ**) Nelson and co-workers[57] were able to effect an enantio-selective synthesis of a variety of *cis*-β-lactones (cf. **2059**) from structurally diverse acid chlorides (e.g., **2053**) and aldehydes (e.g., **2056**, Scheme 28). The reaction likely proceeds through a ketene intermediate (cf. **2054**), which is generated by dehydro-halogenation of the acid chloride with DIEA. Aldol reaction of ammonium *Z*-enolate **2055** with aldehyde **2056** forms acyl pyridinium alkoxide **2058**. The aldol reaction is doubly diastereo- and enantioselective for the newly formed stereocenters via transition structure **2057**. Specifically, simultaneous coordination of lithium cation between the oxygen atoms forms a chair-like six-atom transition structure, and the phenylethylene substituent is thought to adopt a pseudo-equatorial position to minimize steric

[56] Wynberg, H.; Staring, E. G. J. Catalytic asymmetric synthesis of chiral 4-substituted 2-oxetanones. *J. Org. Chem.* **1985**, *50*, 1977–1979.
[57] Zhu, C.; Shen, X.; Nelson, S. G. Cinchona alkaloid-Lewis acid catalyst systems for enantioselective ketene-aldehyde cycloadditions. *J. Am. Chem. Soc.* **2004**, *126*, 5352–5353.

interactions. Lactonization then occurs by condensation of the lithium alkoxide moiety with the acyl pyridinium affords the β-lactone **2059** and regenerates the cinchona alkaloid catalyst **TMSQ**.

Scheme 28 | Stereoselective alkaloid and Lewis acid-catalyzed ketene-aldehyde [2+2] cycloaddition (adapted from ref 57).

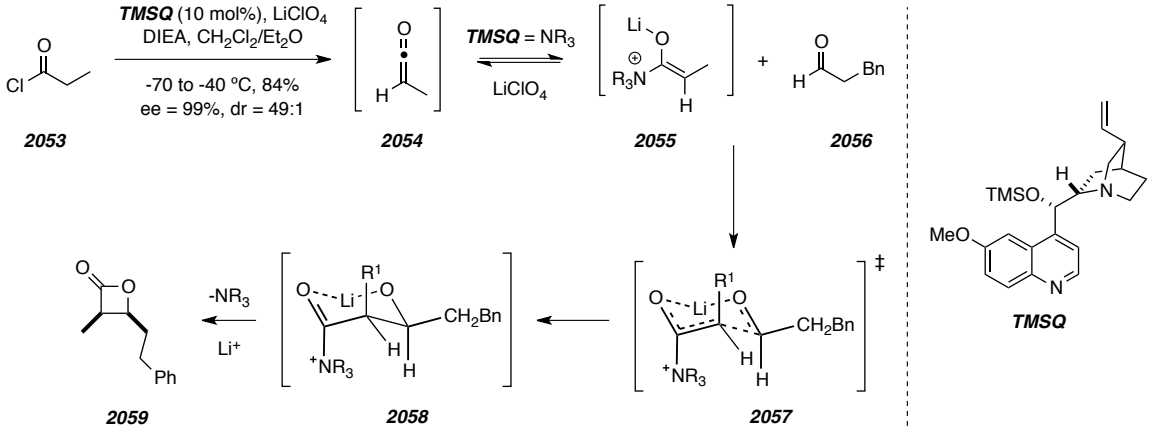

Fu and co-workers[58] have demonstrated that planar-chiral 4-(pyrrolidino)pyridine (PPY) **2062** is a competent promoter of nucleophile-catalyzed ketene-aldehyde [2+2] cycloadditions to enantioselectively prepare β-lactones (cf. **2064**, Scheme 29). The reaction conditions involve generation of a solution of diethylketene (**2060**) followed by addition of the reactant aldehyde (cf. benzaldehyde) and only 5 mol% of catalyst **2062**. Though the mechanism is presumably similar to that of Wynberg (cf. Scheme 27) and Nelson (cf. Scheme 28), use of the PPY catalyst allowed for broader scope of both the aldehydes and ketenes reactants. Additionally, application of Nelson's conditions to the reactants shown in Scheme 29 led to low yields (i.e. 21%) and trace amounts of enantioinduction. Overall, a marginal scope of β-lactones could be generated demonstrating the utility of PPY **2062** for catalyzing the enantioselective ketene-aldehyde [2+2] cycloaddition.

[58] Wilson, J. E.; Fu, G. C. Asymmetric synthesis of highly substituted β-lactones by nucleophile-catalyzed [2+2] cycloadditions of disubstituted ketenes with aldehydes. *Angew. Chem. Int. Ed.* **2004**, *43*, 6358–6360.

Scheme 29 | Chiral PPY-catalyzed ketene-aldehyde [2+2] cycloaddition (adapted from ref 58).

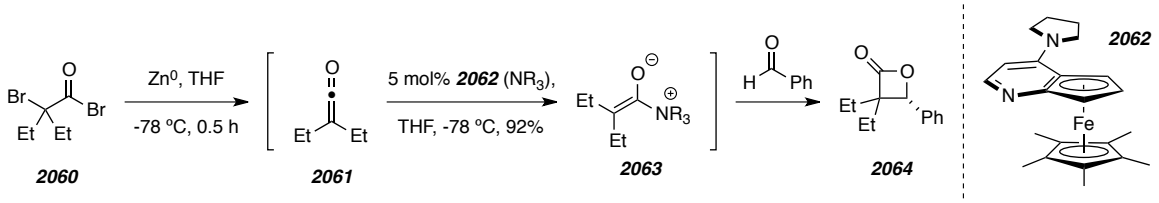

Romo and co-workers[59] developed conditions for a zinc-mediated formal ketene-carbonyl [2+2] cycloaddition to stereoselectively produce β-lactones (Scheme 30). The reaction involves initial Mukaiyama aldol reaction of a silyl ketene thioacetal (cf. **2066**) with an aldehyde (cf. **2065**) in the presence of Zn(II) followed by intramolecular lactonization. The authors termed the overall process a tandem aldol-lactonization (TAL). Mechanistically, it is believed that **2066** is activated with $ZnCl_2$ to form tetrahedral complex **2067**, which further chelates to the carbonyl oxygen of aldehyde **2065**. The Mukaiyama aldol reaction then proceeds through the highly ordered, boat-like transition structure **2068** to give the Zn-coordinated aldolate **2069**.[60] Intramolecular acylation of the zinc alkoxide by the silylated thioester and aqueous workup affords β-lactone **2070**. This methodology has been extensively utilized in the preparation of fused bicyclic β-lactones[61] and in the total synthesis of (–)-panclicin D,[59] okinonellin B,[62] brefeldin A,[63] belactosin,[64] and orlistat.[65]

---

[59] Yang, H. W.; Romo, D. A highly diastereoselective, tandem Mukaiyama aldol-lactonization route to β-lactones: Application to a concise synthesis of the potent pancreatic lipase inhibitor, (–)-panclicin D. *J. Org. Chem.* **1997**, *62*, 4–5.

[60] Zhao, C.; Mitchell, T. A.; Vallakati, R.; Pérez, L. M.; Romo, D. Mechanistic investigations of the $ZnCl_2$-mediated tandem Mukaiyama aldol lactonization: Evidence for asynchronous, concerted transition states and discovery of 2-oxopyridyl ketene acetal variants. *J. Am. Chem. Soc.* **2012**, *134*, 3084–3094.

[61] Mitchell, T. A.; Zhao, C.; Romo, D. Highly diastereoselective, tandem, three-component synthesis of tetrahydrofurans from ketoaldehydes via silylated β-lactone intermediates. *Angew. Chem. Int. Ed.* **2008**, *47*, 5026–5029.

[62] Schmitz, W. D.; Messerschmidt, N. B.; Romo, D. A β-Lactone-based strategy applied to the total synthesis of (8*S*, 21*S*, 22*S*, 23*R*)-and (8*R*, 21*S*, 22*S*, 23*R*)-okinonellin B. *J. Org. Chem.* **1998**, *63*, 2058–2059.

[63] Wang, Y.; Romo, D. Concise total synthesis of (+)-brefeldin A: A combined β-lactone/cross-metathesis-based strategy. *Org. Lett.* **2002**, *4*, 3231–3234.

[64] Cho, S. W.; Romo, D. Total synthesis of (–)-belactosin C and derivatives via double diastereoselective tandem Mukaiyama aldol-lactonizations. *Org. Lett.* **2007**, *9*, 1537–1540.

Scheme 30 | Representative bimolecular Zn(II)-mediated TAL reaction (adapted from refs 59–61).

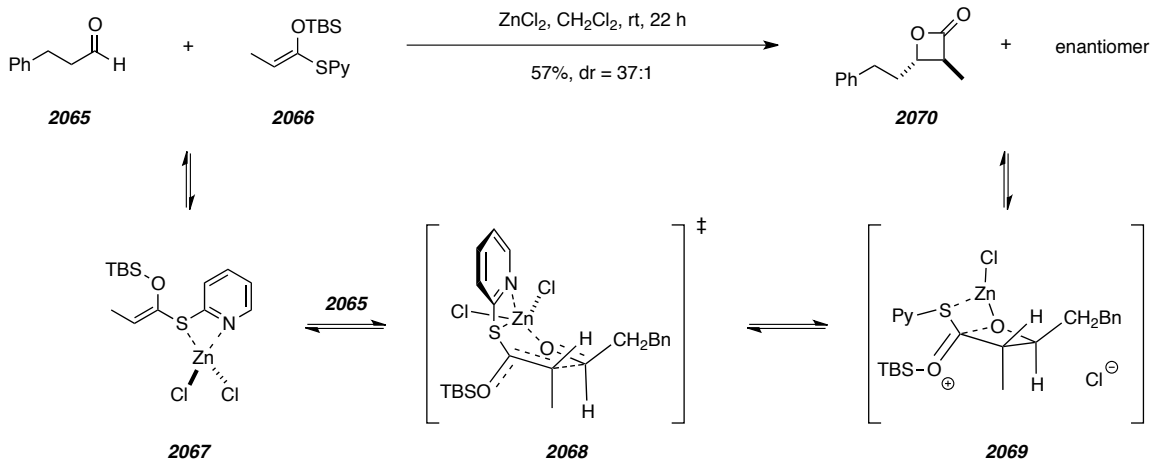

The key step in Romo's total synthesis of **1** (see Schemes 19-21 in Chapter 1) could be considered a formal intramolecular ketene-carbonyl [2+2]-cycloaddition, which would represent a rare example of the carbonyl unit being a ketone. These results represented the culmination of a long-standing effort in the Romo lab that began prior to the isolation **1**. These preliminary studies[66] demonstrated that treating 6-oxohexanoic acid (**2071**) with Mukaiyama's reagent **2033**, DIEA, and a catalytic amount of cinchona alkaloid *O*-acetyl quinidine (**AcQUIND**) gave β-lactone **2076** with excellent diastereo and enantioselectivity (Scheme 31).

[65] Zhang, W.; Richardson, R. D.; Chamni, S.; Smith, J. W.; Romo, D. β-Lactam congeners of orlistat as inhibitors of fatty acid synthase. *Bioorg. Med. Chem. Lett.* **2008**, *18*, 2491–2494.
[66] a) Cortez, G. S.; Tennyson, R. L.; Romo, D. Intramolecular, nucleophile-catalyzed aldol-lactonization (NCAL) reactions: Catalytic, asymmetric synthesis of bicyclic β-lactones. *J. Am. Chem. Soc.* **2001**, *123*, 7945–7946. b) Oh, S. H.; Cortez, G. S.; Romo, D. Asymmetric synthesis of bicyclic β-lactones via the intramolecular, nucleophile-catalyzed aldol lactonization: Improved efficiency and expanded scope. *J. Org. Chem.* **2005**, *70*, 2835–2838.

Scheme 31 | Representative intramolecular nucleophile-catalyzed TAL (adapted from ref 66).

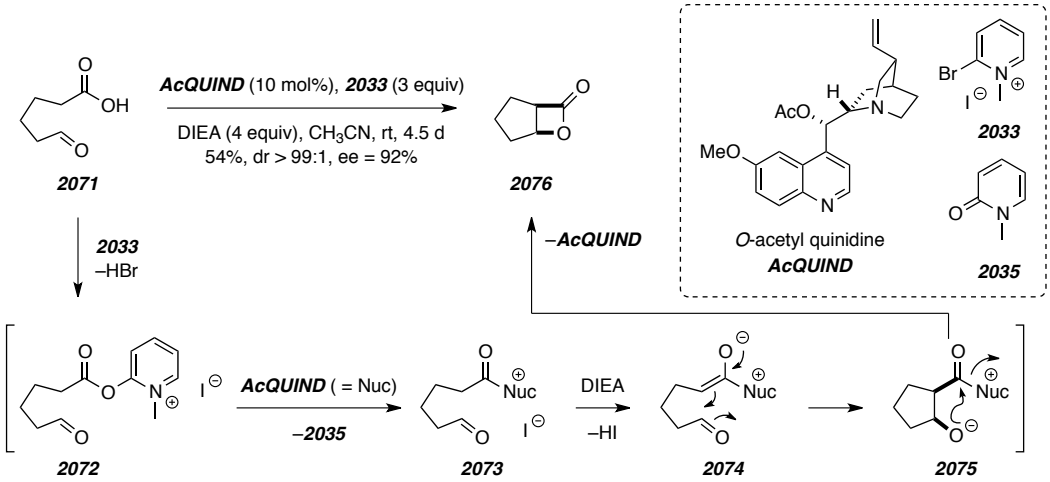

The authors rationalized the transformation with a mechanism similar to that proposed in the total synthesis of **1** (Scheme 11). Namely, acid **2071** reacts with **2033** to form acyl pyridinium **2072**, which is capable of acylating the quinuclidine nitrogen atom of **AcQUIND** to form acyl ammonium halide **2073**. The authors then argue that the ammonium group decreases the C-1 α-proton pKa of **2073** to allow for deprotonation by DIEA to give ammonium enolate **2074**. Intramolecular tandem aldol-lactonization then provides β-lactone **2076** via ammonium alkoxide intermediate **2075**. Similar to the conditions developed by Wynberg,[56] the authors attribute the enantioselectivity to increased steric hindrance around the C-2 *si* face of intermediate **2074**. Furthermore, the high strain energy of *trans*–β-lactones precludes isolation of either diastereomer of **2076**. However, 3-*epi*-**2075** would likely be accessible and subsequent hydrolysis during workup to the corresponding acid is likely responsible for the moderate yield of **2076** in the overall transformation.

These results utilize the same conditions that La Rosa[52] used to prepare spiro-β-lactam **2039** (Scheme 24). Namely, use of Mukaiyama's reagent **2033** on a carboxylic acid precursor generated a ketene intermediate. Romo has demonstrated that intermediates generated from the same conditions can efficiently be trapped with

cinchona alkaloids and subsequently react with an aldehyde to effect an enantioselective ketene-aldehyde [2+2] cycloaddition. Interestingly, and unlike La Rosa, Romo has argued against the involvement of ketene intermediates by arguing for direct transacylation (cf. conversion of **2072** to **2073**).[40]

During their synthesis studies of **1**, Corey and co-workers found that treating acryloyl chloride (**2077**) with amino ketone **2078** in the presence of pyridine gave rise to bicyclic β-lactones (Scheme 32).[30] In a later report,[67] the authors proposed a mechanism for this transformation that involved acid chloride activation by pyridine to form **2081**, which is followed by Michael reaction with amine **2078** to form ammonium enolate, which may eject pyridine to give δ-ketoketene **2083**. Intramolecular, uncatalyzed ketene-ketone [2+2]-cycloaddition of **2083** then affords β-lactone **2080**.

Scheme 32 | Uncatalyzed, intramolecular ketene-ketone [2π + 2π]-cycloaddition (adapted from ref 67).

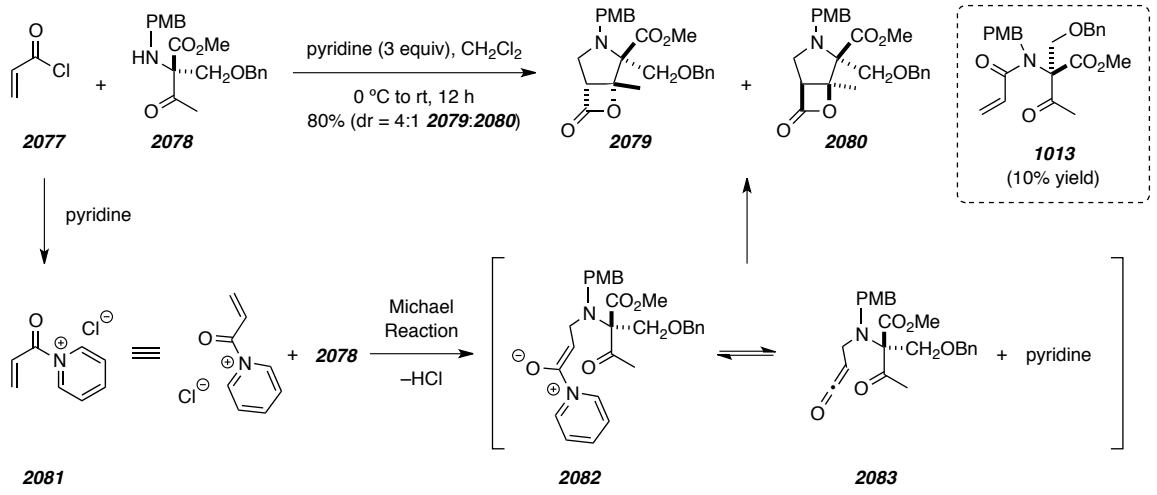

The authors also found that the use of more sterically hindered amines favored direct *N*-acylation. This observation supported the authors' claims that direct *N*-acylation required the use of a Brønsted base to capture HCl produced following condensation of **2077** with **2078**. Use of more nucleophilic amine bases (e.g., pyridine) favored the formation of **2079** and **2080**, presumably because chloride displacement must precede

[67] Reddy, L. R.; Corey, E. J. Novel bicyclization reaction leading to a fused β-lactone. *Org. Lett.* **2006**, *8*, 1717–1719.

Michael addition of amine **2078**. In this report the authors illustrate ketene **2083** and not the corresponding pyridine adducted ammonium enolate **2082** as the immediate precursor to the β-lactones. Considering that Romo and co-workers had already reported their 4-pyrrolidinopyridine (4-PPY) catalyzed TAL,[66b] Corey and co-workers would have found value in studying the effects of more nucleophilic pyridine derivatives on the reaction rate. Such experiments would allow for differentiation between uncatalyzed and nucleophile-catalyzed cycloaddition mechanisms (assuming that cyclization is the rate-limiting step for formation of the final products).

2.3. Previous Studies Into the Stability of Ketenes in Aqueous Media

A major crux of our hypothesis for the biosynthesis of salinosporamide A (**1**) is the transient existence of a ketene in biological media. This is a problematic proposition because ketenes are known to readily hydrolyze to carboxylic acids in water. However, our lab recently reported[68] an example that is both relevant and promising for this audacious postulate. Namely, thermal decomposition of dioxinone **2084** gave α,β-unsaturated macrolactone **2086**, presumably via extrusion of acetone to form an intermediate acylketene (cf. **2085**, Scheme 33). The reactive intermediate **2085** was then trapped intramolecularly by the C-13 hydroxyl group. Subsequent tautomerization to β-ketolactone **2087** followed by hemiketalization produced macrolactone/pyran **2088**. If ketene hydrolysis by adventitious water were occurring the resulting carboxylic acid **2089** would likely decarboxylate spontaneously to give methyl ketone **2090**. While anhydrous benzene was used as solvent in the optimized conditions, running the reaction in a biphasic mixture of benzene-water at 0.5 M still provided desired product **2088** as the predominant product in addition to the expected products of hydrolysis (ratio of **2088**:**2090** = 2:1). This demonstrates that certain ketenes are able to react intramolecularly reactivity under aqueous conditions.

[68] Hoye, T. R.; Danielson, M. E.; May, A. E.; Zhao, H. Dual macrolactonization/pyran-hemiketal formation via acylketenes: Applications to the synthesis of (–)-callipeltoside A and a lyngbyaloside B model system. *Angew. Chem. Int. Ed.* **2008**, *47*, 9743–9746.

Scheme 33 | A tandem lactonization/hemi-ketal formation that demonstrates the possible stability of ketenes in aqueous systems (adapted from ref 68).

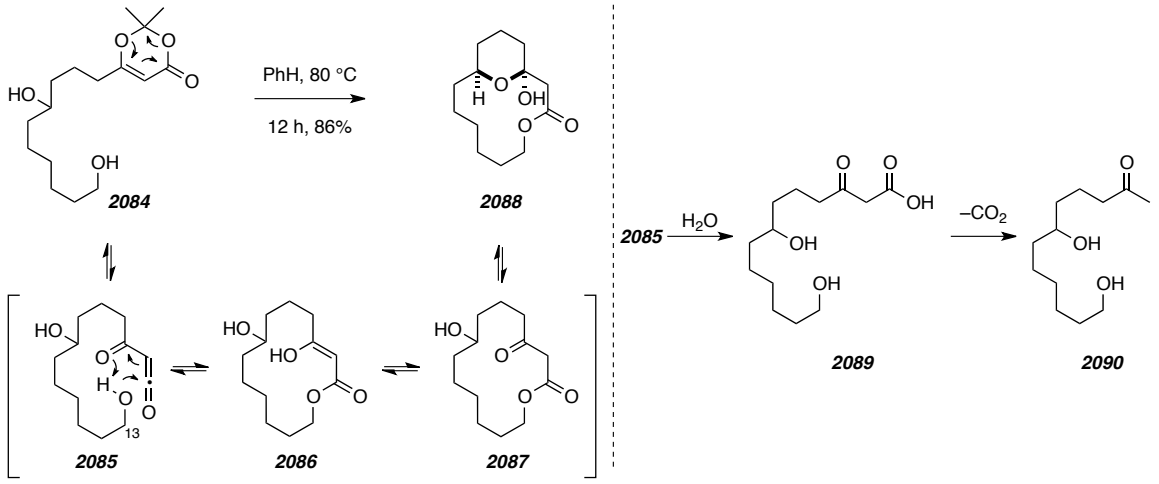

2.4 Concluding Remarks

The efforts by Romo and co-workers represent the only total synthesis of **1** from an activated β-ketoamido acid precursor.[42] Reports on the biosynthesis of **1** from Moore and co-workers[28d,e] demonstrated that subjecting the α-amido acid-derived thioester **1050** (Schemes 7 and 8) to biosynthetic conditions affords **1**. With this in mind, Romo and co-workers argue that the bis-cyclization methodology they employ to form the fused γ-lactam/β-lactone framework of **1** is biomimetic. Although the authors propose a TAL mechanism (Scheme 8), a concerted ketene-ketone $[2\pi_a+2\pi_s]$-cycloaddition involving ketene intermediate **2091** (Scheme 34) is also possible. The authors found that the use of less nucleophilic promoters [e.g., *N,N*-dimethylaminopyridine (DMAP) or pyridine] led to lower conversions, and 5% conversion was observed when the reaction was carried out without a nucleophilic promoter. The authors interpret these results to indicate that the nucleophilic promoter is involved in the rate-determining step of the bis-cyclization event, which may be consistent with a TAL mechanism.

Scheme 34 | Alternative bis-cyclization mechanism for the conversion of mixed anhydride **1063** into β-lactone **1062** via a ketene-ketone [$2\pi_a+2\pi_s$]-cycloaddition.

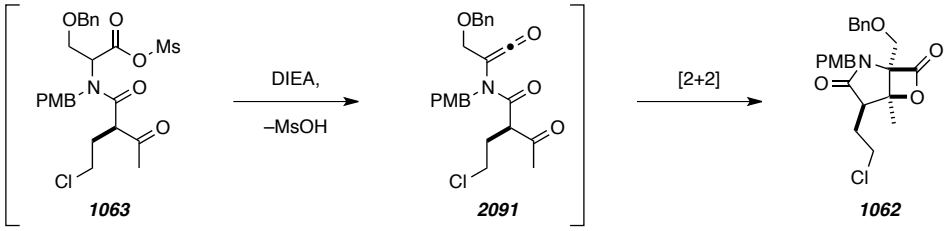

Even though the authors have mechanistic evidence in support of a TAL mechanism over a concerted [$2\pi_a+2\pi_s$] cycloaddition, the cyclization resulted in low yields (34%) of a racemic mixture of epimers **1062** and 2-*epi*-**1062** **(**dr = 5:1, Scheme 10).[40] Two research groups independently reported more favorable dr's from isolation of the natural product (ca. **1**:2-*epi*-**1** dr 40:1),[1,26] which might suggest that bis-cyclization occurs by a different and more stereoselective mechanism. These results led us to formulate an alternative hypothesis for the biosynthesis of **1**, namely one that includes elimination of MsOH to ketene **2091** followed by spontaneous, intramolecular ketene-ketone [2+2] cycloaddition.

Chapter 3. Model Studies for a Spontaneous Biosynthesis of the Salinosporamides

3.1. Synthesis Studies of Thioester Model Substrates

In addition to the results by Romo, the inability of Moore to identify the details of the final biscyclization event in the biosynthesis of **1** led us to propose an alternative mechanism, namely one that involves a spontaneous ketene-ketone [2+2] cycloaddition (summarized in Section 2.1). Chapter 3 of this Thesis will detail our attempts to probe this mechanistic hypothesis. Unfortunately, a series of unsuccessful results led us to abandon the approach, but our efforts certainly provided extensive insight and many important questions regarding the chemical properties of heterocycles related to **1** were addressed. Eventually, deeper insight related to the biosynthesis of **1** revealed itself to us, and these studies are described in Chapter 4.

3.1.1. Initial Approach to the Synthesis of a Thioester Model Substrate

The key intermediate that we initially identified as the entry point to our biomimetic studies was amido thioester **3001**. While the putative biosynthetic intermediate of **1** is likely the cyclohexenyl congener, we believe that **3001** is the biosynthetic precursor to antiprotealide (**2**, Scheme 35). Because Potts and co-workers isolated both **1** and **2** from the same organic extracts conditions that effect the conversion of **3001** into **2** should also be amenable to the production of **1** from its biosynthetic precursor.[69] That is to say, anything we can learn from studying thioester **3001** will greatly increase our understanding of the more potent **1**. Our initial approach to the preparation of **3001** is outlined as a retrosynthetic analysis in Scheme 35. We envision that **3001** will arise from the corresponding amido ester **3002** following ester displacement by an aluminum thiolate.[70] Treating known α-amino ester **3003**[71] with the mixed ketene dimer **1058** will give **3002**.

---

[69] Manam, R. R.; Macherla, V. R.; Tsueng, G.; Dring, C. W.; Weiss, J.; Neuteboom, S. T. C.; Lam, K. S.; Potts, B. C. Antiprotealide is a natural product. *J. Nat. Prod.* **2009**, *72*, 295–297.

[70] Crich, D.; Yao, Q. The 4,6-*O*-[α-(2-(2- iodophenyl)ethylthiocarbonyl)benzylidene] protecting group: Stereoselective glycosylation, reductive radical fragmentation, and synthesis of β-D-rhamnopyranosides and other deoxy sugars. *Org. Lett.* **2003**, *5*, 2189–2191.

Scheme 35 | Retrosynthetic analysis for the preparation of thioester **3001**, the key biosynhetic precusor to **2**.

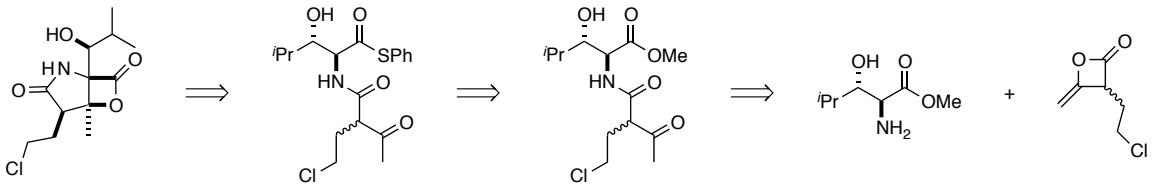

Antiprotealide
2

3001

3002

3003

1058

While the synthesis of **3001** outlined in Scheme 35 is not without precedence, we quickly learned that several steps were problematic, which would result in limited production of the desired thioester. To thoroughly evaluate potential conditions to address the feasibility of our biosynthetic hypothesis, we chose to prepare thioester **3008** (Scheme 36) because it is likely to be easily prepared on larger scales. The synthesis of heteroketene dimer **1058** is known to be accompanied by a slew of impurities, which is exemplified by its low yield (cf. 13%) and inability to be scaled-up beyond 2.3 g in an optimal setting. To ameliorate these challenges **1058** was substituted by the homoketene dimer of methyl ketene (**3005**) because it was both more easily isolated with greater yields from propionyl chloride (**3004**) and more amenable to scale-up. Non-natural α-aminoester **3003** was replaced by the commercially available benzyl ester of L-phenylalanine (**3006**). Acetoacylation of **3006** by **3005** proceeded in high yield to give amido ester **3007**. After screening a variety of conditions for installation of the thioester group, we found that a mixture of benzenethiol and $Al(CH_3)_3$ rapidly produced desired *S*-phenyl thioester **3008** in good yield to give a suitable model substrate in three steps and 29% overall yield.

[71] Thayumanavan, R.; Tanaka, F.; Barbas III, C. F. Direct organocatalytic asymmetric aldol reactions of α-amino aldehydes: Expedient syntheses of highly enantiomerically enriched anti-β-hydroxy-α-amino acids. *Org. Lett.* **2004**, *6*, 3541–3544.

Scheme 36 | Preparation of thioester **3008** from phenylalanine derivative **3006** and propionyl chloride (**3004**).

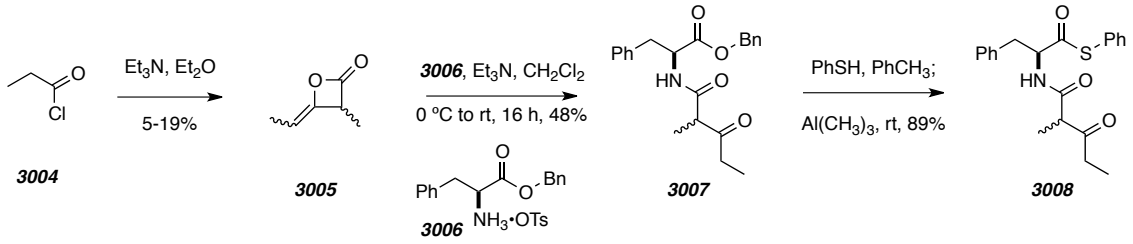

3.1.2. Model Studies of the Reactivity of Thioesters Under Aqueous Conditions

With model thioester **3008** in hand, we were in position to screen a variety of biologically relevant conditions to test for the production of desired β-lactone **3009**. Because our biosynthetic hypothesis requires initial enolate formation to initiate the tautomeric cascade (cf. Scheme 17), we began by studying the stability of thioester **3008** in water at various pH levels. Specifically, **3008** was mixed with a series of aqueous, phosphate buffered solutions with pH values ranging from 6-11. The results of these studies are shown in Figure 5. In summary, no reaction was detected after several weeks when **3008** was mixed in solutions having a pH ≤ 6, which demonstrates that amido thioesters are stable under acidic, non-nucleophilic, aqueous conditions. At neutral pH, hydrolysis of **3008** to the corresponding carboxylic acid was observable by LC-MS after one week. Hydrolysis occurred rapidly in more basic solutions (pH = ca. 8–10) and complete conversion was observed after 6 h at solution pH = 10.5 ($t_{1/2}$ = ca. 0.5 h).

Figure 5 | Studies in to the reactivity of thioester **3008** under aqueous conditions of varying pH.

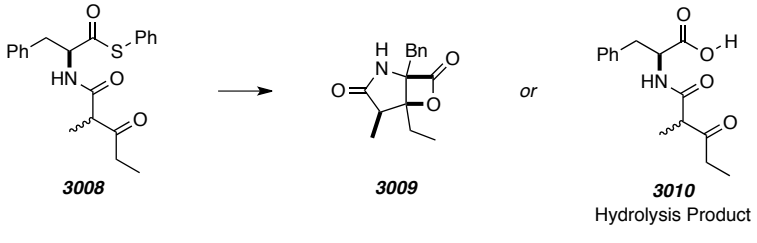

Conditions	Results
pH 6	No Reaction
pH 7	Slow Hydrolysis
pH 8-10	Rapid Hydrolysis
pH > 10	Rapid Hydrolysis ($t_{1/2}$ = 0.5 h)

It is known that azlactones rapidly hydrolyze to carboxylic acids under basic conditions.[72] Hence, base-induced thioester hydrolysis may occur by way of internal acylation of enolate **3011** to form hydrolytically sensitive azlactone **3012** (Scheme 37). An alternative and more conventional mechanism for the hydrolysis of **3008** under basic conditions would be hydroxide-mediated addition-elimination via tetrahedral intermediate **3014**. Alternatively, Douglas[73] has reported evidence that base-mediated thioester hydrolysis proceeds by an elimination-addition mechanism with *in situ* generation of a ketene intermediate (cf. **3016**) from a thioketene enolate (cf. **3015**). Rapid hydrolysis of the ketene by adventitious water forms the corresponding carboxylic acid. Distinguishing between these mechanisms then becomes critical in evaluating the viability of our biosynthetic hypothesis.

Scheme 37 | Possible mechanisms to account for the aqueous base-mediated conversion of thioester **3008** into acid **3010**: A) Transacylation converts the β-ketoamido thioester (cf. **3008**) into a hydrolytically sentitive azlactone (cf. **3012**), B) Addition-elimination via a tetrahedral intermediate (cf. **3014**), and C) Elimination-addition to form a ketene intermediate (cf. **3016**), which is rapidly hydrolyzed.

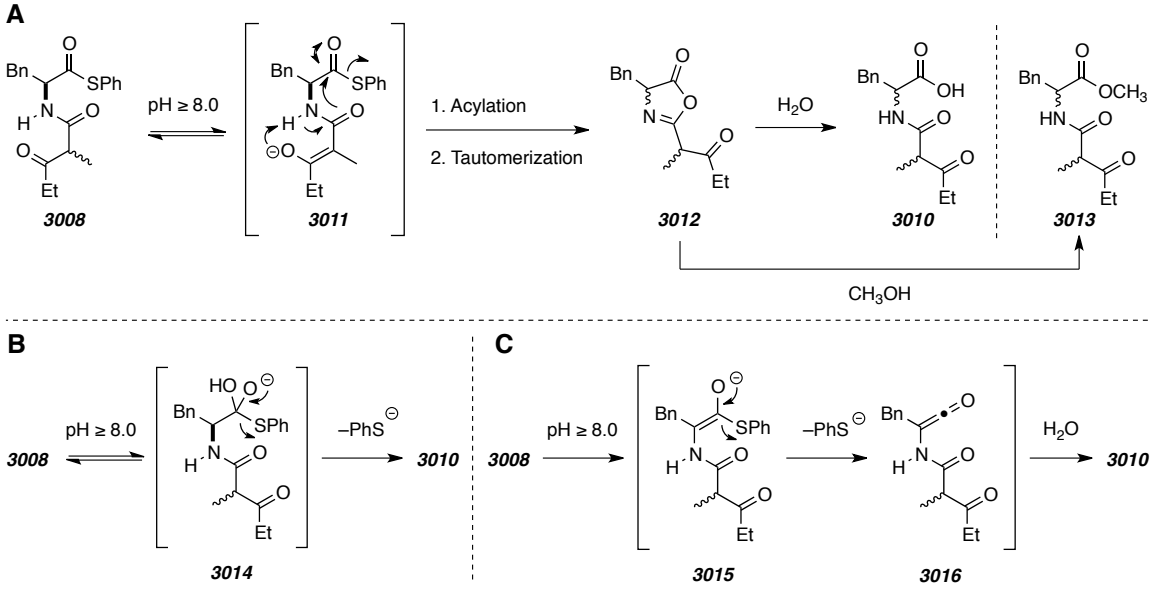

[72] Fisk, J. S.; Mosey, R. A.; Tepe, J. J. The diverse chemistry of oxazol-5-(4*H*)-ones. *Chem. Soc. Rev.* **2007**, *36*, 1432–1440.
[73] Douglas, K. T. Elimination-addition pathways for thiol esters. *Acc. Chem. Res.* **1986**, *19*, 186–192.

In an attempt to differentiate among the potential mechanisms for base-mediated thioesterification we studied the fate of **3008** in the presence of $LiOH•H_2O$ in a solution of CD_3OD by ^1H NMR (Scheme 38). Previous experiments suggested that complete conversion would be achieved in 10 h. Indeed, by collecting spectra at various time points, the half-life for ester formation was found to be 1.25 h. Unfortunately, we were unable to observe evidence for the formation of intermediates in the methanolysis pathway to the deuterated methyl ester. Interestingly, ^1H NMR and LC-MS results indicated that deuterium incorporation occurred at C-2 and the amido-N*H* to give the pentadeutero ester **3017**. This indicates that, under the described conditions, direct ketene formation must not be occurring because deuterium incorporation would likely be observed at C-4 if the α-hydrogen atom was deprotonated in an elimination-addition pathway. Unfortunately, the results presented in this section led us to conclude that the conversion of **3008** into the corresponding β-lactone (cf. **3009**) is not possible under aqueous conditions.

Scheme 38 | Deuterium incorporation and methanolysis of **3008** under basic conditions.

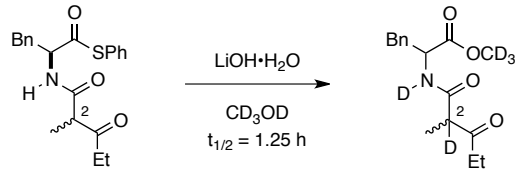

3008 ***3017***

3.1.3. Model Studies for the Thermal Activation of Relevant Thioesters

Analysis of purified **3008** by GC-MS gave a single peak in all cases with molecular ions of $[M^+–PhSH]$ alluding to the possibility of a thermally induced intramolecular thiolate ejection from the parent compound. Thermal entry into the tautomeric cascade outlined in our biosynthetic hypothesis (see Scheme 17) demonstrates an alternative mechanistic pathway. To test this hypothesis we monitored the fate of **3008** at various temperatures by ^1H NMR spectroscopy. No reaction occurred below 150 ºC, while temperatures higher than 150 ºC afforded complicated, overlapping multiplets that impeded deeper spectral interpretation. Electrospray ionization (ESI) mass spectrometry analysis of the resulting reaction mixtures did show a desired mass that possibly

corresponds to a dethiolated product, but no relevant products were isolable by normal phase chromatography.

To supplement these results we attempted to differentiate the possible products that possess a molecular weight equal to that of the dethiolated starting material. However, our hypothesis complicates this endeavor because loss of thiolate could lead to an equilibrating mixture of azlactone **3012**, Münchnone **3018**, ketene **3016**, β-lactone **3009**, and tricarbonyl byproduct **3019**, the latter resulting from *C*-acylation of **3016** (Scheme 39). Each of the aforementioned intermediates has an identical molecular weight, and with the exception of **3019**, is not amenable to LC/MS analysis due to its inherent sensitivity to hydrolysis or methanolysis. Not surprisingly, LC/MS analysis of the reaction mixture resulting from prolonged heating at 150 ºC gave a single peak corresponding to methyl ester **3013**. Even though desired β-lactone **3009** is likely unstable under mildly basic methanolic conditions, comparison of previously recorded retention times suggests that the observed peak corresponds to the acyclic ester **3013**, and a product of β-lactone methanolysis was not observed. Additionally, we found that heating a small sample of **3008** led to no observable reaction (from subsequent ^{1}H NMR analysis). Even though we were unable to fully understand the details of the thermal activation of **3008**, enough evidence was gathered to suggest that this approach was not promising.

Scheme 39 | The potential tautomeric cascade resulting from thermal activation of thioester **3008**. The promsing *m*/*z* observed by GC/MS and ESI-MS analysis could correspond to any of **3009**, **3012**, **3016**, **3018**, or **3019**.

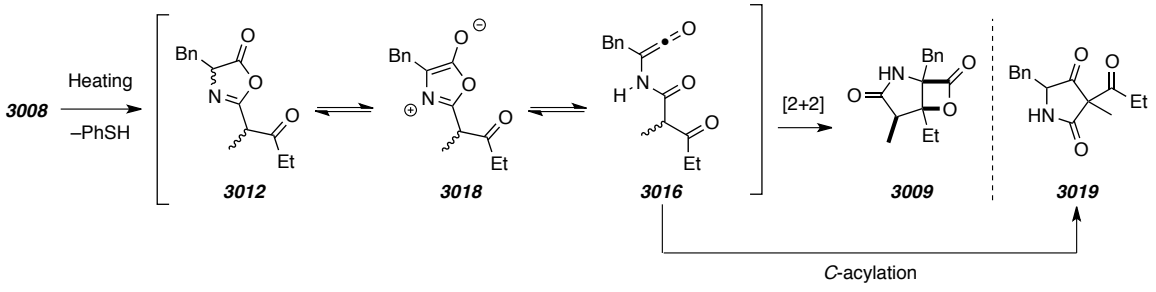

3.1.4. Miscellaneous Strategies for the Activation of Relevant Thioesters

Many soft Lewis acids are known to selectively activate sulfur atoms in the presence of other nucleophilic heteroatoms providing an opportunity to explore the possibility of Lewis acid-promoted entry into our biosynthetic cascade. Precedence exists for thioester activation followed by amido-oxygen acylation to furnish azlactones with silver[74]- and mercury[75]-based Lewis acids. Similarly, we proposed that treating thioester **3008** with Ag(I) might effect its conversion into azlactone **3012** via silver thiolate **3020** (cf. Scheme 40). Ag(I) triflate decomposed thioester **3008** to baseline material by TLC after stirring in CH_2Cl_2 and ^1H NMR analysis after filtration indicated that a complex mixture of products was formed. Repeating the experiment with Ag(I) trifluoroacetate led to slower conversion of the thioester to baseline material by TLC. Interestingly, analysis of the reaction mixture by low-resolution ESI-MS gave an *m*/*z* consistent with the molecular ion of a dethiolated product coordinated to Ag(I). Unfortunately, all attempts to isolate a discreet product were unsuccessful.

Scheme 40 | Proposed mechanism for Ag(I)-mediated activation of thioester **3008** and conversion into azlactone **3012**.

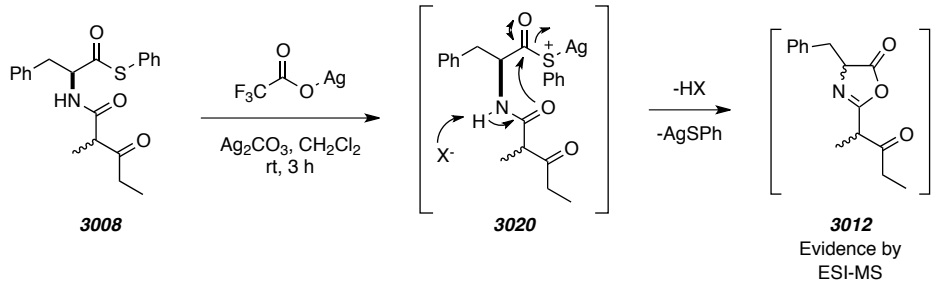

3008 ***3020*** ***3012*** Evidence by ESI-MS

Thioester **3008** was also exposed to a myriad of basic conditions in an attempt to induce intramolecular transacylation to initiate our proposed tautomeric cascade. In general, no reaction occurred in the presence of inorganic bases (e.g., alkali metal acetates, alkoxides, and carbonates) and the use of amine bases (e.g., DBU, DMAP, Et_3N, DIEA, etc.) gave either no reaction or baseline TLC data with complicated ^1H NMR

[74] Haeusler, J. Synthesis of (–)-detoxine D1. *Liebigs Annalen der Chemie* **1986**, *1986*, 114–126.
[75] Homami, S. -S.; Mukerjee, A. K. Reactions of 4-heteromethylene- and 4-heteroethylidene-2-phenyl-2-oxazolin-5-ones with different nucleophiles and related studies. *Indian J. Chem., Sect. B: Org. Chem. Incl. Med. Chem.* **1992**, *31*, 411–414.

spectra. We were unsure if azlactones would be stable to silica gel so the reaction mixtures were also analyzed by low-resolution ESI-MS. In all cases where the starting material was consumed to products with baseline TLC R_f values, ESI-MS data provided no mass evidence corresponding to loss of thiolate and entry into the tautomeric cascade. Collectively, these results provided no promising evidence for the formation of β-lactone **3009**. While progress was made in the preparation of the corresponding azlactone **3012**, no discreet products were isolated. Upon considering these limitations, we ceased to continue probing model thioester **3008**.

3.1.5. Synthesis Studies of β-Hydroxy- and Methyl Ketone-Containing Thioesters

Our inability to observe any promising evidence of β-lactone **3009** from the corresponding thioester (cf. **3008**) led us to consider alternative model substrates. Specifically, we hypothesized that our inability to observe promising conversion of **3008** might be due to the absence of the β-hydroxy and methyl ketone moieties that are present in the natural product. With this in mind, we decided to model the synthesis of key intermediate thioester **3001** and its conversion into **2** with the L-threonine-derived congener, **3033** (Scheme 42). Introduction of the methyl ketone required use of mixed ketene dimer **3025**, which was prepared by concomitant dehydrohalogenation of valeroyl chloride (**3021**) and acetyl chloride (**3022**) to form a mixture of the corresponding ketenes **3025** and **2026** (Scheme 41). The ketene monomers dimerized in the presence of Et_3N by a ketene-ketene [2+2] cycloaddition[76] giving rise to an inseparable mixture of ketene dimers **3025** and **3026**. Ketene dimers resulting from self-dimerization of **3021** and **3022** were removed by fractional vacuum distillation.

Scheme 41 | Preparation of a mixture of ketene heterodimers **3025** and **3026**.

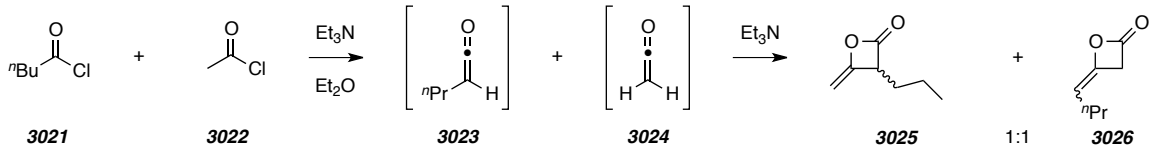

3021 ***3022*** ***3023*** ***3024*** ***3025*** ***3026***

Treatment of L-threonine (**3027**) with a methanolic solution of thionyl chloride afforded L-threonine methyl ester hydrochloride (**3028**) in 99% isolated yield.

[76] Calter, M. A. Catalytic, asymmetric dimerization of methylketene. *J. Org. Chem.* **1996**, *61*, 8006–8007.

Acetoacylation of **3028** with the mixture of ketene dimers **3025** and **3026** gave a separable mixture of β-ketoamido esters **3029** and **3030** in 45% and 39% isolated yield, respectively. Amido ester **3029** was protected at the β-hydroxy position as the triethylsilyl (TES) ether **3031** in 88% isolated yield. Subjecting **3031** to a premixed toluene solution of trimethylaluminum and benzenethiol formed the phenyl thioester **3032**, which was characterized as a clear, colorless oil in 71% isolated yield. Intermediates **3027**-**3031** were stable for months at ambient temperature and open to air, but **3032** desilylated upon standing (12 h) to afford crystalline **3033** in 66% isolated yield from **3031**. Thioester formation was not observed if the C5-hydroxyl group was not protected as the silyl ether.

Scheme 42 | Preparation of thioester **3033** from L-threonine (**3027**).

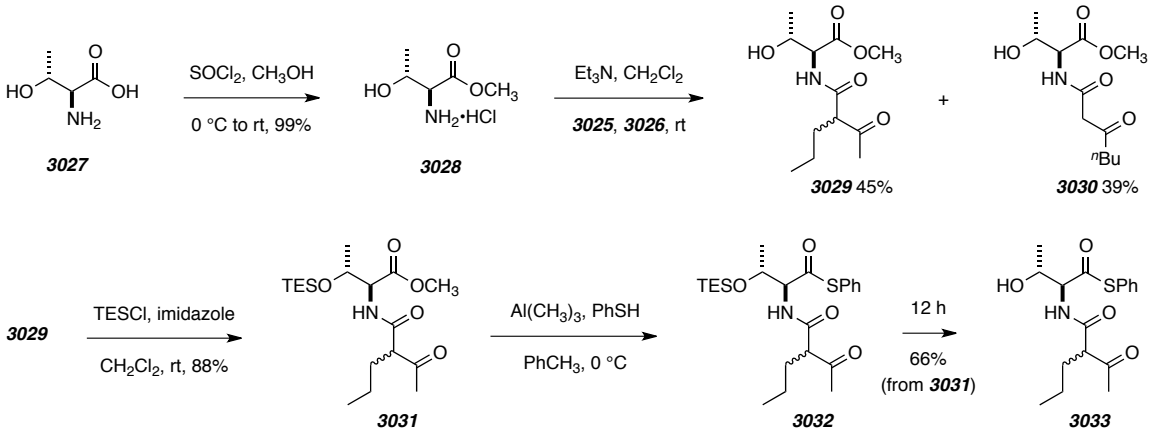

Unfortunately, treating **3033** with reagents that could induce β-lactone formation via the proposed tautomeric cascade led to results similar to those observed with the previous model thioester **3008**. Specifically, mixing **3033** in aqueous solution of pH > 7 led to hydrolysis to the corresponding carboxylic acid. Treating with amine bases led to slow formation of a complex mixture of products, which did not yield any meaningful, isolable compounds. Additionally, adding Ag(I) trifluoroacetate led to slow conversion to base material by TLC analysis. In all cases where apparent decomposition occurred, we carefully analyzed for evidence of thiolate elimination by examining for either benzenethiol or diphenyl disulfide. However, GC/MS indicated that only a trace of each had been formed.

3.2. Synthesis Studies Related to the Preparation of Relevant Azlactones

To increase our understanding of the reactivity of the intermediates in the tautomeric cascade, we sought to develop methodology for the independent synthesis of azlactones derived from *N*-acetyl-α-amido acids (cf. **3034**, Scheme 43). Our concern over the potential instability of azlactones to silica gel encouraged us to explore derivatization strategies or procedures that would allow for efficient isolation from the crude reaction mixtures.

3.2.1. Synthesis of an Azlactone Surrogate: Preparation of 2-Siloxyoxazoles

Takagaki and co-workers[77] have demonstrated that in the presence of Et_3N and a trialkylsilyl chloride, an *in situ*-formed azlactone (cf. **3035**) is converted to the corresponding siloxyoxazole (cf. **3036**). In our hands, *in situ* cyclization of *N*-acetyl-α-amido acid **3034** to azlactone **3035** was accomplished by treating acid **3034** with ethyl chloroformate in the presence of DIEA. Azlactone **3035** intermediate then tautomerized to the corresponding hydroxyoxazole, which upon treatment with chlorosilane gave siloxyoxazole **3036**. The choice of silyl chloride greatly affects the rate of silylation and sensitivity of the resulting siloxyoxazole to hydrolysis. Isolation and purification was found to be easier with the triethylsiloxyoxazole than with the trimethylsiloxyoxazole.

Scheme 43 | Synthesis of siloxyoxazole **3036** from amido acid **3034** via an azlactone intermediate (cf. **3035**).

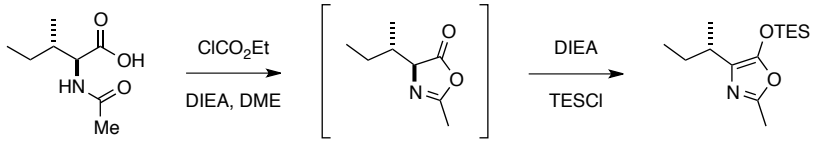

3034 ***3035*** ***3036***

Surprisingly, the reaction is very substrate dependent as the use of different amino acids afforded a mixture of substantially different product mixtures. Cyclization of the L-isoleucine-derived α-amido acid **3034** efficiently provided siloxyoxazole **3036**, whereas substituting a benzyl appendage (**3037**, Scheme 44) led to formation of carbonate **3038** as

[77] Takagaki, H.; Yasuda, N.; Asaoka, M.; Takei, H. Preparation of 5-trimethylsiloxyoxazoles from 2-oxazolin-5-ones and their Diels–Alder reaction: Synthesis of vitamin B_6 derivatives. *Chem. Lett.* **1979**, 183–186.

the major product in low to moderate yields. These results lead us to believe that β-branching (in the case of isoleucine) leads to a sterically hindered transition structure en route to ethyl carbonate generation making siloxyoxazole formation kinetically favored. Steric hindrance about the acylating reagent does not appear to affect the ratio of products because carbonate formation occurred in reproducible yields with methyl, allyl, and isobutyl chloroformates.

Scheme 44 | Unexpected carbonate byproduct in the attempted synthesis of 2-siloxyoxazoles.

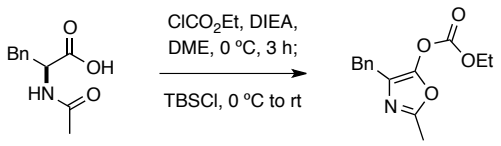

3037 ***3038***

The mechanism for carbonate formation requires two equivalents of alkyl chloroformate for the full transformation to occur. If the chloroformates were to react faster with the hydroxyoxazole than the amido acid, as a result of greater nucleophilicity at the hydroxyl group, complete consumption of ethyl chloroformate by the newly formed azlactones would compete for consumption of the remaining amido acid. The low isolated yields of **3038** could be attributed to incomplete consumption of starting material **3037**. Monitoring the reaction by LC/MS further supports this hypothesis as the conversion of **3037** into **3038** did not progress beyond ca. 40% when 1.0 equivalents of chloroformate is used. Increasing the amount of alkyl chloroformate to 2.0 equivalents increases the isolated yield of **3038** from 12% to 34%, providing further evidence that more than one equivalent of alkyl chloroformate is utilized in the mechanism of alkoxyoxazole formation.

Another approach to improving the yield of the desired siloxyoxazole **3039** (Scheme 45) was to study the effect of varying the reaction mixture incubation time prior to the addition of chlorosilane. To probe this we treated a CH_2Cl_2 solution of Et_3N, **3037**, and methyl chloroformate with TBSCl after varying lengths of incubation times (summarized in Scheme 45). The incubation time had a dramatic effect on the observed

ratio of silyl ether **3039** to carbonate **3040**. Following literature precedent,[77] we first waited three hours after addition of methyl chloroformate before adding TBSCl, but this gave rise to nearly exclusive formation of **3040**. Surprisingly, when the incubation time was halved and TBSCl was added after 1.5 h, the ratio changed to dramatically favor the formation of silyl ether **3039**. Further reducing the incubation time to 0.5 h led to nearly exclusive formation of the desired silyl ether and subsequent experiments allow for isolation of **3039** in high yield. It is interesting to note the subtle change in incubation time leads to a dramatic effect in the ratio of carbonate to silyl ether products. Collectively, the optimization studies suggest that 2-hydrooxazole acylation by chloroformate proceeds at a faster rate than the mixed anhydride formation and cyclization. By optimizing the incubation time before addition of the quenching agent, we were able to prevent unwanted carbonate formation and consumption of the chloroformate reagent. This led to a significant increase in the isolated yield of siloxyoxazole **3040**.

Scheme 45 | Optimization of incubation time prior to TBSCl addition in the chloroformate-mediated synthesis of siloxyoxazole **3039** from *N*-acetyl-L-phenylalanine (**3037**).

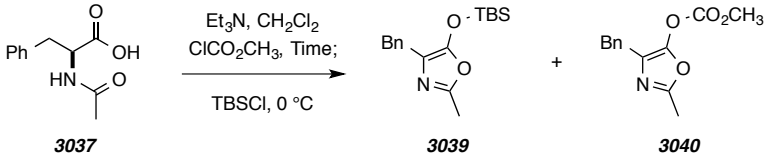

3037 ***3039*** ***3040***

Time Before TBSCl Addition	Ratio ***3039*:*3040*** (GC/MS)
3 h	<1:99
1.5 h	4:1
0.5 h	>99:1 (93% yield of ***3039***)

The methodology was further tested on β-ketoamido acids (cf. **3043**), which were generated in moderate purity by direct acetoacylation of the corresponding α-amino acids in a biphasic mixture under Schotten-Baumenn conditions.[78] Specifically, a mixture of L-phenylalanine (**3041**) and ketene dimer **3042** were added to a biphasic mixture of aqueous NaOH and Et_2O. This methodology allowed for rapid access to β-ketoamido acid **3043**, but with reduced purity. A major contaminant was amide **3044**, and treating the mixture of **3043** and **3044** with ethyl chloroformate and TESCl under the optimized

[78] Bello, C. D.; Filira, F.; Giormani, V.; D'Angeli, F. An investigation of racemisation during the use of acetoacetyl-L-valine in peptide synthesis. *J. Chem. Soc. (C)* **1969**, 350–352.

conditions gave only 5% yield of the desired siloxyoxazole. LC/MS analysis of the crude reaction mixture following scale up indicated that the desired siloxyoxazole was formed as a very minor component and carbonates **3046** and **3047** were the major products.

Scheme 46 | Efforts toward the preparation of acylated siloxyoxazole **3045** from **3043**.

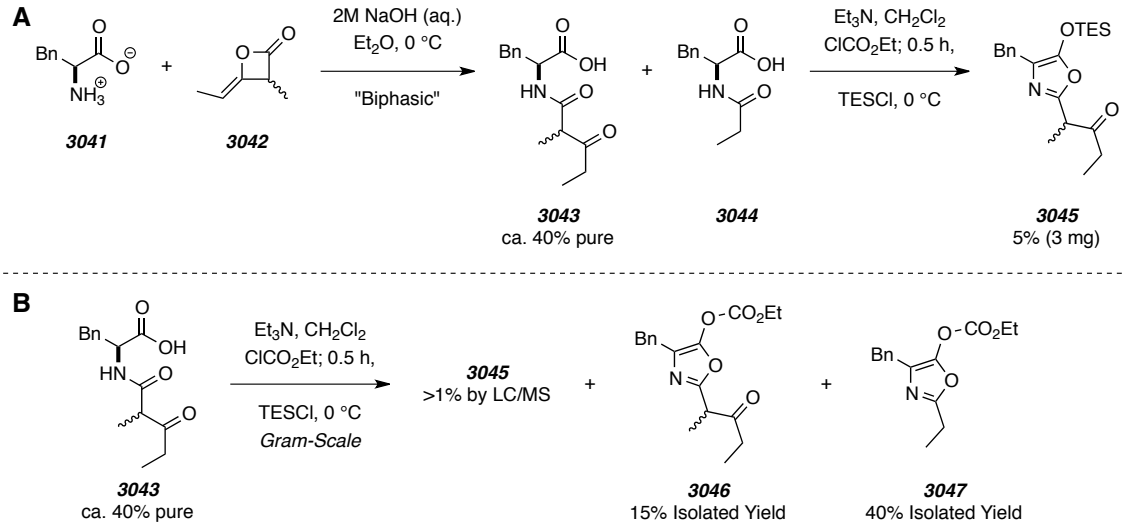

Alternatively, hydrolysis of methyl ester **3048** with LiOH•H_2O gave the β-ketoamido acid **3043** in good yield, and without undesired amide contamination (Scheme 47). Unfortunately, treating **3043** with ethyl chloroformate, followed by TBSCl gave only 2% of the desired silyl ether **3049** along with carbonate **3046** as the major product. In an attempt to prepare a β-hydroxy-containing substrate, we applied the hydrolysis methodology to preparation of acid **3051** from ester **3050**. Specifically, treating ester **3050** with LiOH•H_2O followed by extraction by careful acidification to pH 3 with phosphate buffer gave acid **3051** without observable cleavage of the silyl ether. Unfortunately, the corresponding acid was obtained with reduced purity. In retrospect, we realized that the major contaminant was the *N*-propionyl analogue of **3051**. Unfortunately, application of the chloroformate-mediated cyclization methodology resulted in a complex mixture that included an inseparable mixture of siloxyoxazoles **3052** and **3053**. These results suggest that β-ketoamido acids are not amenable to chloroformate-induced cyclization into the corresponding siloxyoxazole products. This

led us to further consider the direct preparation of azlactones instead of their silylated surrogates.

Scheme 47 | Attempted preparation of acylated siloxyoxzoles by chloroformate-mediated cyclization of the corresponding β-ketoamido acids derived from A) L-phenylalanine and B) threonine.

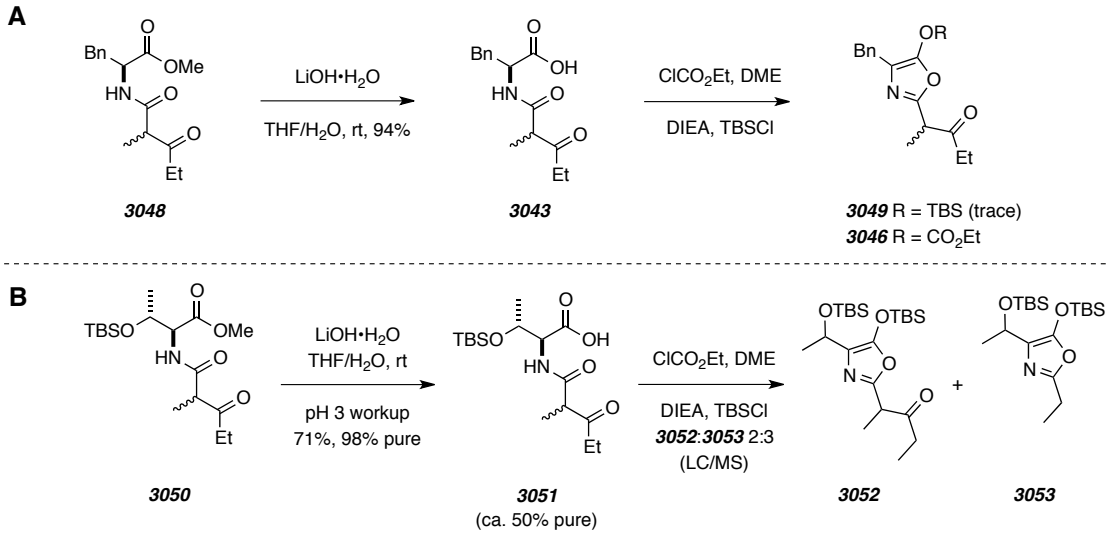

3.2.2. Direct Synthesis of Acylated Azlactones

Our primary goal at this juncture was to optimize conditions for the synthesis of azlactone **3056** from either the corresponding β-ketoamido acid **3054** or thioester **3055** (Scheme 48). Optimization of the reaction conditions would give rise to large amounts of **3056**, which are necessary for us to study its potential entry into a tautomeric cascade analogous to that presented in Scheme 17.

Scheme 48 | Current objectives for modeling the proposed biosynthesis of the salinosporamides.

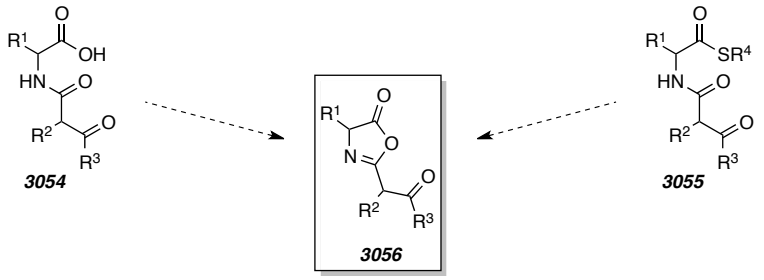

Having identified our primary objective, we sought new methods for azlactone generation and silylation that would be applicable to our β-ketoamido acids. Chen and co-workers[79] demonstrated that treatment of α-amido acids with *N*-(3-dimethylamino propyl)-*N*′-ethylcarbodiimide hydrochloride (EDCI) in CH_2Cl_2 afforded the corresponding azlactones in high purity following aqueous workup. Applying this methodology followed by *in situ* ^{1}H NMR analysis revealed that azlactone **3057** was produced from the corresponding phenylalanine-derived amido acid **3037** (Scheme 49). However, attempts to remove the urea byproduct by aqueous extraction led to hydrolysis of **3057** to give acid **3037**.

Scheme 49 | Carbodiimide-mediated cyclization of *N*-acteyl-L-phenylalanine into azlactone **3057**.

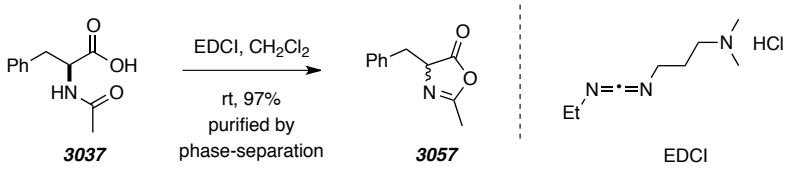

We avoided aqueous workup entirely by treating the reaction mixture with hexanes after 3 h of incubation time to induce phase separation of the urea from the rest of the organic material. Following multiple extractions with 1:1 CH_2Cl_2/hexanes, the combined organic layers were concentrated to afford **3057** in high yield (97%) and purity

[79] Chen, F. M. F.; Kudroda, K.; Benoiton, N. L. A simple preparation of 5-oxo-4,5-dihydro-1,3-oxazoles (oxazolones). *Synthesis* **1979**, 230–232.

(≥ 90%). To better understand the equilibrium between azlactones and 2-hydroxy-oxazoles, we attempted to observe the respective tautomers of **3057** by ^{1}H NMR. The presence of EDCI and the corresponding urea complicated spectral analysis of the crude reaction, but only azlactone **3057** was observed.

Although we identified a protocol for the isolation of azlactones, we were unable to apply it to the approach toward the synthesis of purified samples of acylated azlactones from β-ketoamido acids. For example, early attempts to activate and cyclize β-ketoamido acid **3051** with EDCI gave complex ^{1}H NMR spectra indicating a complex mixture of products despite careful workup and phase separation of known impurities. Despite developing a careful approach to the purification of azlactones, we were able to isolate the products that were completely devoid of impurities from the EDCI reaction. We realized that chromatographic purification was necessary to prepare more complex substrates. We realized that purification of crude reaction mixtures by column chromatography were previously unsuccessful because concentrating the samples for proper loading onto silica gel led to rapid hydrolysis of the desired azlactones. For example, neat samples of purified **3057** completely hydrolyzed in ten minutes under ambient moisture. We assumed that our failure to recover any material was due to hydrolysis to acid **3037** prior to column loading, which did not elute through silica gel with 100% EtOAc.

Despite these attempts, we still had not confirmed if the azlactones themselves were amenable to chromatography. Two-dimensional TLC analysis suggested that azlactone **3057** may decompose on silica gel (i.e. streaked to an R_f = 0.4 in hexanes:EtOAc 7:3), albeit to a lesser extent than we expected considering that azlactones themselves are so sensitive to hydrolysis. With this in mind we proceeded with the EDCI conditions previously described. Instead of working up, the reaction mixture was loaded directly onto a plug of silica gel (EtOAc eluent). This provided a sample of azlactone in 89% yield with excellent purity (Scheme 50). As expected, **3057** could not be stored neat so the sample was diluted in ethanol-free chloroform (usually pre-dried $CDCl_3$).

Scheme 50 | Carbodiimide-mediated cyclization of *N*-acteyl-L-phenylalanine into azlactone **3057** with chromatographic purification.

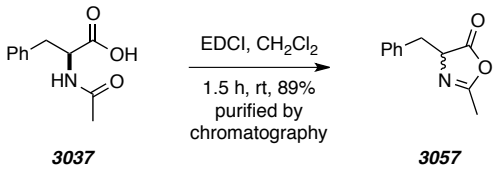

3037 ***3057***

We then turned our attention to applying this approach to the synthesis of acylated azlactones (cf. **3058**, Scheme 51). The first substrate we tested the azlactone preparation protocol on was threonine-derived β-ketoamido acid **3051**. Treating acid **3051** with EDCI and, after 90 minutes, filtering the reaction mixture through a plug of silica gel gave seemingly pure material (cf. one spot by TLC). However, ^{1}H NMR analysis indicated that a complex mixture had formed with very convoluted spectral data. This led us to conclude that the desired cyclization was occurring, but the resulting azlactone was formed as a mixture diastereomers because the starting material was itself prepared as a mixture of inseparable and rapidly equilibrating diastereomers. Furthermore, it is well-known that azlactones exist in equilibrium with their hydroxy oxazoles tautomers (cf. the mechanism for racemization in solid-phase peptide synthesis).[80] This equilibrium leads to an epimerization of the C-2 stereogenic center, thus dehydrative cyclization of **3051** will provide a mixture of four diastereomers of desired azlactone **3058**, in addition to several enolized diastereomers.

Scheme 51 | Attempted preparation of a threonine-derived azlactone **3058**.

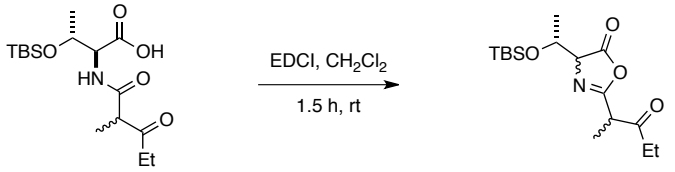

3051 **3058**
Complex Mixture After Chromatography

[80] Bodanszky, M.; Bodanszky, A. Racemization in peptide synthesis. Mechanism-specific models. *Chem. Commun.* **1967**, 591–593.

To simplify the interpretation of the ^{1}H NMR spectra of our model substrate studies, we elected to truncate our target azlactone to the glycine-derived variant **3060** (Scheme 52). The preparation of precursor acid **3059** involved an esterification, acetoacylation, and hydrolysis sequence that was similar to that used prepare acid **3043**. The procedure was modified to include the ketene dimer resulting from butyryl chloride and glycine methyl ester hydrochloride in place of **3005** and **3006**, respectively (see experimental section for details). Using the EDCI-mediated dehydrative cyclization, the desired azlactone **3060** was isolated in moderate yield and excellent purity. Furthermore, the lack of addition a stereogenic centers in the starting material greatly eased the interpretation of the NMR spectral data because **3060** contains only one stereogenic carbon atom.

Scheme 52 | Preparation of a racemic mixture of azlactone **3060** from acid **3059** using carbodiimide-mediated dehydrative cyclization.

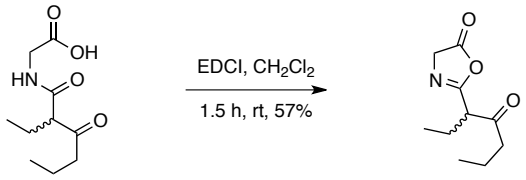

3059 ***3060***

3.3. Investigations Into the Chemical Properties of Acylated Azlactones

With a suitable azlactone model substrate in hand we were prepared to search for conditions that would effect the conversion of azlactone **3060** into the corresponding β-lactone **3061**. However, because our hypothesis relies on the spontaneous generation of **3061** from a thioester precursor, we would predict that **3060** should also readily proceed to product. Our ability to isolate **3060** seems to suggest that acylated azlactones are more stable than we previously thought.

Scheme 53 | The current aim for identifying conditions necessary to effect the conversion of azlactone **3060** into β-lactone **3061.**

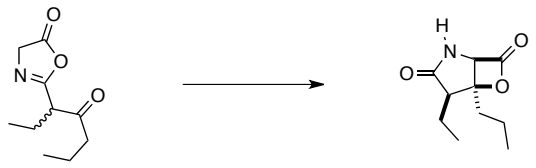

3060 ***3061***

3.3.1. Studies into the Thermal Activation of Acylated Azlactones

The necessary involvement of zwitterionic intermediate Münchnone **3062** would suggest that the rate of azlactone tautomerization and subsequent valence bond isomerism to amidoketene **3063** is strongly solvent dependent. To this end we monitored the fate of **3060** by ^{1}H NMR in a variety of deuterated solvents (see tabular entry in Scheme 54). To summarize, no reaction was observed in all solvents at room temperature over one week. At refluxing temperatures, no reaction was observed in $CDCl_3$ and benzene-d_6. At 120 ºC and in benzene-d_6, peaks corresponding to carboxylic acid **3059** became observable after 24 h. Complete conversion of azlactone **3060** into **3059** was found when either DMSO-d_6 or DMF-d_7 was used as solvent and the reaction heated to 150 ºC for 24 h. These results suggest that the conversion of **3060** into β-lactone **3061** does not proceed under thermal conditions without additional reagents/catalysts. It should be noted that both **3060** and ketene **3063** are sensitive to aqueous hydrolysis, and we were unable to conclude which was involved in the formation of **3059**.

Scheme 54 | Screened conditions for the attempted thermal valence bond isomerism and subsequent [2+2] cylization of azlactone **3060**.

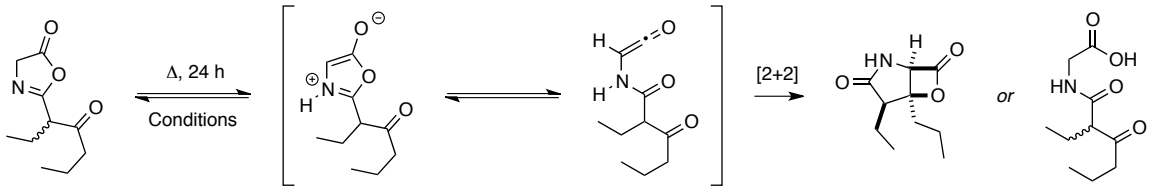

Conditions	Results
$CDCl_3$ (50-80 °C)	NR
C_6D_6 (80 °C)	NR
C_6D_6 (120 °C)	3% Hydrolysis
DMSO-D_6 (150 °C)	Hydrolysis
DMF-D_7 (150 °C)	Hydrolysis

3.3.2. Studies into Activation of Acylated Azlactones by Lewis Acids

Although the aforementioned results clearly indicate that the azlactone is thermally stable, it might also be possible that its nonenzymatic conversion into β-lactone **3061** is promoted by extracellular Lewis acidic metal ions. It is known that certain metal ions are reported to be capable of generating azlactones from thioester precursors.[74,75] Additionally, these same metal ions might also be responsible for promoting tautomerization of the resulting azlactone into a metal-coordinated Münchnone (cf. **3064**, Scheme 55). Tepe has reported that azlactones similar to **3060** react with unsaturated esters via 1,3-dipolar cycloaddition and enol ethers via Alder-ene reaction.[81] Both of these processes likely involve a metallo-Münchnone intermediate similar to **3064**. Toste has also demonstrated that Au(I) is capable of generating Münchnones from azlactones.[82] With this in mind we screened several silver, copper, and lanthanide salts for catalytic activity with azlactone **3060**. Unfortunately, we found that nearly of the all metal salts promoted room temperature hydrolysis to acid **3059**. Sm(III) and Eu(III) were the only exceptions and no conversion of the starting material was observed. Again, we were unable to conclude if Lewis acid-coordinated amidoketene **3065** was involved in the hydrolysis to **3059**.

[81] Mosey, R. A.; Tepe, J. J. New synthetic route to access (+/-) salinosporamide A via an oxazolone-mediated ene-type reaction. *Tetrahedron Lett.* **2009**, *50*, 295–297.
[82] Melhado, A. D.; Luparia, M.; Toste, F. D. Au(I)-catalyzed enantioselective 1,3-dipolar cycloadditions of Münchnones with electron-deficient alkenes. *J. Am. Chem. Soc.* **2007**, *129*, 12638–12639.

Scheme 55 | Screened conditions for the attempted Lewis acid-mediated sequential tautomerization, valence bond isomerism and subsequent [2+2] cylization to convert azlactone **3060** into **3061**.

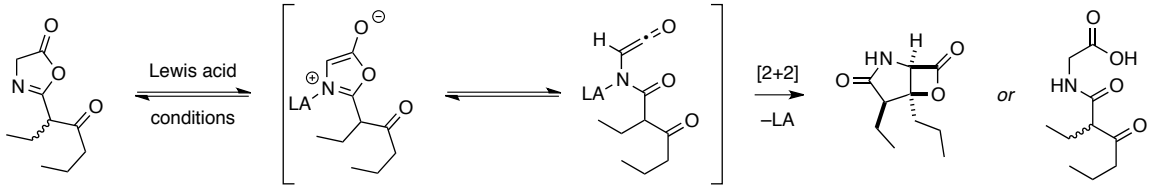

3060 ***3064*** ***3065*** ***3061*** ***3059*** hydrolysis product

Conditions	Results
AgOTf	Slow Hydrolysis
AgTFA	Slow Hydrolysis
AgOAc	Slow Hydrolysis
$Cu(OTf)_2$	Slow Hydrolysis
$Eu(OTf)_3$, 2,6-lutidine	Rapid Hydrolysis
AgOTf, 2,6-lutidine	Rapid Hydrolysis
$Sm(OTf)_3$, 2,6-lutidine	NR

These results had me skeptical about the water content in my reaction mixtures because all of the metal salts were reported to be hydroscopic. However, drying $Cu(OTf)_2$ in a vacuum oven overnight followed by immediately mixing it into a pre-dried solution of $CDCl_3$ did not noticeably change the rate or extent to which **3060** was hydrolyzed to acid **3059**. We then attempted addition of a hindered amine addition to promote Münchnone formation by deprotonating the metal-coordinated azlactone. With this in mind, we repeated the experiments that included AgOTf, Eu(III), and Sm (III) with 2,6-lutidine additive. Except for Sm(III), addition of 2,6-lutidine promoted rapid hydrolysis with full consumption of starting material.

3.3.3. Studies into the Activation of Acylated Azlactones by Brønsted Acids

In lieu of our inability to observe reactivity other than hydrolysis with Lewis acids we turned to use of Brønsted acids. Terada and co-workers reported the use of Brønsted acid-mediated addition of azlactones to 3-vinylindoles.[83] With these results in mind, we screened a series of Brønsted acids for their reaction with azlactone **3060**. Treating **3060** with carboxylic acids and ammonium hydrochloride salts gave hydrolysis to acid **3059**.

[83] Terada, M.; Moriya, K.; Kanomata, K.; Sorimachi, K. Chiral Brønsted acid catalyzed stereoselective addition of azlactones to 3-vinylindoles for facile access to enantioenriched tryptophan derivatives. *Angew. Chem. Int. Ed.* **2011**, *50*, 12586–12590.

Interestingly, ^{1}H NMR analysis of the reaction mixture resulting from treating azlactone **3060** with trifluoromethanesulfonic acid (TfOH) showed only enolization of the exocyclic ketone to presumably give the protonated enol **3066**.

Scheme 56 | Screened conditions for the attempted Brønsted acid-mediated sequential tautomerization, valence bond isomerism and subsequent [2+2] cylization to convert azlactone **3060** into **3061**.

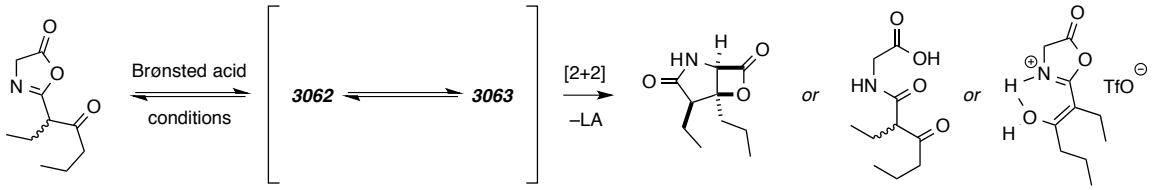

3060 ***3061*** ***3059*** hydrolysis product ***3066*** protonated enol tautomer

Conditions	Results
Py•HCl	Hydrolysis
TFA	Hydrolysis
TfOH	Protonated Enol Tautomer
Py•AcOH	Hydrolysis
Lut.•HCl	Hydrolysis
PPTS	>90% Conv. Byproduct

The mechanism for Brønsted acid-mediated azlactone hydrolysis likely involves protonation of the imine nitrogen (cf. **3067**) and subsequent nucleophilic attack by adventitious water at the lactone carbonyl. However, the TfOH result contradicts this hypothesis because of all of the acids screened, TfOH would be expected to have the highest water content. An alternative mechanistic hypothesis is shown in Scheme 57. We propose that the reaction proceeds by imine protonation followed by nucleophilic addition by carboxylate to form mixed anhydride **3068**. Subsequent reaction of **3068** with a second molecule of carboxylate would cleave the mixed anhydride to give acid **3059** and an anhydride byproduct. In the case of TfOH, the trifluoromethanesulfonate counterion is not nucleophilic enough to ring-open the protonated azlactone, and enolization ensues via intramolecular hydrogen bonding to give **3066**.

Scheme 57 | Proposed mechanism for the carboxylate-mediated azlactone hydrolysis under anhyrous conditions.

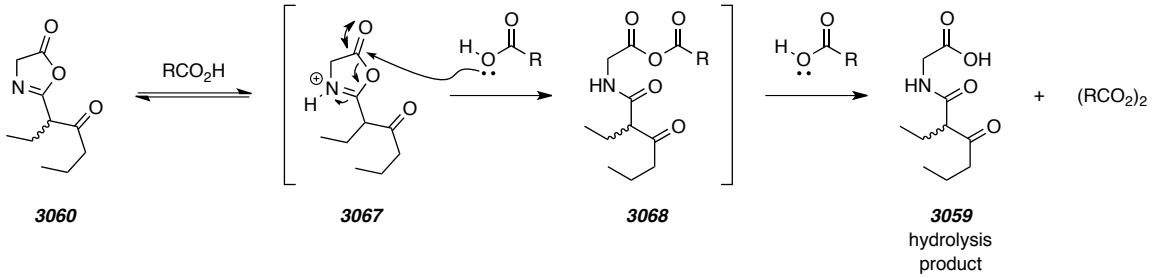

We then studied the reaction of azlactone **3060** with pyridinium *p*-toluenesulfonate (PPTS) because it is a weaker acid with a non-nucleophilic conjugate base. Interestingly, **3060** was readily consumed when treated with 1.5 equivalents of PPTS giving rise to a new set of resonances in the range of 4-5 ppm, which we propose corresponded to a single product. While initially optimistic, we were able rule out the formation of the desired β-lactone **3060** or a structurally related γ-lactam analogue. Still, the cleanliness of the byproduct formation encouraged us to pursue this unexpected outcome a point where we would be confident in assigning a structure. Unfortunately, despite intense effort (e.g., several MPLC purifications, and 2D NMR analysis) we were unable to both isolate the resonances and assign even a tentative structure. It is noteworthy that the outcome was reproduced several times, on various scale, and at increased temperature.

3.4. Modeling the Mechanistic Hypothesis for the Biosynthesis of the Salinosporamides by Direct Generation of β-Ketoamido Ketenes

At this juncture we turned to a different, albeit more important, aspect of the hypothesis–the intramolecular ketene-ketone [2+2] cycloaddition. While studying the azlactone model system was proving to be less and less promising, we began to consider alternative strategies for the generation of amidoketene intermediates. To that end, we prepared Meldrum's acid-derived β-ketoamide **3069**. Heating α-substituted Meldrum's acid is known to generate ketene intermediates with concerted elimination of acetone and

CO_2.[84] We felt that heating Meldrum's acid derivative **3069** would similarly form the desired ketene **3068** without passing through other reactive intermediates.

Scheme 58 | Proposed mechanism for the thermal decomposition of Meldrum's acid derivative **3069** into ketene **3063** and subsequent [2+2] cycloaddition to β-lactone **3061**.

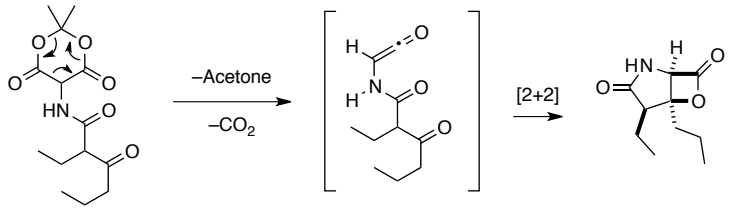

Preparation of **3069** began with preparing the α-oxime of Meldrum's acid with $NaNO_2$, followed by Pd/C-catalyzed hydrogenation and acidification to give the HCl salt of α-amino Meldrum's acid (**3071**). Reaction of **3071** with ketene dimer **3072** gave the desired model substrate in good yield, which was recovered as an orange crystalline solid. Upon measuring the melting point of **3069** we observed the solid began to melt and bubble vigorously at ca. 140 ºC. We hypothesized that the gas that had evolved from the melted product was the released CO_2 and acetone. ^{1}H NMR analysis of the sample after cooling to room temperature and transferring to an NMR tube showed a mixture of starting material and acid **3059**. Additionally, GC/MS analysis produced a single peak with an identical retention time, molecular ion, and fragmentation pattern as the corresponding authentic azlactone **3060**. This suggests that **3069** occurs on the injection port on the GC/MS to the corresponding ketene **3063** which spontaneously cyclizes into the corresponding azlactone **3060**.

[84] Leibfarth, F. A.; Kang, M.; Ham, M.; Kim, J.; Campos, L. M.; Gupta, N.; Moon, B.; Hawker, C. J. A facile route to ketene-functionalized polymers for general materials applications. *Nat. Chem.* **2010**, *2*, 207–212.

Scheme 59 | Synthesis of Meldrum's acid-derived β-ketoamide **3073**.

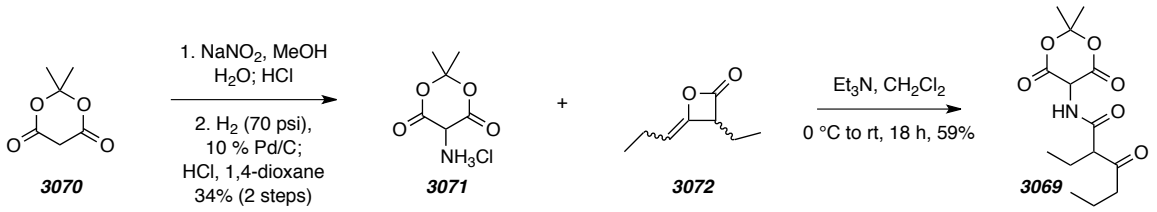

3070 ***3071*** ***3072*** ***3069***

The preliminary observations we made during melting point determination and GC/MS analysis were promising for the generation of ketene **3063** from **3069**. We hypothesized that the carboxylic acid we detected during melting point determination arose from reaction **3063** with ambient moisture. To limit the amount of water present in the system we heated **3069** in benzene-d_6 at 80 ºC for 24 h, but we could only observe ca. 5% conversion to acid **3059** without any detectable production of either **3060** or **3061**. To reproduce the gas evolution we had observed on the melting point apparatus, we heated **3069** neat in an oven-dried NMR tube and under an atmosphere of Ar. Immediately upon submerging the solid into an oil bath at 160 ºC we observed melting and vigorous gas evolution. After five minutes gas evolution ceased and the sample was cooled to ambient temperature and diluted with $CDCl_3$ that was pre-dried with 4Å MS. ^{1}H NMR analysis indicated analysis of the residue showed that complex mixture formed. The major product was acid **3059**, however, we were also able to identify azlactone **3060** with a ratio of **3059**:**3060** ca. 9:1. These studies suggest that thermal decomposition of **3069** gives rise to azlactone **3060**. To account for this we must assume that spontaneous elimination of acetone and CO_2 are occurring, but the resulting ketene is undergoing intramolecular cyclization to generate Münchnone **3062**, which tautomerizes to azlactone **3060**. Reaction of either **3060** or **3063** with adventitious water then gives rise to acid **3059**.

Scheme 60 | Investigations into the thermal activation of Meldrum's acid-derived β-ketoamide **3069**.

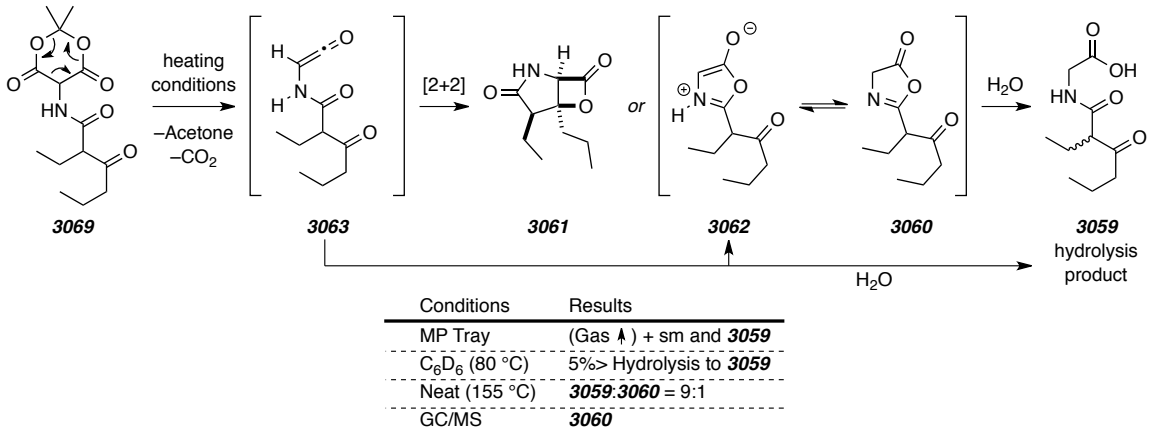

3.5. Computational Analysis of the Energetics of the Proposed Mechanism for the Biosynthesis of the Salinosporamides

Our observation that **3069** spontaneously forms azlactone **3060** when heated neat or subjected to GC/MS analysis led us to consider the energetics of the proposed mechanism depicted in Scheme 17. We turned to DFT computation to determine the energetics of tautomerization of an azlactone to the corresponding amidoketene by way of a Münchnone intermediate. Additionally, we located a transition structure for the uncatalyzed $[2\pi_{s(ketone)} + 2\pi_{a(ketene)}]$ cycloaddition and determined the H and $\Delta H^{\ddagger}$. The "sum of thermal and free enthalpies" was computed for each of the truncated structures **3073**–**3078** were computed using Gaussian 09.[85] The results are summarized in Figure 6, Panel A (enthalpy change for azlactone **3073** to ketene **3075** valence bond isomerization via Münchnone intermediate (**3074**) and B (ΔH and $\Delta H^{\ddagger}$ for the $[2\pi_{s(ketone)} + 2\pi_{a(ketene)}]$

[85] Gaussian 09, Revision **A.1**, Frisch, M. J.; Trucks, G. W.; Schlegel, H. B.; Scuseria, G. E.; Robb, M. A.; Cheeseman, J. R.; Scalmani, G.; Barone, V.; Mennucci, B.; Petersson, G. A.; Nakatsuji, H.; Caricato, M.; Li, X.; Hratchian, H. P.; Izmaylov, A. F.; Bloino, J.; Zheng, G.; Sonnenberg, J. L.; Hada, M.; Ehara, M.; Toyota, K.; Fukuda, R.; Hasegawa, J.; Ishida, M.; Nakajima, T.; Honda, Y.; Kitao, O.; Nakai, H.; Vreven, T.; Montgomery, Jr., J. A.; Peralta, J. E.; Ogliaro, F.; Bearpark, M.; Heyd, J. J.; Brothers, E.; Kudin, K. N.; Staroverov, V. N.; Kobayashi, R.; Normand, J.; Raghavachari, K.; Rendell, A.; Burant, J. C.; Iyengar, S. S.; Tomasi, J.; Cossi, M.; Rega, N.; Millam, J. M.; Klene, M.; Knox, J. E.; Cross, J. B.; Bakken, V.; Adamo, C.; Jaramillo, J.; Gomperts, R.; Stratmann, R. E.; Yazyev, O.; Austin, A. J.; Cammi, R.; Pomelli, C.; Ochterski, J. W.; Martin, R. L.; Morokuma, K.; Zakrzewski, V. G.; Voth, G. A.; Salvador, P.; Dannenberg, J. J.; Dapprich, S.; Daniels, A. D.; Farkas, Ö.; Foresman, J. B.; Ortiz, J. V.; Cioslowski, J.; Fox, D. J. Gaussian, Inc., Wallingford CT, 2009.

cycloaddition of ketene **3076** to β-lactone **3078** via transition structure **3077**). The energies shown in Panel A suggest that it is energetically uphill to proceed from an azlactone to a ketene via a Münchnone intermediate. While this assertion is not unexpected, the observation that it is ca. 20 kcal•mol^{-1} uphill to the reactive intermediates was surprising. Additionally, the results presented in Panel B indicate that activation barrier for the ketene ketone [2+2] cycloaddition is also greater than 20 kcal•mol^{-1}. This data is consistent with the experimental results presented in Section 3.4 where direct generation of a ketene like **3076** is unable to form the corresponding β-lactone. Instead the intermediate cyclizes via the amido oxygen atom to form an azlactone like **3073** in what is likely a low barrier event.

Figure 6 | Summary of computation studies performed on structures relevant to the proposed biosynthesis of the salinosporamides.

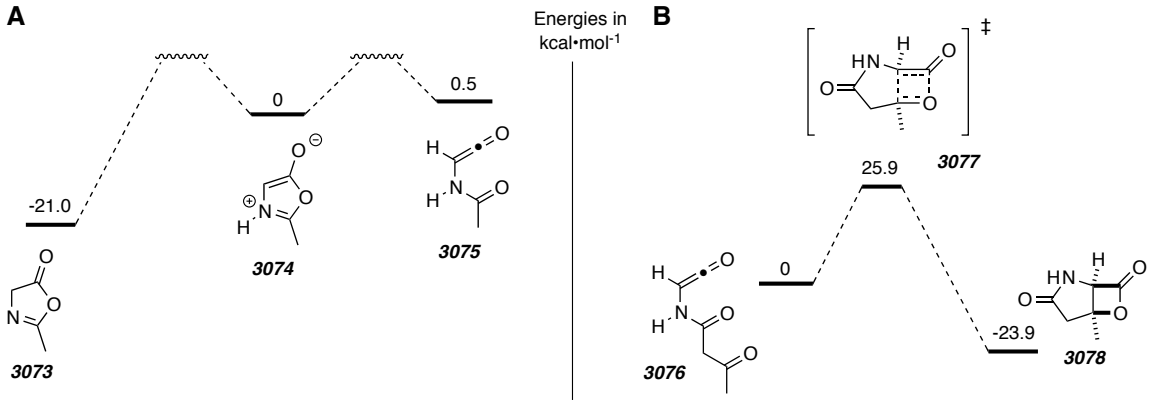

3.6. Concluding Remarks

Unfortunately, the results presented in Chapter 3 seem to exclude the possibility that the biosynthesis of the salinosporamides proceeds via a spontaneous and uncatalyzed [2+2] cycloaddition of an amido ketene intermediate. Still, much was learned in the way of the preparation thioesters, azlactones, and analogues thereof. Additionally, insight was gained into the chemical properties of these reactive functional groups to a variety of conditions. Chapter 4 presents more successful approaches to studying processes related to the biosynthesis of the salinosporamides. Those discoveries would not have been possible without the foundation that was gained from the studies presented in Chapter 3.

Chapter 4. A Biomimetic Approach to the Synthesis of the Salinosporamides

4.1. Revisiting the Proposed Biosynthesis of the Salinosporamides

In lieu of our inability to identify conditions necessary to produce a β-lactone related to **1** from an amido thioester, siloxyoxazole, acylated azlactone, or a Meldrum's acid-derived β-ketoamide, we began to consider an alternative hypothesis for the biosynthetic conversion of a thioester precursor (cf. **4001**) into **1** (Scheme 61). The biosynthetic hypothesis put forth by Moore,[28a] involves an enzyme-catalyzed intramolecular aldol reaction of **4001** to form γ-lactam **4002**. Subsequent esterase-catalyzed lactonization would then deliver the natural product. The aldol reaction to convert **4001** into **4002** is likely to be a challenging transformation to carry out in the laboratory because the β-hydroxy thioester starting material is already the product of a net aldol reaction (i.e. an aldolate). The key reaction would then require the quaternization at C-2 by an aldol reaction of an aldolate. While such processes have been reported,[86,87] rarely do they generate quaternary centers due to the inherent difficulty of enolizing the α-substituted β-hydroxy-carbonyl starting materials.

Scheme 61 | Relevant structures to the biosynthesis of salinosporamide A as proposed by Moore.[28a]

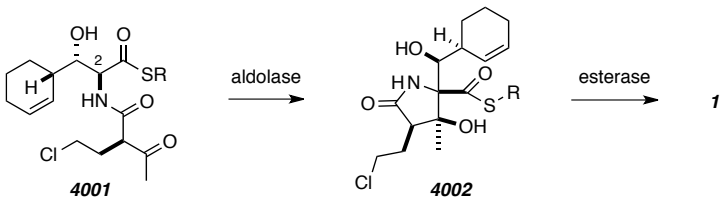

[86] Baitinger, I.; Mayer, P.; Trauner, D. Toward the total synthesis of maoecrystal V: Establishment of contiguous quaternary stereocenters. *Org. Lett.* **2010**, *12*, 5656–5659.
[87] Shimoda, Y.; Kotani, S.; Sugiura, M.; Nakajima, M. Enantioselective double aldol reaction catalyzed by chiral phosphine oxide. *Chem. Eur. J.* **2011**, *17*, 7992–7995.

4.2. An Approach to the Biomimetic Synthesis of the Salinosporamides via a Malonic Acid Half Thioester

To carryout Moore's proposed biosynthesis of the salinosporamides in the laboratory thioester **4001** would be deprotonated at C-2 to form enolate **4003** (Scheme 62). Intramolecular aldol reaction with the β-ketone would form lactam **4004**. However, studying a similar thioester under a variety basic conditions has led to either no reaction or unpromising mixtures of products (cf. **3008**, Section 3.1.3). Additionally, it is likely that an additional complication is presented by our proposed biosynthetic intermediate. Base-mediated enolization at C-2 is likely thwarted by the more acidic α-hydrogen atom of the 1,3-dicarbonyl moiety (i.e. C-2'). Deprotonation at C-2' in **4001** generates either enolate **4005** or the enol conjugate acid. Enolization of the β-ketone in **4005** (or the corresponding enol) precludes an intramolecular aldol reaction to form desired lactam **4004**. Additionally, in our original hypothesis, we proposed that an enolate like **4005** might induce azlactone formation (cf. **4006**). Such a transacylation would be problematic considering our previous studies of azlactones, similar to **4006**, under basic conditions were unproductive for the formation of β-lactone products (cf. Scheme 56, Section 3.3.2).

Scheme 62 | Two potential enolizaiton pathways for the thioester biosynthetic precursor to natural product **1**. Depronation at C-2 affords the natural product via Moore's[28a] proposed biosynthesis, whereas deprotonation at C-2' might give azlactone **4006**.

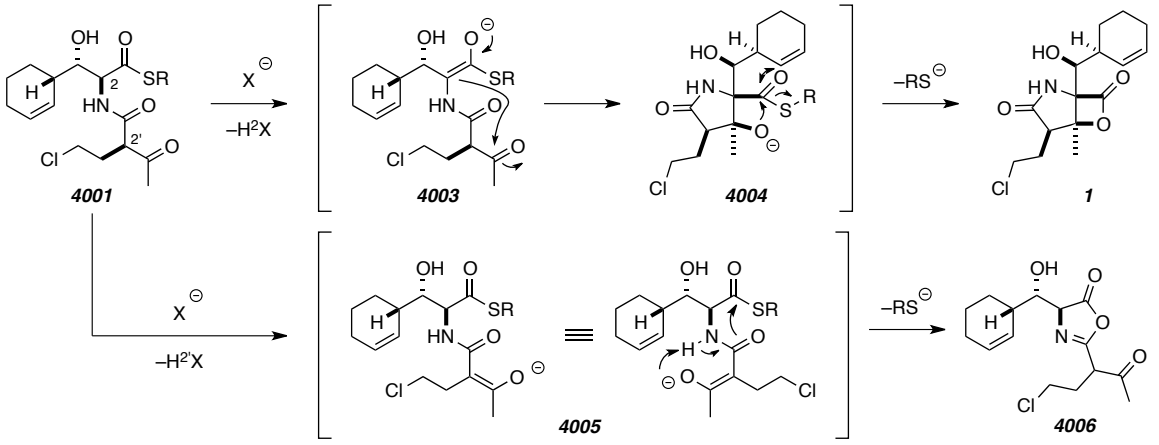

An alternative approach for the generation of a thioester enolate involves direct anion generation by decarboxylation of a malonic acid half thioester (MAHT, cf. **4007** and **4008**, Scheme 63). Such ester enolate equivalents are proposed to be involved in the biosynthesis of fatty acids and polyketides [(e.g., from methylmalonyl CoA (**4007**)].[88] Shair and co-workers[89] have shown that MAHT **4008** will undergo Cu(II)-catalyzed decarboxylation to directly generate thioester enolate **4010**, which is capable of reacting with aldehydes (cf. **4014**) intermolecularly via a Cu(II)-catalyzed aldol reaction. In the presence of C_2-symmetric chiral bisoxazoline ligands (cf. **4015**), the authors were able to effect an enantioselective aldol reaction. The authors also reported that analysis of the reaction kinetics and extensive deuterium labeling studies supports a mechanism involving initial deprotonation of a MAHT-Cu(II) complex (cf. **4009**) to form enolate **4010**. Reaction of **4010** with an aldehyde then generates Cu(II)-stabilized aldolate **4011**. Decarboxylation of **4011** gives another thioester enolate **4012**, which is protonated to give desired β-hydroxy thioester **4013**.

Scheme 63 | Proposed mechanism for the Cu(II)/**4015** complex-catalyzed decarboxylative aldol reaction of MAHT **4008** with an aldehyde (adapted from ref 89b).

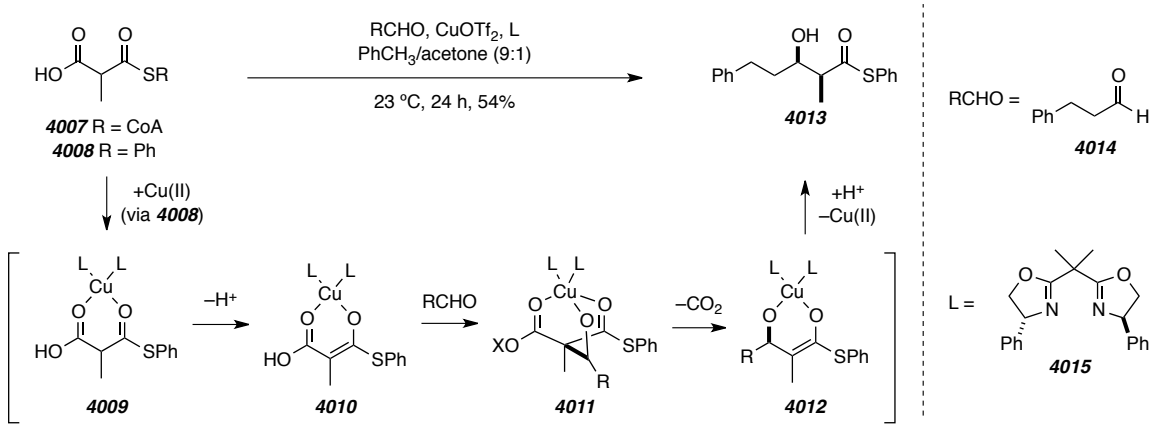

[88] a) Staunton, J.; Weissman, K. J. Polyketide biosynthesis: A millennium review. *Nat. Prod. Rep.* **2001**, *18*, 380–416. b) Hill, A. M. The biosynthesis, molecular genetics and enzymology of the polyketide-derived metabolites. *Nat. Prod. Rep.* **2006**, *23*, 256–320.

[89] a) Lalic, G.; Aloise, A. D.; Shair, M. D. An exceptionally mild catalytic thioester aldol reaction inspired by polyketide biosynthesis. *J. Am. Chem. Soc.* **2003**, *125*, 2852–2853. b) Fortner, K. C.; Shair, M. D. Stereoelectronic effects dictate mechanistic dichotomy between Cu(II)-catalyzed and enzyme-catalyzed reactions of malonic acid half thioesters. *J. Am. Chem. Soc.* **2007**, *129*, 1032–1033.

Shair's approach to thioester enolate generation was attractive because we could directly achieve thioester enolate formation under weakly basic conditions. Our hope was to form the desired thioester enolate, which would likely react intramolecularly to give the desired aldolate. While a model substrate to test this hypothesis could be α-amidomalonate **4016** (Scheme 64), we were skeptical in our abilities to apply the methodology with the α,α-disubstituted variant. However, we realized that the β-hydroxy enolate (cf. **4012**) in the catalytic cycle proposed by Shair[89b] could undergo a subsequent aldol reaction to give rise to a double aldol product. With this in mind, a substrate capable of modeling the synthesis of lactam precursor to **1** would then be **4017**.

Scheme 64 | Proposed mechanism for the conversion of a β-ketoamido MAHT (cf. **4017**) into the bicyclic core of the salinosporamides (cf. **4019**) via lactam precursor (cf. **4018**).

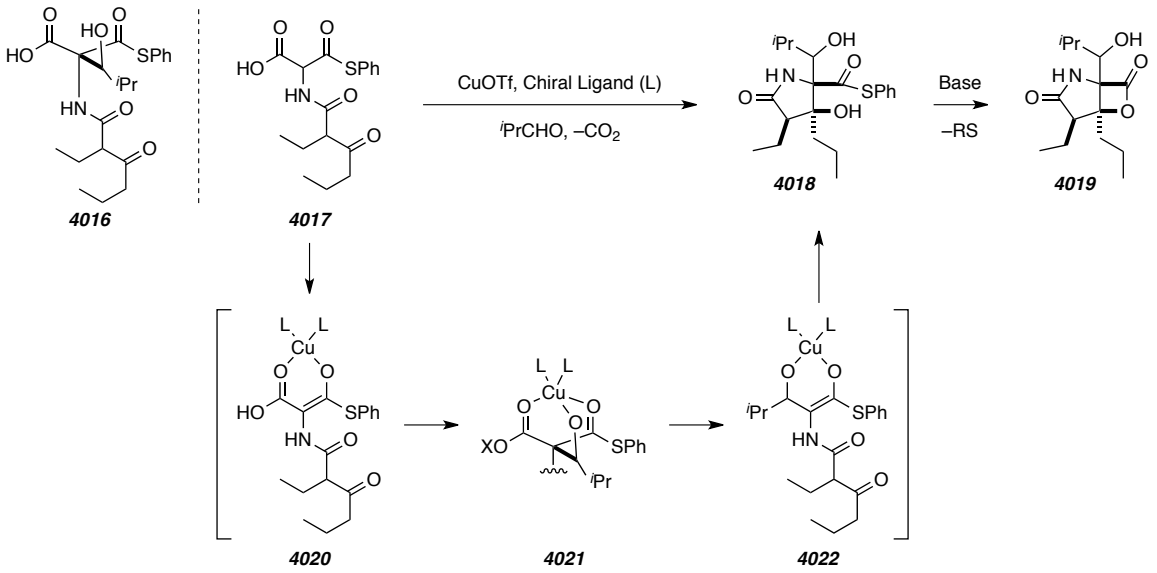

Treating MAHT **4017** with Cu(II) under weakly basic conditions would generate thioester enolate **4020**. Enolate **4020** could react via intramolecular aldol reaction either intramolecularly with the β-ketone or intermolecularly with an aldehyde. For the sake of argument, we have proposed an initial reaction with an excess of isobutyraldehyde to form aldolate **4021**. Isobutyraldehyde was chosen because the isopropyl group is reminiscent of the side chain in antiprotealide **2** (Section 3.1.1, Scheme 35).

Decarboxylation of aldolate **4021** would then generate β-hydroxy thioester enolate **4022**. Intramolecular aldol reaction of **4022** could then give rise to lactam **4018**. Isolation of **4018** might be a challenge because the mildly basic conditions might promote lactonization to the desired β-lactone **4019**. We were certainly aware that the proposed mechanism was bold, but we felt that the rewards for application of this biomimetic process to the synthesis of the salinosporamide core substantially outweighed the risk of failure. Additionally, if the rate of the intramolecular aldol reaction was significantly faster than the intermolecular aldol reaction isobutyraldehyde, decarboxylation of that aldolate would generate another thioester enolate capable of subsequent aldol reaction.

A retrosynthetic plan for the synthesis of MAHT model substrate **4017** is presented in Scheme 65. The carboxylic acid of **4017** would be revealed last by de-*t*-butylation of the corresponding malonate monothioester, **4023**. The thioester could be introduced by standard conditions from the corresponding malonic acid half oxy ester (MAHO), **4024**, which would be available by hydrolysis of the methyl ester of mixed malonate **4025**. The acetoacetyl moiety would be introduced by treating α-aminomalonate **4026** with ketene dimer **3072**. Standard malonate amination conditions could give **4026** from malonate **4027**.

Scheme 65 | Retrosynthetic analysis for the preparation of β-ketoamido MAHT **4017**.

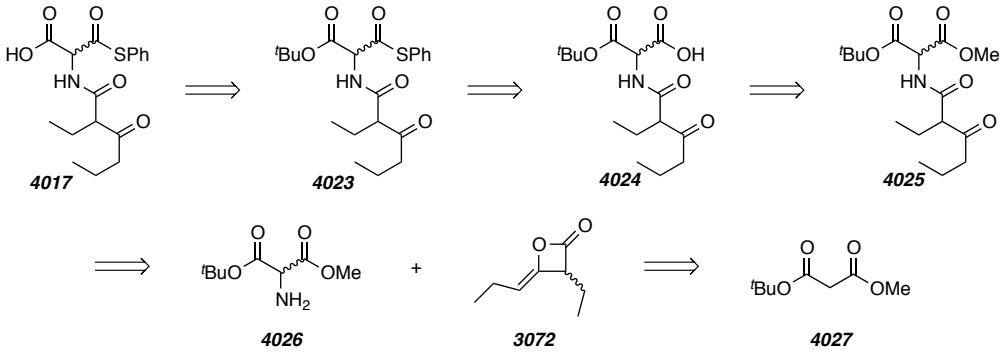

The synthesis of **4017** began with the straightforward preparation of *t*-butyl methyl malonate (**4027**) by following from the known procedure esterification of acid

4028 with methyl chloroformate (Scheme 66).[90] The conventional method[91] for α-amination of malonates involves reacting the malonate with $NaNO_2$ to give an oxime intermediate (cf. **4029**), which can be hydrogenated to the amine in the presence of Pd(0). However, both of these transformations were problematic when applied to malonate **4027**. Slow addition of $NaNO_2$ to **4027** with careful control of reaction temperature (ca. 10 ºC) led to inefficient formation of the desired oxime **4029** (ca. 10% conversion, 95% yield BRSM). Alternatively, deprotonation with NaH and subsequent treatment with isoamyl nitrite gave **4029** in good yield and as a 1:1 mixture of *E*/*Z* isomers. Palladium-catalyzed hydrogenation of **4029** was completely unsuccessful up to 100 psi in a Fischer-Porter reactor. After screening several conditions we found that carefully adding Zinc dust to solution of **4029** in AcOH and heating to 60 ºC gave the desired amine **4026** after filtration, albeit in very low yields.

Scheme 66 | Preparation of α-aminomalonate **4026**.

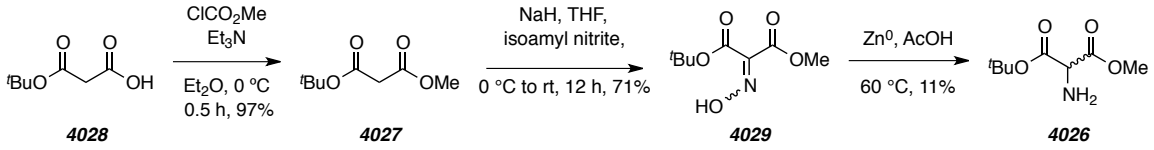

Despite the inefficient synthetic route to **4026**, we were able to prepare enough of the desired aminomalonate to push forward in the synthetic route. Acetoacylation of **4026** by reaction with ketene-dimer **3072** gave desired amidomalonate **4030** (Scheme 67). We then attempted a $Al(CH_3)_3$-mediated transesterification of **4030** with benzenethiol to give thioester **4032** directly, but no reaction was detected. However, selective hydrolysis of the methyl ester of **4030** was straightforward and gave *t*-butyl MAHO **4031**. Thioesterification was achieved by treating acid **4031** with EDCI to give malonate monothioester **4032**. From our previous studies (cf. Section 3.3) we proposed that thioesterification involved generation of an azlactone intermediate, which in the presence

[90] Smith, A. M. R.; Rzepa, H. S.; White, A. J. P.; Billen, D.; Hii, K. K. M. Delineating origins of stereocontrol in asymmetric Pd-catalyzed α-hydroxylation of 1,3-ketoesters. *J. Org. Chem.* **2010**, *75*, 3085–3096.
[91] Hartung, W. H.; Beaujon, J. H. R.; Cocolas, G. *Org. Syn.* **1960**, *40*, 24–26.

of excess PhSH ring-opened to give thioester **4032**. We attempted the acid-mediated de-*t*-butylation of **4032** by addition of TFA, however, a mixture of desired MAHT **4017** in addition to other acid and thioester impurities resulting from decarboxylation and/or thioester hydrolysis. Due to our limited supply of malonate monothioester **4032** we chose to instead focus on studying the more easily accessible MAHO congener **4037** (Scheme 68).

Scheme 67 | Preparation of MAHT **4017** from α-aminomalonate **4026**.

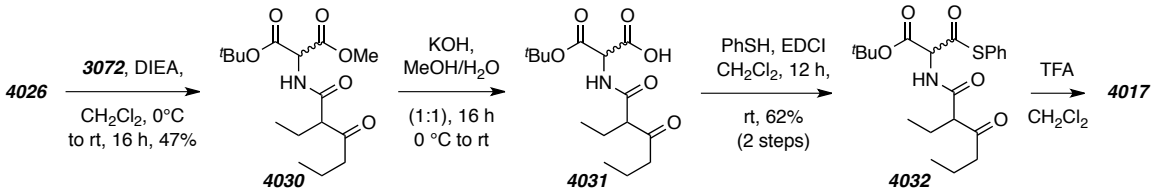

The synthesis of MAHO model substrate **4037** was much more straightforward. Diethyl aminomalonate hydrochloride (**4035**) was prepared following the known procedure[91] by treating diethyl malonate (**4033**) with $NaNO_2$ to give oxime **4034**, followed by hydrogenation (90 psi), and acidification to give **4035**. Reaction of **4035** with ketene dimer **3072** gave β-ketoamido **4036**. Monohydrolysis was achieved by treating **4036** with KOH in 1:1 EtOH/H_2O, which gave desired MAHO **4037**.

Scheme 68 | Synthesis of MAHO **4037**.

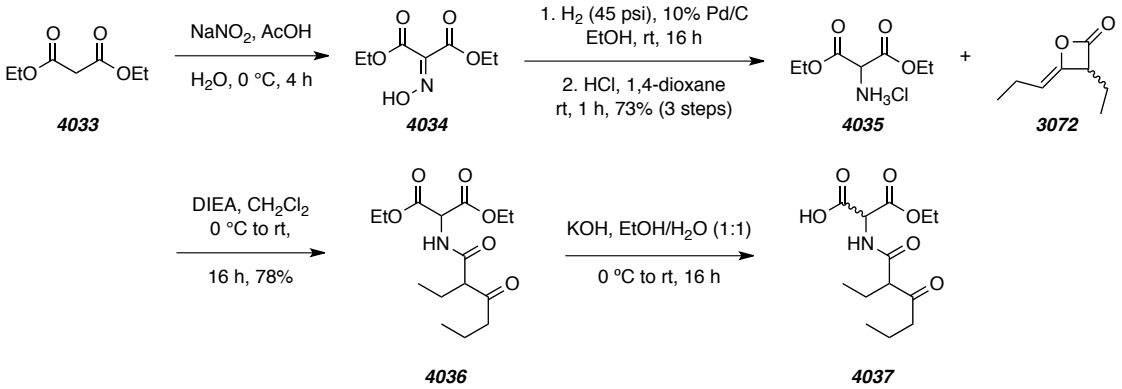

Unfortunately, treating a mixture of **4037** and isobutyraldehyde with myriad acids and bases gave no evidence for either inter- or intramolecular aldol reaction. Removing

isobutyraldehyde gave similar results in all cases. This led us to propose that decarboxylation was occurring to form an enolate, but subsequent protonation was neutralizing the intermediate. The source of proton could be either the α-hydrogen atom of the 1,3-dicarbonyl moiety or the hydroxy group of the enol tautomer. Additionally, the reaction conditions that were attempted likely promoted enolization of the β-ketone to an intermediate that is unable to engage in the necessary intramolecular aldol reaction. At this juncture we had decided to set aside these endeavors in order to study Romo's conditions for the synthesis of structures related to **1**. The insight gained from those studies would be useful in the successful implementation of the mechanism proposed in Scheme 64.

4.3. Studies of Romo's Conditions for the Synthesis of Fused γ-Lactams-β-Lactones

In order to ensure that we had not overlooked the formation of β-lactone **3061** from any of the previously attempted model systems, we choose to prepare an authentic sample of **3061** by the method of Romo and co-workers.[40] With an authentic sample in hand, we would be able detect the presence of **3061** by ^{1}H NMR and TLC analysis of crude reaction mixtures. Additionally, β-lactones are thermally unstable toward decarboxylation, therefore GC/MS analysis of **3061** would likely provide a molecular ion equivalent to the molecular weight of enamide **4038**. Still, GC/MS analysis of the authentic material would provide us with a characteristic retention fragmentation pattern. A similar study would be performed using LC/MS because β-lactones similar to **3061** are known to be prone to methanolysis or hydrolysis, therefore LC/MS analysis of **3061** would likely form acid **3059** or ester **4039**.[21,92]

[92] Hogan, P. C.; Corey, E. J. Proteasome inhibition by a totally synthetic β-lactam related to salinosporamide A and omuralide. *J. Am. Chem. Soc.* **2005**, *127*, 15386–15387.

Scheme 69 | Potential decomposition pathways of β-lactone **3061** under conditions for either GC/MS or LC/MS analysis.

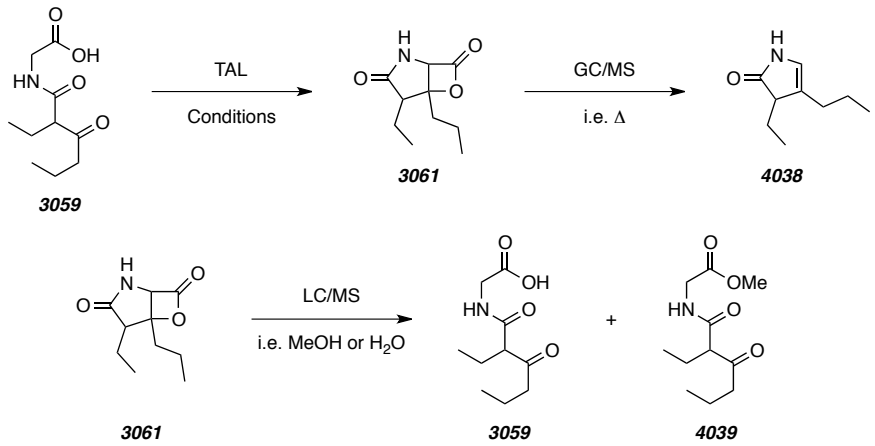

To prepare **3061** we chose to follow conditions from one of Romo's earlier reports in which substrates similar to those we had already prepared, (e.g., acid **4040**) were studied.[42] These conditions involved treating a mixture of the carboxylic acid with 4-PPY, DIEA, and *N*-propyl-2-bromopyridinium triflate (an acid-activating reagent derived from Mukaiyama's reagent).[93,94] Other than our choice to use an alternative pyridinium reagent (cf. **4041**, available from treating 2-bromopyridine with trimethyloxonium tetrafluoroborate) we followed the procedure developed by Romo. Monitoring of the reaction mixture by GC/MS indicated that a complex mixture of products was forming. The crude reaction mixture gave poor mass balance with trace amounts of starting material **3059** as the only identifiable product by ^{1}H NMR. Even after several attempts, none of the desired β-lactone **3061** was recovered.

[93] The most recent report by Romo and co-workers on the total synthesis (–)-**1** (summarized in Section 1.6.2) used MsCl as the acid-activating agent (see ref 40). These studies were reported after we performed the experiments presented in Section 4.1.2.

[94] The authors noted that the commercially available reagent (i.e. 2-chloro-1-methylpyridinium iodide) led to reduced yields, which they attribute to the nucleophilic iodide counterion.

Scheme 70 | Attempted preparation of β-lactone **3061** by the TAL methodology previously described by Romo.[42]

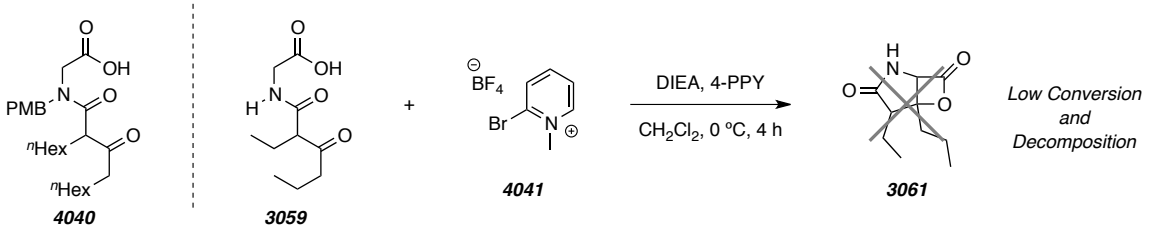

Our inability to synthesize **3061** was unexpected considering the only deviations between our attempt and the report by Romo was the absence of an *N*-PMB protecting group and the substitution of the acid-activating reagent. We initially thought that Romo had chosen to install the *N*-PMB group to enhance the stereoselectivity in the addition of Corey's cyclohexenyl zinc regent to their late-stage aldehyde intermediate (cf. reaction of **1066** with **1019** to give **1067**, see Scheme 12).[95] However, this being the only major difference between Romo's substrate and **3059** led us to consider a deeper role for the *N*-alkyl moiety, namely one that involves its use as a protecting group against azlactone formation and/or ketone enolization.

Romo's conditions involve acid-activation of **3059** or **4042** with **4041** in the presence of an amine (Scheme 71). Under these conditions a ketene intermediate (cf. **4044**) could be generated from activated acid intermediate **4043**. We have shown evidence that ketenes spontaneously isomerize to azlactones (presented throughout Section 3.3). In the case of acid **3059**, acid activation and elimination would form amidoketene **3060**. The ketene-azlactone isomerization mechanism likely involves amidoketene cyclization to form a Münchnone intermediate, which could undergo a net [1,5] hydrogen shift to generate **3060**. Substitution of the *N*-H with *N*-alkyl would preclude azlactone formation and reaction of corresponding ketene **4044** (R = PMB) with 4-PPY would form ammonium enolate **4055** (R = PMB). TAL of intermediate **4055** would then give rise to β-lactone **4056**. Without the *N*-alkyl moiety, application of

[95] Danishefsky and co-workers also noted that a similar reaction proceeded with poor stereoselectivity when adding to lactams lacking *N*-PMB functionalization (see Section 1.4.2).

Romo's methodology to **3059** likely generates **3060**, which reforms **3059** by direct hydrolysis or via ring opening with 4-PPY followed by hydrolysis of the activated intermediate. Washing the resulting reaction mixture with aqueous solutions during workup likely hydrolyzed the electrophilic intermediates to regenerate **3059**.

Scheme 71 | Potential reaction pathways for acids **3059** and **4043** under TAL conditions.

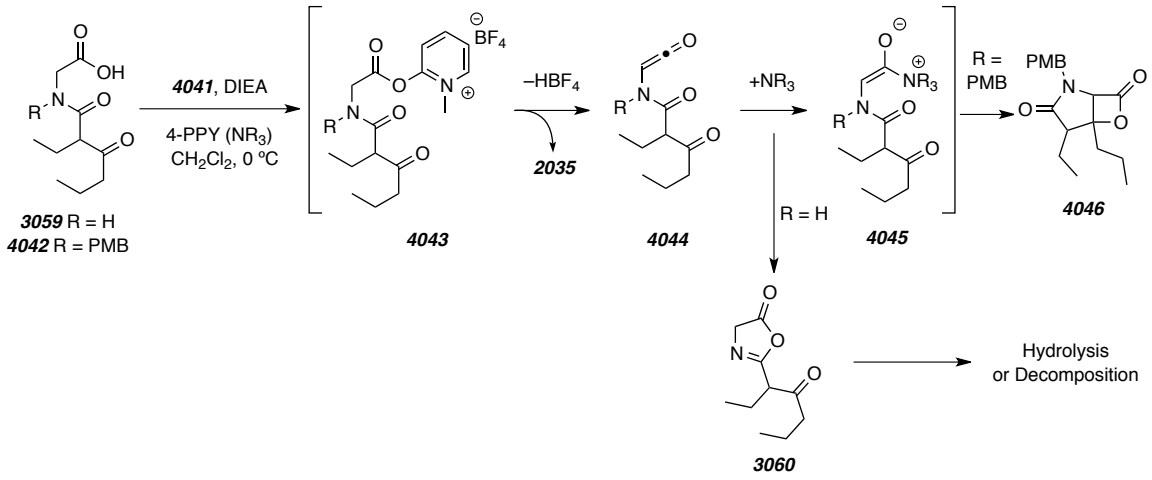

Romo and co-workers demonstrated that deprotonation of relevant tertiary β-keto amides (e.g., **4042**) is sluggish.[40] This suggests that enolization of these substrates introduces substantial $A_{1,3}$-strain, which destabilizes the corresponding enolates and enols.[41] The authors were able to take advantage of this and develop a synthesis of enantioenriched (–)-**1** because the configuration of the C-2' stereogenic center was stable. We predicted that for substrates lacking the *N*-PMB group (cf. **3059**), in addition to azlactone formation, reaction with DIEA led to deprotonation at the more acidic C-2' position of the secondary β-ketoamide instead of C-2 to give an enolate necessary for intramolecular aldol reaction. Enolization at C-2' precludes the opportunity for the productive aldol reaction because the reacting carbonyl is no longer electrophilic. This provides an additional explanation for our inability to observe the formation of β-lactones under the conditions described Romo.

To test the hypothesis that the tertiary amide is necessary for the success of Romo's conditions, we prepared the *N*-PMB amide congener of our previous substrate, **4042**. Treating *N*-PMB amino ester **4047** with ketene dimer **3072** and hydrolyzing the

resulting amido methyl ester **4048** with LiOH gave desired acid **4042**. Subjecting **4042** to the same conditions (i.e. pyridinium **4041**, DIEA, and 4-PPY in CH_2Cl_2) gave an *equimolar* mixture of the desired β-lactone **4049** and 2-*epi*-**4049** in good crude mass recovery. This experiment provided support for the hypothesis we previously proposed and provided us with authentic samples of **4049** and 2-*epi*-**4049**, but, more importantly, demonstrated that *N*-PMB functionalization was necessary for Romo's tandem aldol-lactonization to take place.

Scheme 72 | Synthesis of **4042** and application of Romo's TAL for the preparation of β-lactones **4049** and 2-*epi*-**4049**. and biscyclization of acid **4042**

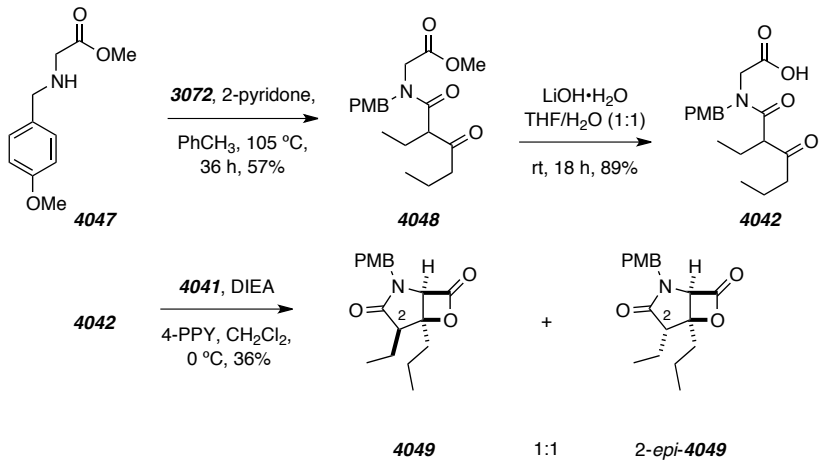

4.4. Studies of the Reactivity of Relevant *N*-PMB Amido Thioesters

Having confirmed that *N*-PMB functionalization was necessary to effect tandem aldol-lactonization led us to study *N*-alkylated analogues of substrates we had previously prepared (e.g. **4050**). We hypothesized that *N*-alkyl functionalization is necessary to convert the thioester-containing biosynthetic precursor of **1** (or antiprotealide **2**) to the corresponding fused γ-lactam-β-lactone-containing natural product. Mechanistically, we proposed that base-mediated elimination of benzenethiol from S-phenyl thioester **4050** would generate an equilibrating mixture of Münchnone **4051** and amido ketene **4052**. The *N*-PMB group would prevent **4051** from isomerizing to an azlactone. Instead **4051**

could revert back to ketene valence bond isomer **4052**, which could react with the β-keto group via [2+2] cycloaddition to form the desired β-lactone **4049**.

Scheme 73 | Proposed mechanism for the conversion of *N*-PMB amdiothioester **4050** into β-lactone **4049** via ketene intermediate **4052**.

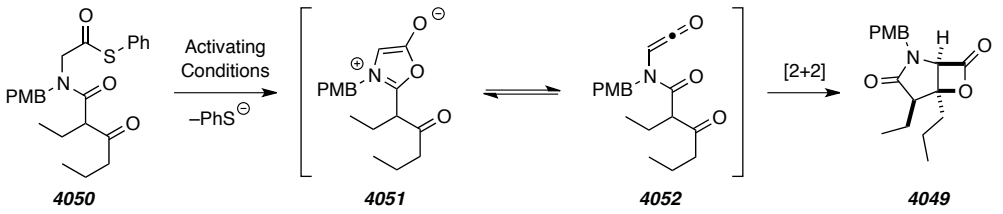

4050 ***4051*** ***4052*** ***4049***

To prepare thioester **4050** we treated acid **4042** with a slight excess of EDCI and five equivalents of benzenethiol. After fourteen hours, LC/MS analysis of the reaction mixture showed >95% consumption of starting material and four discreet peaks with a molecular ion identical to anticipated product **4050**. Crude ^{1}H NMR analysis showed peaks corresponding to the anticipated thioester along with peaks similar (but not identical) in chemical shift to those of β-lactones **4049** and 2-*epi*-**4049**. After chromatographic purification, we isolated and characterized the anticipated thioester **4050**, and γ-lactam thioesters **4053** and **4054** in low yields.

Scheme 74 | Preparation of *N*-PMB amido thioester **4050** and unexpected isolation of γ-lactams **4053** and **4054**.

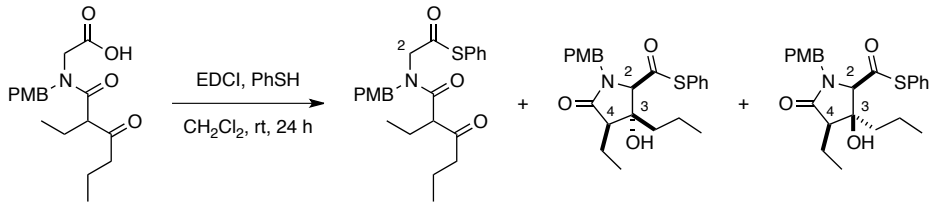

4042 ***4050*** 10% ***4053*** 4% ***4054*** 7%

The structures of lactam thioesters **4053** and **4054** were assigned based upon 1D and 2D NMR analysis. Initial inspection of each of the diastereomers showed an absence rotamers, which were present in ester **4048** and acid **4042** precursors as well as the

acyclic thioester co-isolate **4050**. Additionally, each the ^{1}H NMR spectrum of lactams **4053** and **4054** contained a methine singlet (δ 2.80 vs. 2.26 ppm, respectively) whereas the chemical shifts the C-2 α-hydrogen atoms in the acyclic thioester **4050** exhibited a doublet splitting patter with a *J*-value constituent with geminal coupling (ca. 17 Hz). To determine the relative configuration we first noticed a difference in the chemical shifts of the C-2 methine resonances suggesting that the downfield-shifted resonance was *cis* to the C-3 hydroxy group. A combination of nOe and NOESY techniques also supported the proposed relative configurations. For **4053**, the C-2 methine showed correlations with the C-4 methine and the C-3 O*H*, but not the C-3 methylene; the C-4 also showed correlation with the C-3 O*H* and not the C-3 methylene. For **4054**, the C-2 methine showed correlations with the C-4 methine, the C-3 methylene, and not the C-3 O*H*; the C-4 methine also showed correlation with the C-3 methylene and not the C-3 O*H*.

The structural similarities between **4054** and Moore's proposed intermediate in the biosynthesis of **1** (cf. **4002**) led us to believe that we had serendipitously encountered conditions that mimic a key event in the biosynthesis of the salinosporamides. By uncovering the mechanistic details of this transformation of we would likely shed light onto the mysterious facets of the biosynthetic pathways of the salinosporamides. Additionally, these studies would likely provide access to superior synthetic routes to the natural products and their biologically active analogues.

Following our unexpected isolation of γ-lactam **4054**, we first wanted to probe the possibility that in the absence of benzenethiol EDCI alone might able to induce cyclization of **4042** into β-lactone **4049**. One mechanistic hypothesis was that EDCI was converting the acid starting material into a β-lactone intermediate, which would readily react with benzenethiol to form the corresponding lactam.[96] To test this hypothesis we again treated acid **4042** with EDCI but *without* a thiol nucleophile and in $CDCl_3$ (Scheme 75). Monitoring the reaction mixture by ^{1}H NMR showed a complex mixture was forming while **4042** was being consumed. After 24 h no starting material was detected, but only a trace amount of β-lactone **4049** was observed. Following workup and

[96] Potts and co-workers have demonstrated that salinosporamide A (**1**) readily reacts with mercaptan under dilute (cf. 0.01 M) basic conditions (Et_3N) to convert the β-lactone into a mixture of γ-lactam-containing thioesters (see ref 26).

chromatographic purification **4049** was isolated as a single diastereomer in 5% yield. While the overall reaction is inefficient from a preparative perspective, the stereoselectivity is noteworthy. Crude ^{1}H NMR analysis indicated that 2-*epi*-**4049** was not detectable in even trace quantities. Recall that application of Romo's conditions to acid **4042** gave an equimolar mixture of diastereomers, albeit in much higher yields (cf. 36%).

Scheme 75 | EDCI-mediated conversion of acid **4042** into β-lactone **4049**.

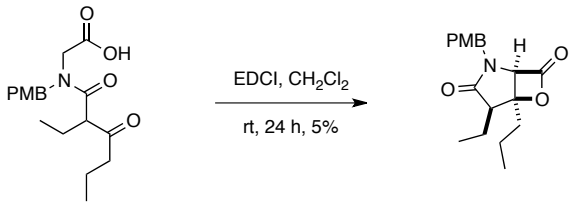

4042 ***4049***

After elucidating the structure of the lactam thioesters, we carefully reviewed the crude ^{1}H NMR spectrum of acid **4042**, which showed that the acyclic acid was contaminated with several resonances consistent with those of γ-lactam thioesters **4053** and **4054**.[97] This led us to hypothesize that LiOH-mediated aldol reaction was occurring under our hydrolysis conditions for the conversion of ester **4048** into **4042**. Attempts at integrating the complex mixture of products lead us to estimate that the aldol products comprise roughly half of the crude reaction mixture. In retrospect, this result is not unexpected considering Potts had reported use of *t*-BuOK to effect a related intramolecular aldol reaction of a tertiary amido methyl ester (see Scheme 13).[43] We then speculated that a reasonable mechanism for the formation of thioester lactams **4053** and **4054** might simply be thioesterification of the corresponding γ-lactam carboxylic acids, **4055** and **4056** (Scheme 76). In the case of the all-*cis*-γ-lactam, we predict that EDCI would induce lactonization to make *cis*-β-lactone **4049** and subsequent thioesterification would proceed by ring opening of the β-lactone with benzenethiol to give **4054**.[96] However, recall that when benzenethiol was omitted from the reaction mixture, β-lactone

[97] Two doublets present at 5.19 and 5.01 ppm with large coupling constants (J = 14.6 Hz for each) likely correspond to diastereotopic, benzylic methylene hydrogen atoms of two diastereomers. By treating the reaction mixture with $TMSCH_2N_2$ we were able to isolate several γ-lactam-containing methyl esters.

4049 was isolated in low yields from a complex mixture of intractable byproducts. The isolation of **4049** in reproducibly low yields when benzenethiol is omitted suggests that the generation of lactam thioester **4054** is proceeding by an alternative mechanism.

Scheme 76 | A proposed mechanism for the formation of γ-lactam thioesters **4053** and **4054** that involves the thioesterification of acids **4055** and **4056**.

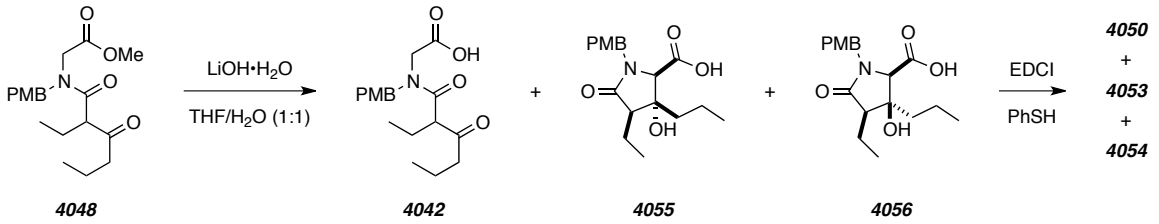

To gain insight into the role of EDCI on the formation of γ-lactams **4053** and **4054** we repeated the same experiment (i.e. synthesis of thioester **4050** from acid **4042**) with other common acid-activating reagents (Scheme 77). To summarize, use of DCC and DMAP gave a crude reaction mixture nearly identical to that obtained when EDCI was used. Standard HATU {1-[Bis(dimethylamino)methylene]-1*H*-1,2,3-triazolo[4,5-*b*]pyridinium 3-oxid hexafluorophosphate} acid-activating conditions (i.e. with Et_3N and HOBT) also gave acyclic thioester **4050**, and the γ-lactams thioesters in ratios comparable to those obtained with DCC and EDCI (cf. 14% and 4% yields for **4053** and **4054** respectively), in addition to β-lactone **4049** (14% yield). Standard with both HBTU [*O*-(Benzotriazol-1-yl)-*N,N,N′,N′*-tetramethyluronium hexafluorophosphate] and BOP [(Benzotriazol-1-yloxy)tris(dimethylamino)phosphonium hexafluorophosphate] acid-activating conditions (i.e. with Et_3N) gave the acyclic thioester **4042**, **4053**/**4054**, and β-lactone **4049** (ratio ca. 2:1:2). The conditions that included HBTU were repeated without benzenethiol, but only a trace amount of β-lactone **4049** was detected. Similar to the EDCI conditions, this suggests that β-lactone **4049** is not an intermediate in the generation of lactam products. Use of diphenyl disulfide and triphenylphosphine gave only the acyclic thioester **4050**, however still in low yields (cf. 14-24%).

Scheme 77 | Screened conditions for the thioesterification of acid **4042**.

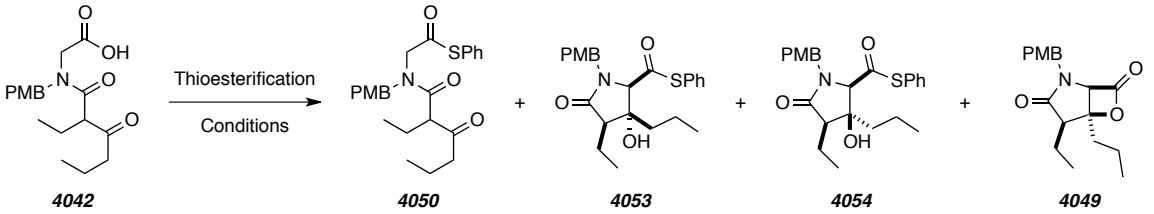

Acid-Activating Reagent(s)	Ratio of ***4050*:*4053*:*4054*:*4049***
EDCI	10:4:7:-
DCC/DMAP	10:4:7:-
HATU	10:7:2:7
HBTU	4:1:1:4
BOP	4:1:1:4

Collectively, the results obtained from screening a handful of peptide coupling reagents suggest that the conversion of acid **4042** into lactams **4053** and **4054** is general, but the mechanism does not proceed through a β-lactone intermediate. This led us to propose that the acyclic thioester **4050** is first formed, as expected, and continues to react via an intramolecular aldol reaction (Scheme 78). The intramolecular aldol reaction would proceed by deprotonation of **4050** at C-2 to form thioester enolate **4057**, which adds to the β-ketone to form aldolate **4058**. Protonation would generate lactams **4053** and **4054**, or, in the case of *cis*-lactam **4054**, reversible lactonization would occur to form of β-lactone **4049**. A basic amine was present in all conditions suggesting that simply treating the acyclic thioester **4050** with an amine might provide the same mixture of products. Unfortunately, we found that treating **4050** with 2 equivalents of DIEA in $CDCl_3$ provided less than 10% conversion after 18 h to a mixture of aldol products. This control experiment would suggest that an amine alone is not capable of generating the thioester enolate necessary for the intramolecular aldol reaction.

Scheme 78 | Proposed mechanism and initial attempt for the base-mediated intramolecular aldol reaction of thioester **4050**.

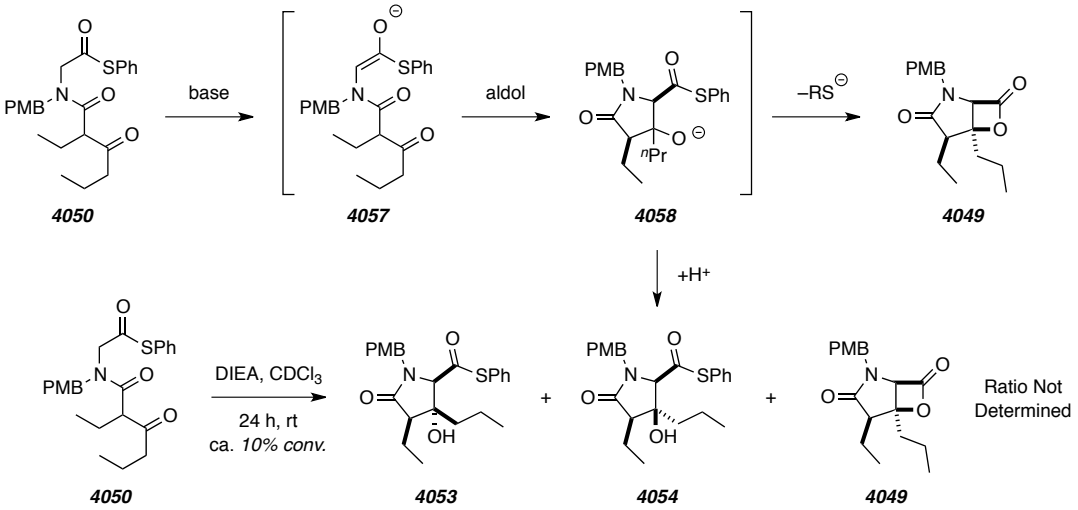

During the course of these studies, Coltart and co-workers reported conditions for a bifunctional urea-catalyzed (cf. **4061**), bimolecular Mannich reaction of a thioester donor (cf. **4059**) with an *N*-sulfonyl imine acceptor (cf. **4060**) to give a β-ketoamido thioester (cf. **4062**) with good diastereo- and enantioselectivity (Scheme 79).[98] The mechanism involves reversible deprotonation of the C-2 α-hydrogen atom to form a thioester enolate (cf. **4064**), which adds to the electron-deficient imine. The authors propose that the urea moiety of catalyst **4061** coordinates to the thioester carbonyl via two hydrogen bonding interactions (cf. **4063**), which orients the basic quinuclidine nitrogen in close proximity to the α-hydrogen atom leading to rapid and reversible deprotonation. The resulting thioester enolate **4064** forms three hydrogen bonds to the protonated catalyst, each of which stabilizes the resulting enolate and provides a chiral environment for inducing enantioselectivity in the conversion to **4062**.

[98] Kohler, M. C.; Yost, J. M.; Garnsey, M. R.; Coltart, D. M. Direct carbon-carbon bond formation via soft enolization: A biomimetic asymmetric Mannich reaction of phenylacetate thioesters. *Org. Lett.* **2010**, *12*, 3376–3379.

Scheme 79 | A noteworthy result and proposed mechanism for the urea-catalyzed, bimolecular Mannich reaction between a thioester (cf. **4059**) and a sulfonyl imine (cf. **4060**) (adapted from ref. 98).

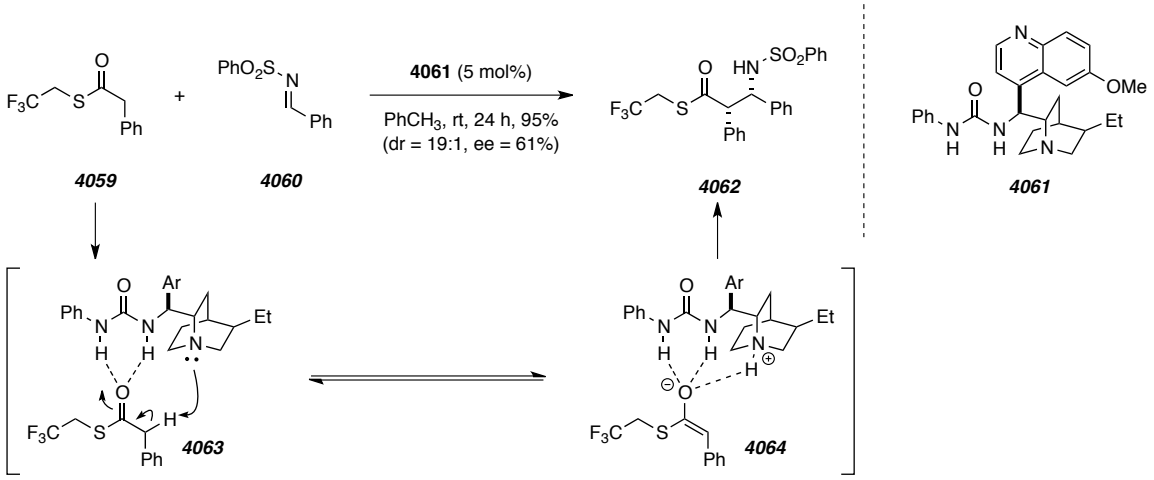

The mechanistic proposal put forth by Coltart led us to consider that a similar process was occurring in the EDCI-mediated conversion of acid **4042** into lactams **4053** and **4054**. The use of carbodiimide coupling reagents (e.g., EDCI) for acid activation gives urea byproducts. EDCI is often chosen in place of DCC because the corresponding urea **4065** (Scheme 80) is more easily removed by aqueous workup.[99] Treating **4065** with dilute HCl or saturated NH_4Cl protonates the basic dimethylamino moiety to give a water-soluble ammonium salt. The position of the basic amino group in urea **4065** with respect to the urea moiety is similar to that of the cinchona alkaloid-derived urea **4061** used by Coltart. This led us to propose a mechanism for the conversion of acid **4042** into thioesters **4050**, **4053**, and **4054** that involves soft-enolization of **4050** to form a thioester enolate that is likely stabilized by hydrogen bonding interactions similar to those of Coltart's proposed intermediate **4064**. Intramolecular aldol reaction and subsequent proton transfer then gives rise to lactams **4053** and **4054**. To test this hypothesis we prepared amine-containing urea **4069** (a.k.a. a bifunctional urea) from phenyl isocyanate (**4067**) and *N*,*N*-dimethylethylenediamine (**4068**).

[99] Sheehan, J.; Cruickshank, P.; Boshart, G. A convenient synthesis of water-soluble carbodiimides. *J. Org. Chem.* **1961**, *26*, 2525–2528.

Scheme 80 | Synthesis of relevant urea catalysts that for the aldol reaction of thioesters.

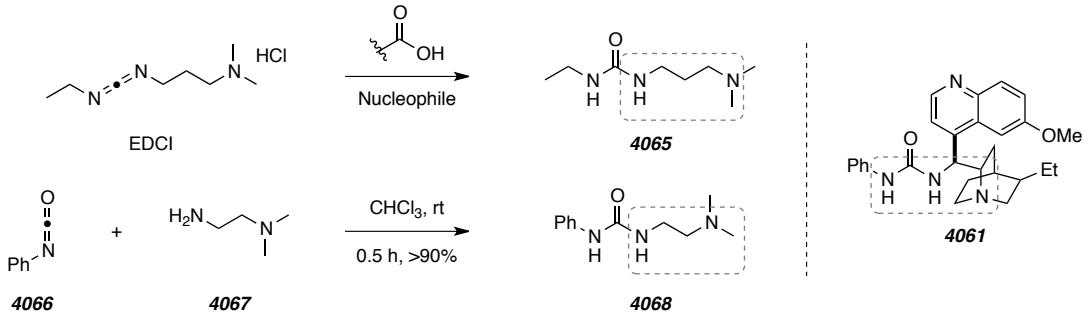

Treating a CH_2Cl_2 solution of thioester **4050** with five equivalents of urea **4068** at room temperature for 48 h gave a mixture of lactam thioesters **4053** (49%) and **4054** (12%), as well as β-lactone **4049** (Scheme 81). Consistent with our hypothesis, we propose the mechanism involves deprotonation at C-2 by the dimethylamino group in **4068**. The resulting thioester enolate then adds to the β-ketone intramolecularly and, following proton transfer from the protonated dimethylamino group, forms aldolates **4053** and **4054**. We were surprised to observe β-lactone **4049** because base-mediated lactonization of *cis*-lactam would release a thiolate nucleophile. Potts[96] and Jacobsen[100] have independently demonstrated that, under basic conditions, the equilibrium between β-hydroxy thioester and β-lactone strongly favors the monocyclic thioester.

Scheme 81 | Urea **4068**-mediated intramolecular aldol reaction of thioester **4050**.

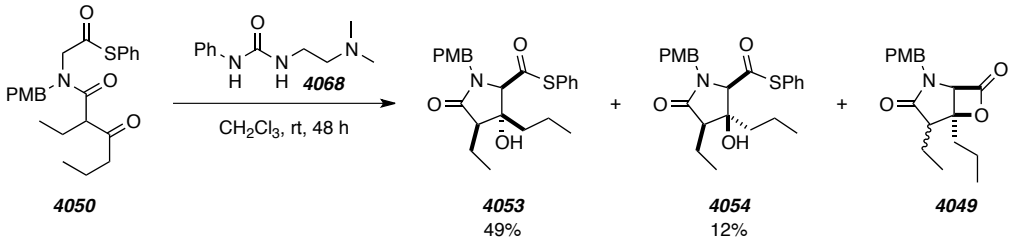

The difference in the rate of the amine-mediated intramolecular aldol reaction when thioester **4050** was treated with DIEA versus urea **4068** (cf. $t_{1/2}$ ca. 90 h vs. 13 h)

[100] Balskus, E. P.; Jacobsen, E. N. α,β-Unsaturated β-silyl imide substrates for catalytic, enantioselective conjugate additions: A total synthesis of (+)-lactacystin and the discovery of a new proteasome inhibitor. *J. Am. Chem. Soc.* **2006**, *128*, 6810–6812.

merits further comment. Similar to the mechanism put forth by Coltart,[98] we propose that the urea forms hydrogen bonds to the thioester carbonyl to place the basic amine in close proximity to the α-hydrogen (cf. **4069**, Scheme 82). Soft-enolization then ensues to deprotonate the α-hydrogen at C-2 and give rise to thioester enolate **4070**. Reversible deprotonation is encouraged by conjugate base stabilization via the triply hydrogen bound enolate-urea complex. Intramolecular aldol reaction between the enolate carbon and the β-keto group then gives protonated urea **4071** and aldolate **4072**. Proton transfer from **4071** completes the catalytic cycle and affords the mixture of γ-lactams.

Scheme 82 | Proposed mechanism for the urea-mediated aldol reaction of thioester **4050**.

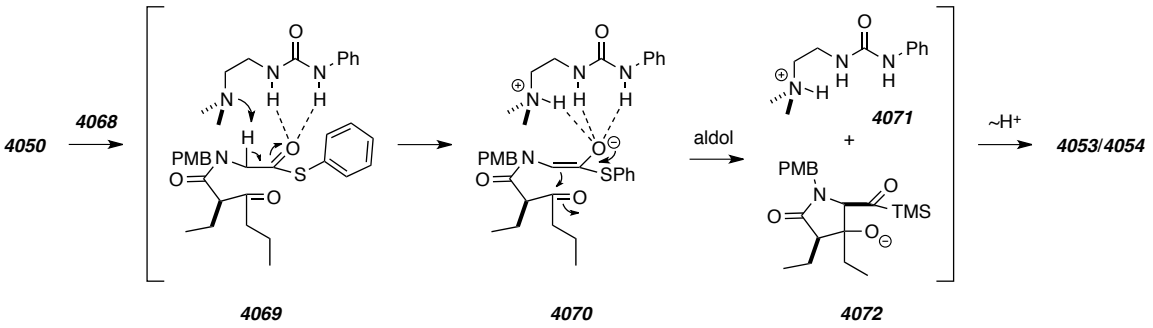

The reaction conditions were optimized by studying the effects of the aldol-promoting reagent had on the reaction outcome (see tabular inset in Figure 7). Substituting the aldol-promoting reagent with thiourea **4073** gave a mixture of the diastereomeric aldol products in a similar ratio, but the rate of the reaction was slower and the amount of β-lactone observed had decreased. Performing the same reaction in CH_2Cl_2 instead of $CDCl_3$ gave a noticeably faster reaction and led to an increased production of β-lactone. However, the ratio of *trans*-aldolate **4053** to *cis*-aldolate **4054** was increased with the solvent change, which suggests that solvent plays an important role in the reaction. To probe the effect of changing the phenyl substituent of urea **4068**, we prepared cyclohexyl-containing urea **4074** and 3,5-bis-trifluoromethyl urea **4075**. Treating thioester **4050** with **4074** led to full consumption of starting material in less than 12 h to give a mixture of aldol and β-lactone products that included a lesser amount of undesired lactam **4053**. Reaction of the electron-deficient urea **4075** with thioester **4050**

proceeded to give a similar ratio of products that we observed with **4068** and **4073** and at a rate intermediate between *N*-phenyl and *N*-cyclohexyl ureas. Consistent with the proposed mechanism, treating thioester **4050** with amide **4076** and di-*n*-butylamine led to no observable reaction.

Figure 7 | Studies of the effect of the aldol-promoting reagent for the intramolecular aldol reaction thioester **4050**.

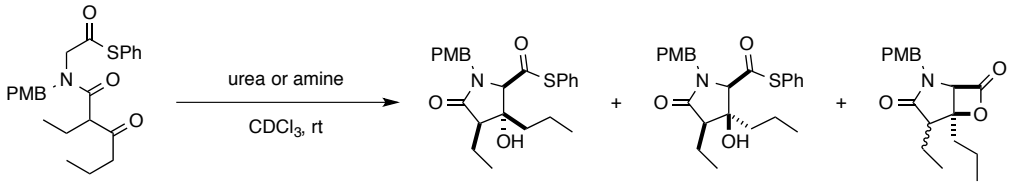

4050 ***4053*** ***4054*** ***4049***

Aldol-Promoting Reagent	Reaction Rate ($t_{1/2}$)	Ratio of ***4053***:***4054***:***4049***
4073	20 h	10:2.5:1.0
4073 (CH_2Cl_2)	13 h	2.4:0.1:1
4074	4 h>	3.7:1.3:1.0
4075	8 h	2.2:1.3:1
4076	NR	-
($^nBu)_2$-urea	NR	-
^{n}BuN($CH_3)_3$	1 h>	13:3:1
Et_3N	4 h>	8.5:1.8:1

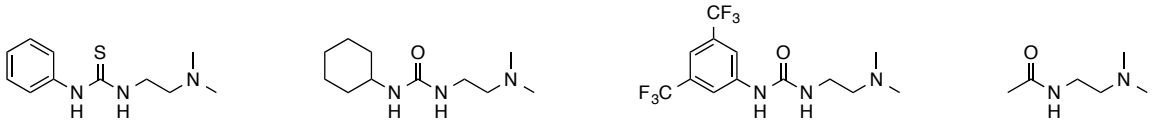

4073 ***4074*** ***4075*** ***4076***

It seemed apparent that the urea functionality was necessary for the aldol reaction to take place considering that the reaction rate had slowed dramatically when DIEA was used instead of urea **4068**. Still, to make sure we were not overlooking an opportunity for use of a simpler catalyst we screened other, less hindered, amine bases. Surprisingly, treating thioester **4050** with 2 equivalents of *N*,*N*-dimethylbutylamine led to full consumption of starting material in 6 hours to selectively give **4053** as the major product in addition to **4054** and **4049**. It was unexpected to find that simply treating the thioester with an amine base would give such an efficient reaction. In light of this new result, we screened several other amine bases. Treating thioester **4050** with 2 equivalents of Et_3N

gave a mixture of aldol products at a rate similar to that of *N*,*N*,-dimethylbutylamine. These results suggest that simple amine bases could be used to effect the intramolecular aldol reaction when the precursor is not readily enolized by ureas conditions.

The aldol-promoting urea reagent is not consumed in our proposed mechanism, so it should be possible to decrease the amount of urea to catalytic levels. The reaction mixture containing thiourea **4073** and the partially converted mixture of **4050** and the corresponding aldol products from above in CH_2Cl_2 were heated in a 95 ºC oil bath (the reaction mixture that had already originally converted to 58% of **4050**, cf. second entry in tabular inset of Figure 7). After 2 h, the reaction mixture became dark brown and ^{1}H NMR indicated that all of **4050** had been consumed. Interestingly, the ratio of aldolate epimers **4053** and **4054** had changed to favor the *trans*-lactam (cf. ratio of **4053**:**4054** = 4:1 to 15:1), the amount of β-lactone had increased, and enamide **4077** was also observed.

Scheme 83 | Sequential intramolecular aldol, lactonization, and decarboxylation reactions of thioester **4050** when heated in the presence of base.

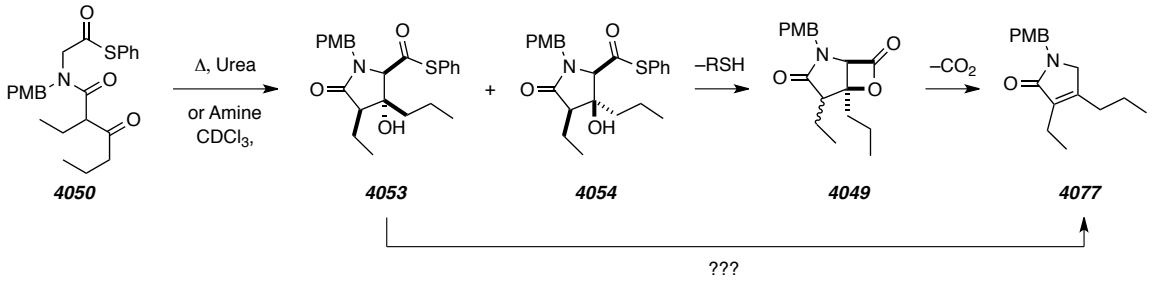

Unfortunately, heating the reaction mixture greatly complicated its subsequent analysis. However, we were encouraged by the increase in reaction rate, so we next considered decreasing loading of the urea catalyst. Heating a mixture of thioester **4050** and 10 mol% of urea **4068** at 95 ºC led to full consumption of starting material in ca. 12 h and the amount of β-lactone **4049** observed was now greater than either of the aldolates. This suggests that heating to 95 ºC enables a retro-aldol process allowing aldolate **4053** and **4054** to interconvert, whereby lactonization to **4049** siphons the equilibrium. However, the major component in the reaction was the unsaturated lactam **4077**, which indicates that the β-lactone is unstable to thermal decarboxylation at 95 ºC. Furthermore,

we cannot rule out the possibility that **4053** is also transforming into **4077**. Overall, we viewed the decomposition to be substrate dependent, and so the effect of temperature was not further screened.

The varying amounts of β-lactone formed under the previously described reaction conditions led us to consider developing conditions that would promote lactonization following the intramolecular aldol reaction. Additionally, spontaneous lactonization of the corresponding aldol precursor **4078** to chloroethyl-containing natural products **1** and antiprotealide **2** would prevent the unwanted intramolecular S_N2 side-reaction (i.e. conversion of **4079** into **4081**). To achieve this we needed to identify a reagent that would trap free thiol without interfering with the intramolecular aldol reaction [e.g., *N*-phenylmaleimide (**4080**)]. This would force the equilibrium between thioester **4078** and β-lactone **1** or **2** to favor lactonization.

Scheme 84 | An approach to tandem aldol-lactonization of thioester precursor **4078** to avoid unwanted S_N2 reaction to form THF-containing byproduct **4081**.

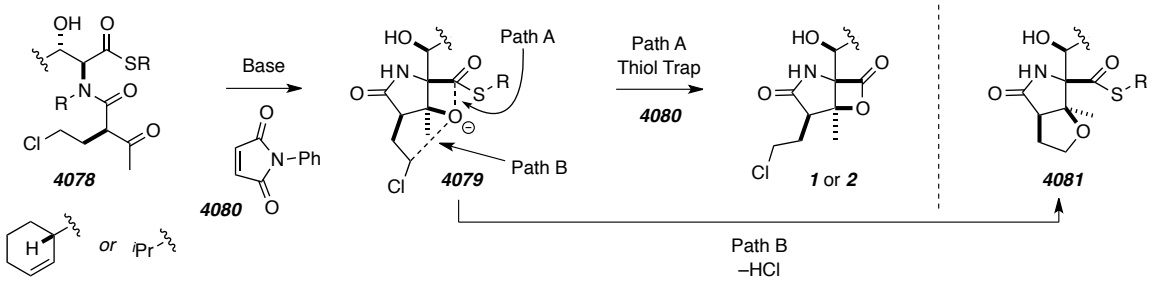

A clear first choice for a thiophilic trap was *N*-phenyl maleimide (**4080**). Adding **4080** to a room temperature mixture of thioester **4050** and Et_3N in $CDCl_3$ gave a mixture of lactam **4053**, β-lactone **4049**, 2-*epi*-**4049**, and unsaturated lactam **4077** (ratio = 1:1.5:3.0:1.5, respectively). Using a substoichiomertric amount of urea **4068** instead of Et_3N and heating an otherwise identical reaction mixture at 95 ºC gave unsaturated lactam **4077** as the exclusive product.[101] Room temperature decarboxylation of **4049**

[101] This result of this experiment was not unexpected given our previous attempts at heating thioester **4050** with a substoichiometric amount of urea **4068**. However, it should be noted that it was not until this experiment was performed that we were able to isolate and elucidate the structure of unsaturated lactam **4077**.

would be surprising, but Romo[40] reported similar results for related substrates. Substituting **4080** for the milder Michael acceptor, 3-methyl-2-cyclohexenone, gave results similar to those observed when the Michael acceptor was absent from the reaction mixture.

To gain additional insight into the mechanism of the room temperature decarboxylation, we treated an authentic sample of β-lactone **4049** separately with **4080** and Et_3N. No reaction was observed with *N*-phenylmaleimide, but Et_3N, by itself, induced C-2 epimerization to give a final dr = 5:1 for the β-lactone diastereomers. Interestingly, none of the unsaturated lactam **4077** was observed, which may suggest an alternative mechanism that does not require a β-lactone intermediate.

We observed moderate to good conversion (i.e. $t_{1/2} \leq 10$ h in most cases) with the use of many aldol-promoting bases, unfortunately, conditions that gave good selectivity for either the all-*cis*-aldolate **4054** or β-lactone **4049** were not identified. In almost every case, lactam **4053** was the major product. This was unexpected because positioning the propyl and ethyl chains *cis* to one another would likely introduce strain and destabilize lactam **4053**. Total electronic energy calculations in MacroModel[102]/Maestro[103] were performed on a series of conformers for **4053** and **4054** (the lowest energy conformer of each is depicted in Figure 8). In general, conformers of the all-*cis*-lactam were approximately 2.6 kcal/mol lower in energy than the monoepimeric analogue.[104] This suggests that desired lactam **4054** is indeed the thermodynamic product, which led us to hypothesize that the observed stereoselectivities for the intramolecular aldol reaction imply that undesired lactam **4053** is the kinetic product.

---

[102] MacroModel, version 9.9, Schrödinger, LLC, New York, NY, 2012.
[103] Maestro, version 9.4, Schrödinger, LLC, New York, NY, 2013.
[104] The structure of both lactam **4053** and **4054** was subjected to Monte-Carlo conformational analysis using the mixed-torsional/low-mode sampling method with the OPLS_2005 molecular mechanics force field potential in MacroModel. In total, 301 conformers were found for **4053**, and 225 conformers were found for **4054**. The range of energies calculated for each conformer of both diastereomers were compared by inspection.

Figure 8 | Computed[104] lowest energy conformers of **4053** and **4054**.

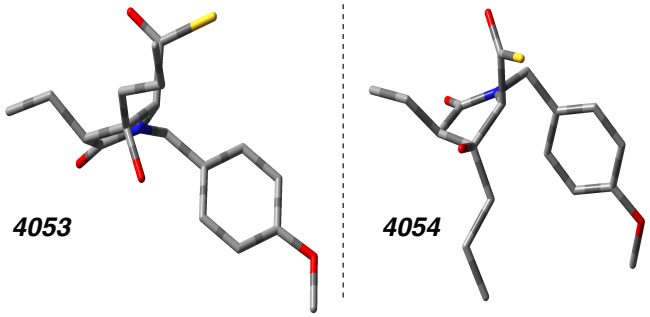

To verify the energetic relationship between lactams **4053** and **4054** experimentally, we studied the rate of epimerization of each in the presence of **4068**. Treating isolated lactams **4053** and **4054** with urea **4068** led to no detectable epimerization or reaction (Scheme 85). This indicates that the ratio of **4053**:**4054** observed when acyclic thioester **4050** was treated with bifunctional urea **4068** reflects the kinetic selectivity for each of the aldol products (cf. 4:1). Even though epimerization was not observed and it seemed that **4054** and **4053** were not interconverting, epimerization at C-3 is still possible. A mechanism to account for this would involve lactam ring opening by a retro-aldol process to give thioester enolate **4083** via **4082**. Subsequent aldol reaction and proton transfer or lactonization with loss of thiolate would give rise to a mixture of the lactam thioesters and β-lactones.

Scheme 85 | Proposed mechanism for the equilibration of lactam thioesters **4053** and **4054** under basic conditions.

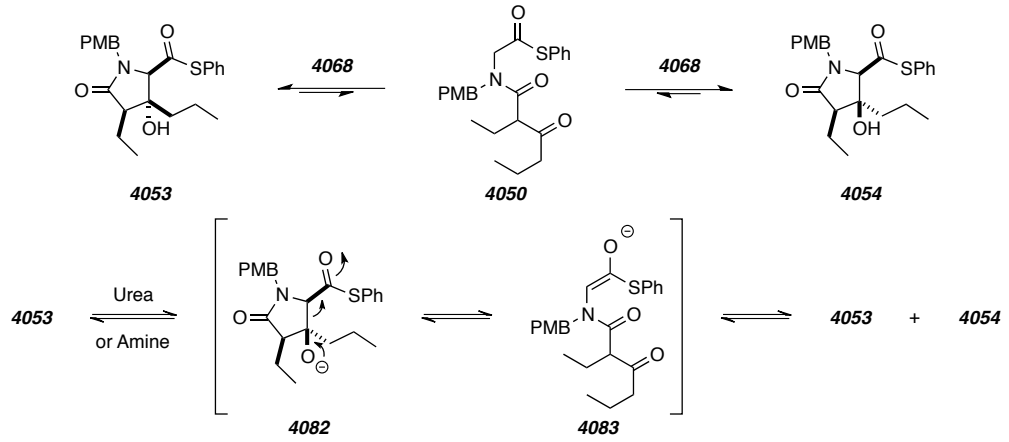

Because replacement of urea **4068** with Et_3N led to a faster reaction for the highly stereoselective formation of undesired *trans*-lactam **4053**, we were curious if all-*cis*-lactam **4054** would epimerize under the same conditions. To probe this we treated an authentic sample all-*cis*-β-lactone **4049** with 10 equivalents of benzenethiol and Et_3N in $CDCl_3$. After 18 h, ^1H NMR analysis of the reaction mixture showed that all of the β-lactone starting material had been converted into the ring-opened lactam products and the only detectable products were the *trans* and *cis* lactams (ratio **4053**:**4054** = ca. 1:3). The reaction likely proceeds by ring opening of the β-lactone to form all-*cis*-lactam **4054**. The presence of epimeric lactam **4053** (ca. 25%) suggests that the retro-aldol reaction of the all-*cis*-lactam is occurring and the epimeric lactam is being formed prior to reaching equilibrium, which implies that lactam **4053** is both the kinetic and thermodynamic product. One could argue that this result indicates that the free energy difference between the two diastereomers is much less than the 2.5 kcal mol^{-1} predicted by calculations. However, in light of the ca. 5:1 stereoselectivity from the final entry of the tabular inset in Figure 7, we predicted that the reaction proceeds through a slow equilibration process that strongly favors lactam **4053**. It then appears that, experimentally, lactam **4053** is both the kinetic and thermodynamic product (as is usually the case).

Scheme 86 | Et_3N-Mediated ring opening of β-lactone **4049** with PhSH to give lactams **4053** and **4054** via alkoxide **4082**.

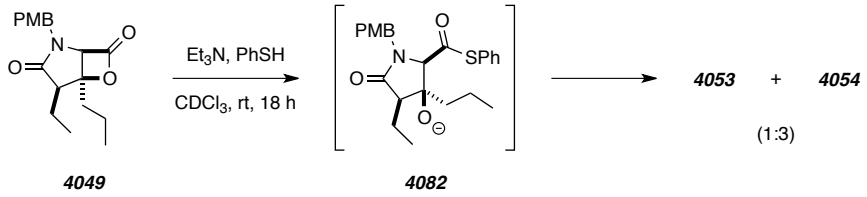

4.5. Alternative Substrates for Studying the Amine-Mediated, Intramolecular Aldol Reaction of Amido Thioesters

Although acyclic thioester **4050** served as a good model substrate for discovering the base-mediated intramolecular aldol reaction, the biosynthesis of **1** is proposed to involve thioester **4001**, which differs from model substrate **4050** at several sites (Figure 9). The C-2' chloroethyl of **4001** has been substituted by ethyl, the C-4' methyl has been replaced by propyl, the β-hydroxy-γ-cyclohexenyl has been replaced by hydrogen, the amide nitrogen has been alkylated with PMB, and the *S*-peptidyl carrier protein thioester has been replaced by *S*-phenyl. Each of these differences could give rise to a substrate that exhibits markedly different reactivity with a bifunctional urea. To systematically assess the structure-*re*activity relationship of the aforementioned substituents, a series of model substrates were prepared and their reactivity with amines and bifunctional ureas was studied.

Figure 9 | Comparison of the structural differences between Moore's[28a] putative biosynthetic precursor **4001** and model substrate **4050**.

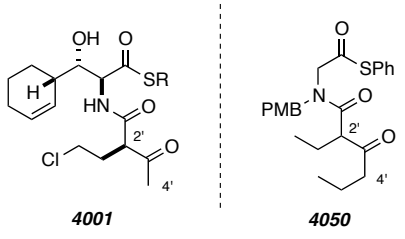

4.5.1. Re-examination of *N*-H Amido Thioesters Under Basic Amine Conditions

We first choose to probe the effect of the *N*-PMB group. This structural modification was what led to our initial discovery of the urea-promoted intramolecular aldol reaction. As previously mentioned, we proposed that alkylation of the amide nitrogen increased the pKa of the α-hydrogen atom in the 1,3-dicarbonyl system due to the increased $A_{1,3}$-strain in the corresponding enol/enolate. By preventing enolization of the β-ketone, deprotonation occurs at C-2 and the thioester enolate readily reacts via an intramolecular aldol reaction. We had prepared several *N*-H analogues of thioester **4050** using EDCI-mediated thioesterification of the corresponding acids, however aldol products were not detected in the corresponding reaction mixture (see Section 3.1). Still, we have shown that treating the glycine-derived amido thioester with bifunctional urea (e.g. **4068**) and Et_3N gave a mixture of aldolates. With this recent insight, we re-examined the reactivity of *N*-H-containing, glycine-derived thioester **4084**. However, treating secondary amido thioester **4084** with urea **4068**, or Et_3N showed no conversion. Other *N*-H substrates were examined that contained, for example, C-2 substitution and β-hydroxy groups, but no reaction was observed in all cases (Scheme 87).

Scheme 87 | Attempted amine-mediated, intramolecular aldol reaction of *N*-H-containing thioester **4084**.

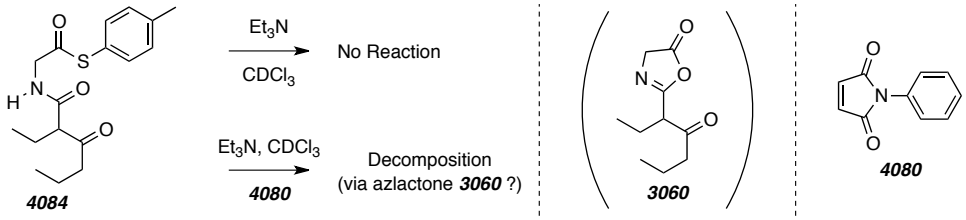

At this point, it was still not entirely clear why the *N*-PMB group was required for the aldol reaction. We originally predicted that *N*-alkylation both prevented unproductive azlactone formation and decreased the acidity of the α-hydrogen atom between the 1,3-dicarbonyl moiety. If the former was relevant, we would expect that treating the *N*-H thioester with an amine base would lead to an observable amount of azlactone **3060**. However, this would be reversible and the equilibrium may favor the acyclic thioester.

Addition of thiol trap **4080** led to a complex mixture, which could have resulted from unproductive side reaction of an unstable azlactone.

4.5.2. Studies of the Intramolecular Aldol Reaction of *N*-CH_3 Amido Thioesters

Alternatively, the role of the *N*-PMB group might be more complicated by, for example, providing a subtle π-stacking interaction[105] or by promoting isomerization into a more reactive conformer. To gain insight into these questions we studied the corresponding *N*-methyl thioester **4088** (Scheme 88). Thioester **4088** was prepared by reaction of sarcosine methyl ester hydrochloride (**4085**) with ketene dimer **3072** to give amide **4086**. Methyl ester hydrolysis to acid **4087** and thioesterification with PPh_3 and diphenyldisulfide then gave thioester **4088**.

Scheme 88 | Synthesis of *N*-methyl thioester **4088**.

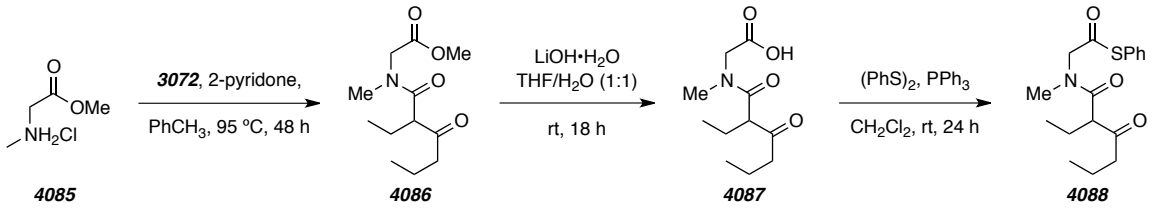

Treating **4088** with urea **4068** did provide the corresponding aldol products, albeit at a slower rate than the corresponding *N*-PMB analogue ($t_{1/2}$ ca. 36 h) to give the corresponding thioesters **4089** and **4090** (ratio ca. 1:3, Scheme 89). The structure of both **4089** and **4090** was assigned by comparison to *N*-PMB lactams **4053** and **4054**. Additionally, we were able obtain a crystalline sample of **4090** suitable for X-ray analysis. The X-ray structure of **4090** confirms the assigned structure and supports our assignment of the relative configuration for the *N*-PMB analogue (cf. **4054**). The isolation of lactams **4089** and **4090** further supports the need for *N*-alkylation for the aldol reaction to proceed. The decreased rate we observed with the *N*-methyl substrate is noteworthy and suggests that the role of the *N*-PMB group is greater than simply preventing azlactone formation.

[105] For references that propose similar roles for π-stacking interactions see Knowles, R. R.; Jacobsen, E. N. Attractive noncovalent interactions in asymmetric catalysis: Links between enzymes and small molecule catalysts. *Proc. Natl. Acad. Sci. USA* **2010**, *107*, 20678–20685.

Scheme 89 | Urea **4068**-mediated aldol reaction of thioester **4088** to form lactams **4089** and **4090**. The structure of **4090** was confirmed by X-ray crystallography.

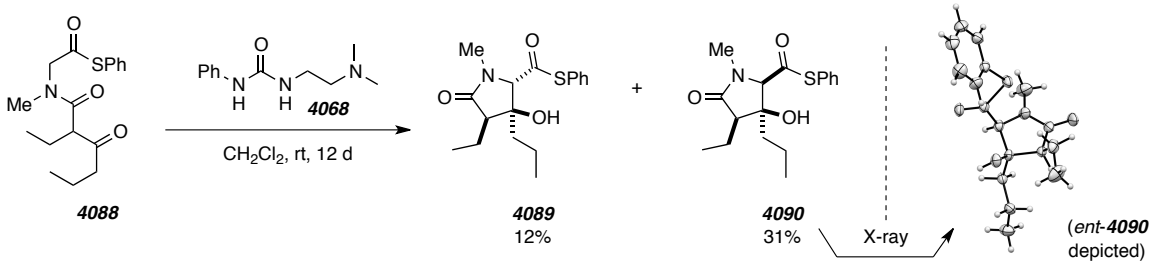

4.5.3. Studies of the Intramolecular Aldol Reaction of *N*-Cbz Amido Thioesters

To better understand the effect of *N*-substitution, we studied carbamate analogue **4095**, which was prepared from the *t*-butyl ester of *N*-Cbz glycine (**4091**, Scheme 90). Esterificaiton of *N*-Cbz glycine with *t*-BuOH gave **4091**, which reacted with ketene dimer **3072** to give β-ketoimido ester **4092**. Acid-mediated de-*t*-butylation to **4093** and subsequent thioesterification with EDCI and 4-methylbenzenethiol gave thioester **4094**. The thioesterification reaction provided the **4094** in low yields, but the reaction was otherwise clean. This indicated to us, similar to *N*-H analogue **4084**, that **4094** may not be amenable to the urea-mediated aldol reaction. Surprisingly, treating **4094** with an excess of bifunctional urea **4068** led to full conversion to a byproduct with a structure tentatively assigned to heterocycle **4095**.

Scheme 90 | Synthesis of *N*-Cbz thioester **4094** and its unexpected side reaction to form **4095** (tentative structure assignment).

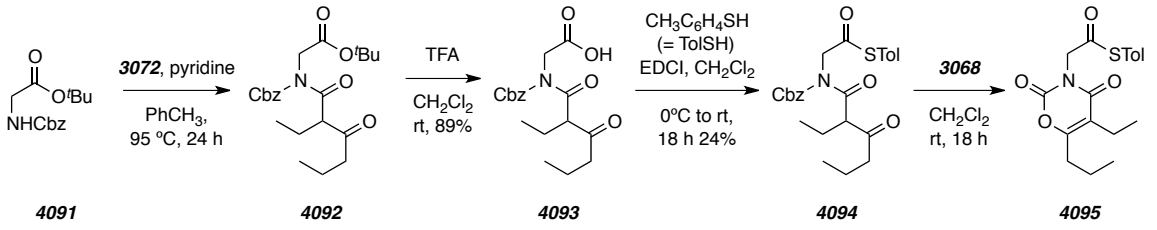

We proposed that a substrate lacking a α-hydrogen in the 1,3-dicarbonyl moiety would be unable to form the heterocyclic byproduct. We viewed the cyclopropyl-

containing substrate **4096** as an interesting candidate because the intramolecular aldol reaction could be followed with HCl-mediated ring opening to give the chloroethyl and isolated methyl substituents of the natural product. Additionally, the undesired cyclization and loss of benzyl alcohol would be inaccessible with this substrate because the cyclopropyl group precludes the necessary enolization. To introduce the acetylcyclopropyl amide we prepared known acid **4100** in one step from ethyl acetoacetate (**4098**) and 1,2-dibromoethane (**4099**).[106] While the reaction seemed to proceed as described[107] the chemical shift of the methyl and cyclopropyl groups in the ^{1}H NMR spectral data were inconsistent to those reported by Danishefsky. We attributed the spectral deviations to differences in the effective pH of the product, which would affect the extent of intramolecular hydrogen bonding of the carboxylic acid to the β-ketone.

Scheme 91 | Alternative, cyclopropane-containing, model substrate **4096** and the synthesis of synthesis of carboxylic acid **4100**.

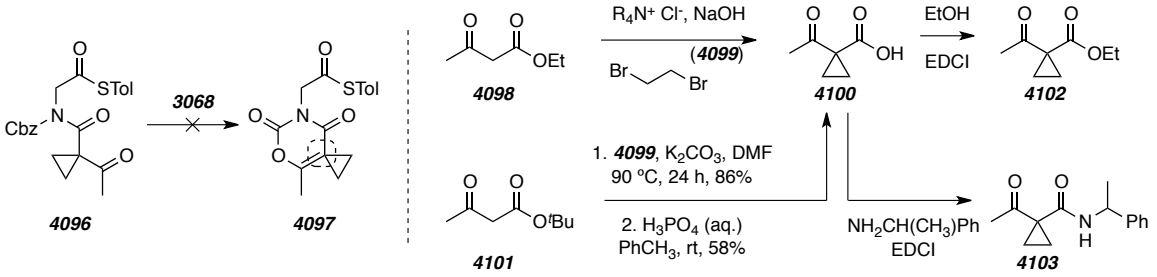

Unfortunately, coupling of acid **4100** and carbamate **4091** was more difficult than anticipated. Activating acid **4100** with EDCI prior to addition of **4091** gave no promising products. Additionally, following previously reported procedures for converting acid **4100** into either a mixed anhydride[108] or an acyl imidazole[109] were also unsuccessful.

[106] Singh, R. K.; Danishefsky, S. Preparation of activated cyclopropanes by phase transfer alkylation. *J. Org. Chem.* **1975**, *40*, 2969–2970.
[107] When preparing acid **4100** from ethyl acetoacetate following the procedure in ref. 106 we found the use of tetra-*n*-butylammonium hydroxide instead of benzyltrimethylammonium chloride led to reduced yields (ca. 0-15%).
[108] Kimura, Y.; Atarashi, S.; Kawakami, K.; Sato, K.; Hayakawa, I. (Fluorocyclopropyl)quinolones. 2. Synthesis and stereochemical structure-activity relationships of chiral 7-(7-amino-5-azaspiro[2.4]heptan-5-yl)-1-(2-fluorocyclopropyl)quinolone antibacterial agents. *J. Med. Chem.* **1994**, *37*, 3344–3352.

These results, along with our inconsistent spectral data led us to believe that we had not prepared **4100**. To test this we prepared the acid by de-*t*-butylation of the corresponding ester, which was prepared by dialkylation of *t*-butyl acetoacetate **4101**. Although the two step route to acid **4100** appeared more robust, the resulting ^{1}H NMR spectral data matched those of our previously prepared batch. Treating these batches of material with EDCI and either ethanol or α-methylbenzyl amine gave known ethyl ester **4102**[110] and amide **4103**,[108] Both acylation products matched the previously reported spectral data. This suggests that the material we prepared is cyclopropane-containing acid **4100**.

Although we had successfully prepared a sample of **4100**, we were unsure if it would prove to be an efficient coupling partner en route to thioester **4096**. We next turned to developing conditions for the conversion of **4100** into the potentially isolable acid chloride (**4104**, Scheme 92). Addition of oxalyl chloride to a solution of **4100** and 0.1 equivalents of DMF readily gave acid chloride **4104** in good yield and modest purity.[111] An approach for acylation of *N*-Cbz protected amino esters includes heating with an acid chloride without additional base.[112] Interestingly, when heating a mixture of **4104** and **4091** we obtained desired imide **4105** along with chloroethyl-containing imide **4106**. This demonstrates that the cyclopropane is amenable to ring-opening by HCl. While interesting, the reaction also gave several products of acid-mediated de-*t*-butylation, which reduced yields and complicated purification.

---

[109] Padwa, A.; Curtis, E. A.; Sandanayaka, V. P. Generation and cycloaddition behavior of spirocyclic carbonyl ylides. Application to the synthesis of the pterosin family of sesquiterpenes. *J. Org. Chem.* **1996**, *61*, 73–81.

[110] Yao, Y.; Fan, W.; Li, W.; Ma, X.; Zhu, L.; Xie, X.; Zhang, Z. Synthesis of (*S*)-7-amino-5-azaspiro[2.4]heptane via highly enantioselective hydrogenation of protected ethyl 1-(2-aminoaceto)cyclopropanecarboxylates. *J. Org. Chem.* **2011**, *76*, 2807–2813.

[111] Acid chloride **4104** was obtained with increased yields and purity were observed when freshly distilled oxalyl chloride was used. Attempts to purify either **4104** or its acid precursor **4100** by Kugelrohr distillation were unsuccessful.

[112] Lee, Y.-T.; Jang, Y.-J.; Syu, S.-E.; Chou, S.-C.; Lee, C.-J.; Lin, W. Preparation of functional benzofurans and indoles via chemoselective intramolecular Wittig reactions. *Chem. Commun.* **2012**, *48*, 8135–8137.

Scheme 92 | Synthesis of cyclopropane-containing ester **4105** and observation of its ring-opened congener **4106**.

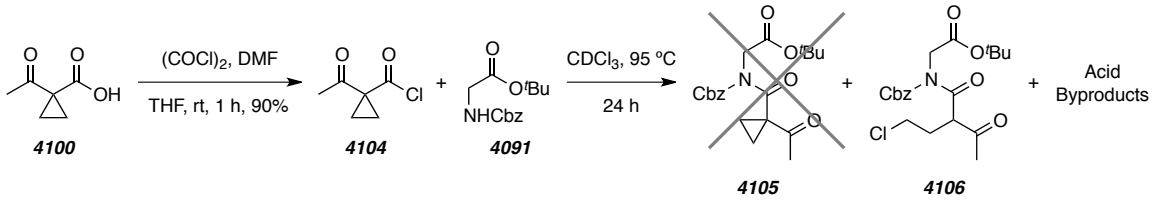

Alternatively, addition of **4104** to a solution containing the *N*-lithiated ester **4107** cleanly gave the corresponding cyclopropane-containing ester, **4105**, in moderate yield (Scheme 93).[113] Sequential acid-mediated de-*t*-butylation and thioesterification under standard conditions converted **4105** into thioester **4096**. Unfortunately, we were unable to induce a urea-mediated intramolecular aldol reaction using urea **4096**. This suggests that *N*-alkylation is necessary as opposed to *N*-carbamate functionalization. This was disappointing considering the effort spent developing a route to thioester **4096**. Additionally, we greatly appreciated the ease with which the spectral data could be interpreted, unlike the *N*-methyl and *N*-PMB congeners, due to the absence of rotamers were not observed in the ^{1}H NMR spectral data at room temperature. Still, our efforts did yield an alternative approach to the introduction of the chloroethyl moiety, which might prove useful when preparing salinosporamide A (**1**) or analogues thereof.

Scheme 93 | Alternative approach to the preparation of **4105** en route to the synthesis of **4096** and our attempt at inducing an intramolecular aldol reaction by addition of **4068**.

[113] We followed a related procedure cited in: Williams, D. R.; Cortez, G. S.; Bogen, S. L.; Rojas, C. M. Total synthesis of lankacyclinol. *Angew. Chem. Int. Ed.* **2000**, *39*, 4612–4615.

4.5.4. Studies of the Aldol Reaction of *N*-PMB, cyclopropane-containing Amido Thioesters

Despite our inability to effect the intramolecular aldol reaction on the cyclopropyl-containing *N*-Cbz thioester **4096**, we were inspired to study *N*-PMB analogue **4112** (Scheme 94). We could most easily prepare **4112** by thioesterification of acid **4111**, which is available from hydrolysis of ester **4109**. EDCI-mediated acetoacylation of secondary-amine **4108** provided ester **4109** in moderate yield. Hydrolysis of **4109** with LiOH gave the corresponding acid in good yield, without observable cyclopropane ring opening. Although HBTU-mediated thioesterification provided the other *N*-PMB amido thioesters in the highest yield, we assumed that use of EDCI would be more instructional with regard to the feasibility of the aldol reaction. Not surprisingly, treating acid **4111** with EDCI and 4-methylbenzenethiol gave a mixture of thioesters in low yields. It should be noted that two other compounds were isolated in low yield, but we were unable to determine their structure. The major product of the reaction mixture was β-keto thioester **4112**, but γ-lactams **4113** and **4114** resulting from an intramolecular aldol reaction, were also isolated (ratio **4113**:**4114** = 55:45).

Scheme 94 | Synthesis of acid **4111** and its tandem thioesterification-aldol reaction to form a mixture of thioesters **4112-4114**.

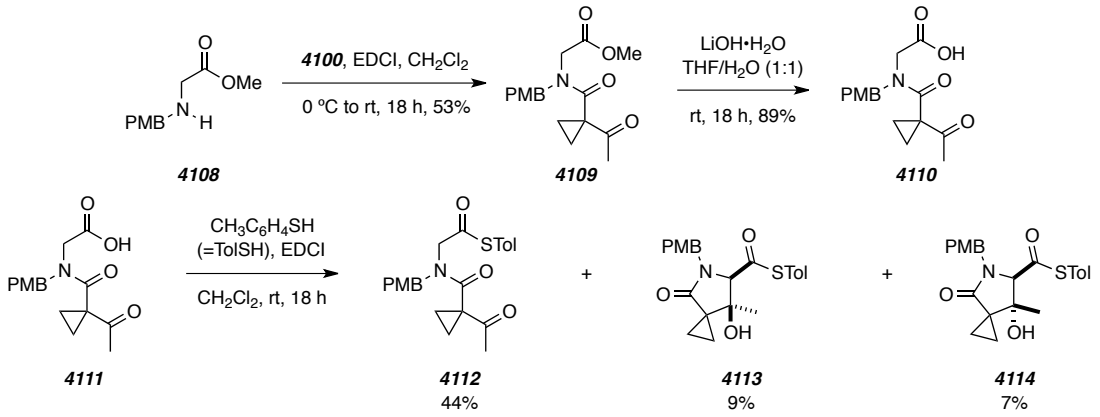

This latter result demonstrates that thioester **4112** is capable of reacting through the intramolecular aldol reaction, at a slower rate than previously studied substrates. We

treated a small amount of β-keto thioester **4112** with bifunctional urea **4068** to probe the effect of substituting the substituents at C-2' and C-4' with cyclopropyl and methyl, respectively (Scheme 95). As expected, the reaction proceeded at a slower rate with 2 equivalents of the urea catalyst (i.e. 16% conversion after 13 h), and the ratio of lactams **4113** to **4114**, was ca. 1:3, again in favor of the undesired *trans*-diastereomer. It is interesting to note the discrepancy in the diastereoselectivity between the EDCI- and urea-mediated cyclizations, but it remains unclear as to the cause for the observed difference in stereoselectivity.[114] A purified sample of *trans*-lactam **4113** was treated with anhydrous HCl (4 M in dioxane) and heated at temperatures up to 150 ºC, but only decomposition was observed. This suggests that conversion of the cyclopropyl into the chloroethyl group requires a second carbonyl electron-withdrawing group (cf. **4106** in Scheme 92).

Scheme 95 | Urea **4068**-mediated intramolecular aldol reaction of **4112** into γ-lactams **4113** and **4114**.

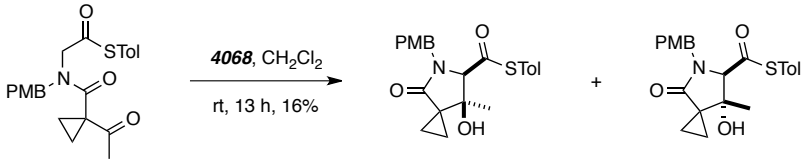

4112 ***4113*** (1:3) ***4114***

To this point, all base-mediated intramolecular aldol reactions that we have studied have favored products that bear a *trans* relative configuration between C-2 and C-3. This was surprising considering that calculations predicted that such relative configuration would be more strained than the desired all-*cis*-epimer. We considered that changing the C-3 propyl group to a methyl group, similar to the natural product, may influence the kinetic selectivity of the aldol reaction. However, observing that a urea-mediated aldol reaction of the methyl-bearing thioester **4112** also favored the *trans* diastereomer made us less optimistic.

[114] Re-inspection of the crude ^{1}H NMR of acid **4111** revealed two sets of resonances at 5.21 (d, J = 14.6 Hz) and 5.08 (d, J = 14.6 Hz). These peaks may correspond to products resulting from a LiOH-mediated intramolecular aldol reaction. Treating either of these aldolates with EDCI would likely form a β-lactone, which would be ring-opened in the presence of thiol to give either lactam **4113** or **4114**.

Mindful of our recent discovery that heating acid halide **4104** with an amine gives a chloroethyl-containing amide, a future substrate for consideration should certainly be the thioester analogue of **4106** (cf. **4119**). Synthetic efforts towards this substrate are shown in Scheme 96. We substituted α-amino methyl ester **4047** for allyl ester **4115**, which was prepared by S_N2 reaction between allyl bromoacetate and 4-methoxybenzylamine. Heating a mixture of *N*-PMB aminoester **4115** with acid halide **4104** gave chloroethyl-containing ester **4117** in addition to the cyclopropyl-containing ester **4116**. We later found that adding 10 mol% $AlCl_3$ to a mixture of anhydrous HCl and **4116** in 1,4-dioxane gave full conversion with ester **4117** as a major product. Deallylation with Pd(0) under standard conditions gave desired carboxylic acid **4118**. With acid **4118** in hand, we felt nearly ready to prepare the corresponding thioester **4119** and study its reactivity under basic conditions.

Scheme 96 | Progress towards a *N*-PMB, glycine-derived congener of the putative biosynthetic precursor to **1** and **2**.

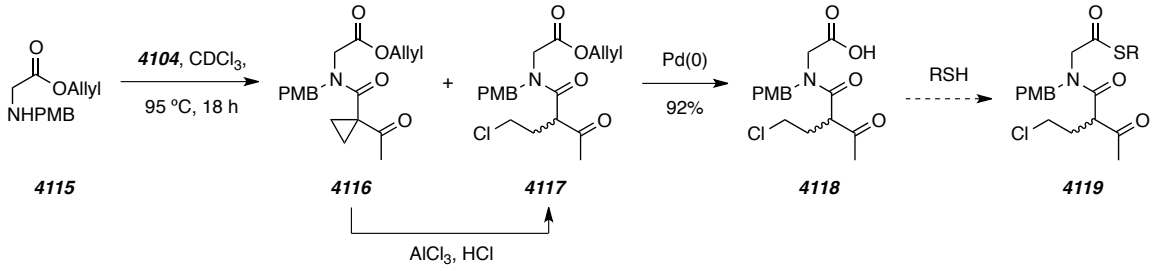

While we had identified a route to **4118**, we were nervous about subjecting our small quantity of **4118** to thioesterification conditions because previous reactions have given rise to low yields and mixtures of thioesters (cf. tabular inset in Scheme 77). Upon revisiting the data, we realized that many of these conditions contained Et_3N to deprotonate the carboxylic acid starting material. Recall that during our optimization of aldol-mediating bases we had found that Et_3N efficiently induces intramolecular aldol reaction of *N*-PMB amido thioesters while DIEA gives only trace conversion (cf. Figure 7). With this in mind, we attempted to prepare our initial model substrate **4050** from acid **4042** using BOP as the acid-activating reagent and DIEA as base instead of Et_3N

(Scheme 97). As expected, the major product in the reaction mixture was acyclic thioester **4050** and products of aldol reaction (e.g., **4053** and **4054**) were not observed. Still, the yield of the reaction was marginal (ca. 40%), which led us to conclude that more work is to be done to fully optimize the efficient synthesis of *N*-PMB amido thioesters from the corresponding carboxylic acids.

Scheme 97 | Improved conditions for the synthesis *N*-PMB amido thioester **4050** from carboxylic acid **4042**.

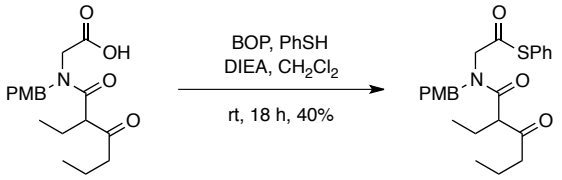

4042 ***4050***

4.6. Concluding Remarks

The results in Chapter 4 of this Thesis represent a tremendous breakthrough in our endeavor to develop conditions that will effect the conversion of a β-ketoamido thioester similar to **4001** into congeners of natural product **1**. It was gratifying to find that treating the thioester starting material with a simple amine base will induce thioester enolization and subsequent aldol reaction. The crux of these studies was identifying the need for *N*-alkylation to promote C-2 enolization over the traditionally more acidic C-2' position. Through these studies we also identified an approach for the preparation and reaction of acid halide **4104** to give cyclopropane-containing ester analogues. Additionally, we demonstrated that simply heating the cyclopropane-containing amides with HCl will effect ring opening to the corresponding chloroethyl-containing compounds. This represents a significant advance for the practical introduction of such groups into complex structures.

Chapter 5. Progress Toward the Total Synthesis of Salinosporamide A and Antiproteaolide

5.1. A Proposed Biomimetic Synthesis of the Salinosporamides

Although we had not discovered conditions that would both cleanly and selectively convert a glycine-derived amido thioester into a β-lactone, we thought it wise to begin pursuing a synthesis of salinosporamide A (**1**). Antiprotealide (**2**) is proposed to be biosynthesized in the same manner as **1**.[69] To avoid unnecessary complications introduced by the chiral cyclohexene ring of **1**, we choose to prepare the biosynthetic precursor of **2** instead (cf. **5002**, Figure 10). The most efficient preparation of **5002** would likely revolve around functionalization of a 3-hydroxyamino acid core prepared from 3-hydroxyleucine (**5001**). Because we had not yet assigned a role to the 3-hydroxy group in the biosynthesis, we felt it was wise to prepare **5001** as the single (2*S*,3*S*)-enantiomer. The 2*S* stereogenic center is enolized during the biosynthetic aldol process, but the 3*S* stereogenic remains intact and likely plays a role in defining the absolute configuration of the natural product.

Figure 10 | Key intermediates in the proposed total synthesis of antiprotealide **2**.

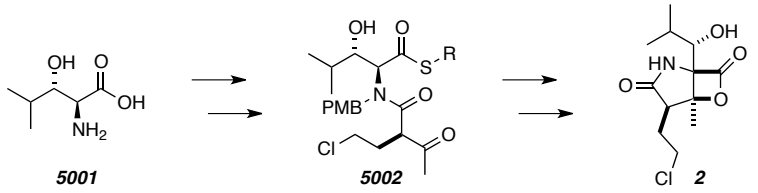

5.2. Enantioselective synthesis of (2*S*,3*S*)-3-hydroxyleucine

Barbas and co-workers recently disclosed a highly stereoselective L-proline-catalyzed bimolecular aldol reaction for the synthesis of β-hydroxy-α-amino acids that is ideally suited for accessing **5001**.[71] The authors reported good diastereoselectivities (ca. anti:syn dr ≥ 100:1), and enantioselectivies (ca. *ee* ≥ 99.5%) along with high yields (87%) for myriad substrates. For the preparation of **5001**, the procedure involves aldol reaction between donor aldehyde phthalimidoacetaldehyde (**5004**, Scheme 98) and

isobutyraldehyde. Subsequent Pinnick oxidation, esterification, and hydrazine-mediated phthalimide cleavage gives the methyl ester analogue of **5001**. The donor aldehyde **5004** was readily prepared by condensing allylamine with phthalic anhydride (**5003**) in DMF followed by ozonolysis and reductive workup. When the described L-proline-catalyzed aldol reaction was conducted at room temperature, the only aldol product observed was enal **5006**, which likely resulted from elimination of the desired β-hydroxy aldehyde **5005**. As Barbas and co-workers indicated, cooling the reaction mixture to 0 °C suppressed dehydration, but 36 h of incubation time was required for full consumption of aldehyde **5004**. These conditions, still gave a significant amount of dehydration (LC/MS ratio **5005**:**5006** 3:2), although the β-hydroxy aldehyde was apparently as a single diastereomer.

Scheme 98 | Our attempted preparation of desired aldehyde **5005** by a proline-catalyzed intermeolcular aldol reaction of aldehyde **5004** with isobutyraldehyde.

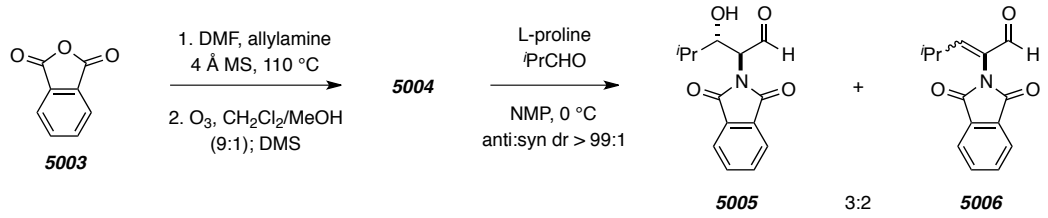

The crude mixture of aldehydes was recovered in 25% yield, and, following a straightforward sodium chlorite oxidation, the corresponding carboxylic acids **5007** and **5008** (Scheme 12) were subjected to esterification protocol with *N*,*N*-dimethylformamide dimethylacetal in pyridine at elevated temperatures (Methyl-8® conditions).[115] Further dehydration occurred under these conditions and methyl enoate **5010** instead of desired ester **5009** was found to be the major product by crude analysis. The authors prescribed esterification with $TMSCHN_2$, which might suppress further dehydration as the reaction can be done at reduced temperatures. However, we felt that suppressing elimination in

[115] Thenot, J.-P., and Horning, E.C. Amino acid *N*-dimethyllaminomethylene alkyl esters. New derivatives for GC and GC-MS studies. *Anal. Lett.* **1972**, *5*, 519–529.

the preparation of intermediate **5005** must first be achieved before considering the esterification.

Scheme 99 | Efforts toward the preparation of ester **5009** from a crude reaction mixture of aldehydes **5005** and **5006**.

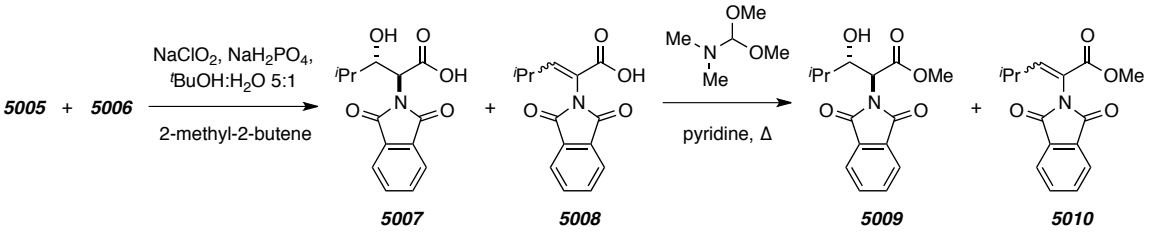

We speculated that replacing the doubly electron-withdrawing phthalimide protecting group might also reduce elimination. A general complication of early solid-phase peptide synthesis procedures was racemization. This likely occurred via azlactone formation and tautomerization to an achiral oxazole intermediate similar to that outlined in our original biosynthetic hypothesis (see Scheme 17). The carbonyl α-hydrogen in a polypeptide is not as acidic as a typical carbonyl α-hydrogen due to the geminal electron-donating amine. However, the α-hydrogen of a α-phthalimido carbonyl has a lower pKa than the corresponding α-amino or α-amido carbonyl due to the strong electron withdrawing nature of the phthalimido group. Choosing a less electron-withdrawing protecting group could make the resulting β-hydroxy aldehyde less prone to elimination.

Unfortunately, considering a less electron-withdrawing amine protecting group presents an additional complication. A competing aldol pathway exists in which the protected nitrogen atom of the enamine intermediate (cf. **5012**, formed from condensation of the *N*-protected aminoaldehyde with L-proline) acts as the nucleophilic center (**Path A**, Scheme 100). If the protected amino electron density is suitably nucleophilic, then **Path A** is dominates and electrophilic attack is favored at C1 to generate iminium ion **5013**. Protecting the amine with an electron-withdrawing group shuts down this pathway allowing the proline nitrogen to enhance the nucleophilicity at C2 resulting in high regioselectivity for the desired α-electrophilic attack to give iminium ion **5014** (**Path B**).

In an attempt to balance these complementary complications we tested the *N*-Cbz substrate, which was readily prepared by a similar sequence used to prepare **5004**. Indeed, our attempts at an L-proline-catalyzed aldol reaction with isobutyraldehyde seemed to indicate that elimination was minimal, but the rate of the reaction proceeded more slowly and greater than ca. 25% conversion was never achieved.

Scheme 100 | Competing reaction pathways for L-proline-catalyzed aldol reactions of α-amino aldehydes.

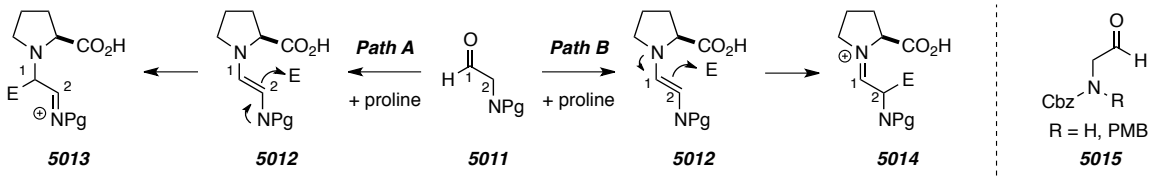

Although we were unable to prepare desired amino acid **5001** by the Barbas route, two noteworthy reports from the Evans[116] and Corey[117] labs describe alternative strategies for the stereoselective preparation of **5001**. Our prior experience with related auxiliary-based chemistry led us to follow the Evans procedure, at least initially. *N*-Acylation of oxazolidinone **5017** with bromoacetyl bromide (**5016**) gave imide **5018**. Treating **5018** with dibutylboryl triflate (DBBT) and Et_3N generated the corresponding boron enolate, which was treated with isobutyraldehyde to stereoselectively give aldol product **5019**. The aldol reaction proceeded with poor conversion, which suggests that enolate formation was inefficient in our hands. The methyl ester of 3-hydroxyleucine was prepared in three steps from the aldol product. Treating **5019** with NaN_3 gave the corresponding azide **5020** in good yield and only a single diastereomer was detected. Methoxide-mediated imide cleavage to azido ester **5021** followed by hydrogenolysis completed the synthesis of **5022**.

[116] Evans, D. A.; Sjogren, E. B.; Weber, A. E.; Conn, R. E. Asymmetric synthesis of *anti*-β-hydroxy-α-amino acids. *Tetrahedron Lett.* **1987**, *28*, 39–42.
[117] Saravanan, P.; Corey, E. A short, stereocontrolled, and practical synthesis of alpha-methylomuralide, a potent inhibitor of proteasome function. *J. Org. Chem.* **2003**, *68*, 2760–2764.

Scheme 101 | Preparation of desired a-amino methyl ester **5022** by the method of Evans.[116]

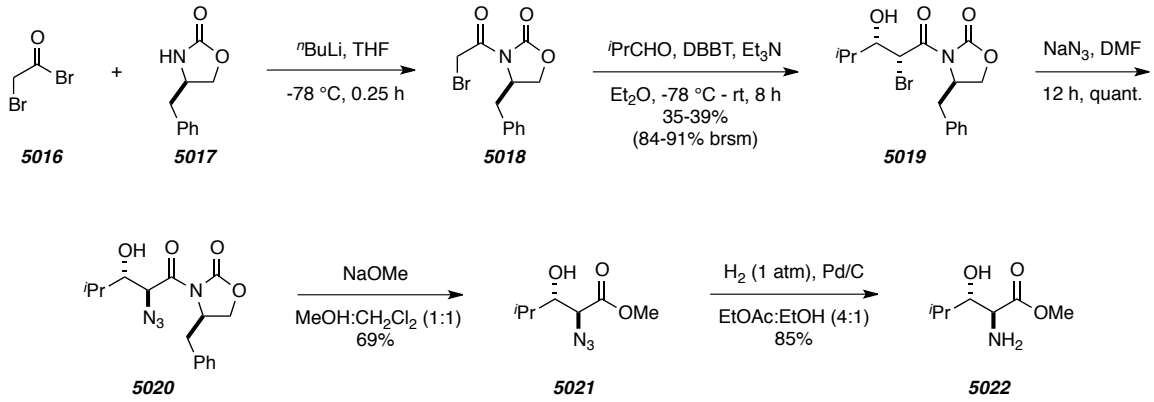

Evans' procedure provided a straightforward route to amino ester **5022**, but the aldol reaction was low-yielding and not amenable to scale up. Corey also reported a stereoselective synthesis of **5022** that utilizes Sharpless asymmetric dihydroxylation (SAD) to introduce the desired chirality. In our hands the procedure was carried out without an issues. The SAD substrate **5024** was prepared via a Doebner-modified Knoevenagel condensation of isobutyraldehyde with malonic acid, followed by Fischer esterification of the resulting acid, **5022**. SAD was carried out with in-house prepared AD-mix-β, which provided the desired diol **5025** in good yield and with excellent stereoselectivity. To finish the preparation of aminoester **5022** we reacted diol **5025** with sulfuryl chloride to give the cyclic sulfite **5026**, and subsequent Ru(III)-mediated oxidation gave sulfate **5027**. Treating **5027** with NaN_3 effected a regioselective addition to form a ring-opened sulfate intermediate, which was readily hydrolyzed to **5021** by washing with H_2SO_4.

Scheme 102 | Preparation of desired α-azido methyl ester **5021** by the method of Corey.[117]

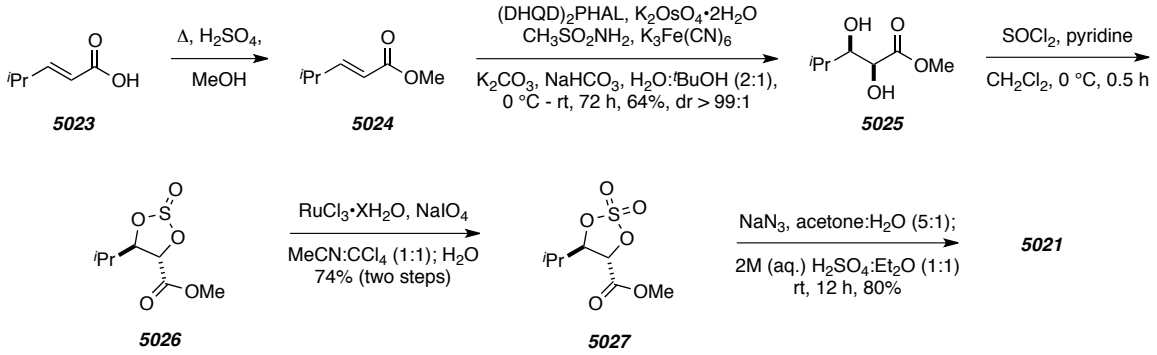

5.3. Synthesis of the Ketene Dimer Necessary for Chloroethyl Introduction

At the outset, we felt it wise to introduce the chloroethyl substituent using the ketene dimer previously reported by Romo (**1058**, Scheme 103).[42] Unfortunately, the preparation of **1058** suffers from low yields because the product arises from a [2+2] ketene-ketene cycloaddition of two different ketene intermediates. The two coupling partners are the ketenes arising from dehydrohalogenation of acetyl chloride and 4-chlorobutyryl chloride (cf. **5028** and **5029**). Cycloaddition can proceed by either a homodimerization or heterodimerization pathway. Heterodimerization of **5028** and **5029** can proceed to give two ketene dimer products (cf. **1058** and **5031**) and homodimerization would give both diketene and ketene dimer **5030**. The low yields of **1058** reported by Romo suggest that the reaction is not selective for the formation of the desired ketene dimer.

Scheme 103 | Studies of the preparation of known[42] ketene dimer **1058**.

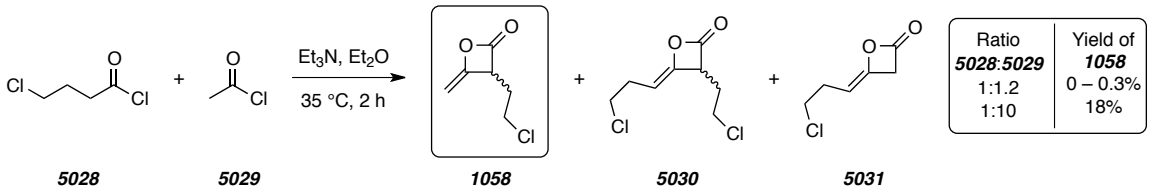

In our hands, numerous attempts provided yields that were much lower than those reported by Romo. Additionally, chromatographic purification was required to isolate the desired heteroketene dimers from the competing dimers. Separating the two heteroketene dimers required serial MPLC purifications with sample loadings >50 mg. This demonstrates that the procedure, while certainly valid, does require a great deal of skill in order to isolate **1058** in even low yields. We did find that increasing the amount of acetyl chloride from 1.2 to 10 equivalents increased the isolated yield of **1058** considerably(cf. 18% vs. 0.3%). Increasing the amount of **5029** likely increases the rate of heterodimerization relative to homodimerization of the ketene derived from **5028**. This also increases the amount of the parent diketene that is formed, but it was easily removed by evaporation. However, increasing the amount of acetyl chloride made the reaction mixture much more difficult to handle, and additional optimization is likely still necessary.

5.4. Synthesis of the Methyl Ester, *N*-PMB Analogue of the Penultimate Intermediate of Antiprotealide

Having prepared both aminoester **5022** and ketene dimer **10588** we proceeded with the synthesis of an aldol precursor similar to **5002**. Reductive amination of **5022** with *p*-anisaldehyde gave *N*-PMB amino ester **5032**, and subsequent treatment with TESCl gave α-amino ester **5033**. Treating **5033** with Romo's ketene dimer **1058** gave amido ester **5034** in good yield.

Scheme 104 | Synthesis of 3-hydroxyleucine-derived amido ester **5034**.

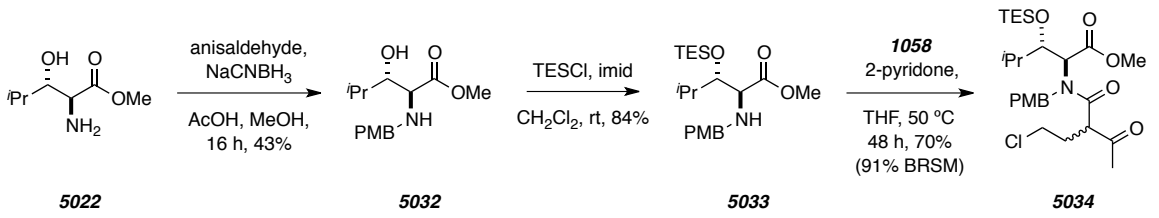

5022 ***5032*** ***5033*** ***5034***

We assumed that the desired thioester would be readily prepared by hydrolysis of **5034** and BOP-mediated thioesterification. Unfortunately, following the procedure previously developed for LiOH-mediated hydrolysis of methyl ester gave a mixture of

products. Low-resolution LC/MS of the reaction mixture suggested that elimination of HCl had occurred and that the methyl ester remained intact. This led us to propose dihydrofuran **5036** as a possible product. However, inspection of the crude ^{1}H NMR indicated that the reaction gave a complex mixture of products. Despite much effort, we were unable to isolate any discreet products. No reaction or similar results were also obtained when the reaction was attempted using *t*-BuOOLi, *n*-Bu_3SnOH, and $KOSi(CH_3)_3$. Although we spent a great deal of effort preparing **5034**, we were discouraged by our inability to hydrolyze the methyl ester and the substrate was abandoned. We thought it wise to consider alternative substrates that bore the thioester prior acetoacetylation.

Scheme 105 | Attempted hydrolysis of **5034** under standard conditions and a tentative structure for a major byproduct observed in the majority of hydrolysis attempts.

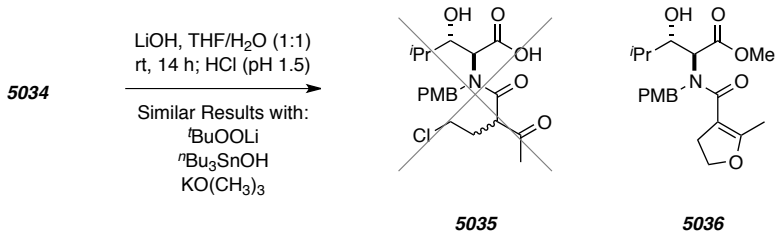

We next attempted to convert **5034** into a thioester by direct Al(III)-mediated thioesterification, even though similar reactions failed on our model substrates. Treating ester **5034** with a solution of $Al(CH_3)_3$ and thiol **5037** gave no reaction desirable reaction and the majority of the methyl ester **5034** was recovered, consistent with our previous attempts. This led us to consider a route wherein the thioester is introduced much earlier in the sequence of events. We recognized an opportunity in the Corey protocol for the synthesis of 3-hydroxyleucine by substituting methyl ester **5024** with the *n*-butyl thioester

analogue. Acid **5023** was converted into the thioester with EDCI and *n*-butanethiol.[118] Both SAD and cyclic sulfite formation proceeded as expected, but Ru(III)-oxidation to the corresponding cyclic sulfate was problematic and often gave reduced yields and complex mixtures. We were able to isolate enough of the desired cyclic sulfate to carry out the regioselective nucleophilic ring-opening with NaN_3, which cleanly gave desired azide **5038**. However, reduction of the azide to the desired aminothioester was unsuccessful despite numerous attempts with either H_2 (various pressures) and Pd/C or prototypical Staudinger reaction conditions. While were not able to identify the specific reason for the inability to isolate thioester **5039**, we felt trying to prepare the β-hydroxy-α-amino thioester was inherently problematic due to its potential for various side reaction.

Scheme 106 | Attempts at preparing a 3-hydroxyleucine-derived thioester.

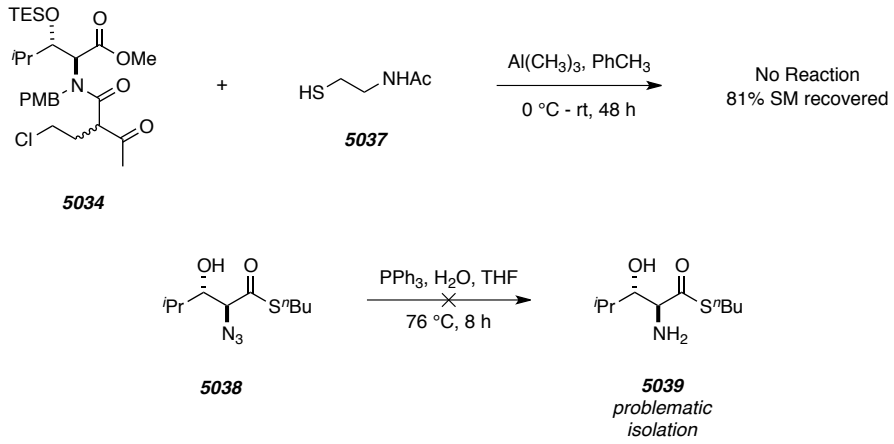

5.5. Synthesis of the *S*-Phenyl, *N*-PMB Analogue of the Penultimate Precursor to Antiprotealide

Although we were frustrated by our inability to readily prepare thioester analogue **5034**, revisiting the literature we found a report by Jackson and coworkers which

[118] *n*-Butanethiol possesses an unpleasant odor that is nearly as detectable as EtSH, however, glassware contaminated with either EtSH or BuSH can be readily de-odorized by leaving in a well-ventilated hood space for one week and then soaking overnight with bleach. I prefer both evaporation and bleaching because bleaching is slow, and I often 'missed' spots in my soaking. This was problematic when it was time to take the glassware to the sink for a thorough scrubbing. Ethanethiol should be avoided because the packing material is contaminated with trance amounts of ethanethiol, which is more difficult to manage than contaminated glass and leads to disgruntled delivery personnel.

describes the preparation of silyl-protected, *N*-Bn, α-aminothioester.[119] The report describes stereoselective ring-opening of a thionitroepoxide (cf. **5044**) by benzylamine with subsequent loss of NO_2 to give an α-aminothioester. The only alteration we opted to make was to substitute benzylamine with 4-methoxybenzylamine, but we felt this would not dramatically affect the outcome of the route. The sequence began by preparing (4-methylphenylthio)nitromethane (**5042**), which was generated by adding 4-methylbezenesulfenyl chloride[120] to *in situ*-generated sodium nitromethylate. The resulting sulfide was sequentially treated with 2 equivalents of *n*-BuLi and aldehyde **5041** was prepared from L-valine (**5040**) to give alkene **5043**. Desilylation with BF_3•Et_2O followed by hydroxy-directed epoxidation with *t*-BuOOLi and reintroduction of the silyl either protecting group with TBSOTf gave thionitroepoxide **5044**.

Scheme 107 | Synthesis of nitrothioepoxide **5044**.[119]

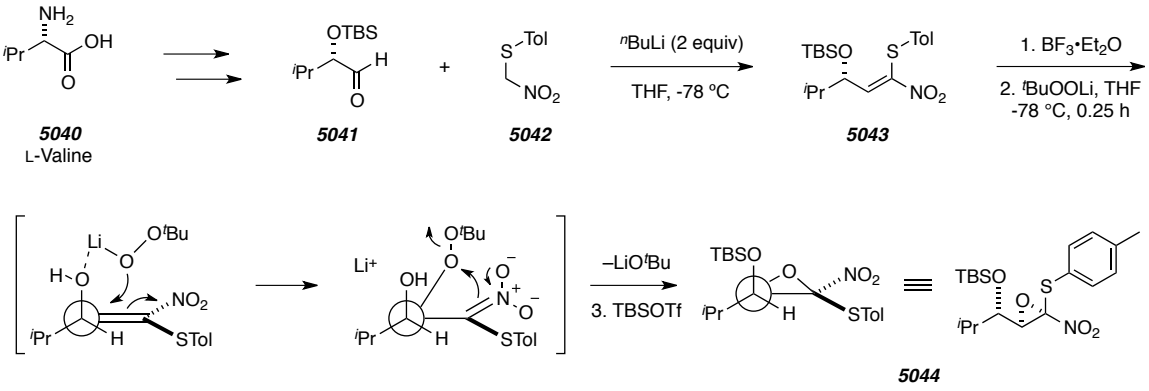

Nucleophilic addition of 4-methoxybenzylamine to epoxide **5044** did provide the desired aminothioester **5046**, however, the reaction was not straightforward. The procedure called for a biphasic medium of *n*-hexane and aqueous $NaHCO_3$ in order to provide a reaction rate that was practical without introducing side reactions. Indeed the

[119] Adams, Z. M.; Jackson, R. F. W.; Palmer, N. J.; Rami, H. K.; Wythes, M. J. Stereoselective syntheses of protected β-hydroxy-α-amino acids using (arylthio)nitrooxiranes. *J. Chem. Soc., Perkin Trans. 1* **1999**, 937–948.

[120] CAUTION! Storing benzenesulfenyl chloride neat for several weeks will result in spontaneously dimerization to form diphenyl disulfide and Cl_2. I have personally witnessed a vial explode that had pressurized from the Cl_2 gas that had formed. While the same observations have not been made for the 4-methyl analogue, caution should certainly be exercised and the reactant should be used immediately after preparation.

prescribed reaction conditions needed to be followed strictly. Namely, the reaction required 5 days of reaction time at 70 ºC with vigorous stirring for sufficient conversion to be achieved. Heating to higher temperatures led to the appearance of byproducts that included an amide resulting from bis-addition of 4-methoxybenzylamine. The reaction was extremely sensitive to the extent of phase mixing and reactions performed in smaller culture tubes provided lower conversions, which is likely due to inefficient phase mixing. Additionally, the reaction provided lower yields on scale up. Still, the reaction did provide a sufficient quantity of aminothioester **5046**, and all steps to **5046** provided yields that were in good agreement to those reported by Jackson.

Scheme 108 | Synthesis of thioester **5046** by reaction of nitroepoxide **5044** and amine **5045**.

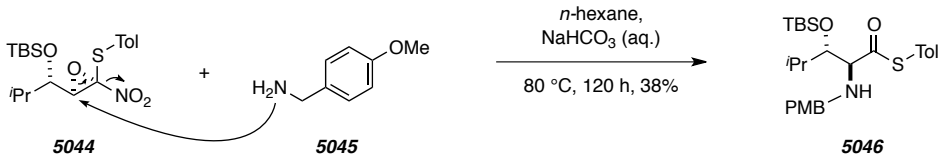

With an adequate amount of aminothioester **5046** in hand, we were now in position to complete the synthesis of our model biosynthetic precursor. Heating a solution of thioester **5046** and Romo's ketene dimer **1058** gave the desired amido thioester **5047** in good yields. Unfortunately, treating **5047** with urea **4068** provided no reaction. We considered that the bulky silyl ether might be discouraging hydrogen bonding and/or deprotonation. Desilylation of **5047** required HF•pyridine conditions, which cleanly provided β-hydroxythioester **5048**. Reaction of **5048** with urea **4068** did not occur below 80 ºC, at which point LC/MS analysis of the crude reaction mixture gave a peak with a molecular ion *m/z* that could be interpreted as a β-lactone resulting from sequential aldol lactonization of **5048**. Unfortunately, the reaction was performed on small scale (ca. 2 mg of starting thioester **5048**), and ^{1}H NMR analysis did not provide enough evidence in support of the desired product. Attempted chromatographic purification of the reaction

mixture in order to remove excess urea **4068** provided no products with the desired LC/MS behavior.

Scheme 109 | Synthesis of thioester **5048** and its attempted urea-promoted intramolecular aldol reaction with **4068**.

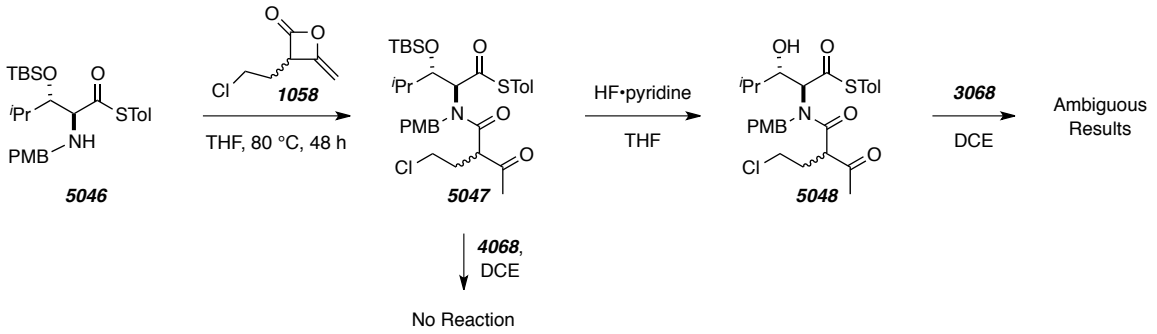

5.6. A Formal Synthesis of Salinosporamide A and Efforts Toward the Synthesis of the *S*-Phenyl, *N*-PMB Analogue of the Penultimate Precursor to Antiprotealide

At this juncture we realized that we had not yet successfully demonstrated that a β-ketoamido thioester similar to the proposed biosynthetic precursor of **1** (and antiprotealide **2**) could be converted into the corresponding natural product. Although it was unsatisfying to come so far only to encounter ambiguous results, we were still able to describe a synthesis for a congener of a biosynthetic precursor of **2** (cf. **5048**). Additionally, the crude LC/MS data was promising, which inspired us to continue studying this interesting question. A major shortcoming in our first- and second-generation synthetic approaches to **5048** was our inability to readily prepare the substrate on a practical scale.

A first step in improving the scalability of the preparation of **5048** was to find an alternative, more efficient method for introducing the chloroethyl moiety. In the course of studying the cyclopropyl-containing substrates we found that heating aminoesters with acid chloride **4104** gave the corresponding chloroethyl-containing amides (cf. **4116** to **4117**). This observation led us to consider developing the HCl-mediated ring-opening as an alternative to Romo's ketene heterodimer **1058**. Keeping Romo's studies in mind, we

realized that the serine-derived amido ester **5052** could be efficiently synthesized from **5049** and was reasonably complex to serve as an effective platform to begin our studies (Scheme 110). HCl-mediated ring opening of **5050** would give **5051** and intercept Romo's total synthesis of (–)-**1**. This would allow us to directly compare our approach to the introduction of the chloroethyl substrate to that of Romo.

Scheme 110 | Proposed formal synthesis of **1** (via **5051**)[42] and synthesis of advanced thioester model substrate **5052**.

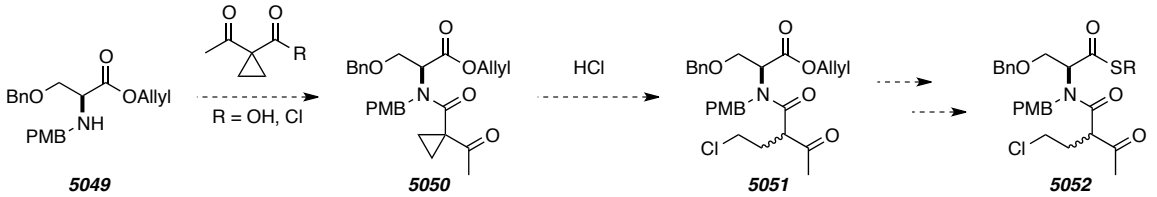

Synthesis of **5050** began with serine-derived amino ester **5049**, which was prepared from commercially available *N*-Boc-*O*-benzyl-L-serine (**5053**) by allyl ester formation, followed by acid-mediated Boc cleavage and reductive amination with *p*-anisaldehyde. Several traditional approaches to couple amine **5049** with acid **4100** were screened, including EDCI, HBTU, HATU, BOP, and DCC. EDCI was most promising because the resulting amide formation was most cleanly formed, albeit, at low conversion. Starting amine **5049** and desired amidoester **5050** co-eluted on TLC, but they were separable by careful flash chromatography.

Scheme 111 | First-generation synthesis of ester **5050**.

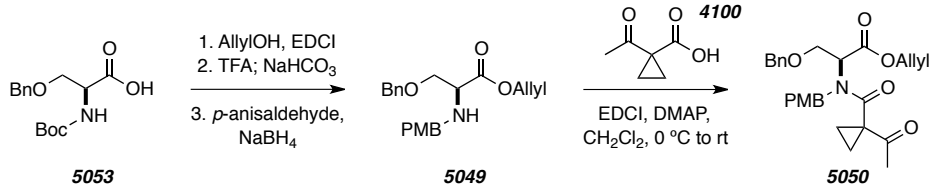

These challenges led us to consider simply heating amine **5049** with the acid chloride **4104** because previous results suggest that the major byproduct would be the chloroethyl-containing compound. This was indeed the case as heating a mixture of

amine **5049** and acid chloride **4104** gave a mixture of cyclopropyl-containing amide **5050**, chloroethyl-containing amide **5051**, in addition to small quantities of **5054**, resulting from *N*-PMB cleavage (Scheme 110-A). To ensure a higher yield of the desired chloroethyl compound we opted to strive for cleaner conditions to prepare cyclopropyl precursor **5050**. Buffering the acid halide solution with Et_3N cleanly gave desired amido ester **5050** in good yield. The use of ambient temperature and short reaction time ($t_{1/2}$ ca. 15 min) is noteworthy when compared to Romo's conditions for reaction of amino ester **5053** with ketene dimer **1058** (μW irradiation 50 ºC, 2 h; or oil-bath, 50 ºC, 48 h).[40]

Scheme 110 | Obsered products from acylation of amine **5049** with acid chloride **4014** under purely thermal and Et_3N-buffered conditions.

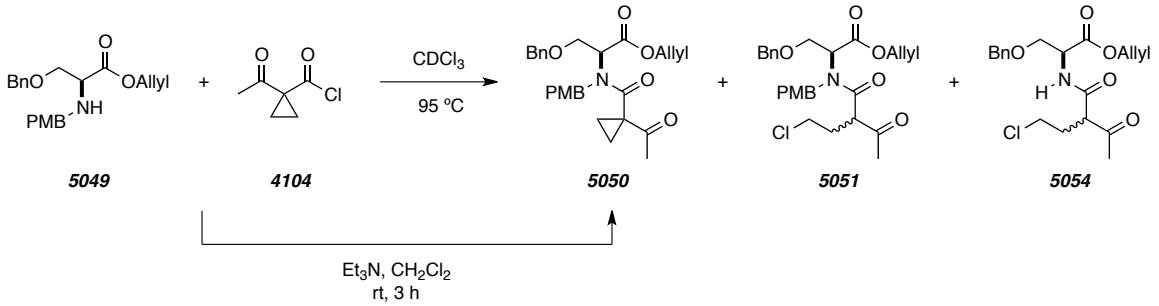

With amidoester **5050** in hand, we began optimizing conditions for the acid-mediated cyclopropane ring opening reaction. Re-subjecting **5050** to anhydrous HCl (4 M in dioxane) conditions led to poor conversion of the starting material, and prolonged heating led to increased amounts of *N*-H amidoester **5054**. Other organic acids, Brønsted acids, and transition metal Lewis acids were screened, but in all cases either poor conversion or *N*-PMB cleavage was observed. In all cases the product of *N*-PMB cleavage also possessed a chloroethyl moiety suggesting that the cyclopropane ring opening proceeds amide dealkylation. Interestingly, the conditions that provided the highest conversion with the least amount of amide dealkylation were those involving heating aminoester **5050** with acid chloride **4104**. Under these conditions the amine likely condenses with the acid chloride in the usual manner, which releases one molecule of HCl. In the majority of our attempts we used an excess of HCl to improve conversion.

This suggests that decreasing the HCl loading to stoichiometric levels might reduce the amount dealkylation.

When one to five equivalents of HCl was added, the reaction proceeded very slowly, and when the reaction temperature was increased, dealkylation with loss of PMB was observed. After screening myriad conditions we found that heating acid chloride **4104** with amine **5049** gave the largest ratio of **5051**:**5054** (ca. 5:1). We speculated that the *in situ* generated HCl was buffered by something in the reaction mixture. When considering that the reaction was carried in CH_2Cl_2, we were left with only amide-containing products esters **5050** and **5051**. We felt that it was possible that the amides were able to buffer low amounts of HCl and prevent dealkylation. Heating an authentic sample cyclopropyl amidoester **5050** in an equivolume mixture of DMF and anhydrous HCl (4 M in 1,4-dioxane) gave the desired chloroethyl-containing amido ester **5051** as a mixture of diastereomers in good yield.

Scheme 111 | Synthesis of chloroethyl-containing amidoester **5051** by HCl-mediated cyclopropane ring opening.

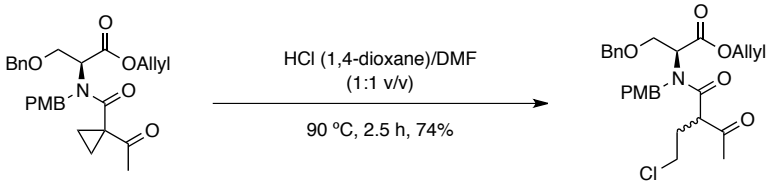

5050 ***5051***

Because reaction between amine **5049** and acid chloride **4104** gives rise to both amides **5050** and **5051**, we considered preparing **5051** from amine **5049** by a two-step, one-pot procedure (Scheme 112). Treating amine **5049** with acid chloride **4104** at 95 ºC for 1 h gave a mixture of **5050** and **5051** with only a trace amounts of **5054**. The reaction mixture was diluted in DMF and an excess of anhydrous HCl (4 M 1,4-dioxane) was added. After heating for an additional 3 h, LC/MS and TLC analysis indicated that the reaction mixture completely converted to **5051**. Overall, the procedure gave the desired chloroethyl-containing amido ester, **5051**, in comparable yields to the two-pot procedure

(ca. 75% yield for both acylation and ring opening). Following Romo's procedure,[40] the mixture of diastereomers was separated by MPLC (7:3 hexanes:EtOAc) to give **5055** and **5056**. Because Romo used the D-serine of **5049**, we had prepared the enantiomers of those reported by Romo. Comparison of our supporting data for **5055** showed the ^{1}H and ^{13}C NMR spectral data was identical to that reported by Romo, and the optical rotation was opposite in sign. This demonstrates that we had achieved a formal synthesis of salinosporamide A [(+)-**1**]. It should be mentioned that use **5056** under Romo's conditions would provide the biologically active enantiomer of the natural product, (–)-**1**. In an attempt to improve the ratio of **5055**:**5056**, we treated amidoester **5050** with a mixture of tetraalkylammonium chlorides and variety of chiral Brønsted acids, but the ratio of epimers **5055** and **5056** that were produced was near equimolar in all cases.

Scheme 112 | One-pot procedure for the preparation of **5051** and seaparation of C-2' diastereomers by MPLC.

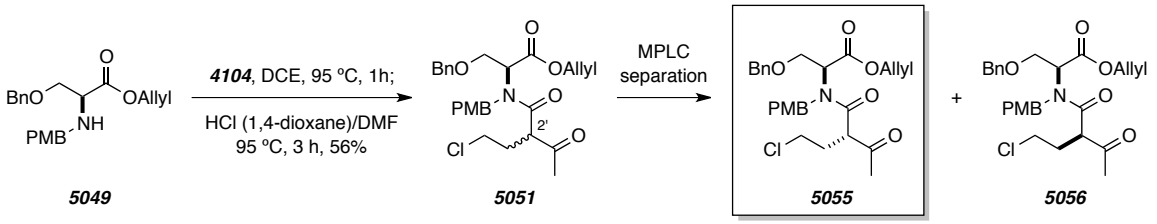

5049 *5051* *5055* *5056*

With a seemingly improved approach for the introduction of the chloroethyl-bearing acetoacyl group, we were in a position to prepare a larger quantity of our biomimetic aldol substrate (cf. amido thioester **5047**). Unfortunately, treating previously prepared amine **5046** with acid chloride **4104** in the presence of DIEA gave a low yield of the desired cyclopropane-containing thioester **5057** (Scheme 113). Also treating amine **5057** with acid chloride in the absence of base gave a mixture of products, which, crude ^{1}H NMR analysis indicates contains only a trace amount of the desired amidoester **5047**. Although some material was recovered, our current, limited understanding of the acid-mediated cyclopropane ring opening suggests that additional model studies need to be carried out before using more of our precious material.

Scheme 113 | Efforts toward the synthesis of aldol precursor **5047** by acylation of **5046** with **4104** and subsequent HCl-mediated ring opening.

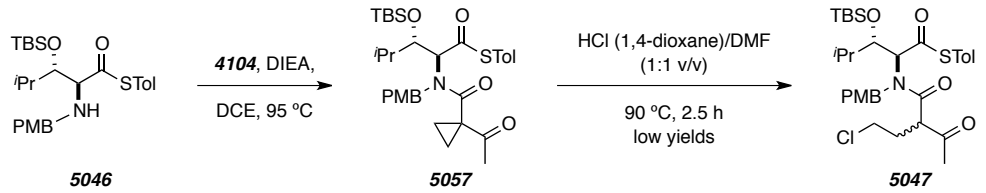

5.7. Future direction and concluding remarks to our efforts to carryout a biomimetic synthesis of salinosporamide A

Fortunately, the studies presented in Chapter 5 have resulted in more interesting questions. There is still much that could be accomplished with regard to our approach to a biomimetic synthesis of the salinosporamides. An alternative, and likely easier, approach to preparing the elusive biosynthetic precursor includes treating methyl amidoester **5032** (likely protected at OH) with acid halide **4104** under buffered conditions to prevent ring-opening and *N*-PMB cleavage (Scheme 114). The resulting product **5058** should be amenable to LiOH-mediated ester hydrolysis to give acid **5059**. The cyclopropane moiety would likely preclude the decomposition pathway that was observed in the chloroethyl analogue, **5034** (Section 5.4, Scheme 105). Performing HCl-mediated ring opening on **5059** under the conditions optimized for the conversion of **5050** into **5051** would give rise to acid **5060**, which should be amenable to thioesterification to give **5047**.

Scheme 114 | Proposed alternative route to biometic precursor **5047** via late-stage introduction of the thioester moiety.

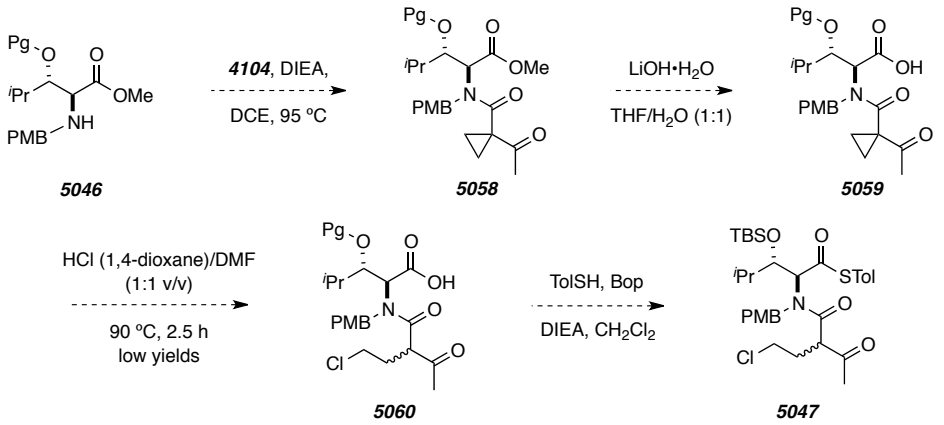

Our ability to utilize acid halide **4104** in the formal synthesis of **1** provides an opportunity to prepare a series of unique analogues of **1** that are potentially biologically active. For example, application of Romo's methodology would allow for the synthesis of **5061** from **5050**, albeit, as a racemic mixture. Although we were unable to open the cyclopropane of lactam **4114** (Scheme 95) under acidic conditions, an opportunity still exists for base-mediated ring opening under biological conditions following interaction of **5061** with the 20SP. Such an event would intercept the same THF-containing intermediate formed when **1** complexes with the 20SP (cf. **1009** in Figure 2).

Additionally, in an attempt to prepare the corresponding precursor (cf. **5062**, **Scheme 114**) to fluorosalinosporamide (**5063**),[28h] we heated a mixture of HF•pyridine and amide **5050**. Unfortunately, only dealkylation of the *N*-PMB group was observed and the cyclopropane remained intact. Still, other fluoride sources could be screened for the opportunity to prepare **5062**. As previously mentioned (see Section 1.3), substituting the C-3 methyl group of **1** with ethyl (cf. salinosporamide I, **1011**) dramatically decreases the potency for inhibition of the 20SP. To date, no analogues other than the naturally occurring **1011** have been isolated or prepared. Although, it seems unwise to consider substituents larger than a methyl group, hydrogen and trifluoromethyl analogues of acid chloride **4104** (cf. **5065**) could be prepared from the corresponding known *t*-butyl esters

5064 (R = H,[121] and CF_3[122]). These would each allow for the preparation of the C-3 H, and CF_3 analogues of **1** (cf. **5066**). The hydrido and trifluoromethyl analogues of **5061** could also be prepared if the cyclopropane-containing substrate, **5061**, showed promising biological activity (cf. **5067** R = H, CF_3).

Scheme 115 | Potentially biologically active analogues of **1** that could be readily prepared using the methodology described in Chapter 5.

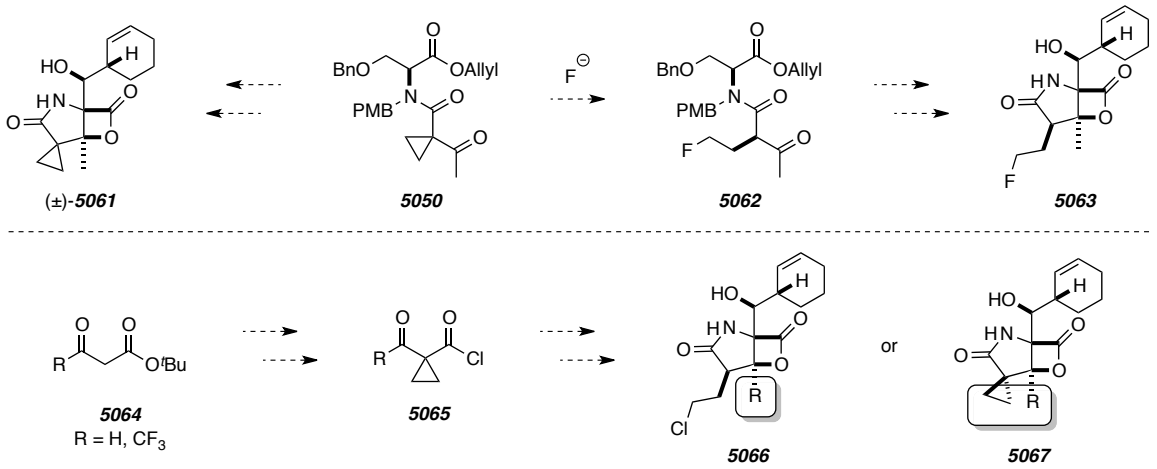

With access to a substrate Romo used in his total synthesis of **1**, we have an opportunity to consider an alternative aldol-lactonization route. The Romo total synthesis is the most efficient synthetic sequence from the perspective of step count, but the overall yields suffer due to the ketene dimer preparation and the key aldol-lactonization event.[8b] We have already improved the introduction of the chloroethyl moiety, but the aldol-lactonization route could be improved with respect to yield and stereoselectivity. Alternative nucleophiles could be probed for their ability to influence the stereoselectivity. Based on Romo's mechanistic studies, chiral DMAP-derivatives (e.g., Fu ferrocene complexes[58]) are most likely to have the strongest influence. Alternative

[121] Padwa, A.; Dean, D. C.; Osterhout, M. H.; Precedo, L.; Semones, M. A. Synthesis of functionalized azomethine ylides via the Rh(II)-catalyzed cyclization of α-diazo carbonyls onto imino π-bonds. *J. Org. Chem.* **1994**, *59*, 5347–5357.

[122] Morita, Y.; Kamakura, R.; Takeda, M.; Yamamoto, Y. Convenient preparation of trifluoroacetyl Meldrum's acid and its use as a building block for trifluoromethyl-containing compounds. *Chem. Commun.* **1997**, 359–360.

substrates to Romo's acid (**1061**, Scheme 10) could also be considered. An obvious example would the thioester analogue, which could be treated with amine to induce an intramolecular aldol reaction with spontaneous lactonization under the conditions presented in Chapter 4 of this Thesis. Still, the thioester is likely only decreasing the pKa of the α-hydrogen atom at C-2, and electron-deficient oxyesters may also be amenable (e.g., phenylesters or 2,2,2,-trifluoroethylesters).

◊ Part II ◊

Hexadehydro-Diels–Alder (HDDA) Reaction Cascade

Chapter 6. Studies of HDDA-Generated Arynes with Intramolecular Trapping

6.1. Introduction and Background to the History of *o*-Benzyne and Related Arynes

1,2-Dehydrobenzene or *o*-benzyne (**3**, Scheme 116) is among the earliest chemical reactive intermediates to be discovered and developed.[123] *o*-Arynes are the broader class of strained triple bond-containing aromatic compounds.[124] With hindsight, the first reaction involving an aryne was reported in 1902 by Stoermer and Kahlert.[125] The authors reported that treating 3-bromobenzofuran (**6001**) with ethanolic KOH gave a mixture of 2- and 3-ethoxybenzofuran (**6003** and **6004**). To account for the formation of **6003** the authors proposed intermediacy of **6002**, which is capable of reacting with ethoxide at either C-2 or C-3. It is interesting to consider that the authors boldly, and correctly, proposed an, at the time unprecedented, intermediate that possessed a strained triple bond within a fused bicyclic aromatic ring system.

Scheme 116 | The structure of *o*-benzyne (**3**) and early reports that propose the intermediacy of arynes (cf. **6002**) (adapted from ref 125).

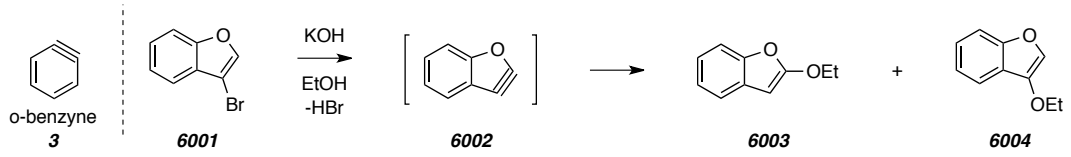

In 1927, Bachmann and Clarke were the first to propose the intermediacy of *o*-benzyne (**6006**, Scheme 117) or "free phenylene."[126] The authors found that adding Na(0) to refluxing chlorobenzene (**6005**) gave myriad products including triphenylene (**6007**) and biphenyl (**6008**). The authors implied that the reaction conditions were producing the

[123] Hoffman, R. W. *Dehydrobenzene and Cycloalkynes*; Organic Chemistry, A Series of Monographs 11; Academic, 1967.
[124] Wenk, H. H.; Winkler, M.; Sander, W. One century of aryne chemistry. *Angew. Chem. Int. Ed.* **2003**, *42*, 502–528.
[125] Stoermer, R; Kahlert, B. Ueber das 1- und 2-brom-cumaron. *Ber. Dtsch. Chem. Ges.* **1902**, *35*, 1633–1640.
[126] Bachmann, W. E.; Clarke, H. T. The mechanism of the Wurtz-Fittig reaction. *J. Am. Chem. Soc.* **1927**, *49*, 2089–2098.

diradical reactive intermediate **6006** (an open-shell resonance structure of benzyne), which trimerized to give **6007**. It was later shown by Wittig that the formation of biphenyl (**6008**), which was also isolated by Bachmann and Clarke in the same reaction mixtures that gave **6007**, likely proceeds via singlet *o*-benzyne.[127]

Scheme 117 | Earliest report of a process that involves **3** as an intermediate (adapted from ref 126).

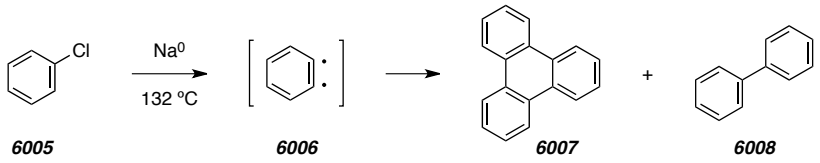

The proposed structure of **3** contains two identical sp-hybridized carbon atoms. In 1945, Gilman found that reaction of $NaNH_2$ with 2-chloroanisole (**6009**) gave *m*-anisidine (**6011**) as the major product (Scheme 118-A).[128] Aryne intermediate **6010** is proposed to account for the net substitution at C-3 instead of C-2. With hindsight, this demonstrates that haloarenes form benzyne by dehydrohalogenation, by the general mechanism shown in Scheme 118-B. The amide anion likely induces dehydrohalogenation to generate an aryne similar to **3**. Nucleophilic addition of another equivalent of amide then occurs at either of the two reactive sp-hybridized carbon atoms to give an aryl anion (cf. **6013**), which is neutralized to give the benzenoid product (cf. **6014**). The electronics of the methoxy group of aryne **6010** likely discourage nucleophilic addition to C-2. More definitive evidence that demonstrated the intermediacy of **3** came from the Roberts labs in 1953 (Scheme 118-C).[129] The authors treated chlorobenzene-1-^{14}C (**6015**) with $NaNH_2$ and isolated both aniline-1- and 2-^{14}C isotopers (**6017** and **6018**, respectively). This demonstrates that parent *o*-benzyne contains two equally reactive

[127] Wittig, V. G.; Phenyl-lithium, der Schlüssel zu einer neuen Chemie metallorganischer Verbindungen. *Naturwissenschaften* **1942**, *30*, 696–703.
[128] Gilman, H.; Avakian, S. Dibenzofuran. XXIII. Rearrangement of halogen compounds in amination by sodamide. *J. Am. Chem. Soc.* **1945**, *67*, 349–351.
[129] Roberts, J. D.; Simmons, H. E., Jr.; Carlsmith, L. A.; Vaughan, C. W. Rearrangement in the reaction of chlorobenzene-1-C^{14} with potassium amide. *J. Am. Chem. Soc.* **1953**, *75*, 3290–3291 and references cited therein.

carbon atoms and the ^{14}C labeled intermediate is an unsymmetrical variant of **3**. These results led the authors to conclude that **3** is a highly strained, cyclic alkyne.

Scheme 118 | A) Evidence for the involvement of aryne **6010** by the unexpected formation of *m*-anisidine from *o*-chloroanisole (adapted from ref 128). B) Mechanism for the reaction of chlorobenzene with sodium amide to give the net substitution product (adapted from ref 124). C) ^{14}C-Labeling studies demonstrate that **3** is a symmetrical intermediate with two degenerate, highly reactive carbon atoms (adapted from ref 129).

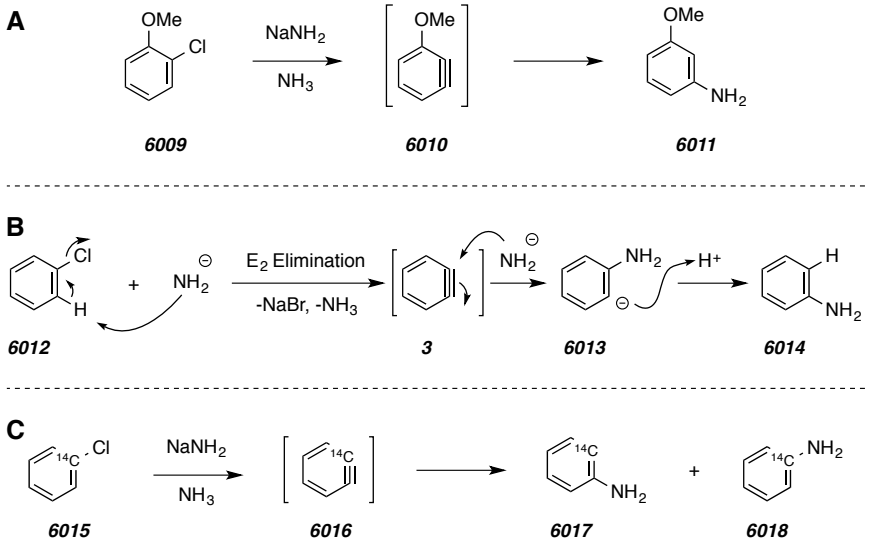

The structure of **3** contains two vicinal sp-hybridized carbon atoms and could be described by four additional, unique resonance structures (cf. **6006**, **6019**, **6020**, and **6021**, Figure 11). Investigations by Leopold[130] into the photoelectron spectral properties indicate that the LUMO of **3** is an alkyne π* orbital. Furthermore, the singlet-triplet splitting was found to be ca. 38 kcal•mol^{-1}, which is consistent with singlet **3** as opposed to the open-shell diradical **6006**.[130] In 1992, Radziszewski[131] measured the IR absorption frequency of the carbon-carbon triple bond to be 1846 cm^{-1}. Collectively, these data suggests that **3** is the major contributing resonance structure of *o*-benzyne. This is

[130] Leopold, D. G.; Miller, A. E. S.; Lineberger, W. C. Determination of the singlet-triplet splitting and electron affinity of *o*-benzyne by negative ion photoelectron spectroscopy. *J. Am. Chem. Soc.* **1986**, *108*, 1379–1384.

[131] Radziszewski, J. G.; Hess, B. A., Jr.; Zahradnik, R. Infrared spectrum of *o*-benzyne: Experiment and theory. *J. Am. Chem. Soc.* **1992**, *114*, 52–57.

consistent with the myriad of reagents that clearly react with **3** via concerted cycloaddition or ionic stepwise pathways.[123,124]

Figure 11 | Various resonance contributors to the structure of **3**.

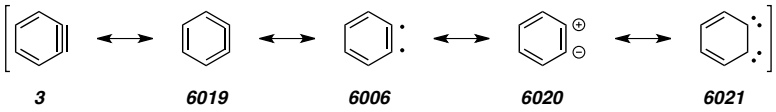

Beyond its theoretical intrigue, **3** has also been a valuable reactive intermediate for the preparation of myriad benzenoids (i.e. benzene-containing molecules). Trapping **3** efficiently gives rise to benzenoids with diverse structures that would be challenging to prepare by convention approaches. Having been discovered over sixty years ago, the scope of trapping methods is now tremendously broad and has been used in the preparation of, for example, fine organics, natural products, and polymers. These methods have been extensively reviewed,[123,124] and, for the most part, have been omitted from this Thesis. In general, **3** reacts with most nucleophiles, π-donors, and 1,3-dipoles.

6.2. A Brief Review of Common Methods for Generating *o*-Benzyne

Developments in the practical application of arynes in organic synthesis have been extensive and consistently remarkable. The evolution of methods that utilize these intermediates has been greatly influenced by the discovery of new methods for their practical generation. Shortly after Roberts confirmed the unorthodox structure of *o*-benzyne,[129] several alterative approaches to the generation of **3** were described (summarized in Figure 12).[132] In addition to the treatment of simple aryl halides with strong base (cf. **6022**, entry 1), *o*-dihalides have also been shown to react with *n*-BuLi or Mg(0) to form aryne intermediates (cf. **6023**, entry 2). Fluoroarenes can be metallated to form either the aryl lithium or aryl Grignard reagents (cf. **6024** and **6025**, entries 3 and 4). Each of these has been shown to react with a variety of aryne-trapping reagents at low temperatures, which demonstrates milder alternatives for the preparation of **3**. A yet even

[132] a) Tadross, P. M.; Stoltz, B. M. A comprehensive history of arynes in natural product total synthesis. *Chem. Rev.* **2012**, *112*, 3550–3577. b) Gampe, C. M.; Carreira, E. M. Arynes and cyclohexyne in natural product synthesis. *Angew. Chem. Int. Ed.* **2012**, *51*, 3766–3778.

milder approach to the transition metal-mediated generation of **3** includes Pb(IV)-mediated oxidation of 2-aminobenzotriazole at room temperature (cf. **6026**, entry 5).[133]

Figure 12 | Classic methods for the generation of **3** (adapted from ref 132a).

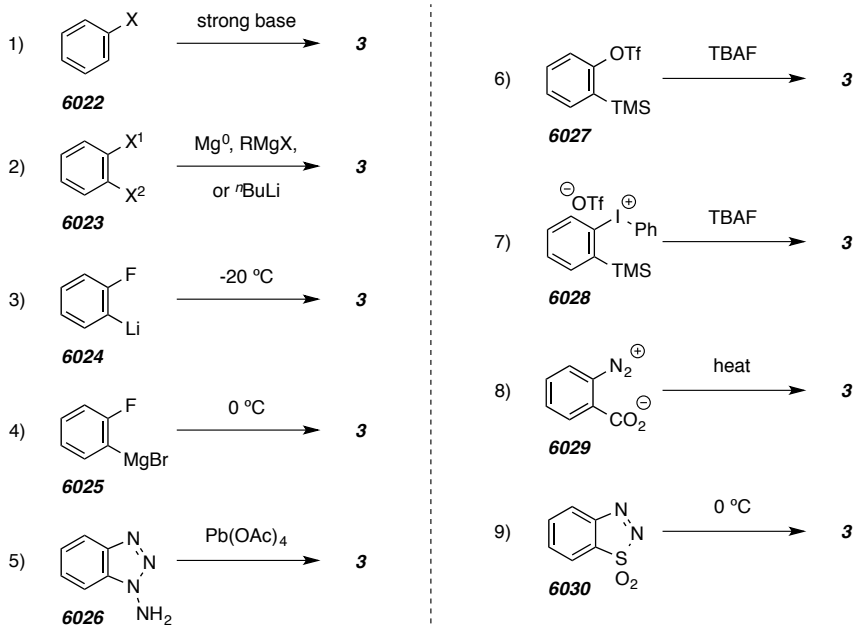

In 1983, Kobayashi and co-workers reported that treating *o*-trimethylsilylphenyl triflate (**6027**, cf. entry 6 of Figure 12) with a variety of fluoride sources in the presence of furan gave products resulting from cycloaddition with intermediate **3**.[134] The fluoride-mediated conditions necessary to effect benzyne generation were much milder than the strongly basic conditions. Additionally, the straightforward preparation of more complex *o*-trimethylsilyl triflate-containing benzenoids has allowed for the application of benzyne reactivity in the synthesis of natural products.[132] For example, Stoltz and co-workers generated an aryne from *o*-trimethylsilylaryl triflate **6031** and trapped the intermediate with β-ketoester **6032** to give the fused tetracyclic benzenoid **6033** (Scheme 119).[135] The

[133] Campbell, C. D.; Rees, C. W. Reactive intermediates. Part I. Synthesis and oxidation of 1- and 2-aminobenzotriazole. *J. Chem. Soc., C* **1969**, 742.
[134] Himeshima, Y.; Sonoda, T.; Kobayashi, H. Fluoride-induced 1, 2-elimination of *o*-trimethylsilylphenyl triflate to benzyne under mild conditions. *Chem. Lett.* **1983**, 1211–1214.
[135] Tambar, U. K.; Ebner, D. C.; Stoltz, B. M. A Convergent and enantioselective synthesis of (+)-amurensinine via selective C−H and C−C bond insertion reactions. *J. Am. Chem. Soc.* **2006**, *128*, 11752–11753.

authors subsequently demonstrated that **6033** could be converted into the biologically active natural product amurensinene (**6034**) in eleven steps.

Scheme 119 | Stoltz's approach to the application of Koboyashi's method for aryne generation to the total synthesis of (+)-amurensinene (adapted from ref 135).

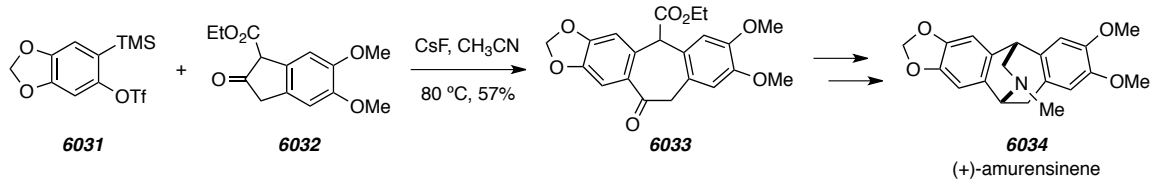

In addition to the Kobayashi reagent **6027**, Kitamura has demonstrated that phenyl[*o*-(trimethylsilyl)phenyl]iodonium triflate (**6028**, cf. entry 7 of Figure 12) will also cleanly form *o*-benzyne in the presence of a mild fluoride source.[136] The authors demonstrate that aryne trapping is efficient and that the resulting benzenoids are obtained in high yield. The authors argue that the preparation of **6028** is also more straightforward than that of **6027**, which may suggest that **6028** is a superior reagent for the generation of arynes. However, the preparation of **6027** has been further optimized[137] and the reagent is now commercially available from Aldrich.

In 1960, Stiles and Miller demonstrated that **3** could be generated by thermal decomposition of *o*-benzenediazonium carboxylate (cf. **6029**, cf. entry 8 of Figure 12) with mild heating (ca. 50 ºC).[138] This discovery allowed **3** to be studied in the absence of additional reagents providing the opportunity to study the reactivity of **3** with potential trapping reagents that are sensitive to, for example, strongly basic conditions or transition metals. The authors used **6029** to cleanly generate and trap **3** with both benzoic acid and *t*-butanol under otherwise neutral reaction conditions.

Because carboxylate **6029** is insoluble in many organic solvents, Wittig and Hoffmann described the preparation and thermal decomposition of diazosulfonamide

[136] Kitamura, T.; Yamane, M. (Phenyl)[*o*-(trimethylsilyl)phenyl]iodonium triflate. A new and efficient precursor of benzyne. *Chem. Commun.* **1995**, 983–984.
[137] Bronner, S. M.; Garg, N. K. Efficient synthesis of 2-(trimethylsilyl)phenyl trifluoromethanesulfonate: A versatile precursor to *o*-benzyne. *J. Org. Chem.* **2009**, *74*, 8842–8843.
[138] Stiles, M.; Miller, R. G.; Burckhardt, U. Reactions of benzyne intermediates in non-basic media. *J. Am. Chem. Soc.* **1963**, *85*, 1792–1797.

6030 into **3** at 10 ºC.[139] The improved organic solubility of **6030** was advantageous, but isolation and handling of both **6029** and **6030** is difficult and hazardous due to the explosive diazo moiety. Safer alternatives include diphenyl-iodonium-2-carboxylate (thermolysis at 160 ºC)[140] and phthalic anhydride (thermolysis microwave flash pyrolysis at 300 ºC for ca. 1 min).[141]

Collectively, the arsenal of methods that have been developed for the generation of **3** have armed the chemistry community with the ability to exploit the unique reactivity of this interesting intermediate. The reagent-free nature of the methods that allow for thermal *o*-benzyne generation is advantageous, and allows for investigations of the trapping by otherwise unstable reactants. Additionally, eliminating reagents necessary for aryne generation will minimize the potential for side-reactions, which would complicate crude reactions mixtures and ultimately reduce reaction efficiencies. However, preparation of the precursors is difficult and/or hazardous, and is not amenable to arynes more complicated than *o*-benzyne itself. Because of these shortcomings, the Kobayashi reagent has been the most utilized reagent for the generation of **3**.[142] Still, a reagent that is i) simple to prepare, ii) not explosive, and iii) generates *o*-benzyne under mild thermal conditions would further expand the utility of aryne intermediates in organic synthesis.

6.3. Our Serendipitous Encounter with a Novel Method for Generating Arynes

The studies presented in this section, and sporadically throughout the rest of Chapters 6 and 7 have been recently disclosed in *Nature*.[143] In order to tell a complete story, portions of the published story have been included even though the author of this Thesis did not personally carry out the experiments. Only data for the experiments performed by the author of this Thesis have been included in the experimental. For an otherwise unrelated study, a postdoctoral research assistant in our group, Beeraiah Baire,

---

[139] Wittig, G.; Hoffmann, R. W. 1,2,3-Benzothiadiazole 1,1-dioxide. *Org. Syn.* **1967**, *47*, 4–9.
[140] Le Goff, E. Aprotic generation of benzyne from diphenyliodonium-2-carboxylate. *J. Am. Chem. Soc.* **1962**, *84*, 3786–3786.
[141] Cho, H. Y.; Ajaz, A.; Himali, D.; Waske, P. A.; Johnson, R. P. Microwave flash pyrolysis. *J. Org. Chem.* **2009**, *74*, 4137–4142.
[142] Kitamura, T. Synthetic Methods for the Generation and Preparative Application of Benzyne. *Aust. J. Chem.* **2010**, *63*, 987.
[143] a) Hoye, T. R.; Baire, B.; Niu, D.; Willoughby, P. H.; Woods, B. P. The hexadehydro-Diels–Alder reaction. *Nature* **2012**, *490*, 208–212. Niu, D.; Willoughby, P. H.; Woods, B. P.; Baire, B.; Hoye, T. R. Alkane desaturation via concerted double hydrogen atom transfer to benzyne. *Nature* **2013**, *accepted*.

was attempting to prepare ketotetrayne **6036** (Scheme 120) by oxidation of the corresponding allylic alcohol **6035**. However, treating **6035** with MnO_2 gave an unexpectedly low yield of the undesired *trans* enone and a separable byproduct with an LC/MS molecular ion identical to the molecular weight of enone **6036**. After extensive NMR analysis, the structure of the byproduct was assigned to indenone **6037**. Evidence for the arylsilane moiety was present in the ^{1}H NMR spectrum by the downfield shift of the dimethylsilyl resonances from 0.1 to 0.36 ppm. Evidence for the formation of the benzenoid core was provided by the ^{13}C NMR spectrum, which included several peaks with δ values in the range for aromatic carbons of ^{13}C NMR spectrum, which indicated that the product was highly aromatic. Additionally, only two resonances corresponding to alkynes were observed.

Scheme 120 | Our initial finding that tetrayne **6035** undergos oxidation to ketotetrayne **6036** with subsequent cycloisomerization to aryne intermediate **6038**/**6039** and trapping (via **6040**) to form benzenoid **6037**.

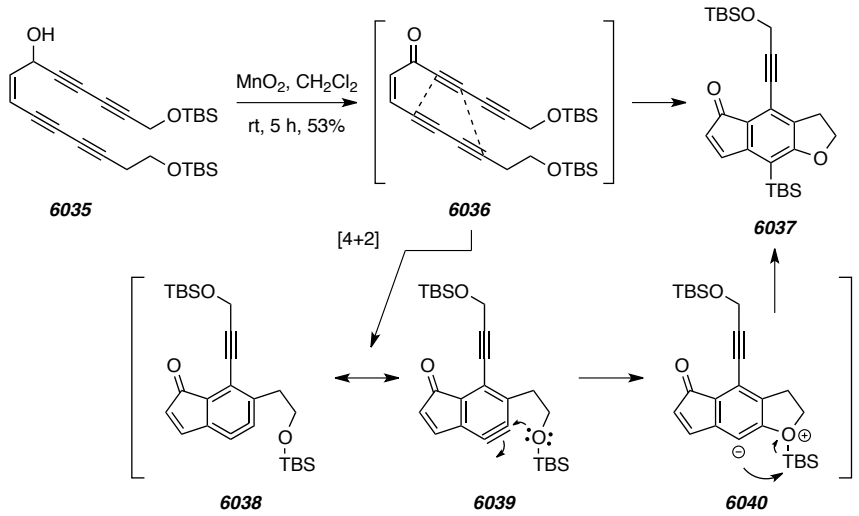

To account for the formation of **6037**, it was assumed that the MnO_2 oxidation was proceeding as predicted, but that *cis*-enone **6036** was further rearranging to indenone **6037**. The formation of **6037** is remarkable for several reasons. First and foremost, three of the alkynes of the starting enone have been transformed into a benzene ring. Secondly, the silyl ether has been cleaved to give rise to a 2,3-dihydro-1-benzofuran and an

arylsilane motif. To account for the conversion of the silyl ether into the arylsilane, we invoked aryne intermediate **6039**. To account for **6039**, we propose a net [4+2] cycloaddition between an alkyne and a conjugated diyne. If a prototypical [4π +2π] mechanism is assumed, then cycloaddition would give rise to a highly strained cyclic cumulene (cf. **6038**). Interestingly, the cumulene ring system is just a less-often considered resonance structure of *o*-benzyne. To account for formation of the product **6037** we propose that the aryne intermediate could engage the nucleophilic oxygen of the silyl ether to form zwitterion **6040**, which could undergo an oxygen-to-carbon migration and give rise to the indenone product. While unprecedented, the mechanism of the aryne-mediated silyl ether cleavage is reminiscent of a retro-Brook[144] rearrangement.

Reflecting on our unexpected preparation of indenone **6037** led us to consider possible reasons for the moderate 53% yield. MnO_2 oxidation of alcohol **6035** was complicated by *E*/*Z*-alkene isomerization as evidenced from isolation of the corresponding *trans* olefin. Additionally, tetrayne **6036** possesses two triyne units that are capable of reacting via differing [4+2] cycloaddition pathways. The pathway that ultimately gives rise to the observed product **6037** (see Scheme 121) proceeds via an aryne containing a suitable, well-positioned silyl ether to trap the reactive intermediate. However, the other cycloaddition pathway gives rise to aryne intermediate **6042** (and cyclic cumulene **6041**), which contains a silyl ether that is only four atoms away from the reactive aryne. If the same trapping mechanism would occur, then the product would result in a strained fused aryloxetane (cf. **6043**). The inherent strain of **6043** or the unflavored four-atom transition structure necessary for its formation would likely prevent the trapping event from even occurring. If aryne **6042** was not efficiently trapped, then we would expect the reactive intermediate to decompose via rapid bimolecular side reactions to give intractable byproducts. Because of these reasons it is not surprising that we were unable to obtain evidence that the alternative cycloaddition pathway was even occurring.

---

[144] Bailey, W. F.; Jiang, X. Stereochemistry of the cyclization of 4-(*t*-butyldimethyl)siloxy-5-hexenyllithium: *cis*-Selective ring-closure accompanied by retro-[1,4]-Brook rearrangement. *ARKIVOK* **2005**, *6*, 25–32.

Scheme 121 | A proposed mechanism for an alternative diyne-alkyne [4+2] cycloaddition of ketotetrayne **6036** to form aryne **6041**/**6042**, which is unable to be cleanly trapped by the pendant silyl ether to form **6043**.

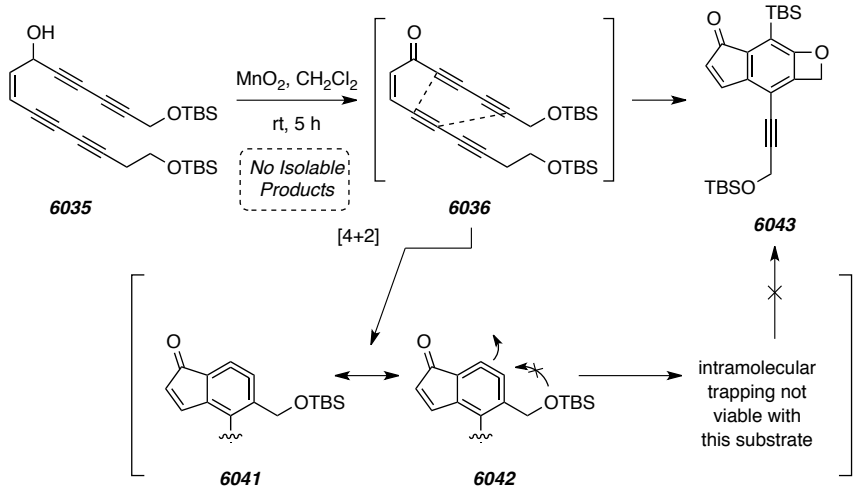

To preclude both *E*/*Z*-alkene isomerization and a second mode of [4+2] cycloaddition we opted to prepare cyclohexene-containing *tri*yne **6048** (Scheme 122). We predicted that eliminating these potential side reactions should lead to increased yields for the benzenoid product. Triyne **6048** was prepared in three steps and with excellent yield from enal **6044** and diyne **6045**. Sonagashira coupling of **6044** with **6045** gave aldehyde **6046** in good yield with a small contamination by the dimer of **6045**. Treating **6046** with *in situ*-generated lithium (trimethylsilyl)acetylide gave the corresponding propargyl alcohol **6047** in near quantitative yield. Oxidation of **6047** with MnO_2 at ambient temperature gave a mixture of the expected ketotriyne **6048** in addition to tetracyclic benzenoid **6049**. The mechanism for the formation of **6049** is likely the same one that was operative in the preparation of indenone **6037**. Specifically, diyne-alkyne [4+2] cycloaddition of **6048** gives an aryne intermediate, which is trapped by the pendant silyl ether to give tetracyclic indenone **6049**. When the mixture of **6048** and **6049** was kept at ambient temperature and monitored by TLC, we found that all of ketotriyne **6048** had converted into benzenoid **6049**. Subsequent chromatographic purification gave the benzenoid in 92% isolated yield from alcohol **6047**.

Scheme 122 | Synthesis of ketotriyne **6048** and its room temperature conversion into benzenoid **6049**.

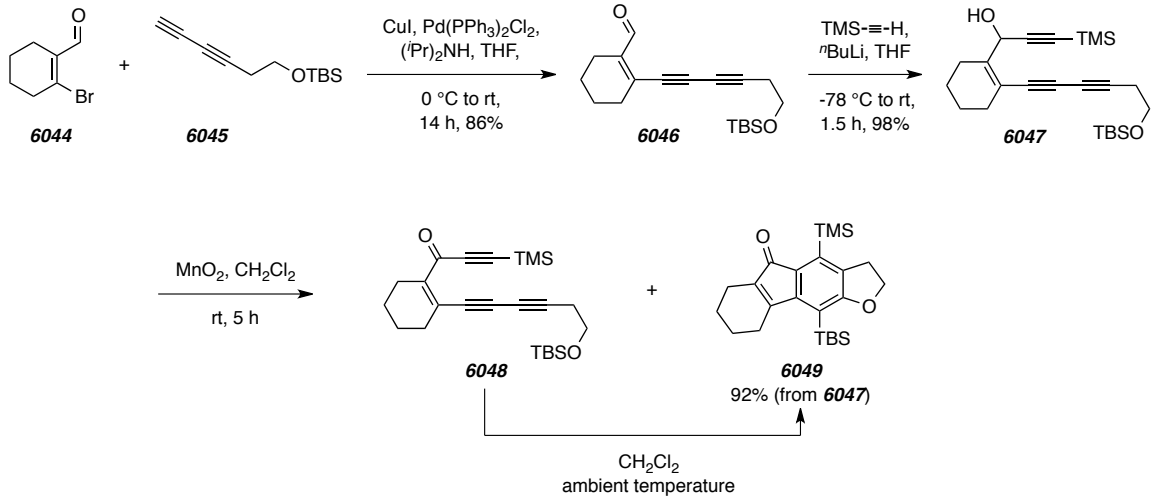

To better understand the kinetics of the cycloisomerization, we performed the MnO_2 oxidation of **6047** at 0 ºC, rapidly filtered through Celite®, and concentrated on a rotary evaporator with a 0 ºC ice-bath to ensure minimal cycloisomerization of the ketotriyne **6048** (Scheme 123). With this approach we were able to cleanly isolate and fully characterize **6048**. It is worth mentioning that performing the reaction under standard Swern conditions provided less pure crude samples of **6048**, and attempted chromatographic purification was complicated by the ensuing cycloisomerization. With a pure sample of **6048**, we studied the rate of cycloisomerization in $CDCl_3$ at ambient temperature by submerging an NMR tube containing the reaction mixture into an oil-bath set to 26 ºC. ^{1}H NMR spectral data of the reaction mixture were collected at several time intervals, which indicated that the $t_{1/2}$ for the cycloisomerization was ca. 7 h at 26 ºC. After 46 h, the conversion was found to be greater than 95% so the mixture was concentrated and purified to give the tetracyclic indenone **6049** in 93% yield. These results clearly demonstrate that a triyne is capable of cycloisomerizing without additional reagents (e.g., MnO_2), and the reaction is inherently very efficient if the substrate bears an efficient aryne trap.

Scheme 123 | "Cold" oxidation of ketotriyne **6048** and its reagent-free, room temperature conversion into benzenoid **6049**.

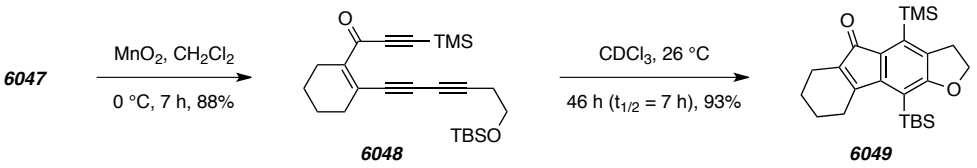

As exciting as it was to have encountered this interesting result, we were curious as to why we were unaware of reports describing related transformations. To our surprise, re-examination of the literature led us to reports from the labs of R. P. Johnson and Ikuo Ueda. In the same year, 1997, independent reports from both the Johnson[145] and Ueda[146] labs described polyyne systems that were capable of generating polycyclic aromatic hydrocarbons. Johnson and co-workers found that subjecting 1,3,8-nonatriyne (**6050**) to flash vacuum pyrolysis conditions led to a mixture of indan (**6052**) and indene (**6053**) with excellent mass recovery and a small amount of 'soot' (Scheme 124). To account for products **6052** and **6053**, the authors proposed that triyne **6050** was cycloisomerizing to form an aryne intermediate (cf. **6051**), which receives dihydrogen to give **6052**, subsequent heating was shown to induce dehydrogenation of **6052** to give **6053**. The source of dihydrogen for the generation of **6052** was unclear, but the authors cited another case where high temperatures have led to products of benzyne hydrogenation.[147]

Scheme 124 | Thermal cycloisomerizaiton of triyne **6050** (adapted from ref 145).

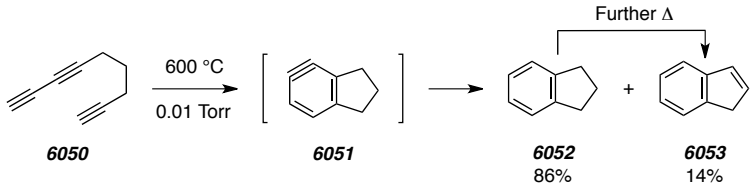

[145] Bradley, A. Z.; Johnson, R. P. Thermolysis of 1,3,8-nonatriyne: Evidence for intramolecular [2+ 4] cycloaromatization to a benzyne intermediate. *J. Am. Chem. Soc.* **1997**, *119*, 9917–9918.
[146] Miyawaki, K.; Suzuki, R.; Kawano, T.; Ueda, I. Cycloaromatization of a non-conjugated polyenyne system: Synthesis of 5*H*-denzo[*d*]fluoreno[3,2-*b*]pyrans via diradicals generated from 1-[2-{4-(2-alkoxymethylphenyl)butan-1,3-diynyl}]phenylpentan-2,4-diyn.l-ols and trapping evidence for the 1,2-didehydrobenzene diradical. *Tetrahedron Lett.* **1997**, *38*, 3943–3946.
[147] Brown, R. F.; Coulston, K. J.; Eastwood, F. W. Formation of biphenylene by elimination of C_2 from 9, 10-didehydrophenanthrene at 1100 ºC. *Tetrahedron Lett.* **1996**, *37*, 6819–6820.

In his seminal report,[146] Ueda described the preparation of tetrayne **6054** and its spontaneous conversion into benzenoids **6055** and **6056** when added to a solution of anthracene with Et_2O and THF co-solvents (Scheme 125). To account for the formation of **6055** and **6056**, the authors proposed that monocyclization of tetrayne **6054** ensues to give an equilibrating mixture of diradical intermediates **6058** and **6059**. Both of these diradical intermediates undergoes a second cyclization to give 1,2-dehydroarene diradicals **6060** and **6061**, each of which is trapped by anthracene to give **6055** and **6056**, respectively. When no trapping reagent was present the authors report observing the formation arene **6057**, but details regarding the reaction rate, storage temperature and reaction medium were omitted in the report. Additionally, the authors reported that tetrayne **6054** also cycloisomerized into other interesting polycyclic aromatic hydrocarbons with mechanisms similar to those that we propose for the silyl ether cleavage (see Scheme **120**). In several follow-up reports, Ueda demonstrated similar reactions of polyalkyne systems with interesting applications including, for example, DNA cleavage.[148]

[148] a) Miyawaki, K.; Kawano, T.; Ueda, I. Multiple cycloaromatization of novel aromatic enediynes bearing a triggering device on the terminal acetylene carbon. *Tetrahedron Lett.* **1998**, *39*, 6923–6926. b) Ueda, I.; Sakurai, Y.; Kawano, T.; Wada, Y.; Futai, M. An unprecedented arylcarbene formation in thermal reaction of non-conjugated aromatic enetetraynes and DNA strand cleavage. *Tetrahedron Lett.* **1999**, *40*, 319–322. c) Miyawaki, K.; Kawano, T.; Ueda, I. Domino thermal radical cycloaromatization of non-conjugated aromatic hexa- and heptaynes: Synthesis of fluoranthene and benzo[*a*]rubicene skeletons. *Tetrahedron Lett.* **2000**, *41*, 1447–1451. d) Kawano, T.; Inai, H.; Miyawaki, K.; Ueda, I. Synthesis of indenothiophenone derivatives by cycloaromatization of non-conjugated thienyl tetraynes. *Tetrahedron Lett.* **2005**, *46*, 1233–1236. e) Kawano, T.; Inai, H.; Miyawaki, K.; Ueda, I. Effect of water molecules on the cycloaromatization of non-conjugated aromatic tetraynes. *Bull. Chem. Soc. Jpn.* **2006**, *79*, 944–949. f) Kawano, T.; Suehiro, M.; Ueda, I. Synthesis and inclusion properties of 6,6′-Bi(benzo[*b*]fluoren-5-ol) derivative by cycloaromatization. *Chem. Lett.* **2006**, *35*, 58–59. g) Kimura, H.; Torikai, K.; Miyawaki, K.; Ueda, I. Scope of the thermal cyclization of nonconjugated ene–yne–nitrile system: A facile synthesis of cyanofluorenol derivatives. *Chem. Lett.* **2008**, *37*, 662–663. h) Torikai, K.; Otsuka, Y.; Nishimura, M.; Sumida, M.; Kawai, T.; Sekiguchi, K.; Ueda, I. Synthesis and DNA cleaving activity of water-soluble non-conjugated thienyl tetraynes. *Bioorgan. Med. Chem.* **2008**, *16*, 5441–5451.

Scheme 125 | Thermal HDDA cycloisomerization of tetrayne **6054** and its initially proposed mechanism involving diradical interemediates (adapted from 146).

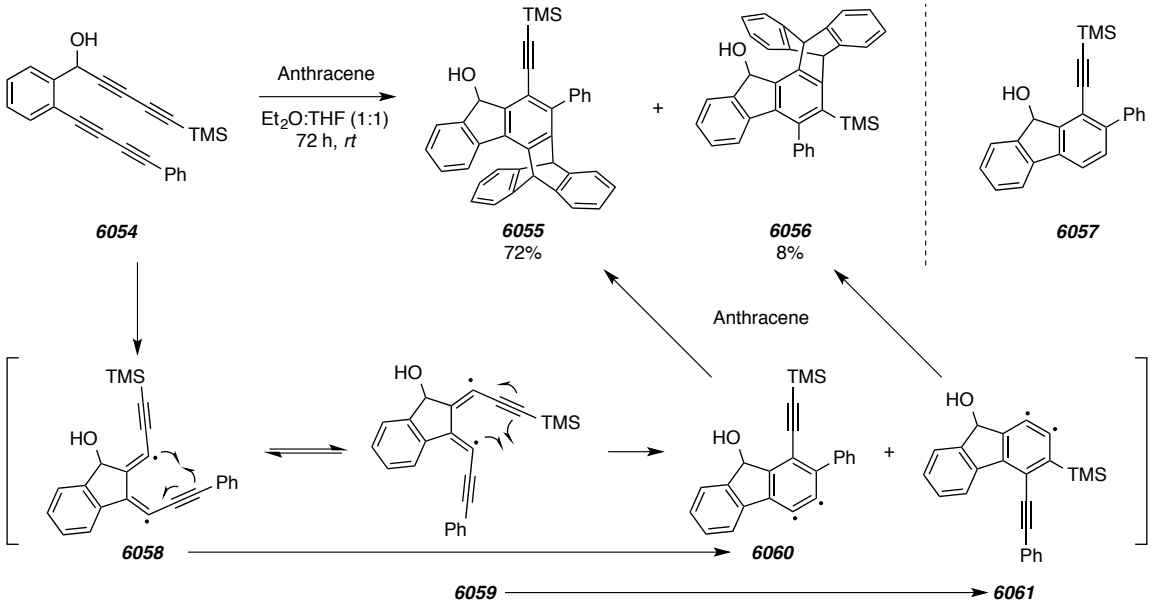

More recently, Sterenberg and co-workers reported the chemical properties of bis-diyne-bridged, dinuclear metal complex **6062** (Scheme 126).[149] They found that *in situ* generation of **6062** in furan and THF cleanly gave strained cyclic alkynes **6064** and **6065**, respectively. The authors proposed that **6062** readily undergoes intramolecular [4+2] cycloaddition to form aryne intermediate **6063**, which is rapidly trapped by furan via [4+2] cycloaddition to form **6064**. To account for the formation of **6065** the authors proposed that aryne **6063** abstracts hydrogen from THF. The authors repeated the experiment in THF-d_8, which gave rise to the dideuterated analogue of **6065** and strongly supported their claim that THF is the source of hydrogen. The authors propose that the aryne-forming reaction is proceeding by a concerted [4+2] cycloaddition mechanism, which they concede is a process that is expected to have a large activation barrier. However, highly organized, metal-templated precursor, **6062**, brings the reacting diynes

[149] Tsui, J. A.; Sterenberg, B. T. A metal-templated 4 + 2 cycloaddition reaction of an alkyne and a diyne to form a 1,2-aryne. *Organometallics* **2009**, *28*, 4906–4908.

to within 3.2 Å of one another, which is within the known "reactivity threshold" for related systems.[150]

Scheme 126 | The HDDA reaction in the context of a bis-diyne-bridged, dinuclear metal complex (cf. **6062**).

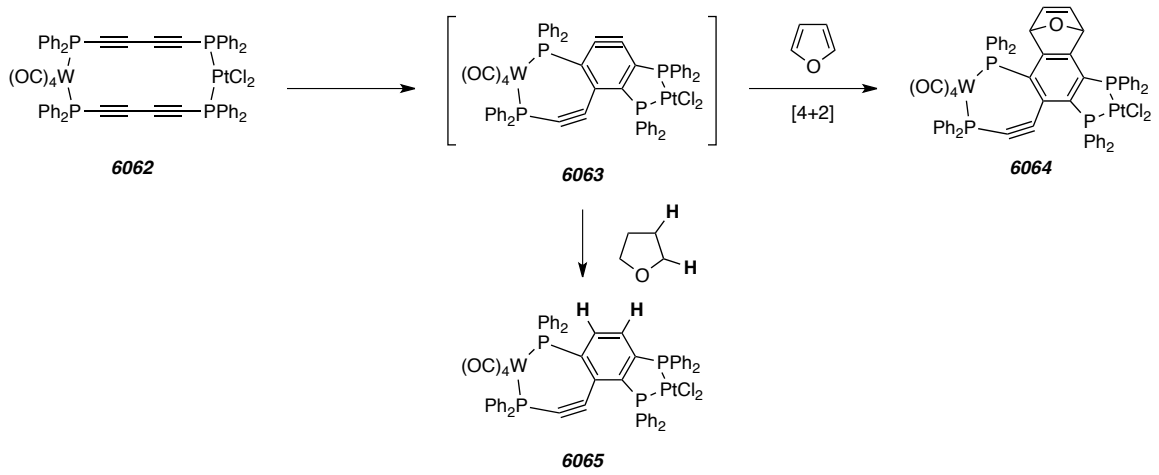

The diyne-alkyne [4+2] cycloaddition could proceed by two potential mechanisms: i) a concerted pathway that proceeds in the same manner as the textbook Diels–Alder reaction, and ii) a stepwise pathway that involves one or more diradical intermediates (cf. Ueda's proposed mechanism in Scheme 125). While a concerted pathway seems unlikely when considering the highly strained transition structure necessary for such a transformation, Houk and co-workers reported theoretical support for alkyne vibrational modes that give rise pseudo *E* and *Z* geometries (cf. **6068** and **6069**, Scheme 127).[151] With these studies in mind, we propose that the concerted mechanism for [4+2] cycloaddition between acetylene (**6066**) and 1,3-butadiyne (**6067**) could proceed through a transition structure where the alkynyl moieties have adopted a pseudo *Z* geometry (cf. **6070**).

[150] Tsui, J. A.; Bolton, T. M.; Sterenberg, B. T. Tungsten coordination chemistry of 1,4-bisdiphenylphosphinobutadiyne–synthesis of coordination macrocycles and factors controlling diyne cycloaddition. *Can. J. Chem.* **2009**, *87*, 197–204.

[151] Strozier, R. W.; Caramella, P.; Houk, K. N. Influence of molecular distortions upon reactivity and stereochemistry in nucleophilic additions to acetylenes. *J. Am. Chem. Soc.* **1979**, *101*, 1340–1343.

Scheme 127 | Proposed reactive geometries (cf. **6068** and **6069**), and transition structure (**6070**) for the concerted HDDA cycloisomerization.

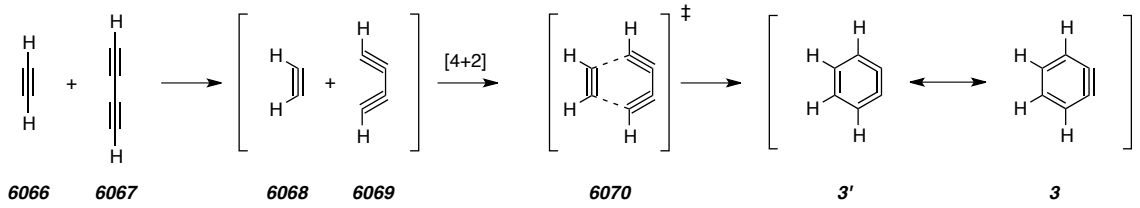

In a recent report, Johnson and co-workers computed the energetics for the aryne formation and found that both concerted and stepwise mechanisms are kinetically viable.[145,152] It should be mentioned that the Johnson report describes a stepwise pathway that involves a single diradical intermediate. Results from a recent report by Tantillo suggest that when computing mechanisms that involve vinyl radical intermediates, both *E* and *Z* isomers need to be considered.[153] The computational analysis put forth by Johnson was performed on the parent system (acetylene + 1,3-butadiyne), wherein, *E* and *Z* vinyl radical isomers are not applicable. In more complex settings, consideration of the possible radical intermediates in the stepwise mechanism for the diyne-alkyne [4+2] cycloaddition will likely affect the difference in reaction barriers between the two proposed mechanisms.

Regardless of whether the generation of aryne intermediates from triyne precursors is concerted or stepwise, the net result is an example of an additional mode the Diels–Alder [4+2] cycloaddition. The normal mode of the Diels–Alder reaction involves the reaction of an alkene with a diene, and as Johnson[152] and we[143] have pointed out, there are a total of four modes of the Diels–Alder [4+2] cycloaddition reaction. The textbook example of ethylene (**6071**) reacting with 1,3-butadiene (**6072**) is shown in Figure 13-A. If an alkyne (cf. **6066**) is used as the dienophile, then [4+2] cycloaddition would give rise to an nonconjugated cyclohexadiene (cf. **6074**). The product

[152] Ajaz, A.; Bradley, A. Z.; Burrell, R. C.; Li, W. H. H.; Daoust, K. J.; Bovee, L. B.; DiRico, K. J.; Johnson, R. P. Concerted vs stepwise mechanisms in dehydro-Diels–Alder reactions. *J. Org. Chem.* **2011**, 9320–9328

[153] Siebert, M. R.; Osbourn, J. M.; Brummond, K. M.; Tantillo, D. J. Differentiating mechanistic possibilities for the thermal, intramolecular [2 + 2] cycloaddition of allene−ynes. *J. Am. Chem. Soc.* **2010**, *132*, 11952–11966.

cyclohexadiene contains two fewer hydrogen atoms compared to cyclohexene, the product of the standard Diels–Alder reaction.[154] Hence, we refer to this process as the didehydro-Diels–Alder reaction (cf. reaction of the parent system show in Figure 13-B).[143] If the diene is substituted with an enyne (cf. **6075**), then reaction with an alkyne dienophile would give rise to a cyclic allene intermediate (cf. **6076**), which spontaneously undergoes [1,5] hydrogen shift to generate a benzenoid (cf. **6077**).[154] We refer to this process as the *tetra*dehydro-Diels–Alder reaction because the cyclic allene resulting from the initial [4+2] cycloaddition contains four fewer hydrogen atoms than cyclohexene (cf. the parent system shown in Figure 13-C). Cycloaddition of a triyne system similar to those encountered by us, Johnson, Ueda, and Sterenberg generates an aryne intermediate that contains six fewer hydrogens than cyclohexene (cf. Figure 13-D). For this reason we refer to the alkyne-diyne [4+2] cycloaddition to an aryne (cf. **3'** and **3**) intermediate and its subsequent trapping as the *hexa*dehydro-Diels–Alder (HDDA) reaction.[143] The cycloaddition reaction that comprises the HDDA reaction involves formation of an aryne, which must be trapped. For this reason we commonly refer to the overall process as the HDDA reaction cascade.

[154] Wessig, P.; Müller, G. The dehydro-Diels−Alder reaction. *Chem. Rev.* **2008**, *108*, 2051–2063.

Figure 13 | Several reported modes for the [4+2] Diels–Alder cycloaddition; A) The prototypical Diels–Alder reaction, B) The didehydro-Diels–Alder reaction, C) the tetradehydro-Diels–Alder reaction, and D) the hexadehydro-Diels–Alder (HDDA) reaction cascade.

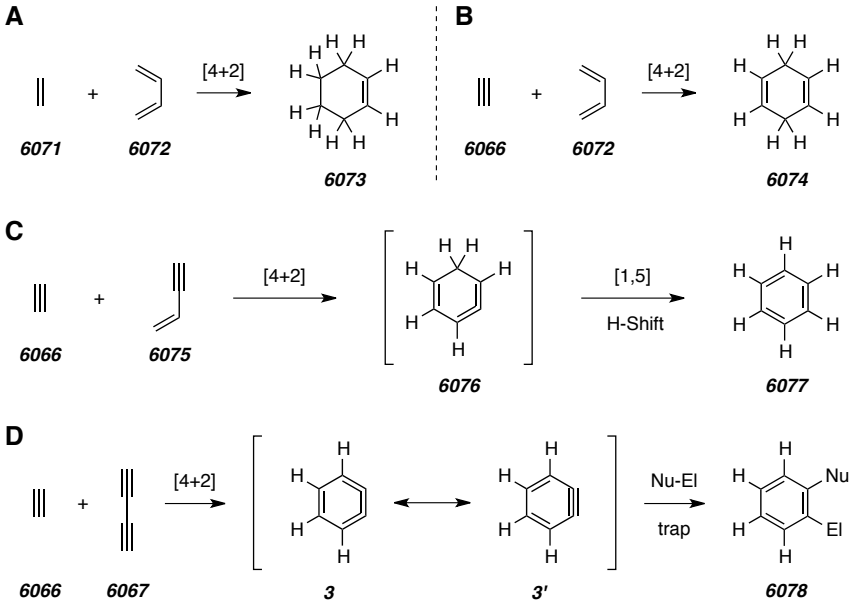

The reports by Johnson and Ueda were pioneering, but there is still much to be done to further develop this interesting cycloaddition. We viewed our discovery that indenones are readily formed from triyne precursors as an excellent opportunity to probe the limits and scope of the HDDA reaction. We often joked that if we had prior knowledge of the extreme conditions used by Johnson, and/or the complicated diradical intermediates proposed by Ueda we would have been dissuaded from studying the process entirely. Additionally, we were very fortunate to have encountered this transformation with substrates that i) thermally generated benzyne at ambient temperatures and ii) possessed a fortuitously positioned aryne-trapping group. Had our initial substrate lacked either of these traits then we would have either observed low

conversion or a complex mixture of products. Overall, our initial discovery represents yet another example of scientific breakthroughs being guided by serendipitous discovery.[155]

6.4. Initial Scope of Substrates Amenable to HDDA Cycloisomerization with Silyl Ether- and Hydroxy-Mediated Aryne Trapping

While mechanistically very interesting, the HDDA reaction is also useful for the preparation of densely functionalized benzene rings. Altering the functional groups that tether the diyne to the monoyne represents an approach to introducing diversity in the scope of benzenoid products that can be synthesized via the HDDA reaction. Additionally, the effects of changing the tethering groups might also provide fundamental insight into the mechanism for the aryne-generating phase of the HDDA reaction. To this end, we prepared several substrates that contained different tethering functionality, and the results are summarized in Figure 14.

Allylic alcohol **6047** was acylated to give triyne **6079**. Similar to its keto variant, cycloisomerization of **6079** gave rise to tetracyclic benzenoid **6080**. However, much higher temperatures were required to effect the HDDA reaction, which suggests that conjugation with electron withdrawing groups accelerate the HDDA reaction. This was further supported when studying ether (cf. **6081**) and sulfonamide tethers (cf. **6083**), which underwent the HDDA reaction at approximately the same rate to give the corresponding benzenoids (cf. **6082** and **6084**, respectively). However substituting CO_2Et with hydrogen led to no observed conversion under the same conditions. Ester **6085** and amide **6087** triynes were also amenable to HDDA reaction to give the corresponding benzenoids **6086** and **6088**, respectively. Not surprisingly, the conformationally restricted amide **6087** underwent cycloisomerization much faster than ester **6085**. Ring systems larger than five were also prepared, where, for example, heating triyne **6089** in *o*-dichlorobenzene effected HDDA cycloisomerization to give the seven-membered ring-containing benzenoid **6090**. Similar to the silyl ether-containing triynes, alcohol-containing substrates malonate **6091** and sulfonamide **6093** also cleanly underwent HDDA cycloisomerization. Substrates **6091** and **6093** give rise to pentasubstituted benzenoids **6092** and **6094**, respectively, by a net insertion into the O–H bond of the

[155] McNally, A.; Prier, C. K.; MacMillan, D. W. C. Discovery of an α-amino C–H arylation reaction using the strategy of accelerated serendipity. *Science* **2011**, *334*, 1114–1117.

alcohol trap. In the case of malonate **6091**, trapping by the propylene alcohol gave a six-membered ring in the benzenoid product.

Figure 14 | Early studies into tether scope for the HDDA reaction cascade with intramolecular trapping by oxy-nucleophiles.

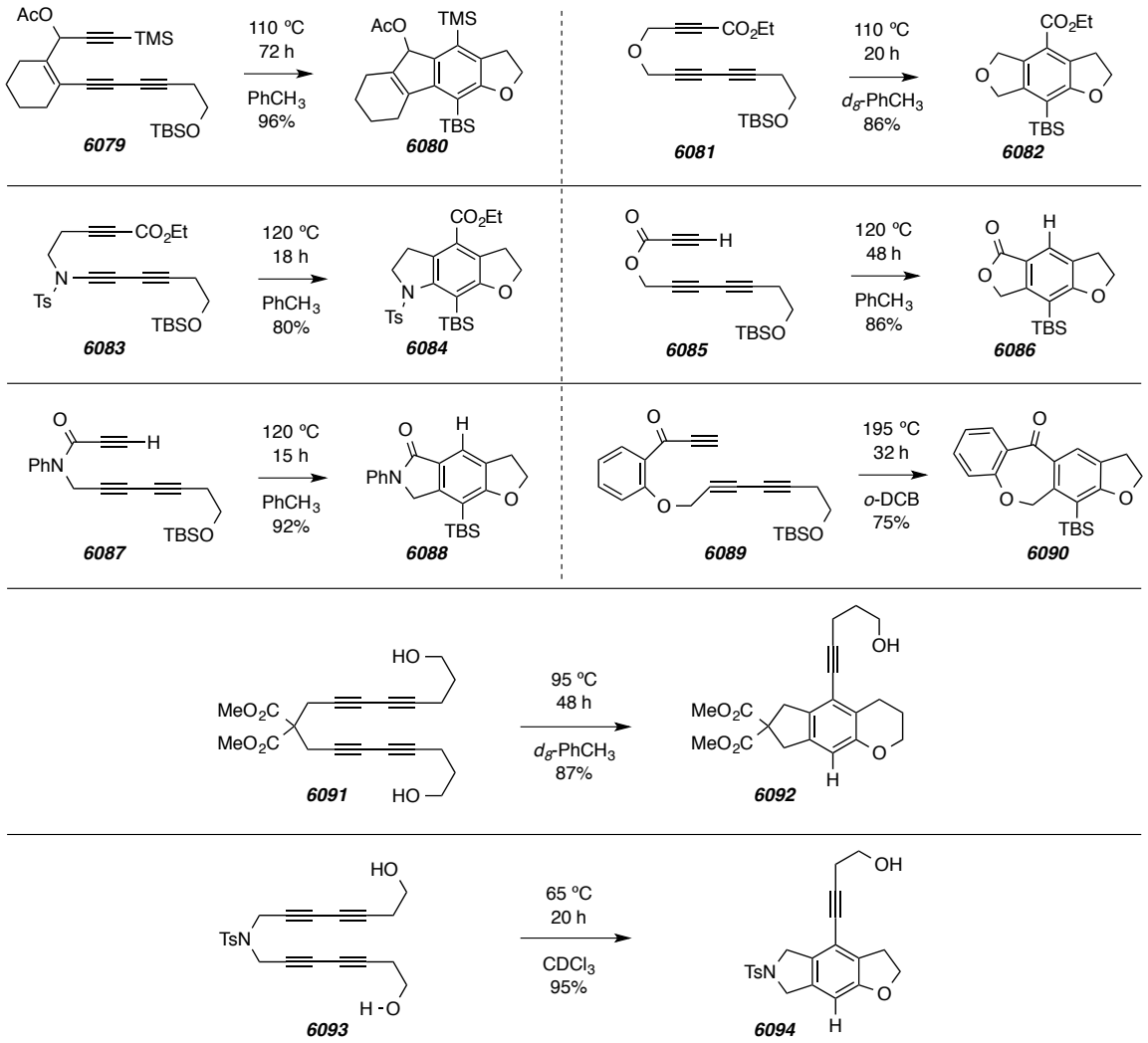

6.5. An Improved Substrate for the Synthesis of HDDA Precursors with Varying Trapping Functionalities

To begin studying new modes of intramolecular benzyne trapping, we had to prepare a substrate by which new trapping groups could be readily attached and screened. Additionally, the substrate needed to be easy to prepare and possess a convenient $t_{1/2}$ for

the aryne generation. An attractive approach was an aromatic analogue of ketotriyne **6048**, which could be prepared by Cadiot-Chodkiewicz coupling of known diyne **6098**[156] with an alkyne bearing the trapping group and subsequent MnO_2 oxidation (Scheme 128). Preparation of known diyne **6098** required Sonagashira coupling of 2-bromo-benzaldehyde (**6095**) with trimethylsilylacetylene to give arylacetylene **6096**, which was desilylated with K_2CO_3 in MeOH to give **4097**, and immediately treated with lithium trimethylsilylacetylide to give desired diyne **6098**. Rapid quenching of the acetylide addition reaction led to increased yields, which is likely because the resulting lithium alkoxide may cyclize onto the pendant alkyne. If the procedure was performed with care, diyne **6098** could be cleanly prepared in decagram quantities.

Scheme 128 | Synthesis of diyne **6098**.

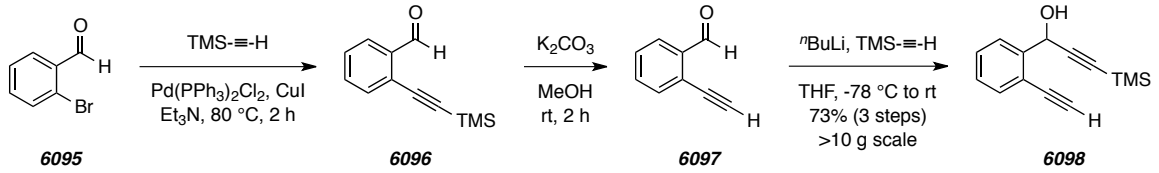

6.6. Trapping HDDA-Generated Arynes with Alkenes–The Tandem HDDA/Alder-Ene Reaction Cascade

We tested the viability of our new substrate in the context of the HDDA reaction by preparing a ketotriyne containing a novel aryne-trapping moiety. Cheng[157] and Lautens[158] independently reported instances where alkene and alkyne π-bonds react with arynes via an Alder-ene mechanism. To study this mode of aryne reactivity in the context of the HDDA reaction we coupled diyne **6098** with a bromoalkyne containing a pendant alkene (c.f., **6101**, Scheme 129) and oxidized the resulting alcohol **6102** with MnO_2 to give ketotriyne **6103**. It should be noted that **6101** was prepared by propargylation of allylic alcohol **6099** and bromination of the resulting ether, **6100**. The aromatic ketotriyne

[156] J. Suffert, E. Abraham, S. Raeppel, R. Brückner, Synthesis of 5-/10-membered ring analogues of the dienediyne core of neocarzinostatine chromophore by palladium(0)-mediated ring-closure reaction. *Liebigs Ann.* **1996**, 447–456.
[157] Jayanth, T. T.; Jeganmohan, M.; Cheng, M.-J.; Chu, S.-Y.; Cheng, C.-H. Ene reaction of arynes with alkynes. *J. Am. Chem. Soc.* **2006**, *128*, 2232–2233.
[158] Candito, D. A.; Panteleev, J.; Lautens, M. Intramolecular aryne–ene reaction: Synthetic and mechanistic studies. *J. Am. Chem. Soc.* **2011**, *133*, 14200–14203.

was readily isolated and stable at room temperature for several days. However, heating to 100 ºC for 22 h led to full conversion of **6103** to give tetracyclic fluorenone **6105**. The benzenoid is formed by HDDA cycloisomerization to give aryne **6104** (a.k.a. a fluorynone), which undergoes an intramolecular ene reaction with the pendant alkene. The reaction was clean, but the process gave of mixture of the *cis* or *trans* alkene isomers.

Scheme 129 | Synthesis of ketotriyne **6103** and subsequent HDDA reaction cascade with Alder-ene trapping to give benzenoid **6105** as a mixture of *E* and *Z* isomers.

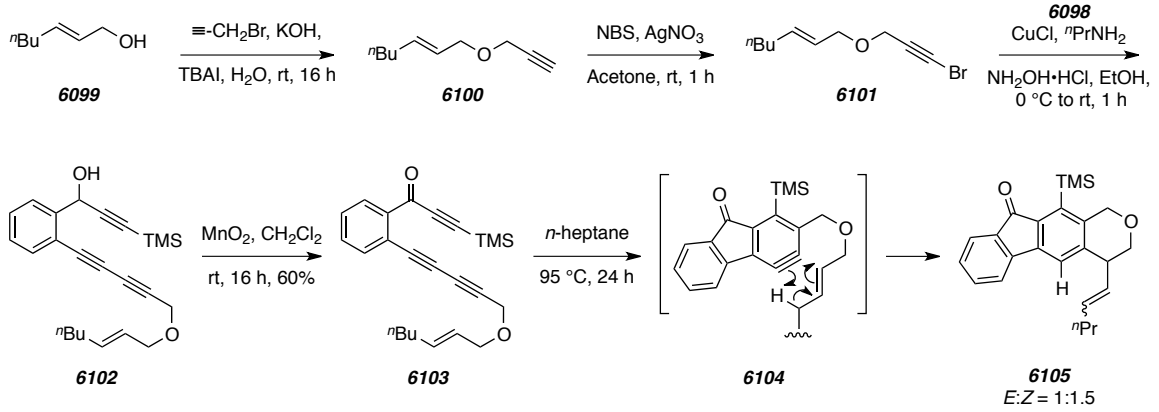

An alternative substrate, ketotriyne **6109**, was prepare in a manner similar to **6103** and it also underwent the tandem HDDA/ene reaction (Scheme 130). Specifically, the synthesis of **6109** began with bromination of ether **6106** and coupling the resulting alkynyl bromide **6107** to diyne **6098** gave alcohol **6108**. Subsequent MnO_2 oxidation of **6108** gave ketotriyne **6109**, and, similar to **6103**, it too was heated in *n*-heptane at 100 ºC. The tandem HDDA/Alder-ene reaction cascade was clean and provided the corresponding benzenoid **6111** in good yield. The previous examples of a tandem HDDA-ene reaction also demonstrate that ketotriynes with an aromatic tether are conveniently prepared, easy to handle, and readily undergo HDDA reaction (cf. $t_{1/2}$ ca. 4 h at 85 ºC). Additionally, peaks corresponding to the aromatic resonances are distinct in the ^{1}H NMR spectrum allowing for facile structure elucidation of the product. Collectively, these perspectives suggest that the aromatic tether in **6103** and **6109** is ideal for studying novel intramolecular trapping reactions of HDDA-generated arynes.

Scheme 130 | Synthesis of ketotriyne **6109** and subsequent HDDA reaction cascade with Alder-ene trapping to give benzenoid **6111** as a single product.

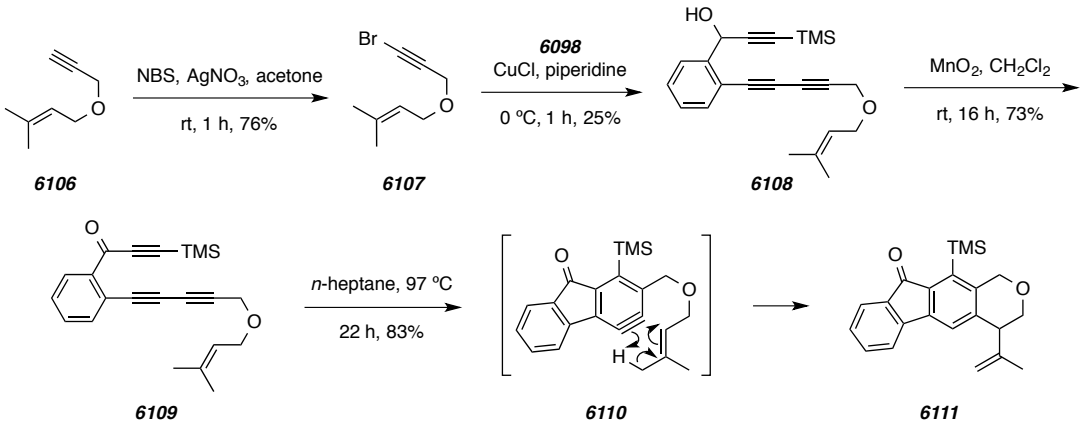

We viewed there to be additional opportunity with regard to the type of alkenes that could react with the aryne intermediates. Allylic alcohol-containing triyne **6116** was an interesting substrate because the tandem HDDA/Alder-ene process would form an enol intermediate that would spontaneously tautomerize to aldehyde **6117** (Scheme 131). Triyne **6116** was prepared by silyl ether cleavage of ketotriyne **6115**, which itself was prepared using previously-described methods. Specifically, coupling of enyne **6113** with diyne **6098** gave alcohol **6114**. The alcohol was oxidized with MnO_2 and heating in $CDCl_3$ led to conversion of resulting triyne **6116** into the aldehyde-containing benzenoid, **6117**. Again, a mechanism to account for this transformation involves HDDA cycloisomerization to form a fluorynone, which is trapped by an Alder-ene reaction with the allylic alcohol functionality to give an enol. Spontaneous enol to aldehyde tautomerization then gives rise to aldehyde **6117**.

Schem 131 | Synthesis of ketotriyne **6116** and subsequent HDDA reaction cascade with Alder-ene trapping to give aldehyde **6117** presumably via the corresponding enol (not pictured).

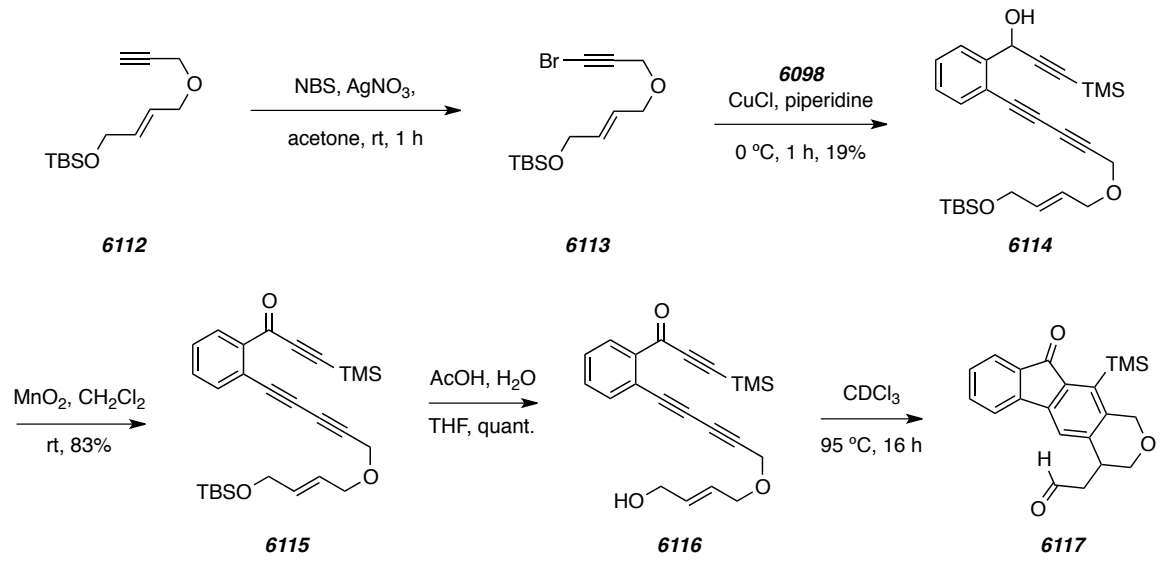

In addition to the allylic alcohol functionality, we became interested in the reaction of vinylcyclopropane with arynes. Wender and co-workers reported several studies of Ru-mediated [5+2] cycloadditions involving vinylcyclopropanes.[159] If we could demonstrate that a similar mechanism was applicable using an HDDA-generated aryne to induce vinylcyclopropane ring-opening, a novel aryne-trapping reaction would be discovered. Alternatively, if the Alder-ene process were the dominant mechanism then the corresponding product would be a methylene cyclopropane (cf. **6121**, Scheme 132). Vinylcyclopropane-containing ketotriyne **6120** was prepared in the usual manner by coupling enyne **6118** with diyne **6098** under Glaser conditions (Scheme 132). We found that Ag(I)-mediated alkyne bromination of vinylcyclopropane **6118** failed to give the corresponding alkynyl bromide. Accordingly, we turned to a modified Glaser protocol,[160] which provided desired triyne **6119**, albeit in low yields. MnO_2 oxidation of **6119** gave

[159] Liu, P.; Cheong, P. H.-Y.; Yu, Z.-X.; Wender, P. A.; Houk, K. N. Substituent effects, reactant preorganization, and ligand exchange control the reactivity in Rh^I-catalyzed (5+2) cycloadditions between vinylcyclopropanes and alkynes. *Angew. Chem. Int. Ed.* **2008**, *47*, 3939–3941.
[160] Yin, W.; He, C.; Chen, M.; Zhang, H.; Lei, A. Nickel-catalyzed oxidative coupling reactions of two different terminal alkynes using O_2 as the oxidant at room temperature: Facile syntheses of unsymmetric 1,3-diynes. *Org. Lett.* **2009**, *11*, 709–712.

the ketotriyne HDDA precursor. Heating **6120** under the usual conditions cleanly gave methylenecyclopropane **6121**. This demonstrates the efficiency with which the Alder-ene reaction with arynes takes place, and provides a new route to methylenecyclpropanes, a functional group that has recently gained interest.[161]

Scheme 132 | Synthesis of ketotriyne **6120** and subsequent HDDA reaction cascade with Alder-ene trapping to give methylenecyclopropane-containing benzenoid **6121**.

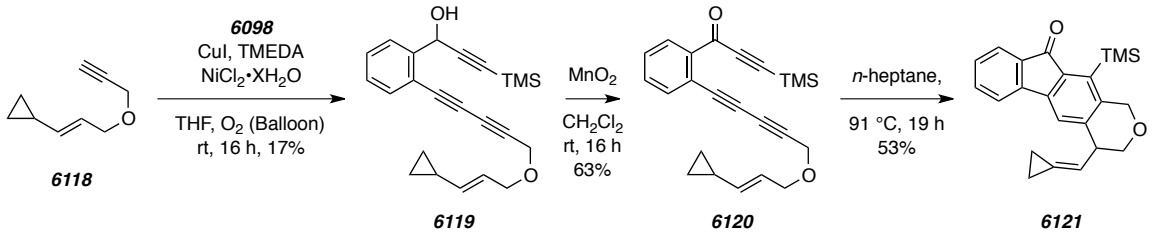

The efficiency with which the HDDA/Alder-ene reaction proceeds led us to consider if atoms other than hydrogen are capable of transferring to the aryne, namely halogen atoms. To test this hypothesis we prepared allyl chloride-containing triyne **6125** by MnO_2 oxidation of alcohol **6124**, which itself is prepared by Cadiot-Chodkiewicz coupling between diyne **6098** and alkyne **6123** (Scheme 133). Enyne coupling partner **6123** was prepared by mono-etherification of *trans*-1,4-dichloro-2-butene (**6122**) with propargyl alcohol. Interestingly, heating **6125** in *n*-heptane gave the corresponding vinyl chloride-containing fluorenones **6126** with an equimolar *E*/*Z* ratio. The mechanism for the formation of **6126** is again likely HDDA cyclization with aryne trapping via an Alder-ene reaction with the pendant alkene functionality. Even though we were unsuccessful in identifying a suitable substrate for the transfer of an atom other than hydrogen, we did demonstrate that it was possible to use the HDDA cascade reaction to prepare other useful functional groups, for example vinyl halides.

[161] a) Shi, M.; Lu, J.-M.; Wei, Y.; Shao, L.-X. Rapid generation of molecular complexity in the Lewis or Brønsted acid-mediated reactions of methylenecyclopropanes. *Acc. Chem. Res.* **2012**, *45*, 641–652. b) Nakamura, I.; Yamamoto, Y. Transition metal-catalyzed reactions of methylenecyclopropanes. *Adv. Synth. Catal.* **2002**, *344*, 111–129.

Scheme 133 | Synthesis of allyl chloride-containing ketotriyne **6125** and subsequent tandem HDDA/Alder-ene reaction to form vinyl chloride **6126**.

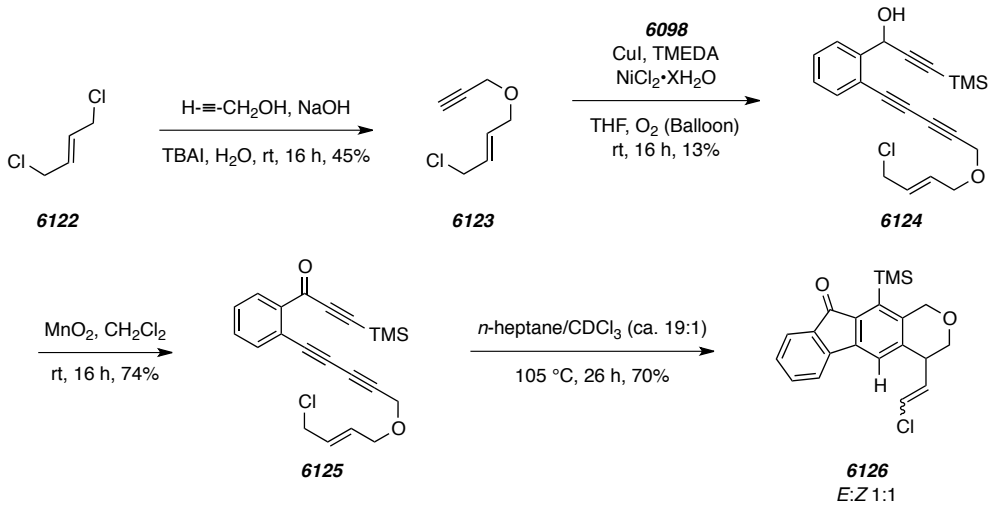

Cheng and co-workers demonstrated that propynes react with arynes through a propargyl ene mechanism to give allene products.[157] The broad substrate scope that they demonstrated inspired us to study the process with HDDA-generated arynes. To this end, we prepared ketotetrayne **6130** in the usual manner by coupling diyne **6098** with alkynyl bromide **6128** and oxidizing the resulting the alcohol, **6129** (Scheme 134). The alkynyl bromide was prepared from **6127** under standard conditions. Interestingly, heating a 0.1 M solution of tetrayne **6130** in $CDCl_3$ gave only modest yields of desired allene **6131** with several unidentifiable, non-isolable, and discreet byproducts. As we previously described, in certain instances the yield and product purity resulting from aryne trapping by certain reagents was substantially improved by further diluting the substrate. Heating 0.01 M solution of tetrayne **6130** in $CDCl_3$ and ^1H NMR analysis of the reaction mixture showed only traces of the byproducts previously observed and fluorenone **6130** was formed in excellent purity and good isolated yield. The mechanism for the formation of **6130** is likely HDDA cyclization and propargyl-ene trapping of the aryne intermediate. It is likely that the propargyl-ene trapping reaction represents a 'slow trap,' which we had not yet observed for intramolecular trapping reactions. We demonstrated that the inherent inefficiency of the process can be overcome by further diluting the triyne substrate. After

these studies were completed a report by Lee and co-workers was published which included a similar result of a Ag-mediated tandem HDDA/propargyl ene reaction on a similar substrate.[162]

Scheme 134 | Synthesis of ketotetrayne **6130** and subsequent tandem HDDA/propargyl ene to form allene **6131**.

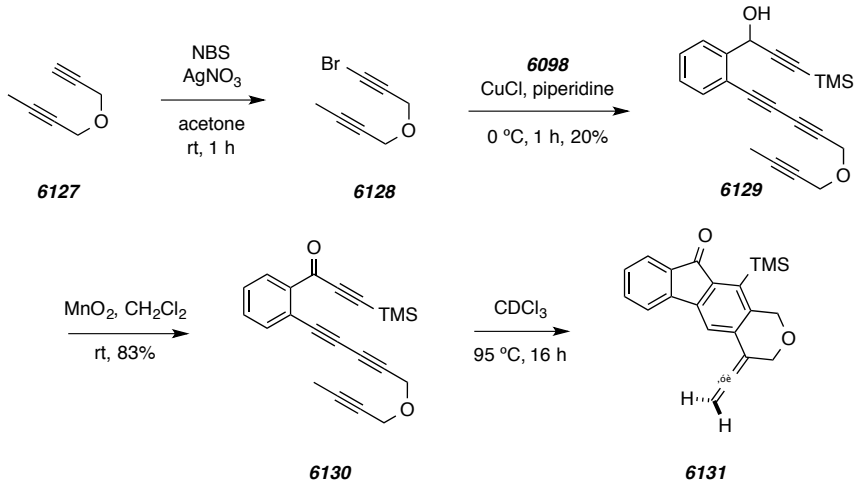

Following our initial disclosure of the HDDA reaction cascade, Lee and co-workers reported other Alder-ene reactions of aryne intermediates generated from polyalkyne substrates.[162] A specific example is shown in Scheme 135. The authors found that heating a mixture tetrayne **6132** in AgOTf gave rise to benzenoid **6133**. To account for the formation of **6133**, the authors proposed the involvement of an aryne intermediate, which reacts by an Alder-ene mechanism (cf. **6110**, Scheme 130). The Ag(I) additive was not found to improve yields of the reaction in every case, but the authors noted that further investigations are underway to determine the effect of metals on the HDDA reaction cascade.

[162] Karmakar, R.; Mamidipalli, P.; Yun, S. Y.; Lee, D. Alder-ene reactions of arynes. *Org. Lett.* **2013**, *15*, 1938–1941.

Scheme 135 | An example from Lee's recent reoprt of Ag(I)-medaited HDDA-cyclization with Alder-ene trapping (adapted from ref 162).

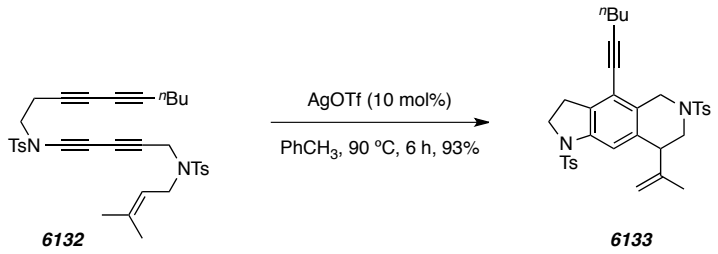

6132 *6133*

6.7. Trapping HDDA-Generated Arynes with Arenes via [4+2] Cycloaddition

With such a promising substrate for preparing ketotriyne precursors, we began considering alternative trapping reactions that could be studied in the context of the HDDA-generated arynes. An obvious follow-up to the ene substrates presented in the previous section is the diene-containing ketotriyne **6137** (Scheme 136). We envisioned that the HDDA-generated aryne would undergo an intramolecular *di*dehydro-Diels–Alder reaction with the diene of **6137** (cf. Figure 13-B) to give a benzocyclohexadiene-containing fluorenone. Unfortunately, a byproduct of the alkyne coupling was cyclohexadiene **6138**, which likely results from didehydro-Diels–Alder cycloaddition of triyne **6135** between the diene moiety and the proximal alkyne. Unfortunately, immediately subjecting recovered triyne **6135** to MnO_2 oxidation conditions cleanly gave ketoarene **6136**, which could result from reaction of benzocyclohexadiene **6138** with MnO_2 to convert the alcohol to the ketone and oxidatively aromatize the cyclohexadienyl to the benzenoid. The substrate was then abandoned because even if ketotriyne could be prepared, subsequent heating would likely induce a didehydro-Diels–Alder reaction instead of the desired HDDA reaction.

Scheme 136 | Unexpected observation of **6136** during the attempted synthesis of ketotriyne **6137**.

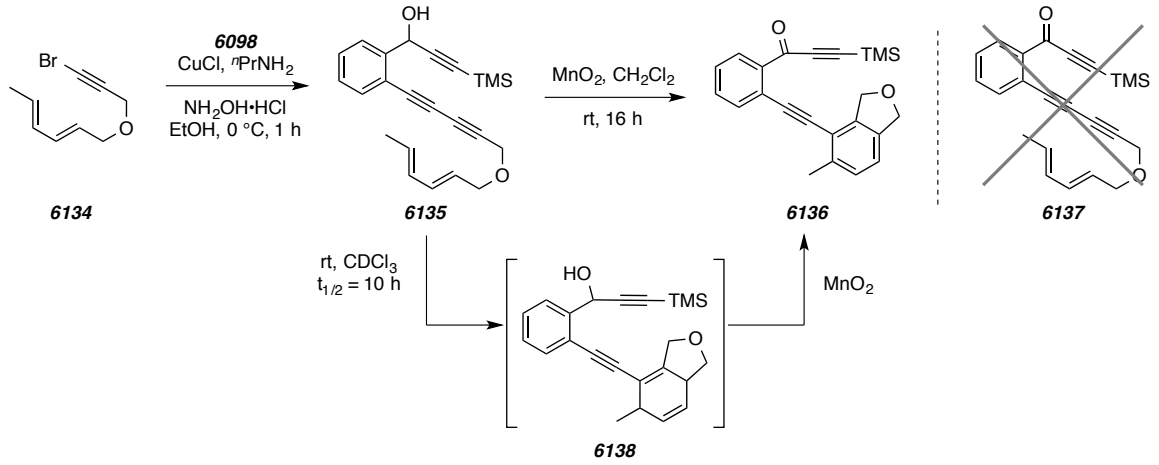

An alternative approach to the introduction of a Diels–Alder trap was use of a pendant benzene ring. Benzene itself has long been known to undergo [4+2] cycloaddition with **3**.[123] To test its ability to trap HDDA-generated arynes, we prepared the *m*-xylene-containing ketotriyne **6139** in the usual manner. Heating **6139** to 85 ºC in $CHCl_3$ gave fluorenone **6141**, which results from HDDA cycloisomerization to aryne **6140** and intramolecular didehydro-Diels–Alder reaction (Scheme 137). This result also demonstrated that the HDDA cascade can be used to cleanly generate a significant amount of structural complexity in a single step.

Scheme 137 | HDDA cycloisomerization of ketotriyne **6139** with subsequent trapping by aryne-arene [4+2] cycloaddition.

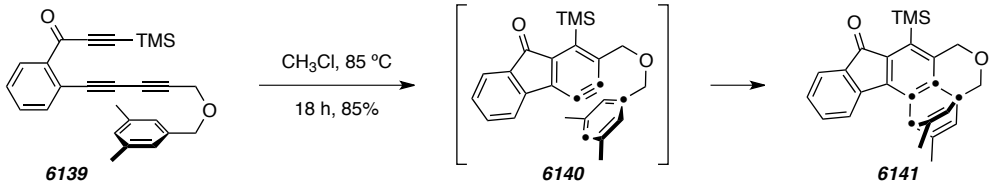

Having identified a robust route to allylic diol-containing triyne **6114**, we considered studying the corresponding enal **6142** for the possibility of a hetero-

*di*dehydro-Diels–Alder reaction via intramolecular aryne enal [4+2] cycloaddition (Scheme 138). Treating previously prepared **6114** sequentially with AcOH and MnO_2 effected TBS cleavage and bis-oxidation to enal-bearing ketotriyne **6142**. Heating **6142** gave fluorenone **6144** without any observable byproducts. This result demonstrates that HDDA-generated arynes can be efficiently trapped by hetero-Diels–Alder processes even though the corresponding all-carbon diene failed (cf. Scheme 136).

Scheme 138 | Synthesis of ketrotriyne **6142** and subsequent HDDA cycloisomerization with hetero [4+2] cycloaddition.

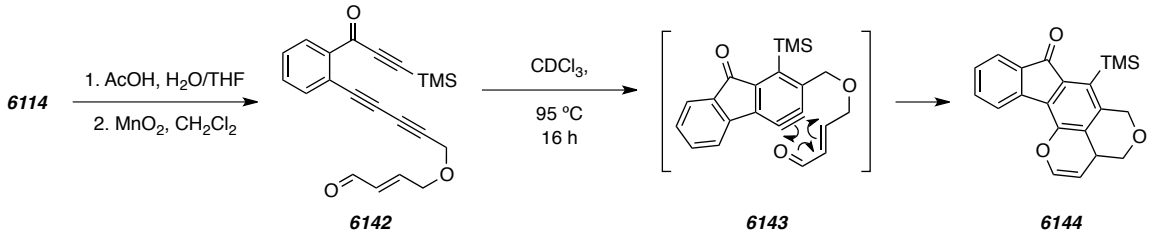

Scheme 139 | Synthesis of diphenylcyclopropane-containing ketotriyne **6148**.

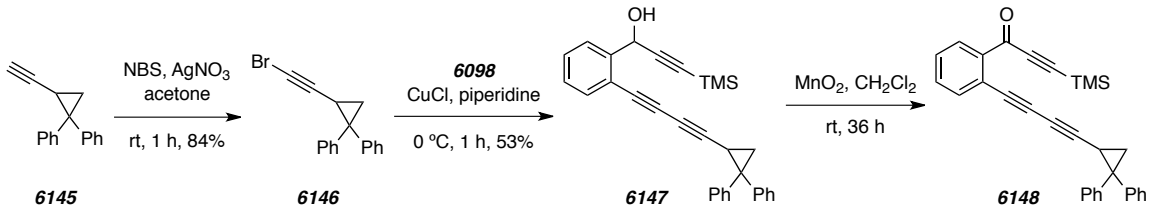

We envisioned that heating **6148** would result in either i) cyclization by a concerted mechanism with trapping by phenyl to give **6152** or ii) a stepwise mechanism would ensue and be interrupted by cyclopropane ring-opening of **6149** to form and give rise to an intractable mixture of products. Similar to the studies by Tantillo,[153] if a complex mixture was observed then we could take recourse by adding efficient hydrogen atom donors in an attempt isolate products consistent with cyclopropane ring-opening. To our delight the reaction was clean and **6152** was isolated as the sole major product! This demonstrates that aryne **6151** and the radical clock remains intact throughout the reaction (Scheme 140). While this result does support a concerted mechanism for aryne generation, it should be mentioned that the extended cumulene in **6150** would be so unstable that the reverse reaction with cyclopropane reformation back to **6149** might be favored. Unfortunately, this would ultimately allow for the stepwise mechanism to also give aryne **6151** with subsequent phenyl trapping.

Scheme 140 | Potential mechanistic pathways of the radical clock-containing ketotriyne **6148** and the observed formation of polycycle **6152**.

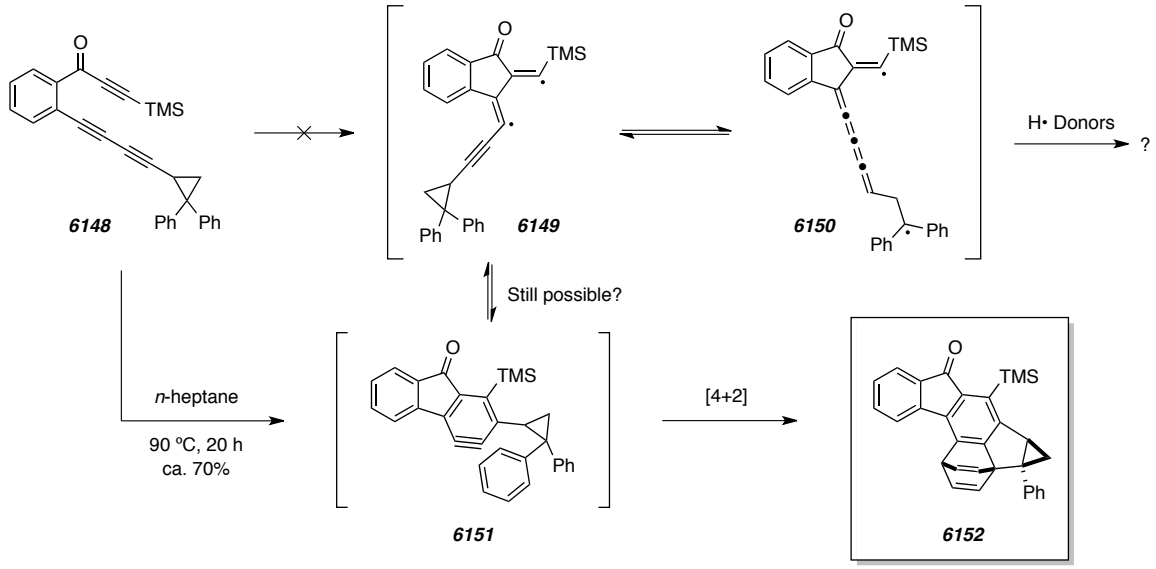

To avoid the ambiguity inherent to ketotriyne, we considered the alternative substrate ketotriyne **6156**, in which the radical clock is in conjugation with the monoyne portion of the substrate. If a stepwise mechanism were operable, the intermediate vinyl radical would surely isomerize and induce cyclopropane ring opening to form cumulene **6158** (Scheme 141). To prepare **6156**, 2-Ethynylbenzaldehyde (**6097**) was first treated with the lithium of acetylide of **6145** to give diyne **6153**. Cadiot-Chodkiewicz coupling with silyl ether **6154** and subsequent MnO_2 oxidation of alcohol **6155** gave desired ketotriyne **6156**. Based on the previous result (cf. conversion of **6148** to **6152**), we expected that **6156** would undergo HDDA cycloisomerization to form an aryne, which would be efficiently trapped by the pendant silyl ether to form fluorenone **6157**. Unfortunately, heating **6156** at 100 ºC for 18 h led to a complex mixture of products. The generation of a complex reaction mixture suggests that aryne generation proceeds through a stepwise mechanism involving diradical intermediates. Following the precedence set forth by Tantillo,[153] we repeated the experiment, this time in the presence of the hydrogen-atom donor, γ-terpinene, but no identifiable products were isolated. Still,

this result adds more ambiguity to our studies of providing experimental evidence for either the concerted or stepwise mechanistic pathways.

Scheme 141 | Synthesis of the altnerative, radical clock-containing ketotriyne, **6131** and attempts to induce HDDA cycloisomerization.

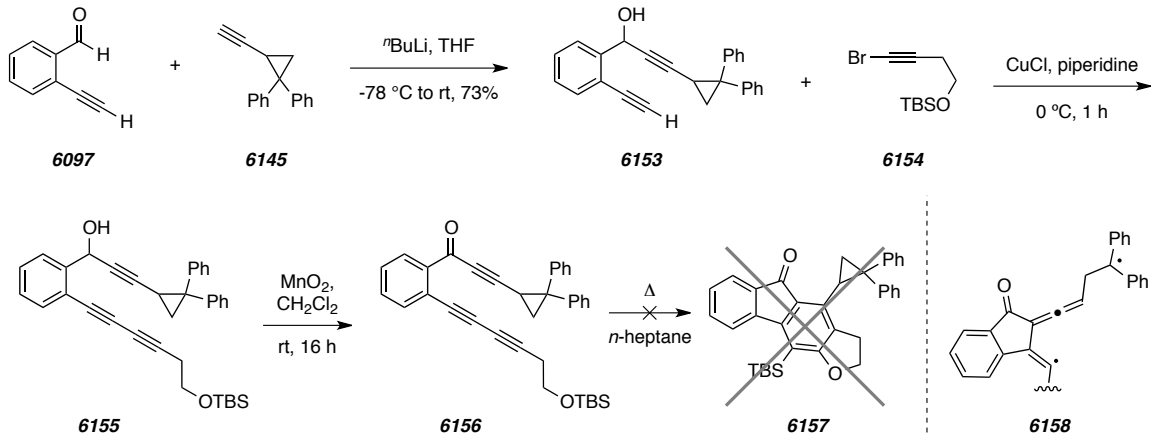

The ambiguity presented in the previous studies led us to consider other reasons for the intractable reaction mixture generated when ketotriyne **6156** was heated. We realized that **6156** was the first substrate we studied that contained an aliphatic group both bound to the monoyne and not part of the tethering moiety. Danheiser and co-workers have shown that intramolecular propargyl ene reactions are possible on related diyne systems.[163] With this in mind we prepared a propynyl-containing ketotriyne **6160** (Scheme 142). Propynyllithium was generated *in situ* and added to a solution of 2-bromobenzyaldehyde, and the resulting product was coupled to TMS-acetylene and desilylated to give diyne **6159**. Ketotriyne **6160** was prepared from **6159** by the previously described methods. Similar to **6156**, heating ketotriyne **6160** gave an intractable mixture of products from which no identifiable products were isolable.

[163] Robinson, J. M.; Sakai, T.; Okano, K.; Kitawaki, T.; Danheiser, R. L. Formal [2+2+2] cycloaddition strategy based on an intramolecular propargylic ene reaction/Diels−Alder cycloaddition cascade. *J. Am. Chem. Soc.* **2010**, *132*, 11039–11041.

Scheme 142 | Synthesis of **6160** and subsequent attempts to induce HDDA cyclo-isomerization.

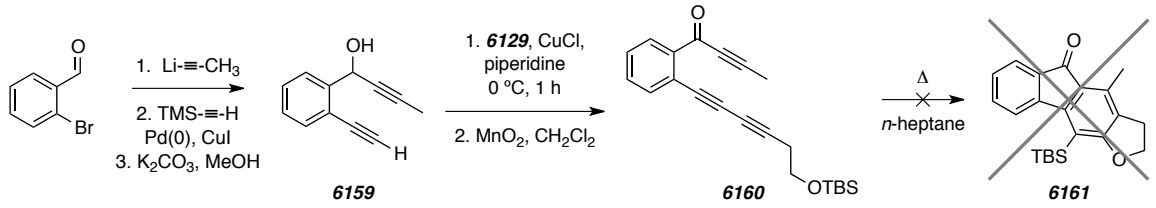

Our failure to effect HDDA reaction of ketotriyne **6160** was likely because of the aliphatic cyclopropyl group and not necessary due to the involvement of a stepwise mechanism. To verify this we considered that an intramolecular propargyl ene reaction of **6160** would generate a vinylallene, and Danheiser has efficiently trapped similar substrates with DMAD and maleimide.[163] Unfortunately, heating ketotriyne **6160** in the presence of either reagent gave no identifiable products. Collectively these results suggest that HDDA reaction cascade is not compatible with monoynes bearing certain aliphatic groups. Unfortunately, these results also demonstrate that related substrates will also not provide experimental support for either the concerted or stepwise reaction mechanism.

6.8. Intramolecular C–H Insertion by HDDA-Generated Arynes

Recently, Lee and co-workers reported a Ag(I)-mediated, intramolecular C–H insertion of substrates that typically undergo HDDA reaction (cf. **6162**, Scheme 143).[164] Specifically, the authors found that treating a polyyne like tetrayne **6162** gave rise to a benzenoid like **6164**. To account for the formation of **6164** the authors propose the intermediacy of carbene **6163**, which is capable of inserting into a C–H bond of the pendant *n*-propyl moiety. The authors show some scope with respect to substrate, but the process is more intriguing from a mechanistic perspective and ultimately limited with respect to preparative value.

[164] Yun, S. Y.; Wang, K.-P.; Lee, N.-K.; Mamidipalli, P.; Lee, D. Alkane C–H insertion by aryne intermediates with a silver catalyst. *J. Am. Chem. Soc.* **2013**, *135*, 4668–4671.

Scheme 143 | Tandem HDDA/C–H insertion reported by Lee (adapted from ref 164).

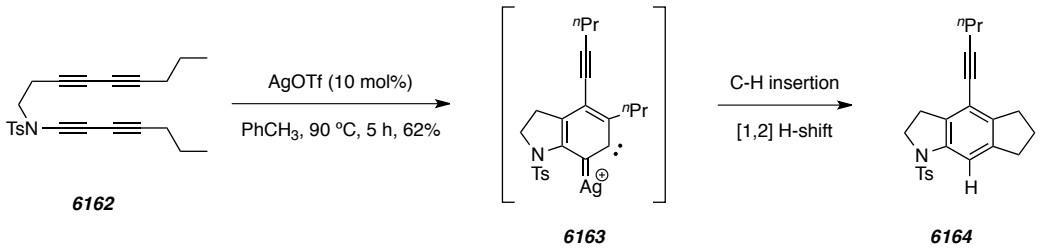

6162 ***6163*** ***6164***

When screening other intermolecular traps, we found that heating ketotriyne **6165** in the presence of modified Mukaiyama reagent **4041** cleanly gave a product with a molecular weight identical to the starting triyne (Scheme 144). Interestingly, products having a mass of an adduct with **4041** were not observed. Subsequent ^{1}H NMR analysis led us to assign the product's structure to be tetracyclic fluorenone **6166**. The product likely results from a net C–H insertion of the aryne intermediate into the methyl group of the propyl chain. The mechanism was not immediately clear because the reagent did not seem capable of supporting the formation of the necessary carbenoid. Pyridinium **4041** was previously used in our studies of the tandem aldol-lactonization reaction (see Section 4.3), and analogues of the reagent are commonly used for activating acids toward acylation reactions. Shortly after making this observation, another graduate student in our group isolated a similar product when 20 equivalents trimethyloxonium tetrafluoroborate was heated with a triyne similar to **6165**. This led us to consider that trace HBF_4 was inducing the C–H insertion. Indeed, C–H insertion product **6166** was isolated in 80% yield when **6165** was treated with an excess of HBF_4. Contrary to the report by Lee, this represents an efficient, metal-free approach to aryne C–H insertion.

Scheme 144 | Unexpected observation of C–H insertion mediated by pyridinium reagent **4041**.

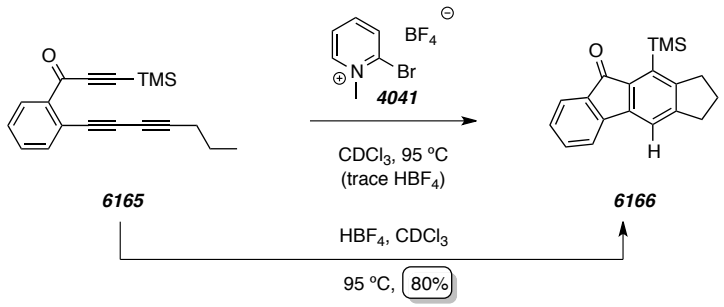

Having discovered a metal-free, acid-mediated C–H insertion we began considering possible mechanisms for this interesting reaction. While the mechanism is still unclear, we hypothesized that the strong acid protonates aryne **6167** to give aryl cation **6168**. A resonance structure of **6168** is carbene **6169**, which is capable inserting into the pendant methyl C–H to give **6170**. Loss of proton regenerates both aromaticity to give fluorenone **6166** and the acid catalyst. Similar reactions have been observed for aryl cations,[165] but we still have no definitive evidence that this was the mechanistic pathway we were observing. It is interesting to note that Lee and co-workers reported that use of HBF_4 as an additive significantly improved the outcome of their Ag-mediated C–H insertion.[164] Consistent with the mechanism we have proposed, we are skeptical as to the actual need of the Ag catalyst beyond slightly increasing the rate of aryne formation.

Scheme 145 | Proposed mechanism for acid-mediated, intramolecular C–H insertion reacitons of aryne **6167** to form **6166**.

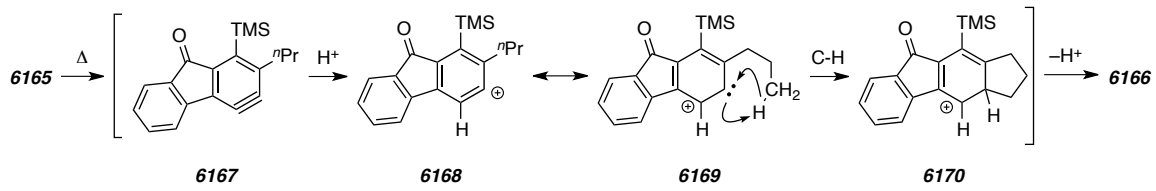

[165] Manet, I.; Monti, S.; Fagnoni, M.; Protti, S.; Albini, A. Aryl cation and carbene intermediates in the photodehalogenation of chlorophenols. *Chem. Eur. J.* **2005**, *11*, 140–151.

Still, with this as our best guess, we began our optimization by exploring alternative acid catalysts. Of all of the acids screened, TFA was the only acid that provided a measureable amount of the C–H insertion product, albeit, as a mixture with the acid O–H insertion product. On the surface, our inability to identify more than two acids capable of inducing the C–H insertion suggests our mechanistic hypothesis is incorrect. However, it can be argued that the reaction is very dependent upon the anionic counter ion, and we have been fortunate to have found two suitable anions to encourage C–H insertion. Changing the solvent from $CDCl_3$ to cyclohexane led to cleaner crude reaction mixtures, but the yield was not significantly greater than the initial result. Use of other solvents led to inferior outcomes. Because the acid is catalytic under our proposed mechanism, we decreased the acid loading to substoichiometric levels. Unfortunately, decreasing the loading of HBF_4 below two equivalents led to substantially reduced yields with less clean reaction mixtures. Studies of the scope of the reaction and more in-depth mechanistic analysis are still ongoing.

6.9. Efforts Toward HDDA-Generated Pyridynes

An obvious extension of the HDDA reaction cascade would be the generation and trapping of aza-*o*-benzynes or pyridynes. In the latest account, Ueda and co-workers attempted to form a pyridyne by HDDA reaction of propionitrile **6171** (Scheme 146-A), however TDDA reaction occurred between the alkyne and the enyne to give benzenoid **6172** as the only product.[148g] We had previously prepared nitrile **6173** (Scheme 146-B), but attempts at inducing an HDDA reaction were unsuccessful.

Scheme 146 | A) Previous effort by Ueda and co-workers to generate a pyridyne via a HDDA process (adapted from ref 148g). B) Previous substrate attempted in our laboratory for the generation of a pyridyne.

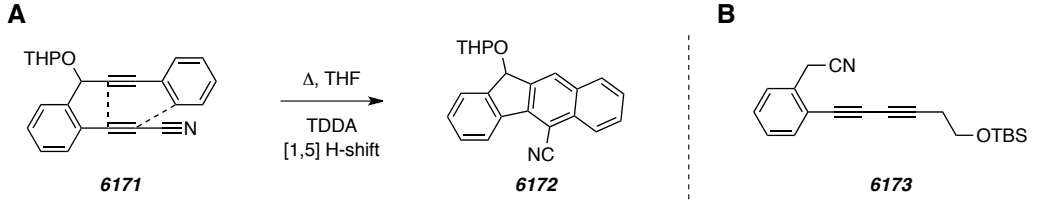

6171 *6172* *6173*

The previous failed attempts to form an HDDA-generated pyridyne led us to consider preparing the cyclohexenone tethered substrate **6145** because the all-carbon variant has been one of the most efficient substrates studied thus far. Acyl cyanide **6145** was prepared by treating the previously prepared aldehyde **6046** with TMSCN and followed by MnO_2 oxidation of the resulting cyanohydrin **6174**. Acyl cyanide **6175** was stable at temperatures up to 150 ºC. When heated in *o*-dichlorobenzene at 150 ºC for 13 h, the majority of the starting material had been consumed, but the resulting reaction mixture had no identifiable products and chromatographic purification failed. Due to a limited supply of starting materials and unpromising initial results, further studies into acyl cyanide were abandoned. However, studies of the HDDA reaction cascade with nitrogen-containing substrates are still ongoing.

Scheme 147 | Synthesis of acyl cyanide **6175** and efforts toward the generation of pyridyne **6176**.

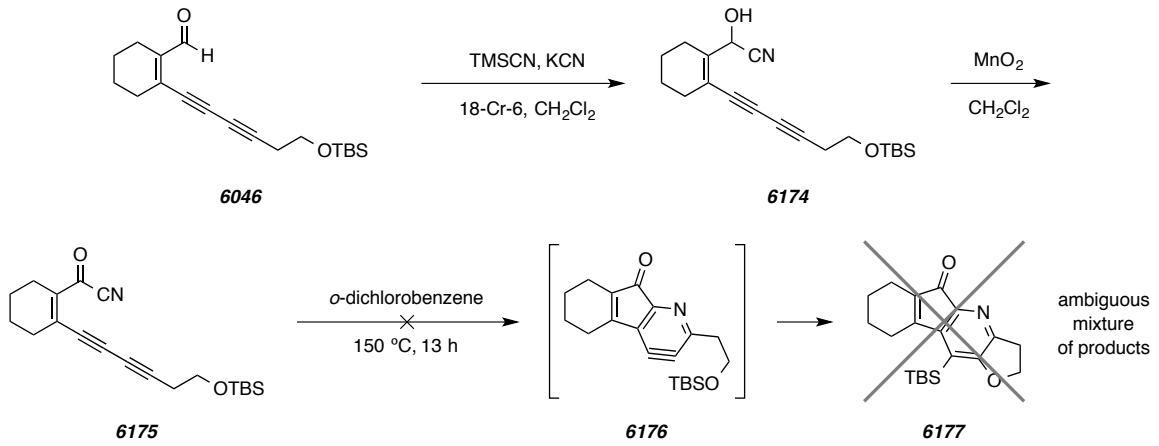

6.10. Concluding Remarks

The results included in this chapter undergird our notion that there is an incredible opportunity to uncover new reactivity of aryne reactive intermediates via the HDDA reaction cascade. In this chapter we have demonstrated that HDDA generation of arynes is efficient and can be accomplished with a large scope of precursors. Furthermore, we have shown that these aryne intermediates can be trapped intramolecularly in a variety of ways to give rise to a high degree of structural complexity. This trend continues in the

following chapter, which includes several examples of intermolecular trapping of HDDA-generated arynes. These processes greatly increase the versatility of the HDDA reaction cascade by both expanding scope of benzenoid products that can be made and increasing the rate by which new reactions of arynes are discovered.

Chapter 7. Intermolecular Trapping of HDDA-Generated Arynes

7.1. Intermolecular Trapping of HDDA-Generated Arynes

An obvious extension of the HDDA reaction cascade is the use of aryne-trapping reagents that are not attached to the substrates because intermolecular trapping would greatly expands the utility of the overall process. We often joke that "benzyne reacts with anything," hence every chemical on the shelf possesses the opportunity to reveal modes of aryne trapping. We found that heating acetate **7001a** gave an intractable mixture of products that did not contain an identifiable fluorenone. We proposed that fluorynone intermediate **7002** was forming, but the acetate functionality was not a competent trap. This led to a buildup of the aryne reactive intermediate, which ultimately decomposed. When benzene was used as solvent instead of $CDCl_3$, fluorenone **7003**, was isolated from an otherwise clean reaction mixture. This demonstrates that acetate **7001a** will generate an aryne intermediate that is capable of reacting with a competent trap *inter*molecularly.

Scheme 148 | HDDA cycloisomerization of ketotriyne **7001a** and intermolecular trapping of resulting aryne **7002** with benzene to give benzenoid **7003**.

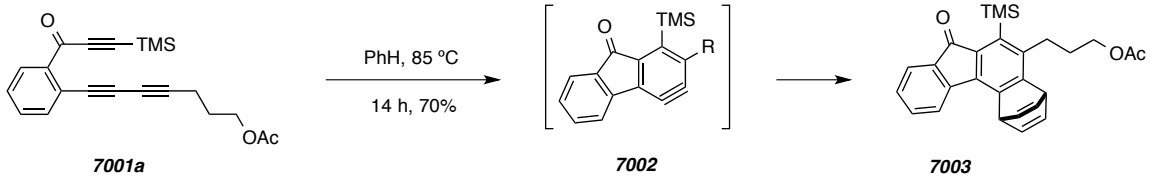

7001a *7002* *7003*

With a suitable substrate for studying intermolecular traps we screened other nucleophiles for their ability to trap HDDA-generated arynes. When a mixture of acetate **7001a** and excess norbornene was heated, the (exo) norbornane-containing fluorenone, **7004**, was isolated as a single diastereomer (Scheme 149). This demonstrates that HDDA-generated arynes are capable of reacting with alkenes via a [2+2] cycloaddition to give highly complex and strained benzenoids. The 63% yield that we have observed is much higher than those typically reported for similar reactions of *o*-benzyne.[123]

Bimolecular aryne-trapping by amides and carboxylic acids is also efficient and proceeds via net H-heteroatom insertion. Specifically, heating a mixture of acetate **7001a** with either acetanilide or acetic acid leads to a clean, high-yielding reaction giving amide **7005** and ester **7006**, respectively. Heating a mixture of acetate **7001a** with phenol cleanly gave biaryl **7007** in high yield. Treating HDDA precursor **7001b** (R^2, *n*-Pr) demonstrated that the bimolecular tandem HDDA/Alder-ene reaction is efficient, but the product, **7008**, was recovered as a mixture of regioisomers (ratio ca. 1:1.5). A novel form of aryne trapping was also found by heating a mixture of HDDA precursor **7001c** (R^3, TMS) with TMSCN in *n*-heptane, whereby aryl nitrile **7009** was isolated as the major product.

Scheme 149 | Examples of intermoelcular trapping of aryne **7002**.

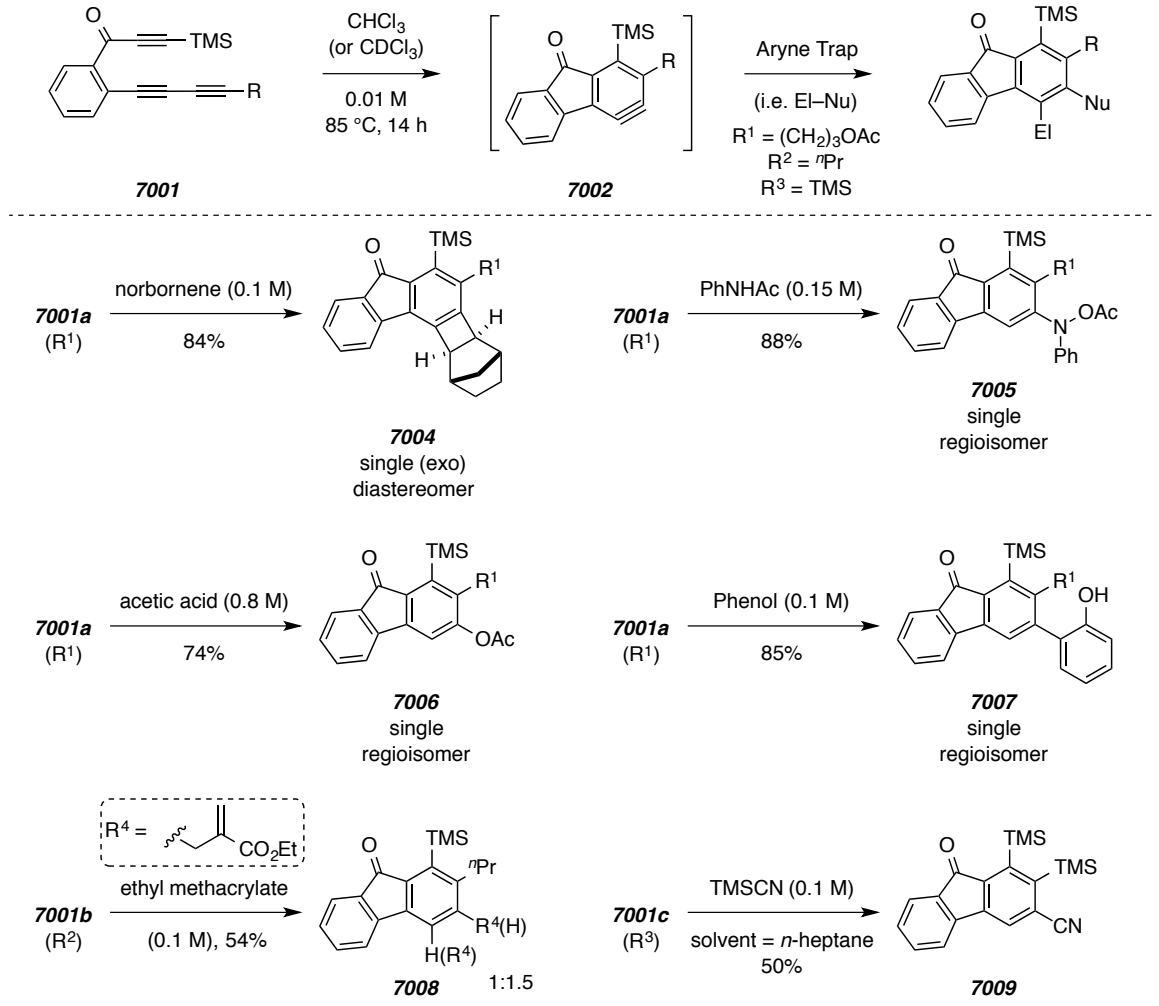

The mechanism for the formation of **7007** likely involves an oxy-ene reaction of phenol with aryne **7002** to give a dione intermediate which readily tautomerizes to product. This result is unique because arynes typically react with phenol via O–H insertion to give the corresponding ethers.[166] However, previous studies required the use of additional reagents to induce aryne generation, which likely affected the mode of addition. We predict that a similar mechanism is occurring in the case of acetic acid, which remains an effective trapping reagent with increased solvent concentration 0.1 M to 0.8 M. These results demonstrate that the reagent-free nature of the HDDA cascade provides platform for the discovery of complementary aryne trapping reactions.

Many of the aforementioned trapping reagents (i.e. acetanilide, acetic acid, and phenol) gave the corresponding benzenoids with excellent regioselectivity. In a related process, heating a mixture of acetate **7001a** and ammonium bromide was found to effect aryne hydrohalogenation (Scheme 150). However, the regioselectivity was much lower and both aryl halides **7011** and **7012** were isolated. After screening a variety of ammonium bromides, we found that **7010** provided the greatest regioselectivity by giving a ratio of **7011**:**7012** = 6:1.

Scheme 150 | HDDA-generated aryne bromination to give the regioisomeric fluorenones **7011** and **7012**.

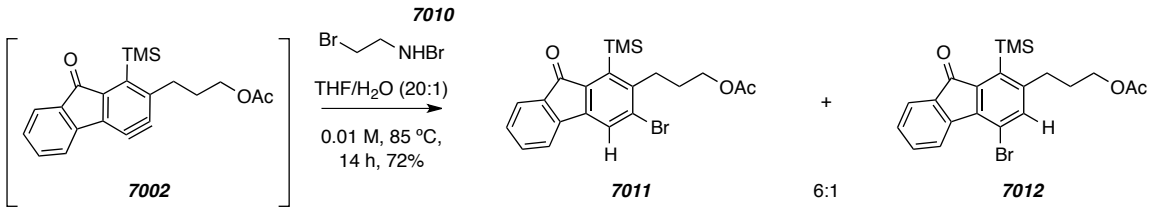

7.2 A Computational Model to Account for the Observed Regioselectivity of Intermolecular Trapping Reactions.

Interestingly, the dominant regioisomer in almost every case was addition of the nucleophile to C-3 of fluorynone **7002**. In 2003, Suzuki and co-workers described a strong preference in fused bicyclic arynes for nucleophilic attack at the sp-hybridized

[166] Liu, Z.; Larock, R. C. Facile *O*-arylation of phenols and carboxylic acids. *Org. Lett.* **2004**, *6*, 99–102.

carbon atom distal to the ring fusion atoms.[167] The observed regioselectivity increased as the size of the fused ring system became smaller and more strained. The authors proposed the increased strain caused induced differences in the reactivity of each of the reactive sp-hybridized carbon atoms. Computational analysis supported the experimental observations by indicating that both the p-character and the natural atomic charge are larger (more positive for the latter) at the more reactive sp carbon.

Follow-up reports from independent collaborations of Cramer/Buszek[168] and Garg/Houk[169] demonstrated that these effects can be modeled by simply computing an optimized geometry of the aryne intermediate. Specifically, inspection of the optimized geometry of an unsymmetrical aryne reveals differing internal bond angles about the sp-hybridized carbon atoms. The relative difference between the acute and obtuse computed bond angles dictates the preferred site of nucleophilic attack. The more obtuse angle inherently possesses increased p-character implying that it is more electrophilic. This suggests that for a particular HDDA reaction cascade with intermolecular trapping, the favored regioisomer can be accurately predicted from a simple geometry optimization of the aryne intermediate. To probe the utility of this approach in predicting the reactive site of HDDA-generated arynes we computed the optimized geometry of phthalidyne **7014** using DFT [M06-2X/6-31+G(d,p)] (Figure 15). The resulting optimized geometry had bond angles $C_aC_bC_c$=122º, and $C_aC_bC_c$=132º, which suggest that the more reactive sp carbon atom is at C-5 (i.e. C_c).

[167] Hamura, T.; Ibusuki, Y.; Sato, K.; Matsumoto, T.; Osamura, Y.; Suzuki, K. Strain-induced regioselectivities in reactions of benzyne possessing a fused four-membered ring. *Org. Lett.* **2003**, *5*, 3551–3554.
[168] Garr, A. N.; Luo, D.; Brown, N.; Cramer, C. J.; Buszek, K. R.; VanderVelde, D. Experimental and theoretical investigations into the unusual regioselectivity of 4,5-, 5,6-, and 6,7-indole aryne cycloadditions. *Org. Lett.* **2010**, *12*, 96–99.
[169] Cheong, P. H. Y.; Paton, R. S.; Bronner, S. M.; Im, G.-Y. J.; Garg, N. K.; Houk, K. N. Indolyne and aryne distortions and nucleophilic regioselectivites. *J. Am. Chem. Soc.* **2010**, *132*, 1267–1269.

Figure 15 | Computed bond angles for the reactive carbons of phthalidyne **7014**.

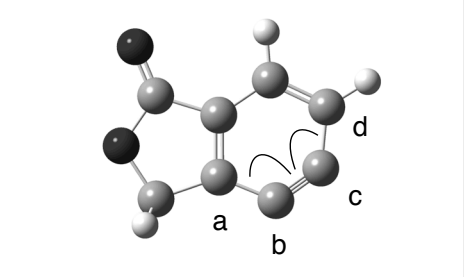

It was surprising that such a subtle difference in bond angle could lead to such a dramatic difference in selectivity for nucleophilic addition to the sp-hybridized carbon atoms. To validate the computed results with experiment we prepared an authentic sample of the precursor to aryne **7014**, triyne **7013**. Heating a solution of **7013** in *t*-butanol gave phthalide **7015** as a single regioisomer (Scheme 151). The structure of **7015** was supported by nOe analysis, and the regioselectivity predicted by computation was confirmed.

Scheme 151 | Experimentally observed regioselectivity for intermolecular nucleophilic addition to phthalidyne **7014**.

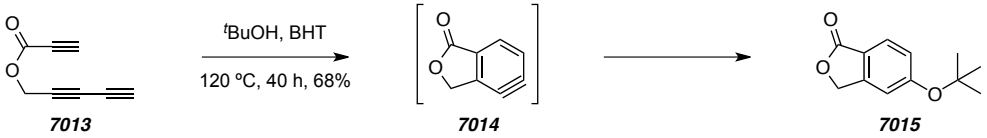

With calculations of aryne **7014** in hand, we though it wise to consider computing the overall energetics of the aryne formation and subsequent trapping by *t*-butanol (summarized in Figure 16). Routine geometry optimization of **7013** and **7015** indicated, as expected, that the overall transformation of the triyne **7013** into aryl ether **7015** was downhill (ca. 125 kcal•mol^{-1}). Surprisingly, the formation of aryne **7014** was also exergonic (ca. 50 kcal•mol^{-1}). This represents a feature of the HDDA cascade reaction that is truly rare and remarkable, the generation of the (aryne) reactive intermediate is itself downhill. The energetics of this process also demonstrate that alkynes store an

incredible amount of potential energy and would likely not exist at all if they were not protected by high kinetic barriers.[170]

Figure 16 | Overall energetics for the HDDA reaction cascade with *t*-BuOH trapping.

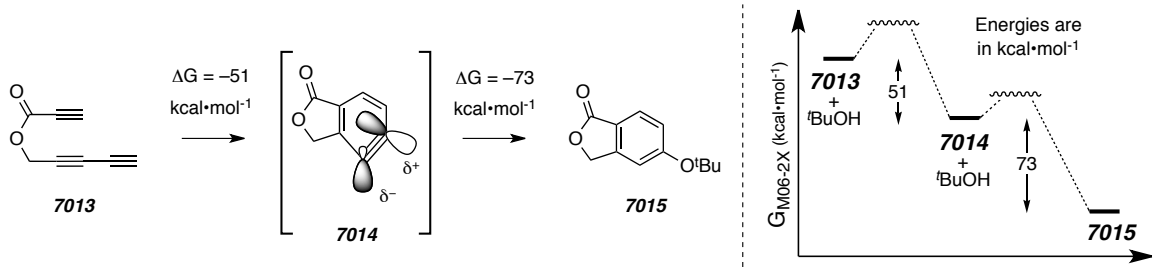

7.3. Alkane Desaturation by HDDA-Generated Arynes

Sterenberg had reported a result that we found very interesting–generating an aryne via the HDDA reaction with THF as solvent gave a product of net aryne hydrogenation (cf. Section 6.2). Inspired by these results, we followed Sterenberg's example and heated a THF solution of acetate **7001a**, which cleanly gave benzenoid **7016**, which is the product of fluorynone **7002** hydrogenation. Similarly when THF-d_8 was used as solvent the corresponding bis-deuterated fluorenone, **7017**, was isolated. At this juncture we recognized that while Sterenberg had certainly proved that THF was the source of hydrogen, the question of whether the two hydrogen atoms came from the same molecule had not been addressed. To probe this question we heated triyne **7001a** in a mixture of 1:1 THF-h_8:THF-d_8, which provided a 6:1 ratio of **7016**:**7017**, and none of the crossover product was detected. For good measure, the experiment was repeated using a mixture of 1:6 THF-h_8:THF-d_8 and, as expected, a 1:1 ratio of **7016**:**7017** was obtained. Again, no cross-over products were detected. These results strongly support the notion that the hydrogen atoms are obtained from the same molecule of THF.

[170] Alabugin, I. V.; Gold, B. Two functional groups in one package: Using both alkyne π-bonds in cascade transformations. *J. Org. Chem.* **2013**, *ASAP*, (DOI: 10.1021/jo401091w).

Figure 17 | Studies of hydrogen atom transfer to aryne **7002** by THF.

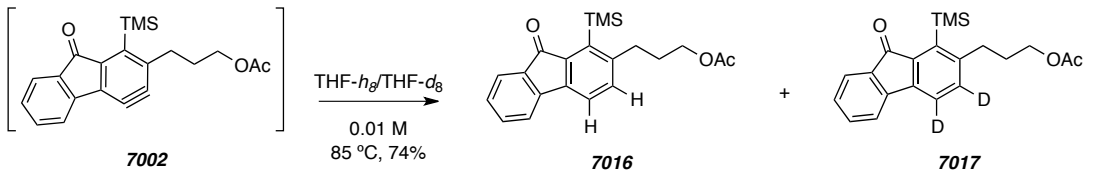

7002 ***7016*** ***7017***

solvent	(*7016* : *7017*)
THF-h_8	100 : 0
THF-d_8	0 : 100
THF-h_8/THF-d_8 (1:1)	6 : 1
THF-h_8/THF-d_8 (1:6)	1 : 1

Crossover H/D or D/H
Not Observed!

With strong support that a single molecule of THF is the source of hydrogen, we began diligently analyzing ^{1}H NMR spectral data of the reaction mixtures for evidence of discreet byproducts from the reaction. Unfortunately, none were observed, but this led us to consider that the byproduct was the "dehydrogenated" THF, or dihydrofuran. Our inability to observe either 2,3- or 2,5-dihydrofuran led us to consider that dihydrofuran was reacting with the aryne intermediate. GC/MS analysis of a reaction mixture resulting from heating a $CDCl_3$ solution containing ketotriyne **7001c** and 20 equivalents of 2,3-dihydrofuran showed a peak with a molecular ion equal to that of the dihydrofuran adduct with **7001c**. Unfortunately, to date we have not been able to isolate the corresponding product.

We next screened 1,4-dioxane for its ability to donate hydrogen to HDDA-generated arynes, but heating a mixture of it and **7001a** provided none of fluorenone **7016**. This led us to consider alternative sources for the hydrogen donor, namely cyclooctane. Cyclooctane has been the reagent of choice for other, usually metal-mediated, dehydrogenation reactions.[171] Still, cyclooctane does not possess an ether oxygen, which may be necessary for weakening the C–H bonds toward aryne hydrogenation. However, heating a cyclooctane solution of triyne **7001a** cleanly gave the corresponding fluorenone **7016** (Scheme 152). No-D ^{1}H NMR analysis[172] of the reaction

[171] Choi, J.; MacArthur, A. H. R.; Brookhart, M.; Goldman, A. S. Dehydrogenation and related reactions catalyzed by iridium pincer complexes. *Chem. Rev.* **2011**, *111*, 1761–1779.
[172] Hoye, T. R.; Eklov, B. M.; Voloshin, M. No-D NMR spectroscopy as a convenient method for titering organolithium (RLi), RMgX, and LDA solutions. *Org. Lett.* **2004**, *6*, 2567–2570.

mixture clearly revealed the presence of cyclooctene. Gratifyingly, the ratio of cylco-octene to fluorenone **7016** was near equimolar, which indicated that cyclooctene was the byproduct of aryne reduction.

Scheme 152 | High-yielding synthesis of benzenoid **7016** by hydrogen transfer from cyclooctane via transition structure **7018**.

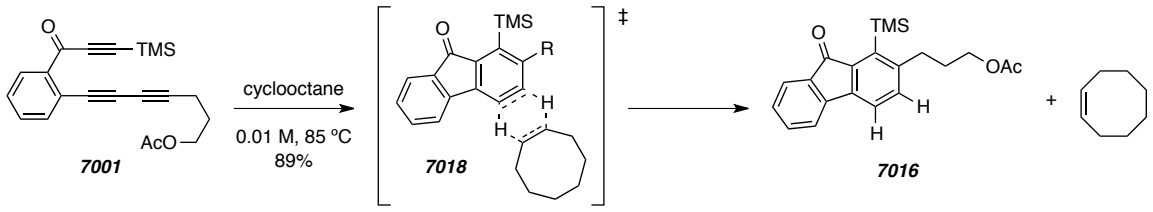

To account for aryne reduction by way of a single molecule of THF or cyclooctane, we proposed the concerted transfer of two hydrogen atoms from vicinal carbon atoms of the reducing agent. Concerted double hydrogen atom transfer (henceforth referred to as 2H atom transfer) has been invoked in other processes such as diimide reduction[173] and type II dyotropic rearrangements.[174] However, the concerted 2H atom transfer from otherwise unactivated alkanes is unprecedented. Assuming the mechanism to be true, aryne reduction by THF must proceed via six-atom transition structure **7018**.

To probe our mechanistic hypothesis we located transition structure **7019** for the 2H atom transfer to *o*-benzyne (**3**) from ethane (Figure 18). The energetics clearly demonstrate that the process is kinetically viable i.e. $\Delta G^{\ddagger}$ = 21 kcal•mol^{-1} [M06-2X/6-31+g(d,p)]. Additionally, and consistent with our hypothesis, the located transition structure contains six atoms that carry out the transformation with a high degree of synchronicity. It is noteworthy that the located transition structure relies on the eclipsed conformation of ethane to ensure a planar transition state. In a related study, Cossío and

[173] a) Hünig, S.; Müller, H.-R.; Thier, W. Reduktionen mit diimid. *Tetrahedron Lett.* **1961**, *2*, 353–357. b) Corey, E. J.; Pasto, D. J.; Mock, W. L. Chemistry of diimide. II. Stereochemistry of hydrogen transfer to carbon-carbon multiple bonds. *J. Am. Chem. Soc.* **1961**, *83*, 2957–2958.
[174] Fernández, I.; Cossío, F. P.; Sierra, M. A. Dyotropic reactions: Mechanisms and synthetic applications. *Chem. Rev.* **2009**, *109*, 6687–6711.

co-workers recently described computational studies of similar processes and noted the decided preference for planar transition structures.[175]

Figure 18 | Computed [M06-2X/6-31+g(d,p)] transition structure **7019** and activation barrier for 2H atom transfer to **3** from ethane.

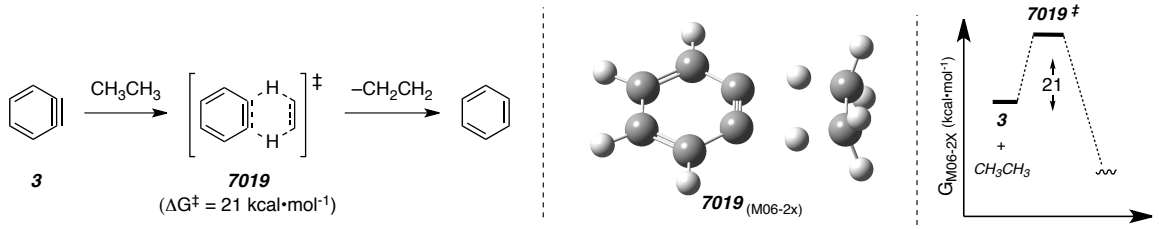

While acetate **7001a** proved to be a worthy substrate for studying intermolecular trapping reactions, we chose to continue our studies with the corresponding propynyl analogue **7021**. We viewed **7021** to potentially be superior for studying 2H atom transfer reaction, due to the absence of additional functionality (e.g. an acetate in the case of **7001a**). To prepare **7021**, we needed to couple diyne **6098** with propyne. This was accomplished using commercial MAPP® gas as an inexpensive source of propyne. MAPP® gas is a welding blend that is advertised as a safer alterative to acetylene. The blend consists of a mixture of propyne (ca. 30%), allene (14%), propene (43%), propane (7%), and butanes (6%). Unfortunately, the North American manufacturer of MAPP gas has stopped production, and the original blend is no longer available for purchase. An alternative product, MAP-Pro®, that does not contain propyne is used in place of the original blend. Still, our current supply of MAPP® gas represented the cheapest source of propyne, which encouraged us to use it as the coupling partner with diyne **6098**. To effect the proposed Glaser coupling, we saturated a 0 ºC THF solution with propyne by bubbling MAPP® gas for one hour. No-D ^{1}H NMR analysis indicated that the solution was 4 M in propyne, which was suitable for our studies. Diyne **6098** and the other necessary reagents[176] were added to the reaction mixture and an O_2 balloon was attached

[175] Fernández, I.; Sierra, M. A.; Cossío, F. P. In-plane aromaticity in double group transfer reactions. *J. Org. Chem.* **2007**, *72*, 1488–1491.

[176] The procedure was adopted from the conditions reported ref 160, namely $NiCl_2$ was used as an additive and THF was used as solvent.

through a septum. After 24 h, GC/MS analysis indicated that diyne **6098** was fully consumed and the corresponding triyne, **7020**, was the major product. Purification and MnO_2-mediated propargyl alcohol oxidation gave **7021**.

Scheme 153 | Synthesis of triyne **7021**.

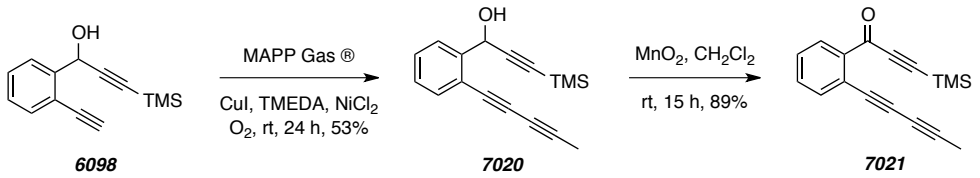

6098 ***7020*** ***7021***

A cyclooctane solution of **7021** was heated to see if the absence of the acetate functionality had would affect the efficiency of the reaction. To our delight, fluorenone **7023** was isolated in nearly quantitative yield (Figure 19). Again, the only substantial byproduct in the reaction was cyclooctene, which was observed in equimolar amounts with fluoreneone **7023**. While the difference between an 89% and 97% yield is not significant, this demonstrates that we had a suitable substrate to study other potential 2H-donors.

Figure 19 | Summary of results obtained for the 2H atom transfer to aryne **7022** from other potential 2H-donors.

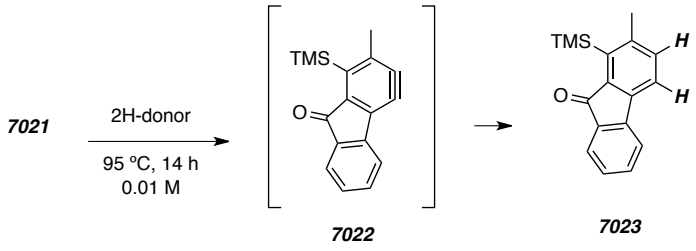

7022 ***7023***

2H-donor	% yield	k_{rel}	$\Delta G^{‡}$
cyclooctane	97%	2.6	17.6
cycloheptane	94%	2.3	17.7
cyclopentane	84%	1.0	18.7
cyclohexane	20%	0.01	24.1
norbornane	66%	0.60	18.5
THF	60%	0.4	19.2
1,4-dioxane	0%	—	27.1
n-heptane	30%	–	–
tetrahydrodi-cyclopentadiene	79%	–	–

Having identified that cyclooctane was a suitable reducing agent represented a critical breakthrough. With this in mind, we probed other seemingly "unactivated" hydrocarbons for their ability to reduce arynes. The results are summarized in the tabular inset of Figure 19. Use of cycloheptane and cyclopentane as solvent provided results

similar to those obtained with cyclooctane and the major byproducts were cycloheptene and cyclopentene, respectively. Interestingly, when cyclohexane was used the solvent, **7023** was recovered in low yield. Additionally, the use of the straight-chain hydrocarbon *n*-heptane gave **7023** in 30% isolated yield. The transition structure found for 2H atom transfer from ethane suggested that eclipsing hydrogen atoms are necessary. This led us to consider norbornane and tetrahydrodicyclopentadiene as potential hydrogen donors because each is imbedded with vicinal eclipsing hydrogen atoms. Heating a mixture of ketotriyne **7021** and excess of either 2H-donor gave benzenoid **7023** in moderate yields. In the case of norbornane, byproduct norbornene was observed in the ^{1}H NMR spectrum of the reaction mixture. No discreet byproducts were observed when tetrahydrodicyclopentadiene was used as the 2H donor.

It was interesting that benzenoid **7023** was obtained in low yields when cyclohexane and *n*-heptane were used as 2H donors as compared to cyclooctane, cycloheptane, and cyclopentane. This led us to consider that there may be a slight structural difference between the various reagents that leads to a difference in 'reducing power.' To measure the 'reducing power' of each solvent, a competition experiment was performed by heating ketotriyne **7021** in an equimolar mixture of cyclopentane and a competing hydrogen source. After 14 h, ^{1}H NMR analysis of the reaction mixtures provided the ratio of cyclopentane to the other alkene byproduct. To ensure accuracy and precision, methods in qNMR[177] were employed. The data are summarized as k_{rel} values in the tabular inset of Figure 19. As implied by the isolated yields, cyclooctane possesses the most inherent reactivity toward dihydrogen transfer followed by cycloheptane and then cyclopentane.

Not surprisingly, cyclohexane was much less reactive than cyclopentane. However, the integral of cyclohexene was within the threshold of the noise in the ^{1}H NMR spectrum, which could introduce error to the measurement. To verify the measured k_{rel} value for cyclohexane, ketotriyne **7021** was heated in a solution consisting of 100:1 molar ratio of cyclohexane and cyclopentane. ^{1}H NMR analysis of the reaction mixture

[177] a) Pauli, G. F.; Jaki, B. U.; Lankin, D. C. Quantitative ^{1}H NMR: Development and potential of a method for natural products analysis. *J. Nat. Prod.* **2005**, *68*, 133–149. b) Pauli, G. F.; Jaki, B. U.; Lankin D. A., Routine experimental protocol for qHNMR illustrated with taxol. *J. Nat. Prod.* **2007**, *70*, 589–595.

showed that the two alkene byproducts, cyclohexene and cyclopentane, were formed in a nearly equimolar ratio. The k_{rel} value for norbornane was found to be intermediate between cyclohexane and cyclopentane. Because the unsaturated byproducts of *n*-heptane- and tetrahydrodicyclopentadiene-mediated aryne hydrogenation were not observable by ^{1}H NMR, the corresponding k_{rel} values could not be determined. The k_{rel} value for THF was found by comparing the ratio of **7023**-h_2:**7023**-d_2 obtained from heating ketrotriyne **7021** in a solution of 1:10 molar ratio of cyclopentane and THF-d_8.

Locating the transition structure for the 2H atom transfer by ethane to *o*-benzyne provided insight into the torsional requirements of the alkane 2H-donor. Namely, the geometry of ethane possessed a 0º dihedral angle between the reacting H–$C_{sp3}C_{sp3}$–H atoms. This suggests that a similar dihedral angle would be required for aryne reduction by each of the cyclic hydrocarbon 2H-donors previously discussed. Cyclooctane, cycloheptane, and cyclopentane consist of conformers with geometries that contain H–$C_{sp3}C_{sp3}$–H dihedral angles < 60º. Whereas, cyclohexane and 1,4-dioxane are dominated by a chair conformation, in which all vicinal dihedral angles are ca. 60º. The six-membered ring 2H-donor hydrocarbon donors must isomerize to the boat-like conformation (ca. 6 kcal•mol^{-1} uphill) to adopt the near-eclipsing dihedral angle required for aryne hydrogenation. We hypothesized that the low reducing power possessed by cyclohexane and 1,4-dioxane can be attributed to the additional energy required to achieve the boat-like reactive conformation.

We turned to computation to find evidence in support of the hypothesis that 2H atom transfer to arynes proceeds via a concerted a mechanism that involves a transition structure with near-planarity among the six reacting atoms.[175] Specifically, computed transition structures were located for 2H atom transfer from the various donors listed in Figure 19 to *o*-benzyne [M06-2X/6-311+G(d,p)]. The lowest energy 'conformer' of each of these transition structures is shown in Figure 20 and was used in determining an estimate for the $\Delta G^{\ddagger}$ (kcal•mol^{-1}). A trend was apparent between the computed $\Delta G^{\ddagger}$ values and the experimentally determined k_{rel} values. This trend suggests that 2H atom transfer to arynes proceeds through the computed transition structures shown in Figure 20. The transition structures that were located correspond to a mechanism involving

concerted 2H atom transfer. Collectively, our experimental and theoretical studies strongly support our overarching hypotheses for the mechanism of alkane-mediated 2H atom transfer to arynes involves concerted transfer of hydrogen through a six-atom transition structure. It should be mentioned that norbornane was expected to have a larger k_{rel} because it contains hydrogen atoms that are locked with an eclipsing dihedral angle. However, this is probably offset by formation of the unstable, strained alkene byproduct, norbornene.

Figure 20 | Computed transition structures and $\Delta G^{\ddagger}$ values for the concerted 2H atom transfer to *o*-benzyne from various cyclic 2H donors.

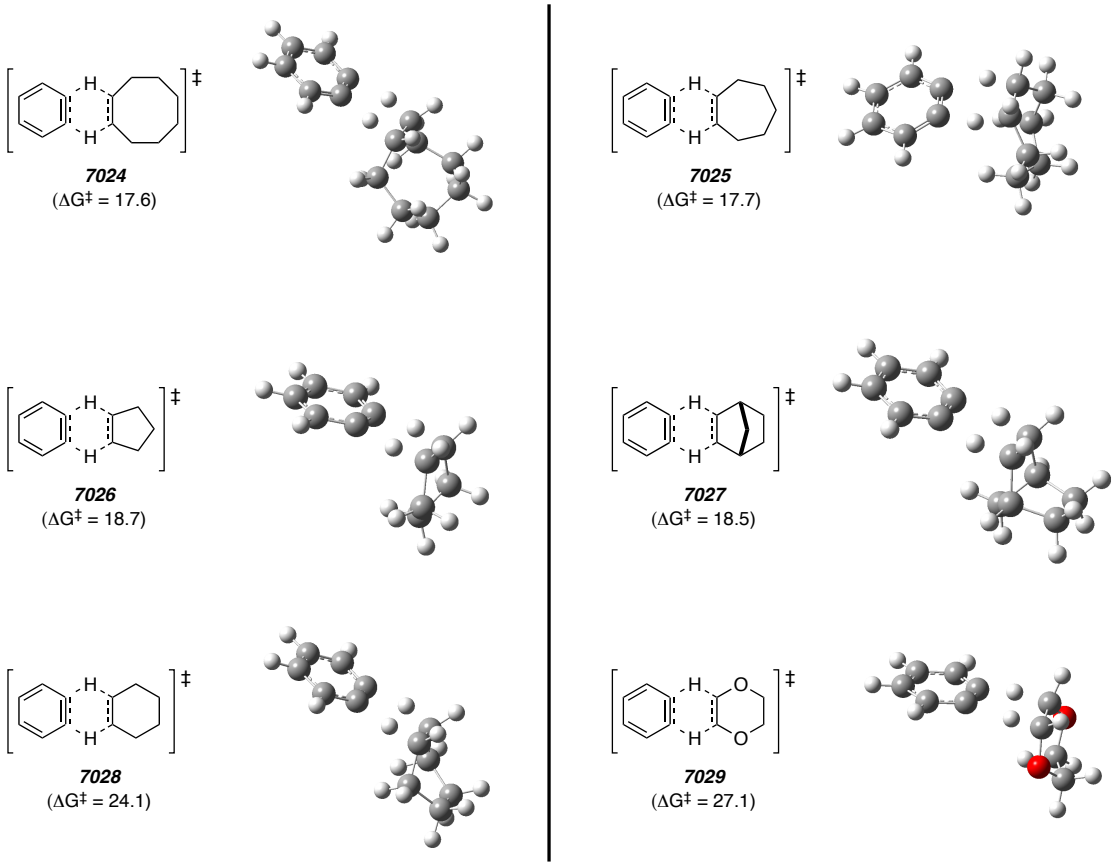

Having gained substantial evidence in support of our proposed mechanism, we began investigating the scope of the reaction with respect to the aryne precursor that can be prepared. To test if ambient temperature 2H atom transfer is possible, we prepared

triyne **7033** from enal **7030** by sequential Glaser coupling with 1-pentyne to give diyne **7031** (Scheme 154). Nucleophilic addition of lithium trimethylsilylacetylide to **7031** gave alcohol **7032**, which was followed by careful MnO_2-mediated alcohol oxidation to give desired triyne **7033**.

Scheme 154 | Synthesis of ketotriyne **7033** and subsequent, cyclooctane-mediated, ambient temperature 2H atom transfer to indenone **7034**.

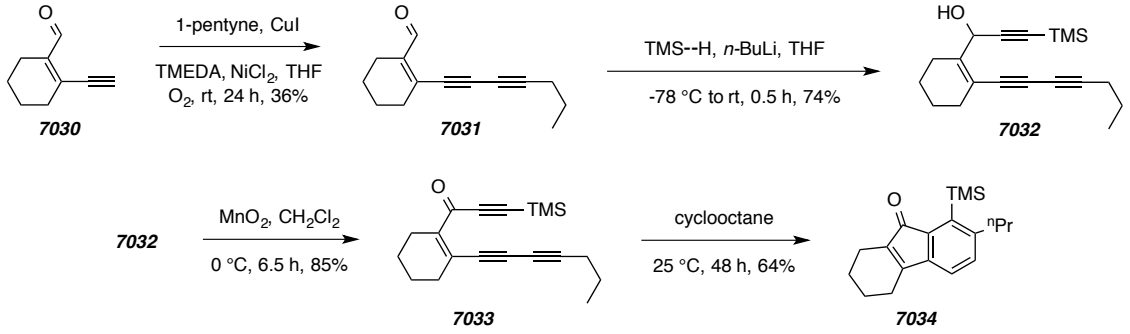

Similar to ketotriyne **6048**, a cyclooctane solution of triyne **7033** gave the corresponding benzenoid **7034** by incubating at 26 ºC for two days. This demonstrates that 2H atom transfer is possible at ambient temperatures if the aryne is able to form. Benzenoids **7035**–**7040** were also prepared by 2H atom transfer from cyclooctane (Figure 21). Additionally, **7040** was prepared on gram-scale, which demonstrates that the efficiency of the reaction is not compromised with larger scales.

Figure 21 | Scope of benzenoids that were made by tandem HDDA/2H atom transfer from cyclooctane.

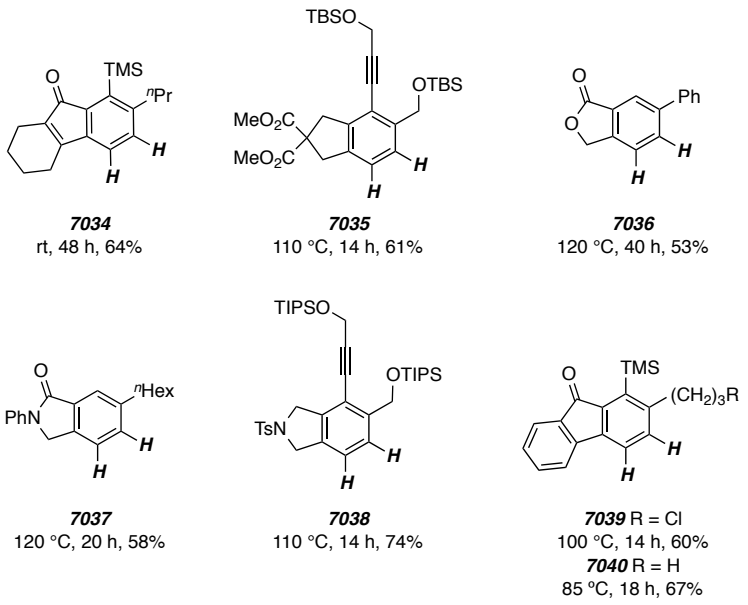

We found it surprising that the 2H atom transfer reaction to arynes has not been observed with non-HDDA-generated arynes. Based on computational results, *o*-benzyne itself should be capable of accepting two hydrogens from a suitable donor. To probe this we heated 2-(trimethylsilyl)phenyl triflate (**6027**) with CsF in THF-h_8 and studied the No-D ^{1}H NMR spectrum of the reaction mixture (Scheme 155). A peak at 7.31 ppm was observed, which, following a series of doping experiments, was confirmed to be benzene. Similarly, use of THF-d_8 as solvent also led to the observed formation of benzene in the reaction mixture (presumably $C_6H_4D_2$). Additionally, ^{1}H NMR analysis was more definitive because of the use of deuterated solvent. When CD_3CN was used as solvent and THF was omitted, benzene was not observed. Not surprisingly, repeating the experiment with 20 equivalents of THF-d_8 (with respect to **6027**) again led to the observed formation of benzene (presumably $C_6H_4D_2$, δ ca. 7.37 ppm, confirmed by doping). These studies strongly suggest that all arynes are, to a certain degree, capable of accepting two hydrogen atoms from THF.

Scheme 155 | Generation of **3** from **6027** and subsequent 2H atom transfer from THF and cyclopentane.

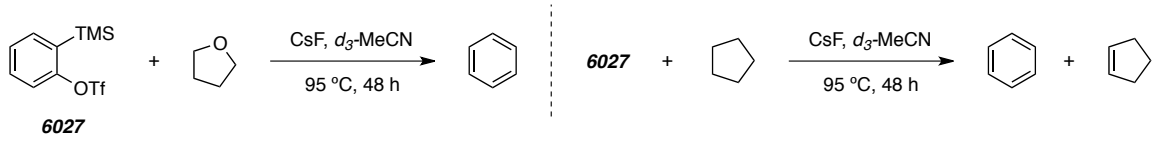

We prepared known norbornadiene **7041**, which forms strained alkyne **7042** in the presence of fluoride ion.[178] Heated a mixture of it, CsF, and cyclopentane in CD_3CN gave a crude reaction mixture in which both norbornadiene and cyclopentene were clearly observable by No-D ^1H NMR (Scheme 156). Recently, Bertozzi and co-workers described dihydrogen transfer from THF-h_8 (and -d_8) to another complex, strained cyclic alkyne.[179] These studies confirm that other strained alkynes are capable of accepting hydrogen atoms from THF. The use of THF as solvent in reactions involving related intermediates are then at risk of unwanted alkyne reduction by solvent. This limitation can be overcome if an efficient trapping reagent rapidly reacts with the strained alkyne. Using Reaxys®, analysis of the solvent used in reactions in which *o*-benzyne precursor **6027** is the starting material indicates that THF is the second most popular solvent generating for *o*-benzyne from **6027**. Specifically, 825 hits were obtained for THF as solvent vs. 1544 for CH_3CN, which was the most popular solvent. Clearly our recent studies, which were guided by discoveries made with HDDA-generated arynes, have shed light on a larger issue in the chemistry of strained alkynes.

Scheme 156 | Example of 2H atom transfer to strained alkyne **7042** from cyclopentane.

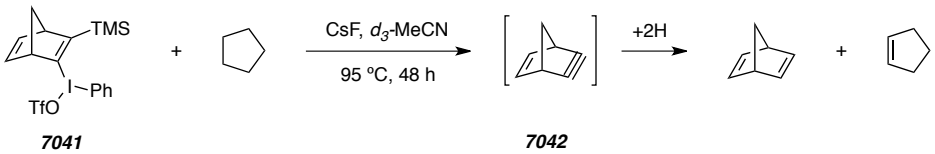

[178] Kitamura, T.; Kotani, M.; Yokoyama, T.; Fujiwara, Y.; Hori, K. A new hypervalent iodine precursor of a highly strained cyclic alkyne. Generation and trapping reactions of bicyclo[2.2.1]hept-2-en-5-yne. *J. Org. Chem.* **1999**, *64*, 680–681.

[179] Almeida, G. de; Townsend, L. C.; Bertozzi, C. R. Synthesis and reactivity of dibenzoselenacycloheptynes. *Org. Lett.* **2013**, *15*, 3038–3041.

7.4. HDDA-Generated Aryne-Mediated Oxidation of Alcohols

One of the oldest aryne trapping groups is the alcohol. An advantage of early precursors that could generate *o*-benzyne under thermal conditions was their ability to efficiently be trapped by acid-sensitive reactants. This was first demonstrated by Stiles and Miller, who observed that heating *o*-benzenediazonium carboxylate **6029** (Section 6.2) in *t*-butanol led to efficient trapping via a net O–H insertion.[138] Roberts had previously reported that a mixture of bromobenzene, $NaNH_2$, and potassium *t*-butoxide did not yield phenyl *t*-butyl ether.[180] Interestingly, reports of similar reactions of *o*-benzyne have been limited to tertiary alcohols or unhindered primary alcohols.[123]

When a mixture of ketotriyne **7043** and cyclooctanol was heated in $CDCl_3$ the expected product, aryl ether **7044**, was isolated in surprisingly low yields. The major byproduct of the reaction was fluorenone **7040**, which is likely formed by 2H atom transfer to the corresponding aryne intermediate. At this point we had a deep working knowledge of the mechanism of 2H atom transfer to arynes from alkanes, but the mechanistic details for aryne hydrogenation in the presence of cyclooctanol were not obvious. The outcome was surprising because we anticipated that addition of the nucleophilic oxygen atom would be much faster than a competing 2H atom transfer process. More importantly, the source of hydrogen was unclear. ^{1}H NMR analysis of the reaction mixture indicated that cyclooctanone was the major byproduct, in equimolar ratio to reduced aryne **7040**. Still, we were not entirely confident that other byproducts were not being formed because the spectral data were convoluted by the remaining cyclooctanol and aryl ether byproduct **7044**. To simplify analysis of the reaction mixture, we repeated the experiment with 1.5 equivalents of alcohol, which gave rise to a different ratio of products (cf. 4:1 **7040**:**7044**) that favored formation of reduced benzenoid **7040**, and cyclooctanone was also formed in equimolar ratio to **7040**. ^{1}H NMR analysis of the reaction mixture was easier because the resulting mixture contained less of both cyclooctanol and aryl ether **7044**. These results led us to hypothesize that cyclooctanol was the source of hydrogen, and also suggested that the rate of aryl ether formation is not first order in alcohol. Additionally, it was surprising that the ^{1}H NMR spectrum of the

[180] Scardiglia, F.; Roberts, J. D. Reactions of non-activated aryl halides with nucleophilic agents induced by alkali amides in liquid ammonia. *Tetrahedron* **1958**, *3*, 197–208.

reaction mixture was clean and fluorenone **7040** was isolated in good yield despite using only 1.5 equivalents of the bimolecular trap. Namely, the data were not contaminated by the intractable resonances in the aromatic region that are typically observed when less than five equivalents of bimolecular trap is present. This suggests that alcohol-mediated 2H atom transfer to arynes is one of the more efficient intermolecular aryne trapping reactions that we have encountered.

Scheme 157 | Product distribution when aryne precusor **7043** is heated in the presence of varying amounts of cyclooctanol.

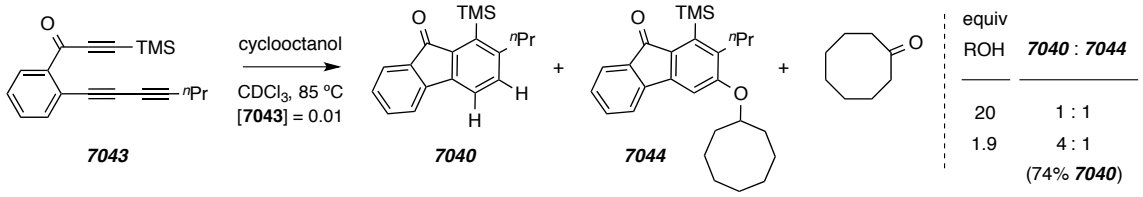

Mindful of our previous mechanistic studies of 2H atom transfer from alkanes to arynes, we initially proposed that the mechanism of cyclooctanol-mediated aryne hydrogenation to benzenoid **7040** and cyclooctanone involved the simultaneous transfer of the weakened carbinol C–H and vicinal methylene C–H to give the fluorenone and enol **7046**. Keto-enol tautomerization of **7046** would then give rise to cyclooctanone. We assumed that the process had not been observed before because i) use of *o*-benzyne precursors would give rise to benzene itself, which is difficult to identify in crude reaction mixtures and ii) similar to cyclooctane, a dominant conformer of cyclooctanol contains a near-eclipsing dihedral angle between the transferred, vicinal hydrogen atoms, and it seemed unlikely that a similar process occurs with other alcohols [postulate ii) was later proven to be incorrect].

Scheme 159 | Initially proposed mechanism for the 2H atom transfer from cyclooctanone to an aryne generated by HDDA cycloisomerization.

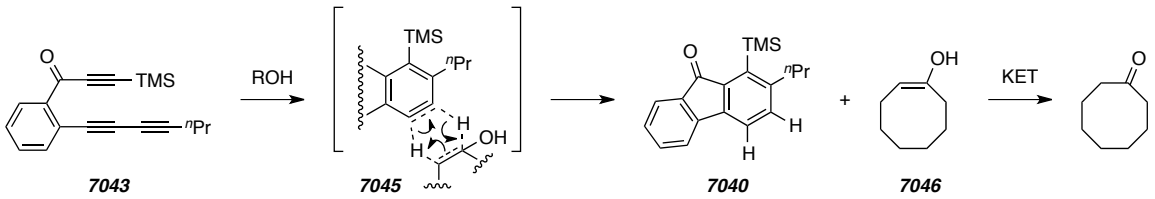

To test our hypothesis that the near-eclipsing dihedral angle of the carbinol C–H to methylene C–H was necessary for efficient 2H atom transfer to arynes, we heated ketotriyne **7043** in an equimolar solution of cyclooctanol and cyclohexanol. Again, fluorenone **7040** was cleanly formed, and, surprisingly, ^{1}H NMR analysis of the reaction mixture indicated that cyclooctanone and cyclohexanone were formed in a nearly equimolar ratio. This result indicates that cyclohexanol is also a competent 2H atom donor, which is in stark contrast to the observed k_{rel} values for the hydrocarbon analogues and suggests an alternative mechanism is involved. Under the assumption that the methylene C–H adjacent to the carbinol carbon was transferred in the alcohol-mediated aryne reduction mechanism, we heated a mixture of ketotriyne **7043** and 2,2,6,6-tetradeuterocyclohexanol (**7047**) in $CDCl_3$ (Scheme 160). ^{1}H NMR analysis, low-resolution GC/MS and low-resolution LC/MS indicated that fluorenone **7040** was the major product, and deuterium incorporation was *not* detected.

Scheme 160 | Studies of deuterium incorporation in the 2H atom transfer reaction from cyclohexanol-$d_{\#}$ to a fluorynone.

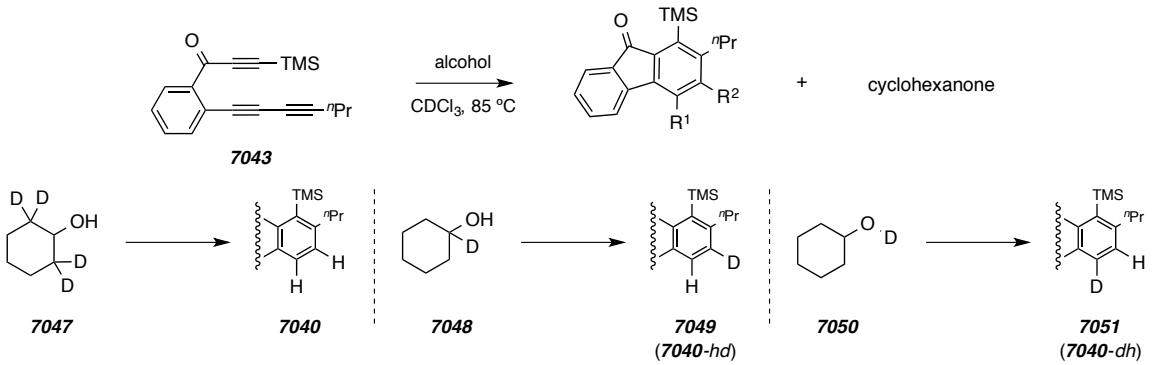

Our inability to incorporate deuterium into the reduced benzenoid led to us to prepare the C-D analogue of cyclohexanol, **7048**.[181] Heating a mixture of **7048** and ketotriyne **7043** in $CDCl_3$ led to exclusive formation of the monodeuterated fluorenone **7049** (henceforth referred to as **7040**-*hd*). Interestingly, the corresponding **7040**-*dh* analogue and the "cross-over products," **7040**-h_2 and **7040**-d_2, were not detected by ^{1}H NMR, low-resolution GC/MS, or low-resolution LC/MS analysis. The complementary experiment was performed with cyclohexanol-OD (**7050**), which was readily prepared by washing cyclohexanol with D_2O. Heating a mixture of **7050** and ketotriyne **7043** in $CDCl_3$ gave a mixture of **7040**-h_2 and **7040**-*dh* (i.e. **7051**) with a ratio of 2:3, which was close to the estimated deuterium incorporation of the cyclohexanol-OD (ca. 70% deuterium). Stirring cyclohexanol with an excess of CD_3OD for one hour and then removing the volatiles led to a greater %-deuterium incorporation of cyclohexanol-OD. The process was repeated five times to give cyclohexanol-OD (**7050**) with >95% *d*. Repeating the alcohol-mediated 2H atom transfer with >95% *d* **7050** gave **7040**-*dh* as the major product with only trace quantities of **7040**-h_2.

The deuterium incorporation studies provided a tremendous amount of mechanistic insight about the alcohol-mediated 2H atom transfer to arynes. Our inability to observe substantial amounts of **7040**-h_2 or **7040**-d_2 when either of the monodeuterated isomers of cyclohexanol was used indicates that the two hydrogen atoms are transferred from one molecule of alcohol. More importantly, the transferred hydrogen atoms were found to be the carbinol methine C–*H* and the hydroxy O–*H*. These results indicate that, similar to 2H atom transfer from alkanes, the mechanism involves the simultaneous transfer of two hydrogens from the alcohol to the aryne intermediate. Additionally, aryne reduction and alcohol oxidation likely occur in concert via transition structure **7052** (Figure 22-A). Interestingly, heating triyne **7043** with either of the monodeuterated isomers of cyclohexanol gave the corresponding monodeuterated product with high and complementary regioselectivities. It is noteworthy that the C–H hydrogen atom prefers addition to what computation has predicted to be the more electrophilic C_{sp} atom (see

[181] Wu, X.; Fors, B. P.; Buchwald, S. L. A single phosphine ligand allows palladium-catalyzed intermolecular C–O bond formation with secondary and primary alcohols. *Angew. Chem. Int. Ed.* **2011**, *50*, 9943–9947.

Section 7.2). This is reminiscent of other processes that utilize the inherent nucleophilicity of a carbinol C–H (e.g., Oppenhauer and Canizzaro reactions). Collectively these data strongly support a concerted 2H atom transfer reaction through transition structure **7052**, in which the C–H adds to the more electrophilic aryne carbon.

Figure 22 | A) Proposed transition structure for the revised mechanism for the alcohol-mediated 2H atom transfer to arynes, B) computed transition structure [M06-2X/6-311+G(d,p)] for 2H atom transfer from methanol to *o*-benzyne (**3**), and C) overall energetics for the alcohol-mediated 2H atom transfer from methanol to **3**.

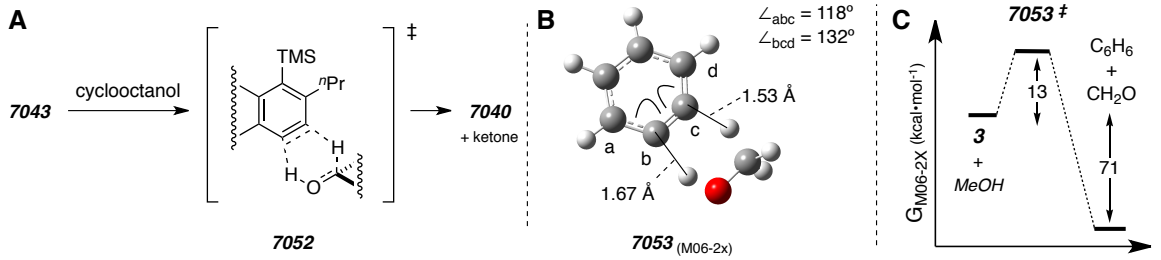

Armed with these mechanistic insights we began studying the energetic feasibility of our current hypothesis for the alcohol-mediated 2H atom transfer reaction with *o*-benzyne itself. Transition structure **7053** was located for the 2H atom transfer reaction between *o*-benzyne and methanol (Figure 22-B). The computed $\Delta G^{‡}$ for the reaction was found to be 13 kcal•mol^{-1} with ΔG_{rxn} = -71 kcal•mol^{-1}. The transition structure suggests that the reaction is asynchronous as seen by difference in H–C_b vs. H–C_c atom distances. Interestingly, symmetric *o*-benzyne had distorted in the transition structure so that the C–H methine was adding to the aryne C_{sp} carbon atom, C_c, with the more obtuse bond angle (132º vs. 118 º for C_b). Recalling the computational model for aryne trapping described in Section 7.1, it is expected that the nucleophilic methine C–H would add to the more electrophilic atom of *o*-benzyne, which is consistent with our deuterium labeling studies summarized in Scheme 160.

We also computed the $\Delta G^{‡}$ of the substrates we were studying experimentally. Specifically, transition structure **7054** was located for the 2H atom transfer reaction between cyclohexanol and fluorynone **7022** (Figure 23). The computed $\Delta G^{‡}$ value of this

more realistic system was found to be 12.2 kcal•mol^{-1}. Comparison between the $\Delta G^{\ddagger}$ values for the transfer of 2H from cyclohexanol vs. cyclopentane (cf. $\Delta G^{\ddagger}$ = 19.4 kcal•mol^{-1}) indicates that 2H atom transfer from alcohols is much faster and suggests why use of only 1.5 equivalents of alcohol is sufficient for efficient preparation of benzenoid **7040**. Computing the transition structure for the inverse addition (i.e. addition of O–H to the more electrophilic aryne carbon) led to location of a transition structure (cf. **7055**) that is 3.4 kcal•mol^{-1} higher in energy than **7054**, which is consistent with the regiochemical preference observed in the deuterium labeling studies. Overall, the computed transition structure strongly supported our proposed mechanism.

Figure 23 | Transition structure calculations and $\Delta G^{\ddagger}$ values for the 2H atom transfer to a model fluorynone, **7056**.

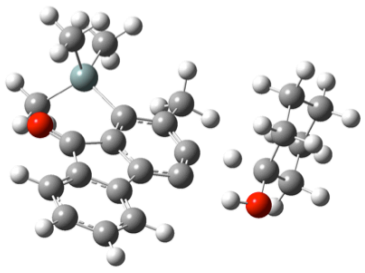

7054
$\Delta G^{\ddagger}$ = 12.2 kcal• mol^{-1}

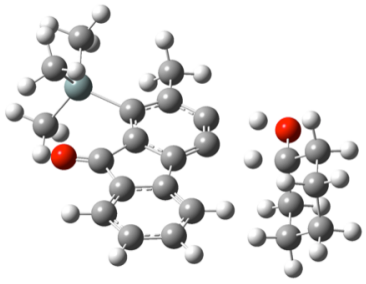

7055
$\Delta G^{\ddagger}$ = 15.4 kcal• mol^{-1}

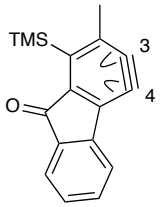

7022
$\angle_{at\ C\text{-}3}$ = 136°
$\angle_{at\ C\text{-}4}$ = 118°

Having established strong support for a mechanism for the 2H atom transfer from alcohols to arynes, we began to examine the scope of alcohol reducing agents. Myriad of alcohol reactants were screened, and almost all were amenable to 2H atom transfer when heated with ketotriyne **7043** (Figure 24). The alcohol screening experiments were performed by heating a mixture of **7043** and the alcohol 2H-donor (1.5 equivalents) in $CDCl_3$. The competency of each reductant was judged based upon the cleanliness of the ^{1}H NMR and GC/MS spectral data. In general, secondary alcohols provided the cleanest spectral data, which suggests that these reagents are superior to primary alcohols. Still, several primary alcohols were found to be competent 2H atom donors, and the major impurities were only the corresponding aryl ethers (cf. **7044**). One noteworthy example

includes the selective mono-oxidation of both *cis* and *trans* 1,2-cyclohexanediol to give 2-hydroxycyclohexanone. Additionally, ^{1}H NMR analysis of the reaction mixture that resulted from heating a mixture of 2-trimethylsilylphenyl triflate (**6027**), CsF, and 5 equivalents of cyclopentanol in CD_3CN clearly indicated that benzene and cyclopentanone were formed. These results suggest that the scope of the 2H atom transfer from alcohols to arynes is general with respect to the alcohol 2H-donor and the aryne acceptor.

Figure 24 | A) Scope of alcohols amenable to 2H atom transfer B) observed cyclopentanol-mediated 2H atom transfer to **3** via **6027**.

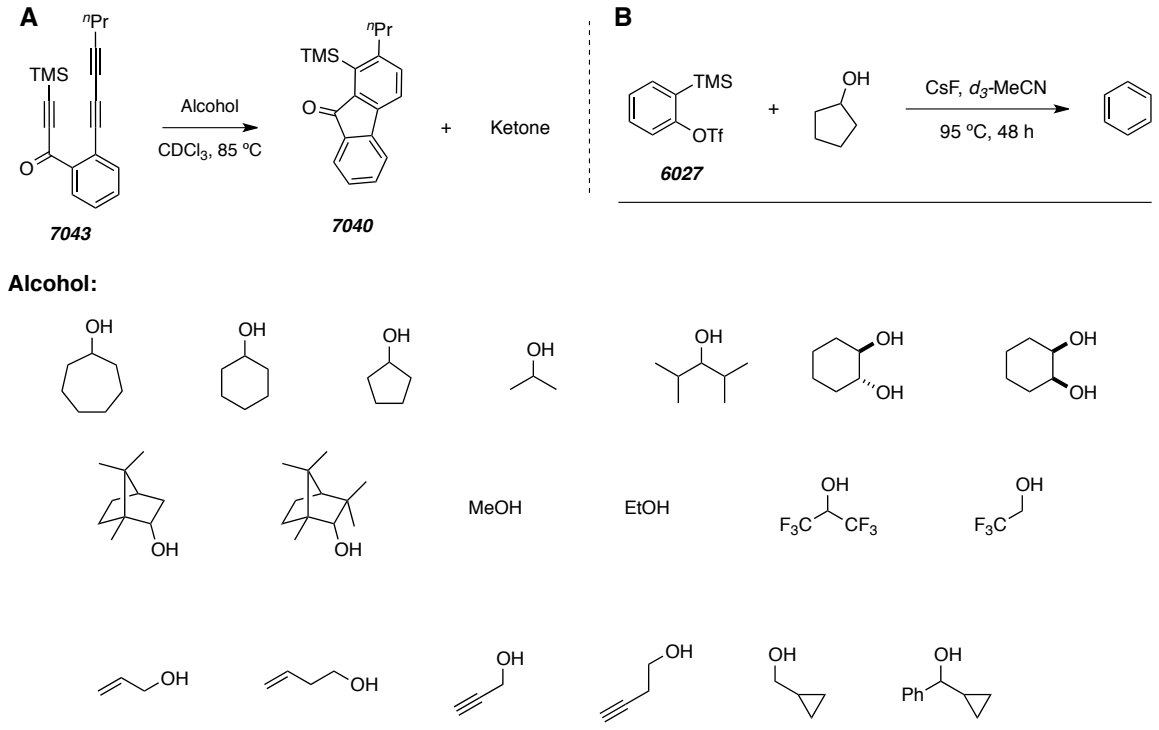

7.5 Implications for the Mechanism of Alcohol Addition to Aryne Intermediates

Our initial observations indicated that increasing the concentration of alcohol led to an increased amount of the aryl ether byproduct (tabular inset of Scheme 157). This suggested to us that the mechanism for alcohol addition to aryne intermediates requires more than one molecule of alcohol. A potential mechanism could be nucleophilic addition of the hydroxy oxygen to aryne **7056** to generate aryl zwitterion **7057**. While intramolecular proton transfer would directly give aryl ether **7058**, this would involve an unfavorable 4-atom transition state. Instead, the aryl anion could deprotonate another alcohol molecule, followed by rapid proton transfer from the oxonium oxygen. Alternatively, ether formation could occur by reaction with a hydrogen-bonded dimer of the trapping alcohol (cf. **7060**). Such a process would simultaneously add oxygen and hydrogen to the aryne via a concerted mechanism (cf. transition structure **7059**). In an attempt to gain further mechanistic insight we attempted to compute **7059**, however all attempts were unsuccessful. As this Thesis was being prepared, another graduate student in our group has performed kinetic studies on the alcohol addition reaction, and strong evidence has been acquired that support a second-order rate dependence on the alcohol concentration.

Figure 25 | Potential mechanisms for the formation of aryl ether **7058** by addition of 2 equivalents of alcohol (R'OH) to aryne **7056**.

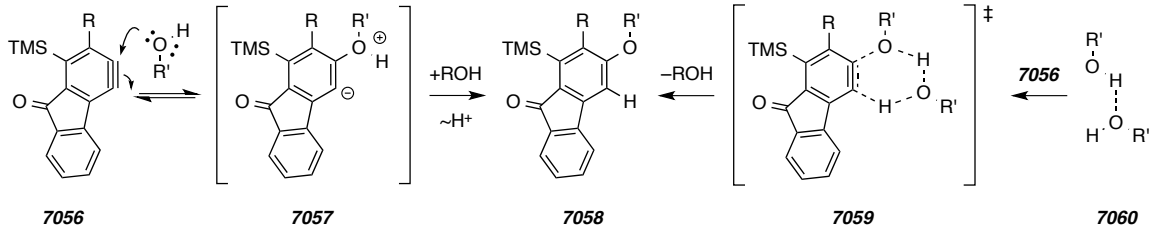

7.6. Concluding Remarks

Collectively, the studies presented in Chapter 7 demonstrate that the generation of aryne intermediates in the absence of additional reagents will lead to fundamental insights about the chemical properties of "one of the oldest, most *interesting*, most *useful*, and most *well-studied* of all reactive intermediates."[143] The highlight of this chapter

includes our studies related to the use of arynes as efficient oxidants for alkanes, cyclic ethers, and alcohols. By simply heating the triyne precursors in THF, the HDDA cyclization allowed for the discovery of a fundamental method of desaturating otherwise inert hydrocarbons. Additionally, a similar process was found to occur between arynes and alcohols. After optimization of each of these processes with the use of HDDA-generated aryne intermediates, we confirmed that each process also occurs with the more conventional aryne precursor, 2-trimethylsilylphenyl triflate (**6027**). We found it surprising that these processes had not been encountered in prior, non-HDDA-related studies. This demonstrates additional advantages of the HDDA reaction cascade, namely i) are sufficiently complex to allow for easier isolation of products when relatively simple trapping reagents are used [e.g., H_2 (net aryne hydrogenation) via 2H atom transfer] and ii) the HDDA reaction cascade is formed in the absence of additional reagents, which reduces the potential for side reactions.

Chapter 8. Developing an Efficient Protocol for the DFT Computation of NMR Chemical Shifts

8.1. Background and Introduction

This chapter describes our recent efforts into developing a routine protocol for the application of modern methods in density functional theory (DFT) to the computation of ^{1}H and ^{13}C NMR chemical shifts. The intended user of this protocol is a chemist who routinely assigns a structure to unknown, often highly complex, organic molecules that exist as a mixture of equilibrating conformers when dissolved in solution. The ultimate goal of the protocol is to empower experimental chemists with the ability to use seemingly complex computational tools to aide in their interpretation of NMR spectral data.

NMR is the most powerful analytical technique for the elucidation of chemical structure. NMR analysis allows for one to gain insight into the local chemical environment surrounding atoms with a particular nucleus (e.g., ^{1}H, ^{13}C, ^{19}F, and ^{31}P). The high degree to which organic molecules are substituted by hydrogen and carbon has made ^{1}H and ^{13}C NMR techniques invaluable to organic chemists. Many recent technological advances have allowed for NMR analysis of organic molecules to be performed in myriad of settings. Examples of these advances include i) application of higher field magnets, ii) development of novel multidimensional experiments, and iii) production of more affordable spectrometers. Use of increasingly higher magnetic fields with better probe technology allows for both greater resolution of over-lapping resonances and vastly improved signal to noise.

Despite these advances, there are several examples of incorrectly assigned structures of complex molecules appearing in the literature.[182] Two recent examples include hexacyclinol (**8002**) and vannusal B (**8004**, Figure 26). Each of these structures was originally assigned to a highly complex, polycyclic architecture that was later found

[182] Nicolaou, K. C.; Snyder, S. A. Chasing molecules that were never there: Misassigned natural products and the role of chemical synthesis in modern structure elucidation. *Angew. Chem. Int. Ed.* **2005**, *44*, 1012–1044.

(with the aide of DFT computation of NMR data)[183] to be incorrect. In the case of hexacyclinol, the originally proposed structure was a constitutional isomer of the natural product. After initial isolation by Gräfe[184] (and a controversial synthesis by La Clair[185]), Rychnovsky[186] challenged the proposed structure (**8001**) for hexacyclinol. Based upon DFT computation of ^{13}C NMR chemical shifts, an alternative structure (cf. **8002**) was proposed and later verified by total synthesis.[187] In the case of vannusal B, synthesis studies by Nicolaou[188] demonstrated that the correct structure (cf. **8004**) is a diastereomer of the originally proposed[189] structure, **8003**. Results from a subsequent collaboration between Nicolaou and Bagno demonstrated that comparison of the DFT computation of the ^{13}C chemical shifts would have allowed for accurate prediction of the relative configuration of vannusal B.[190] These examples demonstrate how DFT computation of NMR data can be used to aide in assigning an accurate structure with regard to constitution (e.g., hexacyclinol) and relative configuration (e.g., vannusal B) of complex and unknown organic molecules.

---

[183] Lodewyk, M. W.; Siebert, M. R.; Tantillo, D. J. Computational prediction of ^{1}H and ^{13}C chemical shifts: A useful tool for natural product, mechanistic, and synthetic organic chemistry. *Chem. Rev.* **2012**, *112*, 1839–1862.

[184] Schlegel, B.; Haertl, A.; Dahse, H. M.; Gollmick, F. A.; Graefe, U.; Doerfelt, H.; Kappes, B. Hexacyclinol, a new antiproliferative metabolite of *Panus rudis* HKI 0254. *J. Antibiot.* **2002**, *55*, 814–817.

[185] La Clair, J. J. Total syntheses of hexacyclinol, 5-*epi*-hexacyclinol, and desoxohexacyclinol unveil an antimalarial prodrug motif. *Angew. Chem. Int. Ed.* **2006**, *45*, 2769–2773.

[186] Rychnovsky, S. D. Predicting NMR spectra by computational methods: Structure revision of hexacyclinol. *Org. Lett.* **2006**, *8*, 2895–2898.

[187] Saielli, G.; Bagno, A. Can two molecules have the same NMR spectrum? Hexacyclinol revisited. *Org. Lett.* **2009**, *11*, 1409–1412.

[188] Nicolaou, K. C.; Ortiz, A.; Zhang, H.; Guella, G. Total synthesis and structural revision of vannusals A and B: Synthesis of the true structures of vannusals A and B. *J. Am. Chem. Soc.* **2010**, *132*, 7153–7176 and references cited therein.

[189] Guella, G.; Callone, E.; Di Giuseppe, G.; Frassanito, R.; Frontini, F. P.; Mancini, I.; Dini, F. Hemivannusal and prevannusadials–new sesquiterpenoids from the marine ciliate protist *Euplotes vannus*: The putative biogenetic precursors to dimeric terpenoid vannusals. *Eur. J. Org. Chem.* **2007**, 5226–5234.

[190] Saielli, G.; Nicolaou, K. C.; Ortiz, A.; Zhang, H.; Bagno, A. Addressing the stereochemistry of complex organic molecules by density functional theory-NMR: Vannusal B in retrospective. *J. Am. Chem. Soc.* **2011**, *133*, 6072–6077.

Figure 26 | Original and revised structures for hexacyclinol and vannusal B.

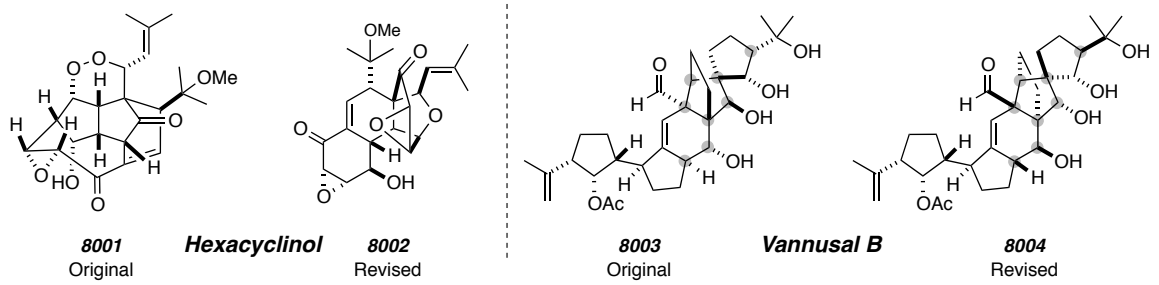

8.2. Modern Approaches to the Computation of NMR Chemical Shifts

Reports of the incorrectly assigned structures for hexacyclinol and vannusal B demonstrate that experimental NMR data can lead to ambiguous conclusions of chemical structure. However, ^{1}H NMR analysis of discreet molecules often provides spectral data that can be fully interpreted even if it cannot be fully explained. Specifically, examination of peaks in a ^{1}H NMR spectrum usually gives rise to i) a chemical shift (δ, in ppm), ii) a coupling constant (*J*, in Hz), and iii) a relative integration (#H). Of each of the pieces of data, the chemical shift is arguably the most instructive about the local chemical environment of a particular atom and is most useful from the perspective of structure elucidation. This is also true of ^{13}C NMR spectroscopy where coupling constant and relative integration are rarely applicable. Fortunately, the chemical shift is amenable to accurate prediction by computational approaches. This provides chemists with the opportunity to predict the chemical shift of known structures for comparison against ambiguous experimental data.

The computation of NMR properties has expanded greatly and modern methods in computational chemistry are now capable of simulating entire ^{1}H and ^{13}C NMR spectra of small molecules. Common software packages that perform these tasks include, for example, ACD/Labs and ChemDraw (ChemBioDraw). These applications use databases and experimental data or increment-based additivity methods, respectively, to generate predicted NMR data. To demonstrate this, we have predicted the ^{1}H NMR spectrum of both *trans*- (**8005**) and *cis*-2-methylcyclohexanol (**8006**) using ACD/Labs software (Figure 27-A). The complexity of the computed spectral data indicates that chemical shifts, coupling constants, and integrations have each been determined with some

reasonably sophisticated algorithms. However, the reliability of this information is not reassuring when these spectra are compared to their experimental counterparts (Figure 27-B). The downfield methine peak has been well predicted, but the upfield resonances are virtually identical in each of the computed spectra. The experimental data of the *cis* diastereomer contains several well-resolved resonances, which is not predicted in the ACD/Labs spectrum. Overall, these similarities suggest that use of this application for predicting data of more complex structures would likely lead to ambiguities and structure assignment would either be inconclusive or incorrect.

Figure 27 | ^{1}NMR spectra for *trans*- (**8005**) and *cis*-3-methylcyclohexanol (**8006**) A) simulated by the software ACD/Labs predictor and B) collected experimentally in chloroform 500 MHz).

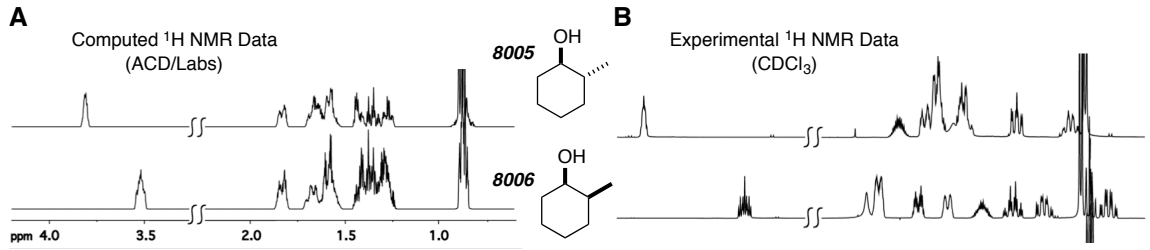

8.3. Use of Mean Absolute Error (MAE) to Assess Goodness of Fit

When comparing computed and experimental NMR chemical shifts it is necessary to be quantitative. The most common approach is to determine the mean absolute error (MAE). The equation of the MAE is shown in Figure 28 where *N* is the number of unique conformers. In the case of the data presented in Figure 27, we determined the MAE for all four modes of comparison: MAE of $trans_{exp}$ vs. $trans_{ACD}$ = 0.13 ppm, MAE of $trans_{exp}$ vs. cis_{ACD} = 0.22 ppm, MAE of cis_{exp} vs. $trans_{ACD}$ = 0.22 ppm, MAE of cis_{exp} vs. cis_{ACD} = 0.26 ppm. Interestingly, comparison of the MAE values between the experimental values for the *cis* and the computed values of both diastereomers would suggest that the structure of the molecule that produced the experimental data should be *trans*-2-methycyclohexanol (**8005**). It should be mentioned that determining the MAE is only one

approach to assessing the best fit. Other statistical approaches include, for example, regression analysis (R^2), corrected mean absolute error (CMAE),[183] and DP4 analysis.[191]

Figure 28 | A) Equation for mean absolute error (MAE) and B) MAE values obtained from comparing experimental and predicted (ACD/Labs) δ values of **8005** and **8006**.

A

$$\mathrm{MAE} = |\Delta\delta_{\mathrm{ave}}| = \frac{1}{N}\sum_{i=1}^{N}|\delta_i^{\mathrm{comp}} - \delta_i^{\mathrm{exp}}|$$

Where N = the number of unique conformers.

B

MAE of Experiment vs. Predicted (ACD/Labs)

Experiment	Predicted (ACD/Labs): 8005$_{(cis)}$	Predicted (ACD/Labs): 8006$_{(trans)}$
8005$_{(cis)}$	0.13	0.22
8006$_{(trans)}$	0.22	0.26

8.4. Use of Density Functional Theory to Compute NMR Properties

In the last twenty years, density functional theory (DFT) has emerged as the most practical approach for accurately computing the physical properties of chemical systems.[192] Previous reports from our lab have shown that chemical shift values of ^{1}H and ^{13}C atoms are most reliably and practically computed using DFT.[193] Armed with the ability to compute the NMR spectral properties of several candidate structures, the task of structure elucidation reduces to five steps i) acquiring experimental NMR data, ii) proposing tentative structures, iii) assigning specific resonances to their corresponding atoms in the proposed structures, iv) computing the chemical shifts of each candidate structure with a high degree of accuracy, and v) comparing the experimental and computed NMR data to determine a 'best fit.' Unfortunately, use of computational methods to aide in structure elucidation (step iv) is not yet routine, which is likely due to the seemingly complex tools used in computational chemistry. Chapter 8 of this Thesis

[191] Smith, S. G.; Goodman, J. M. Assigning stereochemistry to single diastereoisomers by GIAO NMR calculation: The DP4 probability. *J. Am. Chem. Soc.* **2010**, *132*, 12946–12959.
[192] Bachrach, S. M. *Computational Organic Chemistry*, 1st ed.; Wiley Interscience, Hoboken, New Jersey, 2007.
[193] a) Wiitala, K. W.; Al-Rashid, Z. F.; Dvornikovs, V.; Hoye, T. R.; Cramer, C. J. Evaluation of various DFT protocols for computing ^{1}H and ^{13}C chemical shifts to distinguish stereoisomers: Diastereomeric 2-, 3-, and 4-methylcyclohexanols as a test set. *J. Phys. Org. Chem.* **2007**, *20*, 345–354. b) Wiitala, K. W.; Hoye, T. R.; Cramer, C. J. Hybrid density functional methods empirically optimized for the computation of ^{13}C and ^{1}H chemical shifts in chloroform solution. *J. Chem. Theory Comput.* **2006**, *2*, 1085–1092.

will describe our efforts to develop a protocol to guide prototypical synthetic chemists in their efforts to use DFT computation of NMR data to aide with structure elucidation.

Molecules with a high degree of structural complexity are most often the culprits of ambiguous NMR spectral data. Use of DFT to compute these structures requires substantial computational resources. Fortunately, recent advances in processor technologies, parallel computing, and manufacturing of super computers have mitigated these issues and made DFT computation of complex systems more practical. This has allowed for the application of DFT to the computation of many complex properties of organic molecules (e.g., thermochemistry).[194] For this reason, it was not until recently that reports detailing DFT computation of NMR data of complex molecules have begun to surface.[183]

8.5. The Importance of Considering Conformers

An additional barrier exists when computing NMR data, namely with regard to how conformers are to be dealt with. Due to free rotation about the ubiquitous carbon-carbon single bond most organic molecules exist in solution as a mixture of structurally unique conformers. The rapid rate at which conformers equilibrate makes them, for the most part, inconsequential to the study of their physical and chemical properties. NMR spectrometers have a shutter speed, and the data recorded represent an average across the distribution of conformers. Because the atoms of each unique conformer are in differing chemical environments they each have a unique chemical shift. A useful example to consider is cyclohexane, in which the ^{1}H NMR spectrum ($CDCl_3$) contains a single resonance at δ = 1.44 ppm that reflects the time-averaged chemical shift of cyclohexane at ambient temperature. Low temperature ^{1}H NMR analysis of cyclohexane indicates that the chemical shift of the equatorial and axial hydrogen atoms are actually different (H_{eq} δ = 1.68 ppm, H_{ax} δ = 1.19 ppm).[195] Cyclohexane exists in solution as two rapidly interconverting, degenerate conformers, which serves to average these resonances into the one observed resonance [cf. (1.68+1.19)•0.5 = 1.44 ppm]. The accurate consideration

[194] Zhao, Y.; Truhlar, D. G. Density functionals with broad applicability in chemistry. *Acc. Chem. Res.* **2008**, *41*, 157–167.
[195] Garbisch, E. W., Jr; Griffith, M. G. Proton couplings in cyclohexane. *J. Am. Chem. Soc.* **1968**, *90*, 6543–6544.

of conformers is straightforward in the case of cyclohexane because it exists as only two degenerate conformers. However, this is a rare case and most molecules do not possess such a high degree of symmetry.

Substitution by a single substituent breaks this symmetry of the molecule and its constituent conformers are no longer degenerate. A straightforward example, methyl-cyclohexane also exists as a pair of conformers that equilibrate via chair-flip where the methyl group can be positioned either equatorially (cf. **8007**) or axially (cf. **8008**, Figure 29-A). Positioning the methyl group in the axial position introduces 1,3-diaxial strain energy, and increases the overall free energy of axial conformer **8008**. This strain energy creates an energy difference between the two conformers, which also leads to a difference in concentration of either at equilibrium. If the energy difference is known, then the equilibrium concentration can be determined as a mole fraction via the Boltzmann equation (Figure 29-B). The energy difference between **8007** and **8008** is 1.74 kcal•mol^{-1}, favoring equatorial positioning of the methyl group.[196] Using the Boltzmann equation with $\Delta E = 1.74$ gives a ratio of 97:3 for **8007**:**8008**. The mole fraction value resulting from the Boltzmann equation is typically referred to as the Boltzmann factor. The Boltzmann factor is 0.97 for **8007** and 0.03 for **8008**.

Figure 29 | A) The conformers of methyl cyclohexane (**8007** and **8008**) and their known free energy difference and B) the Boltzmann equation, and its application to dteremine the population (i.e. mole fraction) of **8007** and **8008** at equilibrium.

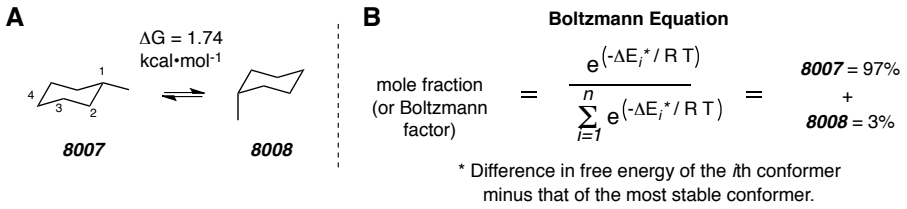

To demonstrate the effect conformers have on ^{1}H NMR δ value, we have computed the δ values for both **8007** and **8008** (Figure 30). The chemical shifts of the

[196] Booth, H.; Everett, J. R. Conformational free energy difference (–ΔG^o value) of the methyl group in methylcyclohexane: An accurate determination by the direct, low-temperature nuclear magnetic resonance method. *J. Chem. Soc., Chem. Commun.* **1976**, 278–279.

equatorial isomer are in good agreement with the experimental values, but differ greatly from the axial conformer. To generate a Boltzmann-weighted chemical shift for each hydrogen atom, we must multiply the corresponding chemical shift of each conformer by its respective structure's Boltzmann factor. The resulting scaled chemical shift must be added for each conformer that is considered. The process should be repeated for all hydrogen atoms that are going to be considered in the best-fit analysis. Comparison of the computed, Boltzmann-weighted chemical shifts [determined by computation with B3LYP/6-311+G(2d,p)//M06-2X/6-31+G(d,p)] to experimental[197] values gives an MAE value of 0.02 (0.0188), which is well within an acceptable range. It is noteworthy that considering both conformers, as opposed to the conformer with the lowest energy, led to reduced error in a molecule as simple as methylcyclohexane (MAE = 0.0188 vs. 0.0225).

Figure 30 | DFT Computed chemical shifts [using B3LYP/6-311+G(2d,p)//M06-2X/6-31+G(d,p)][198] for each of the conformers of methylcyclohexane, application of the Boltzmann equation ($\Delta E = 1.74$ kcal•mol^{-1})[196] to generate Boltzmann-weighted chemical shifts, and determination of the $|\Delta\delta|$ for each resonance and overall MAE value.[183]

8007		***8008***	Boltzmann-weighted			
δ(comp)		δ(comp)	δ(comp)	δ(exp)		| Δδ |
1.27	H1	1.83	1.29 –	1.34	=	0.05
1.62	H2eq	1.52	1.62 –	1.65	=	0.03
0.86	H2ax	1.47	0.88 –	0.88	=	0.00
1.66	H3eq	1.52	1.66 –	1.68	=	0.02
1.25	H3ax	1.34	1.25 –	1.23	=	0.02
1.62	H4eq	1.20	1.60 –	1.62	=	0.02
1.13	H4ax	1.63	1.14 –	1.14	=	0.00
0.85	CH_3	1.01	0.85 –	0.86	=	0.01
						MAE = 0.0188

[197] Gogoll, A.; Grennberg, H.; Axen, A. Chemical shift assignment of geminal protons in 3,7-diazabicyclo-[3.3.1]nonanes: An unexpected deviation from the axial/equatorial chemical shift order. *Magn. Reson. Chem.* **1997**, *35*, 13–20.

[198] Zhao, Y.; Truhlar, D. G. The M06 suite of density functionals for main group thermochemistry, thermochemical kinetics, noncovalent interactions, excited states, and transition elements: Two new functionals and systematic testing of four M06-class functionals and 12 other functionals. *Theor. Chem. Acc.* **120,** 215–241 (2008).

8.6. An Overview of the General Protocol for Obtaining DFT-Computed, Boltzmann-Weighted NMR Chemical Shifts

Computing the chemical shifts of a single molecule requires three separate tasks: i) geometry optimization, ii) NMR shielding tensor calculation, and iii) referencing via either the subtraction of the chemical shift of a known standard (e.g., TMS) or use of previously determined scaling factors. It is often the case that different levels of computational theory are used for geometry optimization and NMR shielding tensor calculation, and the calculations are usually executed from separate input files. If conformers are to be considered, then these steps need to be repeated for each unique conformer. Additionally, determining the reference chemical shift requires previous geometry optimization and NMR calculation of the reference molecule. Scaling factors are tedious to generate, but they often result in more accurate data. Tantillo has developed a practical protocol to determining scaling factors at a given level of theory.[183]

For complex molecules that require consideration of several conformers these tasks becomes much more cumbersome. For convenience, we have broken these steps into a series of operations and depicted them in Figure 31. To begin, the family of conformers must be determined (Operation 1). While this could be done manually, automated stochastic approaches based upon molecular mechanics are readily available and require minimal computational resources for even the most complex molecules. We routinely use the program MacroModel,[102] which is distributed by Schrödinger and run via Maestro[103] graphical user interface. Within MacroModel we use the Monte Carlo/molecular mechanics conformational search tool.

Figure 31 | An overview of the nine operations necessary to obtain DFT-computed, Boltzmann-weighted chemical shifts for a complex organic molecule that exists as many conformers.

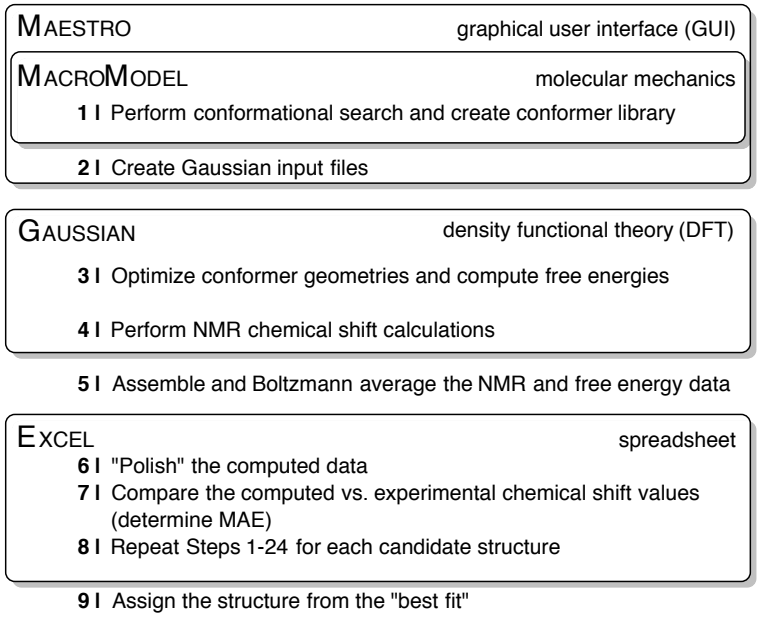

After the family of conformers has been generated, the structures are individually exported as input files to be executed by Gaussian 09 (Operation 2), which is an efficient platform for *ab initio* calculations. The input file to be read by Gaussian 09 will execute the geometry optimization (Operations 3). The M06-2X/6-31+G(d,p) level of theory is used for geometry optimizations because it has been shown to provide both reliable geometries and accurate energies. Frequency analysis is also performed at during this operation in conjunction with the geometry optimization. Frequency analysis is necessary to compute thermochemical quantities that are necessary for determining the free energy of the molecule of interest. These values are used as input for determining the Boltzmann factor (i.e. used for ΔE_i) for the final Boltzmann-weighting of the computed chemical shifts.

After geometry optimization and frequency analysis, NMR data are computed using the simple "NMR" keyword in Gaussian 09 at the B3LYP/6-311+G(2d,p) level of theory (Operation 4). By default, NMR shielding tensors are computed using gauge-

independent atomic orbital (GIAO) method. Following this task, resulting shielding tensors must be referenced to either a known standard or linear scaling factors. To reference a known standard (e.g., TMS) the previous steps must be repeated (i.e. geometry optimization/frequency analysis and NMR calculations of the standard molecule).

It should be mentioned that we elected to model solvation effects in the geometry optimization, frequency analysis, and NMR calculations using integrated equation formalism polarized continuum model (IEFPCM). Solvation cavities are used, specifically, united-atomic radii (UA0) and individual atomic radii (Bondi). In general, use of UA0 results in faster computations, and Bondi gives rise to more accurate results.[193] Typically, $CHCl_3$ solvent is chosen because most experimental data is acquired in $CDCl_3$.

With the computed NMR shielding tensors in hand, the next step is performing the Boltzmann analysis on all conformers (Operation 5). This requires first determining the Boltzmann factor (mole fraction) of each conformer, which itself requires extracting the relevant thermochemical quantity from the Gaussian 09 output file. After determining the Boltzmann factor for each conformer, the product of this percentage and the chemical shift (shielding tensor) is found for each carbon or hydrogen atom of the conformer. This weighted chemical shift is summed with the weighted chemical shifts of the corresponding atom across all conformers to give the scaled chemical shift for that individual atom. The process is repeated for each atom of the candidate structure. With a set of weighted chemical shifts for the candidate structure in hand, the data are "polished" by, for example, averaging atoms or functional groups that are degenerate due to rotation about carbon-carbon single bonds (e.g., hydrogen atoms of a methyl group and methyls of a *t*-butyl group, Operation 6). Comparison to the experimental chemical shifts will give an MAE value (Operation 7). After repeating the protocol for each candidate structure, the user is in position to assign a best fit based upon set of computed chemical shifts are in strongest agreement with experimental data (Operation 8).

8.7. An Automated Approach to Computing Boltzmann-Weighted Chemical Shifts

For structures of great complexity (e.g., hexacyclinol and vannusal B), the process of computing NMR chemical shifts is overwhelming from the standpoint of computational resources required and actual manpower necessary to carry out the Boltzmann weighting. To substantially mitigate these inconveniences we have prepared several Python scripts that automate the laborious operations. Firstly, we have developed a script, entitled "write-g09-inputs.py" that automatically creates two sets of Gaussian 09 input files for each structure found in the conformational search. The first set of input files (cf. those labeled "freq-opt") instructs Gaussian 09 to perform a geometry optimization and frequency analysis of the structure obtained from the conformational search. The second set of input files (cf. those labeled "nmr") is written to instruct Gaussian 09 to perform the NMR calculation on the optimized geometry resulting from the first input file. With these files in hand, one only needs submit them to Gaussian 09 in the correct order and wait for the computations to finish.

With all Gaussian 09 jobs complete and all ".out" files in hand, the Boltzmann-weighted NMR chemical shifts can be determined. The script entitled "nmr-data_compilation.py" has been written to accomplish this chore. Executing the script within the same directory as all of the Gaussian 09 ".out" files will write several spreadsheet files (in ".csv" format, which is Excel readable) that include i) a master list of all energetic and ^{1}H NMR data for each conformer, ii) a master list of all energetic and ^{13}C NMR data for each conformer, iii) the list of Boltzmann-weighted ^{1}H chemical shifts for the candidate structure, and iv) the list of Boltzmann-weighted ^{13}C chemical shifts for the candidate structure. If the user wishes to use a different level of theory, he/she must compute the referencing standard (e.g., TMS) at the new of theory. We have also prepared the script, "get-ref-shifts.py," which extracts NMR shielding tensor information from Gaussian 09 output file for the NMR calculation of the reference standard.

Because much of the protocol is automated, several facets of the data should be reviewed after determining the Boltzmann-weighted chemical shifts. Assuming that all Gaussian 09 calculations terminated normally, it is suggested that the computed data be reviewed to ensure all optimized geometries are i) unique so as to prevent double

counting when determining the Boltzmann weighted shifts and ii) true minimums on the potential energy surface so as to ensure that the computed energies are reliable. The master .csv files list the energy and the number of imaginary frequencies for each conformer. Because it is possible that two MacroModel-generated conformers could optimize to the same DFT geometry, the DFT-computed energies can be reviewed to ensure each conformer is unique (as evidenced by a unequal free energies). If equal or close energy values are observed in the master spreadsheets then geometries of the corresponding conformers should be viewed in, for example, Gaussview, to assess the extent of structural differences.

Inspection of the number of imaginary frequencies will ensure that all conformers have minimized to a reliable geometry. If the geometry optimization calculation gave a structure that is a minimum on the potential energy surface, then the resulting number of imaginary frequencies will be zero. If the geometry optimization mistakenly found a transition structure or "saddle point," then the number of imaginary frequencies will be greater than zero (most typically one). Because the NMR data is calculated in a separate Gaussian 09 job, the number of imaginary frequencies can be checked prior to the NMR job. To do this we have written a third script, entitled "duplicate_conf_and_imag_freq-check.py" to be executed in the same directory as all of the "opt-freq" output files and before the NMR calculations are submitted. This script is just a truncated version of the Boltzmann-weighting script, whereby the output files from the geometry optimization are analyzed and a spreadsheet file is created containing the energies and number of imaginary frequencies of each optimized geometry. Performing this check prior to the NMR calculations will allow erroneous structures to be dealt with or eliminated before spending additional resources computing their NMR properties.

8.8. Future Direction and Concluding Remarks

The computation of analytical data will continue to support the elucidation of chemical structure for complex molecules. This is especially true for the computation of NMR data. However, the extent to which these computations are performed by an expert theoretical chemist vs. a synthetic/natural product will continue to favor computations being done by the same persons who acquire the spectral data. While the continued

evolution of DFT methodologies makes these computations more practical for the novice user, myriad scripting languages are freely available to provide the opportunity to make the tedious and burdensome tasks routine. The Python scripts we developed significantly decreases the amount of active effort required by the user to obtain DFT-computed chemical shifts, and eliminates the chance to mishandle the computed data, which would give rise to erroneous conclusions.

Supplementary Information For Chapters 3–8

General Experimental for Chapters 3–7

^{1}H and ^{13}C NMR spectra were recorded on Varian Inova 500 (500 MHz), Varian Inova 300 (300 MHz), Varian VXR 300 (300 MHz), and Bruker Avance 500 (500 MHz) spectrometers. ^{1}H NMR chemical shifts in $CDCl_3$ are referenced to TMS (δ 0.00 ppm). Non-first order multiplets are identified as "nfom". Intractable multiplets resulting from overlap of one or more peaks are labeled as "m" and denoted with a range of δ. ^{13}C NMR chemical shifts in $CDCl_3$ are referenced to chloroform (δ 77.16 ppm). The following format is used to report resonances: chemical shift in ppm [multiplicity, coupling constant(s) in Hz, integral, and assignment (when possible)]. ^{1}H NMR assignments are indicated by structure environment, e.g., CH_aH$_b$. Some complex structures are numbered in order to simplify proton assignment numbering and naming. Coupling constant analysis was guided by methods we have described elsewhere.[199,200] Quantitative ^{1}H NMR (i.e. qNMR) spectra were obtained on a Bruker Avance 500 (500 MHz) spectrometer. Acquisition parameters were modified as described by Pauli and co-workers[177] (e.g., 256 transients and d1 delay time of 13.0 seconds).

Infrared spectra were recorded on a Midac Corporation Prospect 4000 FT-IR spectrometer. The most intense and/or diagnostic peaks are reported, and all spectra were collected in attenuated total reflectance (ATR) mode as thin films on a germanium window.

High-resolution mass spectrometry (HRMS) measurements were made on one of two instruments. Chemical ionization mass spectrometry was performed on a Finnigan MAT 95 (CIMS) mass spectrometer. Samples were introduced via capillary gas chromatography using an oven temperature profile of 25-320 ºC ramped at 50 ºC/min. Electrospray ionization (ESI) mass spectrometry was performed on a Bruker BioTOF II (ESI-TOF) instrument using PEG or PPG as an internal standard/calibrant. Samples were introduced as solutions in methanol or acetonitrile.

---

[199] Hoye, T. R.; Hanson, P. R.; Vyvyan, J. R. A practical guide to first-order multiplet analysis in ^{1}H NMR spectroscopy. *J. Org. Chem.* **1994**, *59*, 4096–4103.

[200] Hoye, T. R.; Zhao, H. A method for easily determining coupling constant values: An addendum to "A practical guide to first-order multiplet analysis in ^{1}H NMR spectroscopy." *J. Org. Chem.* **2002**, *67*, 4014–4016.

MPLC refers to medium pressure liquid chromatography (25-200 psi) using hand-packed columns of Silasorb silica gel (18-32 μm, 60 Å pore size), a Waters HPLC pump, a Waters R401 differential refractive index detector, and a Gilson 116 UV detector. Flash chromatography was performed using E. Merck silica gel (230-400 mesh). Thin layer chromatography was performed on glass or plastic backed plates of silica gel and visualized by UV detection and/or a solution of ceric ammonium molybdate, anisaldehyde, potassium permanganate, or phosphomolybdic acid.

Reactions requiring anhydrous conditions were performed under an atmosphere of nitrogen or argon in flame or oven dried glassware. Piperidine, diisopropylamine and triethylamine for cross-coupling reactions were deaerated by a freeze-pump-thaw cycle and then stored in a Schlenk flask or by direct purging with N_2 gas immediately prior to use. Anhydrous THF, Et_2O, toluene, and CH_2Cl_2 were taken immediately prior to use after being passed through a column of activated alumina. Reported (external) reaction temperatures are the temperature of the heating bath. HDDA reactions, including those that were carried out at temperatures above the boiling point of the solvent, were typically performed in a screw-capped vial or culture tube fitted with an inert, teflon-lined cap. Those carried out in deuterated solvents were often performed directly in a capped 5 mm NMR sample tube.

Experimental Section for Chapters 3–5

(2*S*)-Benzyl 2-(2-Methyl-3-oxopentanamido)-3-phenylpropanoate (3007)

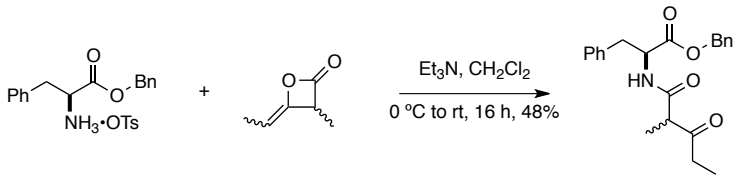

3006 ***3005*** ***3007***

[*PHW 3070*] Ketene dimer **3005**[76] was added to stirred a solution of amine **3006** (200 mg, 0.46 mmol) and Et_3N (100 µL, 0.72 mmol) in CH_2Cl_2 (1.06 mL) at 0 ºC with stirring. After 0.5 h, the ice-bath was removed and the reaction mixture was allowed to warm to rt. After 16 h, the reaction mixture was diluted in EtOAc and washed with sat. aq. NH_4Cl. The organic extract was washed with 2 M aq. NaOH and brine. The crude mixture was dried ($MgSO_4$) and concentrated to give **3007** as a white solid (80 mg, 0.22 mmol, 48%). The crude material was used without further purification.

^{1}H NMR [500 MHz, $CDCl_3$ diastereomer A(*): diastereomer rotB(^) = ~33:67]: δ 7.16-7.47 (m, 8H, $C_{aryl}H$), 6.96-7.08 (m, 2H, $C_{aryl}H$), 6.69* (br d, J = 8.3 Hz, 1H, N*H*), 6.59^ (br d, J = 8.7 Hz, 1H, N*H*), 5.19 (br d, J = 12.1 Hz, 1H, $OCH_aH_bC_{aryl}$), 5.12 (br d, J = 12.1 Hz, 1H, $OCH_aH_bC_{aryl}$), 4.83-5.02 (m, 1H, $CHCO_2$), 3.33-3.46 [m, 1H, C*H*C(O)N], 2.99-3.25 (m, 2H, $CHCH_2C_{aryl}$), 2.34-2.56 (m, 2H, CH_2CH_3), and 0.92-1.42 (m, 6H, CH_3 x2).

LR ESI-MS: [M+Na^+] requires 390.2; found 390.1.

TLC: R_f 0.2 (7:3 Hex/EtOAc).

(2*S*)-*S*-Phenyl 2-(2-Methyl-3-oxopentanamido)-3-phenylpropanethioate (3008)

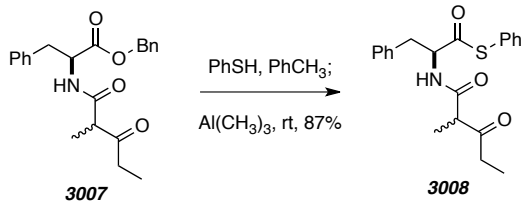

3007 ***3008***

[*PHW 3091*] Benzyl ester **3006** (98.3 mg, 0.27 mmol) was added to a stirred mixture of benzenethiol (125 µL, 1.09 mmol) and $Al(CH_3)_3$ (0.70 mL, 1.39 mmol, 2 M in hexanes), in $PhCH_3$ (0.91 mL) at rt. After 4 h the reaction mixture was diluted in Et_2O and carefully treated with 1 M aq. HCl until gas evolution had ceased. The resulting mixture was further washed with H_2O and brine. The organic phase was separated, dried ($MgSO_4$), and concentrated to give thioester **3008** (87 mg, 0.24 mmol, 89%) as a white solid.

^{1}H NMR [500 MHz, $CDCl_3$ diastereomer A(*): diastereomer rotB(^) = ~1:1]: δ 7.11-7.47 (m, 10 H, $C_{aryl}H$), 6.83* (br d, J = 8.5 Hz, 1H, N*H*), 6.79^ (br d, J = 8.7 Hz, 1H, N*H*), 5.01-5.10 [m, 1H, C*H*C(O)S], 3.45* [ap t, J = 7.2 Hz, 1H, C*H*C(O)N], 3.43^ [ap t, J = 7.2 Hz, 1H, C*H*C(O)N], 3.22-3.32 (m, 2H, CHCH_aH$_b$C$_{aryl}$), 2.99-3.08 (m, 2H, CHCH$_a$$H_bC_{aryl}$), 2.31-2.58 (m, 2H, C$H_2CH_3$), 1.39* (d, J = 7.3 Hz, CHCH_3), 1.25^ (d, J = 7.2 Hz, CHCH_3), 1.00* (t, J = 7.2 Hz, CHCH_3), and 0.99^ (t, J = 7.2 Hz, CHCH_3).

LR ESI-MS: [M+Na$^+$] requires 392.1; found 392.0.

TLC: R_f 0.3 (7:3 Hex/EtOAc).

MP: 144–149 ºC.

(2*S*,3*R*)-Methyl 2-[(2*R*/*S*)-Acetylpentanamido]-3-hydroxybutanoate (3029)

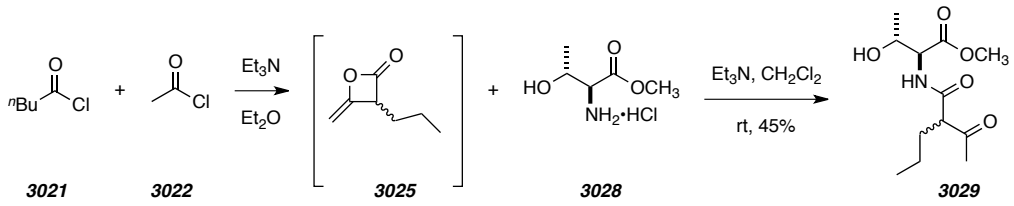

3021 ***3022*** ***3025*** ***3028*** ***3029***

To an oven dried 3-neck round-bottom flask fitted with a mechanical stirrer and reflux condenser was added acetyl chloride (**3022**, 22.5 mL, 317 mmol, 19.1 equiv), valeroyl chloride (**3021**, 19.2 mL, 158 mmol, 9.5 equiv), and dry Et_2O (235 mL) under an N_2 atmosphere. The solution was heated to reflux and Et_3N was added down the sides of the flask over 10 minutes at a rate sufficient to maintain reflux. During the course of addition, a white solid precipitated. After complete addition of Et_3N, the reaction mixture was stirred for 1.5 h, cooled to ambient temperature, and filtered through a pad of Celite® and silica gel. The filtrate was concentrated under reduced pressure and the crude residue was distilled under reduced pressure (2 mmHg) to afford a mixture of mixed ketene dimers. The mixed ketene dimer mixture was added to a stirred solution of methyl ester (**3028**, 2.83 g, 16.6 mmol, 1.0 equiv), and Et_3N (5.0 mL, 36 mmol, 2.6

equiv) in dry CH_2Cl_2 (50 mL) at 0 °C under an atmosphere of N_2. The resulting solution was allowed to warm to ambient temperature during 16 h. The reaction mixture was then diluted with 5% aq. HCl and the aqueous phase was extracted with EtOAc. The combined organic extracts were washed with brine, dried ($MgSO_4$), filtered, and concentrated under reduced pressure. Purification by medium pressure liquid chromatography (SiO_2, 2:1 hexanes:EtOAc) afforded a 1:1 mixture of diastereomers of **3029** as a white crystalline solid (1.94 g, 7.5 mmol, 45%). The mixture of diastereomers equilibrated to 2:1 mixture of diastereomers in $CDCl_3$ after 72 hours.

^{1}H NMR (500 MHz, $CDCl_3$, **3029** diastereomer 1): δ 6.81 (br d, *J* = 8.8 Hz, 1H, N*H*), 4.579 (dd, *J* = 8.8, 2.1 Hz, 1H, C*H*CO_2CH_3), 4.34-4.43 [m, 1H, C*H*(OH)CH_3], 3.77 (s, 3H, CO_2CH_3), 3.43 (t, 1H, *J* = 7.4 Hz C*H*CH_2CH_2), 2.271 [s, 3H, CHC(O)C*H*$_3$], 2.16 (br s, 1H, O*H*), 1.91-1.83 (m, 2H, CHC*H*$_2$$CH_2$), 1.29-1.43 (m, 2H, C*H*$_2$$CH_3$), 1.22 [d, *J* = 6.3 Hz, 3H, C*H*$_3$CH(OH)] and 0.95 (t, *J* = 7.4 Hz, 3H, CH_2C*H*$_3$).

^{1}H NMR (500 MHz, $CDCl_3$, **3029** diastereomer 2): δ 6.82 (br d, *J* = 8.8, 1H, N*H*), 4.580 (dd, *J* = 8.8, 2.2 Hz, 1H, C*H*CO_2CH_3), 4.36-4.44 (m, 1H, C*H*(OH)CH_3), 3.78 (s, 3H, CO_2CH_3), 3.44 (t, *J* = 7.4 Hz, 1H, C*H*CH_2CH_2), 2.272 (s, 3H, CHC(O)C*H*$_3$), 2.18 (br s, 1H, O*H*), 1.91-1.83 (m, 2H, CHC*H*$_2$$CH_2$), 1.42-1.29 (m, 2H, C*H*$_2$$CH_3$), 1.21 [d, *J* = 6.4 Hz, 3H, C*H*$_3$CH(OH)] and 0.95 (t, *J* = 7.2 Hz, 3H, CH_2C*H*$_3$).

^{13}C NMR (125 MHz, $CDCl_3$, for the mixture of diastereomers): δ 206.8, 206.4, 171.2, 169.5, 68.9, 68.0, 67.3, 61.5, 61.4, 57.4, 52.8, 32.3, 32.1, 29.4, 20.8, 20.7, 20.7, 20.2, 20.1, 20.1, 20.1, and 14.0.

HR ESI-MS calcd for $C_{12}H_{21}O_5N$ $[M + Na]^+$ 282.1312, found 282.1305.

IR: 3329, 2959, 2934, 1739, 1718, 1650, 1538, 1522, 1203, 1148, 1115, 1079, and 987 cm^{-1}.

TLC R_f 0.41 (1:2 hexanes:EtOAc).

MP: = 66-74 °C.

(2*S*,3*R*)-Methyl 2-(2-Acetylpentanamido)-3-((triethylsilyl)oxy)butanoate (3031)

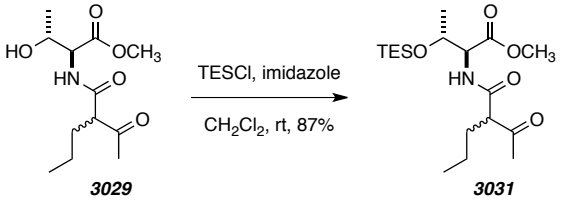

3029 ***3031***

[*PHW 3207*] Triethylsilylchloride (121 mg, 0.80 mmol) was added to a solution of alcohol **3029** (160 mg, 0.62 mmol) and imidazole (90 mg, 1.30 mmol) in CH_2Cl_2 (1 mL) at 0 ºC with stirring. After 48 h the reaction mixture was filtered through a plug of silica gel (EtOAc eluent) to give **3031** (203 mg, 0.54 mmol, 87%).

^{1}H NMR [500 MHz, $CDCl_3$ diastereomer A(*): diastereomer rotB(^) = ~67:33]: δ 6.6-6.7 [m, 1H, N*H*), 4.46-4.52 (m, 2H, C*H*CO_2CH_3 and C*H*(O)CH_3], 3.723^ (s, 3H, CO_2CH_3), 3.717* (s, 3H, CO_2CH_3), 3.42* (t, *J* = 7.4 Hz, 1H, C*H*CH_2CH_2), 3.41^ (t, *J* = 7.4 Hz, 1H,C*H*CH_2CH_2), 2.27 [s, 3H, CHC(O)C*H*$_3$], 1.82-1.91 (m, 2H, CHC*H*$_2CH_2$), 1.29-1.43 (m, 2H, C*H*$_2CH_3$), 1.17* [d, *J* = 6.3 Hz, 3H, C*H*$_3$CH(O)], 1.16^ [d, *J* = 6.3 Hz, 3H, C*H*$_3$CH(O)], 0.90-0.97 (m, 12H, C*H*$_3$ x4), and 0.51-0.61 (m, 6H, SiC*H*$_2$ x3).

(2*S*,3*R*)-*S*-Phenyl 2-[(2*R*/*S*)-Acetylpentanamido]-3-hydroxybutanethioate (130).

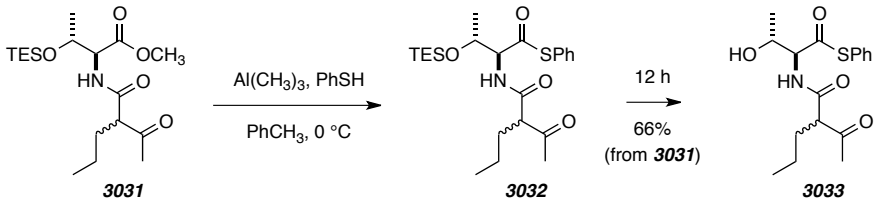

[*PHW 3213*] To a stirred solution of benzenethiol (0.225 mL, 2.14 mmol, 6 equiv) and trimethylaluminum (1.2 mL, 2.14 mmol, 6 equiv, 1.7 M in hexanes), in dry toluene (1.2 mL) at 0 °C under an atmosphere of N_2 was added ester (**3031**, 133 mg, 0.36 mmol, 1.0 equiv). The resulting solution was allowed to warm to ambient temperature during 3 h. The reaction mixture was diluted with EtOAc (30 mL) and quenched with pH 7 buffer (30 mL), and the aqueous phase was extracted with EtOAc. The combined organic extracts were dried ($MgSO_4$), filtered, and concentrated under reduced pressure. The residue was filtered through a pad of silica gel (EtOAc elutent) and concentrated under reduced pressure to afford a clear colorless oil. After standing at ambient temperature for 12 h a white solid precipitated. Purification by flash chromatography (SiO_2, 2:1 hexanes:EtOAc) afforded a 1:1 mixture of diastereomers of **3033** as a white crystalline solid (80 mg, 0.24 mmol, 66%). The mixture of diastereomers equilibrated to 2:1 mixture of diastereomers in $CDCl_3$ after 168 hours.

^{1}H NMR (500 MHz, $CDCl_3$, **3033** diastereomer 1): δ 7.45-7.37 (m, 5H, C_6H_5), 7.12 (d, *J* = 9.1 Hz, 1H, N*H*), 4.75 [dd, *J* = 9.1, 1.9 Hz, 1H, C*H*C(O)SAr], 4.56 (br q, *J* = 5.4 Hz, 1H, C*H*(OH)CH_3), 3.56 (t, *J* = 7.5 Hz, 1H, C*H*CH_2CH_2), 2.33 (s, 3H, CHC(O)C*H*$_3$), 2.00-1.89 (m,

2H, CHCH_2CH$_2$), 1.53-1.31 (m, 2H, CH_2CH$_3$), 1.20 [d, J = 6.4 Hz, 3H, CH_3CH(OH)] and 0.98 (t, J = 7.3 Hz, 3H, CH$_2$CH_3).

^{1}H NMR (500 MHz, $CDCl_3$, **3033** diastereomer 2): δ 7.45-7.37 (m, 5H, C$_6H_5$), 7.00 (br d, J = 9.2 Hz, 1H, N*H*), 4.74 [dd, J = 9.2, 1.9 Hz, 1H, C*H*C(O)SAr], 4.56 (br q, J = 5.4 Hz, 1H, C*H*(OH)CH$_3$), 3.56 (t, J = 7.5 Hz, 1H, C*H*CH$_2$CH$_2$), 2.32 (s, 3H, CHC(O)CH_3), 2.00-1.89 (m, 2H, CHCH_2CH$_2$), 1.53-1.31 (m, 2H, CH_2CH$_3$), 1.23 [d, J = 6.4 Hz, 3H, CH_3CH(OH)] and 0.97 (t, J = 7.3 Hz, 3H, CH$_2$CH_3).

HR ESI-MS calcd for $C_{17}H_{23}O_4NS$ $[M + Na]^+$ 360.1240, found 360.1254.

IR (film, mixture of diastereomers): 3346, 2959, 2930, 2916, 2848, 1727, 1711, 1667, 1642, 1530, 1509, 1167, 1111, 1067, 745, and 689 cm^{-1}; TLC R_f 0.64 (1:2 hexanes:EtOAc).

MP = 134-143 ºC.

(*S*)-4-(*sec*-Butyl)-2-methyl-5-((triethylsilyl)oxy)oxazole (3036)

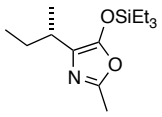

3036

^{1}H NMR (500 MHz, $CDCl_3$): δ 2.44 (ddq, J = 8.3, 8.4, 6.9 Hz, 1H, CH$_2$C*H*(CH$_3$), 2.92 (s, 3H, =CCH_3), 1.55-1.64 (m, 1H, CHCH_aCH$_b$), 1.45-1.55 (m, 1H, CHCH$_a$CH_b), 1.16 (d, J = 7.0 Hz, 3H, CHCH_3), 1.00 (t, J = 8.0 Hz, 9H, SiCH$_2$CH_3), 0.84 (t, J = 7.4 Hz, 3H, CHCH$_2$CH_3), and 0.75 (q, J = 8.0 Hz, 6H, SiCH_2).

(4-Benzyl-5-((*tert*-butyldimethylsilyl)oxy)-2-methyloxazole (3039)

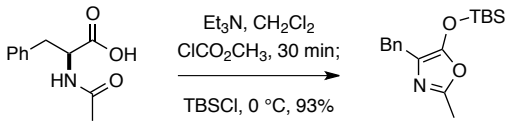

3037 ***3039***

[*PHW 4134*] Methyl chloroformate (43 µL, 0.56 mmol) was added to a solution of amide **3037** (105 mg, 0.51 mmol) and Et_3N (280 µL, 2.0 mmol) in CH_2Cl_2 (1.3 mL) at 0 ºC with stirring. After 30 min, TBSCl (191 mg, 1.27 mmol) was added and the reaction mixture was allowed to

warm to room temperature overnight. After 16 h, the reaction mixture was loaded directly onto a column of silica gel and purified (4:1 hexanes:EtOAc) to give **4039** (144 mg, 0.48, 93%).

^{1}H NMR (500 MHz, $CDCl_3$): δ 2.44 (ddq, *J* = 8.3, 8.4, 6.9 Hz, 1H, $CH_2CH(CH_3)$), 2.92 (s, 3H, $=CCH_3$), 1.55-1.64 (m, 1H, $CHCH_aCH_b$), 1.45-1.55 (m, 1H, $CHCH_aCH_b$), 1.16 (d, *J* = 7.0 Hz, 3H, $CHCH_3$), 1.00 (t, *J* = 8.0 Hz, 9H, $SiCH_2CH_3$), 0.84 (t, *J* = 7.4 Hz, 3H, $CHCH_2CH_3$), and 0.75 (q, *J* = 8.0 Hz, 6H, $SiCH_2$).

2-(4-Benzyl-5-((triethylsilyl)oxy)oxazol-2-yl)pentan-3-one (3045)

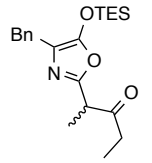

3045

^{1}H NMR (500 MHz, $CDCl_3$): δ 7.16-7.30 (m, 5H, Aryl-*H*), 3.71 (s, 2H, $C_{aryl}CH_2$), 2.38-2.52 (m, 2H, $O=CCH_2$), 1.43 (d, *J* = 7.2 Hz, $CHCH_3$), 1.02 (t, *J* = 1.02 Hz, 3H, CCH_2CH_3), 0.95 (t, *J* = 8.1 Hz, $SiCH_2CH_3$), and 0.70 (q, *J* = 8.0 Hz, $SiCH_2$).

TLC R_f 0.5 (9:1 hexanes:EtOAc).

LC / LR-MS [ES+APCI, 100 % MeOH, 4 min run]: t_R 0.6 min; *m/z* 374 [$M+H^+$].

(2*S*)-Methyl 3-((*tert*-Butyldimethylsilyl)oxy)-2-(2-methyl-3-oxopentanamido)butanoate (3050)

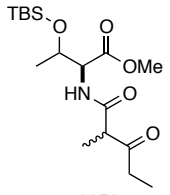

3050

^{1}H NMR [500 MHz, $CDCl_3$ diastereomer A(*): diastereomer rotB(^) = ~1:1.3]: δ 6.72 (br d, *J* = 9 Hz, 1H, N*H*), 4.42-4.52 (m, 2H, $CHCO_2CH_3$ and $CH(O)CH_3$], 3.72* (s, 3H, CO_2CH_3), 3.71^ (s, 3H, CO_2CH_3), 3.537^ (q, *J* = 7.2 Hz, 1H, $CHCH_3$), 3.534* (q, *J* = 7.2 Hz, 1H, $CHCH_3$), 2.49-2.78 (m, 2H, $O=CCH_2CH_3$), 1.43 (d, *J* = 7.1 Hz, 3H, $CH_3CHC=O$), 1.17* [d, *J* = 6.0 Hz, 3H, $CH_3CH(O)$], 1.15^ [d, *J* = 6.3 Hz, 3H, $CH_3CH(O)$], 1.081^ (t, *J* = 7.2 Hz, 3H,

C*H*$_3$CH$_2$), 1.078* (d, *J* = 7.2 Hz, 3H, C*H*$_3$CH$_2$), 0.875* [s, 9H, SiC(C*H*$_3$)$_3$], 0.873* [s, 9H, SiC(C*H*$_3$)$_3$], 0.060 (s, 3H, SiCH$_3$), -0.009* (s, 3H, SiCH$_3$), and -0.012 (s, 3H, SiCH$_3$).

LC / LR-MS [ES+APCI, 100 % MeOH, 4 min run]: t_R 0.144 min; *m/z* 360 [M+H$^+$].

(2*S*,3*R*)-3-((*tert*-Butyldimethylsilyl)oxy)-2-(2-methyl-3-oxopentanamido)butanoic Acid (3051)

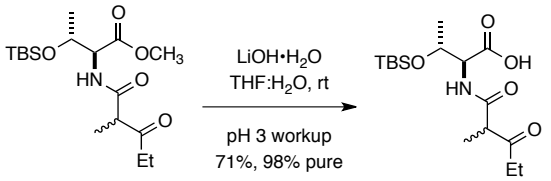

3050 ***3051***

[*PHW 4168* and *4198*] A solution of methyl ester **3050** (4.92 mg, 13.7 mmol) in THF (70 mL) was added to a solution of LiOH•H$_2$O (1.8 mg, 41.1 mmol) in water (70 mL) at room temperature with vigorous stirring. After 7 h the reaction mixture was diluted with water (50 mL), acidified to pH 3 with phosphate buffer, and extracted with EtOAc (6 x 50 mL). The combined organic extracts were washed with brine, dried (MgSO$_4$), and concentrated to give acid **3051** (3.36 mg, 9.74 mmol, 71%).

^{1}H NMR [500 MHz, CDCl$_3$ major diastereomer only]: δ 9.5 (br s, CO$_2$*H*), 6.88 (br d, *J* = 8.7 Hz, 1H, N*H*), 4.43-4.50 (m, 2H, C*H*CO$_2$H and C*H*(O)CH$_3$], 3.54 (q, *J* = 7.2 Hz, 1H, C*H*CH$_3$), 2.46-2.72 (m, 2H, O=CC*H*$_2$CH$_3$), 1.39 (d, *J* = 7.2 Hz, 3H, C*H*$_3$CHC=O), 1.14 [d, *J* = 6.4 Hz, 3H, C*H*$_3$CH(O)], 1.03 (t, *J* = 7.2 Hz, 3H, C*H*$_3$CH$_2$), 0.85 [s, 9H, SiC(C*H*$_3$)$_3$], 0.048 (s, 3H, SiC*H*$_3$), and 0.003 (s, 3H, SiC*H*$_3$).

LC / LR-MS [ES+APCI, 100 % MeOH, 4 min run]: t_R 0.144 min; *m/z* 346 [M+H$^+$].

4-Benzyl-2-methyloxazol-5(4*H*)-one

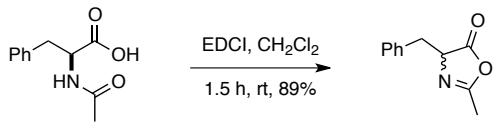

3037 ***3057***

Azlactone **3057** was prepared following the reported procedure by Benoiton, and the data matched the literature precedent.[79]

^{1}H NMR (500 MHz, $CDCl_3$): δ 7.19-7.32 (m, 5H, aryl-*H*), 4.42-4.46 (ddq, *J* = 6.8, 8.9, 2.1 Hz, 1H, NC*H*), 3.26 (dd, *J* = 4.8, 14.0 Hz, 1H, $C_{aryl}CH_aH_b$), 3.06 (dd, *J* = 6.8, 14.0 Hz, 1H, $C_{aryl}CH_aH_b$), and 2.1 (d, *J* = 2.0 Hz, 3H, CH_3).

Methyl 2-(2-Ethyl-3-oxohexanamido)acetate (3072)

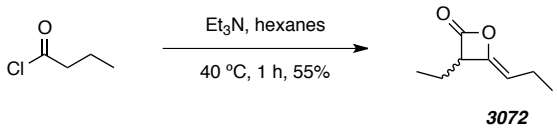

3072

[*PHW 5039*] Et_3N (116 mL, 0.833 mol) was added dropwise through a condenser to a solution of butyryl chloride (80 mL, 0.77 mol) in hexanes (1500 mL) at 40 ºC in an oven-dried round-bottom flask equipped with a mechanical stirrer and under inert atmosphere. After 1 h the reaction mixture was filtered sequentially filtered through a plug of Celite® (hexanes eluent) and silica gel (hexanes eluent) to remove the Et_3N•HCl byproduct. The filtrates were concentrated and purified by flash chromatography (hexanes:EtOAc 19:1) to give ketene dimer **3072** (29.4 g, 0.210 mol, 55%) as a clear yellow oil.

^{1}H NMR (500 MHz, $CDCl_3$): δ 4.72 (ddd, *J* = 1.3, 7.5, 7.5 Hz, 1H, =C*H*), 3.92 (ddddd, *J* = 1.2, 1.2, 1.2, 6.9, 6.9 Hz, 1H, O=CC*H*), 2.153 (dq, *J* = 7.5, 7.5 Hz, 1H, $=CHCH_aH_b$), 2.151 (dq, *J* = 7.5, 7.5 Hz, 2H, $=CHCH_aH_b$), 1.82 (dq, *J* = 7.5, 7.5 Hz, 2H, O=CCHCH_2), 1.06 (t, *J* = 7.4 Hz, 3H, CH_3), and 1.03 (t, *J* = 7.6 Hz, 3H, CH_3).

^{13}C NMR (125 MHz, $CDCl_3$): δ 169.7, 144.9, 103.5, 55.1, 20.9, 18.3, 14.3, and 10.7.

Methyl 2-(2-Ethyl-3-oxohexanamido)acetate (9001)

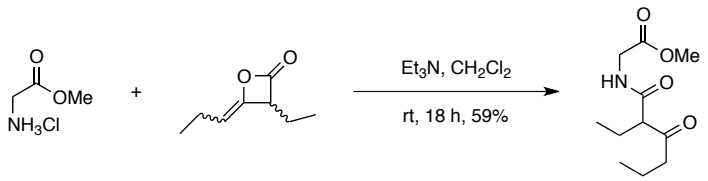

3072 ***S3001***

[*PHW 5041*] A solution of ketene dimer **3072** (2.94 g, 21.0 mmol) in CH_2Cl_2 (21 mL) was added to a suspension of glycine methyl ester hydrochloride (3.16 g, 25.0 mmol) in CH_2Cl_2 (26 mL) at 0

ºC with stirring. After stirring for 1 h the reaction mixture became homogeneous and the ice-bath was removed to allow the reaction mixture to warm to room temperature. After 18 h the reaction mixture concentrated under reduced pressure, diluted in EtOAc (100 mL) and sequentially washed with sat. aq. NH_4Cl (100 mL) and brine. The organic extract was dried ($MgSO_4$) and concentrated. Purification by recrystallization (EtOAc/hexanes) gave β-keto amido ester **S3001** (2.86 g, 12.4 mmol, 59%) as a white solid.

^{1}H NMR (500 MHz, $CDCl_3$): δ 6.81 (br dd, *J* = 7.2, 7.2 Hz, 1H, N*H*), 4.07 (dd, *J* = 5.6, 18.2 Hz, 1H, CH_aH$_b$CO$_2$CH$_3$), 3.99 (dd, *J* = 5.4, 18.2, 1H, CH$_a$$H_bCO_2CH_3$), 3.75 (s, 3H, CO$_2CH_3$), 3.38 (dd, *J* = 7.6, 7.6 Hz, 1H, C*H*), 2.54 (m, 2H, C(O)CH_2), 1.91 (m, 2H, CHCH_2), 1.61 (hex, *J* = 7.3 Hz, 2H, CH$_2$CH_2CH$_3$), 0.96 (t, *J* = 7.4 Hz, 3H, CH$_2$CH_3), and 0.91 (t, *J* = 7.4 Hz, 3H, CH$_2$CH_3).

^{13}C NMR (125 MHz, $CDCl_3$): δ 209.6, 170.1, 169.2, 61.8, 52.48, 44.8, 41.3, 24.6, 16.9, 13.7, and 11.9.

GC / LR EI-MS [5027016]: t_R 7.35 min, and 7.43 min; *m/z* 229 [$M^{+\bullet}$], 214 [$M^{+\bullet}$–$CH_3^\bullet$], 198 [$M^{+\bullet}$–$OCH_3^\bullet$], and 170 [$M^{+\bullet}$–$CO_2CH_3^\bullet$].

TLC: R_f 0.2 (1:1 Hex/EtOAc).

MP: 56–58 ºC.

Methyl 2-(2-Ethyl-3-oxohexanamido)acetate (3059)

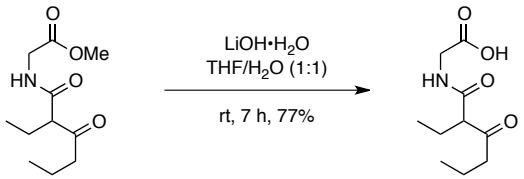

S3001 ***3059***

[*PHW 5053*] A solution of methyl ester **S3001** (2.78 g, 12.1 mmol) in THF (12.2 mL) was added to a solution of LiOH•H_2O (1.57 g, 37.3 mmol) in water (12.2 mL) at room temperature with vigorous stirring. After 7 h the reaction mixture was diluted with water (50 mL), acidified to pH 1 with concentrated HCl, and extracted with EtOAc (6 x 50 mL). The combined organic extracts were washed with brine, dried ($MgSO_4$), and concentrated. Recrystallization (EtOAc/hexanes) of the crude product gave acid **3059** as a while crystalline solid (2.00 g, 9.31 mmol, 77%).

^{1}H NMR (500 MHz, $CDCl_3$): δ 7.04 (br dd, *J* = 4.7, 5.2 Hz, 1H, N*H*), 4.12 (dd, *J* = 5.6, 18.4 Hz, 1H, CH_aH$_b$CO$_2$CH$_3$), 4.04 (dd, *J* = 5.4, 18.4, 1H, CH$_a$$H_bCO_2CH_3$), 3.43 (dd, *J* = 7.2, 7.3 Hz, 1H, C*H*), 2.55 (m, 2H, C(O)CH_2), 1.91 (m, 2H, CHCH_2), 1.61 (hex, *J* = 7.3 Hz, 2H, CH$_2$CH_2CH$_3$), 0.95 (t, *J* = 7.4 Hz, 3H, CH$_2$CH_3), and 0.91 (t, *J* = 7.4 Hz, 3H, CH$_2$CH_3).

^{13}C NMR (125 MHz, $CDCl_3$): δ 210.0, 173.2, 169.9, 61.3, 45.0, 41.4, 24.9, 16.8, 13.7, and 11.9.

LC / LR-MS [ES + APCI, 50:50 to 0:100 (%) H_2O:MeOH, 22 min run]: t_R 2.2 min; *m/z* 216 [M+H$^+$].

MP: 119–120 ºC.

Methyl 2-(2-Ethyl-3-oxohexanamido)acetate (3060)

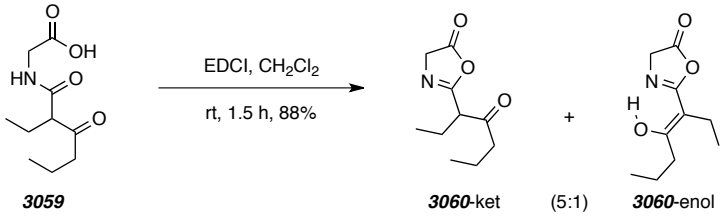

3059 ***3060***-ket (5:1) ***3060***-enol

[*PHW 5037, 5061, 5099*] EDCI (221 mg, 1.15 mmol) was added to an oven-dried screw-capped vial containing a solution of acid **3059** (225 mg, 1.05 mmol) in CH_2Cl_2 (1.3 mL) with stirring. The headspace of the reaction mixture was displaced by gentle stream of Ar and the vial was fitted with a Teflon®-lined cap. After 1.5 h the reaction had become clear and colorless indicating complete consumption of starting material. The reaction mixture was diluted in hexanes (2 mL) and cooled to -20 ºC. After 4 h the reaction mixture quickly filtered and concentrated so as to minimize exposure to moisture. Purification by flash chromatography (hexanes:EtOAc 7:3) gave a mixture (5:1) of keto azlactone and enol tautomers of azlactone **3060** (182 mg, 0.923 mmol, 88%) as a colorless oil.

^{1}H NMR (keto) (500 MHz, $CDCl_3$): δ 4.242 (d, *J* = 1.3 Hz, 1H, O=CCH_aH$_b$N), 4.237 (d, *J* = 1.6 Hz, 1H, O=CCH$_a$$H_b$N), 3.52 (dddd, *J* = 1.4, 1.4, 6.6, 8.0 Hz, 1H, C*H*), 2.55 (m, 2H, O=CCH_2), 1.98 (m, 2H, CHCH_2) 1.64 (hex, *J* = 7.4 Hz, 2H, CH$_2$CH_2CH$_3$), 1.01 (t, *J* = 7.4 Hz, 3H, CH_3), and 0.93 (t, *J* = 7.4 Hz, 3H, CH_3).

^{13}C NMR (keto) (125 MHz, $CDCl_3$): δ 204.8, 175.5, 164.9, 55.1, 54.4, 44.2, 21.4, 17.0, 13.7, and 12.1.

^{1}H NMR (enol) (500 MHz, $CDCl_3$): δ 4.26 (s, 2H, O=CC*H*$_2$N), 3.52 (dd, *J* = 7.4, 7.7 Hz, 2H, C*H*$_2$CH$_2$CH$_3$), 2.31 (q, *J* = 7.4 Hz, 2H, =CC*H*$_2$CH$_3$), 1.65 (m, 2H, CH$_2$C*H*$_2$CH$_3$), 1.05 (t, *J* = 7.4 Hz, 3H, C*H*$_3$), and 0.97 (t, *J* = 7.4 Hz, 3H, C*H*$_3$).

^{13}C NMR (enol) (125 MHz, $CDCl_3$): δ 171.1, 47.9, 37.6, 19.4, 19.0, 15.6, and 14.1. These represent the resonances observable by 1D ^{13}C NMR and/or HSQC and, while incomplete, they do lend support to the structure of enol **3060**.

TLC: R_f 0.4 (7:3 Hex/EtOAc).

5-Ammonium-2,2-dimethyl-1,3-dioxane-4,6-dione Chloride (3071)

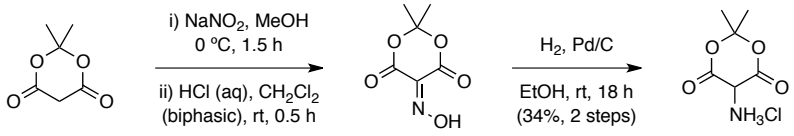

3070 ***3071***

[*PHW 5191*] An aqueous solution (10 mL) of $NaNO_2$ (4.14 g, 60.7 mmol) was added to a solution of Meldrum's acid (**3070**, 7.2 g, 50 mmol) in methanol (50 mL) at 0 ºC with stirring. As the reaction progressed, the mixture became dark red. The reaction mixture was vacuum filtered and the resulting solid added to a vigorously stirred biphasic mixture of CH_2Cl_2 and 10% aq. HCl at room temperature. After 0.5 h the organic phase was separated and the aqueous phase saturated with NaCl and extracted with CH_2Cl_2. The organic phases were combined, dried ($MgSO_4$), and concentrated to give the crude oxime. The crude product was added to a suspension of 10% palladium on carbon (800 mg) and EtOH (36 mL) in a Fischer-Porter reactor. The vessel was sealed and pressurized with H_2 at 70 psi. After 18 h the suspension was filtered. The filtrate was treated anhydrous HCl (4M in dioxane) and concentrated to give ammonium chloride **3071** as a red solid (3.4 g, 17 mmol, 34%). Meaningful spectral data for this material was not obtained. The structure was assigned based following treatment with ketene dimer **3072** in the following procedure.

_N_-(2,2-Dimethyl-4,6-dioxo-1,3-dioxan-5-yl)-2-ethyl-3-oxohexanamide (3069)

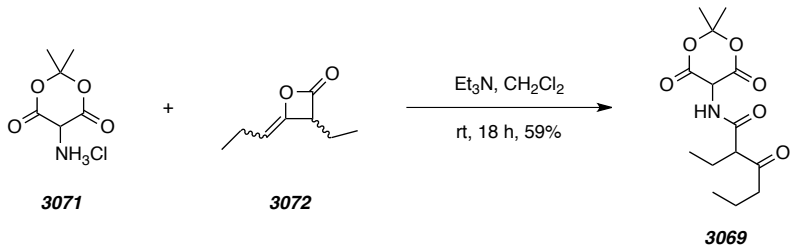

3071 ***3072*** ***3069***

[*PHW 5198*] Diisopropylethylamine (4.51 mL, 25.9 mmol), was added to a suspension of ammonium chloride **3071** (3.37 g, 17.3 mmol) and ketene dimer **3072** (5.85 g, 41.8 mmol) in CH_2Cl_2 (35 mL) at room temperature with stirring and under an inert atmosphere. After 18 h the reaction mixture was diluted in EtOAc and sequentially washed with sat. aq. NH_4Cl and brine. The organic extract was dried ($MgSO_4$) and concentrated. The crude product was purified by recrystallization (EtOAc/hexanes) to give β-ketoamide **3069** (1.98 g, 6.62 mmol, 38%) as an organic crystalline solid.

^{1}H NMR (500 MHz, $CDCl_3$): δ 7.52 (br d, *J* = 7.2 Hz, 1H, N*H*), 5.52 [br d, *J* = 7.0 Hz, 1H, C(O)C*H*C(O)], 3.48 (dd, *J* = 6.6, 7.7 Hz, 1H C*H*CH_2), 2.57 (ddd, *J* = 2.8, 7.2, 7.2 Hz, 2H, O=CC*H*$_2$), 1.83-2.05 (m, 2H, CHC*H*$_2$), 1.90 (s, 3H, C*H*$_3$), 1.83 (s, 3H, C*H*$_3$), 1.64 (hex, *J* = 7.3 Hz, 2H, CH_2C*H*$_2$$CH_3$), 1.00 (t, *J* = 7.4 Hz, 3H, C*H*$_3$), and 0.93 (t, *J* = 7.4 Hz, 3H, C*H*$_3$).

^{13}C NMR (125 MHz, $CDCl_3$): δ 209.2, 170.0, 162.5 (x 2), 106.1, 60.7, 52.3, 44.6, 28.6, 26.9, 24.6, 16.8, 13.7, and 11.7.

IR (neat): 3221, 3063, 2969, 2924, 1808, 1768, 1714, 1639, 1561, 1386, 1351, 1293, 1278, and 1207 cm^{-1}.

HRMS (ESI-TOF): Calcd for $C_{14}H_{21}NNaO_6^+$ [M+Na^+] requires 322.1261; found 322.1287.

TLC: R_f 0.2 (1:1 Hex/EtOAc).

MP: 143–145 ºC (decomposed).

3-(*tert*-Butoxy)-3-oxopropanoic Acid (4028)

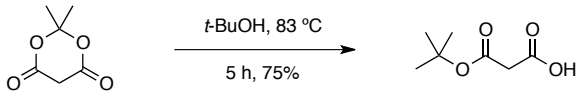

3070 ***4028***

[*PHW 7012*] Malonic acid half oxyester (MAHO) **4028** was prepared following a reported procedure[90] from Meldrum's acid (**3070**, 20.1 g, 140 mmol), *t*-BuOH (40 mL), EtOH (80 mL), and ammonium hydroxide (9.5 mL). The crude acid (16.84 g, 105.4 mmol, 75%) was sufficiently pure, and spectral data matched those from the reported literature.

^{1}H NMR (500 MHz, $CDCl_3$): δ 10.77 (br s, 1H, CO_2H), 3.36 (s, 2H, CH_2CO_2), and 1.49 [s, 9H, $CO_2C(CH_3)_3$].

^{13}C NMR (75 MHz, $CDCl_3$): δ 171.6, 166.9, 83.4, 41.7, and 28.1.

***tert*-Butyl Methyl Malonate (4027)**

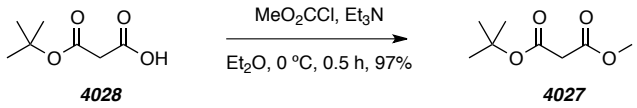

[*PHW 7013*] Malonate **4027** was prepared following a reported procedure[90] from MAHO **4028** (16.75 g, 104.7 mmol), methyl chloroformate (8.5 mL, 110 mmol, Et_3N (14.5 mL, 104 mmol), and Et_2O (500 mL). The crude malonate (17.73 g, 101.8 mmol, 97%) was sufficiently pure, and spectral data matched those from the reported literature.

^{1}H NMR (500 MHz, $CDCl_3$): δ 3.75 (s, 3H, CO_2CH_3), 3.30 (s, 2H, $O{=}CCH_2CO_2$), and 1.47 [s, 9H, $CO_2C(CH_3)_3$].

^{13}C NMR (75 MHz, $CDCl_3$): δ 167.6, 165.9, 82.2, 52.5, 42.8, and 28.0.

1-*tert*-Butyl 3-Methyl 2-(Hydroxyimino)malonate 4029)

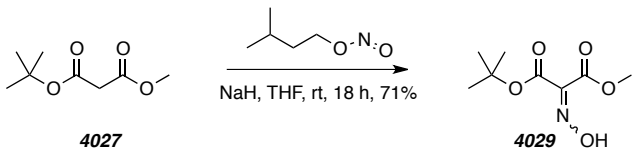

[*PHW 5285, 6048 and 6051*] NaH (246 mg, 10.3 mmol) was added to a solution of malonate **4027** (1.63 g, 9.37 mmol) in THF (31 mL) at rt and under an inert atmosphere. After 1.5 h isoamylnitrite (1.9 mL, 14 mmol) was added. After 16 h the mixture was carefully acidified to pH 3 with 10% aq. HCl and extracted with EtOAc. The combined organic extracts were dried ($MgSO_4$) and concentrated. Purification by flash chromatography (hexanes:EtOAc 4:1) gave oxime **4029** (1.35 g, 6.65 mmol, 71%) as a clear yellow oil.

^{1}H NMR [300 MHz, $CDCl_3$, E/Z isomerA(*):E/Z isomerB(^) = ~55:45]: δ 9.72* (br s, 1H, O*H*), 9.62^ (br s, 1H, O*H*), 3.92^ (s, 3H, CO_2CH_3), 3.89* (s, 3H, CO_2CH_3), 1.57* [s, 9H, $CO_2C(CH_3)_3$], and 1.54^ [s, 9H, $CO_2C(CH_3)_3$].

GC / LR EI-MS [5027016]: t_R 7.35 min, and 7.43 min; *m/z* 188 [$M^{+\bullet}$–$CH_3^{\bullet}$].

TLC: R_f 0.2 (4:1 Hex/EtOAc).

1-*tert*-Butyl 3-Methyl 2-Aminomalonate (4026)

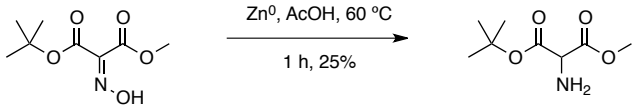

4029 ***4026***

[*PHW 5289*] Zinc dust (5 g, 77 mmol) was carefully added to a stirred solution of oxime **4029** (1.05 g, 5.17 mmol) in AcOH (20 mL) at 60 ºC. After 1 h the mixture as vacuum filtered and the filtrate was diluted in $PhCH_3$ and concentrated. The residue was diluted CH_2Cl_2 and sequentially washed with sat. aq. $NaHCO_3$ and brine. The organic phase was dried ($MgSO_4$) and concentrated to give amine **4026** (241 mg, 1.28 mmol, 25%). The crude material was used immediately without further purification.

^{1}H NMR [500 MHz, $CDCl_3$]: δ 4.10 (s, 1H, O=CC*H*), 3.78 (s, 3H, CO_2CH_3), 1.90 (br s, 2H, NH_2), and 1.48 (s, 9H, $CO_2C(CH_3)_3$).

LC / LR-MS [APCI, 50:50 to 0:100 (%) H_2O:MeOH, 22 min run]: t_R 6.6 min; *m/z* 190 [$M+H^+$].

1-*tert*-Butyl 3-Methyl 2-(2-Ethyl-3-oxohexanamido)malonate (4030)

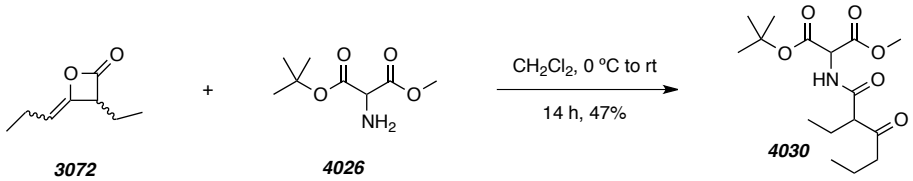

3072 ***4026*** ***4030***

[*PHW 5295 and 5299*] Ketene dimer **3072** (111 mg, 1.43 mmol) was added dropwise to a stirred solution of amine **4026** (100 mg, 0.53 mmol) in CH_2Cl_2 (1 mL) at 0 ºC and under an inert atmosphere. After 0.5 h the ice-bath was removed. After 13 h, the reaction mixture was diluted in EtOAc and washed with 10% aq. NaOH and brine. The organic phase was dried ($MgSO_4$) and concentrated. Purification by flash chromatography (hexanes:EtOAc 4:1) gave amide **4030** (82 mg, 0.25 mmol, 47%).

^{1}H NMR [500 MHz, $CDCl_3$, diastereomer A(*):diastereomer B(^) = ~1:1]: δ 7.27* (br s, 1H, N*H*), 7.21^ (br d, *J* = 6.4 Hz, 1H, N*H*), 5.030* (d, *J* = 6.7 Hz, 1H, NHC*H*), 5.027^ (d, *J* = 6.6 Hz, 1H, NHC*H*), 3.804* (s, 3H, CO_2CH_3), 3.802^ (s, 3H, CO_2CH_3), 3.358* [dd, *J* = 6.8, 8.1 Hz, 1H, NC(O)C*H*], 3.355^ [dd, *J* = 6.5, 7.8 Hz, 1H, NC(O)C*H*], 2.47-2.59 (m, 2H, O=CCH_2), 1.84-1.99 (m, 2H, CHCH_2), 1.61 (ap hex, *J* = 7.3 Hz, 2H, $CH_2CH_2CH_3$), 1.47 [s, 9H, C(CH_3)], 0.95 (t, *J* = 7.3 Hz, 3H, CH_2CH_3), and 0.91 (t, *J* = 7.4 Hz, 3H, CH_2CH_3).

^{13}C NMR [125 MHz, $CDCl_3$, diastereomer A(*):diastereomer B(^) = ~1:1]: δ 208.6*, 208.5^, 168.8*, 168.7^, 167.1*, 167.0^, 164.8*, 164.7^, 84.2*, 84.0^, 61.7*, 61.5^, 57.24*, 57.21^, 53.3*, 53.2^, 44.52*, 44.48^, 27.9, 24.3*, 24.2^, 16.9, 13.69*, 13.68^, 11.92*, and 11.85^.

LC / LR-MS [ES+APCI, 100 % MeOH, 4 min run]: t_R 0.3 min; *m/z* 330 [$M+H^+$].

TLC: R_f 0.3 (4:1 Hex/EtOAc).

3-(*tert*-Butoxy)-2-(2-ethyl-3-oxohexanamido)-3-oxopropanoic Acid (4031)

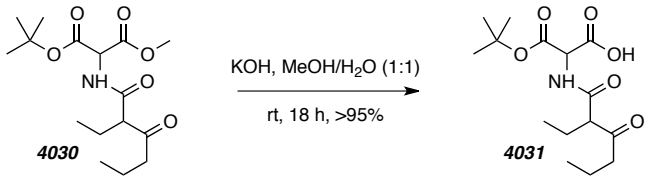

[*PHW 6044*] A solution of KOH (23 mg, 0.41 mmol) in H_2O (2.4 mL) was added to a stirred solution of malonate **4030** (62 mg, 0.19 mmol) in MeOH (2.4 mL) at rt. After 18 h the mixture was acidified to pH 4 with anhydrous HCl (4 M in 1,4-dioxane) and concentrated to give acid **4031** (60 mg, 0.19 mmol, quant). The crude material was used without further purification.

^{1}H NMR [500 MHz, $CDCl_3$]: δ 8.71 (br s, 1H, CO_2H), 6.80 (br s, 1H, N*H*), 5.02 (br d, *J* = 5.9 Hz, 1H, C*H*CO_2H), 3.45 (br t, *J* = 6.6 Hz, 1H, C*H*CH_2), 2.47-2.64 (m, 2H, O=CCH_2), 1.84-2.01 (m, 2H, CHCH_2), 1.54-1.66 (m, 2H, $CH_2CH_2CH_3$), 1.50 [s, 9H, C(CH_3)], 0.95 (t, *J* = 7.3 Hz, 3H, CH_2CH_3), and 0.90 (t, *J* = 7.4 Hz, 3H, CH_2CH_3).

LC / LR-MS [ES+APCI, 100 % MeOH, 4 min run]: t_R 0.3 min; *m/z* 316 [$M+H^+$].

tert-Butyl 2-(2-Ethyl-3-oxohexanamido)-3-oxo-3-(phenylthio)propanoate (4032)

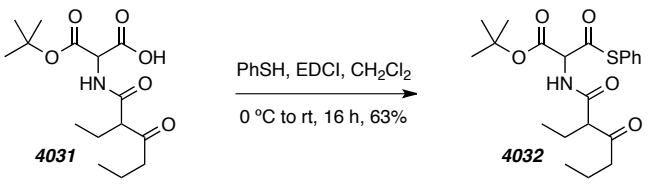

[*PHW 6046*] EDCI (72 mg, 0.38 mmol) was added to a stirred solution of acid **4031** (60 mg, 0.19 mmol) in CH_2Cl_2 (250 µL) at 0 ºC and under an inert atmosphere. After 1 min benzenethiol (200 µL, 1.9 mmol) was added and the ice-bath was removed. After 18 h the reaction mixture was diluted in EtOAc and sequentially washed with sat. aq. NH_4Cl and brine. The organic phase was dried ($MgSO_4$) and concentrated. Purification by flash chromatography (hexanes:EtOAc 4:1) gave thioester **4032** (48 mg, 0.12 mmol, 63%).

^{1}H NMR [300 MHz, $CDCl_3$, diastereomer A(*):diastereomer B(^) = ~5:1]: δ 7.57* (br d, *J* = 7.4 Hz, 1H, N*H*), 7.35-7.45 (m, 5H, Aryl-C_6H_5), 6.55^ (br d, 7.2, 1H, N*H*), 5.38^ (d, *J* = 7.5 Hz, 1H, C*H*CO_2), 5.31* (d, *J* = 7.1 Hz, 1H, C*H*CO_2), 3.41 (dd, *J* = 7.5, 7.1 Hz), 2.41-2.68 (m, 2H, O=CCH_2), 1.83-2.08 (m, 2H, CHCH_2), 1.55-1.67 (m, 2H, $CH_2CH_2CH_3$), 1.522* [s, 9H, C(CH_3)], 1.515 [s, 9H, C(CH_3)], 1.00* (t, *J* = 7.4 Hz, 3H, CH_2CH_3), 0.97^ (t, *J* = 7.4 Hz, 3H, CH_2CH_3), and 0.91 (t, *J* = 7.4 Hz, 3H, CH_2CH_3).

LC / LR-MS [APCI, 50:50 to 0:100 (%) H_2O:MeOH, 22 min run]: t_R 12.3 min; *m/z* 408 [$M+H^+$].

TLC: R_f 0.4 (4:1 Hex/EtOAc).

2-(2-Ethyl-3-oxohexanamido)-3-oxo-3-(phenylthio)propanoic Acid (4017)

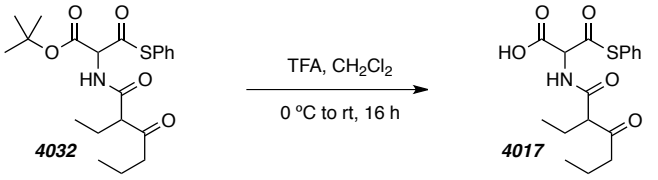

[*PHW 6049*] TFA (4 µL, 0.05 mmol) was added to a solution of *t*-butyl ester **4032** (6 mg, 0.01 mmol) in CH_2Cl_2 at 0 ºC. After 18 h the mixture was concentrated and analysis of the residue suggested that thioester **4017** was formed as a minor component along with acid **3059**.

LC / LR-MS [ES+APCI, 100 % MeOH, 4 min run]: t_R 0.3 min; *m/z* 352 [$M+H^+$], 369 [$M+NH_4^+$], and 380 [$M+K^+$].

1-*tert*-Butyl 3-Methyl 2-(2-Ethyl-3-oxohexanamido)malonate (4036)

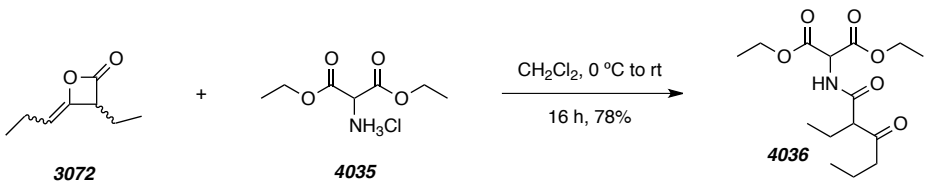

3072 ***4035*** ***4036***

[*PHW 5218*] Ketene dimer **3072** (7.0 g, 50 mmol) was added dropwise to a stirred solution of diethyl aminomalonate hydrochloride (**4035**, 9.03 g, 42.8 mmol) and DIEA (9.7 mL, 56 mmol) in CH_2Cl_2 (60 mL) at 0 ºC and under an inert atmosphere. After 0.5 h the ice-bath was removed. After 15 h, the reaction mixture was diluted in EtOAc and washed with 10% aq. NaOH and brine. The organic phase was dried ($MgSO_4$) and concentrated. Recrystallization of the crude material from EtOAc and hexanes gave amidomalonate **4036** (10.5 g, 33.3 mmol, 78%).

^{1}H NMR [300 MHz, $CDCl_3$]: δ 7.28 (br s, 1H, N*H*), 5.12 (d, *J* = 6.7 Hz, 1H, NHC*H*), 4.18-4.37 (m, 4H, $CO_2CH_2CH_3$), 3.37 [dd, *J* = 6.8, 7.8 Hz, 1H, NC(O)C*H*], 2.43-2.63 (m, 2H, O=CCH_2), 1.82-2.02 (m, 2H, CHCH_2), 1.61 (hex, *J* = 7.3 Hz, 2H, $CH_2CH_2CH_3$), 1.30 (t, *J* = 7.2 Hz, 6H, $CO_2CH_2CH_3$), 0.96 (t, *J* = 7.4 Hz, 3H, $CH_nCH_2CH_3$), and 0.91 (t, *J* = 7.5 Hz, 3H, $CH_nCH_2CH_3$).

LC / LR-MS [ES+APCI, 100 % MeOH, 4 min run]: t_R 0.3 min; *m/z* 316 [$M+H^+$].

3-Ethoxy-2-(2-ethyl-3-oxohexanamido)-3-oxopropanoic Acid (4037)

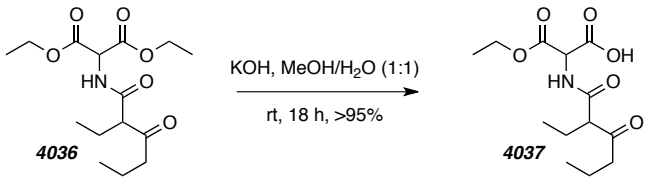

4036 ***4037***

[*PHW 6017* and *6028*] A solution of KOH (60 mg, 1.07 mmol) in H_2O (5 mL) was added to a stirred solution of malonate **4036** (170 mg, 0.54 mmol) in MeOH (5 mL) at rt. After 18 h the mixture was acidified to pH 4 with anhydrous HCl (4 M in 1,4-dioxane) and concentrated to give acid **4037** (173 mg, mmol, quant). The crude material was used without further purification.

^{1}H NMR [500 MHz, $CDCl_3$, diastereomer A(*):diastereomer B(^) = ~6:1]: δ 8.95 (br s, 1H, CO_2H), 5.17^ (d, *J* = 6.5 Hz, 1H, NHC*H*), 5.15* (d, *J* = 6.6 Hz, 1H, NHC*H*), 4.35^ (q, *J* = 7.1 Hz, 2H, $CO_2CH_2CH_3$), 4.29* (q, *J* = 7.1 Hz, 2H, $CO_2CH_2CH_3$), 3.44-3.52 [m, 1H, NC(O)C*H*], 2.46-2.62 (m, 2H, O=CCH_2), 1.81-2.01 (m, 2H, CHCH_2), 1.51-1.74 (m, 2H, $CH_2CH_2CH_3$),

1.31 (t, J = 7.1 Hz, 3H, $CO_2CH_2CH_3$), 0.95* (t, J = 7.4 Hz, 3H, $CH_nCH_2CH_3$), 0.94^ (m, 3H, $CH_nCH_2CH_3$), 0.90* (t, J = 7.5 Hz, 3H, $CH_nCH_2CH_3$), and 0.89^ (t, J = 7.5 Hz, 3H, $CH_nCH_2CH_3$).

^{13}C NMR [125 MHz, $CDCl_3$, diastereomer A(*):diastereomer B(^) = ~6:1]: δ 209.1*, 209.0^, 170.02*, 170.01^, 168.2*, 168.1^, 166.04*, 165.98^, 63.14*, 63.08^, 60.9*, 60.8^, 56.7, 44.47*, 44.46^, 24.36*, 24.35^, 16.77*, 16.75^, 14.0, 13.6, 11.70*, and 11.69^.

LC / LR-MS [ES+APCI, 100 % MeOH, 4 min run]: t_R 0.3 min; *m/z* 288 [$M+H^+$].

Methyl 2-(2-Ethyl-*N*-(4-methoxybenzyl)-3-oxohexanamido)acetate (4048)

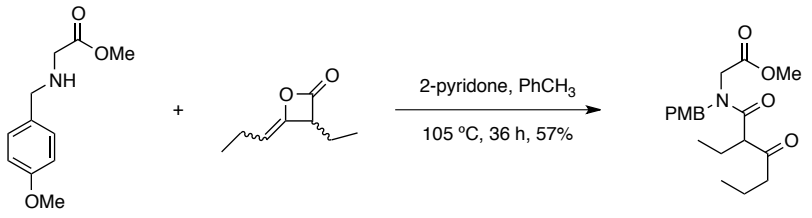

4047 ***3072*** ***4048***

[*PHW 5042* and *9260*] A solution of amine **4047** (2.90 g, 13.9 mmol),[201] ketene dimer **3072** (2.36 g, 16.9 mmol), and 2-hydroxypyridine (2.01 g, 21.0 mmol) in toluene (20 mL) was heated at 105 ºC with stirring and under an inert atmosphere. After 48 h the reaction mixture concentrated under reduced pressure, diluted in EtOAc, sequentially washed with sat. aq. NH_4Cl and brine, dried ($MgSO_4$), and concentrated. Purification by flash chromatography (EtOAc/hexanes 30:70) gave β-keto amido ester **4048** (2.79 g, 7.99 mmol, 57%) as a colorless oil.

^{1}H NMR [500 MHz, $CDCl_3$ rotA(*):rotB(^) = ~70:30]: δ 7.13^ (d, J = 8.6 Hz, 2H, $C_{Ar}HC_{Ar}CH_2$), 7.10* (d, J = 8.7 Hz, 2H, $C_{Ar}HC_{Ar}CH_2$), 6.87* (d, J = 8.7 Hz, 2H, $C_{aryl}HC_{aryl}OCH_3$), 6.84^ (d, J = 8.7 Hz, 2H, $C_{aryl}HC_{aryl}OCH_3$), 4.74* (d, J = 16.4 Hz, 1H, $C_{aryl}CH_aH_b$), 4.63^ (d, J = 14.8 Hz, 1H, $C_{aryl}CH_aH_b$), 4.55^ (d, J = 14.7 Hz, 1H, $C_{aryl}CH_aH_b$), 4.43* (d, J = 16.4 Hz, 1H, $C_{aryl}CH_aH_b$), 4.21* (d, J = 17.1 Hz, 1H, O=CCH_aH_b), 4.10^ (d, J = 18.4 Hz, 1H, O=CCH_aH_b), 3.91^ (d, J = 18.5 Hz, 1H, 1H, O=CCH_aH_b), 3.86* (d, J = 17.2 Hz, 1H, O=CCH_aH_b), 3.81* (s, 3H, $C_{aryl}OCH_3$), 3.79^ (s, 3H, $C_{aryl}OCH_3$), 3.711* (s, 3H, O=$COCH_3$), 3.708^ (s, 3H, O=$COCH_3$), 3.59* (dd, J = 6.4, 7.9 Hz, 1H, O=$CCHCH_2$), 3.35^ (dd, J = 6.6, 7.7 Hz, 1H,

---

[201] Gil, C.; Bräse, S. Efficient solid-phase synthesis of highly functionalized 1,4-benzodiazepin-5-one derivatives and related compounds by intramolecular aza-Wittig reactions. *Chem. Eur. J.* **2005**, *11*, 2680–2688.

O=CC*H*CH_2), 2.47-2.54 (m, 2H, O=CC$H_2$$CH_2$), 1.99-2.12 (m, 1H, O=CCHC$H_a$$H_b$$CH_3$), 1.84-1.95 (m, 1H, O=CCHC$H_a$$H_b$$CH_3$), 1.50-1.64 (m, 2H, O=C$CH_2CH_2$), 0.93* (t, *J* = 7.4 Hz, 3H, CH_3), 0.92^ (t, *J* = 7.4 Hz, 3H, CH_3), 0.90* (t, *J* = 7.4 Hz, 3H, CH_3), and 0.88^ (t, *J* = 7.4 Hz, 3H, CH_3).

^{13}C NMR (125 MHz, $CDCl_3$): δ 207.0, 107.4, 169.6, 160.0, 130.0, 128.4$^+$ (x2), 127.6$^-$, 114.5$^+$ (x2), 114.2$^-$, 60.4$^-$, 59.7$^+$, 55.5, 52.3$^+$, 51.7$^-$, 49.6, 48.1$^-$, 47.3$^+$, 41.3$^+$, 40.7$^-$, 23.03$^+$, 23.01$^-$, 16.9, 13.8, 12.4$^+$, and 12.3$^-$.

TLC: R_f 0.6 (2:1 Hex/EtOAc)

2-(2-Ethyl-*N*-(4-methoxybenzyl)-3-oxohexanamido)acetic Acid (4049)

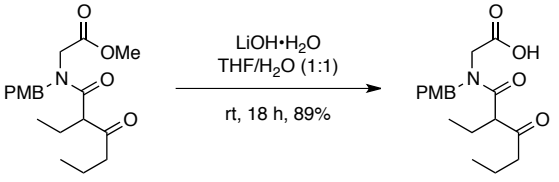

4048 ***4049***

[*PHW 5053*] A solution of methyl ester **4048** (4.24 g, 12.1 mmol) in THF (12 mL) was added to a solution of LiOH•H_2O (2.0 g, 37 mmol) in water (12 mL) at room temperature with vigorous stirring. After 18 h the reaction mixture was diluted with water (50 mL), acidified to pH 1 with concentrated HCl, and extracted with EtOAc (6 x 50 mL). The combined organic extracts were washed with brine, dried ($MgSO_4$), and concentrated to give crude product **4049**. The crude material was of sufficiently pure for subsequent reactions (3.62 g, 10.8 mmol, 89%).

^{1}H NMR [500 MHz, $CDCl_3$ rotA(*):rotB(^) = ~70:30]: δ 7.10 (d, *J* = 8.6 Hz, 2H, C_{Ar}*H*$C_{Ar}$$CH_2$), 6.90 (d, *J* = 8.7 Hz, 2H, C_{aryl}*H*$C_{aryl}$$OCH_3$), 4.74 (d, *J* = 16.3 Hz, 1H, C_{aryl}C$H_a$$H_b$), 4.42 (d, *J* = 16.4 Hz, 1H, $C_{aryl}$$CH_a$$H_b$), 4.26 (d, *J* = 17.6 Hz, 1H, O=CC$H_a$$H_b$), 3.87 (d, *J* = 17.4 Hz, 1H, O=$CCH_a$$H_b$), 3.81$^+$ (s, 3H, C_{aryl}OCH_3), 3.79$^-$ (s, 3H, C_{aryl}OCH_3), 3.59$^+$ (dd, *J* = 6.5, 7.9 Hz, 1H, O=CC*H*CH_2), 3.37$^-$ (dd, *J* = 6.6, 7.8 Hz, 1H, O=CC*H*CH_2), 2.43-2.55 (m, 2H, O=CC$H_2$$CH_2$), 1.98-2.08 (m, 1H, O=CCHC$H_a$$H_b$$CH_3$), 1.85-1.95 (m, 1H, O=CCHC$H_a$$H_b$$CH_3$), 1.49-1.79 (m, 2H, O=C$CH_2CH_2$), 0.83-1.01 (m, 6H, CH_3 (x2)],

^{13}C NMR (125 MHz, $CDCl_3$): δ 207.0, 107.4, 169.6, 160.0, 130.0, 128.4$^+$ (x2), 127.6$^-$, 114.5$^+$ (x2), 114.2$^-$, 60.4$^-$, 59.7$^+$, 55.5, 52.3$^+$, 51.7$^-$, 49.6, 48.1$^-$, 47.3$^+$, 41.3$^+$, 40.7$^-$, 23.03$^+$, 23.01$^-$, 16.9, 13.8, 12.4$^+$, and 12.3$^-$.

HRMS (ESI-TOF): Calcd for $C_{18}H_{25}NNaO_5^+$ [M+Na^+] requires 358.1625; found 358.1639.

***S*-Phenyl 2-(2-Ethyl-*N*-(4-methoxybenzyl)-3-oxohexanamido)ethanethioate (4050)**

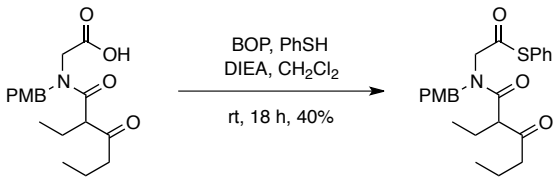

4042 ***4050***

[*PHW xi143*] DIEA (250 µL, 1.44 mmol) and BOP (605 mg, 1.37 mmol) were sequentially added to stirring solution of acid **4042** (380 mg, 1.13 mmol) and benzenethiol (150 µL, 1.5 mmol) at 0 ºC and under an inert atmosphere. After 0.5 h the ice-bath was removed and the reaction mixture was allowed to warm to rt. After 18 h the reaction mixture was loaded onto a column silica gel and purified by gradient flash chromatography (100% hexanes to hexanes:EtOAc 3:1) to give thioester **4050** (194 mg, 0.454 mmol, 40%) as a clear colorless oil.

^{1}H NMR of **4050** [500 MHz, $CDCl_3$, rotA(*):rotB(^) = ~67:33]: δ 7.36-7.47 (m, 5H, Aryl-C_6H_5), 7.16^ (d, *J* = 8.6 Hz, 2H, $C_{aryl}HC_{aryl}CH_2$), 7.09* (d, *J* = 8.7 Hz, 2H, $C_{aryl}HC_{aryl}CH_2$), 6.91* (d, *J* = 8.7 Hz, 2H, $C_{aryl}HC_{aryl}OCH_3$), 6.86^ (d, *J* = 8.7 Hz, 2H, $C_{aryl}HC_{aryl}OCH_3$), 4.82^ (d, *J* = 14.9 Hz, 1H, $C_{aryl}CH_aH_b$), 4.80* (d, *J* = 16.5 Hz, 1H, $C_{aryl}CH_aH_b$), 4.52 (d, *J* = 16.9 Hz, 1H, $C_{aryl}CH_aH_b$), 4.49* (d, *J* = 16.5 Hz, 1H, O=CCH_aH_b), 4.39^ (d, *J* = 18.4 Hz, 1H, O=CCH_aH_b), 4.14* (d, *J* = 16.9 Hz, 1H, O=CCH_aH_b), 4.10^ (d, *J* = 18.6 Hz, 1H, 1H, O=CCH_aH_b), 3.82* (s, 3H, OCH_3), 3.80^ (s, 3H, OCH_3), 3.61* (dd, *J* = 6.5, 7.9 Hz, 1H, O=$CCHCH_2$), 3.43^ (dd, *J* = 6.5, 7.7 Hz, 1H, O=$CCHCH_2$), 2.45-2.56 (m, 2H, O=CCH_2CH_2), 2.01-2.12 (m, 1H, O=$CCHCH_aH_bCH_3$), 1.87-1.98 (m, 1H, O=$CCHCH_aH_bCH_3$), 1.51-1.62 (m, 2H, O=CCH_2CH_2), 0.96^ (t, *J* = 7.3 Hz, CH_3), 0.93* (t, *J* = 7.4 Hz, CH_3), 0.88* (t, *J* = 7.4 Hz, CH_3), and 0.87^ (t, *J* = 7.4 Hz, CH_3).

^{13}C NMR of **4050** (125 MHz, $CDCl_3$, major rot = δ^+, minor rot = δ^-) δ 207.2$^-$, 206.6$^+$, 194.9$^-$, 194.3$^+$, 170.3$^+$, 169.7$^-$, 159.6$^+$, 159.5$^-$, 134.8$^+$ (x2), 134.6$^-$, 130.04$^+$, 130.01$^-$, 129.7$^+$, 129.5$^-$, 129.4$^+$ (x2), 128.33$^+$ (x2), 128.28$^-$, 127.4$^+$, 126.5$^-$, 126.0$^-$, 114.6$^+$ (x2), 114.3$^-$, 60.4$^-$, 59.7$^+$, 55.7$^-$, 55.44$^+$, 55.39$^-$, 55.0$^+$, 51.9$^+$, 41.8$^-$, 41.4$^+$, 40.9$^-$, 23.0, 16.9$^-$, 16.8$^+$, 13.73$^+$, 13.70$^-$, 12.5$^-$, and 12.4$^+$.

HRMS (ESI-TOF): Calcd for $C_{24}H_{29}NNaO_4S^+$ [M+Na^+] requires 450.1710; found 450.1737.

IR (neat): 2965, 2934, 1709, 1650, 1513, 1441, 1249, 1175, and 1033 cm^{-1}.

TLC R_f 0.5 (7:3 Hex/EtOAc).

***S*-Phenyl 4-Ethyl-3-hydroxy-1-(4-methoxybenzyl)-5-oxo-3-propylpyrrolidine-2-carbothioate (4053) and (4054)**

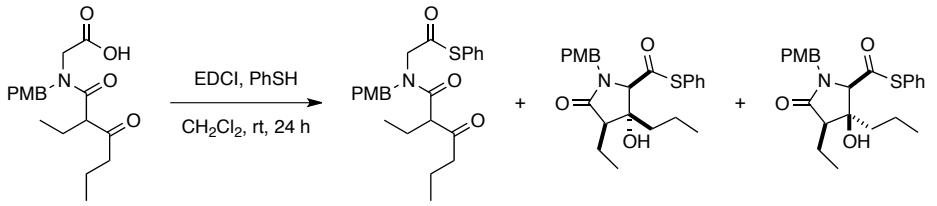

[*PHW 6097* and *7252*] EDCI (318 mg, 1.66 mmol) was added to a solution of acid **4042** (504 mg, 1.42 mmol) in CH_2Cl_2 (3 mL) at 0 ºC with stirring and under an inert atmosphere. After 0.5 h benzenethiol (0.80 mL, 7.8 mmol) was added and the reaction mixture was allowed to warm to room temperature. After 24 h the mixture was loaded onto a bed of silica gel and washed sequentially with hexanes to remove the excess benzenethiol, and ethyl acetate. The hexanes wash was collected in three fractions and each was analyzed by TLC to ensure that no product was lost. The product-containing hexanes fractions and the ethyl acetate fraction were combined and concentrated to provide the crude reaction mixture without benzenethiol. Crude ^{1}H NMR analysis revealed the ratio of lactam products **4053**:**4054** to be 2.7:4.7:1.0 Purification by MPLC (hexanes:EtOAc 2.5:1) gave, in order of elution, thioesters **4050** (59 mg, 0.14 mmol, 10%), **4053** (26 mg, 0.061 mmol, 4%), and **4054** (40 mg, 0.094 mmol, 7%) as colorless oils. The relative configuration of products **4053** and **4054** were assigned based on nOe analysis of the NC*H* and O=CC*H* signals. The spectral data for acyclic thioester **4050** is included in a previous procedure.

^{1}H NMR of **4053** (500 MHz, $CDCl_3$): δ 7.35-7.46 (m, 5H, Aryl-C_6H_5), 7.18 (d, J = 8.6 Hz, 2H, $CH_2C_{aryl}CH$), 6.87 (d, J = 8.6 Hz, 2H, $OC_{aryl}CH$), 5.11 (d, J = 14.5 Hz, 1H, CH_aH_bN), 3.91 (d, J = 14.5 Hz, 1H, CH_aH_bN), 3.84 (s, 1H, O=CC*H*N), 3.81 (s, 3H, OCH_3), 2.80 (dd, J = 6.8, 7.8 Hz, 1H, O=CC*H*CH_2), 2.14 (s, 1H, O*H*), 1.78-1.89 (m, 2H, O=CCHCH_2), 1.47-1.59 (m, 2H, C(OH)CH_2), 1.17-1.30 (m, 2H, $CH_2CH_2CH_3$), 1.14 (t, J = 7.5 Hz, 3H, $CHCH_2CH_3$), and 0.76 (t, J = 7.2 Hz, 3H, $CH_2CH_2CH_3$).

^{13}C NMR of **4053** [6097_right_dia_ChD_C13] (125 MHz, $CDCl_3$): δ 197.8, 174.7, 159.6, 134.5 (x2), 130.6 (x2), 129.9, 129.5 (x2), 127.4, 126.5, 114.3 (x2), 79.3, 70.3, 55.5, 52.3, 45.5, 37.6, 18.0, 16.4, 14.3, and 12.8.

^{1}H NMR of **4054** (500 MHz, $CDCl_3$): δ 7.36-7.47 (m, 5H, Aryl-C_6H_5), 7.16 (d, J = 8.5 Hz, 2H, $CH_2C_{aryl}CH$), 6.88 (d, J = 8.6 Hz, 2H, $OC_{aryl}CH$), 5.18 (d, J = 14.6 Hz, 1H, CH_aH_bN), 3.95 (s, 1H, O=CC*H*N), 3.88 (d, J = 14.6 Hz, 1H, CH_aH_bN), 3.82 (s, 3H, OCH_3), 2.26 (ap t, J = 7.0 Hz, 1H, O=CC*H*CH_2), 2.17 (s, 1H, O*H*), 1.73-1.89 (m, 2H, O=CCHCH_2), 1.55-1.67 (m, 2H, C(OH)CH_2), 1.21-1.33 (m, 2H, $CH_2CH_2CH_3$), 1.14 (t, J = 7.5 Hz, 3H, $CHCH_2CH_3$), and 0.88 (t, J = 7.3 Hz, 3H, $CH_2CH_2CH_3$).

^{13}C NMR of **4054** [6097_wrong_dia_ChD_C13] (125 MHz, $CDCl_3$): δ 197.0, 176.0, 159.5, 134.5 (x2), 130.3 (x2), 130.0, 129.6 (x2), 127.4, 126.5, 114.3 (x2), 77.0, 72.9, 55.4, 52.2, 45.3, 44.2, 20.4, 16.8, 14.3, and 13.4.

Another product was isolated (10 mg), but its structure has not been assigned. We are led to believe it to be the bis-epimer of **4054**.

^{1}H NMR of unknown byproduct (500 MHz, $CDCl_3$): δ 7.28-7.48 (m, 5H, Aryl-C_6H_5), 7.20 (d, J = 8.5 Hz, 2H, $CH_2C_{aryl}CH$), 6.88 (d, J = 8.7 Hz, 2H, $OC_{aryl}CH$), 5.06 (d, J = 14.9 Hz, 1H, CH_aH_bN), 4.00 (d, J = 14.9 Hz, 1H, CH_aH_bN), 3.95 (s, 1H, O=CC*H*N), 3.81 (s, 3H, OCH_3), 2.53 (dd, J = 5.0, 7.6 Hz, 1H, O=CC*H*CH_2), 1.74-1.87 (m, 2H, O=CCHCH_2), 1.68 (br s, 1H, O*H*), 1.41-1.66 (m, 4H, C(OH)CH_2 and $CH_2CH_2CH_3$), 1.21 (t, J = 7.5 Hz, 3H, $CHCH_2CH_3$), and 0.91 (t, J = 7.1 Hz, 3H, $CH_2CH_2CH_3$).

3-Ethyl-1-(4-methoxybenzyl)-4-propyl-1*H*-pyrrol-2(5*H*)-one (4077)

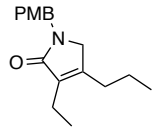

4077

^{1}H NMR (500 MHz, $CDCl_3$): δ 7.16 (d, J = 8.6 Hz, 2H, $C_{aryl}HC_{aryl}CH_2$), 6.85 (d, J = 8.7 Hz, 2H, $OC_{aryl}CH$), 4.54 (s, 2H, $C_{aryl}CH_2$), 3.79 (s, 3H, OCH_3), 3.60 (s, 2H, NCH_2CCH_2), 2.21-2.36 (m, 4H, $=CCH_2CH_3$ and $=CCH_2CH_2$), 1.45 (hexet, J = 7.7 Hz, $CH_2CH_2CH_3$), 1.09 (t, J = 7.6 Hz, 3H, $=CCH_2CH_3$), and 0.91 (t, J = 7.4 Hz, 3H, $CH_2CH_2CH_3$).

4-Ethyl-2-(4-methoxybenzyl)-5-propyl-6-oxa-2-azabicyclo[3.2.0]heptane-3,7-dione (4049)

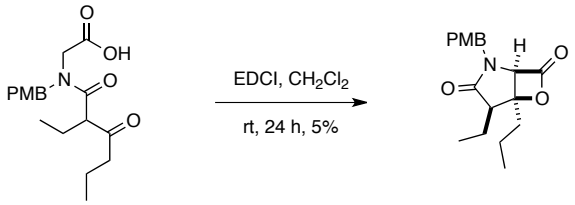

4042 ***4049***

[*PHW xi129*] EDCI (216 mg, 1.09 mmol) was added to a solution of acid **4042** (216 mg, 0.645 mmol) in CH_2Cl_2 (0.8 mL) at 0 ºC with stirring and under an inert atmosphere. The reaction mixture was allowed to warm to room temperature. After 24 h the mixture was diluted in EtOAc and washed with sat. aq. NH_4Cl. The organic phase was washed with brine, dried ($MgSO_4$) and concentrated. Purification by MPLC (hexanes:EtOAc 70:30) gave a single diastereomer of β-lactone **4049** (11 mg, 0.035 mmol, 5%) as a pale yellow oil. The relative configuration was assigned from comparison to structurally related compounds from ref 42.

^{1}H NMR (500 MHz, $CDCl_3$): δ 7.20 (d, J = 8.4 Hz, 2H, $C_{aryl}HC_{aryl}CH_2$), 6.88 (d, J = 8.4 Hz, 2H, $C_{aryl}HC_{aryl}OCH_3$), 5.05 (d, J = 14.6 Hz, 1H, $C_{aryl}CH_aH_b$), 4.37 (s, 1H, $CHCO_2$), 4.04 (d, J = 14.6 Hz, 1H, $C_{aryl}CH_aH_b$), 3.81 (s, 3H, OCH_3), 2.47 (dd, J = 5.6, 9.1 Hz, 1H, $O{=}CCHCH_2$), 1.92-2.04 (m, 2H, $O{=}CCHCH_2$), 1.84-1.92 (m, 1H, $CH_aH_bCH_2CH_3$), 1.73-1.84 (m, 1H, $CH_aH_bCH_2CH_3$), 1.38 (ap hex, J = 7.6 Hz, $CH_2CH_2CH_3$), 1.15 (t, J = 7.5 Hz, CH_3), and 0.94 (t, J = 7.3 Hz, CH_3).

^{13}C NMR: δ 174.3, 166.3, 159.7, 130.2 (x2), 126.9, 114.5 (x2), 82.9, 68.5, 55.4, 49.0, 45.3, 37.8, 19.7, 17.4, 14.0, and 12.8.

HRMS (ESI-TOF): Calcd for $C_{18}H_{23}NNaO_4^+$ [M+Na^+] requires 340.1519; found 340.1517.

IR of (neat): 2965, 2936, 2876, 2838, 1831, 1701, and 1514 cm^{-1}.

TLC: R_f 0.4 (70:30 Hex/EtOAc).

_S_-Phenyl 2-(2-Ethyl-3-oxohexanamido)ethanethioate (S4001)

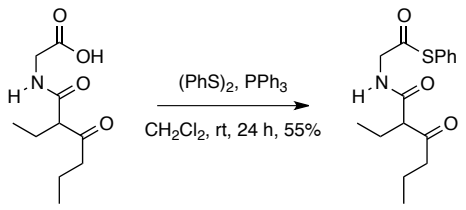

3059 ***s4001***

[*PHW 6011*] PPh_3 (380 mg, 1.45 mmol) was added to a stirred solution of acid **3059** (208 mg, 0.967 mmol) and diphenyl disulfide (380 mg, 1.74 mmol) in CH_2Cl_2 (1.9 mL) at room temperature and under and inert atmosphere. After 24 h the reaction mixture was loaded onto a column of silica gel and purified by gradient flash chromatography (hexanes:EtOAc 9:1 to 4:1) to give thioester **s4001** (163 mg, 0.531 mmol, 55%).

^{1}H NMR [500 MHz, $CDCl_3$]: δ 7.39-7.44 (m, 5H, Aryl-C_6H_5), 7.13 (br dd, 1H, N*H*), 4.35 (dd, *J* = 6.1, 17.8 Hz, 1H, CH_aH_bN), 4.22 (dd, *J* = 5.8, 17.8 Hz, 1H, CH_aH_bN), 3.44 (t, *J* = 7.3 Hz, 1H, O=CC*H*), 2.49-2.63 (m, 2H, O=CCH_2CH$_2$CH$_3$), 1.86-2.01 (m, 2H, O=CCHCH_2CH$_3$), 1.61 (hex, *J* = 7.3 Hz, 2H, O=CCH$_2$CH_2CH$_3$), 0.98 (t, *J* = 7.4 Hz, CH_3), and 0.91 (t, *J* = 7.4 Hz, CH_3).

TLC: R_f 0.3 (4:1 Hex/EtOAc).

_S-p_-Tolyl 2-(2-Ethyl-3-oxohexanamido)ethanethioate (4084)

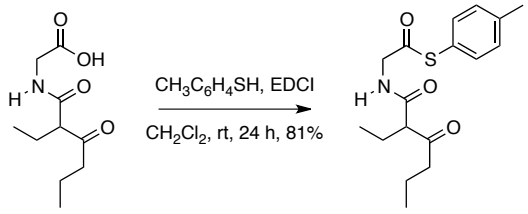

3059 ***4084***

[*PHW 8172*] EDCI (402 mg, 2.10 mmol) was added to a stirred solution of acid **3059** (300 mg, 1.40 mmol) in CH_2Cl_2 (1.8 mL) at room temperature and under and inert atmosphere. After 5 min, 4-methylbenzenethiol (294 mg, 2.37 mmol) was added and the reaction mixture was allowed to warm to room temperature. After 24 h the reaction mixture was diluted in EtOAc and washed with sat. aq. NH_4Cl and brine. The resulting mixture was dried ($MgSO_4$) and concentrated to give thioester **4084** (363 mg, 1.13 mmol, 81%). The crude material was used without further purification.

^{1}H NMR [300 MHz, $CDCl_3$]: δ 7.29 (d, *J* = 8.3 Hz, 2H, $C_{aryl}HC_{aryl}CH_3$), 7.23 (d, *J* = 8.3 Hz, 2H, $C_{aryl}HC_{aryl}S$), 7.04 (br dd, 1H, N*H*), 4.35 (dd, *J* = 6.1, 17.8 Hz, 1H, CH_aH_bN), 4.20 (dd, *J* = 5.8, 17.8 Hz, 1H, CH_aH_bN), 3.43 (t, *J* = 7.3 Hz, 1H, O=CC*H*), 2.56 (dd, *J* = 7.2, 7.3 Hz, 1H O=CC$H_aH_bCH_2CH_3$), 2.55 (dd, *J* = 7.1, 7.2 Hz, 1H O=CC$H_aH_bCH_2CH_3$), 2.38 (s, 3H, $C_{aryl}CH_3$), 1.83-2.02 (m, 2H, O=CCHCH_2CH_3), 1.61 (hex, *J* = 7.3 Hz, 2H, O=C$CH_2CH_2CH_3$), 0.98 (t, *J* = 7.4 Hz, CH_3), and 0.91 (t, *J* = 7.4 Hz, CH_3).

^{13}C NMR (125 MHz, $CDCl_3$): δ 206.7, 170.2 (x2), 169.5 (x2), 59.7, 52.3, 49.9, 41.2, 37.0, 22.5, 16.9, 13.7, and 12.2.

TLC: R_f 0.4 (7:3 Hex/EtOAc).

Methyl 2-(2-ethyl-*N*-Methyl-3-oxohexanamido)acetate (4086)

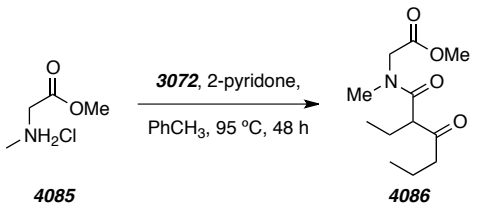

4085 ***4086***

[*PHW 9020* and *xi262*] Ketene dimer **3072** (12.8 g, 90.1 mmol) was added to a stirred solution of amine **4085** (6.26 g, 45.0 mmol), 2-pyridone (4.7 g, 49 mmol), and Et_3N (7 mL, 50 mmol) in toluene (90 mL). After stirring for 1 h, the reaction mixture was heated to 95 ºC. After 24 the reaction mixture was diluted in EtOAc and sequentially washed with sat. aq. NH_4Cl and brine. The organic extract was dried ($MgSO_4$) and concentrated to give the crude ester **4086** (13.73 g, 57 mmol) as a pale yellow oil. The mixture was used without further purification.

^{1}H NMR [500 MHz, $CDCl_3$ rotA(*):rotB(^) = ~75:25]: δ 4.232^ (d, *J* = 18.4 Hz, 1H, CH_aH_bN), 4.425* (d, *J* = 17.3 Hz, 1H, CH_aH_bN), 4.076^ (d, *J* = 18.5 Hz, 1H, CH_aH_bN), 4.067* (d, *J* = 17.2 Hz, 1H, CH_aH_bN), 3.74^ (s, 3H, OCH_3), 3.73* (s, 3H, OCH_3), 3.53* (dd, *J* = 6.8, 7.4 Hz, 1H, O=CC*H*), 3.33^ (dd, *J* = 6.9, 7.6 Hz, 1H, O=CC*H*), 3.11* (s, 3H, NCH_3), 3.00^ (s, 3H, NCH_3), 2.42-2.55 (m, 2H, O=CC$H_2CH_2CH_3$), 1.93-2.07 (m, 2H, O=CCHC$H_aH_bCH_3$), 1.81-1.93 (m, 2H, O=CCH$CH_aH_bCH_3$), 1.69* (hex, *J* = 7.5 Hz, 2H, O=C$CH_2CH_2CH_3$), 1.59^ (hex, *J* = 7.3 Hz, 2H, O=C$CH_2CH_2CH_3$), 0.94 (t, *J* = 7.4 Hz, CH_3), and 0.90 (t, *J* = 7.4 Hz, CH_3).

^{13}C NMR (125 MHz, $CDCl_3$): δ 206.8, 107.2^+, 169.5^+, 169.41^-, 169.39^-, 60.4^-, 59.7^+, 52.6^-, 52.3^+, 51.5^-, 49.4^+, 41.2^+, 40.5^-, 37.0^+, 35.5^-, 22.9^-, 22.6^+, 16.9^+, 16.8^-, 13.72^+, 13.67^-, and 12.2.

LC / LR-MS [ES+APCI, 50:50 to 0:100 (%) H_2O:MeOH, 12 min run]: t_R 2.58 min; *m/z* 244 [$M+H^+$].

2-(2-Ethyl-*N*-methyl-3-oxohexanamido)acetic Acid (4087)

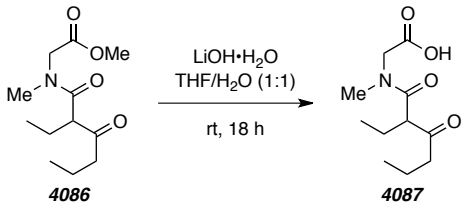

4086 ***4087***

[*PHW xi068*] A solution of methyl ester **4086** (529 mg, 2.18 mmol) in THF (2.2 mL) was added to a solution of LiOH•H_2O (366 mg, 8.5 mmol) in water (2.2 mL) at room temperature with vigorous stirring. After 18 h the reaction mixture was diluted with water (50 mL), acidified to pH 1 with concentrated HCl, and extracted with EtOAc (6 x 50 mL). The combined organic extracts were washed with brine, dried ($MgSO_4$), and concentrated to give crude product **4049**. The crude material was used without further purification (531 mg, 2.32 mmol).

^{1}H NMR (500 MHz, $CDCl_3$, major rotamer only): δ 10.6 (br s, 1H, CO_2H), 4.29 (d, J = 17.5 Hz, 1H, CH_aH_bN), 3.55 (dd, J = 6.7, 7.7 Hz, 1H, O=CC*H*), 3.12 (s, 3H, NCH_3), 2.31-2.51 (m, 2H, $O{=}CCH_2CH_2CH_3$), 1.51-1.73 (m, 2H, $O{=}CCHCH_2CH_3$), 1.60 (hex, J = 7.4 Hz, 2H, $O{=}CCH_2CH_2CH_3$), 0.93 (t, J = 7.3 Hz, CH_3), and 0.89 (t, J = 7.3 Hz, CH_3).

^{13}C NMR (125 MHz, $CDCl_3$): δ 206.7, 173.4, 170.7, 59.6, 50.1, 41.4, 37.2, 22.5, 16.9, 13.7, and 12.2.

HRMS (ESI-TOF): Calcd for $C_{11}H_{19}NNaO_4^+$ [$M+Na^+$] requires 252.1206; found 252.1228.

LC / LR-MS [ES+APCI, 50:50 to 0:100 (%) H_2O:MeOH, 12 min run]: t_R 1.22 min; *m/z* 230 [$M+H^+$].

_S_-Phenyl 2-(2-Ethyl-_N_-methyl-3-oxohexanamido)ethanethioate

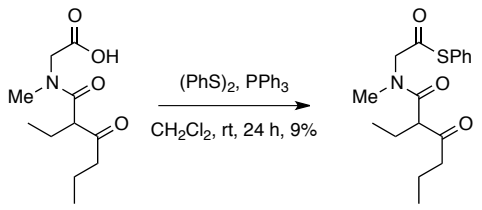

4087 ***4088***

[*PHW 8068*] PPh_3 (1.91 g, 7.29 mmol) was added to a stirred solution of acid **4087** (1.11 g, 4.85 mmol) and diphenyl disulfide (1.4 g, 6.4 mmol) in CH_2Cl_2 (10 mL) at room temperature and under and inert atmosphere. After 24 h the reaction mixture was loaded onto a column of silica gel and purified by gradient flash chromatography (hexanes:EtOAc 9:1 to 5:2) to give thioester **4088** (146 mg, 0.455 mmol, 9.4%).

^{1}H NMR [500 MHz, $CDCl_3$ rotA(*):rotB(^) = ~80:20]: δ 7.40-7.45 (m, 5H, Aryl-C_6H_5), 4.55^ (d, J = 18.3 Hz, 1H, CH_aH_bN), 4.47* (d, J = 17.0 Hz, 1H, CH_aH_bN), 4.37* (d, J = 16.9 Hz, 1H, CH_aH_bN), 4.22^ (d, J = 18.2 Hz, 1H, CH_aH_bN), 3.58* (dd, J = 6.5, 7.8 Hz, 1H, O=CC*H*), 3.41^ (dd, J = 6.5, 7.3 Hz, 1H, O=CC*H*), 3.16* (s, 3H, NCH_3), 3.07^ (s, 3H, NCH_3), 2.34-2.54 (m, 2H, $O{=}CCH_2CH_2CH_3$), 1.84-2.09 (m, 2H, $O{=}CCHCH_2CH_3$), 1.69^ (hex, J = 7.6 Hz, 2H, $O{=}CCH_2CH_2CH_3$), 1.59* (hex, J = 7.3 Hz, 2H, $O{=}CCH_2CH_2CH_3$), 0.97^ (t, J = 7.4 Hz, CH_3), 0.95* (t, J = 7.4 Hz, CH_3), 0.88* (t, J = 7.5 Hz, CH_3), and 0.87^ (t, J = 7.4 Hz, CH_3).

TLC: R_f 0.4 (3:1 Hex/EtOAc).

_N_-(2,2-Dimethyl-4,6-dioxo-1,3-dioxan-5-yl)-2-ethyl-3-oxohexanamide (4089 and 4090)

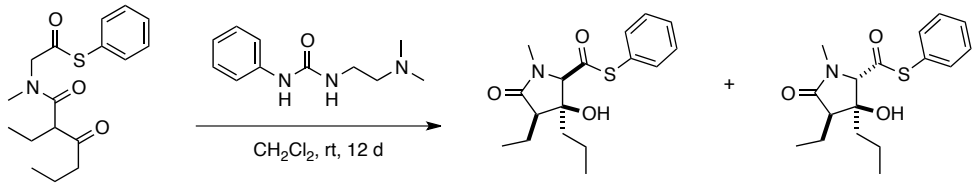

4088 (±)-***4090*** 31% (±)-***4089*** 12%

[*PHW 8121* and *8188*] Urea **4068** (107 mg, 0.52 mmol) was added to a solution of thioester **4088** (80 mg, 0.250 mmol) in CH_2Cl_2 (0.5 mL) at rt with stirring. After 12 days the reaction mixture was diluted in EtOAc and sequentially washed with sat. aq. NH_4Cl and brine. The organic extract was dried ($MgSO_4$) and concentrated. Purification by MPLC (hexanes:EtOAc 3:2) gave, in order

of elution, thioesters **4090** (25 mg, 0.078 mmol, 31%) as a white crystalline solid and **4089** (10 mg, 0.031, 12%) as a colorless oil.

^{1}H NMR of **4090** (500 MHz, $CDCl_3$): δ 7.40-7.47 (m, 5H, Aryl-C_6H_5), 4.14 (s, 1H, NC*H*), 2.93 (s, 3H, NCH_3), 2.25 (ap t, *J* = 7.0, Hz, 1H, C*H*CH_2) 1.73-1.86 (m, 4H, CHCH_2 and C$H_2CH_2CH_3$), 1.37-1.57 (m, 2H, $CH_2CH_2CH_3$), 1.12 (t, *J* = 7.5 Hz, 3H, CH_3), and 1.02 (t, *J* = 7.3 Hz, 3H, CH_3).

^{1}H NMR of **4089** (500 MHz, $CDCl_3$): δ 7.36-7.48 (m, 5H, Aryl-C_6H_5), 4.11 (s, 1H, NC*H*), 2.96 (s, 3H, NCH_3), 2.45 (dd, *J* = 5.2, 7.6, Hz, 1H, C*H*CH_2), 2.05 (s, 1H, O*H*), 1.71-1.86 (m, 4H, CHCH_2), 1.47-1.69 (m, 4H, C$H_2CH_2CH_3$ and $CH_2CH_2CH_3$), 1.20 (t, *J* = 7.5 Hz, 3H, CH_3), and 0.94 (t, *J* = 7.1 Hz, 3H, CH_3).

^{13}C NMR of **4090** (125 MHz, $CDCl_3$): δ 196.9, 176.4, 134.5 (x2), 130.1 (x2), 129.6 (x2), 126.3, 76.8, 51.7, 44.8, 29.8, 20.3, 17.0, 14.4, and 13.4.

IR of **4090** (neat): 3380, 2961, 2932, 2874, 1683, 1682, 1397, and 746 cm^{-1}.

HR ESI-MS of **4090**: $C_{17}H_{23}NNaO_3S^+$ [$M+Na^+$] requires 344.1291; found 344.1303.

TLC of **4090**: R_f 0.2 (7:3 Hex/EtOAc).

MP of **4090**: 112–114 ºC

A crystalline sample of lactam **4090** suitable for X-ray analysis was prepared using vial-in-vial vapor diffusion crystallization. A sample of the purified material (2 mg) was transferred to a 1 dram inner vial and dissolved in EtOAc (ca. 100 µL). The vial was placed inside a 20 mL scintillation vial (the outer vial) containing a shallow layer of cyclohexane (ca. 500 µL). The outer vial was capped and stored at -20 ºC. After two days white crystals formed inside the inner vial. The X-ray analysis full report is attached to this Thesis as an appendix.

***tert*-Butyl 2-(*N*-((Benzyloxy)carbonyl)-2-ethyl-3-oxohexanamido)acetate (4092)**

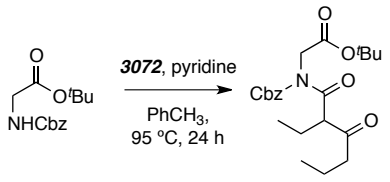

4091 ***4092***

[*PHW xi032*] Ketene dimer **3072** (500 mg, 3.52 mmol) was added to a stirred solution of amine **4091**[202] (683 mg, 2.58 mmol) in pyridine (150 µL) at 95 ºC. After 24 the reaction mixture was diluted in EtOAc and sequentially washed with sat. aq. NH_4Cl and brine. The organic extract was dried ($MgSO_4$) and concentrated. Purification by MPLC (2:1 hexanes:EtOAC) gave ester **4092**. A yield of **4092** was not measured.

^{1}H NMR (500 MHz, $CDCl_3$): δ 7.30-7.39 (m, 5H, Aryl-*H*), 5.20 (d, *J* = 12.2 Hz, $OCH_aH_bC_{aryl}$), 5.15 (d, *J* = 12.2 Hz, $OCH_aH_bC_{aryl}$), 4.56 (d, *J* = 17.2 Hz, $CH_aCH_bCO_2$), 4.45 (dd, *J* = 4.3, 8.9 Hz, 1H, O=CC*H*CH_2CH_3), 4.29 (d, *J* = 17.2 Hz, $CH_aCH_bCO_2$), 2.57-2.67 (m, 1H, O=$CCH_aH_bCH_2$), 2.46-2.54 (m, 1H, O=$CCH_aH_bCH_2$), 1.92-2.02 (m, 1H, O=$CCHCH_aH_bCH_3$), 1.76-1.88 (m, 1H, O=$CCHCH_aH_bCH_3$), 1.61 (ap hexet, *J* = 7.3 Hz, 2H, O=CCH_2CH_2), 1.38 [s, 9H, $C(CH_3)_3$], 0.97 (t, *J* = 7.3 Hz, CH_3), and 0.91 (t, *J* = 7.4 Hz, CH_3).

^{13}C NMR (125 MHz, $CDCl_3$): δ 206.0, 171.9, 167.5, 153.8, 134.8, 128.78, 128.77 (x2), 128.3 (x2), 82.2, 68.9, 62.1, 45.9, 43.1, 28.0 (x3), 22.4, 16.9, 13.8, and 12.8.

LC / LR-MS [ES+APCI, 50:50 to 0:100 (%) H_2O:MeOH, 12 min run]: t_R 8.3 min; *m/z* 423 [$M+NH_4^+$].

2-(*N*-((Benzyloxy)carbonyl)-2-ethyl-3-oxohexanamido)acetic Acid (4093)

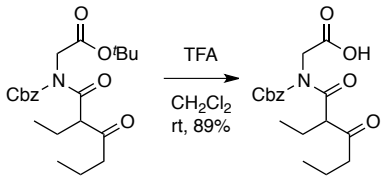

4092 ***4093***

[*PHW xi037*] TFA (100 µL, 1.31 mmol) was added to a solution of ester **4092** (13 mg, 0.032 mmol) in CH_2Cl_2 (300 µL) at ambient temperature. After 2 h, the reaction mixture was concentrated to give crude acid **4093** (10 mg, 0.029 mmol, 89%).

^{1}H NMR (500 MHz, $CDCl_3$): δ 11.0 (br s, 1H CO_2H), 7.29-7.40 (m, 5H, Aryl-*H*), 5.22 (d, *J* = 12.1 Hz, $OCH_aH_bC_{aryl}$), 5.19 (d, *J* = 12.3 Hz, $OCH_aH_bC_{aryl}$), 4.70 (d, *J* = 17.9 Hz, $CH_aCH_bCO_2$), 4.55 (d, *J* = 17.8 Hz, $CH_aCH_bCO_2$), 4.48 (dd, *J* = 4.1, 9.1 Hz, 1H,

---

[202] Muller, D.; Zeltser, I.; Bitan, G.; Gilon, C. Building units for *N*-backbone cyclic peptides. 3. Synthesis of protected *N*α-(ω-aminoalkyl)amino acids and *N*α-(ω-carboxyalkyl)amino acids. *J. Org. Chem.* **1997**, *62*, 411–416.

O=CC*H*CH_2CH_3), 2.37-2.68 (m, 2H, O=CC$H_2$$CH_2$), 1.77-2.03 (m, 1H, O=CCHC$H_2$$CH_3$), 1.60 (ap hexet, J = 7.4 Hz, 2H, O=$CCH_2C$$H_2$), 0.96 (t, J = 7.3 Hz, CH_3), and 0.91 (t, J = 7.4 Hz, CH_3).

_S-p_-Tolyl 2-(_N_-((Benzyloxy)carbonyl)-2-ethyl-3-oxohexanamido)ethanethioate (4094)

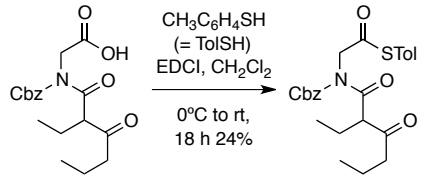

4093 ***4094***

[*PHW xi038*] EDCI (10 mg, 0.052 mmol) was added to a stirred solution of acid **4093** (10 mg, 0.029 mmol) in CH_2Cl_2 at 0 ºC. After 5 minutes, 4-methylbenzenethiol (7 mg, 0.056 mmol) was added to the reaction mixture. After 18 h, the reaction mixture was diluted in hexanes and filtered through a plug of silica gel (gradient elution, hexanes to EtOAc). The EtOAc fraction was concentrated to give crude thioester **4094**. Purification by flash chromatography (9:1 hexanes:EtOAc) gave thioester **4094** (3 mg, 0.007 mmol, 24%).

^{1}H NMR (500 MHz, $CDCl_3$): δ 7.31-7.41 (m, 5H, Aryl-*H*), 7.19 (d, J = 8.6 Hz, 2H, $CH_3C_{aryl}C_{aryl}H$), 7.17 (d, J = 8.6 Hz, 2H, $SC_{aryl}C_{aryl}H$), 5.21 (d, J = 12.1 Hz, $OCH_aH_bC_{aryl}$), 5.16 (d, J = 12.1 Hz, $OCH_aH_bC_{aryl}$), 4.94 (d, J = 17.2 Hz, $CH_aCH_bCO_2$), 4.63 (d, J = 17.2 Hz, $CH_aCH_bCO_2$), 4.46 (dd, J = 4.2, 9.1 Hz, 1H, O=CC*H*CH_2CH_3), 2.55-2.66 (m, 1H, O=$CCH_aH_bCH_2$), 2.42-2.55 (m, 1H, O=$CCH_aH_bCH_2$), 2.37 (s, 3H, $C_{aryl}CH_3$), 1.90-2.04 (m, 1H, O=CCHC$H_aH_bCH_3$), 1.77-1.90 (m, 1H, O=CCHC$H_aH_bCH_3$), 1.60 (ap hexet, J = 7.3 Hz, 2H, O=$CCH_2C$$H_2$), 1.38 [s, 9H, C(C$H_3$)$_3$], 0.97 (t, J = 7.3 Hz, CH_3), and 0.91 (t, J = 7.4 Hz, CH_3).

LC / LR-MS [ES+APCI, 50:50 to 0:100 (%) H_2O:MeOH, 12 min run]: t_R 8.5 min; *m/z* 473 [M+NH_4^+].

tert-Butyl 1-Acetylcyclopropanecarboxylate (S4002)

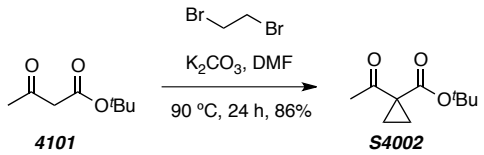

[*PHW xi026*] K_2CO_3 (12.5 g, 0.453 mol) was suspended in a solution of *t*-butyl ester **4101** (22 mL, 0.133 mol) and dibromoethane (14 mL, 0.162 mol) in DMF (150 mL). The resulting mixture was heated at 90 ºC and vigorously sitrred. After 24, the mixture was filtered and the filtrate was diluted in Et_2O and sequentially washed with sat. aq. NH_4Cl and brine. The organic extract was dried ($MgSO_4$) and concentrated. Purification by flash chromatography (4:1 hexanes:EtOAc) gave *t*-butyl ester **S4002** (21.1 g, 0.114 mol, 86%) as a clear colorless oil.

^{1}H NMR (500 MHz, $CDCl_3$): δ 2.45 (s, 3H, O=CC*H*$_3$), 1.49 [s, 9H, (C*H*$_3$)$_3$], 1.44-1.48 (nfom, 2H, C*H*$_a$H$_b$), and 1.37-1.40 (nfom, 2H, CH$_a$*H*$_b$).

1-Acetylcyclopropanecarboxylic Acid (4100)

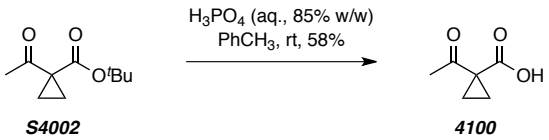

[*PHW xi076*] A mixture of *t*-butyl ester **S4002** (300 mg, 1.63 mmol), 85% aq. H_3PO_4 (600 µL, 8.8 mmol), and toluene (400 µL) was vigorously stirred at ambient temperature. After 6 h the reaction mixture was diluted in H_2O and extracted with EtOAc (x6). The organic extract was dried ($MgSO_4$) and concentrated to give the crude sample of acid **4100** (120 mg, 0.94 mmol, 58%), which was used without further purification.

^{1}H NMR (500 MHz, $CDCl_3$): δ 11.3 (br s, 1H, CO_2*H*), 2.16 (s, 3H, O=CC*H*$_3$), 1.94-2.01 (nfom, 2H, C*H*$_a$H$_b$), and 1.72-1.77 (nfom, 2H, CH$_a$*H*$_b$).

Additional support for the structure **4100** was obtained by preparing the known ethyl ester[110] and α-methylbenzylamide[108] derivatives of **4100**. The procedure involved treating CH_2Cl_2 containing solution of a sample of **4100** with EDCI (1.7 equiv), and DMAP (0.1 equiv) with either EtOH or α-methylbenzylamine (1.1 equiv) at 0 ºC. After 24 h, the reaction mixture was diluted in EtOAc and sequentially washed with sat. aq. NH_4Cl and brine. The organic extract was dried ($MgSO_4$)

and concentrated. Analysis of the crude reaction mixture revealed that the desired ester and amide were the major products.

1-Acetylcyclopropanecarbonyl Chloride (4104)

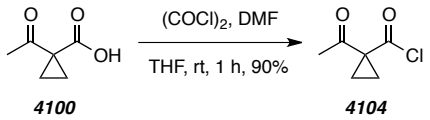

[*PHW xi099*] A solution of oxalyl chloride (2.0 mL, 24 mmol) in THF (10 mL) was added to a solution of acid **4100** (1.47 g, 11.5 mmol) and DMF (75 µL, 0.97 mmol) in THF (26 mL) at rt. After 1 h, the reaction mixture was concentrated with a rotary evaporator equipped with a 0 ºC ice-bath to give the crude acid chloride **4104** (1.52 g, 10.4 mmol, 90%). The crude material was used without further purification.

^{1}H NMR (500 MHz, $CDCl_3$): δ 2.50 (s, 3H, O=CCH_3), 1.87-1.90 (nfom, 2H, CH_aH$_b$), and 1.77-1.80 (nfom, 2H, CH$_a$$H_b$).

GC / LR EI-MS [5010015]: t_R 3.690 min; *m/z* 148 [M(^{37}Cl)$^{+\bullet}$], 146 [M(^{35}Cl)$^{+\bullet}$], 133 [M(^{37}Cl)$^{+\bullet}$–$CH_3^\bullet$], 131 [M(^{35}Cl)$^{+\bullet}$–$CH_3^\bullet$], and 111 [$M^{+\bullet}$–$HCl^\bullet$].

***tert*-Butyl 2-(2-Acetyl-*N*-((benzyloxy)carbonyl)-4-chlorobutanamido)acetate (4106)**

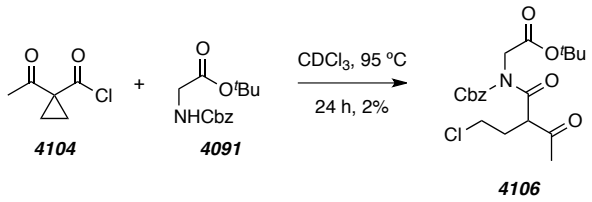

[*PHW xi033*] A solution of acid chloride **4104** (230 mg, 1.58 mmol), carbamate **4091** (337 mg, 1.27 mmol), and DMAP (10 mg,) in toluene (1 mL) was heated at 95 ºC. After 24 h the reaction mixture was diluted in EtOAc and sequentially washed with sat. aq. NH_4Cl and brine. The organic extract was dried ($MgSO_4$) and concentrated. Purification by MPLC (3:1 hexanes:EtOAc) gave **4106** (12 mg, 0.029 mmol, 2%) as a clear yellow.

^{1}H NMR (500 MHz, $CDCl_3$): δ 7.30-7.40 (m, 5H, Aryl-*H*), 5.22 (d, *J* = 12.1 Hz, OCH_aH$_b$C$_{aryl}$), 5.18 (d, *J* = 12.2 Hz, OCH$_a$$H_bC_{aryl}$), 4.82 (dd, *J* = 3.7, 9.5 Hz, 1H, O=CC*H*CH$_2$CH$_2$Cl), 4.52 (d, *J* = 17.2 Hz, CH_aCH$_b$CO$_2$), 4.33 (d, *J* = 17.3 Hz, CH$_a$CH_bCO$_2$), 3.67 (ddd, *J* = 5.0, 6.3,

11.1 Hz, 1H, ClCH_aH$_b$), 3.67 (ddd, J = 5.5, 8.8, 11.1 Hz, 1H, ClCH$_a$$H_b$), 2.49 (nfom, 1H, O=CCHCH_aH$_b$), 2.31 (s, 3H, O=CCH$_3$), 2.16 (nfom, 1H, O=CCHCH$_a$$H_b$), and 1.38 [s, 9H, C(C$H_3$)$_3$].

LC / LR-MS [ES+APCI, 50:50 to 0:100 (%) H_2O:MeOH, 12 min run]: t_R 7.9 min; *m/z* 429 [M(^{35}Cl)+NH_4^+] and 431 [M(^{37}Cl)+NH_4^+].

---

tert-Butyl 2-(1-Acetyl-*N*-((benzyloxy)carbonyl)cyclopropanecarboxamido)acetate (4105)

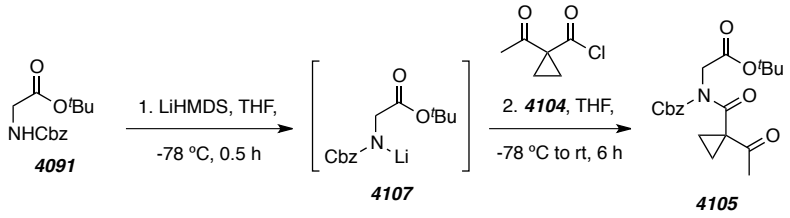

[*PHW xi044*] *n*-BuLi (350 µL, 875 mmol, 2.5 M hexanes) was added to a stirred solution of HMDS (190 µL, 0.91 mmol) in THF (1 mL) at 0 ºC and under an inert atmosphere. After 1 h, the reaction mixture was cooled to -78 ºC and carbamate **4091** (220 mg, 0.83 mmol) was added as a solution in THF (500 µL). After 0.5 h, acid chloride **4104** (200 mg, 1.37 mmol) was added as a solution in THF (500 µL). After 6 h, the reaction mixture was warmed to rt, diluted in EtOAc, and sequentially washed with sat. aq. NH_4Cl and brine. The organic extract was dried ($MgSO_4$) and concentrated. Purification by MPLC (2:1 hexanes:EtOAc) gave ester **4105** (40 mg, 0.11 mmol, 13%) as a clear yellow oil.

^{1}H NMR (500 MHz, $CDCl_3$): δ 7.30-7.39 (m, 5H, Aryl-*H*), 5.19 (s, 2H, OCH_2), 4.43 (s, 2H, NCH_2), 2.15 (s, 3H, CH_3), 1.40-1.52 (m, 4H, CH_2CH_2), and 1.39 [s, 9H, C(CH_3)$_3$].

LC / LR-MS [ES+APCI, 50:50 to 0:100 (%) H_2O:MeOH, 12 min run]: t_R 7.5 min; *m/z* 393 [M+NH_4^+] and 398 [M+Na^+].

Allyl 2-(1-Acetyl-*N*-(4-methoxybenzyl)cyclopropanecarboxamido)acetate (4116)

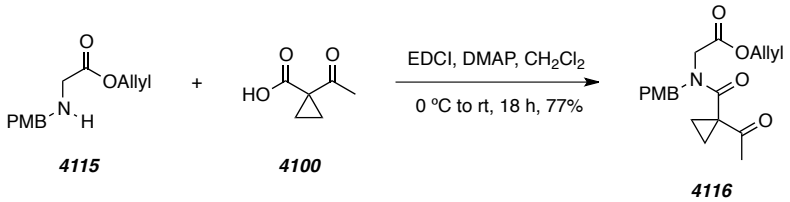

[*PHW xi084*] EDCI (230 mg, 1.20 mmol) was added to a solution of amine **4115** (235 mg, 0.75 mmol), acid **4100** (120 mg, 0.94 mmol) and DMAP (10 mg, 0.08 mmol) in CH_2Cl_2 (1 mL) at 0 ºC with stirring. After 0.5 h the reaction mixture was allowed to warm to room temperature. After 18 h the mixture was diluted in EtOAc, sequentially washed with sat. aq. NH_4Cl and brine, dried ($MgSO_4$), and concentrated. Purification by MPLC (hexanes:EtOAc 65:35) gave amide **4116** (199 mg, 0.58 mmol, 77%) as a clear colorless oil.

^{1}H NMR [500 MHz, $CDCl_3$ rotA(*):rotB(^) = ~75:25]: δ 7.19^ (d, J = 8.6 Hz, 2H, $C_{aryl}HC_{aryl}CH_2$), 7.07* (d, J = 8.7 Hz, 2H, $C_{aryl}HC_{aryl}CH_2$), 6.88* (d, J = 8.8 Hz, 2H, $CH_3OC_{aryl}C_{aryl}H$), 6.86^ (d, J = 9 Hz, 2H, $CH_3OC_{aryl}C_{aryl}H$), 5.88 (dddd, J = 5.8, 5.8, 10.5, 17.2 Hz, 1H, $CH_2CH{=}CH_2$), 5.33^ (dddd, J = 1.4, 1.4, 1.4, 17.2 Hz, 1H, $CH_2CH{=}CH_aH_b$), 5.31* (dddd, J = 1.5, 1.5, 1.5, 17.2 Hz, 1H, $CH_2CH{=}CH_aH_b$), 5.29^ (dddd, J = 1.2, 1.2, 1.2, 10.4 Hz, 1H, $CH_2CH{=}CH_aH_b$), 5.25* (dddd, J = 1.2, 1.2, 1.2, 10.4 Hz, 1H, $CH_2CH{=}CH_aH_b$), 4.65^ (s, 2H, NCH_2), 4.63* (s, 2H, NCH_2), 4.62 (ddd, J = 1.3, 1.7, 5.8 Hz, 2H, $O{=}COCH_2$), 4.03* (s, 2H, $O{=}CCH_2$), 3.98^ (s, 2H, $O{=}CCH_2$), 3.81* (s, 3H, OCH_3), 3.80^ (s, 3H, OCH_3), 2.42* (s, 3H, $O{=}CCH_3$), 2.18^ (s, 3H, $O{=}CCH_3$), 1.48-1.52* (m, 2H, $O{=}CCCH_{2a}CH_{2b}$), 1.41-1.45^ (m, 2H, $O{=}CCCH_{2a}CH_{2b}$), 1.39-1.41* (m, 2H, $O{=}CCCH_{2a}CH_{2b}$), and 1.34-1.37* (m, 2H, $O{=}CCCH_{2a}CH_{2b}$).

^{13}C NMR: δ 204.1, 170.7, 168.9, 159.6, 131.6, 128.9, 126.8, 118.9, 114.6, 65.9, 55.43, 51.5, 45.9, 37.4, 28.1, and 17.2.

^{13}C NMR: δ 203.7, 169.7, 168.7, 159.4, 131.3, 130.1, 128.1, 119.5, 114.3, 66.2, 55.37, 48.9, 47.8, 38.0, 27.2, and 16.5.

Methyl 2-(1-Acetyl-*N*-(4-methoxybenzyl)cyclopropanecarboxamido)acetate (4109)

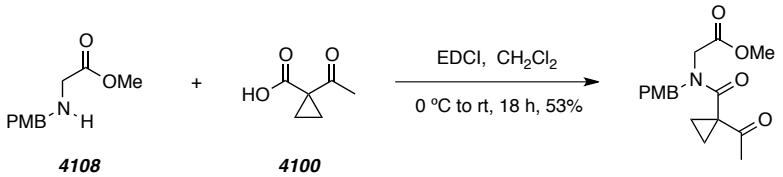

4108 ***4100*** ***4109***

[*PHW 9275*] EDCI (2.0 g, 10.4 mmol) was added to a solution of amine **4108** (899 mg, 4.30 mmol), and acid **4100** (1.057 g, 8.28 mmol) in CH_2Cl_2 (10 mL) at 0 ºC with stirring. After 0.5 h, the reaction mixture was allowed to warm to room temperature. After 18 h, the mixture was diluted in EtOAc, sequentially washed with sat. aq. NH_4Cl and brine, dried ($MgSO_4$), and concentrated. Purification by flash chromatography (hexanes:EtOAc 1:1) gave amide **4109** (720 mg, 2.26 mmol, 77%) as a clear colorless oil.

^{1}H NMR [500 MHz, $CDCl_3$ rotA(*):rotB(^) = ~75:25]: δ 7.19^ (d, *J* = 8.6 Hz, 2H, $C_{aryl}HC_{aryl}CH_2$), 7.06* (d, *J* = 8.6 Hz, 2H, $C_{aryl}HC_{aryl}CH_2$), 6.88* (d, *J* = 8.7 Hz, 2H, $CH_3OC_{aryl}C_{aryl}H$), 6.86^ (d, *J* = 9 Hz, 2H, $CH_3OC_{aryl}C_{aryl}H$), 4.64^ (s, 2H, NCH_2), 4.63* (s, 2H, NCH_2), 4.01* (s, 2H, NCH_2), 3.96^ (s, 2H, NCH_2), 3.81* (s, 3H, $C_{aryl}OCH_3$), 3.80^ (s, 3H, $C_{aryl}OCH_3$), 3.73* (s, 3H, CO_2CH_3), 3.72^ (s, 3H, CO_2CH_3), 2.44* (s, 3H, $O{=}CCH_3$), 2.18^ (s, 3H, $O{=}CCH_3$), 1.47-1.52* (m, 2H, cyclopropyl-C*H*), 1.42-1.52^ (m, 2H, cyclopropyl-C*H*), 1.37-1.41* (m, 2H, cyclopropyl-C*H*), and 1.34-1.37* (m, 2H, cyclopropyl-C*H*).

LC / LR-MS [ES+APCI, 50:50 to 0:100 (%) H_2O:MeOH, 12 min run]: t_R 3.72 min; *m/z* 320 [$M+H^+$].

2-(1-Acetyl-*N*-(4-methoxybenzyl)cyclopropanecarboxamido)acetic Acid (4110)

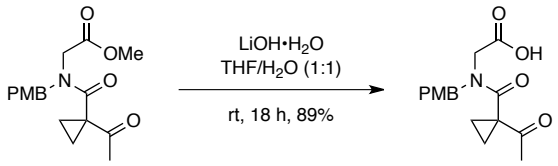

4109 ***4110***

[*PHW 9279*] A solution of methyl ester **4109** (700 mg, 2.19 mmol) in THF (2.2 mL) was added to a solution of $LiOH{\bullet}H_2O$ (300 mg, 7.1 mmol) in water (2.2 mL) at room temperature with vigorous stirring. After 18 h the reaction mixture was acidified to pH 1 with concentrated HCl, and extracted with EtOAc (6 x 50 mL). The combined organic extracts were washed with brine, dried ($MgSO_4$), and concentrated. The crude sample of **4110** was of sufficiently pure for subsequent reactions (593 mg, 1.94 mmol, 89%).

^{1}H NMR of major rotamer (500 MHz, $CDCl_3$): δ 9.54 (br s, 1H, CO_2H), 7.08 (d, *J* = 8.6 Hz, 2H, $C_{Ar}HC_{Ar}CH_2$), 6.89 (d, *J* = 8.7 Hz, 2H, $C_{aryl}HC_{aryl}OCH_3$), 4.62 (s, 2H, NCH_2), 4.04 (s, 2H, NCH_2), 3.81 (s, 3H, $C_{aryl}OCH_3$), 2.36 (s, 3H, $O{=}CCH_3$), 1.50-1.55 (m, 2H, cyclopropyl-C*H*), and 1.41-1.44 (m, 2H, cyclopropyl-C*H*).

LC / LR-MS [ES+APCI, 50:50 to 0:100 (%) H_2O:MeOH, 12 min run]: t_R 1.03 min; *m/z* 306 [$M+H^+$].

_S_-Phenyl 7-Hydroxy-5-(4-methoxybenzyl)-7-methyl-4-oxo-5-azaspiro[2.4]heptane-6-carbothioate (4112), (4113), and (4114)

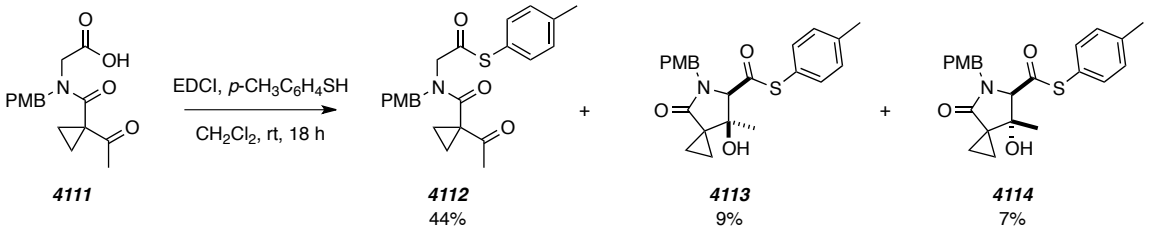

[*PHW 9281*] EDCI (210 mg, 1.09 mmol) was added to a solution of acid **4111** (237 mg, 0.777 mmol) in CH_2Cl_2 (1.6 mL) at 0 ºC with stirring and under an inert atmosphere. After 0.25 h 4-methylbenzenethiol (150 mg, 1.21 mmol) was added and the reaction mixture was allowed to warm to room temperature. After 18 h the mixture was filtered through a bed of silica gel (EtOAc eluent). The filtrate was concentrated and purified by gradient MPLC (hexanes:EtOAc 4:1 to 100% EtOAc). The 100 % EtOAc-containing fractions were combined and concentration. Purification by MPLC (hexanes:EtOAc 1.5:1) gave, in order of elution, thioesters **4112** (141 mg, 0.342 mmol, 44%), **4113** (30 mg, 0.073 mmol, 9%), and **4114** (22 mg, 0.53 mmol, 7%) as orange oils. The relative configuration of **4113** was assigned based on nOe analysis of the NC*H* and O=CCH_3 signals. The relative configuration of **4114** was assigned from comparison to the spectral data of **4113**.

^{1}H NMR of **4112 [**500 MHz, $CDCl_3$ rotA(*):rotB(^) = ~7:3] δ 7.28 (d, J = 8.2 Hz, 2H, $C_{aryl}HC_{aryl}CH_3$), 7.22 (d, J = 8.0 Hz, 2H, $C_{aryl}HC_{aryl}S$), 7.08 (d, J = 8.7 Hz, 2H, $CH_2C_{aryl}CH$), 6.90 (d, J = 8.7 Hz, 2H, $OC_{aryl}C_{aryl}H$), 4.66^ (s, 2H, $C_{aryl}CH_2$), 4.61* (s, 2H, $C_{aryl}CH_2$), 4.30* (s, 2H, NCH_2), 4.21^ (s, 2H, NCH_2), 3.82* (s, 3H, OCH_3), 3.81^ (s, 3H, OCH_3), 2.31-2.42 (m, 5H, $C_{aryl}CH_3$ and O=CCH_2CH_2), 1.48-1.53 (m, 2H, cyclopropyl-C*H*), and 1.40-1.44 (m, 1H, cyclopropyl-C*H*).

LC / LR-MS of **4112** [ES+APCI, 50:50 to 0:100 (%) H_2O:MeOH, 12 min run]: t_R 4.55 min; *m/z* 412 [$M+H^+$].

HRMS of **4112** (ESI-TOF): Calcd for $C_{23}H_{25}NNaO_4S^+$ [$M+Na^+$] requires 434.1397; found 434.1359.

^{1}H NMR of **4113** (500 MHz, $CDCl_3$): δ 7.22-7.28 (m, 4H, Aryl-$C_6H_4CH_3$), 7.18 (d, J = 8.6 Hz, 2H, $CH_2C_{aryl}CH$), 6.88 (d, J = 8.6 Hz, 2H, $OC_{aryl}C_{aryl}H$), 5.20 (d, J = 14.7 Hz, 1H, CH_aH_bN), 3.98 (s, 1H, O=CC*H*N), 3.93 (d, J = 14.7 Hz, 1H, CH_aH_bN), 3.82 (s, 3H, OCH_3), 2.39 (s, 3H,

$C_{aryl}CH_3$), 2.00 (br s, 1H, O*H*), 1.27 [s, 3H, C(OH)C*H*$_3$], 1.22-1.31 (nfom, 1H, cyclopropyl-C*H*), 1.07-1.16 (m, 2H, cyclopropyl-C*H*), and 0.83-0.94 (nfom, 1H, cyclopropyl-C*H*).

^{13}C NMR of **4113** (125 MHz, $CDCl_3$): δ 197.1, 175.2, 159.5, 140.4, 134.5 (x2), 130.4 (x2), 130.3 (x2), 128.8, 127.6, 114.4 (x2), 74.4, 73.2, 55.4, 45.7, 32.9, 26.9, 21.5, 11.9, and 10.0.

HRMS of **4113** (ESI-TOF): Calcd for $C_{23}H_{25}NNaO_4S^+$ [M+H$^+$] requires 434.1397; found 434.1429.

IR of **4113** (neat): 3287, 2967, 2932, 2836, 1700, 1684, and 1513 cm^{-1}.

TLC of **4113**: R_f 0.2 (7:3 Hex/EtOAc).

LC / LR-MS of **4113** [ES+APCI, 50:50 to 0:100 (%) H_2O:MeOH, 12 min run]: t_R 4.40 min; *m/z* 412 [M+H$^+$].

HRMS of **4113** (ESI-TOF): Calcd for $C_{24}H_{29}O_2Si^+$ [M+Na$^+$] requires 377.1931; found 377.1957.

^{1}H NMR of **4114** (500 MHz, $CDCl_3$): δ 7.24 (d, *J* = 8.3 Hz, 2H, $CH_3C_{aryl}C_{aryl}H$), 7.21 (d, *J* = 8.7 Hz, 2H, $CH_2C_{aryl}CH$), 7.20 (d, *J* = 8.4 Hz, 2H, $SC_{aryl}C_{aryl}H$), 6.87 (d, *J* = 8.7 Hz, 2H, $OC_{aryl}CH$), 5.13 (d, *J* = 14.7 Hz, 1H, CH_aH_bN), 4.16 (s, 1H, O=CC*H*N), 4.02 (d, *J* = 14.7 Hz, 1H, CH_aH_bN), 3.80 (s, 3H, OC*H*$_3$), 2.38 (s, 3H, $C_{aryl}CH_3$), 2.12 (br s, 1H, O*H*), 1.22-1.31 (m, 2H, cyclopropyl-C*H*), 1.10 [s, 3H, C(OH)C*H*$_3$], and 0.90-0.98 (nfom, 2H, cyclopropyl-C*H*).

^{13}C NMR of **4114** (125 MHz, $CDCl_3$): δ 197.0, 175.5, 159.5, 140.4, 134.4 (x2), 130.4 (x2), 130.1 (x2), 127.5, 122.9, 114.4 (x2), 76.6, 75.1, 55.4, 45.9, 33.6, 21.5, 20.5, 15.0, and 7.9.

HRMS of **4114** (ESI-TOF): Calcd for $C_{23}H_{25}NNaO_4S^+$ [M+Na$^+$] requires 434.1397; found 434.1407.

LC / LR-MS of **4114** [ES+APCI, 50:50 to 0:100 (%) H_2O:MeOH, 12 min run]: t_R 4.37 min; *m/z* 412 [M+H$^+$].

Allyl 2-(1-Acetyl-*N*-(4-methoxybenzyl)cyclopropanecarboxamido)acetate (4116)

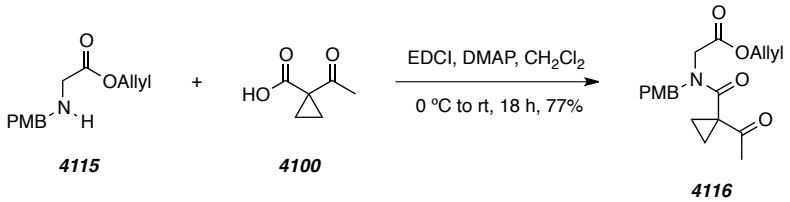

4115 ***4100*** ***4116***

[*PHW xi084*] EDCI (230 mg, 1.20 mmol) was added to a solution of amine **4115** (235 mg, 0.75 mmol), acid **4100** (120 mg, 0.94 mmol) and DMAP (10 mg, 0.08 mmol) in CH_2Cl_2 (1 mL) at 0 ºC with stirring. After 0.5 h the reaction mixture was allowed to warm to room temperature. After 18 h the mixture was diluted in EtOAc, sequentially washed with sat. aq. NH_4Cl and brine, dried ($MgSO_4$), and concentrated. Purification by MPLC (hexanes:EtOAc 65:35) gave amide **4116** (199 mg, 0.58 mmol, 77%) as a clear colorless oil.

^{1}H NMR [500 MHz, $CDCl_3$ rotA(*):rotB(^) = ~75:25]: δ 7.19^ (d, J = 8.6 Hz, 2H, $C_{aryl}HC_{aryl}CH_2$), 7.07* (d, J = 8.7 Hz, 2H, $C_{aryl}HC_{aryl}CH_2$), 6.88* (d, J = 8.8 Hz, 2H, $CH_3OC_{aryl}C_{aryl}H$), 6.86^ (d, J = 9 Hz, 2H, $CH_3OC_{aryl}C_{aryl}H$), 5.88 (dddd, J = 5.8, 5.8, 10.5, 17.2 Hz, 1H, $CH_2CH{=}CH_2$), 5.33^ (dddd, J = 1.4, 1.4, 1.4, 17.2 Hz, 1H, $CH_2CH{=}CH_aH_b$), 5.31* (dddd, J = 1.5, 1.5, 1.5, 17.2 Hz, 1H, $CH_2CH{=}CH_aH_b$), 5.29^ (dddd, J = 1.2, 1.2, 1.2, 10.4 Hz, 1H, $CH_2CH{=}CH_aH_b$), 5.25* (dddd, J = 1.2, 1.2, 1.2, 10.4 Hz, 1H, $CH_2CH{=}CH_aH_b$), 4.65^ (s, 2H, NCH_2), 4.63* (s, 2H, NCH_2), 4.62 (ddd, J = 1.3, 1.7, 5.8 Hz, 2H, $O{=}COCH_2$), 4.03* (s, 2H, $O{=}CCH_2$), 3.98^ (s, 2H, $O{=}CCH_2$), 3.81* (s, 3H, OCH_3), 3.80^ (s, 3H, OCH_3), 2.42* (s, 3H, $O{=}CCH_3$), 2.18^ (s, 3H, $O{=}CCH_3$), 1.48-1.52* (m, 2H, $O{=}CCCH_{2a}CH_{2b}$), 1.41-1.45^ (m, 2H, $O{=}CCCH_{2a}CH_{2b}$), 1.39-1.41* (m, 2H, $O{=}CCCH_{2a}CH_{2b}$), and 1.34-1.37* (m, 2H, $O{=}CCCH_{2a}CH_{2b}$).

^{13}C NMR: δ 204.1, 170.7, 168.9, 159.6, 131.6, 128.9, 126.8, 118.9, 114.6, 65.9, 55.43, 51.5, 45.9, 37.4, 28.1, and 17.2.

^{13}C NMR: δ 203.7, 169.7, 168.7, 159.4, 131.3, 130.1, 128.1, 119.5, 114.3, 66.2, 55.37, 48.9, 47.8, 38.0, 27.2, and 16.5.

Allyl 2-(2-Acetyl-4-chloro-*N*-(4-methoxybenzyl)butanamido)acetate (4117)

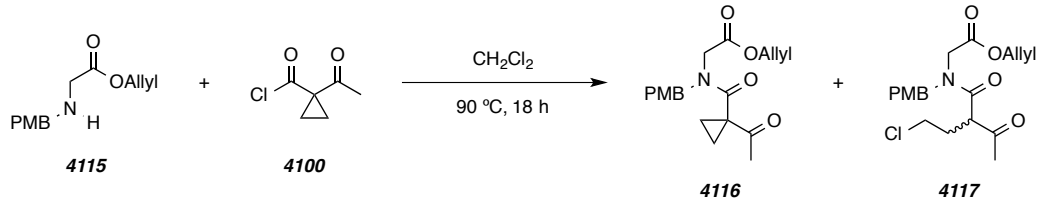

[*PHW xi120*] A solution of **4115** (200 mg, 0.85 mmol) and **4104** (300, 2.1 mmol) in CH_2Cl_2 (1 mL) was heated at 90 ºC. After 18 h the reaction mixture was diluted in EtOAc and sequentially washed with sat. aq. NH_4Cl and brine. The organic extract was dried ($MgSO_4$) and concentrated. Purification by MPLC (hexanes:EtOAc 65:35) gave **4116** and **4117**.

Data for **4117**:

^{1}H NMR [500 MHz, $CDCl_3$ rotA(*):rotB(^) = ~67:33]: δ 7.17* (d, *J* = 8.6, Hz, 2H, $C_{aryl}HC_{aryl}CH_2$), 7.15^ (d, *J* = 8.5 Hz, 2H, $C_{aryl}HC_{aryl}CH_2$), 6.91* (d, *J* = 8.6 Hz, 2H, $CH_3OC_{aryl}C_{aryl}H$), 6.86^ (d, *J* = 8.6 Hz, 2H, $CH_3OC_{aryl}C_{aryl}H$), 5.88 (dddd, *J* = 5.8, 5.8, 10.4, 17.4 Hz, 1H, $CH_2CH{=}CH_2$), 5.32^ (dddd, *J* = 1.4, 1.4, 1.4, 17.2 Hz, 1H, $CH_2CH{=}CH_aH_b$), 5.31* (dddd, *J* = 1.5, 1.5, 1.5, 17.2 Hz, 1H, $CH_2CH{=}CH_aH_b$), 5.28^ (dddd, *J* = 1.2, 1.2, 1.2, 10.5 Hz, 1H, $CH_2CH{=}CH_aH_b$), 5.25* (dddd, *J* = 1.3, 1.3, 1.3, 10.4 Hz, 1H, $CH_2CH{=}CH_aH_b$), 4.69* (d, *J* = 16.18 Hz, 1H, NCH_aH_b), 4.641* (d, *J* = 16.2 Hz, 1H, NCH_aH_b), 4.644^ (d, *J* = 14 Hz, 1H, NCH_aH_b), 4.62* (ddd, *J* = 1.5, 1.5, 5.8 Hz, 2H, $O{=}COCH_2$), 4.58^ (d, *J* = 14.7 Hz, 1H, NCH_aH_b), 4.55^ (ddd, *J* = 1.4, 1.4, 5.9 Hz, 2H, $O{=}COCH_2$), 4.132^ (d, *J* = 18.4 Hz 1H, $O{=}CCH_aH_b$), 4.127* (d, *J* = 17.2 Hz 1H, $O{=}CCH_aH_b$), 4.07* (d, *J* = 17.3 Hz 1H, $O{=}CCH_aH_b$), 4.06^ (d, *J* = 18.5 Hz 1H, $O{=}CCH_aH_b$), 3.81* (s, 3H, OCH_3), 3.80^ (s, 3H, OCH_3), 3.53-3.68 (m, 1H, $O{=}CCHCH_2$), 2.30-2.46 (m, 1H, $O{=}CCHCH_2$), 2.23^ (s, 3H, $O{=}CCH_3$), and 2.18* (s, 3H, $O{=}CCH_3$).

HRMS (ESI-TOF): Calcd for $C_{19}H_{24}ClNNaO_5^+$ [$M+Na^+$] requires 404.1235; found 404.1242.

^{13}C NMR (major rotamer): δ 203.0, 170.0, 168.7, 159.7, 131.6, 128.7 (x2), 127.4, 119.0, 114.7 (x2), 66.1, 55.5, 54.0, 52.3, 47.7, 43.1, 31.96, and 28.2.

^{13}C NMR (minor rotamer): δ 203.3, 169.6, 168.8, 159.5, 131.4, 130.0 (2x), 128.2, 119.6, 114.4 (x2), 66.6, 55.4, 54.5, 49.8, 48.5, 43.3, 31.94, and 27.9.

IR (neat): 2954, 1746, 1724, 1646, 1616, 1513, 1441, 1249, and 1177 cm^{-1}.

***N*-(2-Acetyl-4-chlorobutanoyl)-*N*-(4-methoxybenzyl)glycine (4118)**

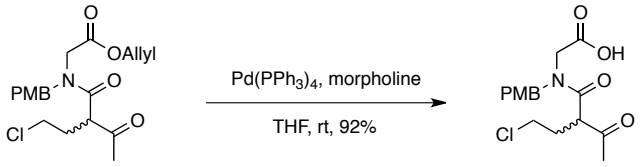

4117 ***4118***

[*PHW xi128*] Morpholine (75μL, 0.86 mmol) and $Pd(PPh_3)$ (9 mg, 8 μmol) was added to a solution of allyl ester **4117** (51 mg, 0.13 mmol) in THF (1 mL) at room temperature with stirring and under an inert atmosphere. After 18 h the reaction mixture was diluted in Et_2O, washed sequentially with 2M HCl and brine, dried ($MgSO_4$), and concentrated to give the acid **4118** (42 mg, 0.12 mmol, 92%). The crude material was used without purification.

^{1}H NMR [500 MHz, $CDCl_3$ rotA(*):rotB(^) = ~1.7:1]: δ 8.6 (br s, 1H, CO_2H), 7.16* (d, *J* = 8.5 Hz, 2H, $C_{aryl}HC_{aryl}CH_2$), 7.14^ (d, *J* = 8.6 Hz, 2H, $C_{aryl}HC_{aryl}CH_2$), 6.91* (d, *J* = 8.4 Hz, 2H, $CH_3OC_{aryl}C_{aryl}H$), 6.84^ (d, *J* = 8.4 Hz, 2H, $CH_3OC_{aryl}C_{aryl}H$), 4.69^ (d, *J* = 14.8 Hz, 1H, NCH_aH_b), 4.68* (d, *J* = 16.2 Hz, 1H, NCH_aH_b), 4.62* (d, *J* = 16.2 Hz, 1H, NCH_aH_b), 4.49^ (d, *J* = 14.7 Hz, 1H, NCH_aH_b), 3.97-4.18 (m, 2H, 1H, O=CCH_2), 3.81* (s, 3H, OCH_3), 3.78^ (s, 3H, OCH_3), 3.55-3.72 (m, 1H, O=$CCHCH_2$), 2.24-2.48 (m, 1H, O=$CCHCH_2$), 2.19^ (s, 3H, O=CCH_3), and 2.16* (s, 3H, O=CCH_3).

^{13}C NMR: δ 203.4$^-$, 203.1$^+$, 170.1$^+$, 169.8$^-$, 159.7$^+$, 159.4$^-$, 132.42$^-$, 132.39$^-$, 132.3$^+$, 132.2$^+$, 131.9$^-$, 131.1$^-$, 129.9$^-$, 128.8$^+$, 128.7$^+$, 128.6$^+$, 128.4$^-$, 127.4$^-$, 114.6$^+$, 114.4$^-$, 114.3$^-$, 55.5$^+$, 55.4$^-$, 54.2$^-$, 53.9$^+$, 52.8$^+$, 49.5$^-$, 43.2$^-$, 43.1$^+$, 31.9$^+$, 30.4$^-$, 29.8$^+$, 28.2$^+$, and 28.0$^-$.

HRMS (ESI-TOF): Calcd for $C_{16}H_{20}ClNNaO_5^+$ [M+Na$^+$] requires 364.0922; found 364.0948.

IR of (neat): 3739, 2919, 1719, 1653, 1249, 1174, and 1120 cm^{-1}.

(2*S*,3*S*)-Methyl 3-Hydroxy-2-((4-methoxybenzyl)amino)-4-methylpentanoate (5032)

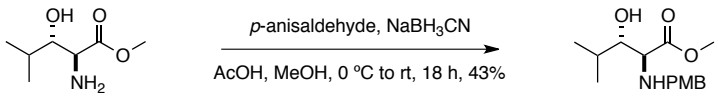

5022 ***5032***

[*PHW 7243*] $NaBH_3CN$ (490 mg, 7.80 mmol) and *p*-anisaldehyde (700 µL, 5.75 mmol) were sequentially added to a stirred solution of amine **5022**[117] (827 mg, 5.14 mmol) and AcOH (650 µL, 11.4 mmol) in MeOH (40 mL) at 0 ºC. After 0.5 h the ice-bath was removed and after 18 h the $NaHCO_3$ (2.0 g, 35 mmol) and the mixture was concentrated. The residue was partitioned between CH_2Cl_2/H_2O (1:1). The layers were separated and the aqueous phase was further extracted with EtOAc. The combined organic extracts were washed with brine, dried ($MgSO_4$), and concentrated. Purification by gradient flash chromatography (hexanes:EtOAc 2:1 to 0:100) gave amine **5032** (623 mg, 2.22 mmol, 43%).

^{1}H NMR [500 MHz, $CDCl_3$]: δ 7.23 (d, *J* = 8.7 Hz, 2H, $C_{aryl}HC_{aryl}CH_2$), 6.85 (d, *J* = 8.7 Hz, 2H, $CH_3OC_{aryl}C_{aryl}H$), 3.79 (s, 3H, OCH_3), 3.78 (d, *J* = 12.3 Hz, 1H, NCH_aH_b), 3.74 (s, 3H, OCH_3), 3.60 (d, *J* = 12.5 Hz, 1H, NCH_aH_b), 3.47 (dd, *J* = 5.3, 6.5 Hz, 1H, C(OH)C*H*), 3.43 (d, *J* = 5.3 Hz, 1H, NC*H*), 2.44 (br s, 1H, O*H*), 1.75 [ap octet, *J* = 6.7 Hz, 1H, $CH(CH_3)_2$], 0.98 (d, *J* = 6.7 Hz, 3H, $CHCH_3$), 0.92 (d, *J* = 6.8 Hz, 3H, $CHCH_3$), and 0.91 (d, *J* = 6.7 Hz, 3H, $CHCH_3$).

^{13}C NMR [125 MHz, $CDCl_3$]: δ 174.6, 159.9, 131.6, 129.6 (x2), 113.9 (x2), 77.4, 63.0, 55.3, 51.9, 51.7, 30.9, 19.6, and 17.9.

IR (neat): 3434, 2958, 1733, 1513, and 1247 cm^{-1}.

(2*S*,3*S*)-Methyl 2-((4-Methoxybenzyl)amino)-4-methyl-3-((triethylsilyl)oxy)pentanoate (5033)

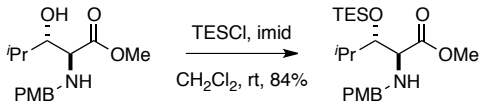

5032 ***5033***

[*PHW 7248*] Triethylchlorosilane (550 μL, 3.29 mmol) was added to stirred solution of alcohol **5032** (623 mg, 2.22 mmol) and imidazole (151 mg, 2.22 mmol) in CH_2Cl_2 at 0 ºC. After 10 h the reaction mixture was diluted in EtOAc and sequentially washed with $NHCO_3$ and brine. The organic extract was dried ($MgSO_4$) and concentrated to give crude silyl ether **5033** (734 mg, 1.86 mmol, 84%).

^{1}H NMR (500 MHz, $CDCl_3$): δ 7.22 (d, J = 8.7 Hz, 2H, $C_{aryl}HC_{aryl}CH_2$), 6.84 (d, J = 8.7 Hz, 2H, $CH_3OC_{aryl}C_{aryl}H$), 3.79 (s, 3H, OCH_3), 3.78 (d, J = 12.7 Hz, 1H, NCH_aH_b), 3.72 (s, 3H, OCH_3), 3.60 (d, J = 12.5 Hz, 1H, NCH_aH_b), 3.65 (dd, J = 4.6, 6.5 Hz, 1H, C(OH)C*H*), 3.54 (d, J = 12.4 Hz, 1H, NC*H*), 1.80 (br s, 1H, N*H*), 1.99 [nfom, 1H, $CH(CH_3)_2$], 0.93 (t, J = 7.9 Hz, 3H, $SiCH_2CH_3$), 0.90 (d, J = 6.9 Hz, 3H, $CHCH_3$), 0.86 (d, J = 6.8 Hz, 3H, $CHCH_3$), and 0.91 (d, J = 6.7 Hz, 3H, $CHCH_3$), and 0.57 (q, J = 8.0 Hz, 2H, $SiCH_2$).

^{13}C NMR (125 MHz, $CDCl_3$): δ 233.1, 175.0, 158.8, 132.1, 129.6, 79.4, 64.4, 55.5, 51.9, 51.5, 31.2, 19.6, 17.5, 7.1, and 5.4.

(2*S*,3*S*)-Methyl 2-(2-Acetyl-4-chloro-*N*-(4-methoxybenzyl)butanamido)-4-methyl-3-((triethylsilyl)oxy)pentanoate (5034)

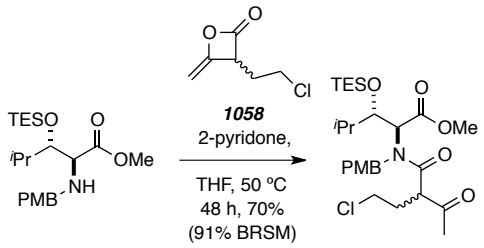

5033 ***5034***

[*PHW 7249*] A stirred solution of amine **5033** (97 mg, 0.25 mmol), ketene dimer **1058** (56 mg, 0.38 mmol), and 2-hydroxy pyridine (32 mg, 0.34 mmol) in THF (2 mL) was heated to 50 ºC in a culture tube equipped with a Teflon®-lined screwcap. After 48 the reaction mixture was diluted in EtOAc and sequentially washed with sat. aq. NH_4Cl and brine. The organic extract was dried ($MgSO_4$) and concentrated. Purification by flash chromatography (6:1 hexanes:EtOAc) gave amidoester **5034** (93 mg, 0.17 mmol, 70%, 91% BRSM) and starting amine **5033** (20 mg, 0.051 mmol).

^{1}H NMR [500 MHz, $CDCl_3$ diastereomer 1(*):diastereomer 2(^) = ~1.1]: δ 7.10* (d, *J* = 8.6 Hz, 2H, $C_{aryl}HC_{aryl}CH_2$), 7.08^ (d, *J* = 8.5 Hz, 2H, $C_{aryl}HC_{aryl}CH_2$), 6.88 (d, *J* = 8.7 Hz, 2H, $CH_3OC_{aryl}C_{aryl}H$), 5.27* (d, *J* = 8.0 Hz, 1H, NC*H*), 5.24^ (d, *J* = 7.8 Hz, 1H, NC*H*), 4.75* (d, *J* = 17.4 Hz, 1H, NCH_aH_b), 4.68^ (d, *J* = 17.6 Hz, 1H, NCH_aH_b), 4.64* (br s, 1H, NCH_aH_b), 4.60^ (d, *J* = 17.4 Hz, 1H, NCH_aH_b), 4.121* (dd, *J* = 8.1, 8.7 Hz, 1H, C*H*OSi), 4.117^ (d, *J* = 8.0, 8.3 Hz, 1H, C*H*OSi), 3.80 (s, 3H, $C_{aryl}OCH_3$), 3.66* (s, 3H, CO_2CH_3), 3.58^ (s, 3H, CO_2CH_3), 3.34-3.57 (m, 3H, O=CC*H* and CH_2Cl), 2.29-2.41 (m, 2H, CH_2CH_2Cl), 2.07* (s, 3H, O=CCH_3), 1.93^ (s, 3H, O=CCH_3), 1.57-1.75 [m, 1H, $CH(CH_3)_2$] 0.84-0.98 (m, 15H, CH_3 x5), and 0.53-0.61 [m, 6H, $Si(CH_2CH_3)_3$].

(2*S*,3*S*)-*S*-Butyl 2-Azido-3-hydroxy-4-methylpentanethioate (5038)

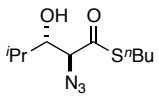

5038

[Data for **5038** from *PHW 7286*]

^{1}H NMR (500 MHz, $CDCl_3$): δ 3.95 (d, *J* = 6.8 Hz, C*H*N_3), 3.72 (br q, *J* = 6.6 Hz, C*H*OH), 2.96 (br dd, *J* = 7.3, 7.4 Hz, SC*H*$_2$), 2.40 (d, *J* = 5.3 Hz, 1H, O*H*), 1.96 [d heptet, *J* = 5.0, 6.8 Hz, 1H, C*H*$(CH_3)_2$], 1.60 (br p, *J* = 7.4 Hz, 2H, $SCH_2CH_2CH_2$), 1.42 (br hexet, *J* = 7.6 Hz, 2H, SCH_2CH_2), 1.02 [d, *J* = 6.9 Hz, 3H, $CH(CH_3)_2$], 0.98 [d, *J* = 6.8 Hz, 3H, $CH(CH_3)_2$], and 0.94 (t, *J* = 7.4 Hz, 3H, CH_2CH_3).

(2*S*,3*S*)-*S*-*p*-Tolyl 3-((*tert*-Butyldimethylsilyl)oxy)-2-((4-methoxybenzyl)amino)-4-methylpentanethioate (5046)

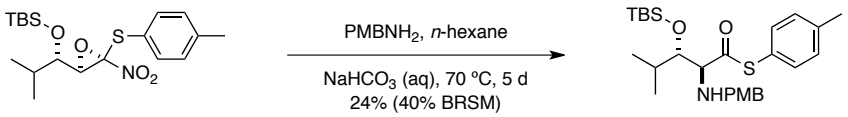

5044 ***5046***

[*PHW 8145* and *xi100*] 4-Methoxybenzylamine (35 μL, 0.27 mmol) was added to a culture tube containing a biphasic mixture of epoxide **5044**[119] (109 mg, 0.274 mmol) in *n*-hexane (1.2 mL) and sat. aq. $NaHCO_3$ (1.2 mL). The culture tube was sealed with a Teflon®-lined cap and the mixture was heated to 70 ºC with vigorous stirring. After 5 days the mixture was cooled to room temperature, diluted in Et_2O, and sequentially washed with sat. aq. NH_4Cl and brine. The organic phase was dried ($MgSO_4$) and concentrated. Purification by MPLC (hexanes:EtOAc 19:1) gave the starting epoxide **5044** (43 mg, 0.11 mmol) and thioester **5046** (32 mg, 0.066 mmol, 24%, 40% BRSM) as a clear yellow oil.

^{1}H NMR (500 MHz, $CDCl_3$): δ 7.36 (d, *J* = 8.6 Hz, 2H, $C_{aryl}HC_{aryl}CH_2$), 7.28 (d, *J* = 8.1 Hz, 2H, $C_{aryl}HC_{aryl}CH_3$), 7.22 (d, *J* = 8.4 Hz, 2H, $SC_{aryl}C_{aryl}H$), 6.89 (d, *J* = 8.6 Hz, 2H, $CH_3OC_{aryl}C_{aryl}H$), 3.94 (d, *J* = 12.5 Hz, 1H, NCH_aH_b), 3.86 (dd, *J* = 4.3, 5.1 Hz, 1H, OC*H*), 3.81 (s, 3H, OCH_3), 3.71 (d, *J* = 12.5 Hz, 1H, NCH_aH_b), 3.58 (d, *J* = 5.2 Hz, 1H, NC*H*), 2.38 (s, 3H, $C_{aryl}CH_3$), 1.99 [d hept, *J* = 4.3, 6.8 Hz, 1H, C*H*$(CH_3)_2$], 0.98 (d, *J* = 6.7 Hz, 3H, CHC*H*$_3$), 0.91 [s, 9H, $SiC(CH_3)_3$], 0.90 (d, *J* = 6.7 Hz, 3H, CHC*H*$_3$), 0.06 (s, 3H, SiC*H*$_3$), and 0.04 (s, 3H, SiC*H*$_3$).

^{13}C NMR (125 MHz, $CDCl_3$): δ 203.0, 158.9, 139.3, 134.5, 132.0, 130.0, 129.7, 125.6, 113.9, 77.9, 72.855.4, 53.2, 31.2, 26.1, 21.5, 20.6, 18.4, 18.1, -4.0, and -4.4.

IR of (neat): 2956, 2929, 2856, 1698, 1249, 1072, and 1039 cm^{-1}.

HRMS (ESI-TOF): Calcd for $C_{27}H_{41}NNaO_3SSi^+$ [M+Na^+] requires 510.2469; found 510.2547.

LC / LR-MS [ES+APCI, 50:50 to 0:100 (%) H_2O:MeOH, 12 min run]: t_R 8.3 min; *m/z* 488 [$M+H^+$].

TLC: R_f 0.4 (19:1 Hex/EtOAc).

[α]$_D$ = -42.8 (*c* = 2.0, CH_2Cl_2)

(2*S*,3*S*)-*S*-*p*-Tolyl 2-(2-Acetyl-4-chloro-*N*-(4-methoxybenzyl)butanamido)-3-((*tert*-butyldimethylsilyl)oxy)-4-methylpentanethioate (5047)

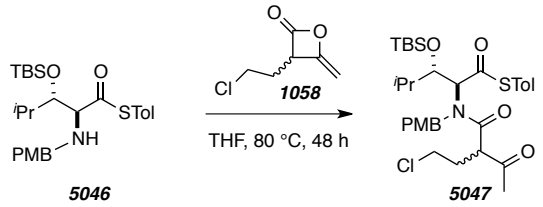

[*PHW 8162*] A culture tube equipped with a Teflon®-lined screwcap containing a mixture of amine **5046** (16 mg, 0.033 mmol), and ketene dimer **1058** (16 mg, 0.11 mmol) in THF was heated at 80 ºC. After 48 h, the reaction mixture was diluted in EtOAc and sequentially washed with sat. aq. NH_4Cl and brine. The organic extract was dried ($MgSO_4$) and concentrated. Purification by MPLC (hexanes:EtOAc 9:1) gave amide **5047** (16 mg, 0.25 mmol, 76%).

^{1}H NMR [500 MHz, $CDCl_3$ diastereomer 1(*):diastereomer 2(^) = ~1.1]: δ 7.12-7.32 (m, 6H, $C_{aryl}HC_{aryl}CH_2$ and SC_6H_4), 6.87* (d, *J* = 8.8 Hz, 2H, $CH_3OC_{aryl}C_{aryl}H$), 6.85^ (d, *J* = 8.6 Hz, 2H, $CH_3OC_{aryl}C_{aryl}H$), 5.60* (br d, *J* = 8.9 Hz, 1H, NC*H*), 4.97^ (br d, *J* = 8.3 Hz, 1H, NC*H*), 4.67* (d, *J* = 17.9 Hz, 1H, NCH_aH_b), 4.61^ (d, *J* = 17.4 Hz, 1H, NCH_aH_b), 4.58* (br s, 1H, NCH_aH_b), 4.51^ (d, *J* = 17.2 Hz, 1H, NCH_aH_b), 4.15-4.21 (m, 1H, C*H*OSi), 3.80 (s, 3H, $C_{aryl}OCH_3$), 3.55-3.69 (m, 3H, O=CC*H* and CH_2Cl), 2.37 (s, 3H, $C_{aryl}CH_3$), 2.28-2.49 (m, 2H, CH_2CH_2Cl), 2.14* (s, 3H, $O=CCH_3$), 1.91^ (s, 3H, $O=CCH_3$), 1.48-1.66 [m, 1H, $CH(CH_3)_2$] 0.83-0.93 (m, 15H, CH_3 x5), and -0.11-0.14 [m, 6H, $Si(CH_3)_2$].

LC / LR-MS [ES+APCI, 50:50 to 0:100 (%) H_2O:MeOH, 12 min run]: t_R 6.7 min; *m/z* 634 [$M(^{35}Cl)+H^+$], 636 [$M(^{37}Cl)+H^+$], 656 [$M(^{35}Cl)+Na^+$], 658 [$M(^{37}Cl)+Na^+$], 692 [$M(^{35}Cl)+K^+$], and 694 [$M(^{37}Cl)+K^+$].

(2*S*,3*S*)-*S*-*p*-Tolyl 2-(2-Acetyl-4-chloro-*N*-(4-methoxybenzyl)butanamido)-3-hydroxy-4-methylpentanethioate (5048)

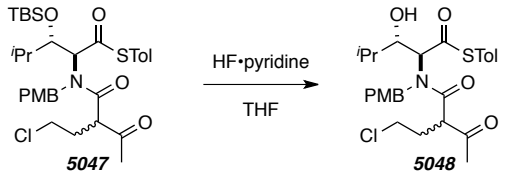

[*PHW 8165*] HF•pyridine (241 µL, 9 mmol HF) was added to a stirred solution of silyl ether **5047** (16 mg, 0.031 mmol) in THF (1.5 mL) in a plastic culture tube. After 16 h, the reaction mixture was diluted in EtOAc and sequentially washed with sat. aq. $NHCO_3$, sat. aq. NH_4Cl, and brine. The organic extract was dried ($MgSO_4$) and concentrated to give alcohol **5048** (8 mg, 0.02 mmol, 66% crude).

LC / LR-MS [ES+APCI, 50:50 to 0:100 (%) H_2O:MeOH, 12 min run]: t_R 4.1 min; *m/z* 520 [M(^{35}Cl)+H^+], and 522 [M(^{37}Cl)+H^+].

(*S*)-Allyl 2-(1-Acetyl-*N*-(4-methoxybenzyl)cyclopropanecarboxamido)-3-(benzyloxy)propanoate (5050)

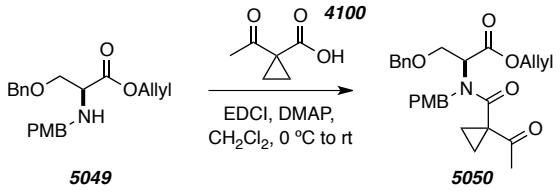

[*PHW xi094*] EDCI (1.4 g, 7.29 mmol) was added to a stirred solution of acid **4100** (1.36 g, 10.6 mmol) and DMAP (75 mg, 0.45 mmol) in CH_2Cl_2 (5.7 mL) at 0 ºC and under and inert atmosphere. After 5 min, amine **5049** (1.63 g, 4.59 mmol) was added and the reaction mixture was allowed to warm to rt. After 16 h, the reaction mixture was diluted in EtOAc and sequentially washed with sat. aq. NH_4Cl and brine. The organic extract was dried ($MgSO_4$) and concentrated. Purification by gradient flash chromatography (30% to 50% EtOAc in hexanes) gave starting amine (595 mg, 1.68 mmol) and desired amide **5050** (455 mg, 0.978 mmol, 21%, 34% BRSM).

^{1}H NMR [500 MHz, $CDCl_3$, rotA(*):rotB(^) = ~ 4:1]: δ 7.25-7.39 (m, 5H, $OCH_2C_6H_5$), 7.22* (br d, *J* = 8.6 Hz, 2H, $NCH_2C_{aryl}C_{aryl}H$), 7.16^ (br d, *J* = 8.7 Hz, 2H, $NCH_2C_{aryl}C_{aryl}H$), 6.85* (br d, *J* = 8.7 Hz, 2H, $C_{aryl}HC_{aryl}OCH_3$), 6.80^ (br d, *J* = 8.7 Hz, 2H, $C_{aryl}HC_{aryl}OCH_3$), 5.86 (dddd,

J = 5.8, 5.8, 10.5, 17.2 Hz, CH_2CH=CH_aH_b), 5.28 (dddd, J = 1.5, 1.5, 1.5, 15.7 Hz, 1H, CH_2CH=CH_aH_b), 5.22 (dddd, J = 1.4, 1.4, 1.4, 10.3 Hz, 1H, CH_2CH=CH_aH_b), 4.83 (d, J = 15.1 Hz, 1H, $CH_aH_bC_{aryl}$), 4.56 (dddd, J = 1.3, 1.3, 5.9, 7.3 Hz, 1H, $NCHCO_2$), 4.48 (d, J = 11.8 Hz, 1H, $CH_aH_bC_{aryl}$), 4.44 (d, J = 11.9 Hz, 1H, $CH_aH_bC_{aryl}$), 4.07 (dd, J = 3.9, 11.6 Hz, 1H, $CO_2CH_aH_b$), 4.04 (dd, J = 3.9, 11.6 Hz, 1H, $CO_2CH_aH_b$), 3.80* (s, 3H, OCH_3), 3.78^ (s, 3H, OCH_3), 2.29* (s, 3H, $O=CCH_3$), 2.20^ (s, 3H, $O=CCH_3$), 1.54 (nfom, 1H, cyclopropyl-CH), 1.47 (nfom, 1H, cyclopropyl-CH), 1.38 (nfom, 1H, cyclopropyl-CH), and 1.30 (nfom, 1H, cyclopropyl-CH).

HRMS (ESI-TOF): Calcd for $C_{27}H_{31}NNaO_6^+$ [$M+Na^+$] requires 488.2044; found 465.2118.

LC / LR-MS [ES+APCI, 50:50 to 0:100 (%) H_2O:MeOH, 12 min run]: t_R 7.5 min; *m/z* 466 [$M+H^+$] and 488 [$M+Na^+$].

TLC: R_f 0.3 (7:3 Hex/EtOAc).

(2*S*)-Allyl 2-(2-Acetyl-4-chloro-*N*-(4-methoxybenzyl)butanamido)-3-(benzyloxy)propanoate (5051)

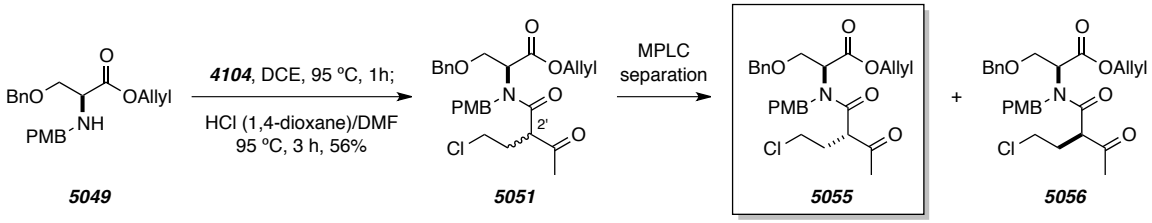

5049 ***5051*** ***5055*** ***5056***

[*PHW xi109*] Acid chloride **4104** (350 mg, 2.40) was added to a solution of amine **5049** (181 mg, 0.51 mmol) in DCE (650 µL) in a glass culture tube. The culture tube was sealed with a Teflon®-lined cap and the mixture was heated to 95 ºC. After 1 h, the mixture was cooled to rt and concentrated. DMF (260 µL) and HCl (260 µL, 1.04 mmol, 4 M in 1,4-dioxane) were sequentially added to the concentrated reaction mixture. The culture was again sealed and the reaction mixture was heated to 95 ºC. After 3 h, the reaction mixture was diluted in EtOAc and sequentially washed with sat. aq. NH_4Cl and brine. The organic extract was dried ($MgSO_4$) and concentrated. Purification by MPLC (hexanes:EtOAc 7:3) allowed for partial separation of **5055** and **5056** (combined mass = 143 mg, 0.285 mmol, 56%). The spectral data of the mixture matched the reported data for the diastereomeric mixture, and the ^{1}H NMR spectrum of purified **5055** was identical to the spectrum reported for its diastereomer.

HRMS (ESI-TOF): Calcd for $C_{27}H_{32}ClNNaO_6^+$ [M+Na^+] requires 524.1810; found 524.1813.

LC / LR-MS [ES+APCI, 50:50 to 0:100 (%) H_2O:MeOH, 12 min run]: t_R 7.9 min; *m/z* 502 [M(^{35}Cl)+H^+] and 504 [M(^{37}Cl)+H^+].

Experimental Section for Chapters 6–7

2-(6-((*tert*-Butyldimethylsilyl)oxy)hexa-1,3-diyn-1-yl)cyclohex-1-enecarboxaldehyde (6046)

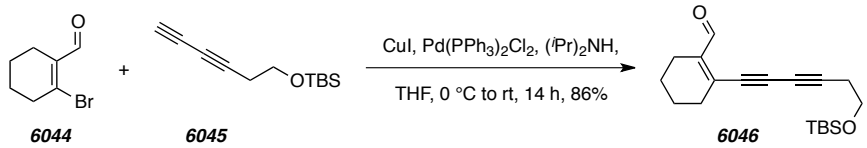

6044 ***6045*** ***6046***

CuI (29 mg, 0.15 mmol) and $Pd(PPh_3)_2Cl_2$ (7 mg, 0.01 mmol) were added to a stirred solution of 2-bromo-1-cyclohexene-1-carboxaldehyde[203] (**6044**, 188 mg, 0.99 mmol), diyne **6045** (250 mg, 1.20 mmol), and freshly deaerated diisopropylamine (3.0 mL, 21 mmol) in THF (5 mL) at 0 ºC and under an atmosphere of N_2. After 1 h the ice-bath was removed and the reaction mixture was allowed to warm to rt. After 14 h the reaction mixture was diluted in Et_2O and washed with satd. aq. NH_4Cl. The aqueous phase was extracted with Et_2O and the combined organic extracts were washed with brine, dried ($MgSO_4$), and concentrated. Purification by MPLC (hexanes:EtOAc 15:1) gave the diyne **6046** (269 mg, 0.85 mmol, 86%) as a clear brown oil.

^{1}H NMR (500 MHz, $CDCl_3$): δ 10.11 (s, 1H, C*H*O), 3.78 (t, *J* = 6.9 Hz, 2H, OSiCH_2), 2.58 (t, *J* = 6.9 Hz, 1H, ≡CCH_2), 2.40 (nfom, 2H, =C-CH_2), 2.27 (nfom, 2H, =C-CH_2), 1.65 [nfom, 4H, $CH_2(CH_2)_2CH_2$], 0.90 [s, 9H, $C(CH_3)_3$], and 0.08 [s, 6H, $Si(CH_3)_2$].

^{13}C NMR (125 MHz, $CDCl_3$): δ 192.3, 146.3, 138.8, 85.7, 83.5, 71.7, 65.9, 61.3, 32.2, 26.0, 24.3, 22.4, 21.9, 21.0, 18.5, and -5.2.

IR (neat): 2933, 2858, 2232, 1677, 1255, 1220, 1108, 839, and 779 cm^{-1}.

HRMS (ESI-TOF): Calcd for $C_{19}H_{28}NaO_2Si^+$ [M+Na^+] requires 339.1751; found 339.1774.

TLC: R_f 0.4 (9:1 Hex/EtOAc).

---

[203] Tang, J.-M.; Bhunia, S.; Sohel, S. M. A.; Lin, M.-Y.; Liao, H.-Y.; Datta, S.; Das, A.; Liu, R.-S. The skeletal rearrangement of gold- and platinum-catalyzed cycloisomerization of *cis*-4,6-dien-1-yn-3-ols: Pinacol rearrangement and formation of bicyclo[4.1.0]heptenone and reorganized styrene derivatives. *J. Am. Chem. Soc.* **2007**, *129*, 15677–15683.

1-(2-(6-((*tert*-Butyldimethylsilyl)oxy)hexa-1,3-diyn-1-yl)cyclohex-1-en-1-yl)-3-(trimethylsilyl)prop-2-yn-1-ol (6047)

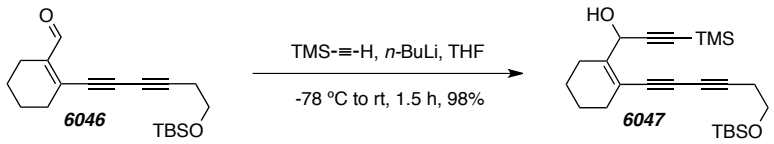

n-BuLi (800 µL, 2.5 M in hexanes, 2.0 mmol) was added to a stirred solution of ethynyltrimethylsilane (350 µL, 2.5 mmol) in THF (2.3 mL) at -78 ºC. After 1 h a solution of diyne **6046** (399 mg, 1.26 mmol) in THF (1.7 mL) was added and the reaction mixture was allowed to warm to rt. After 30 min satd. aq. NH_4Cl was added and the mixture was extracted with EtOAc. The combined organic extracts were washed with brine, dried ($MgSO_4$), and concentrated. The crude product triynol **6047** (508 mg, 1.23 mmol, 98%) was a clear red oil and used directly in the next reaction.

^{1}H NMR (500 MHz, $CDCl_3$): δ 5.58 (d, *J* = 4.2 Hz, 1H, C*H*OH), 3.76 (t, *J* = 7.1 Hz, 2H, SiOCH_2), 2.55 (t, *J* = 7.1 Hz, 2H, ≡CCH_2), 2.33 (nfom, 2H, =C-CH_2), 2.19 (nfom, 2H, =C-CH_2), 1.94 (d, *J* = 4.5 Hz, 1H, O*H*), 1.64 (nfom, 4H, $CH_2(CH_2)_2CH_2$), 0.90 [s, 9H, SiC(CH_3)$_3$], 0.18 [s, 9H, Si(CH_3)$_3$], and 0.08 [s, 6H, Si(CH_3)$_2$C].

^{13}C NMR (125 MHz, $CDCl_3$): δ 146.6, 117.9, 104.1, 90.7, 82.5, 78.3, 73.7, 66.3, 64.7, 61.6, 30.0, 26.0, 24.2, 23.7, 22.2, 21.9, 18.5, 0.0, and -5.2.

IR (neat): 3409, 2933, 2859, 2171, 1251, 1106, 842, and 778 cm^{-1}.

HRMS (ESI-TOF): Calcd for $C_{24}H_{38}NaO_2Si_2^+$ [M+Na$^+$] requires 437.2303; found: 437.2306.

TLC: R_f 0.3 (9:1 Hex/EtOAc).

1-(2-(6-((*tert*-Butyldimethylsilyl)oxy)hexa-1,3-diyn-1-yl)cyclohex-1-en-1-yl)-3-(trimethylsilyl)prop-2-yn-1-one (6048)

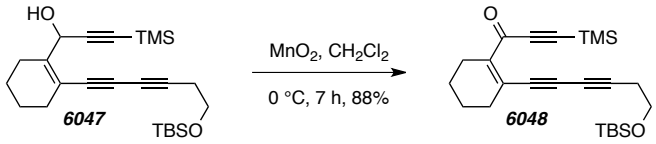

MnO_2 (267 mg, 3.07 mmol) was added in two portions to a stirred solution of alcohol **6047** (41 mg, 0.099 mmol) in CH_2Cl_2 (0.5 mL) at 0 ºC. After 7 h the reaction mixture was filtered through

Celite® (Et_2O eluent) and concentrated at 0 ºC to give ketone **6047** (36 mg, 0.087 mmol, 88%) as a clear amber oil. Because of the high reactivity of this ketone (toward conversion to **6049**) at ambient temperature this sample was characterized without further purification.

^{1}H NMR (500 MHz, $CDCl_3$): δ 3.75 (t, J = 7.2 Hz, 2H, SiOCH_2), 2.57 (t, J = 7.2 Hz, 2H, ≡CCH_2), 2.37-2.44 (m, 4H, =C-CH_2), 1.61-1.66 (m, 4H, CH_2(CH_2)$_2$CH_2), 0.90 [s, 9H, SiC(CH_3)$_3$], 0.27 [s, 9H, Si(CH_3)$_3$], and 0.07 [s, 6H, Si(CH_3)$_2$C].

^{13}C NMR (125 MHz, $CDCl_3$): δ 177.4, 144.4, 131.4, 102.4, 101.4, 85.8, 85.3, 74.3, 67.1, 61.5, 33.4, 26.0, 25.6, 24.3, 21.9, 21.6, 18.4, -0.4, and -5.2.

IR (neat): 2953, 2933, 2859, 2228, 2151, 1612, 1250, 1106, and 844 cm^{-1}.

HRMS (ESI-TOF): Calcd for $C_{24}H_{36}NaO_2Si_2^+$ [M+Na^+] requires 435.2146; found 435.2154.

TLC: R_f 0.4 (9:1 Hex/EtOAc).

10-(*tert*-Butyldimethylsilyl)-4-(trimethylsilyl)-6,7,8,9-tetrahydro-2*H*-fluoreno[3,2-*b*]furan-5(3*H*)-one (6049)

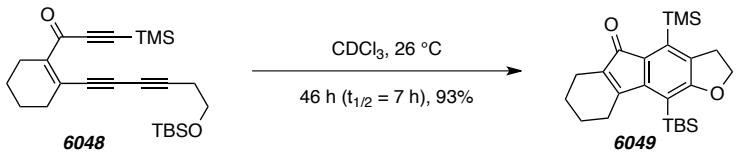

A solution of ketone **6048** (29 mg, 0.070 mmol) in $CDCl_3$ (2 mL) was kept at 26 ºC (external bath temperature). After 46 h the reaction mixture was concentrated and purified by flash chromatography (hexanes:EtOAc 15:1) to give the benzenoid **6049** (27 mg, 0.066 mmol, 93%) as a clear amber oil.

^{1}H NMR (500 MHz, $CDCl_3$): δ 4.42 (t, J = 8.9 Hz, 2H, OCH_2), 3.15 (t, J = 8.9 Hz, 2H, OCH_2CH_2), 2.49 (nfom, 2H, =C-CH_2), 2.23 (nfom, 2H, =C-CH_2), 1.69 (nfom, 4H, CH_2(CH_2)$_2$CH_2), 0.98 [s, 9H, SiC(CH_3)$_3$], 0.36 [s, 6H, Si(CH_3)$_2$C], and 0.33 [s, 9H, Si(CH_3)$_3$].

^{13}C NMR (125 MHz, $CDCl_3$): δ 198.2, 169.1, 157.6, 154.9, 136.2, 133.9, 130.6, 128.2, 115.7, 70.2, 31.3, 28.1, 27.5, 23.2, 21.5, 20.2, 18.9, 1.6, and 1.5.

IR (neat): 2929, 2856, 1737, 1370, 1301, 1255, 1225, 1015, 838, 810, and 760 cm^{-1}.

HRMS (ESI-TOF): Calcd for $C_{24}H_{36}NaO_2Si_2^+$ [M+Na^+] requires 435.2146; found 435.2126.

TLC: R_f 0.6 (9:1 Hex/EtOAc).

(*E*)-1-(Prop-2-yn-1-yloxy)hept-2-ene (6100)

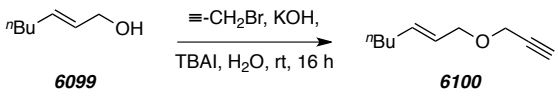

6099 ***6100***

[*PHW 9050*] Propargyl bromide (3.5 mL, 39.3 mmol, 80 wt. % in toluene) was added dropwise to an aqueous (9 mL) solution of (*E*)-hept-2-en-1-ol (4.49 g, 39.3 mmol), tetra-*n*-butylammonium iodide (145 mg, 0.393 mmol), and sodium hydroxide (4.7 g, 118 mmol) at room temperature with stirring. After 16 h the reaction mixture was extracted with Et_2O. The combined organic layers were washed with brine, dried ($MgSO_4$), and concentrated to give crude **6100** (8.88 g, 58.4 mmol, quant), which was used without further purification.

^{1}H NMR (500 MHz, $CDCl_3$): δ 5.75 (ddddd, *J* = 1.3, 1.3, 6.7, 6.8, 15.3 Hz, 1H, =C*H*), 5.54 (ddddd, *J* = 1.5, 1.5, 6.4, 6.5, 15.4 Hz, 1H, =C*H*), 4.13 (d, *J* = 2.4 Hz, 2H, OCH_2CCCH$_3$), 4.02 (dq, *J* = 6.4, 1.1 Hz, 2H, OCH_2C=C), 2.42 (dd, *J* = 2.4, 2.4 Hz, 1H, CC*H*), 2.03-2.09 (m, 2H, =CCH_2CH$_2$), 1.27-1.41 (m, 4H, CH_2CH_2CH$_3$), and 0.89 (t, *J* = 7.2 Hz, CH_3).

(*E*)-1-((3-Bromoprop-2-yn-1-yl)oxy)hept-2-ene (6101)

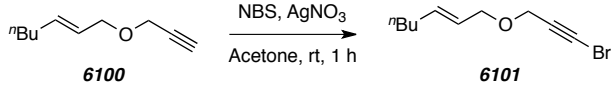

6100 ***6101***

[*PHW 9060*] Powdered $AgNO_3$ (0.819 g, 4.8 mmol) was added to a stirred solution of alkyne **6100** (8.88 g, 58.4 mmol) and NBS (9.5 g, 53 mmol) in acetone (107 mL) at rt. After 1 h the slurry was either partitioned between Et_2O and water, further extracted with Et_2O, washed with brine, dried ($MgSO_4$), and concentrated. The crude bromoalkyne, **6101** (11.6 g, 50.2 mmol, 86%), was used without further purification.

^{1}H NMR (500 MHz, $CDCl_3$): δ 5.75 (ddddd, *J* = 1.3, 1.3, 6.7, 6.8, 15.3 Hz, 1H, =C*H*), 5.54 (ddddd, *J* = 1.4, 1.4, 6.4, 6.4, 15.3 Hz, 1H, =C*H*), 4.15 (s, 2H, OCH_2CCCH$_2$), 4.02 (ap dq, *J* = 6.4, 1.1 Hz, 2H, OCH_2C=C), 2.01-2.11 (m, 2H, =CCH_2CH$_2$), 1.29-1.42 (m, 4H, CH_2CH_2CH$_3$), and 0.89 (t, *J* = 7.0 Hz, CH_3).

GC / LR EI-MS [5025015]: t_R 6.43 min; *m/z* 232 [M(^{81}Br)$^{+\bullet}$], 230 [M(^{79}Br)$^{+\bullet}$], 202 [M(^{81}Br)$^{+\bullet}$–$CH_2CH_3^{\bullet}$], and 200 [M(^{79}Br)$^{+\bullet}$–$CH_2CH_3^{\bullet}$].

(*E*)-1-(2-(5-(hept-2-en-1-yloxy)penta-1,3-diyn-1-yl)phenyl)-3-(trimethylsilyl)prop-2-yn-1-ol (6102)

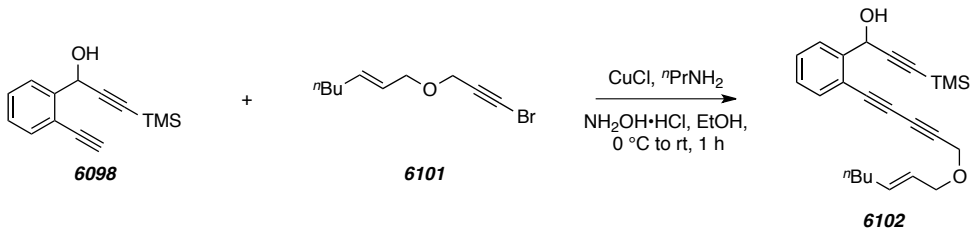

[*PHW 9062*] NH_2OH•HCl (ca. 50 mg, 0.75 mmol) was added to a stirred mixture of CuCl (8 mg, 0.08 mmol) and *n*-propylamine (360 µL, 4.38 mmol) in EtOH (4.4 mL) until the blue solution became colorless. Diyne **6098**[156] (421 mg, 1.85 mmol) was added and the resulting mixture was cooled to 0 ºC and a solution of bromoalkyne **6101** (600 mg, 2.61 mmol) in EtOH (1 mL) was added. After 1 h the reaction mixture was diluted in EtOAc and sequentially washed with sat. aq. NH_4Cl and brine. The organic extract was dried ($MgSO_4$) and concentrated to give crude triyne **6102** (524 mg, 1.39 mmol, 75%). A portion of the crude reaction mixture was purified by MPLC (4:1 hexanes:EtOAc) to give a pure sample of **6102**.

^{1}H NMR (500 MHz, $CDCl_3$): δ 7.71 (dd, *J* = 1.2, 7.8 Hz, 1H, *H3*), 7.53 (dd, *J* = 1.5, 7.7 Hz, 1H, *H6*), 7.42 (ddd, *J* = 1.5, 7.6, 7.6 Hz, 1H, *H4or5*), 7.30 (ddd, *J* = 1.4, 7.5, 7.6 Hz, 1H, *H4or5*), 5.82 [d, *J* = 5.7 Hz, 1H, C*H*(OH)], 5.72-5.82 (nfom, 1H, =C*H*), 5.49-5.60 (nfom, 1H, =C*H*), 4.29 (s, 2H, OCH_2CCCH_2), 4.05 (ap dq, *J* = 6.4, 1.1 Hz, 2H, OCH_2C=C), 2.05-2.12 (m, 2H, =CCH_2CH_2), 1.30-1.44 (m, 4H, CH_2CH_2CH_3), 0.89 (t, *J* = 7.0 Hz, CH_3), and 0.20 [s, Si(CH_3)$_3$].

LC / LR-MS [ES+APCI, 50:50 to 0:100 (%) H_2O:MeOH, 12 min run]: t_R 5.1 min; *m/z* 379 [M+H$^+$], and 396 [M+NH_4^+].

(*E*)-1-(2-(5-(Hept-2-en-1-yloxy)penta-1,3-diyn-1-yl)phenyl)-3-(trimethylsilyl)prop-2-yn-1-one (6103)

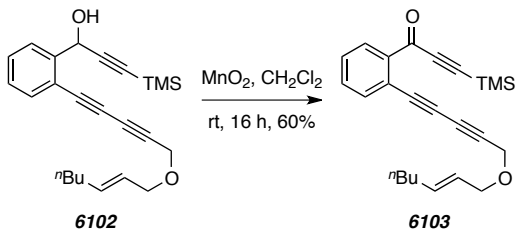

[*PHW 9063*] MnO_2 (575 mg, 6.61 mmol) was added to a solution of alcohol **6102** (125 mg, 0.331 mmol) in CH_2Cl_2 (1 mL). After 16 h the reaction mixture was filtered through a plug of Celite® (EtOAc eluent) and concentrated to give the ketone **6103** (74 mg, 0.20 mmol, 60%) as a clear amber oil.

^{1}H NMR (500 MHz, $CDCl_3$): δ 8.11 (dd, *J* = 1.4, 7.7 Hz, 1H, *H6*), 7.63 (dd, *J* = 1.3, 7.5 Hz, 1H, *H3*), 7.52 (ddd, *J* = 1.4, 7.5, 7.5 Hz, 1H, *H4*), 7.48 (ddd, *J* = 1.4, 7.6, 7.6 Hz, 1H, *H5*), 5.77 (ddddd, *J* = 1.3, 1.3, 6.8, 6.9, 15.3 Hz, 1H, =C*H*), 5.50-5.63 (nfom, 1H, =C*H*), 4.30 (s, 2H, OCH_2CCCH_2), 4.04 (ap dq, *J* = 6.5, 1.1 Hz, 2H, OCH_2C=C), 2.05-2.10 (m, 2H, =CCH_2CH_2), 1.28-1.42 (m, 4H, $CH_2CH_2CH_3$), 0.90 (t, *J* = 7.3 Hz, CH_3), and 0.31 [s, Si(CH_3)$_3$].

LC / LR-MS [ES+APCI, 50:50 to 0:100 (%) H_2O:MeOH, 12 min run]: t_R 5.8 min; *m/z* 377 [M+H$^+$], and 394 [M+NH_4^+].

(*E*)-4-(Pent-1-en-1-yl)-11-(trimethylsilyl)-3,4-dihydroindeno[1,2-*g*]isochromen-10(1*H*)-one (*E*-6105) and (*Z*)-4-(Pent-1-en-1-yl)-11-(trimethylsilyl)-3,4-dihydroindeno[1,2-*g*]isochromen-10(1*H*)-one (*Z*-6105)

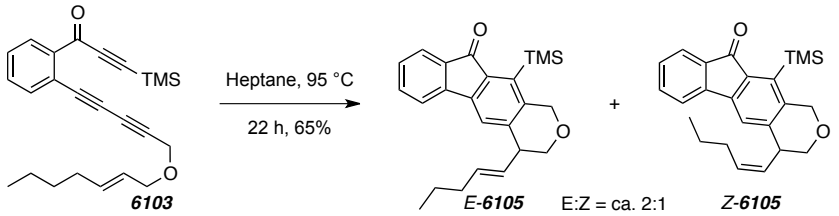

[*PHW 9064*] A solution of the triyne **6103** (51 mg, 0.14 mmol) was heated to 95 °C in heptane (1 mL). After 22 h the reaction mixture was concentrated. Purification by flash chromatography (9:1 hexanes:EtOAc) gave a mixture of *E*-**6105** and *Z*-**6105** (33 mg, .088 mmol, 65%) as a golden yellow oil. Analytical samples for both *E*-**6105** and *Z*-**6105** were prepared by separating the product mixture with MPLC (39:1 hexanes:EtOAc).

[Data for *E*-**6105**]

^{1}H NMR (500 MHz, $CDCl_3$): δ = 7.58 (ddd, *J* = 1.0, 1.0, 7.3 Hz, 1H, C_{aryl}-*H9*), 7.46 (nfom, 1H, C_{aryl}-*H6*), 7.45 (nfom, 1H, C_{aryl}-*H7*), 7.37 (d, *J* = 0.8 Hz, 1H, C_{aryl}-*H5*), 7.26 (nfom, 1H, C_{aryl}-*H8*), 5.73 (dddd, *J* = 0.8, 6.8. 6.8, 15.3 Hz, 1H, =C*H*CHC_2), 5.46 (dddd, *J* = 1.4, 1.4, 8.8, 15.2 Hz, 1H, =C*H*CH_2), 4.88 (d, *J* = 1.3 Hz, 2H), 3.97 (dd, *J* = 5.3, 11.1 Hz, 1H) 3.66 (dd, *J* = 7.1,

11.1 Hz, 1H), 3.55 (nfom, 1H), 2.09 (ddd, 1.5, 7.0, 7.0 Hz, 1H), 2.07 (ddd, *J* = 1.5, 6.8, 6.8 Hz, 1H), 1.46 (sextet, *J* = 7.4 Hz, 2H), 0.95 (t, *J* = 7.4 Hz, 3H), and 0.42 [s, $Si(CH_3)_3$].

GC/MS t_r = 13.59 min; m/z: 376, 361, 331, 306, 287, 202, 189, 137, and 73.

HRMS (ESI-TOF): Calcd for $C_{24}H_{29}O_2Si^+$ [$M+H^+$] requires 377.1931; found 377.1957.

LC / LR-MS [ES+APCI, 50:50 to 0:100 (%) H_2O:MeOH, 12 min run]: t_R 2.9 min; *m/z* 392 [M+16]. When this Thesis was prepared we were not sure what caused the +16 mass in the LC/MS. However, this behavior was characteristic of all fluorenones screened by LC/MS and will be reported as +16.

[Data for *Z*-**6105**]

^{1}H NMR (500 MHz, $CDCl_3$): δ = 7.58 (ddd, *J* = 1.0, 1.0, 7.3 Hz, 1H), 7.45 (nfom, 1H, C_{aryl}-*H6*), 7.44 (nfom, 1H, C_{aryl}-*H7*), 7.32 (d, *J* = 0.7 Hz, 1H), 7.26 (nfom, 1H, C_{aryl}-*H8*), 5.71 (dddd, *J* = 0.8, 7.5, 7.5, 10.8 Hz, 1H), 5.38 (dddd, *J* = 1.7, 1.7, 9.3, 10.8 Hz, 1H), 4.93 (d, *J* = 15.1 Hz, 1H), 4.87 (dd, *J* = 1.28 Hz, 1H), 3.99 (nfom), 3.53 (nfom, 1H, C*H*CH_2O), 2.26 (nfom, 1H), 1.53 (nfom, 1H), 1.02 (t, *J* = 7.4 Hz, 3H), and 0.42 [s, $Si(CH_3)_3$].

GC-MS t_r = 13.68 min; m/z: 376, 361, 331, 287, 215, 202, and 73.

LC / LR-MS [ES+APCI, 50:50 to 0:100 (%) H_2O:MeOH, 12 min run]: t_R 2.9 min; *m/z* 392 [M+16].

1-((3-Bromoprop-2-yn-1-yl)oxy)-3-methylbut-2-ene (6107)

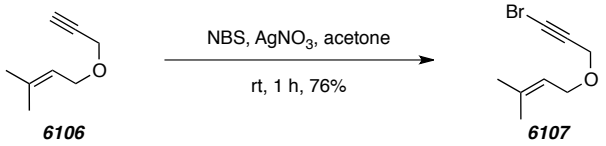

6106 ***6107***

Powdered $AgNO_3$ (312 mg, 1.84 mmol) was added to a stirred solution of 3-methyl-1-(prop-2-yn-1-yloxy)but-2-ene[204] (**6106**, 2.07 g, 16.7 mmol) and NBS (3.35 g, 18.8 mmol) in acetone (40 mL) at rt. After 1 h the slurry was either partitioned between Et_2O and water, further extracted with Et_2O, washed with brine, dried ($MgSO_4$), and concentrated. Purification by flash chromatography (hexanes:EtOAc 9:1) gave the bromoalkyne **6107** (2.56 g, 12.6 mmol, 76%) as a clear colorless oil.

---

[204] M. Nishizawa, V. K. Yadav, M. Skwarczynski, H. Takao, H. Imagawa, T. Sugihara, Mercuric triflate catalyzed hydroxylative carbocyclization of 1,6-enynes. *Org. Lett.* **5**, 1609–1611 (2003).

^{1}H NMR (500 MHz, $CDCl_3$): δ 5.33 (tqq, *J* = 7.1, 1.4, 1.4 Hz, 1H, =C*H*), 4.15 (s, 2H, OCH_2C≡), 4.05 (dqq, *J* = 7.1, 0.8, 0.8 Hz, 2H, OCH_2CH=), 1.76 (dt, *J* = 1.2, 1.2 Hz, 3H, CH_3), and 1.71 (br d, *J* = 1.5 Hz, 3H, CH_3).

^{13}C NMR (125 MHz, $CDCl_3$): δ 138.7, 120.2, 76.7, 66.2, 57.9, 45.7, 25.9, and 18.2.

IR (neat): 2974, 2933, 2913, 2853, 2212, 1673, 1630, 1443, 1378, 1352, 1077, 1027, 1002, 925, and 897 cm^{-1}.

HRMS (CIMS): Calcd for $C_8H_{15}BrNO^+$ [M+NH_4^+] requires 220.0332; found 220.0348.

TLC: R_f 0.4 (19:1 Hex/EtOAc).

1-(2-(5-((3-Methylbut-2-en-1-yl)oxy)penta-1,3-diyn-1-yl)phenyl)-3-(trimethylsilyl)prop-2-yn-1-ol (6108)

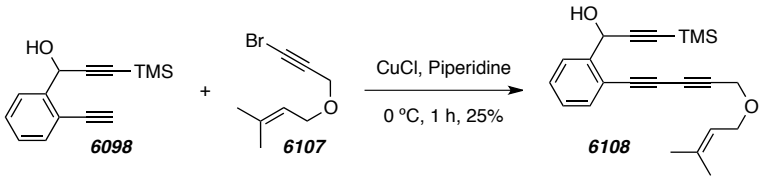

Bromoalkyne **6107** (123 mg, 0.606 mmol) was added to a stirred solution of **6098** (108 mg, 0.474 mmol) and CuCl (3 mg, 0.03 mmol) in piperidine (1.0 mL) at 0 ºC and under an inert atmosphere. After 1 h the reaction mixture was diluted in EtOAc and sequentially washed with sat. aq. NH_4Cl and brine. The organic extract was dried ($MgSO_4$) and concentrated. Purification by MPLC (hexanes:EtOAc 4:1) gave the triyne **6108** (42 mg, 0.12 mmol, 25%) as a clear yellow oil.

^{1}H NMR (500 MHz, $CDCl_3$): δ 7.71 (dd, *J* = 1.3, 7.8 Hz, 1H, *H3*), 7.52 (dd, *J* = 1.5, 7.7 Hz, 1H, *H6*), 7.42 (ddd, *J* = 1.5, 7.7, 7.7 Hz, 1H, *H4or5*), 7.30 (ddd, *J* = 1.4, 7.6, 7.6 Hz, 1H, *H4or5*), 5.82 [d, *J* = 4.9 Hz, 1H, C*H*(OH)], 5.35 [tqq, *J* = 7.1, 1.4, 1.4 Hz, 1H, $(CH_3)_2$C=C*H*], 4.29 (s, 2H, OCH_2C≡), 4.09 (dqq, *J* = 7.1, 0.8, 0.8 Hz, 2H, OCH_2CH=), 2.48 (d, *J* = 5.2 Hz, 1H, O*H*), 1.78 (dt, *J* = 1.2, 1.2 Hz, 3H, CCH_3), 1.73 (br d, *J* = 1.6 Hz, 3H, CCH_3), and 0.20 (s, 9H, SiCH_3).

^{13}C NMR (125 MHz, $CDCl_3$): δ 143.6, 138.9, 133.8, 129.9, 128.5, 127.1, 120.2, 120.1, 104.1, 92.0, 80.9, 78.7, 75.1, 70.6, 66.4, 63.4, 57.6, 26.0, 18.3, and -0.1.

IR (neat): 3437, 2960, 2238, 2172, 1250, 1059, 845, and 760 cm^{-1}.

HRMS (ESI-TOF): Calcd for $C_{22}H_{26}NaO_2Si^+$ [M+Na^+] requires 373.1594; found 373.1604.

TLC: R_f 0.4 (4:1 Hex/EtOAc).

1-(2-(5-((3-Methylbut-2-en-1-yl)oxy)penta-1,3-diyn-1-yl)phenyl)-3-(trimethylsilyl)prop-2-yn-1-one (6111)

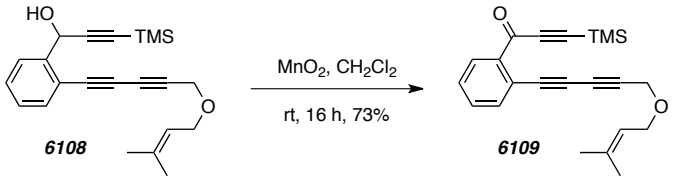

MnO_2 (230 mg, 2.64 mmol) was added to a solution of alcohol **6109** (37 mg, 0.11 mmol) in CH_2Cl_2 (0.25 mL). After 16 h the reaction mixture was filtered through a plug of Celite® (EtOAc eluent) and concentrated to give the ketone **6111** (28 mg, 0.080 mmol, 73%) as a clear amber oil.

^{1}H NMR (500 MHz, $CDCl_3$): δ 8.11 (dd, *J* = 1.6, 7.7 Hz, 1H, *H6*), 7.63 (dd, *J* = 1.6, 7.6 Hz, 1H, *H3*), 7.52 (ddd, *J* = 1.6, 7.5, 7.5 Hz, 1H, *H4*), 7.48 (ddd, *J* = 1.5, 7.6, 7.6 Hz, 1H, *H5*), 5.34 (tqq, *J* = 7.1, 1.5, 1.5 Hz, 1H, $(CH_3)_2C{=}CH$), 4.29 (s, 2H, $OCH_2C{\equiv}$), 4.09 (br d, *J* = 7.1 Hz, 2H, $OCH_2CH{=}$), 1.77 (dt, *J* = 1.2, 1.2 Hz, 3H, CCH_3), 1.73 (d, *J* = 1.4 Hz, 3H, CCH_3), and 0.31 (s, 9H, $SiCH_3$).

^{13}C NMR (125 MHz, $CDCl_3$): δ 176.4, 139.1, 138.8, 135.9, 132.7, 132.1, 128.9, 121.5, 120.2, 101.6, 101.4, 81.6, 79.5, 76.0, 71.1, 66.4, 57.7, 26.0, 18.3, and -0.6.

IR (neat): 2965, 2931, 2872, 2152, 1649, 1236, 1067, 1015, 850, and 757 cm^{-1}.

HRMS (ESI-TOF): Calcd for $C_{22}H_{24}NaO_2Si^+$ $[M+Na^+]$ requires 371.1438; found 371.1436.

TLC: R_f 0.4 (9:1 Hex/EtOAc).

4-(Propen-2-yl)-11-(trimethylsilyl)-3,4-dihydroindeno[1,2-*g*]isochromen-10(1*H*)-one (6111)

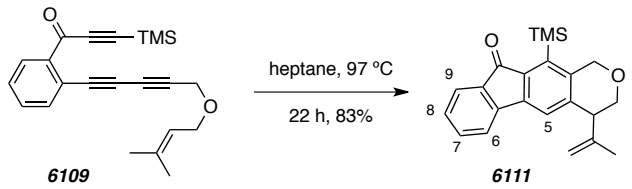

A solution of triynone **S35** (53 mg, 0.15 mmol) in heptane (4 mL) was heated at 97 ºC. After 16 h the mixture was concentrated and the crude material was purified by flash chromatography (hexanes:EtOAc 15:1) to give the fluorenone **S36** (44 mg, 0.13 mmol, 83%) as a golden yellow oil.

^{1}H NMR (500 MHz, $CDCl_3$): δ 7.59 (ddd, *J* = 1.0, 1.0, 7.3 Hz, 1H, *H9*), 7.48 (ddd, *J* = 0.8, 1.5, 7.4 Hz, 1H, *H6*), 7.45 (ddd, *J* = 1.1, 7.2, 7.2 Hz, 1H, *H7*), 7.33 (d, *J* = 0.8 Hz, 1H, *H5*), 7.26 (ddd, *J* = 1.5, 7.2, 7.2 Hz, 1H, *H8*), 5.03 (br dq, *J* = 0.8, 1.5 Hz, 1H, =CH_aH$_b$), 4.91 (ddq, *J* = 0.8, 2.1, 0.8 Hz, 1H, =CH$_a$$H_b$), 4.90 (dd, *J* = 1.2, 15.2 Hz, C$_{Ar}$CH_aH$_b$O), 4.85 (dd, *J* = 1.2, 15.2 Hz, C$_{Ar}$CH$_a$$H_b$O), 3.97 (dd, *J* = 5.5, 11.3 Hz, OCH_aH$_b$CH), 3.84 (dd, *J* = 6.0, 11.3 Hz, OCH$_a$$H_b$CH), 3.63 (dddq, *J* = 0.8, 5.5, 6.0, 0.8 Hz, 1H, C*H*CH$_2$O), 1.73 (dd, *J* = 0.8, 1.5 Hz, 3H, CCH_3), and 0.43 (s, 9H, SiCH_3).

^{13}C NMR (125 MHz, $CDCl_3$): δ 195.1, 145.9, 144.0, 143.1, 142.2, 140.5, 139.0, 138.4, 134.6, 134.2, 128.9, 124.0, 122.1, 119.8, 115.5, 71.2, 68.3, 47.8, 20.3, and 2.7.

IR (neat): 2974, 2933, 2913, 2853, 2212, 1673, 1630, 1443, 1378, 1352, 1077, 1027, 1002, 925, and 897 cm^{-1}.

HRMS (CIMS): Calcd for $C_{22}H_{25}O_2Si^+$ [M+H$^+$] requires 349.1618; found 349.1629.

TLC: R_f 0.4 (9:1 Hex/EtOAc).

(*E*)-((4-((3-Bromoprop-2-yn-1-yl)oxy)but-2-en-1-yl)oxy)(*tert*-butyl)dimethylsilane (6113)

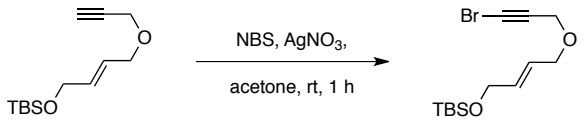

6112 ***6113***

[*PHW x047*] Powdered $AgNO_3$ (36 mg, 0.21 mmol) was added to a stirred solution of enyne **6112**[205] (168 mg, 0.70 mmol) and NBS (189 mg, 1.62 mmol) in acetone (3.5 mL) at rt. After 1 h the slurry was either partitioned between Et_2O and water, further extracted with Et_2O, washed with brine, dried ($MgSO_4$), and concentrated. The crude sample of bromoalkyne **6113** (246 mg, 0.77 mmol, quant) was sufficiently pure for subsequent experiments.

^{1}H NMR (500 MHz, $CDCl_3$): δ 5.74-5.87 (m, 2H, C*H*=C*H*), 4.19 (nfom, 2H, SiOCH$_2$C=), 4.17 (s, 2H, OCH_2C≡), 4.06 (nfom, 2H, COCH_2C=), 0.91 [s, 9H, SiC(CH_3)$_3$], and 0.07 [s, 6H, Si(CH_3)$_2$].

---

[205] DeBoef, B.; Counts, W. R.; Gilbertson, S. R. Rhodium-catalyzed synthesis of eight-membered rings. *J. Org. Chem.* **2007**, *72*, 799–804.

GC / LR EI-MS [5031022H]: t_R 8.3 min; *m/z* 263 [M(^{81}Br)$^{+\bullet}$–C(CH$_3$)$_3^{\bullet}$] and [M(^{79}Br)$^{+\bullet}$–C(CH$_3$)$_3^{\bullet}$].

(*E*)-1-(2-(5-((4-((*tert*-Butyldimethylsilyl)oxy)but-2-en-1-yl)oxy)penta-1,3-diyn-1-yl)phenyl)-3-(trimethylsilyl)prop-2-yn-1-ol (6114)

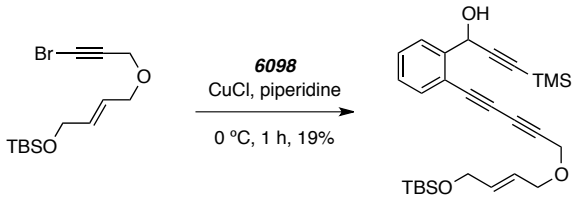

6113 ***6114***

[*PHW x048*] Bromoalkyne **6113** (246 mg, 0.77 mmol) was added to a stirred solution of **6098** (180 mg, 0.79 mmol) and CuCl (4 mg, 0.04 mmol) in piperidine (2.0 mL) at 0 ºC and under an inert atmosphere. After 1 h the reaction mixture was diluted in EtOAc and sequentially washed with sat. aq. NH_4Cl and brine. The organic extract was dried ($MgSO_4$) and concentrated. Purification by flash chromatography (hexanes:EtOAc 9:1) gave the triyne **6114** (72 mg, 0.15 mmol, 19%) as a clear yellow oil.

^{1}H NMR (500 MHz, $CDCl_3$): δ 7.72 (dd, *J* = 1.4, 7.8 Hz, 1H, *H3*), 7.53 (dd, *J* = 1.4, 7.7 Hz, 1H, *H6*), 7.42 (ddd, *J* = 1.5, 7.7, 7.7 Hz, 1H, *H4or5*), 7.30 (ddd, *J* = 1.3, 7.6, 7.6 Hz, 1H, *H4or5*), 5.76-5.91 (m, 3H, C*H*OH and C*H*=C*H*), 4.31 (s, 2H, OCH_2C≡), 4.21 (nfom, 2H, SiOCH_2C=), 4.12 (nfom, 2H, COCH_2C=), 2.49 (br s, 1H, O*H*), 0.92 [s, 9H, SiC(CH_3)$_3$], 0.20 [s, 9H, SiCH_3)$_3$], and 0.08 [s, 6H, Si(CH_3)$_2$].

^{13}C NMR (125 MHz, $CDCl_3$): δ 143.6, 134.0, 133.9, 130.0, 129.6, 128.5, 127.1, 125.1, 120.2, 104.1, 92.0, 92.8, 80.5, 75.2, 70.1, 63.4, 63.1, 57.8, 26.1, 18.6, -0.05, -0.06, and -5.1.

LC / LR-MS [ES+APCI, 50:50 to 0:100 (%) H_2O:MeOH, 12 min run]: t_R 3.4 min; *m/z* 467 [M+H$^+$].

(*E*)-1-(2-(5-((4-((*tert*-Butyldimethylsilyl)oxy)but-2-en-1-yl)oxy)penta-1,3-diyn-1-yl)phenyl)-3-(trimethylsilyl)prop-2-yn-1-one (6115)

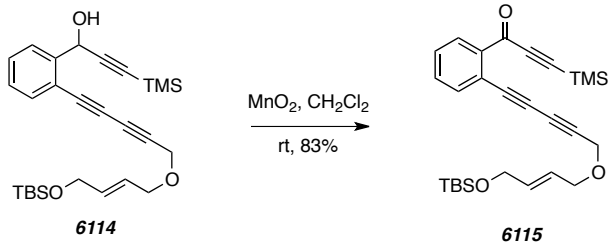

6114 ***6115***

[*PHW X050*] MnO_2 (40 mg, 0.46 mmol) was added to a stirred solution of triyne **6114** (12 mg, 0.026 mmol) in CH_2Cl_2 (300 µL) at room temperature. After 16 h the reaction mixture was filtered through a small column of SiO_2 (EtOAc eluent). The crude reaction mixture was sufficiently pure to give triynone **6115** (10 mg, 0.022 mmol, 83%).

^{1}H NMR (500 MHz, $CDCl_3$): δ 8.11 (d, *J* = 7.8 Hz, 1H, *H6*), 7.63 (d, *J* = 7.6 Hz, 1H, *H3*), 7.52 (dd, *J* = 6.8, 7.6 Hz, 1H, *H4*), 7.47 (dd, *J* = 7.4, 7.6 Hz, 1H, *H5*), 5.73-5.92 (m, 2H, C*H*=C*H*), 4.31 (s, 2H, OCH_2C≡), 4.20 (br d, *J* = 2.6 Hz, 2H, SiOCH_2C=), 4.11 (br d, *J* = 5.5 Hz, 2H, COCH_2C=), 0.91 [s, 9H, SiC(CH_3)$_3$], 0.31 [s, 9H, SiCH_3)$_3$], and 0.08 [s, 6H, Si(CH_3)$_2$].

^{13}C NMR (125 MHz, $CDCl_3$): δ 176.5, 139.2, 135.9, 134.0, 132.7, 132.1, 128.9, 125.2, 121.5, 101.7, 101.4, 81.2, 79.4, 76.1, 71.3, 70.1, 63.1, 57.8, 26.1, 18.6, 0.2, -0.5, and -5.1.

(*E*)-1-(2-(5-((4-hydroxybut-2-en-1-yl)oxy)penta-1,3-diyn-1-yl)phenyl)-3-(trimethylsilyl)prop-2-yn-1-one (6116)

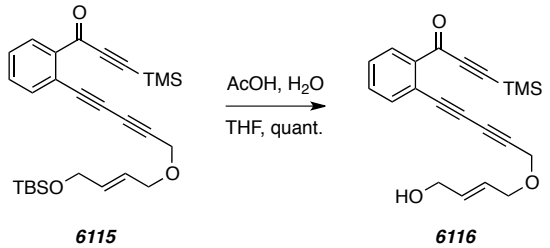

6115 ***6116***

[*PHW x185*] AcOH (60 µL, 1.05 mmol) was added to a stirred mixture of silyl ether **6115** (10 mg, 0.022 mmol) THF (20 µL) and water (20 µL) at rt. After 16 h the mixture was diluted in EtOAc and sequentially washed with $NaHCO_3$ and brine. The organic extract was dried ($MgSO_4$) and concentrated to give alcohol **6116** (8 mg, 0.2 mmol).

^{1}H NMR (500 MHz, $CDCl_3$): δ 8.13 (dd, *J* = 1.7, 7.6 Hz, 1H, *H6*), 7.63 (d, *J* = 1.5, 7.6 Hz, 1H, *H3*), 7.53 (ddd, *J* = 1.6, 7.5, 7.5 Hz, 1H, *H4*), 7.48 (dd, *J* = 1.5, 7.5, 7.5 Hz, 1H, *H5*), 5.97 (ddddd, *J* = 1.4, 1.4, 5.2, 5.2, 15.5 Hz, 1H, =C*H*CH_2OH), 5.83 (nfom, 1H COC=C*H*), 4.33 (s, 2H, OCH_2C≡), 4.18-4.21 (m, 2H, HOCH_2C=), 4.13 (ap dq, *J* = 5.9, 1.2 Hz, 2H, COCH_2C=), 2.27 (dd, *J* = 1.7, 1.7 Hz, 1H, O*H*), and 0.31 [s, 9H, SiCH_3)$_3$].

2-(10-Oxo-11-(trimethylsilyl)-1,3,4,10-tetrahydroindeno[1,2-*g*]isochromen-4-yl)acetaldehyde (6117)

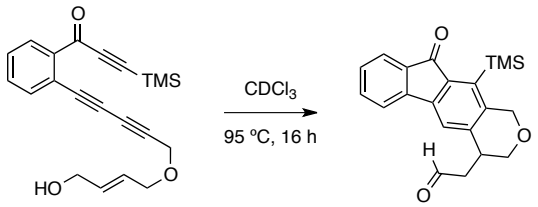

6116 ***6117***

[*PHW x188*] A solution of alcohol **6116** (8 mg, 0.2 mmol) in $CDCl_3$ (700 μL) was heated at 95 ºC in an NMR tube. After 16 h, the mixture was cooled and several resonances from ^{1}H NMR spectrum suggested that aldehyde **6117** had formed.

^{1}H NMR (500 MHz, $CDCl_3$): δ 9.88 (br s, 1H, C*H*O), 7.60 (ddd, *J* = 0.9, 0.9, 7.3 Hz, 1H, *H9*), 7.46-7.48 (m, 2H, *H6andH7*), 7.29 (s, 1H, *H5*), 7.28 (m, 1H, *H8*), 4.97 (d, *J* = 15.4 Hz, $C_{Ar}CH_aH_bO$), 4.80 (d, *J* = 15.4 Hz, $C_{Ar}CH_aH_bO$), 3.90 (dd, *J* = 1.9, 11.5 Hz, OCH_aH_bCH), 3.82 (dd, *J* = 3.4, 11.5 Hz, OCH_aH_bCH), 3.41 (nfom, 1H, C*H*CH_2O), 3.16 (dd, *J* = 9.2, 18.5 Hz, 3H, CH_aH_bCHO), 3.16 (dd, *J* = 3.8, 18.5 Hz, 3H, CH_aH_bCHO), and 0.43 (s, 9H, SiCH_3).

(*E*)-1-(2-(5-((3-Cyclopropylallyl)oxy)penta-1,3-diyn-1-yl)phenyl)-3-(trimethylsilyl)prop-2-yn-1-ol (6119)

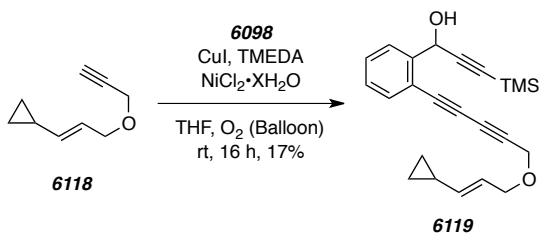

6118 ***6119***

[*PHW 9155*] CuI (5 mg, 0.03 mmol) was added to a stirred solution of diyne **6098**[Error! Bookmark not defined.] (255 mg, 1.12 mmol), alkyne **6118**[206] (53 mg, 0.39 mmol), TMEDA (14 μL, 0.094 mmol), and $NiCl_2•XH_2O$ (5 mg) in THF (3.7 mL) at ambient temperature and under an O_2 atmosphere (via balloon). After 24 h the reaction mixture was diluted in satd. aq. NH_4Cl and extracted with EtOAc. The combined organic extracts were washed with brine, dried ($MgSO_4$), and concentrated. Purification by flash chromatography (hexanes:EtOAc 4:1) gave triyne **6119** (24 mg, 0.066 mmol, 17%).

^{1}H NMR (500 MHz, $CDCl_3$): δ 7.71 (dd, *J* = 1.4, 7.9 Hz, 1H, *H3*), 7.52 (dd, *J* = 1.5, 7.7 Hz, 1H, *H6*), 7.42 (ddd, *J* = 1.5, 7.7, 7.7 Hz, 1H, *H4or5*), 7.30 (ddd, *J* = 1.4, 7.6, 7.6 Hz, 1H, *H4or5*), 5.82 (d, *J* = 5.7 Hz, 1H, C*H*OH), 5.63 (ddd, *J* = 6.6, 6.6, 15.3 Hz, 1H, OCH_2CH=), 5.32 (nfom, 1H, OCH_2CH=C*H*), 4.29 (s, 2H, OCH_2C≡), 4.03 (dd, *J* = 1.3, 6.6 Hz, 2H, =$CHCH_2O$), 2.41 (d, *J* = 5.7 Hz, 1H, O*H*), 1.43 (nfom, 1H, C*H*CH=$CHCH_2$), 0.74 (nfom, 2H, cyclopropyl-CH_2), 0.42 (nfom, 2H, cyclopropyl-CH_2), and 0.20 (s, 9H, $SiCH_3$).

LC / LR-MS [ES+APCI, 50:50 to 0:100 (%) H_2O:MeOH, 12 min run]: t_R 4.8 min; *m/z* 363 [$M+H^+$].

(*E*)-1-(2-(5-((3-Cyclopropylallyl)oxy)penta-1,3-diyn-1-yl)phenyl)-3-(trimethylsilyl)prop-2-yn-1-one (6120)

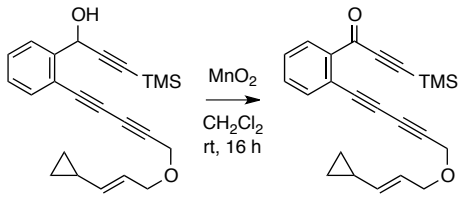

6119 ***6120***

[*PHW 9129*] MnO_2 (162 mg, 1.86 mmol) was added to a stirred solution of triyne **6124** (27 mg, 0.075 mmol) in CH_2Cl_2 (300 μL) at room temperature. After 16 h the reaction mixture was filtered through a small column of SiO_2 (EtOAc eluent). The crude reaction mixture was sufficiently pure to give triynone **6120** (17 mg, 0.047 mmol, 63%).

^{1}H NMR (500 MHz, $CDCl_3$): δ 8.11 (dd, *J* = 1.6, 7.7 Hz, 1H, *H6*), 7.63 (dd, *J* = 1.5, 7.6 Hz, 1H, *H3*), 7.52 (ddd, *J* = 1.6, 7.6, 7.6 Hz, 1H, *H4*), 7.48 (ddd, *J* = 1.6, 7.6, 7.6 Hz, 1H, *H5*), 5.62

---

[206] Lee, S. I.; Park, S. Y.; Park, J. H.; Jung, I. G.; Choi, S. Y.; Chung, Y. K.; Lee, B. Y. Rhodium N-heterocyclic carbene-catalyzed [4+2] and [5+2] cycloaddition reactions. *J. Org. Chem.* **2006**, *71*, 91–96.

(ddd, J = 6.6, 6.6, 15.3 Hz, 1H, OCH_2CH=), 5.30 (dddd, J = 1.3, 1.3, 8.9, 15.3 Hz, 1H, OCH_2CH=C*H*), 4.29 (s, 2H, $OCH_2C\equiv$), 4.03 (dd, J = 1.3, 6.6 Hz, 2H, =$CHCH_2O$), 1.43 (nfom, 1H, C*H*CH=$CHCH_2$), 0.74 (nfom, 2H, cyclopropyl-CH_2), 0.41 (nfom, 2H, cyclopropyl-CH_2), and 0.31 (s, 9H, $SiCH_3$).

4-(Cyclopropylidenemethyl)-11-(trimethylsilyl)-3,4-dihydroindeno[1,2-*g*]isochromen-10(1*H*)-one (6121)

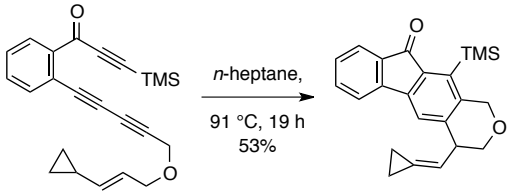

6120 ***6121***

[*PHW 9162*] A solution of triynone **6120** (15 mg, 0.042 mmol) in heptane (1 ml) was heated at 95 °C. After 20 h the reaction mixture was concentrated. The crude material contained **6121** (8 mg, 0.02 mmol, 53%) with sufficient purity to give the following data.

^{1}H NMR (500 MHz, $CDCl_3$): δ = 7.58, (ddd, J = 1.0, 1.0, 7.3 Hz, 1H C_{aryl}-*H9*), 7.48 (nfom, 1H, C_{aryl}-*H6*), 7.44 (nfom, 1H C_{aryl}-*H7*), 7.31 (d, J = 0.9 Hz, 1H, C_{aryl}-*H5*), 7.26 (nfom, 1H), 5.88 (dtt, J = 8.31, 2.0, 2.0 Hz, 1H), 4.93 (dd, J = 1.4, 15.2 Hz, 1H), 4.89 (dd, J = 1.5, 15.1 Hz, 1H), 4.00 (dd, J = 5.0, 10.8 Hz, 1H), 3.83 (nfom, 1H), 3.77 (dd, J = 6.7, 10.8 Hz, 1H), 1.26 (nfom, 1H), 0.88 (nfom, 1H), and 0.42 [s, $Si(CH_3)_3$].

GC-MS t_r = 13.63 min; m/z: 360, 345, 330, 315, 301, 287, and 275.

(*E*)-1-Chloro-4-(prop-2-yn-1-yloxy)but-2-ene (6123)

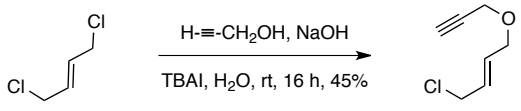

6122 ***6123***

[*PHW 9116*] Propargyl alcohol (1.2 mL, 21 mmol) was added dropwise to an aqueous (10 mL) solution of (*E*)-1,4-dichlorobut-2-ene (6.4 mL, 61 mmol), tetra-*n*-butylammonium iodide (74 mg, 0.20 mmol), and sodium hydroxide (800 mg, 20 mmol) at room temperature with stirring. After 16 h the reaction mixture was extracted with Et_2O. The combined organic layers were washed

with brine, dried ($MgSO_4$), and concentrated. Purification by distillation gave ether **6123** (1.36 g, 9.4 mmol, 45%) as a clear colorless oil.

^{1}H NMR (500 MHz, $CDCl_3$): δ 5.83-5.96 (m, 2H, *H*C=C*H*), 4.16 (d, *J* = 2.4 Hz, 2H, CH_2CCH), 4.06-4.11 (m, 4H, CH_2Cl and =CHCH_2O), and 2.48 (t, *J* = 2.4 Hz, 1H, CC*H*).

GC / LR EI-MS [5025015]: t_R 4.2min; *m/z* 109 [$M^{+\bullet}$–$Cl^{\bullet}$] and 95 [$M^{+\bullet}$–$CH_2Cl^{\bullet}$].

(*E*)-1-(2-(5-((4-Chlorobut-2-en-1-yl)oxy)penta-1,3-diyn-1-yl)phenyl)-3-(trimethylsilyl)prop-2-yn-1-ol (6124)

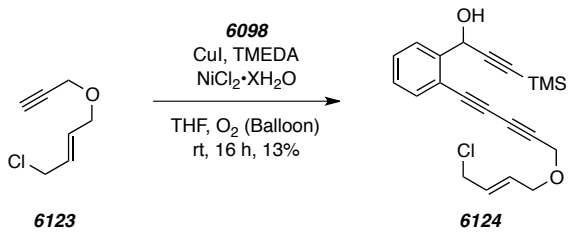

6123 ***6124***

[*PHW 9126*] CuI (8 mg, 0.42 mmol) was added to a stirred solution of diyne **6098**[156] (210 mg, 0.921 mmol), alkyne **6123** (688 mg, 4.78 mmol), TMEDA (35 μL, 0.24 mmol), and $NiCl_2$•XH_2O (6 mg) in THF (3.7 mL) at ambient temperature and under an O_2 atmosphere (via balloon). After 24 h the reaction mixture was diluted in satd. aq. NH_4Cl and extracted with EtOAc. The combined organic extracts were washed with brine, dried ($MgSO_4$), and concentrated. Purification by flash chromatography (hexanes:EtOAc 4:1) gave triyne **6124** (44 mg, 0.12 mmol, 13%).

^{1}H NMR (500 MHz, $CDCl_3$): δ 7.72 (dd, *J* = 1.2, 7.9 Hz, 1H, *H3*), 7.53 (dd, *J* = 1.3, 7.6 Hz, 1H, *H6*), 7.43 (ddd, *J* = 1.5, 7.7, 7.7 Hz, 1H, *H4or5*), 7.31 (ddd, *J* = 1.4, 7.6, 7.6 Hz, 1H, *H4or5*), 5.81-6.02 [m, 3H, C*H*(OH) and C*H*=C*H*], 4.33 (s, 2H, OCH_2C≡), 4.06-4.15 (m, 4H, CH_2Cl and =CHCH_2O), and 0.20 (s, 9H, SiCH_3).

^{13}C NMR (125 MHz, $CDCl_3$): δ 143.7, 133.9, 130.2, 130.0, 129.5, 128.5, 127.1, 120.2, 104.1, 92.1, 80.1, 78.5, 75.5, 71.1, 69.4, 63.5, 58.2, 44.3, and -0.05.

TLC: R_f 0.2 (4:1 Hex/EtOAc).

(*E*)-1-(2-(5-((4-chlorobut-2-en-1-yl)oxy)penta-1,3-diyn-1-yl)phenyl)-3-(trimethylsilyl)prop-2-yn-1-one (6125)

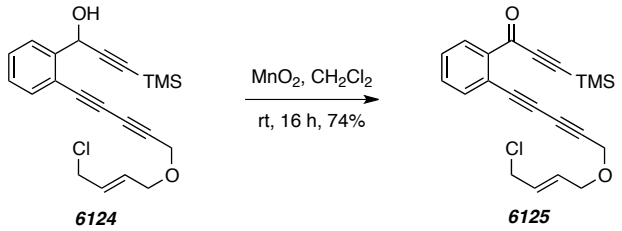

6124 ***6125***

[*PHW 9129*] MnO_2 (60 mg, 0.69 mmol) was added to a stirred solution of triyne **6124** (10 mg, 0.027 mmol) in CH_2Cl_2 (125 μL) at room temperature. After 15 h the reaction mixture was filtered through a small column of SiO_2 (EtOAc eluent). The crude reaction mixture was sufficiently pure to give triynone **12** (8 mg, 0.02 mmol, 74%).

^{1}H NMR (500 MHz, $CDCl_3$): δ 8.12 (dd, *J* = 1.6, 7.7 Hz, 1H, *H6*), 7.63 (dd, *J* = 1.5, 7.6 Hz, 1H, *H3*), 7.53 (ddd, *J* = 1.6, 7.5, 7.5 Hz, 1H, *H4*), 7.48 (ddd, *J* = 1.5, 7.6, 7.7 Hz, 1H, *H5*), 5.84-5.98 [m, 2H, C*H*=C*H*], 4.33 (s, 2H, OCH_2C≡), 4.13 (br dd, *J* = 1.1, 5.2 Hz, 2H, CH_2Cl or =CHCH_2O), 4.08 (br d, *J* = 6.6 Hz, 2H, CH_2Cl or =CHCH_2O), and 0.31 (s, 9H, SiCH_3).

TLC: R_f 0.3 (4:1 Hex/EtOAc).

(*E*)-4-(2-Chlorovinyl)-11-(trimethylsilyl)-3,4-dihydroindeno[1,2-*g*]isochromen-10(1*H*)-one (*E*-6126) and (*Z*)-4-(2-chlorovinyl)-11-(trimethylsilyl)-3,4-dihydroindeno[1,2-*g*]isochromen-10(1*H*)-one (*Z*-6126)

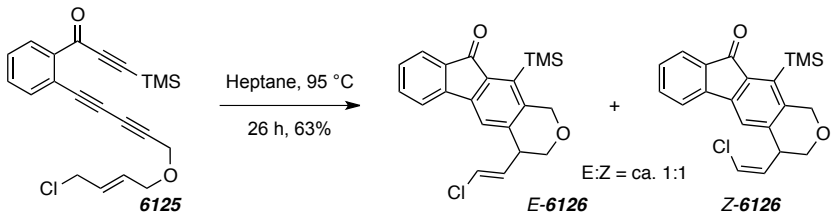

6125 ***E-6126*** ***Z-6126***

[*PHW 9131*] A solution of triynone **6125** (8 mg, 0.02 mmol) in heptane (1 mL) was heated at 95 °C. After 26 h the reaction mixture was concentrated. Purification by flash chromatography (9:1 hexanes:EtOAc) gave a mixture of *E*-**6126** and *Z*-**6126** (5 mg, 0.01 mmol, 63%). Analytical samples for both *E*-**6126** and *Z*-**6126** were prepared by separating the mixture of products with MPLC (39:1 hexanes:EtOAc).

[Data for *E*-**6126**]

^{1}H NMR (500 MHz, $CDCl_3$): δ = 7.30 (ddd, *J* = 0.9, 0.9, 7.4 Hz, 1H), 7.50 (nfom, 1H), 7.47 (nfom, 1H), 7.30 (s, 1H), 7.29 (nfom, 1H), 6.24 (d, *J* = 13.3 Hz, 1H), 6.05 (dd, 9.2, *J* = 13.3 Hz, 1H), 4.93 (d, *J* = 15.6 Hz, 1H), 4.86 (dd, *J* =0.7, 15.6 Hz, 1H), 3.96 (dd, *J* = 4.8, 11.1 Hz, 1H), 3.77 (dd, *J* = 5.6, 11.2 Hz, 1H), 3.62 (nfom, 1H), and 0.42 [s, $Si(CH_3)_3$].

GC-MS t_r = 13.48 min; m/z: 368, 353, 287, 257, 228, 202, 136, and 73.

[Data for *Z*-**6126]**

^{1}H NMR (500 MHz, $CDCl_3$): δ = 7.59 (ddd, *J* = 1.0, 1.0, 7.3 Hz, 1H), 7.48 (nfom, 1H), 7.46 (nfom, 1H), 7.35 (s, 1H), 7.28 (nfom), 6.29 (d, *J* = 7.1 Hz, 1H), 5.96 (dd, *J* = 7.1, 9.7 Hz, 1H), 4.94 (d, *J* = 15.3 Hz, 1H), 4.87 (d, *J* = 15.3 Hz, 1H), 4.25 (nfom, 1H), 4.00 (dd, *J* = 4.9, 11.3 Hz, 1H), 3.73 (dd, *J* = 5.5, 11.3 Hz, 1H), and 0.42 [s, $Si(CH_3)_3$].

GC-MS t_r = 13.52 min; m/z: 368, 353, 287, 257, 228, 202, 136, and 73.

1-(2-(5-(But-2-yn-1-yloxy)penta-1,3-diyn-1-yl)phenyl)-3-(trimethylsilyl)prop-2-yn-1-ol

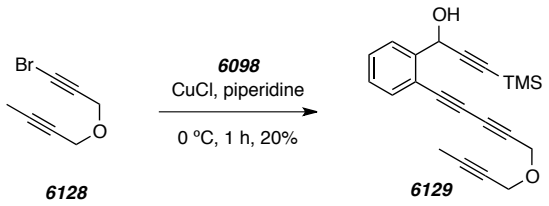

[*PHW X275*] Bromoalkyne **6128** (478 mg, 2.57 mmol) was added to a stirred solution of diyne **6098** (140 mg, 0.614) and CuCl (12 mg, 0.12 mmol) in piperidine (6.0 mL) at 0 ºC and under an inert atmosphere. After 1 h the reaction mixture was diluted in EtOAc and sequentially washed with sat. aq. NH_4Cl and brine. The organic extract was dried ($MgSO_4$) and concentrated. Purification by flash chromatography (4:1 hexanes:EtOAc) gave triyne **6129** (34 mg, 0.099 mmol, 16%).

^{1}H NMR (500 MHz, $CDCl_3$): δ 7.71 (dd, *J* = 1.3, 7.8 Hz, 1H, *H3*), 7.52 (dd, *J* = 1.5, 7.7 Hz, 1H, *H6*), 7.42 (ddd, *J* = 1.4, 7.7, 7.7 Hz, 1H, *H4or5*), 7.30 (ddd, *J* = 1.4, 7.6, 7.6 Hz, 1H, *H4or5*), 5.81 (s, 1H, C*H*(OH), 4.41 (s, 2H, $OCH_2C{\equiv}$), 4.25 (q, *J* = 2.4 Hz, 2H, $OCH_2C{\equiv}CCH_3$), 1.88 (t, *J* = 2.3 Hz, 3H, $C{\equiv}CCH_3$), and 0.20 (s, 9H, $SiCH_3$).

LC / LR-MS [ES+APCI, 50:50 to 0:100 (%) H_2O:MeOH, 12 min run]: t_R 7.7 min; *m/z* 335 [$M+H^+$].

1-(2-(5-(But-2-yn-1-yloxy)penta-1,3-diyn-1-yl)phenyl)-3-(trimethylsilyl)prop-2-yn-1-one (6130)

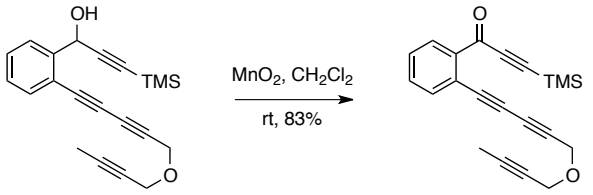

6129 ***6130***

[*PHW x281* and *x299*] MnO_2 (180 mg, 2.07 mmol) was added to a solution of alcohol **6129** (34 mg, 0.099 mmol) in CH_2Cl_2 (0.5 mL). After 16 h the reaction mixture was filtered through a plug of Celite® (EtOAc eluent) and concentrated to give the ketone **6130** (28 mg, 0.20 mmol, 83%).

^{1}H NMR (500 MHz, $CDCl_3$): δ 8.12 (dd, *J* = 1.3, 1.6 Hz, 1H, *H6*), 7.63 (dd, *J* = 1.3, 7.5 Hz, 1H, *H3*), 7.52 (br t, *J* = 1.5, 7.5 Hz, 1H, *H4*), 7.48 (dd, *J* = 1.4, 7.6 Hz, 1H, *H5*), 4.41 (s, 2H, $OCH_2C{\equiv}$), 4.25 (q, *J* = 2.3 Hz, 2H, $OCH_2C{\equiv}CCH_3$), 1.87 (t, *J* = 2.4 Hz, 3H, $C{\equiv}CCH_3$), and 0.31 (s, 9H, $SiCH_3$).

TLC: R_f 0.3 (9:1 Hex/EtOAc).

11-(Trimethylsilyl)-4-vinylidene-3,4-dihydroindeno[1,2-*g*]isochromen-10(1*H*)-one (6131)

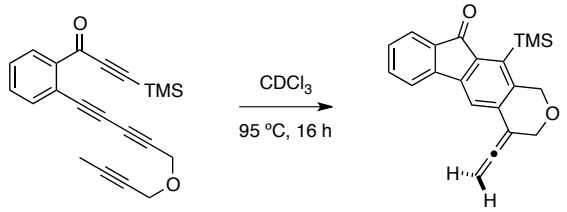

6130 ***6131***

[*PHW xi018*] A solution of triynone **6130** (9 mg, 0.027 mmol) in $CDCl_3$ (3 ml) was heated at 95 °C. After 16 h the reaction mixture was concentrated to a sufficiently pure sample of. Purification by MPLC (hexanes:EtOAc 4:1) gave allene **6131** (7 mg, 0.021, 78%).

^{1}H NMR (500 MHz, $CDCl_3$): δ 7.65 (s, 1H, C_{aryl}-*H5*), 7.60 (ddd, *J* = 1.0, 1.0, 7.3 Hz, 1H, C_{aryl}-*H9*), 7.52 (ddd, *J* = 0.9, 1.5, 7.4 Hz, 1H, C_{aryl}-*H6*), 7.47 (ddd, *J* = 1.2, 7.4, 7.4 Hz, 1H, C_{aryl}-*H7*), 7.28 (ddd, *J* = 1.1, 7.4, 7.4 Hz, 1H, *H8*), 5.34 (t, *J* = 3.0 Hz, 1H, $=CH_2$), 4.90 (s, $C_{aryl}CH_2$), 4.51 (t, *J* = 3.0 Hz, $=CCH_2O$), and 0.42 (s, 9H, $SiCH_3$).

1-(2-((5-Methyl-1,3-dihydroisobenzofuran-4-yl)ethynyl)phenyl)-3-(trimethylsilyl)prop-2-yn-1-one (6136)

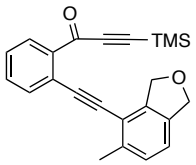

6136

^{1}H NMR (500 MHz, $CDCl_3$): δ 8.22 (dd, *J* = 1.5, 7.9 Hz, 1H, *H6*), 7.64 (dd, *J* = 1.4, 7.7 Hz, 1H, *H3*), 7.56 (ddd, *J* = 1.4, 7.5, 7.5 Hz, 1H, *H4*), 7.47 (ddd, *J* = 1.4, 7.6, 7.6 Hz, 1H, *H5*), 7.15 (d, *J* = 7.8 Hz, 1H, $CH_3C_{aryl}C_{aryl}HC_{aryl}H$), 7.10 (d, *J* = 7.7 Hz, 1H, $CH_3C_{aryl}C_{aryl}HC_{aryl}H$), 5.32 (dd, *J* = 2.2, 2.2 Hz, 2H, $OCH_2C_{aryl}C_{aryl}CC_2$), 5.14 (nfom, 2H, $OCH_2C_{aryl}C_{aryl}CH$), 2.60 (nfom, 3H, CCH_3), and 0.28 (s, 9H, $SiCH_3$).

(*E*)-4-((5-(2-(1-Hydroxy-3-(trimethylsilyl)prop-2-yn-1-yl)phenyl)penta-2,4-diyn-1-yl)oxy)but-2-en-1-ol (S6001)

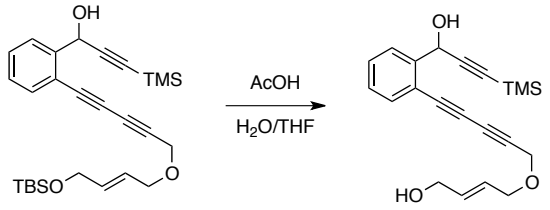

6114 ***S6001***

[*PHW x049*] Acetic acid (60 µL) was added to a stirred mixture of silyl ether **6114** (10 mg, 0.21 mmol), water (20 µL), and THF (20 µL) at rt. After 13 h, the reaction mixture was neutralized with sat. aq. K_2CO_3 and extracted with Et_2O (x6). The combined organic extracts were washed with brine, dried $MgSO_4$, and concentrated to give diol **S6001** (9 mg, 0.03 mmol, quant). The crude material was used without further purification.

^{1}H NMR (500 MHz, $CDCl_3$): δ 7.72 (dd, *J* = 1.2, 7.9 Hz, 1H, *H3*), 7.53 (dd, *J* = 1.4, 7.7 Hz, 1H, *H6*), 7.43 (ddd, *J* = 1.5, 7.7, 7.7 Hz, 1H, *H4or5*), 7.31 (ddd, *J* = 1.4, 7.6, 7.6 Hz, 1H, *H4or5*), 5.97 (ddddd, *J* = 1.4, 1.4, 5.3, 5.3, 15.5 Hz, 1H, $=CHCH_2OH$), 5.84 (nfom, 1H COC=C*H*), 5.82 (s, 1H, C*H*OH), 4.33 (s, 2H, $OCH_2C{\equiv}$), 4.20 (nfom, 2H, $SiOCH_2C=$), 4.13 (nfom, 2H, $COCH_2C=$), 2.54 (br s, 1H, O*H*), 1.60 (br s, 1H, O*H*), and 0.20 [s, 9H, $SiCH_3)_3$].

(*E*)-4-((5-(2-(3-(Trimethylsilyl)propioloyl)phenyl)penta-2,4-diyn-1-yl)oxy)but-2-enal (6142)

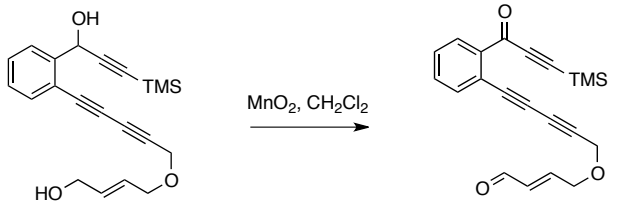

S6001 ***6142***

[*PHW X064*] MnO_2 (125 mg, 1.44 mmol) was added to a stirred solution of triyne **6114** (9 mg, 0.03 mmol) in CH_2Cl_2 (310 µL) at room temperature. After 16 h, the reaction mixture was filtered through a small column of SiO_2 (EtOAc eluent). The crude reaction mixture was sufficiently pure to give triynone **6115** (6 mg, 0.02 mmol, 60%).

^{1}H NMR (500 MHz, $CDCl_3$): δ 9.60 (d, *J* = 7.9 Hz, 1H C*H*O), 8.14 (br d, *J* = 8 Hz, 1H, *H6*), 7.63 (br d, *J* = 8 Hz, 1H, *H3*), 7.54 (br t, *J* = 7.5 Hz, 1H, *H4*), 7.50 (br d, *J* = 7.4 Hz, 1H, *H5*), 6.85 (ddd, *J* = 4.2, 4.2, 15.8 Hz, 1H , =C*H*CH_2O), 6.37 (dddd, *J* = 2, 2, 7.9, 15.8 Hz, 1H =C*H*CHO), 4.41 (s, 2H, OCH_2C≡), 4.39-4.41 (m, 2H, HOCH_2C=), and 0.31 [s, 9H, SiCH_3)$_3$].

7-(Trimethylsilyl)-3a,4-dihydroindeno[2,1-*h*]pyrano[3,4,5-*de*]chromen-8(6*H*)-one (6144)

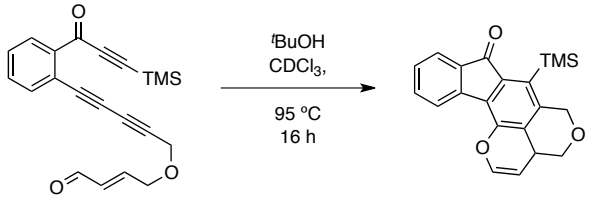

6142 ***6144***

[*PHW x065*] A $CDCl_3$ (2 mL) solution of triyne **6142** (5 mg, 0.015 mmol) and *t*-BuOH (100 µL, 1.0 mmol) was heated at 95 ºC. After 16 h, the reaction mixture was cooled and ^{1}H NMR spectral data were obtained. Several resonances suggested that **6144** was a product of the reaction mixture. Subsequent attempts at chromatographic purification failed, which suggests that **6144** is unstable to silica gel.

^{1}H NMR (500 MHz, $CDCl_3$): δ 7.82 (ddd, *J* = 1.6, 1.6, 7.4 Hz, 1H, *H9*), 7.43-7.65 (m, 3H, *H6*, *H7*, and *H8*), 6.76 (ddd, *J* = 3.0, 5.9 Hz, 1H, OC*H*=), 5.03 (br d, *J* = 15.6 Hz, 1H, $C_{Ar}CH_aH_bO$), 4.96 (dd, *J* = 1.9, 5.9 Hz, 1H, OCH=C*H*), 4.89 (dd, *J* = 1.7, 15.2 Hz,

$C_{Ar}CH_aH_bO$), 4.31 (dd, *J* = 6.7, 6.7 Hz, OCH_aH_bCH),4.14 (dd, *J* = 5.4, 10.0 Hz, OCH_aH_bCH), 3.66 (nfom, 1H, $CHCH_2O$), and 0.40 (s, 9H, $SiCH_3$).

LC / LR-MS [ES+APCI, 50:50 to 0:100 (%) H_2O:MeOH, 12 min run]: t_R 3.9 min; *m/z* 347 [M–H^+] and 364 [M+16].

(2-(Bromoethynyl)cyclopropane-1,1-diyl)dibenzene (6146)

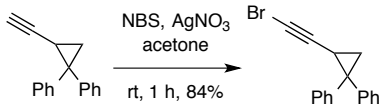

6145 ***6146***

[*SSH 1145*] Powdered $AgNO_3$ (17 mg, 0.10 mmol) was added to a stirred solution of known enyne **6145**[207] (218 mg, 1.00 mmol) and NBS (196 mg, 1.10 mmol) in acetone (17 mL) at rt. After 1 h the slurry was either partitioned between Et_2O and water, further extracted with Et_2O, washed with brine, dried ($MgSO_4$), and concentrated. The crude sample of bromoalkyne **6145** (250 mg, 0.84 mmol, 84%) was sufficiently pure for subsequent experiments.

^{1}H NMR (500 MHz, $CDCl_3$): δ 7.40 (br d, *J* = 8 Hz, 2H, $C_{aryl}H$), 7.32 (br t, *J* = 7.8 Hz, 2H, $C_{aryl}H$), 7.22-7.28 (m, 5H, $C_{aryl}H$), 7.17 (nfom, 1H, $C_{aryl}H$), 2.15 (dd, *J* = 5.9, 9.0 Hz, 1H, ≡C*CH*), 1.69 (dd, *J* = 4.8, 5.9 Hz, 1H, ≡CCHCH_aH_b), and 1.64 (dd, *J* = 4.7, 8.9 Hz, 1H, ≡CCHCH_aH_b).

GC / LR EI-MS [50325015]: t_R 9.79 min; *m/z* 298 [M(^{81}Br)$^{+\bullet}$] and 296 [M(^{79}Br)$^{+\bullet}$].

1-(2-((2,2-Diphenylcyclopropyl)buta-1,3-diyn-1-yl)phenyl)-3-(trimethylsilyl)prop-2-yn-1-ol (6147)

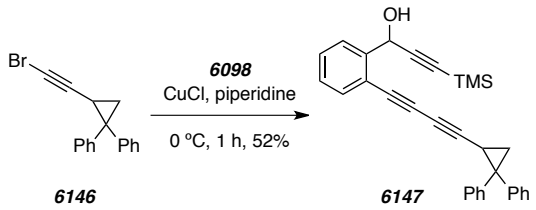

6146 ***6147***

---

[207] Schmittel, M.; Mahajan, A. A.; Bucher, G.; Bats, J. W. Thermal C^2–C^6 cyclization of enyne–allenes. Experimental evidence for a stepwise mechanism and for an unusual thermal silyl shift. *J. Org. Chem.* **2007**, *72*, 2166–2173.

[*SSH 1142* and *1151*] Bromoalkyne **6146** (100 mg, 0.337 mmol) was added to a stirred solution of diyne **6098** (77 mg, 0.337) and CuCl (1 mg, 0.01 mmol) in piperidine (0.7 mL) at 0 ºC and under an inert atmosphere. After 1 h the reaction mixture was diluted in EtOAc and sequentially washed with sat. aq. NH_4Cl and brine. The organic extract was dried ($MgSO_4$) and concentrated. Purification by flash chromatography (9:1 hexanes:EtOAc) gave triyne **6147** (79 mg, 0.18 mmol, 53%).

^{1}H NMR [500 MHz, $CDCl_3$, diastereomer 1(*):diastereomer 2(^)]: δ 7.67 (ddd, *J* = 1.5, 1.6, 7.8 Hz, 1H, *H3*), 7.41-7.45 (m, 3H, $C_{aryl}H$), 7.33-7.38 (m, 3H, $C_{aryl}H$), 7.23-7.29 (m, 7H, $C_{aryl}H$), 7.19 (nfom, 1H, $C_{aryl}H$), 5.74 (d, *J* = 5.6 Hz, 1H, O*H*), 2.39* (dd, *J* = 4.7, 5.7 Hz, 1H, ≡CC*H*), 2.33^ (dd, *J* = 5.9, 8.9 Hz, 1H, ≡CC*H*), 1.80 (nfom, 2H, ≡CCHCH_2), and 0.19 (s, 9H, SiCH_3).

^{13}C NMR (125 MHz, $CDCl_3$): δ 144.3, 143.4, 140.3, 133.6, 130.1, 129.4, 128.6, 128.42, 128.36, 128.0, 127.2, 127.0, 126.8, 120.7, 104.1, 91.8, 85.7, 79.8, 72.6, 66.3, 63.41, 63.39, 39.3, 23.8, 16.9, and -0.05.

LC / LR-MS [ES+APCI, 50:50 to 0:100 (%) H_2O:MeOH, 12 min run]: t_R 5.19 min; *m/z* 445 [M+H$^+$], 462 [M+NH_4^+], and 467 [M+Na$^+$].

TLC: R_f 0.3 (9:1 Hex/EtOAc).

1-(2-((2,2-Diphenylcyclopropyl)buta-1,3-diyn-1-yl)phenyl)-3-(trimethylsilyl)prop-2-yn-1-one (6148)

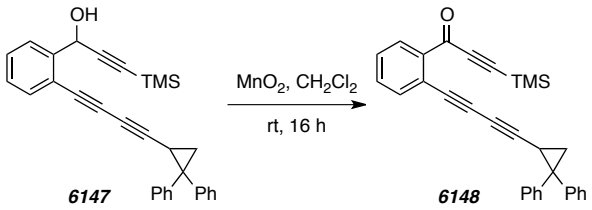

[*SSH 1144*] MnO_2 (85 mg, 0.98 mmol) was added to a stirred solution of triyne **6147** (17 mg, 0.038 mmol) in CH_2Cl_2 (0.1 mL) at room temperature. After 36 h the reaction mixture was filtered through a small column of SiO_2 (EtOAc eluent). The crude reaction mixture was sufficiently pure to give triynone **6148** (17 mg, 0.39, quant).

^{1}H NMR (500 MHz, $CDCl_3$): δ 8.05 (dd, *J* = 1.3, 7.7 Hz, 1H, *H6*), 7.53 (dd, *J* = 1.3, 7.7 Hz, 1H, *H3*), 7.46 (ddd, *J* = 1.5, 7.5, 7.5 Hz, *H4*), 7.41-7.54 (m, 3H, $C_{aryl}H$), 7.41 (ddd, *J* = 1.4, 7.5, 7.5 Hz, 1H, *H5*), 7.23-7.29 (m, 6H, $C_{aryl}H$), 7.18 (nfom, 1H, $C_{aryl}H$), 2.33 (dd, *J* = 6.1, 8.8 Hz,

1H, ≡CC*H*), 1.80 (ap q, *J* = 4.7 Hz, 1H, ≡CCHC$H_a$$H_b$), 1.78 (dd, *J* = 6.4 Hz, 1H, ≡CCHC$H_a$$H_b$), and 0.29 (s, 9H, SiC$H_3$).

TLC: R_f 0.2 (9:1 Hex/EtOAc).

(1*S*,3a*R*,3b*R*,4a*S*)-3b-Phenyl-5-(trimethylsilyl)-4,4a-dihydro-1*H*-1,3a-ethenocyclopropa[2,3]indeno[1,7-*bc*]fluoren-6(3b*H*)-one (6152)

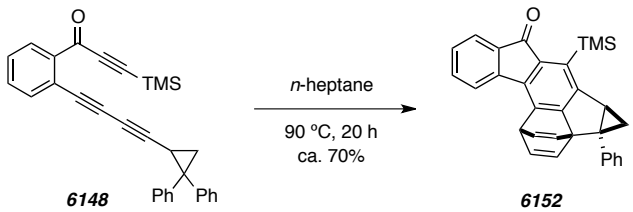

[*SSH-1146*] A solution of triynone **6148** (17 mg, 0.038 mmol) in heptane (8 ml) was heated at 95 °C. After 20 h the reaction mixture was concentrated to a sufficiently pure sample of **6152** (12 mg, 0.27, 70%).

^{1}H NMR (500 MHz, $CDCl_3$): δ = 7.74 (d, *J* = 7.5 Hz, 1H), 7.57 (d, *J* = 7.4 Hz, 1H), 4.45 (nfom, 3H), 7.39 (nfom, 2H), 7.30 (dddd, *J* = 1.3, 1.3, 7.3, 7.3 Hz, 1H), 7.22 (dd, *J* = 7.4, 7.4 Hz, 1H), 7.06 (d, *J* = 6.6 Hz, 1H), 6.90 (dd, *J* = 5.8, 6.5 Hz, 1H), 6.73 (dd, *J* = 5.5, 6.8 Hz, 1H), 6.69 (dd, *J* = 1.4, 6.8 Hz, 1H), 5.50 (dddd, *J* = 1.5, 1.5, 5.5, 5.5 Hz, 1H), 3.20 (dd, *J* = 3.8, 8.3 Hz, 1H), 1.61 (dd, *J* = 4.7, 8.2 Hz, 1H), 1.10 (dd, *J* = 4.0, 4.5 Hz, 1H), and 0.45 [s, $Si(CH_3)_3$].

HRMS (ESI-TOF): Calcd for $C_{31}H_{26}NaOSi^+$ [M+Na^+] requires 465.1645; found 465.1875.

GC-MS t_r = 16.02 min; m/z: 442, 427, 401, 365, 324, 313, 265, 162, and 73.

TLC: R_f 0.4 (9:1 Hex/EtOAc).

3-(2,2-Diphenylcyclopropyl)-1-(2-ethynylphenyl)prop-2-yn-1-ol (6153)

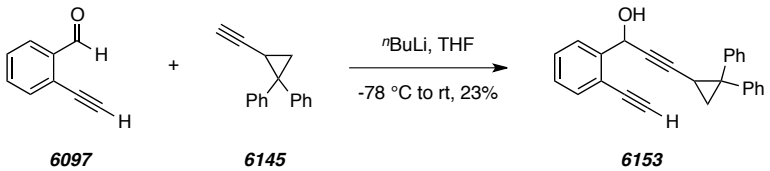

[*PHW x289*] *n*-BuLi (225 µL, 0.56 mmol, 2.5 M hexanes) was added to a stirred solution of alkyne **6145** (135 mg, 0.62 mmol) in THF (1.2 mL) at -78 ºC. After 1 h, a solution of aldehyde **6097** (73 mg, 0.56 mmol) in THF (570 µL) was added to the reaction mixture. After 2 h, the reaction mixture was warmed to room temperature and diluted in EtOAc and sequentially washed with sat. aq. NH_4Cl and brine. The organic extract was dried ($MgSO_4$) and concentrated. Purification by MPLC (4:1 hexanes:EtOAc) gave alcohol **6153** (46 mg, 0.13 mmol, 23%) as a mixture of diastereomers.

^{1}H NMR [500 MHz, $CDCl_3$ diastereomer1(*):diastereomer2(^) = ~1.2:1]: δ 7.38-7.46 (m, 4H, $C_{aryl}H$), 7.14-7.32 (m, 9H, $C_{aryl}H$), 7.04-7.08* (m, 1H, $C_{aryl}H$), 6.95-6.99^ (m, 1H, $C_{aryl}H$), 5.72* (br s, 1H, C*H*OH), 5.70^ (br s, 1H, C*H*OH), 3.28* (s, 1H, ≡C*H*), 3.26^ (s, 1H, ≡C*H*), 2.33 (br s, 1H, O*H*), 2.23-2.29 (m, 1H, ≡CC*H*), 1.79* (dd, *J* = 4.7, 5.7 Hz, 1H, ≡CCHCH_aH_b), 1.71^ (dd, *J* = 4.8, 5.7 Hz, 1H, ≡CCHCH_aH_b), 1.65* (dd, *J* = 4.7, 9.0 Hz, 1H, ≡CCHCH_aH_b), and 1.63^ (dd, *J* = 4.7, 9.0 Hz, 1H, ≡CCHCH_aH_b).

LC / LR-MS [ES+APCI, 50:50 to 0:100 (%) H_2O:MeOH, 12 min run]: t_R 7.7 min; *m/z* 349 [$M+H^+$].

1-(2-(6-((*tert*-Butyldimethylsilyl)oxy)hexa-1,3-diyn-1-yl)phenyl)-3-(2,2-diphenylcyclopropyl)prop-2-yn-1-ol (6155)

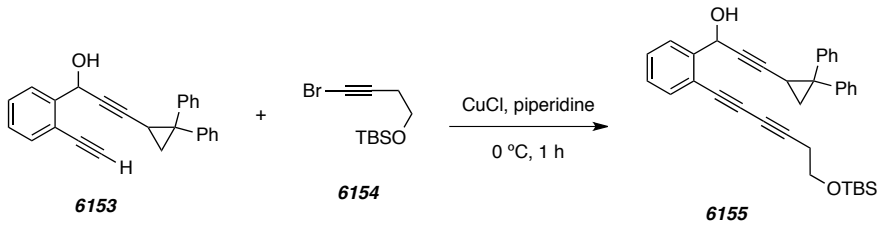

[*PHW x297*] Bromoalkyne **6154** (113 mg, 0.43 mmol) was added to a stirred solution of diyne **6153** (30 mg, 0.086) and CuCl (2 mg, 0.02 mmol) in piperidine (0.2 mL) at 0 ºC and under an inert atmosphere. After 1 h the reaction mixture was diluted in EtOAc and sequentially washed with sat. aq. NH_4Cl and brine. The organic extract was dried ($MgSO_4$) and concentrated. Purification by MPLC (4:1 hexanes:EtOAc) gave triyne **6155** (12 mg, 0.16 mmol, 26%).

^{1}H NMR [500 MHz, $CDCl_3$ diastereomer1(*):diastereomer2(^) = ~1.2:1]: δ 7.36-7.45 (m, 4H, $C_{aryl}H$), 7.14-7.31 (m, 9H, $C_{aryl}H$), 7.03-7.07* (m, 1H, $C_{aryl}H$), 6.94-6.97^ (m, 1H, $C_{aryl}H$), 5.65 (br s, 1H, C*H*OH), 3.79 (t, *J* = 7.0 Hz, 2H, OCH_2CH$_2$), 2.59 (t, *J* = 7.0 Hz, 2H, OCH$_2$CH_2), 2.22-2.29 (m, 1H, ≡CC*H*), 2.09 (br s, 1H, O*H*), 1.80* (dd, *J* = 4.8, 5.7 Hz, 1H, ≡CCHCH_aH$_b$), 1.71^ (dd, *J* = 4.8, 5.7 Hz, 1H, ≡CCHCH_aH$_b$), 1.65* (dd, *J* = 4.7, 9.0 Hz, 1H, ≡CCHCH$_a$$H_b$), 1.63^ (dd, *J* = 4.7, 9.0 Hz, 1H, ≡CCHCH$_a$$H_b$), 0.91 [s, 9H, C(C$H_3$)$_3$], and 0.09 [s, 6H, Si(C$H_3$)$_2$].

1-(2-(6-((*tert*-Butyldimethylsilyl)oxy)hexa-1,3-diyn-1-yl)phenyl)-3-(2,2-diphenylcyclopropyl)prop-2-yn-1-one (6156)

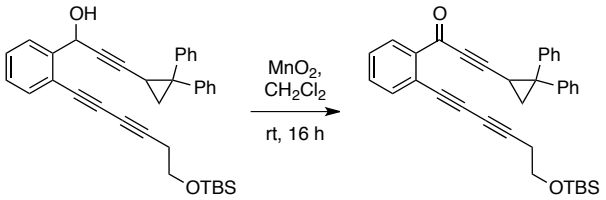

6155 ***6156***

[*PHW xi010*] MnO_2 (40 mg, 5.7 mmol) was added to a stirred solution of triyne **6155** (12 mg, 0.023 mmol) in CH_2Cl_2 (0.2 mL) at room temperature. After 16 h the reaction mixture was filtered through a small column of SiO_2 (EtOAc eluent). The crude reaction mixture was sufficiently pure to give triynone **6156** (9 mg, 0.017 mmol, 74%).

^{1}H NMR (500 MHz, $CDCl_3$): δ 7.45-7.51 (m, 3H, $C_{aryl}H$), 7.18-7.38 (m, 9H, $C_{aryl}H$), 7.06 (ddd, *J* = 1.1, 7.8, 7.8 Hz, 1H, $C_{aryl}H$), 6.96 (dd, *J* = 1.2, 7.9 Hz, 1H, $C_{aryl}H$), 3.77 (t, *J* = 7.2 Hz, 2H, OCH_2CH$_2$), 2.57 (t, *J* = 7.2 Hz, 2H, OCH$_2$CH_2), 2.47 (dd, *J* = 5.6, 9.0 Hz, 1H, ≡CC*H*), 2.00 (dd, *J* = 4.8, 5.6 Hz, 1H, ≡CCHCH_aH$_b$), 1.84 (dd, *J* = 4.8, 9.0 Hz, 1H, ≡CCHCH$_a$$H_b$), 0.90 [s, 9H, C(C$H_3$)$_3$], and 0.08 [s, 6H, Si(C$H_3$)$_2$].

^{13}C NMR (125 MHz, $CDCl_3$): δ 176.2, 143.8, 140.3, 139.0, 135.6, 132.3, 132.1, 130.3 (x2), 128.8 (x2), 128.7 (x2), 128.3, 128.1 (x2), 127.4, 127.1, 97.4, 83.7, 81.5, 79.7, 73.6, 66.8, 61.6, 40.5, 26.0 (x3), 24.3, 24.2, 18.5, 16.2, and -5.1 (x2).

1-(2-(6-((*tert*-Butyldimethylsilyl)oxy)hexa-1,3-diyn-1-yl)phenyl)but-2-yn-1-ol (S6002)

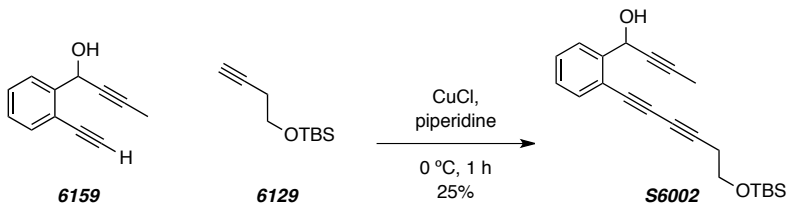

6159 ***6129*** ***S6002***

[*PHW 9143*] Bromoalkyne **6129** (206 mg, 0.786 mmol) was added to a stirred solution of diyne **6159** (110 mg, 0.647) and CuCl (5 mg, 0.05 mmol) in piperidine (1.3 mL) at 0 ºC and under an inert atmosphere. After 1 h the reaction mixture was diluted in EtOAc and sequentially washed with sat. aq. NH_4Cl and brine. The organic extract was dried ($MgSO_4$) and concentrated. Purification by MPLC (4:1 hexanes:EtOAc) gave triyne **S6002** (55 mg, 0.16 mmol, 25%).

^{1}H NMR (500 MHz, $CDCl_3$): δ 7.71 (dd, *J* = 1.4, 7.7 Hz, 1H, *H6*), 7.50 (dd, *J* = 1.5, 7.7 Hz, 1, *H3*), 7.39 (ddd, *J* = 1.5, 7.6, 7.6 Hz, 1H, *H4or5*), 7.27 (ddd, *J* = 1.4, 7.6, 7.6 Hz, 1H, *H4or5*), 5.82 (dq, *J* = 5.1, 2.2 Hz, 1H, C*H*OH), 3.80 (t, *J* = 7.0 Hz, 2H, CH_2OSi), 2.60 (t, *J* = 7.0 Hz, 2H, CH_2CH$_2$OSi), 1.91 (d, *J* = 2.3 Hz, 3H, ≡CCH_3), 0.92 [s, 9H, C(CH_3)$_3$], and 0.10 [s, 6H, Si(CH_3)$_2$].

LC / LR-MS [ES+APCI, 50:50 to 0:100 (%) H_2O:MeOH, 12 min run]: t_R 5.1 min; *m/z* 353 [M+H$^+$] and 370 [M+Na$^+$].

1-(2-(6-((*tert*-Butyldimethylsilyl)oxy)hexa-1,3-diyn-1-yl)phenyl)but-2-yn-1-one (6160)

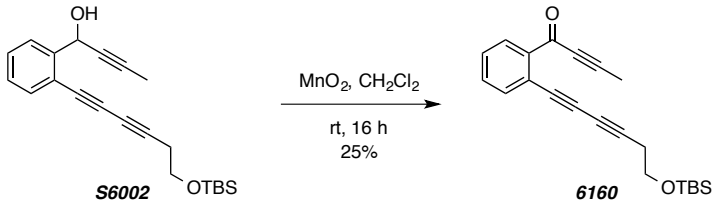

S6002 ***6160***

[*PHW 9145*] MnO_2 (300 mg, 3.4 mmol) was added to a stirred solution of triyne **S6002** (48 mg, 0.14 mmol) in CH_2Cl_2 (6.5 mL) at room temperature. After 16 h the reaction mixture was filtered through a small column of SiO_2 (EtOAc eluent). The crude reaction mixture was sufficiently pure to give triynone **6160** as a brown oil.

^{1}H NMR (500 MHz, $CDCl_3$): δ 8.10 (dd, *J* = 1.6, 7.8 Hz, 1H, *H6*), 7.60 (dd, *J* = 1.5, 7.7 Hz, 1H, *H3*), 7.48 (ddd, *J* = 1.5, 7.6, 7.6 Hz, 1H, *H4*), 7.43 (ddd, *J* = 1.5, 7.6, 7.6 Hz, 1H, *H5*), 3.79 (t,

J = 7.1 Hz, 2H, CH_2OSi), 2.59 (t, J = 7.1 Hz, 2H, CH_2CH$_2$OSi), 2.15 (s, 3H, ≡CCH_3), 0.91 [s, 9H, C(CH_3)$_3$], and 0.09 [s, 6H, Si(CH_3)$_2$].

1-(2-(Hepta-1,3-diyn-1-yl)phenyl)-3-(trimethylsilyl)prop-2-yn-1-ol (S6003)

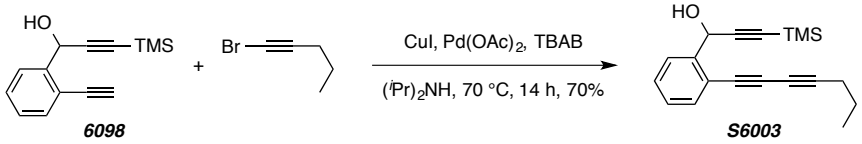

CuI (5 mg, 0.03 mmol) was added to a solution of 1-(2-ethynylphenyl)-3-(trimethylsilyl)prop-2-yn-1-ol[156] (**6098**, 1.52 g, 6.67 mmol), 1-bromopent-1-yne[208] (1.35 g, 9.35 mmol), TBAB (13 mg, 40 mmol), and diisopropylamine (67 mL) at 70 ºC under an inert atmosphere. Pd(OAc)$_2$ (2 mg, 0.009 mmol) was added after five minutes. After 14 h the reaction mixture was diluted in 2 M HCl and extracted with EtOAc. Purification by MPLC (hexanes:EtOAc 6:1) gave the triyne **S6003** (1.38 g, 4.69 mmol, 70%) as a clear yellow oil.

^{1}H NMR (500 MHz, $CDCl_3$): δ 7.69 (ddd, J = 0.5, 1.4, 7.8 Hz, 1H, *H6*), 7.50 (ddd, J = 0.5, 1.5, 7.7 Hz, 1H, *H3*), 7.39 (ddd, J = 1.4, 7.6, 7.6 Hz, 1H, *H4*), 7.28 (ddd, J = 1.3, 7.6, 7.6 Hz, 1H, *H5*), 5.83 (d, J = 5.7 Hz, 1H, C*H*OH), 2.48 (d, J = 5.7, 1H O*H*), 2.36 (t, J = 7.0 Hz, 2H, CH_2CH$_2$CH$_3$), 1.62 (sext, J = 7.3 Hz, 2H, CH_2CH$_3$), 1.04 (t, J = 7.4 Hz, 3H, CH$_2$CH_3), and 0.20 (s, 9H, SiCH_3).

^{13}C NMR (125 MHz, $CDCl_3$): δ 143.4, 133.7, 129.4, 128.4, 127.1, 120.9, 104.2, 91.9, 86.5, 79.9, 71.8, 65.2, 63.6, 21.9, 21.8, 13.7, and 0.0.

IR (neat): 3439, 2963, 2239, 2173, 1701, 1250, 1038, 985, 844, and 761 cm^{-1}.

HRMS (ESI-TOF): Calcd for $C_{19}H_{22}NaOSi^+$ [M+Na$^+$] requires 317.1332; found 317.1318.

TLC: R_f 0.3 (9:1 Hex/EtOAc).

1-(2-(Hepta-1,3-diyn-1-yl)phenyl)-3-(trimethylsilyl)prop-2-yn-1-one (6165)

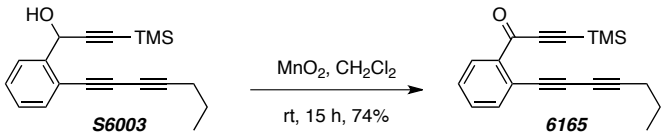

[208] Brandsma, L.; Verkruijsse, H. D. Practical and safe procedures for the preparation of the lower homologues of bromoacetylene. *Synthesis* **1990**, *11*, 984–985.

MnO_2 (1.79 g, 20.6 mmol) was added to a solution of alcohol **S6003** (611 mg, 2.08 mmol) in CH_2Cl_2 (10 mL) and the resulting suspension was vigorously stirred for 15 h. The reaction mixture was filtered through a plug of Celite® (EtOAc eluent) and concentrated to give the ketone **6165** (450 mg, 1.54 mmol, 74%) as a clear amber oil.

^{1}H NMR (500 MHz, $CDCl_3$): δ 8.07 (dd, *J* = 1.5, 7.8 Hz, 1H, *H6*), 7.61 (dd, *J* = 1.5, 7.7 Hz, 1H, *H3*), 7.49 (ddd, *J* = 1.5, 7.6, 7.6 Hz, 1H, *H4*), 7.43 (ddd, *J* = 1.5, 7.6, 7.6 Hz, 1H, *H5*), 2.36 (t, *J* = 7.0 Hz, 2H, C*H*$_2$CH$_2$CH$_3$), 1.61 (sext, *J* = 7.2 Hz, 2H, C*H*$_2$CH$_3$), 1.03 (t, *J* = 7.4 Hz, 3H, CH$_2$C*H*$_3$), and 0.31 (s, 9H, SiC*H*$_3$).

^{13}C NMR (125 MHz, $CDCl_3$): δ 176.7, 139.1, 135.7, 132.6, 131.8, 128.4, 122.3, 101.6, 101.5, 87.2, 80.9, 72.8, 65.8, 21.8 (x2), 13.7, and -0.6.

IR (neat): 2965, 2242, 2152, 1648, 1234, 1014, 847, and 756 cm^{-1}.

HRMS (ESI-TOF): Calcd for $C_{19}H_{20}NaOSi^+$ [M+Na$^+$] requires 315.1176; found 315.1192.

TLC: R_f 0.4 (9:1 Hex/EtOAc).

10-(Trimethylsilyl)-2,3-dihydrocyclopenta[*b*]fluoren-9(1*H*)-one (6166)

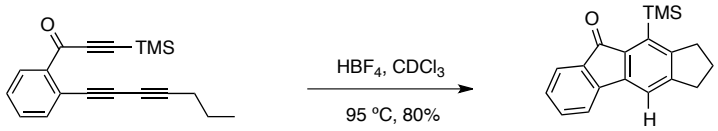

6165 ***6166***

[*PHW xi011*] A mixture of triyne **6165** (10 mg, 0.034 mmol) and HBF_4**.**Et_2O (100 μL, 0.74 mmol) in $CDCl_3$ (3.4 mL) was heated in a culture tube sealed with a Teflon®-lined cap. After 24 h, the reaction mixture was concentrated and the crude material was purified by flash chromatography (hexanes:EtOAc 9:1) to give indenone **6166** (8 mg, 0.03 mmol, 80%) as a yellow solid.

^{1}H NMR (500 MHz, $CDCl_3$): δ 7.55 (ddd, *J* = 1.1, 1.1, 7.3 Hz, 1H, *H9*), 7.40-7.44 (m, 2H, *H6andH7*), 7.38 (s, 1H, *H3*), 7.23 (nfom, 1H, *H7*), 3.00 (t, *J* = 7.5 Hz, 2H, C$_{aryl}$C*H*$_2$), 2.88 (t, *J* = 7.6 Hz, 2H, C$_{aryl}$C*H*$_2$), 2.06 (pentet, *J* = 7.5 Hz, CarylCH$_2$C*H*$_2$), and 0.40 (s, 9H, SiC*H*$_3$).

GC / LR EI-MS [5031022H]: t_R 7.35 min; *m/z* 292 [M$^{+\bullet}$], and 277 [M$^{+\bullet}$–CH$_3^\bullet$].

2-(2-(6-((*tert*-butyldimethylsilyl)oxy)hexa-1,3-diyn-1-yl)cyclohex-1-en-1-yl)-2-hydroxyacetonitrile (6174)

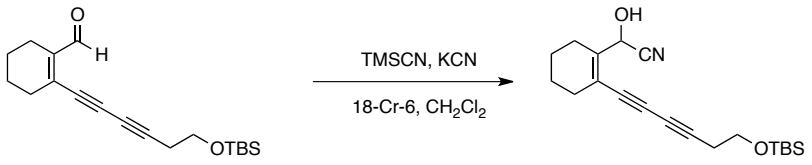

6046 ***6174***

[*PHW 9282*] TMSCN (90 µL, 0.72 mmol) was added to a stirred mixture of aldehyde **6046** (29 mg, 0.092 mmol), 18-crown-6 (ca. 2 mg), and KCN (ca. 2 mg) in CH_2Cl_2 at rt and under and inert atmosphere. After 12 h, additional TMSCN (90 µL, 0.72 mmol) was added due to poor conversion. After 24 h, the reaction mixture was washed with brine and concentrated. The residue was diluted in MeOH (500 µL) and citric acid (20 mg) was added. After 6 h, the reaction mixture was concentrated, diluted in Et_2O, and sequentially washed with H_2O and brine. The organic extract was concentrated to give crude alcohol **6174** (14 mg, 0.041, 45%).

^{1}H NMR (500 MHz, $CDCl_3$): δ 5.67 (s, 1H, C*H*CN), 3.77 (t, *J* = 6.9 Hz, 2H, SiOCH_2), 2.56 (t, *J* = 7.0 Hz, 2H, ≡CCH_2), 2.34 (nfom, 2H, =C-CH_2), 2.22 (nfom, 2H, =C-CH_2), 1.54-1.82 (nfom, 4H, $CH_2(CH_2)_2CH_2$), 0.90 [s, 9H, SiC(CH_3)$_3$], 0.18 [s, 9H, Si(CH_3)$_3$], and 0.08 [s, 6H, Si(CH_3)$_2$C].

GC / LR EI-MS (of the OTMS analogue) [5027016]: t_R 12.0 min; *m/z* 400 [$M^{+\bullet}$–$CH_3^{\bullet}$] and 358 [$M^{+\bullet}$–$C(CH_3)_3^{\bullet}$].

2-(6-((*tert*-Butyldimethylsilyl)oxy)hexa-1,3-diyn-1-yl)cyclohex-1-enecarbonyl Cyanide (6175)

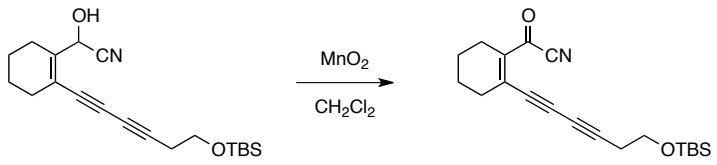

6174 ***6175***

[*PHW 9285*] MnO_2 (110 mg, 1.26 mmol) was added in two portions to a stirred solution of alcohol **6174** (14 mg, 0.041 mmol) in CH_2Cl_2 (0.2 mL) at 0 ºC. After 24 h the reaction mixture was filtered through Celite® (Et_2O eluent) and concentrated at 0 ºC to give acyl cyanide **6175**.

^{1}H NMR (500 MHz, $CDCl_3$): δ 3.78 (t, *J* = 6.9 Hz, 2H, SiOC*H*$_2$), 2.58 (t, *J* = 6.9 Hz, 2H, ≡CC*H*$_2$), 2.30-2.43 (m, 4H, =C-C*H*$_2$), 1.61-1.70 (m, 4H, $CH_2(CH_2)_2CH_2$), 0.90 [s, 9H, $SiC(CH_3)_3$], and 0.07 [s, 6H, $Si(CH_3)_2C$].

Ethyl 2-((9-Oxo-2-propyl-1-(trimethylsilyl)-9*H*-fluoren-3-yl)methyl)acrylate (7008-A) and Ethyl 2-((9-Oxo-2-propyl-1-(trimethylsilyl)-9*H*-fluoren-4-yl)methyl)acrylate (7008-B)

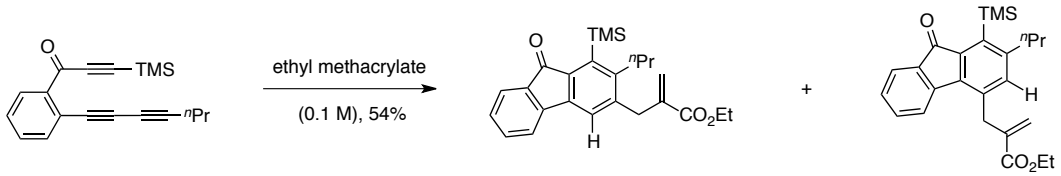

[*PHW x295* and *xi020*] A solution of triyne **7043** (20 mg, 0.068 mmol) and ethyl methacrylate (170 µL, 2.7 mmol) in $CDCl_3$ (7 mL) was heated to 85 ºC with stirring. After 14 h the reaction mixture was concentrated and the crude mixture was purified by MPLC (hexanes:EtOAc 4:1) to give a mixture of fluorenones **7008-A** and **7008-B** (15 mg, 0.037 mmol, 54%). An analytical sample of each regioisomer was obtained by partial separation via MPLC (hexanes:EtOAc 9:1) to give, in order of elution, **7008-B** and **7008-A**.

[Data for **7008-A**]

^{1}H NMR (500 MHz, $CDCl_3$): δ 7.56 (ddd, *J* = 0.9, 1.0, 7.3 Hz, 1H, C_{aryl}-*H9*), 7.43 (m, 2H, C_{aryl}-*H5* and -*H6*), 7.28 (s, 1H, C_{aryl}-H4), 7.26 (ddd, *J* = 1.5, 7.2, 7.2 Hz, 1H, *H8*), 6.31 (ap q, *J* = 1.3 Hz, 1H, =CH_aH$_b$), 5.35 (ap q, *J* = 1.4 Hz, 1H, =CH$_a$$H_b$), 4.26 (q, *J* = 7.1 Hz, 2H, $CO_2CH_2CH_3$), 3.70 (dd, *J* = 1.6, 1.6 Hz, 2H, $C_{aryl}CH_2C$=), 2.68 (br t, *J* = 8.5 Hz, 2H, $CH_2CH_2CH_3$), 1.47 (br sext, *J* = 7 Hz, 2H, CH_2CH_3), 1.32 (t, *J* = 7.1 Hz, 3H, $CO_2CH_2CH_3$), 0.98 (t, *J* = 7.3 Hz, CH_2CH_3), and 0.44 (s, 9H, $SiCH_3$).

GC / LR EI-MS [5031022H]: t_R 13.22 min; *m/z* 406 [$M^{+\bullet}$], 391 [$M^{+\bullet}$–$CH_3^\bullet$], and 363 [$M^{+\bullet}$–$CH_2CH_2CH_3^\bullet$].

TLC: R_f 0.3 (9:1 Hex/EtOAc).

[Data for **7008-B**]

^{1}H NMR (500 MHz, $CDCl_3$): δ 7.60 (br d, *J* = 7.2 Hz, 1H, C_{aryl}-*H9*), 7.39 (ddd, *J* = 1.1, 7.5, 7.5 Hz, 1H, C_{aryl}-*H6*), 7.34 (br d, *J* = 7.5 Hz, 1H, C_{aryl}-*H5*), 7.22 (br t, *J* = 7.3 Hz, 1H, *H8*), 6.96 (s, 1H, C_{aryl}-H4), 6.28 (ap q, *J* = 1.2 Hz, 1H, =CH_aH$_b$), 5.30 (ap q, *J* = 1.1 Hz, 1H, =CH$_a$$H_b$),

4.31 (q, J = 7.1 Hz, 2H, $CO_2CH_2CH_3$), 3.89 (ap t, J = 1.8 Hz, 2H, $C_{aryl}CH_2C$=), 2.71 (br t, J = 8.0 Hz, 2H, $CH_2CH_2CH_3$), 1.53 (br sext, J = 8 Hz, 2H, CH_2CH_3), 1.35 (t, J = 7.1 Hz, 3H, $CO_2CH_2CH_3$), 0.95 (t, J = 7.3 Hz, CH_2 CH_2CH_3), and 0.44 (s, 9H, $SiCH_3$).

GC / LR EI-MS [5031022H]: t_R 13.15 min; *m/z* 406 [$M^{+\bullet}$], 391 [$M^{+\bullet}$–$CH_3^{\bullet}$], and 363 [$M^{+\bullet}$–$CH_2CH_2CH_3^{\bullet}$].

TLC: R_f 0.3 (9:1 Hex/EtOAc).

3-(Trimethylsilyl)-1-(2-((trimethylsilyl)buta-1,3-diyn-1-yl)phenyl)prop-2-yn-1-ol (S7001)

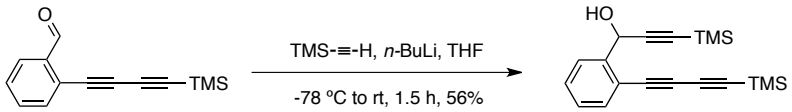

S7001

[*PHW 9146*] *n*-BuLi (370 µL, 2.5 M in hexanes, 0.93 mmol) was added to a stirred solution of ethynyltrimethylsilane (160 µL, 1.1 mmol) in THF (1.1 mL) at -78 ºC. After 1 h a solution of 2-[(trimethylsilyl)buta-1,3-diyn-1-yl]benzaldehyde[146] (122 mg, 0.54 mmol) in THF (550 µL) was added and the reaction mixture was allowed to warm to rt. After 30 min satd. aq. NH_4Cl was added and the mixture was extracted with EtOAc. The combined organic extracts were washed with brine, dried ($MgSO_4$), and concentrated. Purification by flash chromatography (hexanes:EtOAc 9:1) gave triynol **S7002** (98 mg, 0.30 mmol, 56%).

^{1}H NMR (500 MHz, $CDCl_3$): δ 7.69 (dd, J = 1.3, 7.8 Hz, 1H, *H6*), 7.52 (dd, J = 1.5, 7.7 Hz, 1H, *H3*), 7.41 (ddd, J = 1.4, 7.6, 7.6 1H, *H4*), 7.30 (ddd, J = 1.4, 7.6, 7.6 Hz, 1H, *H5*), 5.81 (d, J = 5.6 Hz, 1H, C*H*OH), 2.42 (d, J = 5.8, 1H O*H*), 0.24 (s, 9H, $SiCH_3$), and 0.20 (s, 9H, $SiCH_3$).

GC / LR EI-MS [5031022H]: t_R 10.3 min; *m/z* 324 [$M^{+\bullet}$], 309 [$M^{+\bullet}$–$CH_3^{\bullet}$], and 251 [$M^{+\bullet}$–$Si(CH_3)_3^{\bullet}$].

TLC: R_f 0.3 (9:1 Hex/EtOAc).

3-(Trimethylsilyl)-1-(2-((trimethylsilyl)buta-1,3-diyn-1-yl)phenyl)prop-2-yn-1-one (S7002)

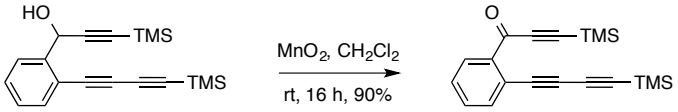

S7001 ***S7002***

[*PHW 9149*] MnO_2 (625 mg, 7.18 mmol) was added to a solution of alcohol **S7001** (93 mg, 0.29 mmol) in CH_2Cl_2 (1.5 mL). After 16 h the reaction mixture was filtered through a plug of Celite® (EtOAc eluent) and concentrated to give the ketone **S7002** (85 mg, 0.26 mmol, 90%) as a clear amber oil.

^{1}H NMR (500 MHz, $CDCl_3$): δ 8.07 (dd, *J* = 1.6, 7.7 Hz, 1H, *H6*), 7.61 (dd, *J* = 1.5, 7.6 Hz, 1H, *H3*), 7.51 (ddd, *J* = 1.6, 7.6, 7.6 Hz, 1H, *H4*), 7.47 (ddd, *J* = 1.5, 7.6, 7.6 Hz, 1H, *H5*), 0.31 (s, 9H, SiC*H*$_3$), and 0.23 (s, 9H, SiC*H*$_3$).

9-Oxo-1,2-bis(trimethylsilyl)-9*H*-fluorene-3-carbonitrile (7009)

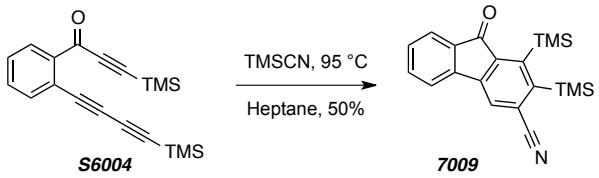

[*PHW 9180*] A solution of triyne **S6004** (16.7 mg, 0.052 mmol) and TMSCN (340 µL, 2.7 mmol) in heptane (2.0 mL) was heated to 95 ºC with stirring. After 96 h the reaction mixture was concentrated and the crude mixture was purified by MPLC (19:1 hexanes:EtOAc) to give fluorenone **7009** (9 mg, 0.03 mmol, 50%).

^{1}H NMR (500 MHz, $CDCl_3$): δ = 7.72 (s, 1H), 7.66 (ddd, *J* = 1.0, 1.0, 7.4 Hz, 1H), 7.55 (nfom, 1H), 7.54 (nfom, 1H) 7.37, (nfom), 0.54 [s, $Si(CH_3)_3$], and 0.42 [s, $Si(CH_3)_3$].

^{13}C NMR (125 MHz, $CDCl_3$): δ = 195.0, 157.4, 153.9, 143.3, 143.0, 142.6, 135.3, 133.6, 130.3, 124.6, 124.4, 123.3, 120.8, 120.3, 2.8, and 2.4.

GC-MS t_r = 12.3 min; 349, 334, 318, 276, 260, 159, and 73.

1-(2-(Penta-1,3-diyn-1-yl)phenyl)-3-(trimethylsilyl)prop-2-yn-1-ol (7020)

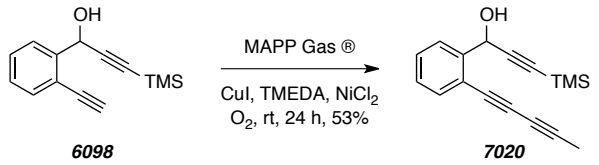

MAPP Gas® was bubbled through THF (50 mL) for 1 h at 0 °C to give a 1.4 M solution of propyne in THF as determined by integrations (solvent vs. $CH_3C{\equiv}CH$, propene, allene, and

propane were also present) of the No-D ^{1}H NMR spectrum[209]. **6098**[156] (433 mg, 1.90 mmol), TMEDA (70 μL, 0.47 mmol), $NiCl_2$ (32 mg, 0.25 mmol), and CuI (41 mg, 0.22 mmol) were added to the propyne/THF solution (14 mL). An oxygen balloon was introduced through a septum and the reaction mixture was allowed to warm to room temperature with stirring. After 24 h the reaction mixture was diluted in satd. aq. NH_4Cl and extracted with EtOAc. The combined organic extracts were washed with brine, dried ($MgSO_4$), and concentrated. Purification by flash chromatography (hexanes:EtOAc 6:1) gave triyne **7020** as an orange-yellow oil (266 mg, 1.00 mmol, 53%).

^{1}H NMR (500 MHz, $CDCl_3$): δ 7.69 (dd, *J* = 1.5, 7.8 Hz, 1H, *H6*), 7.50 (dd, *J* = 1.5, 7.7 Hz, 1, *H3*), 7.39 (ddd, *J* = 1.4, 7.6, 7.6 Hz, 1H, *H4or5*), 7.28 (ddd, *J* = 1.4, 7.6, 7.6 Hz, 1H, *H4or5*), 5.82 (d, *J* = 5.7 Hz, 1H, ArC*H*OH), 2.45 (d, *J* = 5.7 Hz, 1H, O*H*), 2.04 (s, 3H, CC*H*$_3$), and 0.20 [s, 9H, Si(C*H*$_3$)$_3$].

^{13}C NMR (125 MHz, $CDCl_3$): δ 143.5, 133.7, 129.5, 128.4, 127.1, 120.8, 104.2, 91.9, 82.1, 79.9, 71.3, 64.4, 63.5, 4.8, and -0.1.

IR (neat): 3406, 2960, 2242, 2173, 1482, 1449, 1250, 1037, 983, 846, and 761 cm^{-1}.

HR ESI-MS: $C_{17}H_{18}NaOSi^+$ [M+Na^+] requires 289.1019; found 289.1013.

TLC: R_f 0.5 (4:1 Hex/EtOAc).

1-(2-(Penta-1,3-diyn-1-yl)phenyl)-3-(trimethylsilyl)prop-2-yn-1-one (7021)

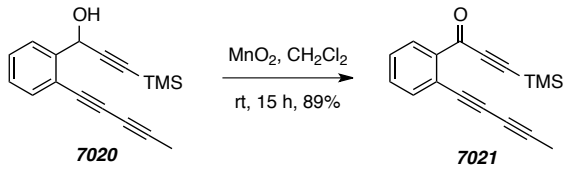

MnO_2 (2.21 g, 25 mmol) was added to a stirred solution of triyne **7020** (247 mg, 0.93 mmol) in CH_2Cl_2 (2.5 mL) at room temperature. After 15 h the reaction mixture was filtered through a small column of SiO_2 (EtOAc eluent). The crude reaction mixture was sufficiently pure to give triynone **7021** (220 mg, 0.83 mmol, 89%) as a brown oil.

---

[209] Hoye, T. R.; Aspaas, A. W.; Eklov, B. M.; Ryba, T. D. Reaction titration: A convenient method for titering reactive hydride agents (Red-Al, $LiAlH_4$, DIBALH, L-Selectride, NaH, and KH) by no-D NMR spectroscopy. *Org. Lett.* **2005**, *7*, 2205–2208.

^{1}H NMR (500 MHz, $CDCl_3$): δ = 8.08 (dd, *J* = 1.6, 7.8 Hz,1H, *H6*), 7.60 (dd, *J* = 1.5, 7.7 Hz, 1H, *H3*), 7.49 (ddd, *J* = 1.5, 7.5, 7.5 Hz, 1H, *H4*), 7.44 (ddd, *J* = 1.5, 7.6, 7.6 Hz, 1H, *H5*), 2.04 (s, 3H, C*H*$_3$), and 0.31 [s, 9H, Si(C*H*$_3$)$_3$].

^{13}C NMR (125 MHz, $CDCl_3$): δ = 176.6, 139.2, 135.7, 132.6, 131.8, 128.5, 122.2, 101.6, 101.5, 82.9, 80.9, 72.3, 65.0, 4.9, and -0.5.

IR (neat): 2961, 2246, 2152, 1648, 1480, 1235, 1014, 850, and 757 cm^{-1}.

HR ESI-MS: $C_{17}H_{16}NaOSi^+$ [M+Na^+] requires 287.0863; found 287.0866.

TLC: R_f 0.4 (9:1 Hex/EtOAc).

2-Methyl-1-(trimethylsilyl)-9*H*-fluoren-9-one (7023)

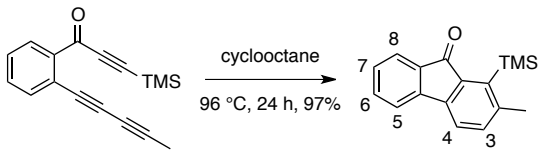

7021 ***7023***

A solution of triyne **7021** (38 mg, 0.144 mmol) in cyclooctane (14 mL) was heated at 96 ºC in a culture tube fitted with an inert, Teflon®-lined cap. After 24 h the reaction mixture was loaded onto a bed of silica gel and washed sequentially with hexanes, to remove the excess cyclooctane, and ethyl acetate. The ethyl acetate fraction was concentrated and purified by flash chromatography (hexanes:EtOAc 19:1) to give fluorenone **7023** (37 mg, 0.139 mmol, 97%) as a yellow solid.

^{1}H NMR (500 MHz, $CDCl_3$): δ 7.57 (ddd, *J* = 1.1, 1.0, 7.3 Hz, 1H, *H8*), 7.44 (m, 2H, *H5* and *H6*), 7.39 (d, *J* = 7.6 Hz, 1H, *H4*), 7.24 (nfom, 1H, *H7*), 7.19 (ddd, *J* = 0.8, 1.5, 7.6 Hz, 1H, *H3*), 2.47 (s, 3H, C*H*$_3$), and 0.42 [s, 9H, Si(C*H*$_3$)$_3$].

^{13}C NMR (125 MHz, $CDCl_3$): δ 195.6, 145.3, 144.2, 143.0, 141.4, 140.3, 135.7, 134.6, 134.0, 128.6, 124.0, 120.8, 119.5, 25.3, and 2.6.

IR (neat): 2946, 1714, 1606, 1249, 862, 843, and 763 cm^{-1}.

HR ESI-MS: $C_{17}H_{18}NaOSi^+$ [M+Na^+] requires 289.1019; found 289.1047.

TLC: R_f 0.5 (9:1 Hex/EtOAc).

MP: 65–69 ºC.

2-(Hepta-1,3-diyn-1-yl)cyclohex-1-enecarbaldehyde (7031)

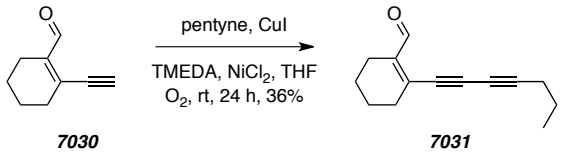

CuI (5 mg, 0.03 mmol) was added to a stirred solution of **7030**[210] (82 mg, 0.61 mmol), pentyne (1.0 mL, 10 mmol), TMEDA (20 µL, 0.13 mmol), and $NiCl_2$ (5 mg, 0.04 mmol) in THF solution (2 mL) at room temperature. An oxygen balloon was attached through a septum. After 24 h the reaction mixture was diluted in satd. aq. NH_4Cl and extracted with EtOAc. The combined organic extracts were washed with brine, dried ($MgSO_4$), and concentrated. Purification by MPLC (hexanes:EtOAc 19:1) gave the sample of diyne **7031** as a clear brown oil (43 mg, 0.22 mmol, 36%).

^{1}H NMR (500 MHz, $CDCl_3$): δ 10.13 (s, 1H, C*H*O), 2.40 (m, 2H, =C-C*H*$_2$), 2.35 (t, *J* = 7.0 Hz, 2H, ≡CC*H*$_2$), 2.27 (m, 2H, =C-C*H*$_2$), 1.60-1.70 [m, 4H, $CH_2(CH_2)_2CH_2$], 1.61 (sext, *J* = 7.3 Hz, 2H, ≡CCH_2CH_2), and 1.02 [t, *J* = 7.4 Hz, 3H, C*H*$_3$].

^{13}C NMR (125 MHz, $CDCl_3$): δ 192.4, 146.1, 139.0, 88.7, 83.7, 71.5, 64.9, 32.3, 22.3, 22.0, 21.83, 21.79, 21.1, and 13.7.

IR (neat): 2933, 2869, 2229, 1742 w, 1677, and 1221 cm^{-1}.

HRMS (ESI-TOF): Calcd for $C_{14}H_{16}NaO^+$ [M+Na$^+$] requires 223.1093; found 223.1102.

TLC: R_f 0.4 (19:1 Hex/EtOAc).

1-(2-(Hepta-1,3-diyn-1-yl)cyclohex-1-en-1-yl)-3-(trimethylsilyl)prop-2-yn-1-ol (7032)

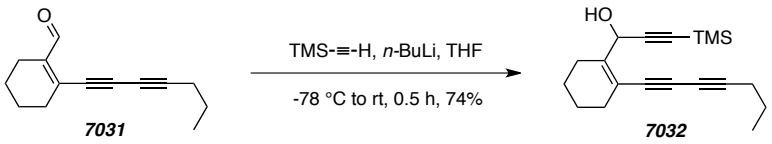

n-BuLi (130 µL, 2.5 M in hexanes, 0.33 mmol) was added to a stirred solution of ethynyltrimethylsilane (54 µL, 0.38 mmol) in THF (380 µL) at -78 ºC. After 1 h a solution of

---

[210]. Eberbach, W., Roser, J. Thermally initiated reaction of (*Z*)-epoxyhexenynes; a facile preparation of 3,4-annulated furans. *Tetrahedron* **1986**, *42*, 2221–2234.

aldehyde **7031** (38 mg, 0.19 mmol) in THF (200 μL) was added and the reaction mixture was allowed to warm to rt. After 30 min satd. aq. NH_4Cl was added and the mixture was extracted with EtOAc. The combined organic extracts were washed with brine, dried ($MgSO_4$), and concentrated. The crude product triynol **7032** (43 mg, 0.14 mmol, 74%) was a clear red oil and used directly in the next reaction.

^{1}H NMR (500 MHz, $CDCl_3$): δ 5.59 (s, 1H, C*H*OH), 2.32 (t, *J* = 7.0 Hz, 2H, ≡CC*H*$_2$), 2.33 (m, 2H, =C-C*H*$_2$), 2.19 (m, 2H, =C-C*H*$_2$), 1.94 (br s, 1H, O*H*), 1.55-1.75 (m, 4H, $CH_2(CH_2)_2CH_2$), 1.58 (sext, *J* = 7.2 Hz, 2H, ≡CCH_2CH_2), 1.01 [t, *J* = 7.4 Hz, 3H, C*H*$_3$], and 0.18 [s, 6H, $Si(CH_3)_2C$].

^{13}C NMR (125 MHz, $CDCl_3$): δ 146.3, 118.0, 104.1, 90.7, 85.7, 78.4, 73.4, 65.3, 64.7, 30.1, 23.7, 22.2, 22.0, 21.9, 21.7, 13.7, and 0.0.

IR (neat): 3440, 2934, 2235, 2170, 1250, 1028, and 845 cm^{-1}.

HRMS (ESI-TOF): Calcd for $C_{19}H_{26}NaOSi^+$ [M+Na^+] requires 321.1645; found: 321.1658.

TLC: R_f 0.4 (6:1 Hex/EtOAc).

1-(2-(Hepta-1,3-diyn-1-yl)cyclohex-1-en-1-yl)-3-(trimethylsilyl)prop-2-yn-1-one (7033)

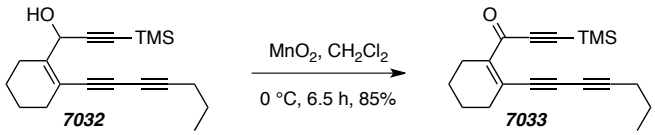

MnO_2 (160 mg, 1.84 mmol) was added to a stirred solution of alcohol **7032** (20 mg, 0.067 mmol) in CH_2Cl_2 (0.8 mL) at 0 ºC. After 6.5 h the reaction mixture was rapidly filtered through Celite® (Et_2O eluent) and concentrated (0 ºC bath) to give ketone **7033** (17 mg, 0.057 mmol, 85%) as a clear red oil. Because of the high reactivity of this ketone at ambient temperature this sample was characterized without further purification.

^{1}H NMR (500 MHz, $CDCl_3$): δ 2.41 [m, 4H, =C-(CH_2)$_2$], 2.34 (t, *J* = 7.0 Hz, 2H, ≡CC*H*$_2$), 1.63 (m, 4H, $CH_2(CH_2)_2CH_2$), 1.58 (sext, *J* = 7.2 Hz, 2H, ≡CCH_2CH_2), 1.00 [t, *J* = 7.4 Hz, 3H, C*H*$_3$], and 0.28 [s, 6H, $Si(CH_3)_2C$].

^{13}C NMR (125 MHz, $CDCl_3$): δ 177.4, 144.2, 131.9, 102.5, 101.4, 89.2, 85.7, 73.9, 66.1, 33.5, 25.6, 21.9, 21.8 (2x), 21.6, 13.7, and -0.5.

IR (neat): 2936, 2225, 2149, 1610, 1591, 1249, 861, and 846 cm^{-1}.

HRMS (ESI-TOF): Calcd for $C_{19}H_{24}NaOSi^+$ [M+Na^+] requires 319.1489; found 319.1474.

TLC: R_f 0.4 (9:1 Hex/EtOAc).

7-Propyl-8-(trimethylsilyl)-1,2,3,4-tetrahydro-fluoren-9-one (7034)

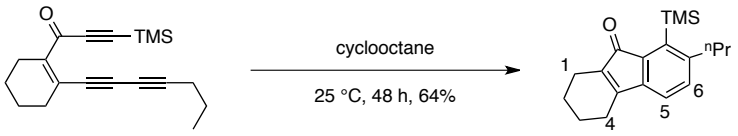

7033 ***7034***

A solution of triyne **S4** (17 mg, 0.057 mmol) in cyclooctane (6 mL) was heated at 25 ºC in a culture tube fitted with an inert, Teflon®-lined cap. After 24 h the reaction mixture was loaded onto a bed of silica gel and washed sequentially with hexanes, to remove the excess cyclooctane, and ethyl acetate. The ethyl acetate fraction was concentrated and purified by MPLC (hexanes:EtOAc 39:1) to give the indenone **7034** (11 mg, 0.037 mmol, 64%) as a clear amber oil.

^{1}H NMR (500 MHz, $CDCl_3$): δ 7.02 (d, *J* = 7.3 Hz, 1H, *H5*), 6.83 (d, *J* = 7.3 Hz, 1H, *H6*), 2.66 (br t, *J* = 8.0 Hz, 2H, ArCH_2), 2.38 (tt, *J* = 6.0, 2.7 Hz, 2H, *H1*$_2$), 2.19 (tt, *J* = 6.1, 2.7 Hz, 2H, *H4*$_2$), 1.79 (nfom, 2H, $CH_2(CH_2)_2CH_2$), 1.71 (nfom, 2H, $CH_2(CH_2)_2CH_2$), 1.49 (br sext, *J* = 7 Hz, 2H, CH_2CH_3), 0.94 (t, *J* = 7.3 Hz, 3H,CH_3), and 0.38 [s, 9H, $Si(CH_3)_3$].

^{13}C NMR (125 MHz, $CDCl_3$): δ 199.2, 157.0, 149.2, 143.4, 138.6, 138.4, 133.1, 132.7, 118.7, 39.0, 27.1, 22.6, 22.21, 22.20, 19.7, 13.9, and 2.5.

IR (neat): 2953, 2874, 1714, 1607, 1248, 968, 862, 849, and 769 cm^{-1}.

HRMS (ESI-TOF): Calcd for $C_{19}H_{26}NaOSi^+$ [M+Na^+] requires 321.1645; found: 321.1677.

TLC: R_f 0.5 (9:1 Hex/EtOAc).

2-Propyl-1-(trimethylsilyl)-9*H*-fluoren-9-one (7040)

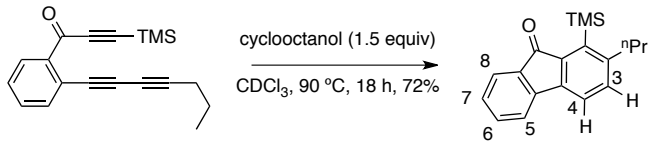

7043 ***7040***

A solution of triynone **7043** (22 mg, 0.075 mmol) in cyclooctanol (18 mg, 0.14 mmol) in $CDCl_3$ (7.5 mL) was heated at 90 ºC. After 18 h the mixture was concentrated and the crude material was purified by flash chromatography (hexanes:EtOAc 19:1) to give the fluorenone **7040** (16 mg, 0.054 mmol, 72%) as a golden yellow oil.

^{1}H NMR (500 MHz, $CDCl_3$): δ 7.56 (ddd, *J* = 1.0, 1.0, 7.3 Hz, 1H, *H8*), 7.43 (m, 2H, *H5* and *H6*), 7.42 (d, *J* = 7.6 Hz, 1H, *H4*), 7.23 (nfom, 1H, *H7*), 7.21 (d, *J* = 7.6 Hz, 1H, *H3*), 2.73 (br t, *J* = 8.0 Hz, 2H, C*H*$_2$CH$_2$CH$_3$), 1.54 (br sext, *J* = 7 Hz, 2H, C*H*$_2$CH$_3$), 0.97 (t, *J* = 7.3 Hz, CH$_2$C*H*$_3$), and 0.43 (s, 9H, SiC*H*$_3$).

^{13}C NMR (125 MHz, $CDCl_3$): δ 195.6, 150.7, 144.2, 143.2, 141.0, 140.4, 135.4, 134.5, 134.0, 128.6, 124.0, 120.8, 119.5, 39.0, 27.1, 14.0, and 2.5.

IR (neat): 2955, 2935, 2875, 1713, 1606, 1248, 968, 861, and 846 cm^{-1}.

HRMS (ESI-TOF): Calcd for $C_{19}H_{22}NaOSi^+$ [M+Na$^+$] requires 317.1332; found 317.1358.

TLC: R_f 0.5 (9:1 Hex/EtOAc).

2-Propyl-1-(trimethylsilyl)-9*H*-fluoren-9-one-3-*d* (7049 or 7040-hd)

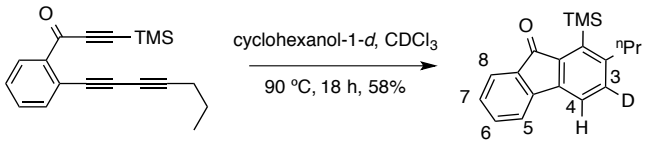

7043 ***7049*** (***7040-hd***)

A solution of triynone **7043** (12 mg, 0.041 mmol) and cyclohexanol-1-*d*[181] (6 mg, 0.06 mmol) in $CDCl_3$ (4 mL) was heated at 90 ºC. After 18 h the mixture was concentrated and the crude material was purified by flash chromatography (hexanes:EtOAc 19:1) to give the mono-deuterated fluorenone **7049** (7 mg, 0.023 mmol, 58%) as a golden yellow oil.

^{1}H NMR (500 MHz, $CDCl_3$): δ 7.57 (ddd, *J* = 7.3, 1.0, 1.0 Hz, 1H, *H8*), 7.44 (m, 2H, *H5* and *H6*), 7.42 (s, 1H, *H4*), 7.23 (nfom, 1H, *H7*), 2.73 (br t, 8.0 Hz, 2H, C*H*$_2$CH$_2$CH$_3$), 1.54 (br sext, 2H, C*H*$_2$CH$_3$), 0.97 (t, J = 7.3 Hz, 3H, CH$_3$), and 0.43 (s, 9H, SiC*H*$_3$).

2-Propyl-1-(trimethylsilyl)-9*H*-fluoren-9-one-4-*d* (7051 or 7040-dh)

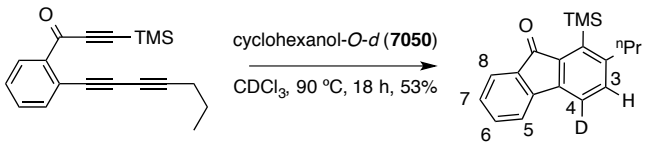

7043 ***7051*** (***7040-dh***)

A solution of triynone **7043** (17 mg, 0.058 mmol) and cyclohexanol-*O*-*d* (**7050**, 9 mg, 0.09 mmol) in $CDCl_3$ (6 mL) was heated at 90 ºC. After 18 h the mixture was concentrated and the crude material was purified by flash chromatography (hexanes:EtOAc 19:1) to give the mono-deuterated fluorenone **7051** (9 mg, 0.031 mmol, 53%) as a golden yellow oil.

^{1}H NMR (500 MHz, $CDCl_3$): δ 7.57 (ddd, *J* = 7.3, 1.0, 1.0 Hz, 1H, *H8*), 7.44 (m, 2H, *H5* and *H6*), 7.22 (s, 1H, *H3*), 7.23 (nfom, 1H, *H7*), 2.73 (br t, 8.0 Hz, 2H, $CH_2CH_2CH_3$), 1.54 (br sext, 2H, CH_2CH_3), 0.97 (t, J = 7.3 Hz, 3H, CH_3), and 0.43 (s, 9H, $SiCH_3$).

Cyclohexanol-*O*-*d* (**7050**) was prepared by treating cyclohexanol in methanol-d_4 and concentrating the mixture on a rotary evaporator. This procedure was repeated several times. ^{1}H NMR analysis suggested ca. 95% deuterium incorporation.

Computational Data for Chapters 3, 6–7

General Computational Details

DFT calculations were carried out in Gaussian 09[85] using the M06-2X/6-311+G(d,p) functional[198]/basis set for geometry optimizations and frequency calculations (unless otherwise specified, e.g., 2H atom transfer from ethane). To identify starting geometries for the DFT calculations of the various hydrocarbon donors, Monte Carlo conformational searches were carried out in MacroModel version 9.9.[102] Each of the identified conformers was subjected to geometry optimization using the above DFT method. The optimized reactant and product geometries were found to have no imaginary frequencies and the optimized transition structure geometries were found to have only one imaginary frequency. The values for the "Sum of electronic and thermal Free Energies=" were used to determine the free energy (G) of each of the two reactants (e.g., $G_{Benzyne}$ and $G_{H2\text{-}Donor}$) and of the transition structure (G_{TS}) for each H2-donor. The $\Delta G^{‡}$ value for the dihydrogen transfer between the benzyne and each H2-donor were determined using the following equation:

$$\Delta G^{‡} = G_{TS} - (G_{Benzyne} + G_{H2\text{-}Donor})$$

where the G values were those of the lowest energy conformer of the 2H atom donor, the *o*-benzyne, and the transition structure.

Energies and geometries for all of the entries in Figure 6

Computed energy and geometry of azlactone **3073**

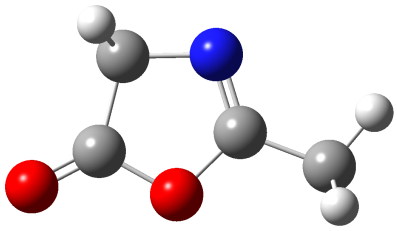

Sum of electronic and thermal Free Energies[a] = -360.537198 A.U.[b]

Atom Type	Cartesian Coordinates (x,y,z)		
C	0.992264	0.047988	0.000061
C	-0.834666	1.229061	0.000073
C	-1.202003	-0.244796	-0.000066
O	0.002483	-0.918494	-0.000078
H	-1.2472	1.722893	-0.882498
H	-1.247286	1.722751	0.882683
O	-2.251209	-0.794922	-0.000153
C	2.378003	-0.479311	0.000029
H	3.07608	0.35409	0.000191
H	2.536792	-1.101924	0.882332
H	2.536866	-1.101629	-0.882472
N	0.618995	1.256214	0.000146

[a] Used for the $\Delta G^{\ddagger}_{M06\text{-}2X}$ calculation.

[b] Atomic Units = Hartrees

Computed energy and geometry of Münchnone **3074**

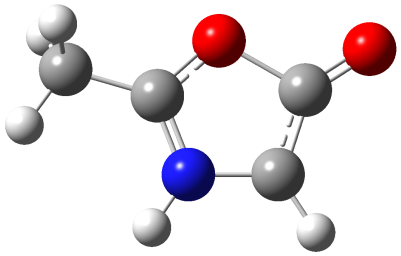

Sum of electronic and thermal Free Energies[a] = -360.503905 A.U.[b]

Atom Type	Cartesian Coordinates (x,y,z)		
C	-0.980348	-0.071537	-0.000014
C	0.86438	1.185344	0.000051
C	1.326346	-0.122377	0.000031
O	0.005008	-0.9114	-0.00002
H	1.429333	2.096055	-0.000099
O	2.346226	-0.744716	0.000017
C	-2.397339	-0.506238	0.000027
H	-3.064761	0.355407	0.000375
H	-2.598702	-1.114819	-0.883478
H	-2.598322	-1.115343	0.88325
N	-0.532826	1.162656	-0.000203
H	-1.125866	1.977892	0.000822

[a] Used for the $\Delta G^{\ddagger}_{M06\text{-}2X}$ calculation.
[b] Atomic Units = Hartrees

Computed energy and geometry of ketene **3075**

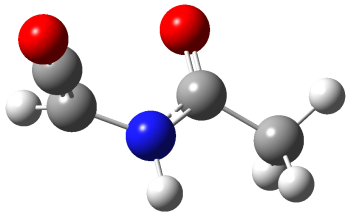

Sum of electronic and thermal Free Energies[a] = -360.507369 A.U.[b]

Atom Type	Cartesian Coordinates (x,y,z)		
N	0.22156	-0.650215	-0.280517
H	0.398653	-1.640557	-0.353289
C	1.279813	0.183228	0.023255
C	2.563926	-0.534541	0.377838
H	2.396113	-1.546432	0.747954
H	3.19188	-0.584159	-0.514413
H	3.088974	0.050873	1.129933
O	1.186769	1.385662	-0.010422
C	-0.994047	-0.139298	-0.799356
H	-1.064213	0.277232	-1.79574
C	-2.047606	-0.042533	-0.009721
O	-2.983624	0.013514	0.660056

[a] Used for the $\Delta G^{\ddagger}_{M06\text{-}2X}$ calculation.
[b] Atomic Units = Hartrees

Computed energy and geometry of ketene **3076**

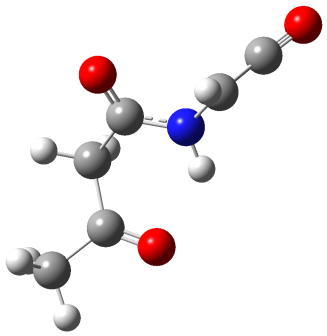

Sum of electronic and thermal Free Energies[a] = -513.100713 A.U.[b]

Atom Type	Cartesian Coordinates (x,y,z)		
C	-2.006161	-0.141256	-0.725183
C	-3.09898	-0.389866	-0.030788
O	-4.060216	-0.642362	0.555177
N	-0.7379	-0.216555	-0.092483
C	0.028811	0.909214	0.036537
O	-0.351453	2.019192	-0.250961
C	1.417271	0.687271	0.635673
C	2.228664	-0.479544	0.089608
O	1.724703	-1.552128	-0.146453
C	3.699546	-0.227458	-0.105212
H	-2.114926	0.196249	-1.747568
H	-0.252847	-1.106239	-0.054848
H	1.958675	1.626787	0.535975
H	1.28616	0.492953	1.707351
H	4.203104	-1.148242	-0.391032
H	3.832682	0.530738	-0.882079
H	4.133274	0.175848	0.813655

[a] Used for the $\Delta G^{\ddagger}_{M06\text{-}2X}$ calculation.
[b] Atomic Units = Hartrees

Computed energy and geometry of [2+2] transition structure **3077**

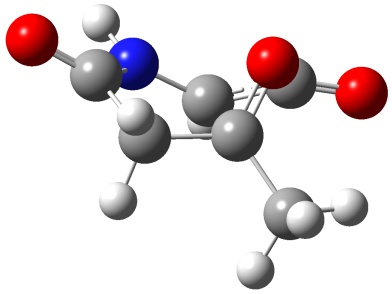

Sum of electronic and thermal Free Energies[a] = -513.053156 A.U.[b]

Atom Type	Cartesian Coordinates (x,y,z)		
C	-1.02093	1.219039	0.158537
C	0.421605	0.976117	-0.137056
C	0.267993	-1.244862	0.680832
H	-1.168264	1.646357	1.152087
H	-1.422528	1.918569	-0.580833
H	0.500043	-1.954815	1.46887
C	1.357928	-0.983562	-0.148655
O	2.520778	-1.094829	-0.20787
O	0.714868	0.281639	-1.169105
C	-1.821548	-0.06771	0.025848
N	-1.091624	-1.185995	0.324115
H	-1.609397	-2.052127	0.24856
O	-2.981728	-0.102339	-0.302728
C	1.477575	1.7787	0.552709
H	1.224508	1.973157	1.593835
H	2.448789	1.290069	0.467098
H	1.541144	2.738654	0.02592

[a] Used for the $\Delta G^{\ddagger}_{M06\text{-}2X}$ calculation.
[b] Atomic Units = Hartrees

Computed energy and geometry of β-lactone **3078**

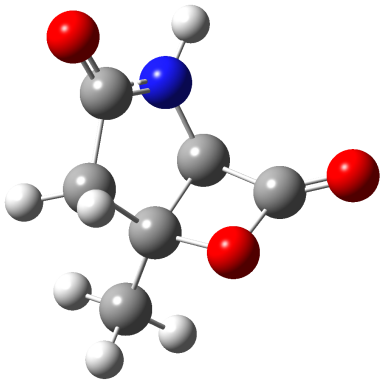

Sum of electronic and thermal Free Energies[a] = -513.131612 A.U.[b]

Atom Type	Cartesian Coordinates (x,y,z)		
C	1.358031	-0.916634	-0.127449
O	1.27657	0.166868	-0.948486
C	-1.758101	-0.202675	-0.048768
C	-1.005181	1.021017	-0.568261
C	0.405767	0.898978	-0.018931
C	0.401559	-0.332295	0.922736
N	-0.940754	-0.840688	0.858508
O	-2.870804	-0.54566	-0.347564
H	-1.512188	1.920532	-0.213439
H	-1.016214	1.02667	-1.658513
C	1.06997	2.1654	0.453004
H	0.79499	-0.224823	1.932899
O	1.968626	-1.915797	-0.289998
H	-1.211968	-1.736653	1.23686
H	2.065377	1.95324	0.847674
H	1.168479	2.867661	-0.376984
H	0.469395	2.632153	1.236353

[a] Used for the $\Delta G^{\ddagger}_{M06\text{-}2X}$ calculation.
[b] Atomic Units = Hartrees

Energies and geometries for the computations in presented in Figures 18, 20, and 22.

Computed energy and geometry of *o*-benzyne [**3**, M06-2X/6-31+g(d,p)]

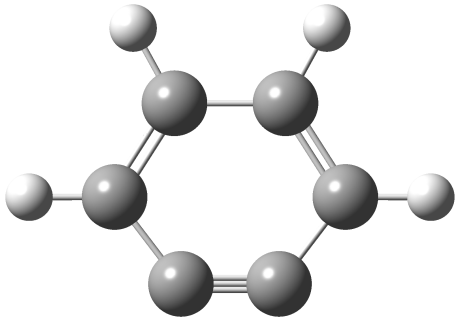

Sum of electronic and thermal Free Energies[a] = -230.771202 A.U.[b]

Atom Type	Cartesian Coordinates (x,y,z)		
C	0.703412	1.053556	-0.000032
C	-0.703355	1.053589	-0.000032
C	-1.462632	-0.132492	0.000132
C	-0.623112	-1.233087	-0.000083
C	0.623034	-1.233078	-0.000084
C	1.462637	-0.132562	0.000133
H	1.225682	2.006452	-0.000146
H	-1.22558	2.006511	-0.000154
H	-2.545934	-0.134193	0.000052
H	2.545937	-0.13433	0.00005

[a] Used for the $\Delta G^{\ddagger}_{M06\text{-}2X}$ calculation.
[b] Atomic Units = Hartrees

Computed energy and geometry of ethane [M06-2X/6-31+g(d,p)]

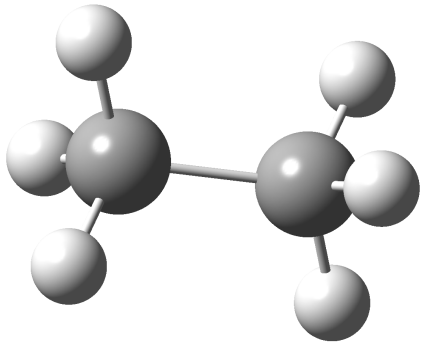

Sum of electronic and thermal Free Energies[a] = -79.726741 A.U.[b]

Atom Type	Cartesian Coordinates (x,y,z)		
C	0	0	0.763578
H	0.507537	0.884016	1.160387
H	0.511811	-0.881548	1.160387
H	-1.019349	-0.002468	1.160387
C	0	0	-0.763578
H	1.019349	-0.002468	-1.160387
H	-0.511811	-0.881548	-1.160387
H	-0.507537	0.884016	-1.160387

[a] Used for the $\Delta G^{\ddagger}_{M06\text{-}2X}$ calculation.
[b] Atomic Units = Hartrees

Computed energy and geometry of transition structure **7019** [M06-2X/6-31+g(d,p)]

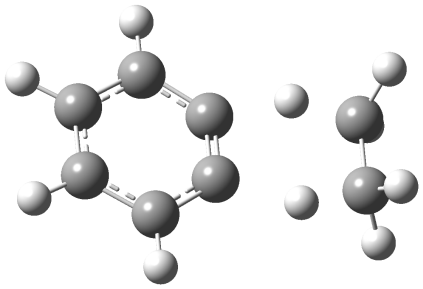

Sum of electronic and thermal Free Energies[a] = -310.464958 A.U.[b]

Atom Type	Cartesian Coordinates (x,y,z)		
C	1.358031	-0.916634	-0.127449
O	1.27657	0.166868	-0.948486
C	-1.758101	-0.202675	-0.048768
C	-1.005181	1.021017	-0.568261
C	0.405767	0.898978	-0.018931
C	0.401559	-0.332295	0.922736
N	-0.940754	-0.840688	0.858508
O	-2.870804	-0.54566	-0.347564
H	-1.512188	1.920532	-0.213439
H	-1.016214	1.02667	-1.658513
C	1.06997	2.1654	0.453004
H	0.79499	-0.224823	1.932899
O	1.968626	-1.915797	-0.289998
H	-1.211968	-1.736653	1.23686
H	2.065377	1.95324	0.847674
H	1.168479	2.867661	-0.376984
H	0.469395	2.632153	1.236353

[a] Used for the $\Delta G^{\ddagger}_{M06\text{-}2X}$ calculation.
[b] Atomic Units = Hartrees

Energies and geometries for all of the entries in Figure 20

Computed energy and geometry of *o*-benzyne (**3**)

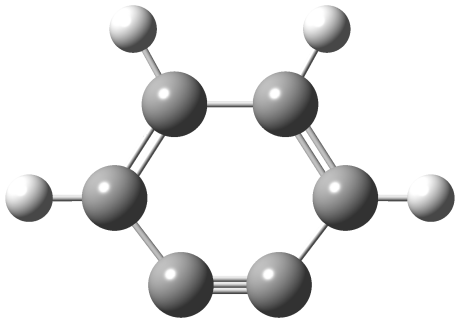

Sum of electronic and thermal Free Energies[a] = -230.818447 A.U.[b]

Atom Type	Cartesian Coordinates (x,y,z)		
C	-1.459052	-0.132412	0.000018
C	-0.619665	-1.230665	-0.000010
C	0.619772	-1.230671	-0.000012
C	1.459048	-0.132316	0.000019
C	0.702178	1.051807	-0.000005
C	-0.702256	1.051763	-0.000003
H	-2.540326	-0.134912	0.000002
H	2.540323	-0.134729	0.000002
H	1.224618	2.002344	-0.000019
H	-1.224760	2.002265	-0.000024

[a] Used for the $\Delta G^{\ddagger}_{M06\text{-}2X}$ calculation.

[b] Atomic Units = Hartrees

Computed energy and geometry of the lowest energy conformation of cyclooctane

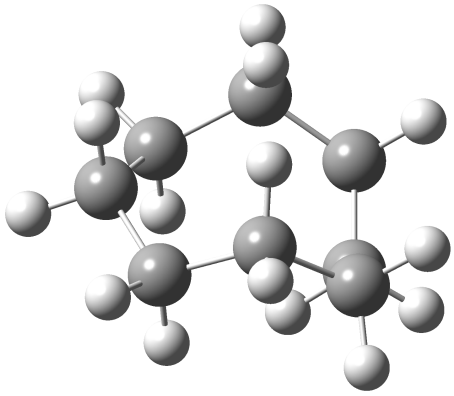

Sum of electronic and thermal Free Energies[a] = -314.211943 A.U.[b]

Atom Type	Cartesian Coordinates (x,y,z)		
C	1.386062	1.302498	0.075459
C	1.555205	0.000013	-0.708312
C	1.386085	-1.302476	0.075458
C	-0.011757	-1.594145	0.645066
C	-1.181610	-1.318856	-0.319334
C	-1.932003	-0.000017	-0.088097
C	-1.181635	1.318835	-0.319336
C	-0.011786	1.594147	0.645064
H	2.116816	1.330163	0.891727
H	1.651515	2.125159	-0.597901
H	0.872340	0.000008	-1.563660
H	2.560936	0.000022	-1.140582
H	1.651548	-2.125132	-0.597905
H	2.116842	-1.330131	0.891723
H	-0.027389	-2.649099	0.932882
H	-0.170345	-1.039328	1.572997
H	-0.833023	-1.373252	-1.357020
H	-1.917232	-2.121427	-0.214552
H	-2.818322	-0.000026	-0.731086
H	-2.306930	-0.000020	0.943276
H	-0.833049	1.373237	-1.357022
H	-1.917272	2.121392	-0.214553
H	-0.027435	2.649103	0.932874
H	-0.170367	1.039333	1.572998

[a] Used for the $\Delta G^{\ddagger}_{M06\text{-}2X}$ calculation.

[b] Atomic Units = Hartrees

Computed energy and geometry of the lowest energy conformation of cycloheptane

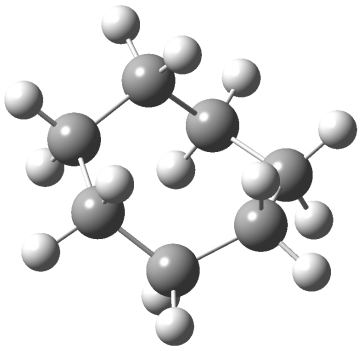

Sum of electronic and thermal Free Energies[a] = -274.941457 A.U.[b]

Atom Type	Cartesian Coordinates (x,y,z)		
C	-0.302164	-1.501933	-0.412011
C	-1.540652	-0.758057	0.103147
C	-1.540629	0.758091	-0.103154
C	-0.302128	1.501937	0.412016
C	0.957234	1.228415	-0.423200
C	1.775429	-0.000027	-0.000010
C	0.957196	-1.228429	0.423215
H	-0.517731	-2.573709	-0.383694
H	-0.121706	-1.254041	-1.465273
H	-2.433889	-1.169259	-0.377531
H	-1.642722	-0.973246	1.173961
H	-1.642680	0.973282	-1.173970
H	-2.433859	1.169320	0.377513
H	-0.517671	2.573718	0.383692
H	-0.121687	1.254047	1.465280
H	0.652717	1.122283	-1.470333
H	1.616574	2.100311	-0.393454
H	2.433845	-0.274850	-0.830377
H	2.433899	0.274763	0.830324
H	1.616513	-2.100345	0.393505
H	0.652673	-1.122254	1.470341

[a] Used for the $\Delta G^{\ddagger}_{M06\text{-}2X}$ calculation.

[b] Atomic Units = Hartrees

Computed energy and geometry of the lowest energy conformation of cyclopentane

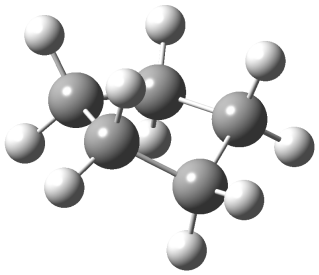

Sum of electronic and thermal Free Energies[a] = -196.390277 A.U.[b]

Atom Type	Cartesian Coordinates (x,y,z)		
C	0.385818	1.231221	-0.105059
C	1.258905	0.011173	0.235529
C	0.429546	-1.170900	-0.272733
C	-0.987219	-0.803866	0.182930
C	-1.080434	0.722828	-0.039973
H	0.567075	2.070685	0.567847
H	0.617753	1.576142	-1.115782
H	1.380797	-0.074487	1.320421
H	2.255624	0.066707	-0.205884
H	0.473479	-1.208453	-1.366795
H	0.767610	-2.135947	0.109375
H	-1.766379	-1.355194	-0.346028
H	-1.090109	-1.033565	1.247707
H	-1.601467	0.943684	-0.973666
H	-1.644074	1.207694	0.758645

[a] Used for the $\Delta G^{\ddagger}_{M06\text{-}2X}$ calculation.
[b] Atomic Units = Hartrees

Computed energy and geometry of the lowest energy conformation of norbornane

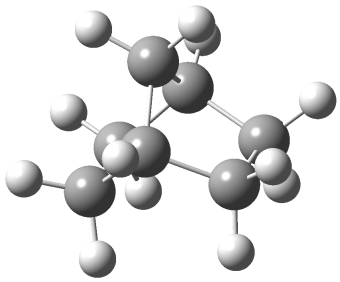

Sum of electronic and thermal Free Energies[a] = -273.756351 A.U.[b]

Atom Type	Cartesian Coordinates (x,y,z)		
C	0.000002	-1.129721	0.339789
C	1.248387	-0.779489	-0.492222
C	1.248383	0.779492	-0.492223
C	-0.000002	1.129721	0.339790
C	-1.248387	0.779489	-0.492222
C	-1.248384	-0.779492	-0.492223
H	1.196535	-1.200976	-1.498320
H	2.151392	-1.170004	-0.017696
H	2.151388	1.170013	-0.017701
H	1.196527	1.200977	-1.498322
H	-2.151392	1.170005	-0.017696
H	-1.196534	1.200976	-1.498320
H	-1.196528	-1.200977	-1.498322
H	-2.151388	-1.170013	-0.017700
C	0.000000	0.000000	1.384438
H	-0.000003	2.147370	0.730337
H	0.000003	-2.147371	0.730336
H	0.891968	0.000001	2.016324
H	-0.891968	-0.000002	2.016324

[a] Used for the $\Delta G^{\ddagger}_{M06\text{-}2X}$ calculation.

[b] Atomic Units = Hartrees

Computed energy and geometry of the lowest energy conformation of cyclohexane

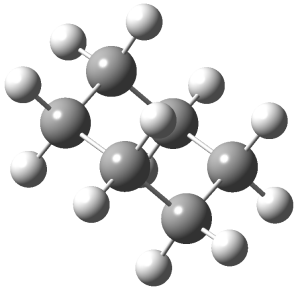

Sum of electronic and thermal Free Energies[a] = -235.674605 A.U.[b]

Atom Type	Cartesian Coordinates (x,y,z)		
C	1.211373	0.811084	-0.233837
C	-0.097080	1.454448	0.233650
C	-1.308099	0.643098	-0.233836
C	-1.211372	-0.811078	0.233847
C	0.097074	-1.454448	-0.233651
C	1.308100	-0.643103	0.233827
H	-2.234114	1.097326	0.129326
H	-0.100726	1.503293	1.329698
H	-0.166880	2.483590	-0.129270
H	1.252818	0.838955	-1.329834
H	2.067958	1.384997	0.130436
H	-1.252793	-0.838932	1.329846
H	-2.067962	-1.385004	-0.130393
H	0.166880	-2.483590	0.129272
H	0.100713	-1.503296	-1.329698
H	1.352108	-0.664365	1.329875
H	2.234109	-1.097319	-0.129368
H	-1.352089	0.664347	-1.329887

[a] Used for the $\Delta G^{\ddagger}_{M06\text{-}2X}$ calculation.

[b] Atomic Units = Hartrees

Computed energy and geometry of the lowest energy conformation of tetrahydrofuran

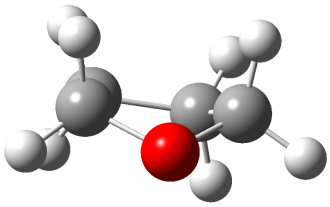

Sum of electronic and thermal Free Energies[a] = -232.317059 A.U.[b]

Atom Type	Cartesian Coordinates (x,y,z)		
C	-0.727053	1.048685	0.001155
C	0.814257	0.971705	-0.102986
C	-1.151828	-0.431331	0.118007
H	-1.051389	1.620296	0.871252
H	-1.157310	1.516745	-0.883978
H	1.321852	1.642671	0.590240
H	1.142241	1.214535	-1.114335
H	-1.402299	-0.679166	1.157989
H	-1.993612	-0.700530	-0.518644
O	-0.032045	-1.195054	-0.293715
C	1.100281	-0.503504	0.196032
H	1.199749	-0.668713	1.278647
H	1.983193	-0.898732	-0.304702

[a] Used for the $\Delta G^{\ddagger}_{M06\text{-}2X}$ calculation.
[b] Atomic Units = Hartrees

Computed energy and geometry of the lowest energy conformation of 1,4-dioxane

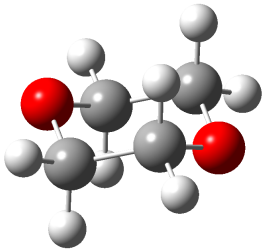

Sum of electronic and thermal Free Energies[a] = -307.522164 A.U.[b]

Atom Type	Cartesian Coordinates (x,y,z)		
C	1.197526	-0.179741	-0.682838
C	-0.140416	-0.670677	-1.209619
O	-1.189925	0.151375	-0.732743
C	-1.197526	0.179741	0.682838
C	0.140416	0.670677	1.209619
O	1.189925	-0.151375	0.732743
H	1.398345	0.828230	-1.072404
H	2.006123	-0.846886	-0.984057
H	-0.305174	-1.707625	-0.884566
H	-0.172068	-0.628468	-2.299057
H	-2.006123	0.846886	0.984057
H	-1.398345	-0.828230	1.072404
H	0.305174	1.707625	0.884566
H	0.172068	0.628468	2.299057

[a] Used for the $\Delta G^{\ddagger}_{M06\text{-}2X}$ calculation.

[b] Atomic Units = Hartrees

Computed energy and geometry of benzene

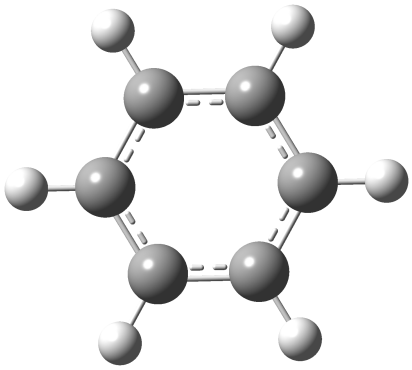

Sum of electronic and thermal Free Energies[a] = -232.124771 A.U.[b]

Atom Type	Cartesian Coordinates (x,y,z)		
C	-1.391337	-0.031931	0.000000
C	-0.667949	-1.220979	0.000009
C	0.723285	-1.188838	0.000001
C	1.391335	0.031992	0.000002
C	0.668002	1.220950	0.000001
C	-0.723336	1.188808	-0.000005
H	-2.474672	-0.056246	-0.000007
H	-1.188429	-2.171454	-0.000018
H	1.286545	-2.114684	-0.000021
H	2.474673	0.056165	-0.000012
H	1.188364	2.171490	0.000009
H	-1.286478	2.114725	0.000000

[a] Used for the $\Delta G^{\ddagger}_{M06\text{-}2X}$ calculation.

[b] Atomic Units = Hartrees

Computed energy and geometry of cyclopentene

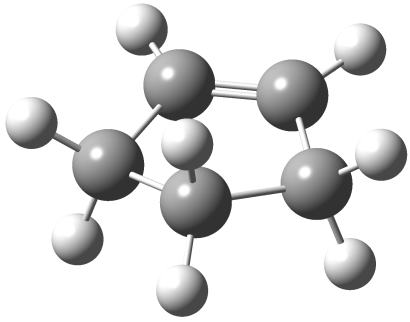

Sum of electronic and thermal Free Energies[a] = -195.188423 A.U.[b]

Atom Type	Cartesian Coordinates (x,y,z)		
C	-0.303216	-1.189786	0.000000
C	0.078190	-0.333163	1.226730
C	0.078190	1.069551	0.665108
C	0.078190	1.069551	-0.665108
C	0.078190	-0.333163	-1.226730
H	-1.384460	-1.346354	0.000000
H	1.075923	-0.586623	1.604461
H	-0.618163	-0.460452	2.058666
H	0.118614	1.956325	1.286629
H	0.118614	1.956325	-1.286629
H	1.075923	-0.586623	-1.604461
H	-0.618163	-0.460452	-2.058666
H	0.174438	-2.170083	0.000000

[a] Used for the $\Delta G^{\ddagger}_{M06\text{-}2X}$ calculation.

[b] Atomic Units = Hartrees

Computed energy and geometry of the lowest energy conformation of methanol

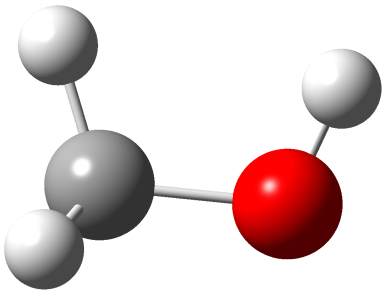

Sum of electronic and thermal Free Energies[a] = -115.674994 A.U.[b]

Atom Type	Cartesian Coordinates (x,y,z)		
C	-0.664628	0.018786	-0.000076
H	-1.080481	-0.464642	-0.887031
H	-1.080567	-0.462708	0.887979
H	-0.976282	1.066354	-0.000784
O	0.746429	-0.124117	0.000094
H	1.153665	0.741212	-0.000458

[a] Used for the $\Delta G^{\ddagger}_{M06\text{-}2X}$ calculation.

[b] Atomic Units = Hartrees

Computed energy and geometry of the lowest energy conformation of benzene

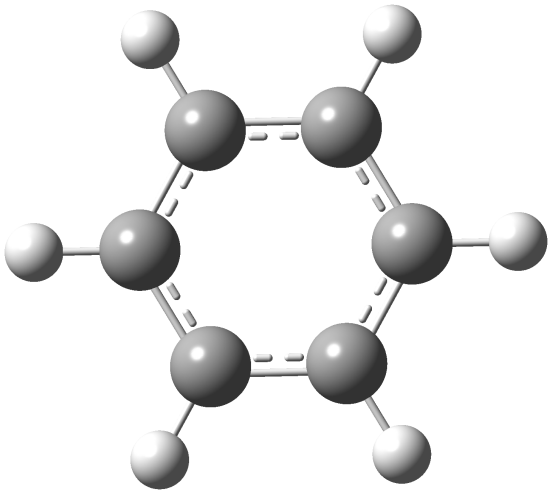

Sum of electronic and thermal Free Energies[a] = -232.124771 A.U.[b]

Atom Type	Cartesian Coordinates (x,y,z)		
C	-1.391337	-0.031931	0
C	-0.667949	-1.220979	0.000009
C	0.723285	-1.188838	0.000001
C	1.391335	0.031992	0.000002
C	0.668002	1.22095	0.000001
C	-0.723336	1.188808	-0.000005
H	-2.474672	-0.056246	-0.000007
H	-1.188429	-2.171454	-0.000018
H	1.286545	-2.114684	-0.000021
H	2.474673	0.056165	-0.000012
H	1.188364	2.17149	0.000009
H	-1.286478	2.114725	0

[a] Used for the $\Delta G^{\ddagger}_{M06\text{-}2X}$ calculation.

[b] Atomic Units = Hartrees

Computed energy and geometry of the lowest energy conformation of cyclohexanol

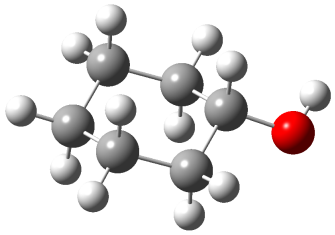

Sum of electronic and thermal Free Energies[a] = -310.892951 A.U.[b]

Atom Type	Cartesian Coordinates (x,y,z)		
C	0.314543	-1.263338	-0.179004
C	-1.162839	-1.249644	0.220059
C	-1.858974	0.017604	-0.282605
C	-1.136643	1.272271	0.214199
C	0.339982	1.246925	-0.190003
C	1.027826	-0.016467	0.320757
H	0.410325	-1.290348	-1.270633
H	0.822636	-2.147781	0.212677
H	-1.245163	-1.295325	1.312796
H	-1.662442	-2.139694	-0.169943
H	-1.861333	0.015613	-1.379139
H	-2.903819	0.030329	0.038415
H	-1.617341	2.172200	-0.177115
H	-1.213097	1.322692	1.307159
H	0.431435	1.263810	-1.282350
H	0.857556	2.133312	0.193968
H	0.999502	-0.013582	1.421808
O	2.375254	-0.099469	-0.121492
H	2.836335	0.700419	0.143874

[a] Used for the $\Delta G^{\ddagger}_{M06\text{-}2X}$ calculation.

[b] Atomic Units = Hartrees

Computed energy and geometry of fluorynone **23**

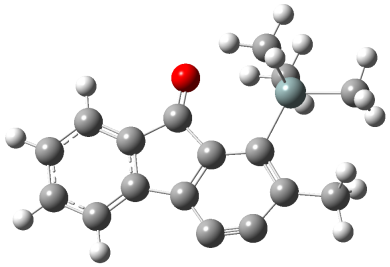

Sum of electronic and thermal Free Energies[a] = -1021.720925 A.U.[b]

Atom Type	Cartesian Coordinates (x,y,z)		
C	-3.376586	-1.568926	0.000097
C	-4.662063	-1.019773	-0.000056
C	-4.840752	0.361839	-0.000211
C	-3.749231	1.236231	-0.000224
H	-3.214349	-2.640635	0.000236
H	-5.527599	-1.670916	-0.000050
H	-5.845969	0.766727	-0.000320
H	-3.892029	2.310480	-0.000332
C	-0.837833	-1.008104	0.000234
C	-2.304416	-0.699238	0.000066
C	-2.479968	0.686666	-0.000093
C	-0.121849	0.323846	-0.000073
C	-1.146687	1.312595	-0.000082
C	-0.655318	2.601049	-0.000016
C	0.575819	2.780441	0.000059
C	1.688362	1.973070	0.000020
C	1.261215	0.600346	-0.000126
C	3.100969	2.487509	0.000205
O	-0.355483	-2.113049	0.000702
C	2.288681	-1.856895	-1.587161
C	4.322963	-0.374847	-0.000942
C	2.289512	-1.855642	1.587784
H	3.647751	2.152402	0.881594
H	3.647737	2.152968	-0.881414
H	3.089526	3.576133	0.000552
H	2.976890	-2.707580	-1.581617
H	1.279030	-2.238808	-1.723083
H	2.548916	-1.228829	-2.443826

H	4.880949	-1.317754	-0.001166
H	4.632825	0.178075	-0.888607
H	4.633637	0.178116	0.886409
H	2.980000	-2.704485	1.584085
H	2.547035	-1.225858	2.444011
H	1.280667	-2.239973	1.722936
Si	2.504424	-0.879762	-0.000135

[a] Used for the $\Delta G^{\ddagger}_{M06\text{-}2X}$ calculation.
[b] Atomic Units = Hartrees

Computed energy and geometry for the benzyne + cyclooctane TS

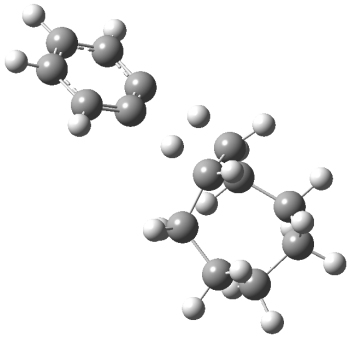

Sum of electronic and thermal Free Energies[a] = -545.002382 A.U.[b]

Atom Type	Cartesian Coordinates (x,y,z)		
C	-3.040245	-1.361495	0.316047
C	-4.247015	-0.809740	-0.125296
C	-4.358290	0.553455	-0.435982
C	-3.270941	1.425609	-0.318634
H	-2.948716	-2.412130	0.563610
H	-5.116561	-1.449755	-0.226857
H	-5.313941	0.938303	-0.776410
H	-3.371011	2.477901	-0.557925
C	-2.022376	-0.425539	0.395875
C	-2.096565	0.821113	0.116074
C	0.648616	0.928510	0.668793
C	0.572092	-0.538036	0.789480
C	1.038190	-1.460510	-0.332431
C	2.520558	-1.856095	-0.299352
C	3.544466	-0.765138	-0.628164
C	3.646551	0.368932	0.409650
C	2.988222	1.680815	-0.022369
C	1.514578	1.561013	-0.418629
H	0.454851	-2.384777	-0.264959
H	0.786471	-1.022880	-1.303738
H	2.751328	-2.267060	0.691415
H	2.656187	-2.678187	-1.009562
H	4.518670	-1.253071	-0.721337
H	3.326379	-0.346024	-1.617992
H	3.211565	0.034442	1.358402
H	4.698776	0.576569	0.622436

H	3.076402	2.406565	0.793908
H	3.546280	2.096839	-0.869052
H	1.131924	2.561941	-0.638484
H	1.419092	0.995813	-1.349229
H	0.830106	1.403597	1.637048
H	0.821655	-0.926838	1.778954
H	-0.454704	1.251789	0.410361
H	-0.651807	-0.740403	0.789043

[a] Used for the $\Delta G^{\ddagger}_{M06\text{-}2X}$ calculation.
[b] Atomic Units = Hartrees

Computed energy and geometry for the benzyne + cycloheptane TS

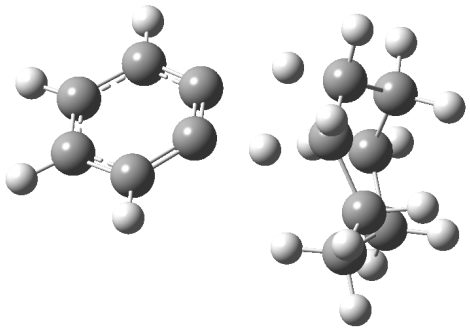

Sum of electronic and thermal Free Energies[a] = -505.731727 A.U.[b]

Atom Type	Cartesian Coordinates (x,y,z)		
C	2.358479	1.403046	0.060657
C	3.495967	0.752452	-0.427241
C	3.562531	-0.646397	-0.503637
C	2.496928	-1.455265	-0.095208
H	2.302392	2.483378	0.122838
H	4.346361	1.341932	-0.752210
H	4.464594	-1.109434	-0.889494
H	2.559396	-2.535682	-0.157045
C	1.354614	0.526931	0.440710
C	1.395998	-0.752587	0.379849
C	-1.984284	-1.251629	-1.004763
C	-2.529686	0.077388	-1.526323
C	-1.832764	1.322139	-0.978831
C	-1.992488	1.536455	0.531186
C	-1.097727	0.683237	1.420838
C	-1.176370	-0.780696	1.405238
C	-2.186496	-1.480841	0.497562
H	-2.481615	-2.060879	-1.548054
H	-0.915618	-1.328306	-1.239294
H	-2.450688	0.085597	-2.617895
H	-3.600512	0.138262	-1.292977
H	-0.765380	1.285451	-1.227790
H	-2.241525	2.197627	-1.492333
H	-1.784253	2.585329	0.760822
H	-3.041388	1.364091	0.810118
H	-2.115162	-2.553337	0.699332

H	-3.206159	-1.183397	0.776341
H	-1.010072	1.095076	2.426728
H	-1.193987	-1.195366	2.414445
H	0.052756	0.920203	0.996440
H	-0.107359	-1.135943	1.009797

[a] Used for the $\Delta G^{\ddagger}_{M06\text{-}2X}$ calculation.
[b] Atomic Units = Hartrees

Computed energy and geometry for the benzyne + cyclopentane TS

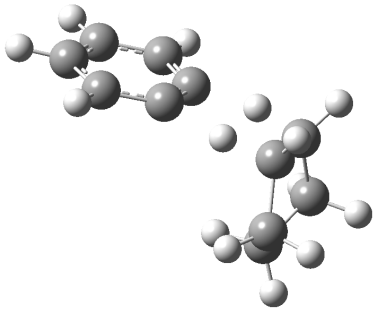

Sum of electronic and thermal Free Energies[a] = -427.178882 A.U.[b]

Atom Type	Cartesian Coordinates (x,y,z)		
C	1.936071	1.419798	-0.070021
C	3.115873	0.758905	0.285953
C	3.188398	-0.641143	0.322237
C	2.086226	-1.442008	0.005123
H	1.877126	2.501027	-0.103869
H	3.995206	1.341273	0.538809
H	4.124348	-1.112727	0.602504
H	2.153516	-2.523320	0.032028
C	0.943597	-0.727851	-0.334072
C	0.895947	0.552441	-0.363669
C	-2.371611	0.035678	1.246519
C	-2.545284	-1.169909	0.313210
C	-1.739723	-0.763853	-0.928924
C	-1.674332	0.702123	-0.946129
C	-2.413744	1.230038	0.283738
H	-3.128781	0.089219	2.029962
H	-1.388913	-0.012579	1.725594
H	-3.601729	-1.289493	0.049659
H	-2.202332	-2.106892	0.755942
H	-3.451493	1.457333	0.014063
H	-1.971928	2.138038	0.699109
H	-1.840205	1.211877	-1.892960
H	-2.003653	-1.252317	-1.865291
H	-0.475229	0.951560	-0.736132
H	-0.614443	-1.118306	-0.733204

[a] Used for the $\Delta G^{\ddagger}_{M06\text{-}2X}$ calculation.

[b] Atomic Units = Hartrees

Computed energy and geometry for the benzyne + norbornane TS

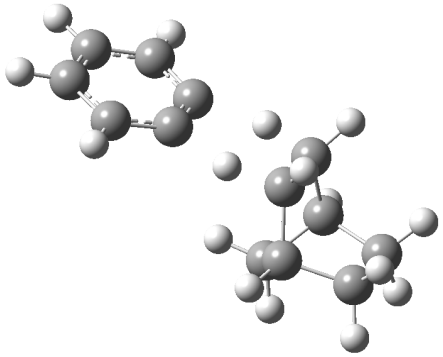

Sum of electronic and thermal Free Energies[a] = -504.545282 A.U.[b]

Atom Type	Cartesian Coordinates (x,y,z)		
C	2.719658	1.430940	-0.014251
C	3.848384	0.646372	0.243223
C	3.788447	-0.754443	0.226184
C	2.596051	-1.430207	-0.050577
H	2.774227	2.513244	0.000175
H	4.794312	1.131091	0.460305
H	4.687618	-1.324789	0.432268
H	2.547979	-2.512544	-0.065152
C	1.568809	0.700687	-0.280430
C	1.526190	-0.582597	-0.294306
C	-1.051181	-0.695977	-0.871667
C	-1.084265	0.771529	-0.864241
C	-1.914618	-1.124874	0.315531
C	-1.618703	0.008129	1.313436
C	-1.981254	1.131378	0.327073
C	-3.426935	0.742384	-0.059008
C	-3.381399	-0.814204	-0.069336
H	-1.746482	-2.142857	0.665394
H	-2.273815	-0.016736	2.187519
H	-0.575866	0.037794	1.635717
H	-1.869742	2.152263	0.690584
H	-4.134618	1.108662	0.688380
H	-3.716244	1.162826	-1.024082
H	-3.646084	-1.239757	-1.039259
H	-4.064838	-1.231953	0.673671
H	-1.201901	-1.213194	-1.818054

H	-1.296611	1.271064	-1.808927
H	0.050370	1.112787	-0.607556
H	0.136599	-0.982596	-0.600762

[a] Used for the $\Delta G^{\ddagger}_{M06\text{-}2X}$ calculation.
[b] Atomic Units = Hartrees

Computed energy and geometry for the benzyne + cyclohexane TS

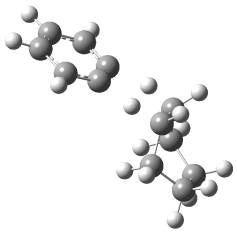

Sum of electronic and thermal Free Energies[a] = -466.454652 A.U.[b]

Atom Type	Cartesian Coordinates (x,y,z)		
C	2.558048	-1.432210	-0.021464
C	3.677709	-0.656503	-0.339859
C	3.625160	0.745027	-0.340818
C	2.449767	1.432749	-0.022447
H	2.606004	-2.514784	-0.020985
H	4.610784	-1.149338	-0.591249
H	4.517502	1.307386	-0.593581
H	2.408576	2.515366	-0.020765
C	1.426086	-0.687701	0.282230
C	1.388866	0.592931	0.279567
C	-1.200384	0.705021	0.847346
C	-1.969783	1.359873	-0.290983
C	-3.397440	0.793354	-0.351894
C	-3.410445	-0.755278	-0.420161
C	-1.998506	-1.356843	-0.331628
C	-1.227653	-0.761596	0.840415
H	-1.456406	1.166837	-1.238606
H	-1.995669	2.444117	-0.163426
H	-3.937019	1.129170	0.538222
H	-3.921522	1.219624	-1.210683
H	-4.011180	-1.155360	0.401264
H	-3.887032	-1.092232	-1.344007
H	-2.055122	-2.443726	-0.240404
H	-1.453144	-1.150661	-1.258306
H	-1.479741	-1.207150	1.803753
H	-1.381706	1.159386	1.822023
H	-0.015245	0.991593	0.651721
H	-0.077625	-1.093173	0.683206

[a] Used for the $\Delta G^{\ddagger}_{M06\text{-}2X}$ calculation.

[b] Atomic Units = Hartrees

Computed energy and geometry for the benzyne + tetrahydrofuran TS

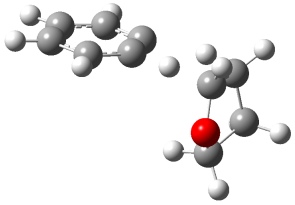

Sum of electronic and thermal Free Energies[a] = -463.104873 A.U.[b]

Atom Type	Cartesian Coordinates (x,y,z)		
C	1.785857	-1.368935	-0.146323
C	3.017036	-0.851078	0.258615
C	3.220388	0.532563	0.356529
C	2.206252	1.443669	0.052873
H	1.608090	-2.434081	-0.230493
H	3.826792	-1.530131	0.500390
H	4.189881	0.899580	0.677842
H	2.389003	2.509880	0.133376
C	0.849913	-0.383946	-0.422008
C	0.980790	0.900737	-0.341891
C	-2.323308	-0.198769	1.211650
O	-2.193127	-1.238526	0.231388
C	-1.667861	-0.661355	-0.897495
C	-1.850454	0.800291	-0.887791
C	-2.656201	1.050157	0.396175
H	-3.094836	-0.508101	1.914434
H	-1.368500	-0.086622	1.735561
H	-3.726387	1.091928	0.182023
H	-2.362042	1.965315	0.909579
H	-1.844114	-1.260206	-1.787280
H	-2.275433	1.204697	-1.803738
H	-0.368824	-0.787448	-0.796966
H	-0.803076	1.263404	-0.767843

[a] Used for the $\Delta G^{\ddagger}_{M06\text{-}2X}$ calculation.
[b] Atomic Units = Hartrees

Computed energy and geometry for the benzyne + 1,4-dioxane TS

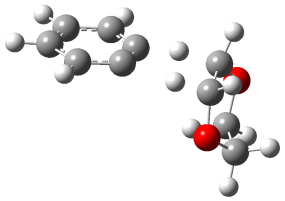

Sum of electronic and thermal Free Energies[a] = -538.297484 A.U.[b]

Atom Type	Cartesian Coordinates (x,y,z)		
C	-2.018263	1.405022	0.046566
C	-3.269890	0.945620	-0.366027
C	-3.551915	-0.426345	-0.425090
C	-2.598541	-1.384806	-0.074682
H	-1.783838	2.461259	0.100855
H	-4.034507	1.661554	-0.645636
H	-4.535858	-0.747012	-0.751723
H	-2.838694	-2.441114	-0.124974
C	-1.355478	-0.896124	0.329851
C	-1.139680	0.380427	0.367537
C	1.340084	0.425284	1.126588
O	2.091019	1.342197	0.440495
C	2.430906	0.939037	-0.882781
C	2.973410	-0.472256	-0.852815
O	1.958984	-1.353024	-0.419304
C	1.421400	-1.013726	0.837652
H	1.536303	0.978851	-1.515285
H	3.167775	1.658484	-1.238271
H	3.269067	-0.798024	-1.850162
H	3.844015	-0.521637	-0.184469
H	1.298249	0.688767	2.180728
H	1.890609	-1.576306	1.651363
H	0.083095	0.683424	0.776074
H	0.311562	-1.374423	0.791167

[a] Used for the $\Delta G^{\ddagger}_{M06\text{-}2X}$ calculation.

[b] Atomic Units = Hartrees

Computed energy and geometry for the benzyne + methanol TS

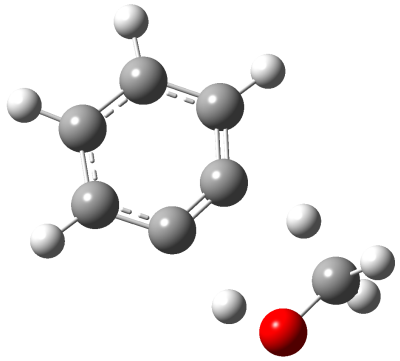

Sum of electronic and thermal Free Energies[a] = -346.472271 A.U.[b]

Atom Type	Cartesian Coordinates (x,y,z)		
C	-0.088381	0.488354	0.000067
C	-0.061082	-0.787721	-0.00013
H	0.780258	2.511681	0.000416
C	0.909007	1.43811	0.000257
C	1.18545	-1.425138	-0.000168
C	2.295661	-0.577068	0.00002
C	2.164715	0.819529	0.000225
H	1.307387	-2.501553	-0.000336
H	3.291269	-1.007104	0.000002
H	3.053649	1.440243	0.000359
C	-2.669298	0.610833	-0.000013
H	-3.071069	1.059936	0.91288
H	-3.071048	1.060246	-0.912761
H	-1.708744	-1.077819	-0.000204
H	-1.533939	0.988119	0.000066
O	-2.683024	-0.734393	-0.000247

[a] Used for the $\Delta G^{\ddagger}_{M06\text{-}2X}$ calculation.

[b] Atomic Units = Hartrees

Computed energy and geometry for the fluorynone **7022** + cyclohexanol TS

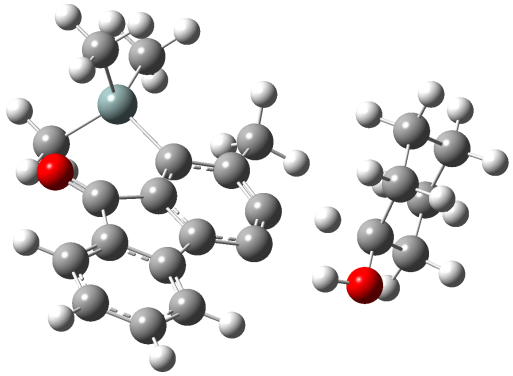

Sum of electronic and thermal Free Energies[a] = -1332.594198 A.U.[b]

Atom Type	Cartesian Coordinates (x,y,z)		
C	-4.548322	-1.944252	0.188748
C	-4.608215	-3.340084	0.197613
C	-3.444017	-4.097826	0.085891
C	-2.189863	-3.491422	-0.037421
H	-5.440992	-1.334625	0.271158
H	-5.564903	-3.839403	0.292029
H	-3.513104	-5.179445	0.094292
H	-1.286101	-4.083438	-0.125367
C	-2.947852	0.098703	0.030738
C	-3.305380	-1.354023	0.070244
C	-2.136000	-2.109320	-0.043169
C	-0.991295	-1.179633	-0.154732
C	-1.443381	0.157573	-0.093224
C	-0.599574	1.281428	-0.180969
C	0.796810	1.039360	-0.362412
C	1.854865	2.086807	-0.566305
O	-3.726523	1.019112	0.068126
C	-0.080155	4.438966	0.060619
C	-2.455767	3.431633	-1.456178
C	-2.191682	3.150814	1.691041
H	-0.652673	5.347046	0.279330
H	0.660136	4.332234	0.855250
H	0.438354	4.609235	-0.883671
H	-1.861310	3.439063	-2.374231
H	-3.269408	2.716992	-1.568556
H	-2.889328	4.428977	-1.335039

H	-1.444599	3.027495	2.480382
H	-2.634531	4.144421	1.809749
H	-2.977431	2.411302	1.830290
H	2.053026	2.650691	0.346826
H	2.783241	1.612030	-0.879248
C	0.375060	-1.401911	-0.295808
C	1.059063	-0.316085	-0.378667
O	2.702577	-2.699154	-0.602392
C	5.310394	-0.023166	-0.736236
C	4.549194	-1.290942	-1.127965
C	3.332372	-1.549269	-0.250937
C	3.602381	-1.425686	1.241700
C	4.309065	-0.115036	1.580954
C	5.597106	0.029626	0.766544
H	4.732334	0.861389	-1.022462
H	6.243438	0.026020	-1.303010
H	5.200880	-2.164710	-1.003745
H	4.238821	-1.273399	-2.175049
H	2.656372	-1.530631	1.781172
H	4.230004	-2.279890	1.522705
H	3.640547	0.727112	1.361496
H	4.524435	-0.073076	2.651087
H	6.279734	-0.786377	1.032608
H	6.105719	0.963816	1.017447
H	1.561974	2.793858	-1.341248
H	1.716882	-2.580015	-0.420614
H	2.564997	-0.644410	-0.486280
Si	-1.355270	3.047181	0.013316

[a] Used for the $\Delta G^{\ddagger}_{M06\text{-}2X}$ calculation.

[b] Atomic Units = Hartrees

Computed energy and geometry for the TS of the regioisomeric mode of addition of H2 to fluorynone **7022** by cyclohexanol

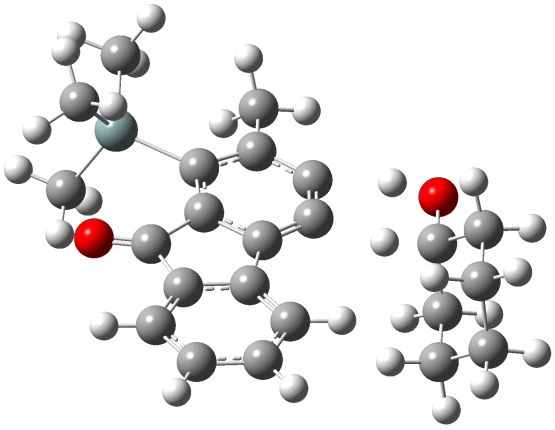

Sum of electronic and thermal Free Energies[a] = -1332.589072 A.U.[b]

Atom Type	Cartesian Coordinates (x,y,z)		
C	0.403221	4.038002	-0.067409
C	-0.865723	4.611356	0.052050
C	-1.988880	3.803707	0.203399
C	-1.884458	2.409213	0.237280
H	1.294941	4.642961	-0.186069
H	-0.978666	5.688301	0.028803
H	-2.965889	4.263329	0.298132
H	-2.768890	1.797322	0.356581
C	-0.626643	1.843677	0.118988
C	0.497543	2.662139	-0.027043
C	1.718171	1.802222	-0.132849
C	-0.167209	0.439196	0.119199
C	1.248894	0.377644	0.024741
C	2.005898	-0.806687	-0.001826
C	1.301749	-2.046953	0.002438
C	1.957303	-3.397065	-0.128770
C	-0.088700	-1.934991	0.098064
C	-0.706523	-0.819699	0.159574
O	-2.451927	-3.133233	0.162421
C	4.533475	-0.194162	-1.684070
C	4.439109	0.543473	1.385638
C	4.798457	-2.277080	0.490582

H	1.192274	-4.156834	-0.280987
H	2.641791	-3.423620	-0.978520
H	2.525855	-3.661712	0.764398
O	2.836946	2.188034	-0.358927
H	4.101659	0.749746	-2.016714
H	5.163787	0.070000	2.052719
H	4.886482	1.443535	0.963108
H	3.584710	0.858519	1.988676
H	5.859370	-2.022875	0.588649
H	4.472867	-2.665198	1.458750
H	4.719635	-3.071918	-0.250544
C	-4.774881	-0.370214	1.115622
C	-4.087649	-1.732586	1.201680
C	-3.089977	-1.940057	0.070775
C	-3.657484	-1.656894	-1.314090
C	-4.328557	-0.285463	-1.378358
C	-5.376501	-0.130880	-0.272437
H	-4.043649	0.413980	1.342613
H	-5.550141	-0.296658	1.882400
H	-4.832193	-2.533866	1.116494
H	-3.576979	-1.869609	2.157539
H	-2.854781	-1.748957	-2.051098
H	-4.386589	-2.447507	-1.530231
H	-3.564020	0.493994	-1.276600
H	-4.787504	-0.140126	-2.359325
H	-6.179793	-0.858266	-0.440589
H	-5.833837	0.861244	-0.320177
H	5.622432	-0.090849	-1.680487
H	4.274985	-0.973447	-2.406457
Si	3.931512	-0.666241	0.028714
H	-1.446055	-2.976681	0.083286
H	-2.256942	-1.083225	0.226624

[a] Used for the $\Delta G^{\ddagger}_{\text{M06-2X}}$ calculation.
[b] Atomic Units = Hartrees

Computed energy and geometry for the fluorynone **7022** + cyclopentane TS

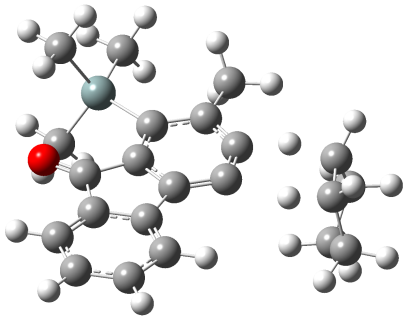

Sum of electronic and thermal Free Energies[a] = -1218.080249 A.U.[b]

Atom Type	Cartesian Coordinates (x,y,z)		
C	-0.362336	3.686943	0.258095
C	0.370684	4.868713	0.111076
C	1.745371	4.845722	-0.116549
C	2.427895	3.629507	-0.203637
H	-1.431241	3.708248	0.437063
H	-0.139373	5.822980	0.176810
H	2.284941	5.778634	-0.225556
H	3.496797	3.587032	-0.379268
C	0.317876	2.485456	0.170220
C	1.695595	2.467757	-0.058036
C	2.158774	1.044103	-0.102145
C	-0.154523	1.088687	0.279565
C	0.928534	0.194351	0.112867
C	0.812697	-1.208560	0.171475
C	-0.486838	-1.735938	0.428616
C	-0.835710	-3.194959	0.566234
O	3.296998	0.679082	-0.265888
C	3.045916	-1.973642	-1.839435
C	3.606383	-2.003784	1.277877
C	2.059289	-4.155060	-0.086679
H	-0.280362	-3.665874	1.378368
H	-1.899496	-3.297848	0.786039
H	-0.624516	-3.751715	-0.347205
C	-1.460393	-0.757142	0.563625
C	-1.400302	0.532781	0.507435
C	-4.436356	-0.435864	-1.476031

C	-4.844517	0.757355	-0.601142
C	-4.191039	0.436154	0.752781
C	-4.021815	-1.019043	0.806064
C	-4.511498	-1.622552	-0.506002
H	-3.404166	-0.305700	-1.814516
H	-5.933806	0.788973	-0.495135
H	-4.517551	1.714808	-1.010414
H	-4.638557	0.895263	1.632770
H	-4.240315	-1.545471	1.732634
H	-5.552526	-1.942633	-0.380522
H	-3.934442	-2.491566	-0.829580
H	3.969778	-2.543307	-1.978809
H	2.325378	-2.328403	-2.581989
H	3.263810	-0.925073	-2.031539
H	3.034937	-4.618060	-0.271851
H	1.701125	-4.536823	0.870208
H	1.389116	-4.498896	-0.876255
H	4.516017	-2.579540	1.081426
H	3.884775	-0.957483	1.387768
H	3.187040	-2.361117	2.222735
H	-5.068363	-0.562713	-2.355671
H	-3.094770	0.871344	0.714339
H	-2.753492	-1.174082	0.766998
Si	2.378655	-2.292823	-0.112813

[a] Used for the $\Delta G^{\ddagger}_{\text{M06-2X}}$ calculation.
[b] Atomic Units = Hartrees

Bibliography and Notes

1. Feling, R. H.; Buchanan, G. O.; Mincer, T. J.; Kauffman, C. A.; Jensen, P. R.; Fenical, W. Salinosporamide A: A highly cytotoxic proteasome inhibitor from a novel microbial source, a marine bacterium of the new genus *Salinospora*. *Angew. Chem. Int. Ed.* **2003**, *42*, 355–357.

2. Potts, B. C.; Albitar, M. X.; Anderson, K. C.; Baritaki, S.; Berkers, C.; Bonavida, B.; Chandra, J.; Chauhan, D.; Cusack, J. C.; Fenical, W.; Ghobrial, I. M.; Groll, M.; Jensen, P. R.; Lam, K. S.; Lloyd, G. K.; McBride, W.; McConkey, D. J.; Miller, C. P.; Neuteboom, S. T. C.; Oki, Y.; Ovaa, H.; Pajonk, F.; Richardson, P. G.; Roccaro, A. M.; Sloss, C. M.; Spear, M. A.; Valashi, E.; Younes, A.; Palladino, M. A. Marizomib, a proteasome inhibitor for all seasons: Preclinical profile and a framework for clinical trials. *Current Cancer Drug Targets* **2011**, *11*, 254–284.

3. Ōmura, S.; Fujimoto, T.; Otoguro, K.; Matsuzaki, K.; Moriguchi, R.; Tanaka, H.; Sasaki, Y. Lactacystin, a novel microbial metabolite, induces neuritogenesis of neuroblastoma cells. *J. Antibiot.* **1991**, *44*, 113–116.

4. Dick, L. R.; Cruikshank, A. A.; Destree, A. T.; Grenier, L.; McCormack, T. A.; Melandri, F. D.; Nunes, S. L.; Palombella, V. J.; Parent, L. A.; Plamondon, L.; Stein, R. L. Mechanistic studies on the inactivation of the proteasome by lactacystin in cultured cells. *J. Biol. Chem.* **1997**, *272*, 182–188.

5. While nOe analysis allowed for assignment of relative configuration, use of NMR spectroscopy to determine the absolute configuration by was a challenge because derivatization of the hindered C-5 hydroxy failed with either Mosher's reagent or *p*-bromobenzoic acid failed.

6. Fenical, W.; Jensen, P. R.; Palladino, M. A.; Lam, K. S.; Lloyd, G. K.; Potts, B. C. Discovery and development of the anticancer agent salinosporamide A (NPI-0052). *Bioorg. Med. Chem.* **2009**, *17*, 2175–2180.

7. All functional groups have been assigned a unique role for 20SP inhibition (see ref 6).

8. a) Shibasaki, M.; Kanai, M.; Fukuda, N. Total synthesis of lactacystin and salinosporamide A. *Chem.-Asian J.* **2007**, *2*, 20–38. b) Gulder, T. A. M.; Moore, B. S. Salinosporamide natural products: Potent 20S proteasome inhibitors as promising cancer chemotherapeutics. *Angew. Chem. Int. Ed.* **2010**, *49*, 9346–9367. c) Rentsch, A.; Landsberg, D.; Brodmann, T.; Bülow, L.; Girbig, A.-K.; Kalesse, M. Synthesis and pharmacology of proteasome inhibitors. *Angew. Chem. Int. Ed.* **2013**, *52*, 5450–5488.

9. Lodish, H.; Berk, A.; Matsudaira, P.; Kaiser, C. A.; Krieger, M.; Scott, M. P.; Zipursky, L.; Darnell, J. *Molecular Cell Biology*, 5th ed.; Scientific American Press, N.Y. 2003, pp. 71–73.

10. Nandi, D.; Tahiliani, P.; Kumar, A.; Chandu, D. The ubiquitin-proteasome system. *J. Biosci.* **2006**, *31*, 137–155.

11. Marques, A. J.; Palanimurugan, R.; Matias, A. C.; Ramos, P. C.; Dohmen, R. J. Catalytic mechanism and assembly of the proteasome. *Chem. Rev.* **2009**, *109*, 1509–1536.

12. Lodish, H.; Berk, A.; Matsudaira, P.; Kaiser, C. A.; Krieger, M.; Scott, M. P.; Zipursky, L.; Darnell, J. *Molecular Cell Biology*, 5th ed.; Scientific American Press, N.Y. 2003, pp. 602–603.

13. a) Karin, M.; Cao, Y.; Greten, F. R.; Li, Z.-W. NF-κB in cancer: From innocent bystander to major culprit. *Nature Reviews Cancer* **2002**, *2*, 301–310. b) Liu, J.-J.; Lin, M.; Yu, J.-Y.; Liu, B.; Bao, J.-K. Targeting apoptotic and autophagic pathways for cancer therapeutics. *Cancer Letters* **2011**, *300*, 105–114.

14. Escárcega, R. O.; Fuentes-Alexandro, S.; García-Carrasco, M.; Gatica, A.; Zamora, A. The transcription factor nuclear factor-kappa B and cancer. *Clinical Oncology* **2007**, *19*, 154–161.

15. Montagut, C.; Rovira, A.; Albanell, J. The proteasome: A novel target for anticancer therapy. *Clin. Transl. Oncol.* **2006**, *8*, 313–317.

16. Sánchez-Serrano, I. Success in translational research: Lessons from the development of bortezomib. *Nat. Rev. Drug Disc.* **2006**, *5*, 107–114.

17. Fenteany, G.; Standaert, R. F.; Lane, W. S.; Choi, S.; Corey, E. J.; Schreiber, S. L. Inhibition of proteasome activities and subunit-specific amino-terminal threonine modification by lactacystin. *Science* **1995**, *268*, 726–726.

18. Groll, M.; Ditzel, L.; Löwe, J.; Stock, D.; Bochtler, M.; Bartunik, H. D.; Huber, R. Structure of 20S proteasome from yeast at 2.4 Å resolution. *Nature* **1997**, *386*, 463–471.

19. Groll, M.; Huber, R.; Potts, B. C. M. Crystal structures of salinosporamide A (NPI-0052) and B (NPI-0047) in complex with the 20S proteasome reveal important consequences of β-lactone ring opening and a mechanism for irreversible binding. *J. Am. Chem. Soc.* **2006**, *128*, 5136–5141.

20. Williams, P. G.; Buchanan, G. O.; Feling, R. H.; Kauffman, C. A.; Jensen, P. R.; Fenical, W. New cytotoxic salinosporamides from the marine actinomycete *Salinispora tropica*. *J. Org. Chem.* **2005**, *70*, 6196–6203.

21. Macherla, V. R.; Mitchell, S. S.; Manam, R. R.; Reed, K. A.; Chao, T.-H.; Nicholson, B.; Deyanat-Yazdi, G.; Mai, B.; Jensen, P. R.; Fenical, W. F.; Neuteboom, S. T. C.; Lam, K. S.; Palladino, M. A.; Potts, B. C. M. Structure−activity relationship studies of salinosporamide A (NPI-0052), a novel marine derived proteasome inhibitor. *J. Med. Chem*. **2005**, *48*, 3684–3687.

22. Nett, M.; Moore, B. S. Exploration and engineering of biosynthetic pathways in the marine actinomycete *Salinispora tropica*. *Pure. Appl. Chem.* **2009**, *81*, 1075–1084.

23. Manam, R. R.; McArthur, K. A.; Chao, T.-H.; Weiss, J.; Ali, J. A.; Palombella, V. J.; Groll, M.; Lloyd, G. K.; Palladino, M. A.; Neuteboom, S. T. C.; Macherla, V. R.; Potts, B. C. M. Leaving groups prolong the duration of 20S proteasome inhibition and enhance the potency of salinosporamides. *J. Med. Chem.* **2008**, *51*, 6711–6724.

24. Stadler, M.; Bitzer, J.; Mayer-Bartschmid, A.; Müller, H.; Benet-Buchholz, J.; Gantner, F.; Tichy, H.-V.; Reinemer, P.; Bacon, K. B. Cinnabaramides A−G: Analogues of lactacystin and salinosporamide from a terrestrial streptomycete. *J. Nat. Prod.* **2007**, *70*, 246–252.

25. Hogan, P. C.; Corey, E. J. Proteasome inhibition by a totally synthetic β-lactam related to salinosporamide A and omuralide. *J. Am. Chem. Soc.* **2005**, *127*, 15386–15387.

26. Reed, K. A.; Manam, R. R.; Mitchell, S. S.; Xu, J.; Teisan, S.; Chao, T.-H.; Deyanat-Yazdi, G.; Neuteboom, S. T. C.; Lam, K. S.; Potts, B. C. M. Salinosporamides D−J from the marine actinomycete *Salinispora tropica*, bromosalinosporamide, and thioester derivatives are potent inhibitors of the 20S proteasome. *J. Nat. Prod.* **2007**, *70*, 269–276.

27. While the reported IC_{50} value of **1005** is lower than that of **1**, the authors reported that they were not able to obtain an authentic sample of **1** for direct comparison.

28. a) Beer, L. L.; Moore, B. S. Biosynthetic convergence of salinosporamides A and B in the marine actinomycete *Salinispora tropica*. *Org. Lett.* **2007**, *9*, 845–848. b) Eustáquio, A. S.; Pojer, F.; Noel, J. P.; Moore, B. S. Discovery and characterization of a marine bacterial SAM-dependent chlorinase. *Nat. Chem. Biol.* **2007**, *4*, 69–74. c) McGlinchey, R. P.; Nett, M.; Eustáquio, A. S.; Asolkar, R. N.; Fenical, W.; Moore, B. S. Engineered biosynthesis of antiprotealide and other unnatural salinosporamide proteasome inhibitors. *J. Am. Chem. Soc.* **2008**, *130*, 7822–7823. d) Eustáquio, A. S.; McGlinchey, R. P.; Liu, Y.; Hazzard, C.; Beer, L. L.; Florova, G.; Alhamadsheh, M. M.; Lechner, A.; Kale, A. J.; Kobayashi, Y.; Reynolds, K. A.; Moore, B. S. Biosynthesis of the salinosporamide A polyketide synthase substrate chloroethylmalonyl-coenzyme A from *S*-adenosyl-L-methionine. *Proc. Natl. Acad. Sci. U.S.A.* **2009**, *106*, 12295–12300. e) Liu, Y.; Hazzard, C.; Eustaquio, A. S.; Reynolds, K. A.; Moore, B. S.

Biosynthesis of salinosporamides from α,β-unsaturated fatty acids: Implications for extending polyketide synthase diversity. *J. Am. Chem. Soc.* **2009**, *131*, 10376–10377. f) Nett, M.; Guider, T. A. M.; Kale, A. J.; Hughes, C. C.; Moore, B. S. Function-oriented biosynthesis of β-lactone proteasome inhibitors in *Salinispora tropica*. *J. Med. Chem.* **2009**, *52*, 6163–6167. g) Gulder, T. A. M.; Moore, B. S. Chasing the treasures of the sea-bacterial marine natural products. *Curr. Opin. Microbiol.* **2009**, *12*, 252–260. h) Eustáquio, A. S.; O'Hagan, D.; Moore, B. S. Engineering fluorometabolite production: Fluorinase expression in *Salinispora tropica* yields fluorosalinosporamide. *J. Nat. Prod.* **2010**, *73*, 378–382. i) Mahlstedt, S.; Fielding, E. N.; Moore, B. S.; Walsh, C. T. Prephenate decarboxylases: A new prephenate-utilizing enzyme family that performs nonaromatizing decarboxylation en route to diverse secondary metabolites. *Biochemistry* **2010**, *49*, 9021–9023.

29. Appel, A. Drugs: More shots on target. *Nature* **2011**, *480*, S40–S42.

30. Reddy, L. R.; Saravanan, P.; Corey, E. J. A simple stereocontrolled synthesis of salinosporamide A. *J. Am. Chem. Soc.* **2004**, *126*, 6230–6231.

31. Miyake, H.; Yamamura, K. Pd(0) catalyzed hydrostannation of conjugated dienes. A facile and highly regio- and stereoselective synthesis of (Z)-2-alkenylstannanes. *Chem. Lett.* **1992**, 507–508.

32. Corey, E. J.; Kürti, L. *Enantioselective Chemical Synthesis*, 1st ed.; Direct Book Publishing, Dallas, Texas, 2010, pp. 218–222.

33. The authors noted that attempts to react other metallo-cyclohex-2-ene reagents with **1024** were unproductive. For example, no product was observed when cyclohex-2-enyl lithium was, which is likely due to retro-aldol cleavage of the intermediate lithium alkoxide. Direct addition of the organostannane via a Lewis acid-catalyzed approach also failed.

34. Reddy, L. R.; Fournier, J.-F.; Reddy, B. V. S.; Corey, E. J. New synthetic route for the enantioselective total synthesis of salinosporamide A and biologically active analogues. *Org. Lett.* **2005**, *7*, 2699–2701.

35. Endo, A.; Danishefsky, S. J. Total synthesis of salinosporamide A. *J. Am. Chem. Soc.* **2005**, *127*, 8298–8299.

36. a) Thottathil, J. K.; Moniot, J. L.; Mueller, R. H.; Wong, M. K.; Kissick, T. P. Conversion of L-pyroglutamic acid to 4-alkyl-substituted L-prolines. The synthesis of *trans*-4-cyclohexyl-L-proline. *J. Org. Chem.* **1986**, *51*, 3140–3143. b) Hamada, Y.; Kawai, A.; Yasushi, K.; Hara, O.; Shioiri, T. Stereoselective total synthesis of AI-77-B, a gastroprotective substance from *Bacillus pumilus* AI-77. *J. Am. Chem. Soc.* **1989**, *111*, 1524–1525.

37. Moore, B. S.; Beer, L.; Eustaquio, A. S. Biosynthesis of salinosporamide A and analogs and methods thereof. U.S. Patent 2009/0325208 A1, December 31, 2009.

38. Mulholland, N. P.; Pattenden, G.; Walters, I. A. S. A concise total synthesis of salinosporamide A. *Org. Biol. Chem.* **2006**, *4*, 2845–2846.

39. Mulholland, N. P.; Pattenden, G.; Walters, I. A. S. A concise and straightforward total synthesis of (±)-salinosporamide A, based on a biosynthesis model. *Org. Biol. Chem.* **2008**, *6*, 2782–2789.

40. Nguyen, H.; Ma, G.; Gladysheva, T.; Fremgen, T.; Romo, D. Bioinspired total synthesis and human proteasome inhibitory activity of (−)-salinosporamide A, (−)-homosalinosporamide A, and derivatives obtained via organonucleophile promoted bis-cyclizations. *J. Org. Chem.* **2011**, *76*, 2–12, and references cited therein.

41. Evans, D. A.; Ennis, M. D.; Le, T.; Mandel, N.; Mandel, G. Asymmetric acylation reactions of chiral imide enolates. The first direct approach to the construction of chiral β-dicarbonyl synthons. *J. Am. Chem. Soc.* **1984**, *106*, 1154–1156.

42. Ma, G.; Nguyen, H.; Romo, D. Concise total synthesis of (±)-salinosporamide A, (±)-cinnabaramide A, and derivatives via a bis-cyclization process: Implications for a biosynthetic pathway? *Org. Lett.* **2007**, *9*, 2143–2146.

43. Ling, T.; Macherla, V. R.; Manam, R. R.; McArthur, K. A.; Potts, B. C. M. Enantioselective total synthesis of (−)-salinosporamide A (NPI-0052). *Org. Lett.* **2007**, *9*, 2289–2292.

44. Satoh, N.; Yokoshima, S.; Fukuyama, T. Total synthesis of (−)-salinosporamide A. *Org. Lett.* **2011**, *13*, 3028–3031.

45. Huisgen, R.; Funke, E.; Schaefer, F. C.; Knorr, R. Possible valence tautomerism of a mesoionic oxazol-5-one with an acylaminoketene. *Angew. Chem. Int. Ed.* **1967**, *6*, 367–368.

46. Tidwell, T. T. *Ketenes*, 2nd ed.; Wiley Interscience, Hoboken, New Jersey, 2006.

47. Wilde, R. G. Generation, cycloadditions, and tautomerism of *N*-acyl munchnones. *Tetrahedron Lett.* **1988**, *29*, 2027–2030.

48. a) Dghaym, R. D.; Dhawan, R.; Arndtsen, B. A. The use of carbon monoxide and imines as peptide derivative synthons: A facile palladium-catalyzed synthesis of α-amino acid derived imidazolines. *Angew. Chem. Int. Ed.* **2001**, *40*, 3228–3230. b) Dhawan, R.; Dghaym, R. D.; Arndtsen, B. A. The development of a catalytic synthesis of Münchnones: A simple four-component coupling approach to α-amino acid derivatives. *J. Am. Chem. Soc.* **2003**, *125*, 1474–1475.

49. Dhawan, R.; Arndtsen, B. A. Palladium-catalyzed multicomponent coupling of alkynes, imines, and acid chlorides: A direct and modular approach to pyrrole synthesis. *J. Am. Chem. Soc.* **2004**, *126*, 468–469.

50. Siamaki, A. R.; Arndtsen, B. A. A direct, one step synthesis of imidazoles from imines and acid chlorides: A palladium catalyzed multicomponent coupling approach. *J. Am. Chem. Soc.* **2006**, *128*, 6050–6051.

51. Dhawan, R.; Dghaym, R. D.; St. Cyr, D. J.; Arndtsen, B. A. Direct, palladium-catalyzed, multicomponent synthesis of β-lactams from imines, acid chloride, and carbon monoxide. *Org. Lett.* **2006**, *8*, 3927–3930.

52. Croce, P. D.; Ferraccioli, R.; La Rosa, C. Cycloaddition reactions of 5H,7H-thiazolo[3,4-*c*] oxazolium-1-oxides with imines. *Tetrahedron* **1995**, *51*, 9385–9392. (b) Cremonesi, G.; Croce, P. D.; La Rosa, C. Synthesis of imidazo[5,1-*b*]thiazoles or spiro-β-lactams by reaction of imines with mesoionic compounds or ketenes generated from *N*-acyl-thiazolidine-2-carboxylic acids. *Tetrahedron* **2004**, *60*, 93–97. (c) Cremonesi, G.; Dalla Croce, P.; La Rosa, C. [2+ 2] Cycloaddition reactions of imines with cyclic ketenes: Synthesis of 1,3-thiazolidine derived spiro‐β‐lactams and their transformations. *Helv. Chim. Acta* **2005**, *88*, 1580–1588.

53. Knunyants, I. L.; Cheburkov, Y. A. Fluorine containing β-lactones I. β,β-Bis(trifluoromethyl)-β-propiolactone and its properties. *Izvest. Akad. Nauk SSSR, Otd. Khim.* **1960**, 678–685.

54. Neidlein, B. Dicyanoketene. *Angew. Chem. Int. Ed.* **1978**, *17*, 369–370.

55. Weyler, W., Jr; Duncan, W. G.; Moore, H. W. Rearrangements of azidoquinones. XVI. Thermal and photolytic rearrangements of 2,5-diazido-1,4-quinones. Synthesis and chemistry of cyanoketenes. *J. Am. Chem. Soc.* **1975**, *97*, 6187–6192.

56. Wynberg, H.; Staring, E. G. J. Catalytic asymmetric synthesis of chiral 4-substituted 2-oxetanones. *J. Org. Chem.* **1985**, *50*, 1977–1979.

57. Zhu, C.; Shen, X.; Nelson, S. G. Cinchona alkaloid-Lewis acid catalyst systems for enantioselective ketene-aldehyde cycloadditions. *J. Am. Chem. Soc.* **2004**, *126*, 5352–5353.

58. Wilson, J. E.; Fu, G. C. Asymmetric synthesis of highly substituted β-lactones by nucleophile-catalyzed [2+2] cycloadditions of disubstituted ketenes with aldehydes. *Angew. Chem. Int. Ed.* **2004**, *43*, 6358–6360.

59. Yang, H. W.; Romo, D. A highly diastereoselective, tandem Mukaiyama aldol-lactonization route to β-lactones: Application to a concise synthesis of the potent pancreatic lipase inhibitor, (–)-panclicin D. *J. Org. Chem.* **1997**, *62*, 4–5.

60. Zhao, C.; Mitchell, T. A.; Vallakati, R.; Pérez, L. M.; Romo, D. Mechanistic investigations of the $ZnCl_2$-mediated tandem Mukaiyama aldol lactonization:

Evidence for asynchronous, concerted transition states and discovery of 2-oxopyridyl ketene acetal variants. *J. Am. Chem. Soc.* **2012**, *134*, 3084–3094.

61. Mitchell, T. A.; Zhao, C.; Romo, D. Highly diastereoselective, tandem, three-component synthesis of tetrahydrofurans from ketoaldehydes via silylated β-lactone intermediates. *Angew. Chem. Int. Ed.* **2008**, *47*, 5026–5029.

62. Schmitz, W. D.; Messerschmidt, N. B.; Romo, D. A β-Lactone-based strategy applied to the total synthesis of (8*S*, 21*S*, 22*S*, 23*R*)-and (8*R*, 21*S*, 22*S*, 23*R*)-okinonellin B. *J. Org. Chem.* **1998**, *63*, 2058–2059.

63. Wang, Y.; Romo, D. Concise total synthesis of (+)-brefeldin A: A combined β-lactone/cross-metathesis-based strategy. *Org. Lett.* **2002**, *4*, 3231–3234.

64. Cho, S. W.; Romo, D. Total synthesis of (–)-belactosin C and derivatives via double diastereoselective tandem Mukaiyama aldol-lactonizations. *Org. Lett.* **2007**, *9*, 1537–1540.

65. Zhang, W.; Richardson, R. D.; Chamni, S.; Smith, J. W.; Romo, D. β-Lactam congeners of orlistat as inhibitors of fatty acid synthase. *Bioorg. Med. Chem. Lett.* **2008**, *18*, 2491–2494.

66. a) Cortez, G. S.; Tennyson, R. L.; Romo, D. Intramolecular, nucleophile-catalyzed aldol-lactonization (NCAL) reactions: Catalytic, asymmetric synthesis of bicyclic β-lactones. *J. Am. Chem. Soc.* **2001**, *123*, 7945–7946. b) Oh, S. H.; Cortez, G. S.; Romo, D. Asymmetric synthesis of bicyclic β-lactones via the intramolecular, nucleophile-catalyzed aldol lactonization: Improved efficiency and expanded scope. *J. Org. Chem.* **2005**, *70*, 2835–2838.

67. Reddy, L. R.; Corey, E. J. Novel bicyclization reaction leading to a fused β-lactone. *Org. Lett.* **2006**, *8*, 1717–1719.

68. Hoye, T. R.; Danielson, M. E.; May, A. E.; Zhao, H. Dual macrolactonization/ pyran-hemiketal formation via acylketenes: Applications to the synthesis of (–)-callipeltoside A and a lyngbyaloside B model system. *Angew. Chem. Int. Ed.* **2008**, *47*, 9743–9746.

69. Manam, R. R.; Macherla, V. R.; Tsueng, G.; Dring, C. W.; Weiss, J.; Neuteboom, S. T. C.; Lam, K. S.; Potts, B. C. Antiprotealide is a natural product. *J. Nat. Prod.* **2009**, *72*, 295–297.

70. Crich, D.; Yao, Q. The 4,6-*O*-[α-(2-(2- iodophenyl)ethylthiocarbonyl) benzylidene] protecting group: Stereoselective glycosylation, reductive radical fragmentation, and synthesis of β-D-rhamnopyranosides and other deoxy sugars. *Org. Lett.* **2003**, *5*, 2189–2191.

71. Thayumanavan, R.; Tanaka, F.; Barbas III, C. F. Direct organocatalytic asymmetric aldol reactions of α-amino aldehydes: Expedient syntheses of highly enantiomerically enriched anti-β-hydroxy-α-amino acids. *Org. Lett.* **2004**, *6*, 3541–3544.

72. Fisk, J. S.; Mosey, R. A.; Tepe, J. J. The diverse chemistry of oxazol-5-(4*H*)-ones. *Chem. Soc. Rev.* **2007**, *36*, 1432–1440.

73. Douglas, K. T. Elimination-addition pathways for thiol esters. *Acc. Chem. Res.* **1986**, *19*, 186–192.

74. Haeusler, J. Synthesis of (–)-detoxine D1. *Liebigs Annalen der Chemie* **1986**, *1986*, 114–126.

75. Homami, S. -S.; Mukerjee, A. K. Reactions of 4-heteromethylene- and 4-heteroethylidene-2-phenyl-2-oxazolin-5-ones with different nucleophiles and related studies. *Indian J. Chem., Sect. B: Org. Chem. Incl. Med. Chem.* **1992**, *31*, 411–414.

76. Calter, M. A. Catalytic, asymmetric dimerization of methylketene. *J. Org. Chem.* **1996**, *61*, 8006–8007.

77. Takagaki, H.; Yasuda, N.; Asaoka, M.; Takei, H. Preparation of 5-trimethylsiloxyoxazoles from 2-oxazolin-5-ones and their Diels–Alder reaction: Synthesis of vitamin B_6 derivatives. *Chem. Lett.* **1979**, 183–186.

78. Bello, C. D.; Filira, F.; Giormani, V.; D'Angeli, F. An investigation of racemisation during the use of acetoacetyl-L-valine in peptide synthesis. *J. Chem. Soc. (C)* **1969**, 350–352.

79. Chen, F. M. F.; Kudroda, K.; Benoiton, N. L. A simple preparation of 5-oxo-4,5-dihydro-1,3-oxazoles (oxazolones). *Synthesis* **1979**, 230–232.

80. Bodanszky, M.; Bodanszky, A. Racemization in peptide synthesis. Mechanism-specific models. *Chem. Commun.* **1967**, 591–593.

81. Mosey, R. A.; Tepe, J. J. New synthetic route to access (+/-) salinosporamide A via an oxazolone-mediated ene-type reaction. *Tetrahedron Lett.* **2009**, *50*, 295–297.

82. Melhado, A. D.; Luparia, M.; Toste, F. D. Au(I)-catalyzed enantioselective 1,3-dipolar cycloadditions of Münchnones with electron-deficient alkenes. *J. Am. Chem. Soc.* **2007**, *129*, 12638–12639.

83. Terada, M.; Moriya, K.; Kanomata, K.; Sorimachi, K. Chiral Brønsted acid catalyzed stereoselective addition of azlactones to 3-vinylindoles for facile access to enantioenriched tryptophan derivatives. *Angew. Chem. Int. Ed.* **2011**, *50*, 12586–12590.

84. Leibfarth, F. A.; Kang, M.; Ham, M.; Kim, J.; Campos, L. M.; Gupta, N.; Moon, B.; Hawker, C. J. A facile route to ketene-functionalized polymers for general materials applications. *Nat. Chem.* **2010**, *2*, 207–212.

85. Gaussian 09, Revision **A.1**, Frisch, M. J.; Trucks, G. W.; Schlegel, H. B.; Scuseria, G. E.; Robb, M. A.; Cheeseman, J. R.; Scalmani, G.; Barone, V.; Mennucci, B.; Petersson, G. A.; Nakatsuji, H.; Caricato, M.; Li, X.; Hratchian, H. P.; Izmaylov, A. F.; Bloino, J.; Zheng, G.; Sonnenberg, J. L.; Hada, M.; Ehara, M.; Toyota, K.; Fukuda, R.; Hasegawa, J.; Ishida, M.; Nakajima, T.; Honda, Y.; Kitao, O.; Nakai, H.; Vreven, T.; Montgomery, Jr., J. A.; Peralta, J. E.; Ogliaro, F.; Bearpark, M.; Heyd, J. J.; Brothers, E.; Kudin, K. N.; Staroverov, V. N.; Kobayashi, R.; Normand, J.; Raghavachari, K.; Rendell, A.; Burant, J. C.; Iyengar, S. S.; Tomasi, J.; Cossi, M.; Rega, N.; Millam, J. M.; Klene, M.; Knox, J. E.; Cross, J. B.; Bakken, V.; Adamo, C.; Jaramillo, J.; Gomperts, R.; Stratmann, R. E.; Yazyev, O.; Austin, A. J.; Cammi, R.; Pomelli, C.; Ochterski, J. W.; Martin, R. L.; Morokuma, K.; Zakrzewski, V. G.; Voth, G. A.; Salvador, P.; Dannenberg, J. J.; Dapprich, S.; Daniels, A. D.; Farkas, Ö.; Foresman, J. B.; Ortiz, J. V.; Cioslowski, J.; Fox, D. J. Gaussian, Inc., Wallingford CT, 2009.

86. Baitinger, I.; Mayer, P.; Trauner, D. Toward the total synthesis of maoecrystal V: Establishment of contiguous quaternary stereocenters. *Org. Lett.* **2010**, *12*, 5656–5659.

87. Shimoda, Y.; Kotani, S.; Sugiura, M.; Nakajima, M. Enantioselective double aldol reaction catalyzed by chiral phosphine oxide. *Chem. Eur. J.* **2011**, *17*, 7992–7995.

88. a) Staunton, J.; Weissman, K. J. Polyketide biosynthesis: A millennium review. *Nat. Prod. Rep.* **2001**, *18*, 380–416. b) Hill, A. M. The biosynthesis, molecular genetics and enzymology of the polyketide-derived metabolites. *Nat. Prod. Rep.* **2006**, *23*, 256–320.

89. a) Lalic, G.; Aloise, A. D.; Shair, M. D. An exceptionally mild catalytic thioester aldol reaction inspired by polyketide biosynthesis. *J. Am. Chem. Soc.* **2003**, *125*, 2852–2853. b) Fortner, K. C.; Shair, M. D. Stereoelectronic effects dictate mechanistic dichotomy between Cu(II)-catalyzed and enzyme-catalyzed reactions of malonic acid half thioesters. *J. Am. Chem. Soc.* **2007**, *129*, 1032–1033.

90. Smith, A. M. R.; Rzepa, H. S.; White, A. J. P.; Billen, D.; Hii, K. K. M. Delineating origins of stereocontrol in asymmetric Pd-catalyzed α-hydroxylation of 1,3-ketoesters. *J. Org. Chem.* **2010**, *75*, 3085–3096.

91. Hartung, W. H.; Beaujon, J. H. R.; Cocolas, G. *Org. Syn.* **1960**, *40*, 24–26.

92. Hogan, P. C.; Corey, E. J. Proteasome inhibition by a totally synthetic β-lactam related to salinosporamide A and omuralide. *J. Am. Chem. Soc.* **2005**, *127*, 15386–15387.

93. The most recent report by Romo and co-workers on the total synthesis (–)-**1** (summarized in Section 1.6.2) used MsCl as the acid-activating agent (see ref 40). These studies were reported after we performed the experiments presented in Section 4.1.2.

94. The authors noted that the commercially available reagent (i.e. 2-chloro-1-methylpyridinium iodide) led to reduced yields, which they attribute to the nucleophilic iodide counterion.

95. Danishefsky and co-workers also noted that a similar reaction proceeded with poor stereoselectivity when adding to lactams lacking *N*-PMB functionalization (see Section 1.4.2).

96. Potts and co-workers have demonstrated that salinosporamide A (**1**) readily reacts with mercaptan under dilute (cf. 0.01 M) basic conditions (Et_3N) to convert the β-lactone into a mixture of γ-lactam-containing thioesters (see ref 26).

97. Two doublets present at 5.19 and 5.01 ppm with large coupling constants (J = 14.6 Hz for each) likely correspond to diastereotopic, benzylic methylene hydrogen atoms of two diastereomers. By treating the reaction mixture with $TMSCH_2N_2$ we were able to isolate several γ-lactam-containing methyl esters.

98. Kohler, M. C.; Yost, J. M.; Garnsey, M. R.; Coltart, D. M. Direct carbon-carbon bond formation via soft enolization: A biomimetic asymmetric Mannich reaction of phenylacetate thioesters. *Org. Lett.* **2010**, *12*, 3376–3379.

99. Sheehan, J.; Cruickshank, P.; Boshart, G. A convenient synthesis of water-soluble carbodiimides. *J. Org. Chem.* **1961**, *26*, 2525–2528.

100. Balskus, E. P.; Jacobsen, E. N. α,β-Unsaturated β-silyl imide substrates for catalytic, enantioselective conjugate additions: A total synthesis of (+)-lactacystin and the discovery of a new proteasome inhibitor. *J. Am. Chem. Soc.* **2006**, *128*, 6810–6812.

101. This result of this experiment was not unexpected given our previous attempts at heating thioester **4050** with a substoichiometric amount of urea **4068**. However, it should be noted that it was not until this experiment was performed that we were able to isolate and elucidate the structure of unsaturated lactam **4077**.

102. MacroModel, version 9.9, Schrödinger, LLC, New York, NY, 2012.

103. Maestro, version 9.4, Schrödinger, LLC, New York, NY, 2013.

104. The structure of both lactam **4053** and **4054** was subjected to Monte-Carlo conformational analysis using the mixed-torsional/low-mode sampling method with the OPLS_2005 molecular mechanics force field potential in MacroModel. In total, 301 conformers were found for **4053**, and 225 conformers were found for

4054. The range of energies calculated for each conformer of both diastereomers were compared by inspection.

105. For references that propose similar roles for π-stacking interactions see Knowles, R. R.; Jacobsen, E. N. Attractive noncovalent interactions in asymmetric catalysis: Links between enzymes and small molecule catalysts. *Proc. Natl. Acad. Sci. USA* **2010**, *107*, 20678–20685.

106. Singh, R. K.; Danishefsky, S. Preparation of activated cyclopropanes by phase transfer alkylation. *J. Org. Chem.* **1975**, *40*, 2969–2970.

107. When preparing acid **4100** from ethyl acetoacetate following the procedure in ref. 106 we found the use of tetra-*n*-butylammonium hydroxide instead of benzyltrimethylammonium chloride led to reduced yields (ca. 0-15%).

108. Kimura, Y.; Atarashi, S.; Kawakami, K.; Sato, K.; Hayakawa, I. (Fluorocyclopropyl)quinolones. 2. Synthesis and stereochemical structure-activity relationships of chiral 7-(7-amino-5-azaspiro[2.4]heptan-5-yl)-1-(2-fluorocyclopropyl)quinolone antibacterial agents. *J. Med. Chem.* **1994**, *37*, 3344–3352.

109. Padwa, A.; Curtis, E. A.; Sandanayaka, V. P. Generation and cycloaddition behavior of spirocyclic carbonyl ylides. Application to the synthesis of the pterosin family of sesquiterpenes. *J. Org. Chem.* **1996**, *61*, 73–81.

110. Yao, Y.; Fan, W.; Li, W.; Ma, X.; Zhu, L.; Xie, X.; Zhang, Z. Synthesis of (*S*)-7-amino-5-azaspiro[2.4]heptane via highly enantioselective hydrogenation of protected ethyl 1-(2-aminoaceto)cyclopropanecarboxylates. *J. Org. Chem.* **2011**, *76*, 2807–2813.

111. Acid chloride **4104** was obtained with increased yields and purity were observed when freshly distilled oxalyl chloride was used. Attempts to purify either **4104** or its acid precursor **4100** by Kugelrohr distillation were unsuccessful.

112. Lee, Y.-T.; Jang, Y.-J.; Syu, S.-E.; Chou, S.-C.; Lee, C.-J.; Lin, W. Preparation of functional benzofurans and indoles via chemoselective intramolecular Wittig reactions. *Chem. Commun.* **2012**, *48*, 8135–8137.

113. We followed a related procedure cited in: Williams, D. R.; Cortez, G. S.; Bogen, S. L.; Rojas, C. M. Total synthesis of lankacyclinol. *Angew. Chem. Int. Ed.* **2000**, *39*, 4612–4615.

114. Re-inspection of the crude ^{1}H NMR of acid **4111** revealed two sets of resonances at 5.21 (d, J = 14.6 Hz) and 5.08 (d, J = 14.6 Hz). These peaks may correspond to products resulting from a LiOH-mediated intramolecular aldol reaction. Treating either of these aldolates with EDCI would likely form a β-lactone, which would be ring-opened in the presence of thiol to give either lactam **4113** or **4114**.

115. Thenot, J.-P., and Horning, E.C. Amino acid *N*-dimethyllaminomethylene alkyl esters. New derivatives for GC and GC-MS studies. *Anal. Lett.* **1972**, *5*, 519–529.

116. Evans, D. A.; Sjogren, E. B.; Weber, A. E.; Conn, R. E. Asymmetric synthesis of *anti*-β-hydroxy-α-amino acids. *Tetrahedron Lett.* **1987**, *28*, 39–42.

117. Saravanan, P.; Corey, E. A short, stereocontrolled, and practical synthesis of alpha-methylomuralide, a potent inhibitor of proteasome function. *J. Org. Chem.* **2003**, *68*, 2760–2764.

118. *n*-Butanethiol possesses an unpleasant odor that is nearly as detectable as EtSH, however, glassware contaminated with either EtSH or BuSH can be readily deodorized by leaving in a well-ventilated hood space for one week and then soaking overnight with bleach. I prefer both evaporation and bleaching because bleaching is slow, and I often 'missed' spots in my soaking. This was problematic when it was time to take the glassware to the sink for a thorough scrubbing. Ethanethiol should be avoided because the packing material is contaminated with trance amounts of ethanethiol, which is more difficult to manage than contaminated glass and leads to disgruntled delivery personnel.

119. Adams, Z. M.; Jackson, R. F. W.; Palmer, N. J.; Rami, H. K.; Wythes, M. J. Stereoselective syntheses of protected β-hydroxy-α-amino acids using (arylthio)nitrooxiranes. *J. Chem. Soc., Perkin Trans. 1* **1999**, 937–948.

120. CAUTION! Storing benzenesulfenyl chloride neat for several weeks will result in spontaneously dimerization to form diphenyl disulfide and Cl_2. I have personally witnessed a vial explode that had pressurized from the Cl_2 gas that had formed. While the same observations have not been made for the 4-methyl analogue, caution should certainly be exercised and the reactant should be used immediately after preparation.

121. Padwa, A.; Dean, D. C.; Osterhout, M. H.; Precedo, L.; Semones, M. A. Synthesis of functionalized azomethine ylides via the Rh(II)-catalyzed cyclization of α-diazo carbonyls onto imino π-bonds. *J. Org. Chem.* **1994**, *59*, 5347–5357.

122. Morita, Y.; Kamakura, R.; Takeda, M.; Yamamoto, Y. Convenient preparation of trifluoroacetyl Meldrum's acid and its use as a building block for trifluoromethyl-containing compounds. *Chem. Commun.* **1997**, 359–360.

123. Hoffman, R. W. *Dehydrobenzene and Cycloalkynes*; Organic Chemistry, A Series of Monographs 11; Academic, 1967.

124. Wenk, H. H.; Winkler, M.; Sander, W. One century of aryne chemistry. *Angew. Chem. Int. Ed.* **2003**, *42*, 502–528.

125. Stoermer, R; Kahlert, B. Ueber das 1- und 2-brom-cumaron. *Ber. Dtsch. Chem. Ges.* **1902**, *35*, 1633–1640.

126. Bachmann, W. E.; Clarke, H. T. The mechanism of the Wurtz-Fittig reaction. *J. Am. Chem. Soc.* **1927**, *49*, 2089–2098.

127. Wittig, V. G.; Phenyl-lithium, der Schlüssel zu einer neuen Chemie metallorganischer Verbindungen. *Naturwissenschaften* **1942**, *30*, 696–703.

128. Gilman, H.; Avakian, S. Dibenzofuran. XXIII. Rearrangement of halogen compounds in amination by sodamide. *J. Am. Chem. Soc.* **1945**, *67*, 349–351.

129. Roberts, J. D.; Simmons, H. E., Jr.; Carlsmith, L. A.; Vaughan, C. W. Rearrangement in the reaction of chlorobenzene-1-C^{14} with potassium amide. *J. Am. Chem. Soc.* **1953**, *75*, 3290–3291 and references cited therein.

130. Leopold, D. G.; Miller, A. E. S.; Lineberger, W. C. Determination of the singlet-triplet splitting and electron affinity of *o*-benzyne by negative ion photoelectron spectroscopy. *J. Am. Chem. Soc.* **1986**, *108*, 1379–1384.

131. Radziszewski, J. G.; Hess, B. A., Jr.; Zahradnik, R. Infrared spectrum of *o*-benzyne: Experiment and theory. *J. Am. Chem. Soc.* **1992**, *114*, 52–57.

132. a) Tadross, P. M.; Stoltz, B. M. A comprehensive history of arynes in natural product total synthesis. *Chem. Rev.* **2012**, *112*, 3550–3577. b) Gampe, C. M.; Carreira, E. M. Arynes and cyclohexyne in natural product synthesis. *Angew. Chem. Int. Ed.* **2012**, *51*, 3766–3778.

133. Campbell, C. D.; Rees, C. W. Reactive intermediates. Part I. Synthesis and oxidation of 1- and 2-aminobenzotriazole. *J. Chem. Soc., C* **1969**, 742.

134. Himeshima, Y.; Sonoda, T.; Kobayashi, H. Fluoride-induced 1, 2-elimination of *o*-trimethylsilylphenyl triflate to benzyne under mild conditions. *Chem. Lett.* **1983**, 1211–1214.

135. Tambar, U. K.; Ebner, D. C.; Stoltz, B. M. A Convergent and enantioselective synthesis of (+)-amurensinine via selective C−H and C−C bond insertion reactions. *J. Am. Chem. Soc.* **2006**, *128*, 11752–11753.

136. Kitamura, T.; Yamane, M. (Phenyl)[*o*-(trimethylsilyl)phenyl]iodonium triflate. A new and efficient precursor of benzyne. *Chem. Commun.* **1995**, 983–984.

137. Bronner, S. M.; Garg, N. K. Efficient synthesis of 2-(trimethylsilyl)phenyl trifluoromethanesulfonate: A versatile precursor to *o*-benzyne. *J. Org. Chem.* **2009**, *74*, 8842–8843.

138. Stiles, M.; Miller, R. G.; Burckhardt, U. Reactions of benzyne intermediates in non-basic media. *J. Am. Chem. Soc.* **1963**, *85*, 1792–1797.

139. Wittig, G.; Hoffmann, R. W. 1,2,3-Benzothiadiazole 1,1-dioxide. *Org. Syn.* **1967**, *47*, 4–9.

140. Le Goff, E. Aprotic generation of benzyne from diphenyliodonium-2-carboxylate. *J. Am. Chem. Soc.* **1962**, *84*, 3786–3786.

141. Cho, H. Y.; Ajaz, A.; Himali, D.; Waske, P. A.; Johnson, R. P. Microwave flash pyrolysis. *J. Org. Chem.* **2009**, *74*, 4137–4142.

142. Kitamura, T. Synthetic Methods for the Generation and Preparative Application of Benzyne. *Aust. J. Chem.* **2010**, *63*, 987.

143. a) Hoye, T. R.; Baire, B.; Niu, D.; Willoughby, P. H.; Woods, B. P. The hexadehydro-Diels–Alder reaction. *Nature* **2012**, *490*, 208–212. Niu, D.; Willoughby, P. H.; Woods, B. P.; Baire, B.; Hoye, T. R. Alkane desaturation via concerted double hydrogen atom transfer to benzyne. *Nature* **2013**, *accepted*.

144. Bailey, W. F.; Jiang, X. Stereochemistry of the cyclization of 4-(*t*-butyldimethyl)siloxy-5-hexenyllithium: *cis*-Selective ring-closure accompanied by retro-[1,4]-Brook rearrangement. *ARKIVOK* **2005**, *6*, 25–32.

145. Bradley, A. Z.; Johnson, R. P. Thermolysis of 1,3,8-nonatriyne: Evidence for intramolecular [2+ 4] cycloaromatization to a benzyne intermediate. *J. Am. Chem. Soc.* **1997**, *119*, 9917–9918.

146. Miyawaki, K.; Suzuki, R.; Kawano, T.; Ueda, I. Cycloaromatization of a non-conjugated polyenyne system: Synthesis of 5*H*-denzo[*d*]fluoreno[3,2-*b*]pyrans via diradicals generated from 1-[2-{4-(2-alkoxymethylphenyl)butan-1,3-diynyl}]phenylpentan-2,4-diyn.l-ols and trapping evidence for the 1,2-didehydrobenzene diradical. *Tetrahedron Lett.* **1997**, *38*, 3943–3946.

147. Brown, R. F.; Coulston, K. J.; Eastwood, F. W. Formation of biphenylene by elimination of C_2 from 9, 10-didehydrophenanthrene at 1100 ºC. *Tetrahedron Lett.* **1996**, *37*, 6819–6820.

148. a) Miyawaki, K.; Kawano, T.; Ueda, I. Multiple cycloaromatization of novel aromatic enediynes bearing a triggering device on the terminal acetylene carbon. *Tetrahedron Lett.* **1998**, *39*, 6923–6926. b) Ueda, I.; Sakurai, Y.; Kawano, T.; Wada, Y.; Futai, M. An unprecedented arylcarbene formation in thermal reaction of non-conjugated aromatic enetetraynes and DNA strand cleavage. *Tetrahedron Lett.* **1999**, *40*, 319–322. c) Miyawaki, K.; Kawano, T.; Ueda, I. Domino thermal radical cycloaromatization of non-conjugated aromatic hexa- and heptaynes: Synthesis of fluoranthene and benzo[*a*]rubicene skeletons. *Tetrahedron Lett.* **2000**, *41*, 1447–1451. d) Kawano, T.; Inai, H.; Miyawaki, K.; Ueda, I. Synthesis of indenothiophenone derivatives by cycloaromatization of non-conjugated thienyl tetraynes. *Tetrahedron Lett.* **2005**, *46*, 1233–1236. e) Kawano, T.; Inai, H.; Miyawaki, K.; Ueda, I. Effect of water molecules on the cycloaromatization of non-conjugated aromatic tetraynes. *Bull. Chem. Soc. Jpn.* **2006**, *79*, 944–949. f) Kawano, T.; Suehiro, M.; Ueda, I. Synthesis and inclusion properties of 6,6′-Bi(benzo[*b*]fluoren-5-ol) derivative by cycloaromatization. *Chem. Lett.* **2006**, *35*, 58–59. g) Kimura, H.; Torikai, K.; Miyawaki, K.; Ueda, I. Scope of the thermal

cyclization of nonconjugated ene–yne–nitrile system: A facile synthesis of cyanofluorenol derivatives. *Chem. Lett.* **2008**, *37*, 662–663. h) Torikai, K.; Otsuka, Y.; Nishimura, M.; Sumida, M.; Kawai, T.; Sekiguchi, K.; Ueda, I. Synthesis and DNA cleaving activity of water-soluble non-conjugated thienyl tetraynes. *Bioorgan. Med. Chem.* **2008**, *16*, 5441–5451.

149. Tsui, J. A.; Sterenberg, B. T. A metal-templated 4 + 2 cycloaddition reaction of an alkyne and a diyne to form a 1,2-aryne. *Organometallics* **2009**, *28*, 4906–4908.

150. Tsui, J. A.; Bolton, T. M.; Sterenberg, B. T. Tungsten coordination chemistry of 1,4-bisdiphenylphosphinobutadiyne–synthesis of coordination macrocycles and factors controlling diyne cycloaddition. *Can. J. Chem.* **2009**, *87*, 197–204.

151. Strozier, R. W.; Caramella, P.; Houk, K. N. Influence of molecular distortions upon reactivity and stereochemistry in nucleophilic additions to acetylenes. *J. Am. Chem. Soc.* **1979**, *101*, 1340–1343.

152. Ajaz, A.; Bradley, A. Z.; Burrell, R. C.; Li, W. H. H.; Daoust, K. J.; Bovee, L. B.; DiRico, K. J.; Johnson, R. P. Concerted vs stepwise mechanisms in dehydro-Diels–Alder reactions. *J. Org. Chem.* **2011**, 9320–9328

153. Siebert, M. R.; Osbourn, J. M.; Brummond, K. M.; Tantillo, D. J. Differentiating mechanistic possibilities for the thermal, intramolecular [2 + 2] cycloaddition of allene−ynes. *J. Am. Chem. Soc.* **2010**, *132*, 11952–11966.

154. Wessig, P.; Müller, G. The dehydro-Diels−Alder reaction. *Chem. Rev.* **2008**, *108*, 2051–2063.

155. McNally, A.; Prier, C. K.; MacMillan, D. W. C. Discovery of an α-amino C–H arylation reaction using the strategy of accelerated serendipity. *Science* **2011**, *334*, 1114–1117.

156. J. Suffert, E. Abraham, S. Raeppel, R. Brückner, Synthesis of 5-/10-membered ring analogues of the dienediyne core of neocarzinostatine chromophore by palladium(0)-mediated ring-closure reaction. *Liebigs Ann.* **1996**, 447–456.

157. Jayanth, T. T.; Jeganmohan, M.; Cheng, M.-J.; Chu, S.-Y.; Cheng, C.-H. Ene reaction of arynes with alkynes. *J. Am. Chem. Soc.* **2006**, *128*, 2232–2233.

158. Candito, D. A.; Panteleev, J.; Lautens, M. Intramolecular aryne–ene reaction: Synthetic and mechanistic studies. *J. Am. Chem. Soc.* **2011**, *133*, 14200–14203.

159. Liu, P.; Cheong, P. H.-Y.; Yu, Z.-X.; Wender, P. A.; Houk, K. N. Substituent effects, reactant preorganization, and ligand exchange control the reactivity in Rh^{I}-catalyzed (5+2) cycloadditions between vinylcyclopropanes and alkynes. *Angew. Chem. Int. Ed.* **2008**, *47*, 3939–3941.

160. Yin, W.; He, C.; Chen, M.; Zhang, H.; Lei, A. Nickel-catalyzed oxidative coupling reactions of two different terminal alkynes using O_2 as the oxidant at room temperature: Facile syntheses of unsymmetric 1,3-diynes. *Org. Lett.* **2009**, *11*, 709–712.

161. a) Shi, M.; Lu, J.-M.; Wei, Y.; Shao, L.-X. Rapid generation of molecular complexity in the Lewis or Brønsted acid-mediated reactions of methylenecyclopropanes. *Acc. Chem. Res.* **2012**, *45*, 641–652. b) Nakamura, I.; Yamamoto, Y. Transition metal–catalyzed reactions of methylenecyclopropanes. *Adv. Synth. Catal.* **2002**, *344*, 111–129.

162. Karmakar, R.; Mamidipalli, P.; Yun, S. Y.; Lee, D. Alder-ene reactions of arynes. *Org. Lett.* **2013**, *15*, 1938–1941.

163. Robinson, J. M.; Sakai, T.; Okano, K.; Kitawaki, T.; Danheiser, R. L. Formal [2+2+2] cycloaddition strategy based on an intramolecular propargylic ene reaction/Diels−Alder cycloaddition cascade. *J. Am. Chem. Soc.* **2010**, *132*, 11039–11041.

164. Yun, S. Y.; Wang, K.-P.; Lee, N.-K.; Mamidipalli, P.; Lee, D. Alkane C–H insertion by aryne intermediates with a silver catalyst. *J. Am. Chem. Soc.* **2013**, *135*, 4668–4671.

165. Manet, I.; Monti, S.; Fagnoni, M.; Protti, S.; Albini, A. Aryl cation and carbene intermediates in the photodehalogenation of chlorophenols. *Chem. Eur. J.* **2005**, *11*, 140–151.

166. Liu, Z.; Larock, R. C. Facile *O*-arylation of phenols and carboxylic acids. *Org. Lett.* **2004**, *6*, 99–102.

167. Hamura, T.; Ibusuki, Y.; Sato, K.; Matsumoto, T.; Osamura, Y.; Suzuki, K. Strain-induced regioselectivities in reactions of benzyne possessing a fused four-membered ring. *Org. Lett.* **2003**, *5*, 3551–3554.

168. Garr, A. N.; Luo, D.; Brown, N.; Cramer, C. J.; Buszek, K. R.; VanderVelde, D. Experimental and theoretical investigations into the unusual regioselectivity of 4,5-, 5,6-, and 6,7-indole aryne cycloadditions. *Org. Lett.* **2010**, *12*, 96–99.

169. Cheong, P. H. Y.; Paton, R. S.; Bronner, S. M.; Im, G.-Y. J.; Garg, N. K.; Houk, K. N. Indolyne and aryne distortions and nucleophilic regioselectivities. *J. Am. Chem. Soc.* **2010**, *132*, 1267–1269.

170. Alabugin, I. V.; Gold, B. Two functional groups in one package: Using both alkyne π-bonds in cascade transformations. *J. Org. Chem.* **2013**, *ASAP*, (DOI: 10.1021/jo401091w).

171. Choi, J.; MacArthur, A. H. R.; Brookhart, M.; Goldman, A. S. Dehydrogenation and related reactions catalyzed by iridium pincer complexes. *Chem. Rev.* **2011**, *111*, 1761–1779.

172. Hoye, T. R.; Eklov, B. M.; Voloshin, M. No-D NMR spectroscopy as a convenient method for titering organolithium (RLi), RMgX, and LDA solutions. *Org. Lett.* **2004**, *6*, 2567–2570.

173. a) Hünig, S.; Müller, H.-R.; Thier, W. Reduktionen mit diimid. *Tetrahedron Lett.* **1961**, *2*, 353–357. b) Corey, E. J.; Pasto, D. J.; Mock, W. L. Chemistry of diimide. II. Stereochemistry of hydrogen transfer to carbon-carbon multiple bonds. *J. Am. Chem. Soc.* **1961**, *83*, 2957–2958.

174. Fernández, I.; Cossío, F. P.; Sierra, M. A. Dyotropic reactions: Mechanisms and synthetic applications. *Chem. Rev.* **2009**, *109*, 6687–6711.

175. Fernández, I.; Sierra, M. A.; Cossío, F. P. In-plane aromaticity in double group transfer reactions. *J. Org. Chem.* **2007**, *72*, 1488–1491.

176. The procedure was adopted from the conditions reported ref 160, namely $NiCl_2$ was used as an additive and THF was used as solvent.

177. a) Pauli, G. F.; Jaki, B. U.; Lankin, D. C. Quantitative ^{1}H NMR: Development and potential of a method for natural products analysis. *J. Nat. Prod.* **2005**, *68*, 133–149. b) Pauli, G. F.; Jaki, B. U.; Lankin D. A., Routine experimental protocol for qHNMR illustrated with taxol. *J. Nat. Prod.* **2007**, *70*, 589–595.

178. Kitamura, T.; Kotani, M.; Yokoyama, T.; Fujiwara, Y.; Hori, K. A new hypervalent iodine precursor of a highly strained cyclic alkyne. Generation and trapping reactions of bicyclo[2.2.1]hept-2-en-5-yne. *J. Org. Chem.* **1999**, *64*, 680–681.

179. Almeida, G. de; Townsend, L. C.; Bertozzi, C. R. Synthesis and reactivity of dibenzoselenacycloheptynes. *Org. Lett.* **2013**, *15*, 3038–3041.

180. Scardiglia, F.; Roberts, J. D. Reactions of non-activated aryl halides with nucleophilic agents induced by alkali amides in liquid ammonia. *Tetrahedron* **1958**, *3*, 197–208.

181. Wu, X.; Fors, B. P.; Buchwald, S. L. A single phosphine ligand allows palladium-catalyzed intermolecular C–O bond formation with secondary and primary alcohols. *Angew. Chem. Int. Ed.* **2011**, *50*, 9943–9947.

182. Nicolaou, K. C.; Snyder, S. A. Chasing molecules that were never there: Misassigned natural products and the role of chemical synthesis in modern structure elucidation. *Angew. Chem. Int. Ed.* **2005**, *44*, 1012–1044.

183. Lodewyk, M. W.; Siebert, M. R.; Tantillo, D. J. Computational prediction of ^{1}H and ^{13}C chemical shifts: A useful tool for natural product, mechanistic, and synthetic organic chemistry. *Chem. Rev.* **2012**, *112*, 1839–1862.

184. Schlegel, B.; Haertl, A.; Dahse, H. M.; Gollmick, F. A.; Graefe, U.; Doerfelt, H.; Kappes, B. Hexacyclinol, a new antiproliferative metabolite of *Panus rudis* HKI 0254. *J. Antibiot.* **2002**, *55*, 814–817.

185. La Clair, J. J. Total syntheses of hexacyclinol, 5-*epi*-hexacyclinol, and desoxohexacyclinol unveil an antimalarial prodrug motif. *Angew. Chem. Int. Ed.* **2006**, *45*, 2769–2773.

186. Rychnovsky, S. D. Predicting NMR spectra by computational methods: Structure revision of hexacyclinol. *Org. Lett.* **2006**, *8*, 2895–2898.

187. Saielli, G.; Bagno, A. Can two molecules have the same NMR spectrum? Hexacyclinol revisited. *Org. Lett.* **2009**, *11*, 1409–1412.

188. Nicolaou, K. C.; Ortiz, A.; Zhang, H.; Guella, G. Total synthesis and structural revision of vannusals A and B: Synthesis of the true structures of vannusals A and B. *J. Am. Chem. Soc.* **2010**, *132*, 7153–7176 and references cited therein.

189. Guella, G.; Callone, E.; Di Giuseppe, G.; Frassanito, R.; Frontini, F. P.; Mancini, I.; Dini, F. Hemivannusal and prevannusadials–new sesquiterpenoids from the marine ciliate protist *Euplotes vannus*: The putative biogenetic precursors to dimeric terpenoid vannusals. *Eur. J. Org. Chem.* **2007**, 5226–5234.

190. Saielli, G.; Nicolaou, K. C.; Ortiz, A.; Zhang, H.; Bagno, A. Addressing the stereochemistry of complex organic molecules by density functional theory-NMR: Vannusal B in retrospective. *J. Am. Chem. Soc.* **2011**, *133*, 6072–6077.

191. Smith, S. G.; Goodman, J. M. Assigning stereochemistry to single diastereoisomers by GIAO NMR calculation: The DP4 probability. *J. Am. Chem. Soc.* **2010**, *132*, 12946–12959.

192. Bachrach, S. M. *Computational Organic Chemistry*, 1st ed.; Wiley Interscience, Hoboken, New Jersey, 2007.

193. a) Wiitala, K. W.; Al-Rashid, Z. F.; Dvornikovs, V.; Hoye, T. R.; Cramer, C. J. Evaluation of various DFT protocols for computing ^{1}H and ^{13}C chemical shifts to distinguish stereoisomers: Diastereomeric 2-, 3-, and 4-methylcyclohexanols as a test set. *J. Phys. Org. Chem.* **2007**, *20*, 345–354. b) Wiitala, K. W.; Hoye, T. R.; Cramer, C. J. Hybrid density functional methods empirically optimized for the computation of ^{13}C and ^{1}H chemical shifts in chloroform solution. *J. Chem. Theory Comput.* **2006**, *2*, 1085–1092.

194. Zhao, Y.; Truhlar, D. G. Density functionals with broad applicability in chemistry. *Acc. Chem. Res.* **2008**, *41*, 157–167.

195. Garbisch, E. W., Jr; Griffith, M. G. Proton couplings in cyclohexane. *J. Am. Chem. Soc.* **1968**, *90*, 6543–6544.

196. Booth, H.; Everett, J. R. Conformational free energy difference ($-\Delta G^o$ value) of the methyl group in methylcyclohexane: An accurate determination by the direct, low-temperature nuclear magnetic resonance method. *J. Chem. Soc., Chem. Commun.* **1976**, 278–279.

197. Gogoll, A.; Grennberg, H.; Axen, A. Chemical shift assignment of geminal protons in 3,7-diazabicyclo-[3.3.1]nonanes: An unexpected deviation from the axial/equatorial chemical shift order. *Magn. Reson. Chem.* **1997**, *35*, 13–20.

198. Zhao, Y.; Truhlar, D. G. The M06 suite of density functionals for main group thermochemistry, thermochemical kinetics, noncovalent interactions, excited states, and transition elements: Two new functionals and systematic testing of four M06-class functionals and 12 other functionals. *Theor. Chem. Acc.* **120,** 215–241 (2008).

199. Hoye, T. R.; Hanson, P. R.; Vyvyan, J. R. A practical guide to first-order multiplet analysis in ^{1}H NMR spectroscopy. *J. Org. Chem.* **1994**, *59*, 4096–4103.

200. Hoye, T. R.; Zhao, H. A method for easily determining coupling constant values: An addendum to "A practical guide to first-order multiplet analysis in ^{1}H NMR spectroscopy." *J. Org. Chem.* **2002**, *67*, 4014–4016.

201. Gil, C.; Bräse, S. Efficient solid-phase synthesis of highly functionalized 1,4-benzodiazepin-5-one derivatives and related compounds by intramolecular aza-Wittig reactions. *Chem. Eur. J.* **2005**, *11*, 2680–2688.

202. Muller, D.; Zeltser, I.; Bitan, G.; Gilon, C. Building units for *N*-backbone cyclic peptides. 3. Synthesis of protected *N*α-(ω-aminoalkyl)amino acids and *N*α-(ω-carboxyalkyl)amino acids. *J. Org. Chem.* **1997**, *62*, 411–416.

203. Tang, J.-M.; Bhunia, S.; Sohel, S. M. A.; Lin, M.-Y.; Liao, H.-Y.; Datta, S.; Das, A.; Liu, R.-S. The skeletal rearrangement of gold- and platinum-catalyzed cycloisomerization of *cis*-4,6-dien-1-yn-3-ols: Pinacol rearrangement and formation of bicyclo[4.1.0]heptenone and reorganized styrene derivatives. *J. Am. Chem. Soc.* **2007**, *129*, 15677–15683.

204. M. Nishizawa, V. K. Yadav, M. Skwarczynski, H. Takao, H. Imagawa, T. Sugihara, Mercuric triflate catalyzed hydroxylative carbocyclization of 1,6-enynes. *Org. Lett.* **5**, 1609–1611 (2003).

205. DeBoef, B.; Counts, W. R.; Gilbertson, S. R. Rhodium-catalyzed synthesis of eight-membered rings. *J. Org. Chem.* **2007**, *72*, 799–804.

206. Lee, S. I.; Park, S. Y.; Park, J. H.; Jung, I. G.; Choi, S. Y.; Chung, Y. K.; Lee, B. Y. Rhodium N-heterocyclic carbene-catalyzed [4+2] and [5+2] cycloaddition reactions. *J. Org. Chem.* **2006**, *71*, 91–96.

207. Schmittel, M.; Mahajan, A. A.; Bucher, G.; Bats, J. W. Thermal C^2–C^6 cyclization of enyne–allenes. Experimental evidence for a stepwise mechanism and for an unusual thermal silyl shift. *J. Org. Chem.* **2007**, *72*, 2166–2173.

208. Brandsma, L.; Verkruijsse, H. D. Practical and safe procedures for the preparation of the lower homologues of bromoacetylene. *Synthesis* **1990**, *11*, 984–985.

209. Hoye, T. R.; Aspaas, A. W.; Eklov, B. M.; Ryba, T. D. Reaction titration: A convenient method for titering reactive hydride agents (Red-Al, $LiAlH_4$, DIBALH, L-Selectride, NaH, and KH) by no-D NMR spectroscopy. *Org. Lett.* **2005**, *7*, 2205–2208.

210. Eberbach, W., Roser, J. Thermally initiated reaction of (*Z*)-epoxyhexenynes; a facile preparation of 3,4-annulated furans. *Tetrahedron* **1986**, *42*, 2221–2234.

211. SMART V5.054, Bruker Analytical X-ray Systems, Madison, WI (2001).

212. Blessing, R. H. An empirical correction for absorption anisotropy. *Acta Cryst. A51* **1995**, 33–38.

213. SAINT+ V6.45, Bruker Analytical X-Ray Systems, Madison, WI (2003).

214. SHELXTL V6.14, Bruker Analytical X-Ray Systems, Madison, WI (2000).

Appendix A: Crystal Structure Data for **4090**

CRYSTAL STRUCTURE REPORT

$C_{17}H_{23}NO_3S$

REFERENCE NUMBER: 11085

Figure 32 | Thermal ellipsoid plot of **4090** showing 50% probability ellipsoids, hydrogen atoms not pictured for clarity.

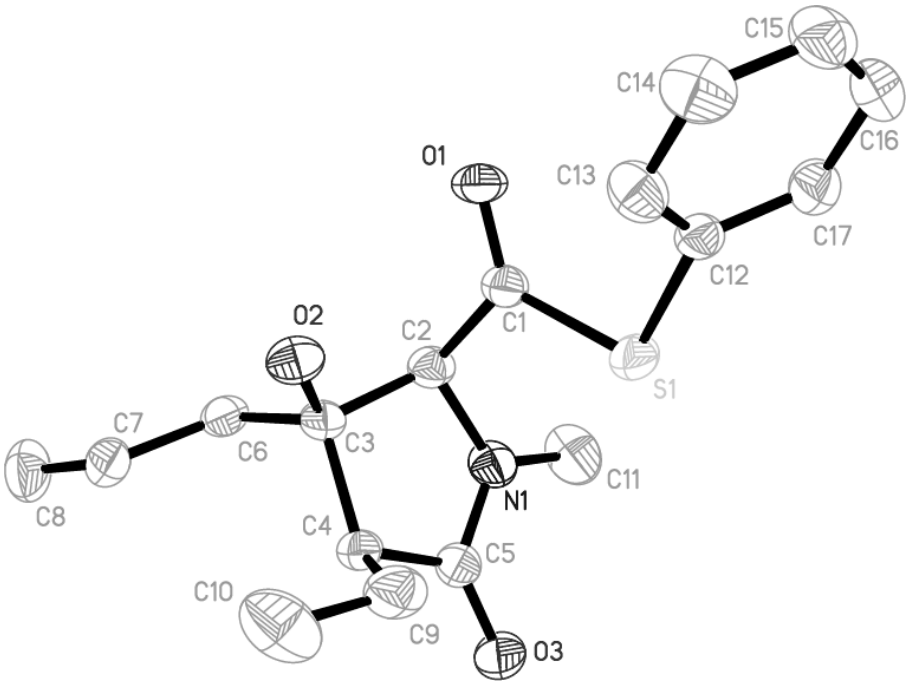

Report was prepared by:
Gregory T. Rohde
X-Ray Crystallographic Laboratory
Department of Chemistry
University of Minnesota
207 Pleasant St. S.E.
Minneapolis, MN 55455

Data Collection

A crystal (approximate dimensions 0.35 x 0.15 x 0.15 mm^3) was placed onto the tip of a 0.1 mm diameter glass capillary and mounted on a Bruker APEX-II CCD diffractometer for a data collection at 173(2) K.[211] A preliminary set of cell constants was calculated from reflections harvested from three sets of 12 frames. These initial sets of frames were oriented such that orthogonal wedges of reciprocal space were surveyed. This produced initial orientation matrices determined from 666 reflections. The data collection was carried out using MoKα radiation (graphite monochromator) with a frame time of 30 seconds and a detector distance of 6.0 cm. A randomly oriented region of reciprocal space was surveyed to the extent of one sphere and to α resolution of 0.77 Å. Four major sections of frames were collected with 0.50º steps in w at four different ϕ settings and a detector position of -28º in 2θ. The intensity data were corrected for absorption and decay (SADABS).[212] Final cell constants were calculated from the xyz centroids of 8716 strong reflections from the actual data collection after integration (SAINT).[213] Please refer to Table 1 for additional crystal and refinement information.

Structure Solution and Refinement

The structure was solved using SHELXS-97 (Sheldrick, 1990)[214] and refined using SHELXL-97 (Sheldrick, 1997).[214] The space group $Pna2_1$ was determined based on systematic absences and intensity statistics. A direct-methods solution was calculated which provided most non-hydrogen atoms from the E-map. Full-matrix least squares / difference Fourier cycles were performed which located the remaining non-hydrogen atoms. All non-hydrogen atoms were refined with anisotropic displacement parameters. All hydrogen atoms were placed in ideal positions and refined as riding atoms with relative isotropic displacement parameters. The final full matrix least squares refinement converged to $R1 = 0.0318$ and $wR2 = 0.0774$ (F^2, all data).

Structure Description

The structure is the one suggested. Both enantiomers of 11085 are present in the unit cell. An intermolecular hydrogen bond between O2 and O3 is present.

---

[211] SMART V5.054, Bruker Analytical X-ray Systems, Madison, WI (2001).
[212] Blessing, R. H. An empirical correction for absorption anisotropy. *Acta Cryst*. *A51* **1995**, 33–38.
[213] SAINT+ V6.45, Bruker Analytical X-Ray Systems, Madison, WI (2003).
[214] SHELXTL V6.14, Bruker Analytical X-Ray Systems, Madison, WI (2000).

Figure 33 | Thermal ellipsoid plot of **4090** showing 50% probability ellipsoids.

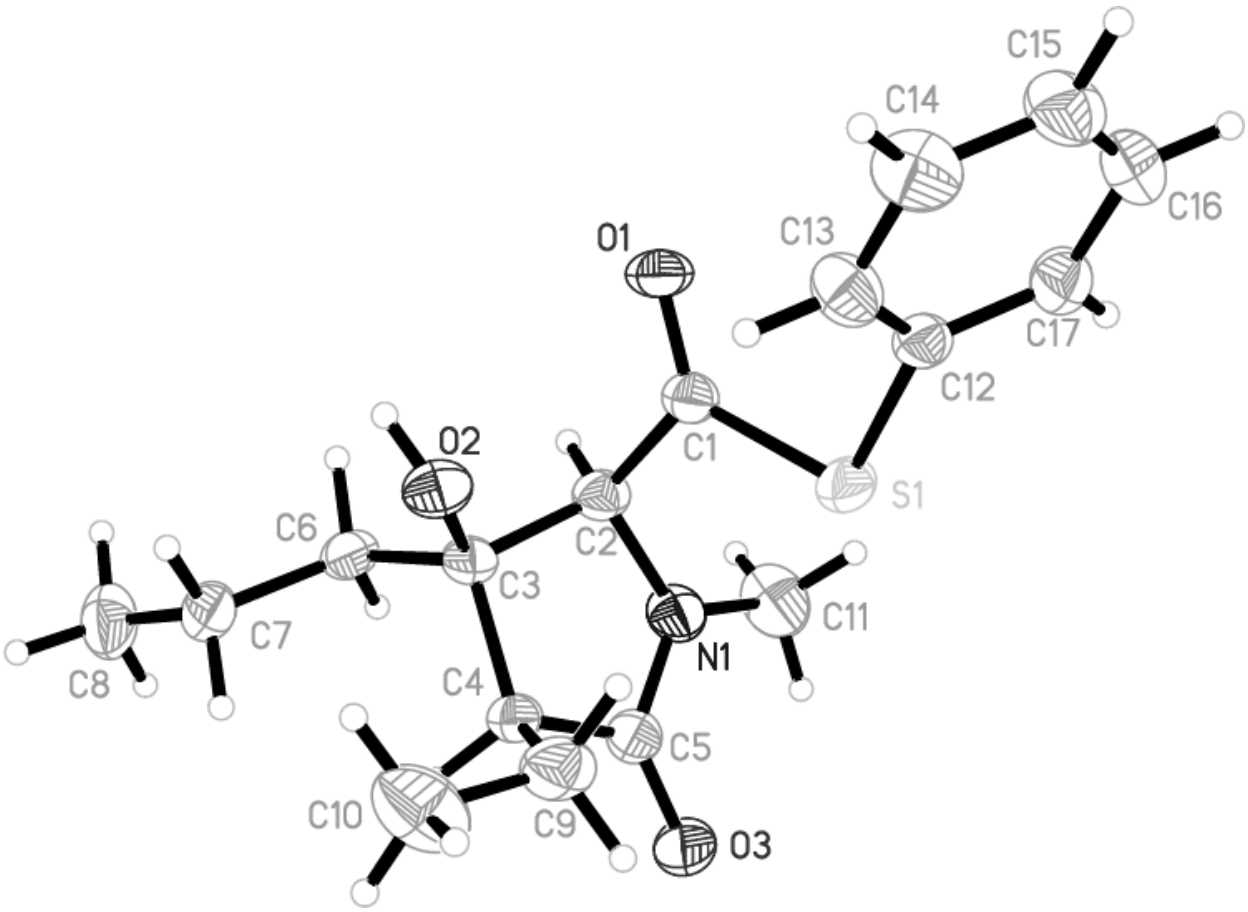

Data collection and structure solution were conducted at the X-Ray Crystallographic Laboratory, S146 Kolthoff Hall, Department of Chemistry, University of Minnesota. All calculations were performed using Pentium computers using the current SHELXTL suite of programs. All publications arising from this report must either 1) include Gregory T. Rohde as a coauthor or 2) acknowledge Gregory T. Rohde, Victor G. Young, Jr., and the X-Ray Crystallographic Laboratory.

Table 1 | Crystal data and structure refinement for **4090**.

Identification code	11085	
Empirical formula	$C_{17}H_{23}NO_3S$	
Formula weight	321.42	
Temperature	173(2) K	
Wavelength	0.71073 Å	
Crystal system	Orthorhombic	
Space group	$Pna2_1$	
Unit cell dimensions	a = 12.4695(6) Å	$\alpha = 90°$
	b = 10.8984(5) Å	$\beta = 90°$
	c = 12.8044(6) Å	$\gamma = 90°$
Volume	1740.09(14) $Å^3$	
Z	4	
Density (calculated)	1.227 Mg/m^3	
Absorption coefficient	0.197 mm^{-1}	
F(000)	688	
Crystal color, morphology	colorless, block	
Crystal size	0.35 x 0.15 x 0.15 mm^3	
Theta range for data collection	2.45 to 27.67°	
Index ranges	$-16 \le h \le 16$, $-14 \le k \le 14$, $-16 \le l \le 16$	
Reflections collected	19178	
Independent reflections	4048 [R(int) = 0.0316]	
Observed reflections	3577	
Completeness to theta = 27.67°	99.9%	
Absorption correction	Multi-scan	
Refinement method	Full-matrix least-squares on F^2	
Data / restraints / parameters	4048 / 1 / 203	
Goodness-of-fit on F^2	1.044	
Final R indices [I>2sigma(I)]	$R1$ = 0.0318, $wR2$ = 0.0731	
R indices (all data)	$R1$ = 0.0387, $wR2$ = 0.0774	
Absolute structure parameter	-0.02(6)	
Largest diff. peak and hole	0.213 and -0.218 e.$Å^{-3}$	

Table 2 | Atomic coordinates ($x10^4$) and equivalent isotropic displacement parameters ($Å^2$ x 10^3) for **4090**. U_{eq} is defined as one third of the trace of the orthogonalized U_{ij} tensor.

	x	y	z	U_{eq}
S1	2573(1)	5699(1)	4056(1)	37(1)
O1	4088(1)	4278(1)	4873(1)	36(1)
O2	2917(1)	2308(1)	3713(1)	34(1)
O3	-422(1)	4021(1)	4621(1)	49(1)
N1	1252(1)	4116(1)	5320(1)	34(1)
C1	3140(1)	4444(1)	4759(1)	28(1)
C2	2303(1)	3565(2)	5204(1)	29(1)
C3	2106(1)	2420(1)	4476(1)	27(1)
C4	1012(1)	2710(1)	3950(1)	29(1)
C5	516(1)	3670(2)	4646(2)	34(1)
C6	2014(1)	1281(2)	5160(1)	31(1)
C7	1849(1)	81(2)	4571(2)	35(1)
C8	1595(2)	-981(2)	5299(2)	48(1)
C9	1035(2)	3136(2)	2809(2)	43(1)
C10	1131(2)	2088(2)	2037(2)	61(1)
C11	1000(2)	5005(2)	6135(2)	51(1)
C12	3742(1)	6401(2)	3543(1)	30(1)
C13	4349(2)	5802(2)	2794(1)	39(1)
C14	5224(2)	6390(2)	2356(2)	48(1)
C15	5487(2)	7567(2)	2660(2)	47(1)
C16	4885(2)	8157(2)	3403(2)	46(1)
C17	4011(1)	7580(2)	3853(2)	38(1)

Table 3 | Bond lengths [Å] and angles [º] for **4090**.

S(1)-C(12)	1.7722(17)	C(11)-H(11B)	0.9800
S(1)-C(1)	1.7838(16)	C(11)-H(11C)	0.9800
O(1)-C(1)	1.2049(18)	C(12)-C(13)	1.385(2)
O(2)-C(3)	1.4114(17)	C(12)-C(17)	1.386(2)
O(2)-H(2B)	0.8400	C(13)-C(14)	1.384(3)
O(3)-C(5)	1.2312(19)	C(13)-H(13A)	0.9500
N(1)-C(5)	1.350(2)	C(14)-C(15)	1.380(3)
N(1)-C(2)	1.449(2)	C(14)-H(14A)	0.9500
N(1)-C(11)	1.458(2)	C(15)-C(16)	1.373(3)
C(1)-C(2)	1.526(2)	C(15)-H(15A)	0.9500
C(2)-C(3)	1.577(2)	C(16)-C(17)	1.384(3)
C(2)-H(2A)	1.0000	C(16)-H(16A)	0.9500
C(3)-C(6)	1.524(2)	C(17)-H(17A)	0.9500
C(3)-C(4)	1.553(2)		
C(4)-C(5)	1.507(2)	C(12)-S(1)-C(1)	101.05(7)
C(4)-C(9)	1.533(3)	C(3)-O(2)-H(2B)	109.5
C(4)-H(4A)	1.0000	C(5)-N(1)-C(2)	113.58(14)
C(6)-C(7)	1.524(2)	C(5)-N(1)-C(11)	123.34(15)
C(6)-H(6A)	0.9900	C(2)-N(1)-C(11)	122.96(15)
C(6)-H(6B)	0.9900	O(1)-C(1)-C(2)	122.11(14)
C(7)-C(8)	1.520(3)	O(1)-C(1)-S(1)	124.41(12)
C(7)-H(7A)	0.9900	C(2)-C(1)-S(1)	113.48(11)
C(7)-H(7B)	0.9900	N(1)-C(2)-C(1)	113.38(13)
C(8)-H(8A)	0.9800	N(1)-C(2)-C(3)	104.31(12)
C(8)-H(8B)	0.9800	C(1)-C(2)-C(3)	112.48(13)
C(8)-H(8C)	0.9800	N(1)-C(2)-H(2A)	108.8
C(9)-C(10)	1.515(3)	C(1)-C(2)-H(2A)	108.8
C(9)-H(9A)	0.9900	C(3)-C(2)-H(2A)	108.8
C(9)-H(9B)	0.9900	O(2)-C(3)-C(6)	112.39(13)
C(10)-H(10A)	0.9800	O(2)-C(3)-C(4)	110.31(12)
C(10)-H(10B)	0.9800	C(6)-C(3)-C(4)	110.45(12)
C(10)-H(10C)	0.9800	O(2)-C(3)-C(2)	111.44(12)
C(11)-H(11A)	0.9800	C(6)-C(3)-C(2)	108.44(13)

C(4)-C(3)-C(2)	103.44(12)	C(4)-C(9)-H(9B)	108.9
C(5)-C(4)-C(9)	111.20(14)	H(9A)-C(9)-H(9B)	107.7
C(5)-C(4)-C(3)	104.18(13)	C(9)-C(10)-H(10A)	109.5
C(9)-C(4)-C(3)	117.30(14)	C(9)-C(10)-H(10B)	109.5
C(5)-C(4)-H(4A)	107.9	H(10A)-C(10)-H(10B)	109.5
C(9)-C(4)-H(4A)	107.9	C(9)-C(10)-H(10C)	109.5
C(3)-C(4)-H(4A)	107.9	H(10A)-C(10)-H(10C)	109.5
O(3)-C(5)-N(1)	123.44(17)	H(10B)-C(10)-H(10C)	109.5
O(3)-C(5)-C(4)	126.14(17)	N(1)-C(11)-H(11A)	109.5
N(1)-C(5)-C(4)	110.42(13)	N(1)-C(11)-H(11B)	109.5
C(7)-C(6)-C(3)	115.11(14)	H(11A)-C(11)-H(11B)	109.5
C(7)-C(6)-H(6A)	108.5	N(1)-C(11)-H(11C)	109.5
C(3)-C(6)-H(6A)	108.5	H(11A)-C(11)-H(11C)	109.5
C(7)-C(6)-H(6B)	108.5	H(11B)-C(11)-H(11C)	109.5
C(3)-C(6)-H(6B)	108.5	C(13)-C(12)-C(17)	120.16(16)
H(6A)-C(6)-H(6B)	107.5	C(13)-C(12)-S(1)	120.19(13)
C(8)-C(7)-C(6)	112.21(16)	C(17)-C(12)-S(1)	119.55(13)
C(8)-C(7)-H(7A)	109.2	C(14)-C(13)-C(12)	119.57(17)
C(6)-C(7)-H(7A)	109.2	C(14)-C(13)-H(13A)	120.2
C(8)-C(7)-H(7B)	109.2	C(12)-C(13)-H(13A)	120.2
C(6)-C(7)-H(7B)	109.2	C(15)-C(14)-C(13)	120.27(19)
H(7A)-C(7)-H(7B)	107.9	C(15)-C(14)-H(14A)	119.9
C(7)-C(8)-H(8A)	109.5	C(13)-C(14)-H(14A)	119.9
C(7)-C(8)-H(8B)	109.5	C(16)-C(15)-C(14)	120.01(18)
H(8A)-C(8)-H(8B)	109.5	C(16)-C(15)-H(15A)	120.0
C(7)-C(8)-H(8C)	109.5	C(14)-C(15)-H(15A)	120.0
H(8A)-C(8)-H(8C)	109.5	C(15)-C(16)-C(17)	120.43(18)
H(8B)-C(8)-H(8C)	109.5	C(15)-C(16)-H(16A)	119.8
C(10)-C(9)-C(4)	113.28(16)	C(17)-C(16)-H(16A)	119.8
C(10)-C(9)-H(9A)	108.9	C(16)-C(17)-C(12)	119.55(17)
C(4)-C(9)-H(9A)	108.9	C(16)-C(17)-H(17A)	120.2
C(10)-C(9)-H(9B)	108.9	C(12)-C(17)-H(17A)	120.2

Table 4 | Anisotropic displacement parameters ($Å^2 x\ 10^3$) for **4090**. The anisotropic displacement factor exponent takes the form: $-2\pi^2[\ h^2\ a^{*2}U_{11} + ...\ + 2\ h\ k\ a^*\ b^*\ U_{12}\ ]$.

	U_{11}	U_{22}	U_{33}	U_{23}	U_{13}	U_{12}
S1	23(1)	33(1)	54(1)	10(1)	2(1)	1(1)
O1	21(1)	41(1)	46(1)	7(1)	-5(1)	-3(1)
O2	24(1)	43(1)	36(1)	1(1)	7(1)	1(1)
O3	21(1)	39(1)	87(1)	0(1)	3(1)	2(1)
N1	26(1)	35(1)	43(1)	-5(1)	10(1)	-2(1)
C1	24(1)	30(1)	31(1)	2(1)	-1(1)	-2(1)
C2	24(1)	32(1)	32(1)	4(1)	1(1)	-2(1)
C3	20(1)	29(1)	30(1)	0(1)	1(1)	-2(1)
C4	22(1)	28(1)	37(1)	4(1)	-3(1)	-1(1)
C5	23(1)	29(1)	50(1)	6(1)	4(1)	-4(1)
C6	24(1)	33(1)	37(1)	6(1)	-2(1)	2(1)
C7	31(1)	30(1)	44(1)	-1(1)	1(1)	4(1)
C8	52(1)	30(1)	62(1)	2(1)	10(1)	-1(1)
C9	42(1)	47(1)	40(1)	13(1)	-11(1)	-4(1)
C10	75(2)	71(2)	36(1)	1(1)	-8(1)	-21(1)
C11	47(1)	49(1)	57(1)	-15(1)	20(1)	-4(1)
C12	25(1)	31(1)	33(1)	7(1)	-2(1)	-1(1)
C13	43(1)	39(1)	36(1)	-6(1)	2(1)	-6(1)
C14	45(1)	60(1)	38(1)	-3(1)	12(1)	-4(1)
C15	40(1)	50(1)	51(1)	12(1)	7(1)	-10(1)
C16	44(1)	33(1)	61(1)	2(1)	1(1)	-8(1)
C17	36(1)	32(1)	46(1)	-1(1)	3(1)	3(1)

Table 5 | Hydrogen coordinates (x 10^4) and isotropic displacement parameters (Å^2 x 10^3) for **4090**.

	x	y	z	U(eq)
H2B	3435	1910	3962	51
H2A	2553	3270	5902	35
H4A	558	1955	3990	35
H6A	2675	1210	5585	37
H6B	1406	1395	5648	37
H7A	1253	182	4067	42
H7B	2506	-113	4169	42
H8A	1542	-1742	4893	72
H8B	913	-825	5654	72
H8C	2168	-1062	5818	72
H9A	370	3599	2658	52
H9B	1648	3701	2710	52
H10A	1161	2418	1325	91
H10B	508	1546	2105	91
H10C	1787	1623	2181	91
H11A	227	5172	6132	77
H11B	1393	5768	6004	77
H11C	1208	4672	6816	77
H13A	4166	4993	2582	47
H14A	5644	5981	1844	57
H15A	6086	7969	2354	56
H16A	5069	8967	3611	55
H17A	3597	7989	4370	45

Table 6 | Torsion angles [º] for **4090**.

C12-S1-C1-O1	5.55(17)		
C12-S1-C1-C2	-173.71(12)	C3-C6-C7-C8	-171.26(15)
C5-N1-C2-C1	110.40(16)	C5-C4-C9-C10	-158.81(16)
C11-N1-C2-C1	-73.6(2)	C3-C4-C9-C10	81.5(2)
C5-N1-C2-C3	-12.30(18)	C1-S1-C12-C13	67.46(15)
C11-N1-C2-C3	163.75(16)	C1-S1-C12-C17	-116.15(14)
O1-C1-C2-N1	159.05(16)	C17-C12-C13-C14	-0.1(3)
S1-C1-C2-N1	-21.67(18)	S1-C12-C13-C14	176.24(15)
O1-C1-C2-C3	-82.9(2)	C12-C13-C14-C15	-0.3(3)
S1-C1-C2-C3	96.39(14)	C13-C14-C15-C16	0.4(3)
N1-C2-C3-O2	137.51(13)	C14-C15-C16-C17	-0.1(3)
C1-C2-C3-O2	14.22(18)	C15-C16-C17-C12	-0.3(3)
N1-C2-C3-C6	-98.27(15)	C13-C12-C17-C16	0.4(3)
C1-C2-C3-C6	138.44(13)	S1-C12-C17-C16	-175.96(15)
N1-C2-C3-C4	19.01(15)		
C1-C2-C3-C4	-104.28(14)		
O2-C3-C4-C5	-138.29(13)		
C6-C3-C4-C5	96.86(15)		
C2-C3-C4-C5	-19.00(15)		
O2-C3-C4-C9	-14.91(19)		
C6-C3-C4-C9	-139.76(15)		
C2-C3-C4-C9	104.37(16)		
C2-N1-C5-O3	-179.89(16)		
C11-N1-C5-O3	4.1(3)		
C2-N1-C5-C4	-0.22(19)		
C11-N1-C5-C4	-176.25(16)		
C9-C4-C5-O3	65.2(2)		
C3-C4-C5-O3	-167.52(17)		
C9-C4-C5-N1	-114.43(16)		
C3-C4-C5-N1	12.82(17)		
O2-C3-C6-C7	-54.88(18)		
C4-C3-C6-C7	68.77(17)		
C2-C3-C6-C7	-178.53(13)		

Table 7 | Hydrogen bonds for **4090** [Å and º].

D-H...A	d(D-H)	d(H...A)	d(D...A)	<(DHA)
O2-H2B...O3#1	0.84	1.94	2.7811(17)	176.3

Symmetry transformations used to generate equivalent atoms:

#1 x+1/2,-y+1/2,z

Appendix B: Python Scripts for Automating Computation of NMR Data

Python Script entitled "write-g09-inputs.py"

```
from schrodinger import maestro
from schrodinger import structure
from schrodinger import project
import os
from math import exp as exp

def main ():
#  Dictionary holding column names for project table properties depending on the force field being used
   columns = {'mm2' : ['r_mmod_Potential_Energy-MM2*', 'r_mmod_Relative_Potential_Energy-MM2*'], 'mm3': ['r_mmod_Potential_Energy-MM3*', 'r_mmod_Relative_Potential_Energy-MM3*'],
   'amber': ['r_mmod_Potential_Energy-AMBER*', 'r_mmod_Relative_Potential_Energy-AMBER*'], 'opls': ['r_mmod_Potential_Energy-OPLSA*', 'r_mmod_Relative_Potential_Energy-OPLSA*'],
   'amber94': ['r_mmod_Potential_Energy-AMBER94', 'r_mmod_Relative_Potential_Energy-AMBER94'], 'mmff': ['r_mmod_Potential_Energy-MMFF94', 'r_mmod_Relative_Potential_Energy-MMFF94'],
   'mmffs': ['r_mmod_Potential_Energy-MMFF94s', 'r_mmod_Relative_Potential_Energy-MMFF94s'], 'opls2001': ['r_mmod_Potential_Energy-OPLS-AA', 'r_mmod_Relative_Potential_Energy-OPLS-AA'],
   'opls2005': ['r_mmod_Potential_Energy-OPLS-2005', 'r_mmod_Relative_Potential_Energy-OPLS-2005']}
```

```
# Start by selecting all entries in the project table, and making sure the first entry is in the
workspace
   maestro.command("entryselectall")
   maestro.command("eplayergotofirst")

# Grab the entire project table
   pt = maestro.project_table_get()

   currentforcefield = ''
   for forcefield in columns.keys():
      if not pt[1][columns[forcefield][0]] == None :
         currentforcefield = forcefield
         break

# Create a directory to store the input files.
   os.popen( "mkdir " + str( pt[1]['s_m_title']+'-gaussian_files' ) )

# Create a dictionary with keys being each conformer name and a list of the
# absolute and relative MM energies for the conformer.
   energies = {}

# Make a loop to operate on every conformation in the project table.
# This loop operates on one conformation.
   conf_num = 1
   for row in pt.selected_rows:
      structure = maestro.workspace_get()

# Open the output file for writing
      outputfile = open( row['s_m_title'] + "-opt_freq-conf-" + str(conf_num) + ".com",
'w' )
```

```
        nmr_outputfile = open( row['s_m_title'] + "-nmr-conf-" + str(conf_num) + '.com',
'w' )

#  Add the conformer energy to the dictionary of energies
        energies[ str( row['s_m_title'] + row['s_m_entry_id'] ) ]
=[ row[columns[currentforcefield][0]], row[columns[currentforcefield][1]] ]



#  Write the Gaussian stuff that goes into every input deck.

        print >> outputfile, gaussian_input( "link", str( pt[1]['s_m_title']),  str( conf_num ))
        print >> nmr_outputfile, gaussian_nmr_input( "link", str( pt[1]['s_m_title']),
str( conf_num ) )
        print >> outputfile, gaussian_input( "route" )
        print >> nmr_outputfile, gaussian_nmr_input( "route" )
        print >> outputfile, gaussian_input( "title", str( pt[1]['s_m_title']),  str( conf_num ))
        print >> nmr_outputfile, gaussian_nmr_input( "title", str( pt[1]['s_m_title']),
str( conf_num ))
        print >> outputfile, gaussian_input( "molecule" )
        print >> nmr_outputfile, gaussian_nmr_input( "molecule" )
        print >> nmr_outputfile, gaussian_nmr_input( "readline" )
        print >> nmr_outputfile, gaussian_nmr_input( "end" )

#  This loop operates on one atom.

        for atom in structure.atom:
           outputstring = "%2s %10.6f %10.6f %10.6f" % (atom.element, atom.x, atom.y,
atom.z)
           print >> outputfile, outputstring

        print >> outputfile, gaussian_input( "readline" )
```

```
        print >> outputfile, gaussian_input("end")

#  Close the opened output file.

        outputfile.flush()
        outputfile.close()
        nmr_outputfile.flush()
        nmr_outputfile.close()
        maestro.command("eplayerstepahead")
        conf_num += 1

#  Move the created input files "-gaussian_files" directory.
    os.popen( "mv " + str( pt[1]['s_m_title'] + '*conf* ' ) + str( pt[1]['s_m_title']+'-
gaussian_files') )

def convert_mmat_symbol(mmat):
#    mmat2Number =
{1:'C',2:'C',3:'C',15:'O',16:'O',24:'N',25:'N',26:'N',41:'H',42:'H',43:'H',49:'S',56:'F',57:'Cl',5
8:'Br',59:'I'}
#    symbol = mmat2Number[mmat]
#    return symbol
    return
{1:'C',2:'C',3:'C',15:'O',16:'O',24:'N',25:'N',26:'N',41:'H',42:'H',43:'H',49:'S',56:'F',57:'Cl',5
8:'Br',59:'I'}[mmat]

def gaussian_input(which_section,candidate_filename="X", conformer_number="Y"):
#  Current acceptable values for which_section: link, route, title, molecule, and end

    ENDLINE   = "\n"
    LINK1     = "%mem=16gb\n"
    LINK2     = "%nproc=8\n"
```

```
   LINK3     = "%%chk=%s \n" % (candidate_filename +'-conf-' + conformer_number +
".chk")
   LINK4     = "\nradii=UA0\n"
   ROUTE1    = "# m062x/6-31+G(d,p) opt freq=noraman integral(ultrafinegrid)
scrf=(iefpcm,read,solvent=chloroform)"
   TITLE1    = "Candidate Structure: %s, Conformer: %s geometry optimization and
frequency calculation with chloroform solvation" %
(candidate_filename,conformer_number)
   MOL1      = "0 1"
   CARTHEAD  = "          X           Y           Z\n"

   LINKZERO = LINK1 + LINK2 + LINK3
   ROUTE    = ROUTE1 + ENDLINE
   TITLE    = TITLE1 + ENDLINE
   MOLECULE = MOL1
   READLINE = LINK4 +ENDLINE
   END      = ENDLINE

   if (which_section == "link"): return LINKZERO
   if (which_section == "route"): return ROUTE
   if (which_section == "title"): return TITLE
   if (which_section == "molecule"): return MOLECULE
   if (which_section == "readline"): return READLINE
   if (which_section == "end"): return END

   return "There is a problem generating the input files."

def
gaussian_nmr_input(which_section,candidate_filename="X",conformer_number="Y"):
   ENDLINE   = "\n"
   LINK1     = "%mem=16gb\n"
```

```
    LINK2     = "%nproc=8\n"
    LINK3     = "%%chk=%s \n" % (candidate_filename + '-conf-' + conformer_number +
'.chk')
    LINK4     = "radii=bondi\n"
    ROUTE1    = "# b3lyp/6-311+G(2d,p) nmr guess=read geom=check
integral(ultrafinegrid) scrf=(iefpcm,read,solvent=chloroform)"
    TITLE1    = "Candidate Structure: %s, Conformer: %s, NMR calculation with
chloroform solvation" % (candidate_filename,conformer_number)
    MOL1      = "0 1"
    CARTHEAD  = "          X           Y           Z\n"

    LINKZERO = LINK1 + LINK2 + LINK3
    ROUTE    = ROUTE1 + ENDLINE
    TITLE    = TITLE1 + ENDLINE
    MOLECULE = MOL1 + ENDLINE
    READLINE = LINK4 + ENDLINE
    END      = ENDLINE

    if (which_section == "link"): return LINKZERO
    if (which_section == "route"): return ROUTE
    if (which_section == "title"): return TITLE
    if (which_section == "molecule"): return MOLECULE
    if (which_section == "readline"): return READLINE
    if (which_section == "end"): return END

    return "There is a problem generating the input files."

main()
```

Python Script “nmr-data_compilation.py”

```
import sys
import re
import math

HARTREE_TO_KCAL = 627.509391
TEMPERATURE = 298.0
GAS_CONSTANT = 0.001986

MENU_SELECTION = raw_input("""Choose from the following options:

A. Enter reference and scaling factor data from regression analysis of a
test set of molecules.

B. Enter reference data from computation of a reference standard (e.g.,
TMS) NMR shielding tensors.

C. Do not reference or scale NMR shielding tensor data.

""")


if MENU_SELECTION.upper() == "A":
   PROTON_INTERCEPT = input("""
Enter the 1H scaling factor INTERCEPT:

""")
   PROTON_SCALING_SLOPE = input("""
Enter the 1H scaling factor SLOPE:
```

```
""")
   CARBON_INTERCEPT = input("""
Enter the 13C scaling factor INTERCEPT:

""")
   CARBON_SCALING_SLOPE = input("""
Enter the 13C scaling factor SLOPE:

""")
   OUTPUT_PREFIX = raw_input("""
Enter the name of the candidate structure:

""") + "-nmr_data_compilation"

if MENU_SELECTION.upper() == "B":
   PROTON_REF_STANDARD = input("""
Enter the computed 1H shielding tensor for the reference standard:
""")
   PROTON_REL_TMS = input("""
Enter the experimental 1H chemical shift of the reference standard:
""")
   PROTON_INTERCEPT = PROTON_REF_STANDARD - PROTON_REL_TMS
   PROTON_SCALING_SLOPE = -1
   CARBON_REF_STANDARD = input("""
Enter the computed 13C shielding tensor for the reference standard:
""")
   CARBON_REL_TMS = input("""
Enter the experimental 13C chemical shift of the reference standard:
""")
   CARBON_INTERCEPT = CARBON_REF_STANDARD - CARBON_REL_TMS
   CARBON_SCALING_SLOPE = -1
```

```
   OUTPUT_PREFIX = raw_input("""
Enter the name of the candidate structure:

""") + "-nmr_data_compilation"

if MENU_SELECTION.upper() == "C":
   PROTON_INTERCEPT = 0
   PROTON_SCALING_SLOPE = -1
   CARBON_INTERCEPT = 0
   CARBON_SCALING_SLOPE = -1
   OUTPUT_PREFIX = raw_input("""
Enter the name of the candidate structure:

""") + "-nmr_data_compilation"



#Below are the index values for the master data structure.
NAME = 0; CONF_NUM = 1; ENERGY = 2; KCAL_E = 3; REL_E = 4;
BOLTZMANN_FACTOR = 5; MOL_X = 6; CARBON_CS = 7; PROTON_CS = 8;
IMAG_FREQUENCIES = 9

#Below are the index values for the proton and carbon chemical shift data substructures.
ATOM_NUMBER = 0 ; ISOTROPIC_VALUE = 1; REF_SHIFT = 2;
WEIGHTED_SHIFT = 3;

def main():
   lofc_freq = read_gaussian_freq_outfiles()
   lofc_nmr = read_gaussian_nmr_outfiles()
   locs = prepare_list_of_chemical_shifts(lofc_nmr)
   lofe = get_list_of_free_energies(lofc_freq)
   lofe = boltzmann_analysis(lofe)
```

```
    lofe = report_chemical_shifts(lofc_nmr, lofe)
    summed_proton_shifts = final_proton_chemical_shifts(lofe)
    summed_carbon_shifts = final_carbon_chemical_shifts(lofe)
    lofe = count_imaginary_freq(lofc_freq, lofe)
    write_final_shift_csv(summed_proton_shifts,summed_carbon_shifts)
    write_master_csv(lofe)



def boltzmann_analysis(lofe):
    lofe = kcal_convert(lofe)
    minE = find_minimum_E(lofe)
    lofe = calc_rel_E(lofe, minE)
    lofe = calc_boltzmann_weights(lofe)
    denom = calc_boltzmann_denomenator(lofe)
    lofe = calc_mol_fraction(lofe,denom)

    return lofe

def report_chemical_shifts(lofc_nmr,lofe):
    get_chemical_shifts(lofc_nmr, lofe)
    ref_chemical_shift(lofe)
    boltzmann_chemical_shifts(lofe)

    return lofe

def write_master_csv(lofe):

    masterpwriter = open(OUTPUT_PREFIX+"-master_proton.csv",'w')
    mastercwriter = open(OUTPUT_PREFIX+"-master_carbon.csv",'w')
```

```
   print>> masterpwriter, "filename, energy (a.u.), energy (kcal), rel energy (kcal),
boltzmann factor, eq mole fraction, imaginary freqs"
   for conformation in lofe:
      print >> masterpwriter, conformation[NAME],",", conformation[ENERGY],",",
conformation[KCAL_E],",",
conformation[REL_E],",",conformation[BOLTZMANN_FACTOR],",",
conformation[MOL_X],",", conformation[IMAG_FREQUENCIES]
   print>>masterpwriter, " "
   for conformation in lofe:
      print >> masterpwriter, "conformation",",", conformation[NAME],",", "mole
fraction",",", conformation[MOL_X]
      print >> masterpwriter, "Atom Number, Isotropic Value, Ref Chemical Shift, Avg
Chemical Shift"
      for proton in conformation[PROTON_CS]:
         print >> masterpwriter, proton[ATOM_NUMBER],",",
proton[ISOTROPIC_VALUE],",", proton[REF_SHIFT],",",proton[WEIGHTED_SHIFT]
      print >> masterpwriter, " "

   print>> mastercwriter, "filename, energy (a.u.), energy (kcal), rel energy (kcal),
boltzmann factor, eq mole fraction"
   for conformation in lofe:
      print >> mastercwriter, conformation[NAME],",", conformation[ENERGY],",",
conformation[KCAL_E],",",
conformation[REL_E],",",conformation[BOLTZMANN_FACTOR],",",
conformation[MOL_X]
   print>>mastercwriter, " "
   for conformation in lofe:
      print >> mastercwriter, "conformation",",", conformation[NAME],",", "mole
fraction",",", conformation[MOL_X]
      print >> mastercwriter, "Atom Number, Isotropic Value, Ref Chemical Shift, Avg
Chemical Shift"
```

```
        for carbon in conformation[CARBON_CS]:
            print >> mastercwriter, carbon[ATOM_NUMBER],",",
carbon[ISOTROPIC_VALUE],",",
carbon[REF_SHIFT],",",carbon[WEIGHTED_SHIFT]
        print >> mastercwriter, " "

def write_final_shift_csv(summed_proton_shifts,summed_carbon_shifts):
    ATOM_NUMBER = 0; SHIFT = 1
    pwriter = open(OUTPUT_PREFIX+"-avg_proton.csv",'w')
    cwriter = open(OUTPUT_PREFIX+"-avg_carbon.csv",'w')

    print >> pwriter, "ATOM NUMBER, CHEMICAL SHIFT"
    for item in summed_proton_shifts:
        print >> pwriter, item[ATOM_NUMBER],",",item[SHIFT]

    print >> cwriter, "ATOM NUMBER, CHEMICAL SHIFT"
    for item in summed_carbon_shifts:
        print >> cwriter, item[ATOM_NUMBER],",",item[SHIFT]

    return 0


def final_proton_chemical_shifts(lofe):
    ATOM_NUMBER = 0; SHIFT = 1
    final_proton_cshift = []

    for proton in lofe[0][PROTON_CS]:

final_proton_cshift.append([proton[ATOM_NUMBER],proton[WEIGHTED_SHIFT]])

    for conformation in lofe[1:]:
```

```
        counter = 0
        for proton in conformation[PROTON_CS]:
            final_proton_cshift[counter][SHIFT] += proton[WEIGHTED_SHIFT]
            counter += 1

    return final_proton_cshift

def final_carbon_chemical_shifts(lofe):
    ATOM_NUMBER = 0; SHIFT = 1
    final_carbon_cshift = []

    for carbon in lofe[0][CARBON_CS]:

final_carbon_cshift.append([carbon[ATOM_NUMBER],carbon[WEIGHTED_SHIFT]])

    for conformation in lofe[1:]:
        counter = 0
        for carbon in conformation[CARBON_CS]:
            final_carbon_cshift[counter][SHIFT] += carbon[WEIGHTED_SHIFT]
            counter += 1

    return final_carbon_cshift

def kcal_convert(lofe):
    NAME = 0; CONF_NUM = 1; ENERGY = 2
    for entry in lofe:
        entry.append(entry[ENERGY] * HARTREE_TO_KCAL)

    return lofe

def find_minimum_E(lofe):
```

```
    minE = 0
    for entry in lofe:  #This finds the minimum energy
        if entry[KCAL_E] < minE:
            minE = entry[KCAL_E]

    return minE

def calc_rel_E(lofe, minE):
    for entry in lofe:
        entry.append(entry[KCAL_E] - minE)

    return lofe

def calc_boltzmann_weights(lofe):
    for entry in lofe:
        entry.append(math.exp( (-1 * entry[REL_E]) / (TEMPERATURE *
GAS_CONSTANT)))

    return lofe

def calc_boltzmann_denomenator(lofe):
    Boltzmann_denomenator = 0
    for entry in lofe:
        Boltzmann_denomenator = Boltzmann_denomenator +
entry[BOLTZMANN_FACTOR]

    return Boltzmann_denomenator

def calc_mol_fraction(lofe,Boltzmann_denomenator):
    for entry in lofe:
        entry.append(entry[BOLTZMANN_FACTOR]/Boltzmann_denomenator)
```

```
    return lofe

def ref_chemical_shift(lofe):
    for conformation in lofe:
        for proton in conformation[PROTON_CS]:
            proton.append(abs((PROTON_INTERCEPT -
float(proton[ISOTROPIC_VALUE])) / PROTON_SCALING_SLOPE))
        for carbon in conformation[CARBON_CS]:
            carbon.append(abs((CARBON_INTERCEPT -
float(carbon[ISOTROPIC_VALUE])) / CARBON_SCALING_SLOPE))
    return lofe

def boltzmann_chemical_shifts(lofe):
    for conformation in lofe:
        for proton in conformation[PROTON_CS]:
            proton.append(proton[REF_SHIFT] * conformation[MOL_X])
        for carbon in conformation[CARBON_CS]:
            carbon.append(carbon[REF_SHIFT] * conformation[MOL_X])

    return lofe

def get_chemical_shifts(lofc_nmr, lofe):
    ATOM_NUMBER = 0; ATOM_SYMBOL = 1; ISOTROPIC_VALUE = 4
    counter = 0
    for file in lofc_nmr:
        proton_chemicalshift_table = []
        carbon_chemicalshift_table = []
        for line in file[2]:
            if "Isotropic" in line:
                linesplit = line.split()
```

```
            if linesplit[ATOM_SYMBOL] == "C":

carbon_chemicalshift_table.append([linesplit[ATOM_NUMBER],linesplit[ISOTROPIC_
VALUE]])
            if linesplit[ATOM_SYMBOL] == "H":

proton_chemicalshift_table.append([linesplit[ATOM_NUMBER],linesplit[ISOTROPIC_
VALUE]])
        lofe[counter].append(carbon_chemicalshift_table)
        lofe[counter].append(proton_chemicalshift_table)
        counter += 1
    return lofe

def prepare_list_of_chemical_shifts(lofc_nmr):
    list_of_chemical_shifts = []
    for file in lofc_nmr:
        list_of_chemical_shifts.append([file[0],file[1]])
    return list_of_chemical_shifts

def count_imaginary_freq(lofc_freq, lofe):
    LINE_POS_OF_FREQUENCY_A = 2; LINE_POS_OF_FREQUENCY_B = 3;
LINE_POS_OF_FREQUENCY_C = 4;
    counter = 0
    for file in lofc_freq:
        IMAG_FREQUENCIES = 0
        for line in file[2]:
            if "Frequencies -- " in line:
                freq_linesplit = line.split()
                if float(freq_linesplit[LINE_POS_OF_FREQUENCY_A]) < 0:
                    IMAG_FREQUENCIES = IMAG_FREQUENCIES + 1
                if float(freq_linesplit[LINE_POS_OF_FREQUENCY_B]) < 0:
```

```
                IMAG_FREQUENCIES = IMAG_FREQUENCIES + 1
            if float(freq_linesplit[LINE_POS_OF_FREQUENCY_C]) < 0:
                IMAG_FREQUENCIES = IMAG_FREQUENCIES + 1

        lofe[counter].append(IMAG_FREQUENCIES)
        counter += 1

    return lofe

def get_list_of_free_energies(lofc_freq):
    LINE_POS_OF_FREE_ENERGY = 7
    list_of_free_energies = []
    for file in lofc_freq:
        for line in file[2]:
            if "Free Energies=" in line:
                free_linesplit = line.split()
                free_energy = float(free_linesplit[LINE_POS_OF_FREE_ENERGY])
                list_of_free_energies.append([file[0],file[1],free_energy])
    return list_of_free_energies

def get_conf_number(filename):
    split_filename = re.findall(r'\w+', filename)
    rev_filename = split_filename[::-1]
    conf_number = rev_filename[1]
    return conf_number

def read_gaussian_nmr_outfiles():
    list_of_nmr_outfiles = []
    list_of_files= sys.argv[1:]
    for file in list_of_files:
        if file.find('nmr-') !=-1:
```

```
list_of_nmr_outfiles.append([file,int(get_conf_number(file)),open(file,"r").readlines()])

   return list_of_nmr_outfiles

def read_gaussian_freq_outfiles():
   list_of_freq_outfiles = []
   list_of_files= sys.argv[1:]
   for file in list_of_files:
      if file.find('freq-') !=-1:

list_of_freq_outfiles.append([file,int(get_conf_number(file)),open(file,"r").readlines()])

   return list_of_freq_outfiles


if __name__ == "__main__":
   main()

print """
The script successfully performed the Boltzmann weighting,
compiled the results of the NMR computation, assembled, scaled,
and/or referenced these data in the following ".csv" files:

%s-master_proton.csv

%s-avg_proton.csv

%s-master_carbon.csv

%s-avg_carbon.csv
```

""" % (OUTPUT_PREFIX,OUTPUT_PREFIX,OUTPUT_PREFIX,OUTPUT_PREFIX)

Python Script "duplicate_conf_and_imag_freq-check.py"

```
HARTREE_TO_KCAL = 627.509391
TEMPERATURE = 298.0
GAS_CONSTANT = 0.001986

FILENAME = raw_input("""Enter the name of the candidate structure:
""") + "-conf_energy_and_imag_freq.csv"

#Below are the index values for the master data structure.
NAME = 0; CONF_NUM = 1; ENERGY = 2; KCAL_E = 3; REL_E = 4;
BOLTZMANN_FACTOR = 5; MOL_X = 6; IMAG_FREQUENCIES = 7

#Below are the index values for the proton and carbon chemical shift data substructures.
ATOM_NUMBER = 0 ; ISOTROPIC_VALUE = 1; REF_SHIFT = 2;
WEIGHTED_SHIFT = 3;

def main():
   lofc_freq = read_gaussian_freq_outfiles()
   lofe = get_list_of_free_energies(lofc_freq)
   lofe = boltzmann_analysis(lofe)
   lofe = count_imaginary_freq(lofc_freq, lofe)
   write_validate_csv(lofe)



def boltzmann_analysis(lofe):
   lofe = kcal_convert(lofe)
   minE = find_minimum_E(lofe)
   lofe = calc_rel_E(lofe, minE)
   lofe = calc_boltzmann_weights(lofe)
```

```
    denom = calc_boltzmann_denomenator(lofe)
    lofe = calc_mol_fraction(lofe,denom)

    return lofe

def report_chemical_shifts(lofc_nmr,lofe):
    get_chemical_shifts(lofc_nmr, lofe)
    ref_chemical_shift(lofe)
    boltzmann_chemical_shifts(lofe)

    return lofe

def write_validate_csv(lofe):

    validate_writer = open(FILENAME,'w')

    print>> validate_writer, "Filename, Energy (a.u.), Energy (kcal/mol), Relative Energy
(kcal/mol), Boltzmann Factor, Equilibrium Mole Fraction, Number of Imaginary
Frequencies"
    for conformation in lofe:
        print >> validate_writer, conformation[NAME],",", conformation[ENERGY],",",
conformation[KCAL_E],",",
conformation[REL_E],",",conformation[BOLTZMANN_FACTOR],",",
conformation[MOL_X],",", conformation[IMAG_FREQUENCIES]
    print>>validate_writer, " "

def kcal_convert(lofe):
    NAME = 0; CONF_NUM = 1; ENERGY = 2
    for entry in lofe:
        entry.append(entry[ENERGY] * HARTREE_TO_KCAL)
```

```
    return lofe

def find_minimum_E(lofe):
    minE = 0
    for entry in lofe:  #This finds the minimum energy
        if entry[KCAL_E] < minE:
            minE = entry[KCAL_E]

    return minE

def calc_rel_E(lofe, minE):
    for entry in lofe:
        entry.append(entry[KCAL_E] - minE)

    return lofe

def calc_boltzmann_weights(lofe):
    for entry in lofe:
        entry.append(math.exp( (-1 * entry[REL_E]) / (TEMPERATURE *
GAS_CONSTANT)))

    return lofe

def calc_boltzmann_denomenator(lofe):
    Boltzmann_denomenator = 0
    for entry in lofe:
        Boltzmann_denomenator = Boltzmann_denomenator +
entry[BOLTZMANN_FACTOR]

    return Boltzmann_denomenator
```

```
def calc_mol_fraction(lofe,Boltzmann_denomenator):
    for entry in lofe:
        entry.append(entry[BOLTZMANN_FACTOR]/Boltzmann_denomenator)

    return lofe



def count_imaginary_freq(lofc_freq, lofe):
    LINE_POS_OF_FREQUENCY_A = 2; LINE_POS_OF_FREQUENCY_B = 3;
LINE_POS_OF_FREQUENCY_C = 4;
    counter = 0
    for file in lofc_freq:
        IMAG_FREQUENCIES = 0
        for line in file[2]:
            if "Frequencies -- " in line:
                freq_linesplit = line.split()
                if float(freq_linesplit[LINE_POS_OF_FREQUENCY_A]) < 0:
                    IMAG_FREQUENCIES = IMAG_FREQUENCIES + 1
                if float(freq_linesplit[LINE_POS_OF_FREQUENCY_B]) < 0:
                    IMAG_FREQUENCIES = IMAG_FREQUENCIES + 1
                if float(freq_linesplit[LINE_POS_OF_FREQUENCY_C]) < 0:
                    IMAG_FREQUENCIES = IMAG_FREQUENCIES + 1

        lofe[counter].append(IMAG_FREQUENCIES)
        counter += 1

    return lofe

def get_list_of_free_energies(lofc_freq):
    LINE_POS_OF_FREE_ENERGY = 7
    list_of_free_energies = []
```

```
    for file in lofc_freq:
        for line in file[2]:
            if "Free Energies=" in line:
                free_linesplit = line.split()
                free_energy = float(free_linesplit[LINE_POS_OF_FREE_ENERGY])
                list_of_free_energies.append([file[0],file[1],free_energy])
    return list_of_free_energies

def get_conf_number(filename):
    split_filename = re.findall(r'\w+', filename)
    rev_filename = split_filename[::-1]
    conf_number = rev_filename[1]
    return conf_number

def read_gaussian_freq_outfiles():
    list_of_freq_outfiles = []
    list_of_files= sys.argv[1:]
    for file in list_of_files:
        if file.find('freq-') !=-1:

list_of_freq_outfiles.append([file,int(get_conf_number(file)),open(file,"r").readlines()])

    return list_of_freq_outfiles

if __name__ == "__main__":
    main()
print """
The script successfully performed the task of creating the
%s
file that shows the conformer number, conformer filename,
total electronic energy, free energy, and total number of
```

imaginary frequencies for each conformer.

""" % (FILENAME)

Python Script "get-ref-shifts.py"

```
import sys
import re
import math
import decimal

OUTPUT_PREFIX = "tms_std-nmr"

#Below are the index values for the master data structure.
CARBON_CS = 0; PROTON_CS = 1;

def main():
   lofc_nmr = read_gaussian_nmr_outfiles()
   locs = prepare_list_of_chemical_shifts(lofc_nmr)
   lofe = report_chemical_shifts(lofc_nmr)
   AVERAGE_PROTON = average_proton_shift_csv(lofe)
   AVERAGE_CARBON = average_carbon_shift_csv(lofe)
   print """
The shielding tensor of the hydrogen atoms = %s

The shielding tensor of the carbon atoms = %s

Additionally, the script has performed the task of creating the
following files, which contain the NMR shielding tensors of the
individual proton and carbon atoms of the reference standard:

%s-protons.csv
```

```
%s-carbons.csv
""" %
(AVERAGE_PROTON,AVERAGE_CARBON,OUTPUT_PREFIX,OUTPUT_PREFIX)
   write_final_shift_csv(lofe)

def report_chemical_shifts(lofc_nmr):
   ATOM_NUMBER = 0; ATOM_SYMBOL = 1; ISOTROPIC_VALUE = 4
   lofe = []
   for file in lofc_nmr:
      proton_chemicalshift_table = []
      carbon_chemicalshift_table = []
      for line in file[2]:
         if "Isotropic" in line:
            linesplit = line.split()
            if linesplit[ATOM_SYMBOL] == "C":

carbon_chemicalshift_table.append([int(linesplit[ATOM_NUMBER]),float(linesplit[ISO
TROPIC_VALUE])])
            if linesplit[ATOM_SYMBOL] == "H":

proton_chemicalshift_table.append([int(linesplit[ATOM_NUMBER]),float(linesplit[ISO
TROPIC_VALUE])])
      lofe.append(carbon_chemicalshift_table)
      lofe.append(proton_chemicalshift_table)

   return lofe


def get_conf_number():
   conf_number = 0
   return conf_number
```

```
def write_final_shift_csv(lofe):
    ATOM_NUMBER = 0; SHIFT = 1
    pwriter = open(OUTPUT_PREFIX+"-protons.csv",'w')
    cwriter = open(OUTPUT_PREFIX+"-carbons.csv",'w')
    proton_list = []
    carbon_list = []
    print >> pwriter, "ATOM NUMBER, CHEMICAL SHIFT"
    for item in lofe[PROTON_CS]:
        print >> pwriter, str(item[ATOM_NUMBER]),",",str(item[SHIFT])
        proton_list.append(item[SHIFT])
    print >> cwriter, "ATOM NUMBER, CHEMICAL SHIFT"
    for item in lofe[CARBON_CS]:
        print >> cwriter, str(item[ATOM_NUMBER]),",",str(item[SHIFT])
        carbon_list.append(item[SHIFT])
    return 0

def average_proton_shift_csv(lofe):
    ATOM_NUMBER = 0; SHIFT = 1
    proton_list = []
    for item in lofe[PROTON_CS]:
        proton_list.append(item[SHIFT])
    AVG_PROTON_SHIFT = round(sum(proton_list)/len(proton_list),4)
    return AVG_PROTON_SHIFT

def average_carbon_shift_csv(lofe):
    ATOM_NUMBER = 0; SHIFT = 1
    carbon_list = []
    for item in lofe[CARBON_CS]:
        carbon_list.append(item[SHIFT])
    AVG_CARBON_SHIFT = round(sum(carbon_list)/len(carbon_list),4)
```

```
    return AVG_CARBON_SHIFT

def prepare_list_of_chemical_shifts(lofc_nmr):
    list_of_chemical_shifts = []
    for file in lofc_nmr:
        list_of_chemical_shifts.append([file[0],file[1]])

    return list_of_chemical_shifts

def read_gaussian_nmr_outfiles():
    list_of_nmr_outfiles = []
    list_of_files= sys.argv[1:]
    for file in list_of_files:
        list_of_nmr_outfiles.append([file,int(get_conf_number()),open(file,"r").readlines()])

    return list_of_nmr_outfiles


if __name__ == "__main__":
    main()
```